Nickel Catalyzed C–H Functionalization: Development, Application and Mechanistic Investigation

by

Mo Chen

A dissertation submitted in partial fulfillment
of the requirements for the degree of
Doctor of Philosophy
(Chemistry)
in the University of Michigan
2023

Doctoral Committee:

Professor John Montgomery, Chair
Assistant Professor Timothy A. Cernak
Professor Anne J. McNeil
Professor John P. Wolfe

Mo Chen

mochem@umich.edu

ORCID iD: 0000-0002-4421-4073

Dedication

This dissertation is dedicated to my family.

Acknowledgements

Looking back at grad school time and beyond that leads me to today, I want to first thank my family for their unconditional love and support. They have taught me all merits with themselves as examples, *putting me on their shoulders to more than I can be*. Five years ago, I left home to pursue this degree in the US, I can still remember it was a seemingly ordinary sunny day when I waved goodbye to my family. I wish I knew at that time; it would be my last chance spending time with those who raised me up; but I am afraid if I knew, I could never make up my mind for this 5-year commitment. Thank you for shaping me to be who I am. I hope what I have achieved in the past, what I am fighting for now, and what I will accomplish in the future can make you proud.

I want to thank my advisor Prof. John Montgomery for his unwavering care and support. Without John's help, I cannot develop into as good a scientist, and I am grateful for the leadership opportunities he provided with insightful suggestions. I am grateful for my peers in the group, who kindly allow me to learn and grow with. I am also grateful for every open door in the department that generously shared expertise and chemicals. I want to thank Prof. Pavel Nagorny for offering me rotation opportunity, my collaborators for their indigenous work and my committee members for their continuous support. I want to thank the supporting staff in the department. I also want to thank NSF Center for Selective C−H Functionalization for offering an outstanding collaborative environment with an awesome group of engaging scientists.

I want to thank my friends who share the highs and lows with me during grad school, it would be much tougher a journey without their support.

I would also like to thank my mentors at Nankai University and University of Illinois at Chicago, Prof. Shou-Fei Zhu, and Prof. Tom Driver, who offered me the chance to work in their labs, encouraged me to pursue my aspirations in grad school.

I, by no means am the lucky guy in lab, with first paper online right before the final year in this program. However, I am blessed with incredible support and help from people around me: from day-to-day research to out of work on basketball court, from getting into lab to perform challenging experiments to finding a job in industry. Motivated by all the helping hands, I have learned and will keep doing my best to get out of my way helping others to achieve their own successes and pass on the kindness I received. Lastly, I want to thank all the hard-working nights and weekends, overcoming different challenges to entitle myself to this PhD degree.

“桃李春风一杯酒，江湖夜雨十年灯”

Table of Contents

List of Tables

List of Schemes

List of Abbreviations

Me	methyl
Et	ethyl
i-Pr	isopropyl
n-Pr	propyl
n-Bu	butyl
n-Pent	pentyl
n-Hex	hexyl
hex	hexanes/hexyl
tBu	tert-butyl
Cy	cyclohexyl
Ph	phenyl
PMP	para-methoxyphenyl
Ar	aryl
Bn	benzyl
Bz	benzoyl
Ac	acetyl
Ts	tosyl
TMS	trimethylsilyl
Py	pyridine
Boc	tert-butyloxycarbonyl

TFA	trifluoroacetic acid
TFE	trifluoroethanol
COD	1,5-cyclooctadiene
NHC	N-heterocyclic carbene
Ni	nickel
Ir	iridium
PF6	hexafluorophosphate
TEMPO	(2,2,6,6-Tetramethylpiperidin-1-yl)oxyl
NHPI	N-hydroxyphthalimide
THF	tetrahydrofuran
DME	dimethoxyethane
Et2O	diethyl ether
EtOAc	ethyl acetate
DCM	dichloromethane
DMF	dimethylformamide
MeCN	acetonitrile
KHMDS	potassium bis(trimethylsilyl)amide
TBADT	tetrabutylammonium decatungstate
DTBP	di-tert-butylperoxide
CDC	cross dehydrogenative coupling
AIBN	azobisisobutyronitrile
TBPB	tert-butylperoxy benzoate
DCP	dicumyl peroxide

TBEC	tert-butylperoxy 2-ethylhexyl carbonate
TDAE	tetrakis(dimethylamino)ethylene
TBACl	tetrabutylammonium chloride
TBAB	tetrabutylammonium bromide
TBAI	tetrabutylammonium iodide
TBHP	tert-butylhydrogenperoxide
bpy	2,2'-bipyridine
dtbbpy	4,4'-di-tert-butyl-2,2'-bipyridine
4,4’-diMebbpy	4,4'-di-methyl-butyl-2,2'-bipyridine
4,4’-diOMebbpy	4,4'-di-methoxy-butyl-2,2'-bipyridine
5,5’-diMebpy	5,5'-di-methyl-butyl-2,2'-bipyridine
5,5’-diCF3bpy	5,5'-di-trifluoromethyl-butyl-2,2'-bipyridine
dcype	1,2-Bis(dicyclohexylphosphino)ethane
dtbbpy	4,4'-di-tert-butyl-2,2'-bipyridine
1,10-phen	1,10-phenanthroline
terpy	2,2’:6’,2” terpyridine
bpp	2,6-di(pyrazol-1-yl)pyridine
PyBiOx	bis(oxazolinyl)pyridine
DPPE	1,2-bis(diphenylphosphino)ethane
DPPF	1,1’-bis(diphenylphosphino)ferrocene
rt	room temperature
ºC	temperature in degrees Celsius
min	minute(s)

h	hours(s)
d	day(s)
ee	enantiomeric excess
er	enantiomeric ratio
dr	diastereomeric ratio
equiv	equivalent
CFL	compact fluorescent lamp
BRSM	based on recovered starting material
GCMS	gas chromatography mass spectrometry
BDE	bond dissociation energy
HAT	hydrogen atom transfer
PCET	proton-coupled electron transfer
NMR	nuclear magnetic resonance
SET	single electron transfer
OA	oxidative addition
CMD	concerted metalation deprotonation
RE	reductive elimination
MI	migratory insertion
TM	transmetallation
LLHT	ligand-to-ligand hydrogen transfer
KIE	kinetic isotope effect
SPO	secondary phosphine oxide
MAD	methylaluminum bis (2,6-di-tert-butyl-4-methylphenoxide)

SFC	supercritical fluid chromatography
Mn	average molecular weight
DP	degree of polymerization
PDI	polymer dispersity index
OLED	organic light-emitting diode
LED	light-emitting diode
PC	photocatalyst
Da	Dalton

Abstract

C–H bonds are ubiquitous in nature. The direct conversion of C–H bonds into desired functionalities holds great promises in fields of natural product total synthesis, agricultural, biomedicine, and material science. However, the fact that C–H bonds being prevalent in organic molecules not only indicates their relative inert nature, but also renders their selective functionalization a daunting challenge. Moreover, the development of C–H functionalization methodology has been long hampered due to the obstacles in mechanistic investigations, thus often preventing further reaction development and application. New opportunities have become available for achieving site-selective C–H functionalization as transition metal (TM) catalyzed cross coupling revolutionized organic synthesis with myriad of methods being developed for diverse categories of coupling partners. Through these studies, the synthetic community started to recognize C–H bonds being latent nucleophiles, the use of which would bypass the reductant synthetic handle installation, offering unprecedented routes towards target structures.

This dissertation focuses on developing C–H functionalization using nickel (Ni) catalysis, a sustainable, earth-abundant transition metal. Application has sequentially been demonstrated by applying the developed methodologies to enantioselective catalysis and polymer synthesis. The reaction development has been guided by the exploration in organometallic catalyst synthesis and mechanistic investigations which were conducted both experimentally and computationally including reaction progress kinetic analysis (RPKA), kinetic isotope effect (KIE) same excess experiments and density functional theory (DFT).

The first chapters revisit a unique, nickel mediated C–H activation pathway, ligand-to-ligand hydrogen transfer (LLHT). The successful synthesis of unprecedented 1,5-hexadiene supported chiral nickel catalysts enabled a novel, intermolecular asymmetric C–C cross coupling. Experimental evidence from RPKA and KIE experiments were consistent with the proposed LLHT pathway, where the C–H activation precedes a rate-determining reductive elimination step. The implication of this methodology was translated to a defect-free polymer synthesis. High molecular weight polymers (M_n >17 kDa) have been synthesized with readily available monomers under mild condition in stereo-regulated manners.

Being not only a cost-effective replacement for precious transition metals, nickel is also appealing for its unique reactivities, single electron transfer (SET) being one of them. The radical nature of odd oxidation states (Ni^{I}, Ni^{III}) has been highlighted in the mechanistic study of α-arylation of *N*-alkylbenzamides catalyzed by a dual nickel/photoredox system where tetrabutylammonium bromide (TBAB) was a potent HAT agent. Moreover, this additive effect was demonstrated with improved reactivities and better access to valuable C(sp3)-arylated products. Intrigued by the versatilities of hydrogen atom transfer (HAT) for activating C–H bonds that are otherwise hard to approach, the final chapters focus on the cross coupling between aldehydes and carbamates via a dual HAT process. Supported both by experimental evidence and quantum chemical simulations, the unconventional combination of oxidants and reductants was deemed vital in this redox-buffered dehydrogenative coupling. Building on this seminal report, ongoing efforts are harvesting nickel as a powerful carbon centered radical mediator to attain modular synthesis of targeted structures under diverse manifolds. Considering the pivotal role that *N*-heterocycles play in the bioactive molecules, we surmise future application in structural elaboration of amine-containing targets.

Chapter 1 Nickel Catalyzed C–H Functionalization, an Overview

1.1 Introduction

In the realm of transition metal catalysis, C–H activation, a fundamental organometallic pathway, precedes C–H functionalization due to the inert nature of C–H bonds.[1] Different manifolds have thus been developed under the regime of nickel (Ni) catalyzed C–H activation, including direct oxidative addition (OA), concerted metalation deprotonation (CMD), hydrogen atom transfer (HAT) and ligand-to-ligand hydrogen transfer (LLHT) (**Scheme 1-1**).[2] C–H bonds are cleaved in different manners among these C–H activation pathway, where only HAT involves a homolytic bond cleavage leading to the formation of carbon centered radicals. Within heterolytic C–H bond breaking events, direct OA is unique for the formation of nickel hydride intermediates while in both CMD and LLHT processes, proton acceptors are required either externally as a base additive or internally on the substrate. This chapter aims at summarizing and clarifying different C–H activation manifolds, paving the way towards the conversion of carbon hydrogen bonds to carbon metal bonds, and ultimately the functionalities of choice which will be further discussed in later chapters.

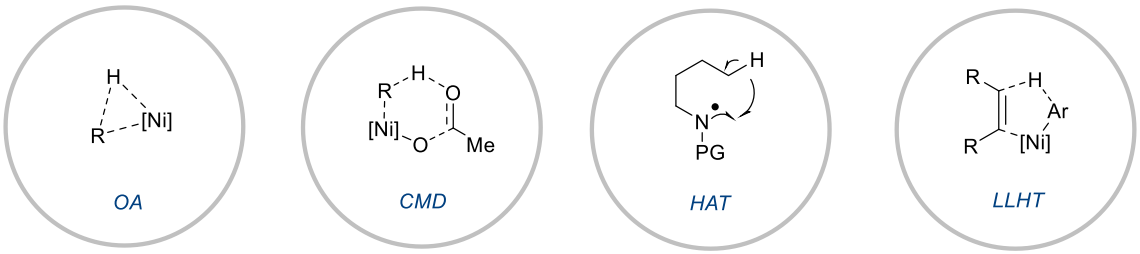

Scheme 1-1 Different modes of C–H activation.

1.2 Oxidative Addition (OA)

To initiate C–H oxidative addition, the formation of a σ-complex is a pre-requisite step for substrate binding. Owing to nickel being a relatively electropositive late transition metal, the sequential three center two electron oxidative addition is rendered kinetically feasible.[3] However, OA is hampered by the significantly lower nickel carbon bond energy compared to heavier metals, resulting in a decreased thermodynamic driving force for the C–H bond cleavage.[4] Despite being a challenging organometallic step, efforts have been made towards the isolation of nickel hydride intermediates to deconvolute this oxidative addition pathway. The first synthesis of a nickel hydride species via oxidative addition can be dated back to 1969 by Wilke and co-workers and their stoichiometric synthesis benefitted from labile hydrogen atoms in the cyclopentadiene scaffold (**Scheme 1-2**, top).[5] Since this seminal report, efforts towards isolating nickel hydride species from direct oxidative addition of C–H bonds with Ni(0) complexes often turned out unsuccessful, yielding only the η^2-arene complexes, let alone the Ni(I) and Ni(II) counterparts. [6]

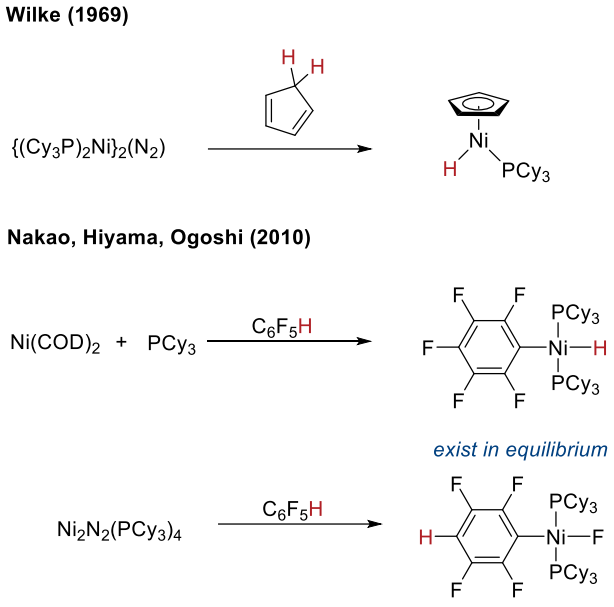

Scheme 1-2 Precedents for stoichiometric OA by nickel.

More recently, polyfluoroarenes have been identified as unique substrates that could undergo OA, resulting in nickel hydride complexes. On the other hand, the simultaneous competing C–F activation cast shadow on the isolation of corresponding nickel hydride complex, as Nakao, Hiyama, and Ogoshi reported the in-situ characterization of *trans*-$(C_6F_5)(H)Ni(PCy_3)_2$ (**Scheme 1-2**, bottom).[7] Of note, bulky ligands (mostly phosphine ligands) are necessary to stabilize the hydride complexes.

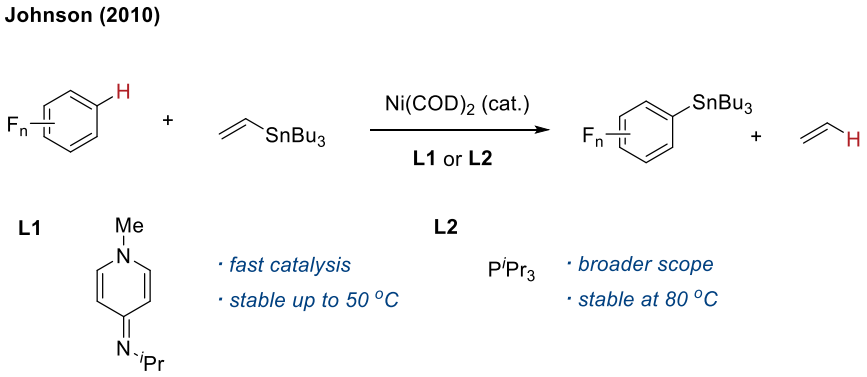

Scheme 1-3 The first C–H stannylation via nickel catalysis.

Other than the stoichiometric synthesis and isolation of via OA, nickel hydrides are among the most reactive metal hydrides species and have been actively employed in catalysis.[8] That said, one of the most explored fields is the insertion into substances that are featured with degree of unsaturation allowing for a concerted migratory insertion step following the initial oxidative addition. In this vein, Johnson and co-workers disclosed the first C–H stannylation with the combination of a catalytic $Ni(COD)_2$ and a carefully designed neutral ancillary ligand (**L1**) yielding a broader scope at variable conditions (**Scheme 1-3**).[9] The major debate of reaction mechanism originated in the lack of understandings whether the C–H bond-breaking step involved oxidative addition coupled with insertion.[10] Mechanistic investigations have been performed both experimentally and computationally to mitigate such gaps where the authors found that a KIE of 2.0 indicated that C–H activation being irreversible. Interestingly, calculation performed using

density functional theory (DFT) did not exclude a direct hydrogen transfer between fluorinated arenes and vinyl stannanes, where the C–H activation fell into the ligand-to-ligand hydrogen transfer (LLHT) mode that will be further discussed later this chapter.[11]

1.3 Concerted Metalation Deprotonation (CMD)

First proposed by Winstein and Traylor in 1955,[12] concerted metalation deprotonation (CMD) has become an ever-growing field especially with the skyrocketing development of palladium catalyzed C–H functionalization.[13] The idea of a carboxylate or carbonate base which deprotonates substrate while allowing for the formation of a new carbon metal bond in a concerted manner turns out to be a prevalent pathway for late transition metals including nickel.[14] Under this framework, two major types of transformation can be classified by directing group strategy and undirected, ligand controlled pathway.

Scheme 1-4 Nickel catalyzed C–H iodination and the computed CMD pathway.

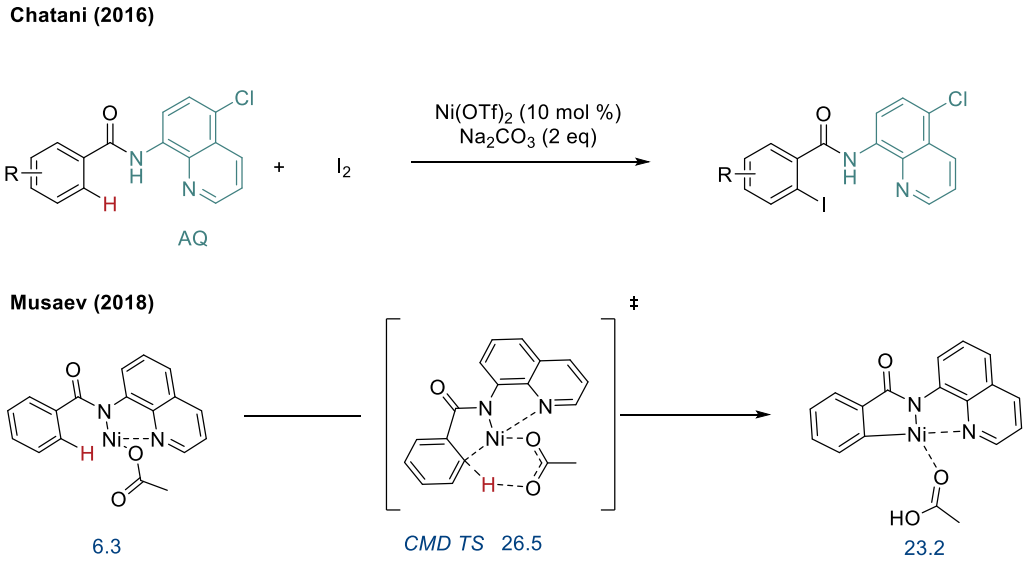

ΔG was displayed with respective to $Ni(OAc)_2$ in kcal/mol.

Recently, Chatani demonstrated the first example of Ni(II) catalyzed C–H iodination using molecular iodine as an iodinating reagent (**Scheme 1-4**, top).[15] The superior reactivity and selectivity lied in aromatic amide substrates bearing amino quinoline moieties as a directing group, incurring a CMD mechanism. Deuterium labeling experiments indicated that the cleavage of C–H bonds is irreversible and could be the rate-determining step which prompted further mechanistic investigations to understand the C–H activation pattern.[16] DFT calculations not only confirmed that the C–H cleavage occurred via 6-membered transition state with an internal acetate base but also examined the energy landscape to verify that the C–H activation being the rate determining step (**Scheme 1-4**, bottom).[17]

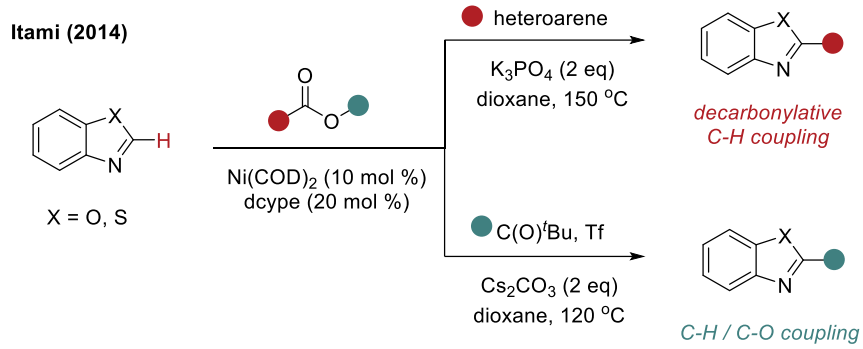

Scheme 1-5 C–O electrophile-controlled chemoselective C–H functionalization of azoles.

Yamaguchi, Itami and co-workers reported the C–O eletrophile-controlled chemoselectivity of Ni-catalyzed coupling reactions between azoles and esters for the synthesis of privileged 2-arylazole scaffolds (**Scheme 1-5**).[18] A systematically study by the Fu group investigated the aforementioned transformations to elucidate the chemoselectivity and a base-promoted C–H activation of azoles.[19] The calculated energy barriers indicated a change of rate-determining step depending on whether CO migration was involved. However, in both scenarios, the C–H bond activation underwent a base promoted 6-membered transition state, foraging a new carbon metal bond, depleting the phosphate base as proton acceptor (**Scheme 1.6**, left).

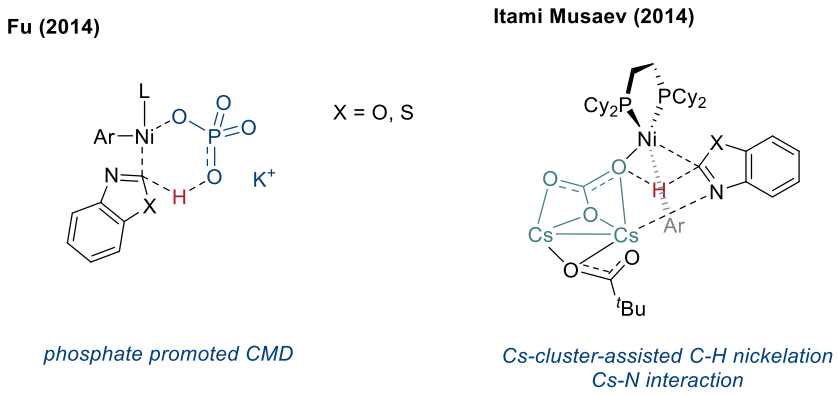

Scheme 1-6 Computed C–H activation pathway via CMD or σ-bond metathesis.

Following this seminal mechanistic report, another computational analysis has been fruitful from the collaboration between the Itami and Musaev groups. When Cs_2CO_3 was used as a base, the calculation suggested that C–H activation could undergo a σ-bond metathesis process promoted by a cesium cluster (**Scheme 1-6**, right).[20] It is worth to note that *σ-bond metathesis* has been a long-standing manifold in the nickel promoted C–H activation and the earliest example can be dated back to 1963 by Dubeck and co-workers (**Scheme 1-7**).[21] However, this overview will be sticking with the manifolds that are more pertinent to later chapters in lieu of further discussing such pathway.

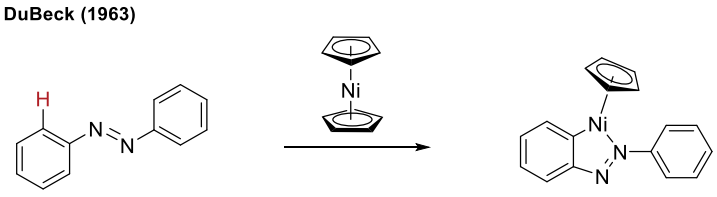

Scheme 1-7 First nickel mediated C–H activation via σ-bond metathesis.

1.4 Hydrogen Atom Transfer (HAT)

Compared with previously discussed two-electron C–H activation pathway, hydrogen atom transfer (HAT) is an inherently different process which involves a concerted movement of a

proton and an electron in a single kinetic step from one group to another.[22] Such radical process contributes a new dimension to traditional organic synthesis and has been long recognized by the chemistry community as the discovery of Hofmann–Löffler–Freytag (HLF) reaction,[23] Barton's nitrite photolysis[24], and application of Bu_3SnH with azobisisobutyronitrile (AIBN)[25]. Despite of these early precedents, developments of HAT mediated C–H functionalization have been hampered due to the harsh reaction condition. Recent breakthroughs of mild methodologies for generation of various carbon centered radical species enabled their utilization in the HAT process, which in turn led to the renaissance of the field.[26] Coupled with transition metal catalysis, HAT has unlocked the potential of chemo- and regioselective functionalization of C–H bonds that are otherwise difficult to be activated.[27] This section will be focusing on nickel mediated processes as they have become a major thrust in the field of C–H functionalization via HAT.[28] Two mainstream revenues have been invented to make the most of the merger of HAT with nickel catalysis, namely photoinduction and thermal-activation.[29]

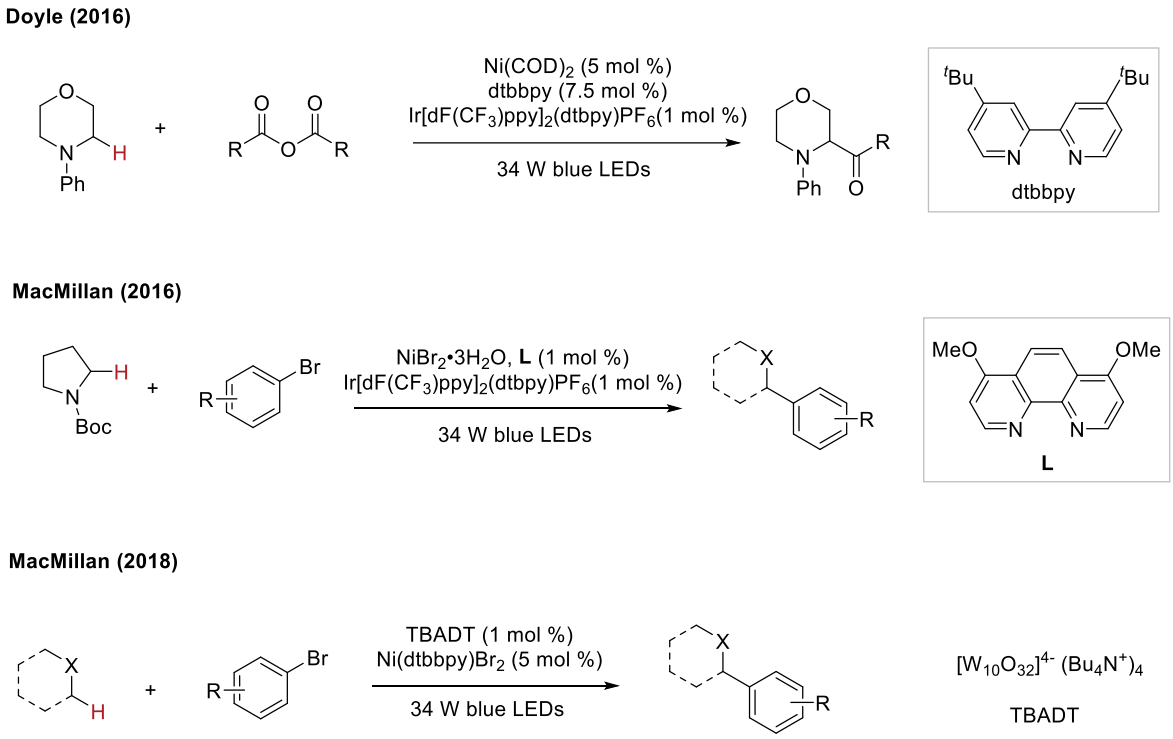

Scheme 1-8 C(sp3)–H arylation through photoinduced HAT and nickel catalysis.

Seminal contribution by Doyle and MacMillan disclosed a proof-of-concept study supporting the idea of converting C(sp3)–H bonds in dimethylaniline into organic radicals which could sequentially undergo cross couplings.[30] Building on these efforts, the Doyle group developed a direct functionalization of C(sp3)–H bonds of *N*-aryl amines by acyl electrophiles under a mild, metallaphotoredox condition with a wide scope (**Scheme 1.8**, top). Shortly after, the MacMillan group followed with the photoinduced α-amino and α-oxy C(sp3)–H arylation using a Ni(II) hydrate pre-catalyst, representing a powerful demonstration of the versatility of C–H bonds as organometallic nucleophile equivalents (**Scheme 1-8**, middle).[31] In 2018, the same group reported another photo-catalytic HAT where direct arylation of C(sp3)–H bonds in a broad range of alkanes have been achieved (**Scheme 1-8**, bottom).[32] The novel application of tetrakis(tetrabutylammonium) decatungstate (TBADT) serving not only as the photosensitizer but also as the HAT reagent was worth highlighting.

Peroxides often come into sight when discussing thermal HAT processes. As compared to various hydrogen peroxides that have been applied to atom transfer chemistry with other transition metals, dialkyl peroxides, a more stable organic peroxide counterpart, are well suited within nickel's redox potential.[29, 33]

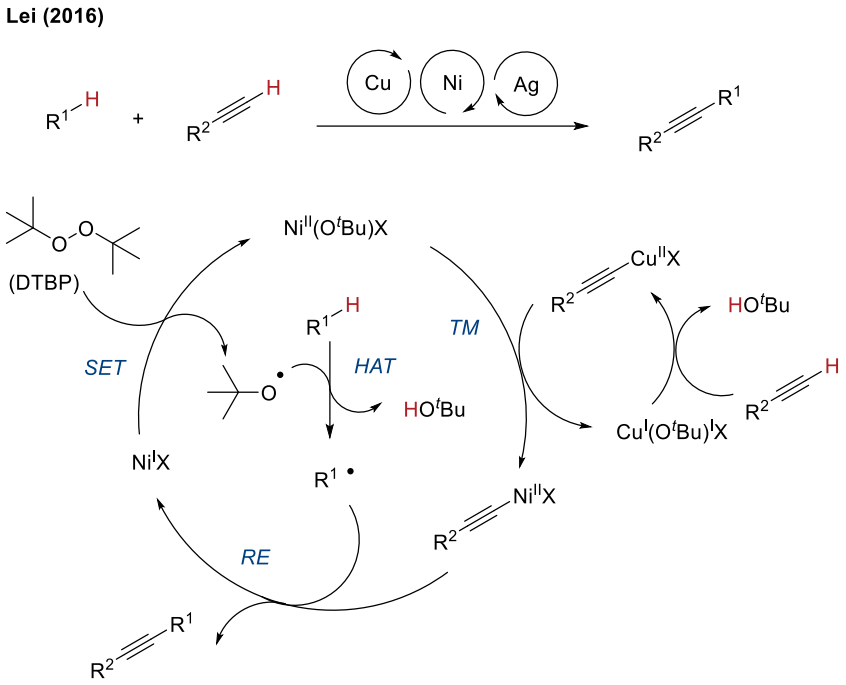

Scheme 1-9 Alkanes and alkynes coupling enabled by multi-metallic catalysis.

In 2016, Lei and co-workers reported a selective radical oxidative C(sp3)–H/C(sp)–H cross coupling of unactivated alkanes with terminal alkynes by using a combined Cu/Ni/Ag catalytic system (**Scheme 1-9**).[34] The proposed mechanism began with the decomposition of di-*tert*-butyl peroxide (DTBP) by a low valent Ni(I) species, releasing one equivalent *tert*-butoxy radical that underwent HAT with alkanes. On the other hand, similar to the Sonogashira coupling, an oxidized Ni(II) intermediate underwent transmetalation (TM) with an alkynyl Cu(II) complex which was separately generated. To complete the catalytic cycle, reductive elimination (RE) took place, producing the desired cross coupled product as well as the reactive Ni(I) catalyst.

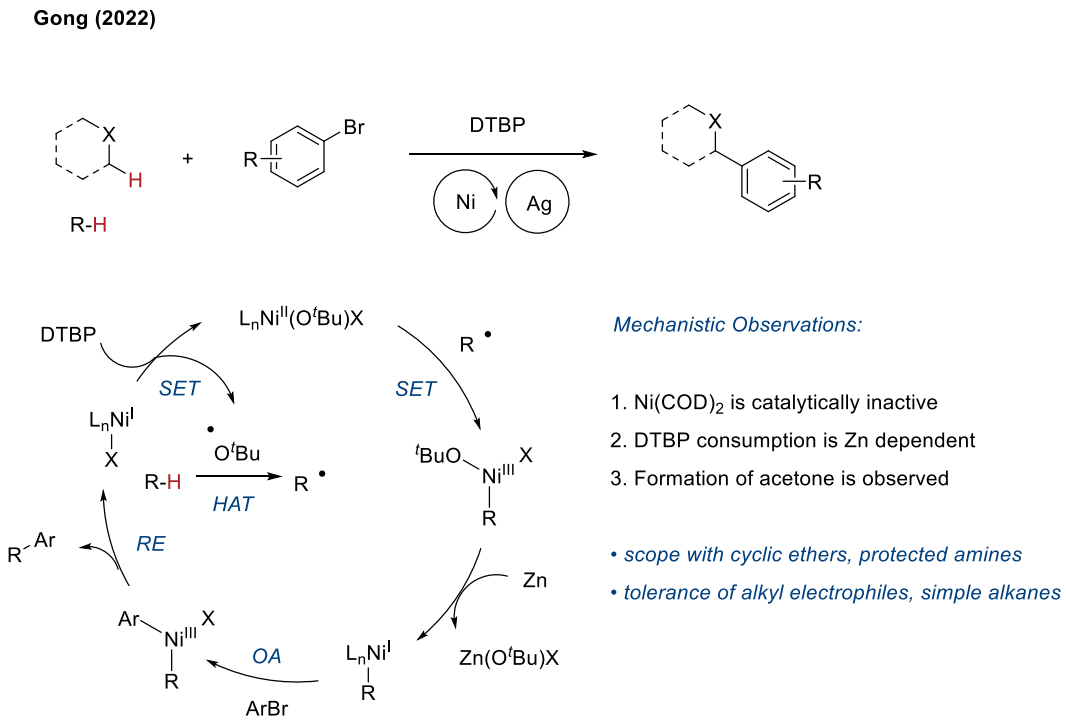

Scheme 1-10 Nickel catalyzed arylation of C(sp3)–H bonds.

Recently, the Gong group reported a nickel catalyzed arylation of C(sp3)–H bonds with organohalides using DTBP as the HAT reagent (**Scheme 1-10**).[35] A strategic merge of Zn as an terminal reductant with oxidant enabled this unique carbofunctionalization while such co-existence has also been seen in redox-buffer systems developed by Stahl.[36] This protocol allowed for the arylation under mild, thermal conditions with a broad substrate scope including cyclic ethers, amines and even cyclohexane. Mechanistic investigations were conducted to elucidate the dual roles of nickel a) serve a crucial electron shuttle between the reductant and oxidant and b) the radical mediator. Unlike the redox-buffer system, Zn in this case played a key role in nickel catalyst turnover, correlating to the formation of *tert*-butoxy radical. Coincidentally, Stahl and co-workers separately developed a benzylic C(sp3)–H methylation strategy harvesting β-scission process of DTBP and applied it also as a methylation reagent.[37] This unique metallaphotoredox enabled peroxide decomposition will be further discussed in **Chapter 5**.

1.5 Ligand-to-Ligand Hydrogen Transfer (LLHT)

As described in **Section 1.2**, the thermodynamic favorability of a C–H bond activation event depends on the formation of a strong carbon metal bond to offset the energy required to break the C–H bond. The beneficial role of an external base promoted CMD (**Section 1.3**) also alluded to the challenge of nickel-mediated C–H activation, which roots in the low thermostability of carbon nickel bond. That said, to facilitate C–H activation, other fundamental organometallic pathways can be coupled in a concerted manner, taking advantages of driving force for the formation of a stable intermediate. Along with this line, nickel-mediated ligand-to-ligand hydrogen transfer (LLHT) was a recently proposed mechanism via computational studies by Perutz and Eisenstein.[11] The authors suggested that the stepwise oxidative addition (OA), migratory insertion (MI) was burdened with high kinetic barriers, presumably due the reasons mentioned above. Alternatively, the calculation indicated that OA and MI could happen in a concerted manner via a relatively low energy transition state (**Scheme 1-11**). Subsequently, isomerization of the vinyl nickel species positioned the complex in an appropriate geometry for the reductive elimination. It should be noted that the isomerization from a Y-shaped three-coordinate complex to the T-shaped nickel structure was computed as the highest transition state of this pathway. In this case, the C–H bond of the fluoroarene was already broken that of the vinyl group was fully made, no longer interacting with the metal fragment and this is in sharp contrast with the OA mechanism where the rate determining step involved a nickel hydride intermediate. This calculation was further supported by the absence of KIE per experimental analysis.[7]

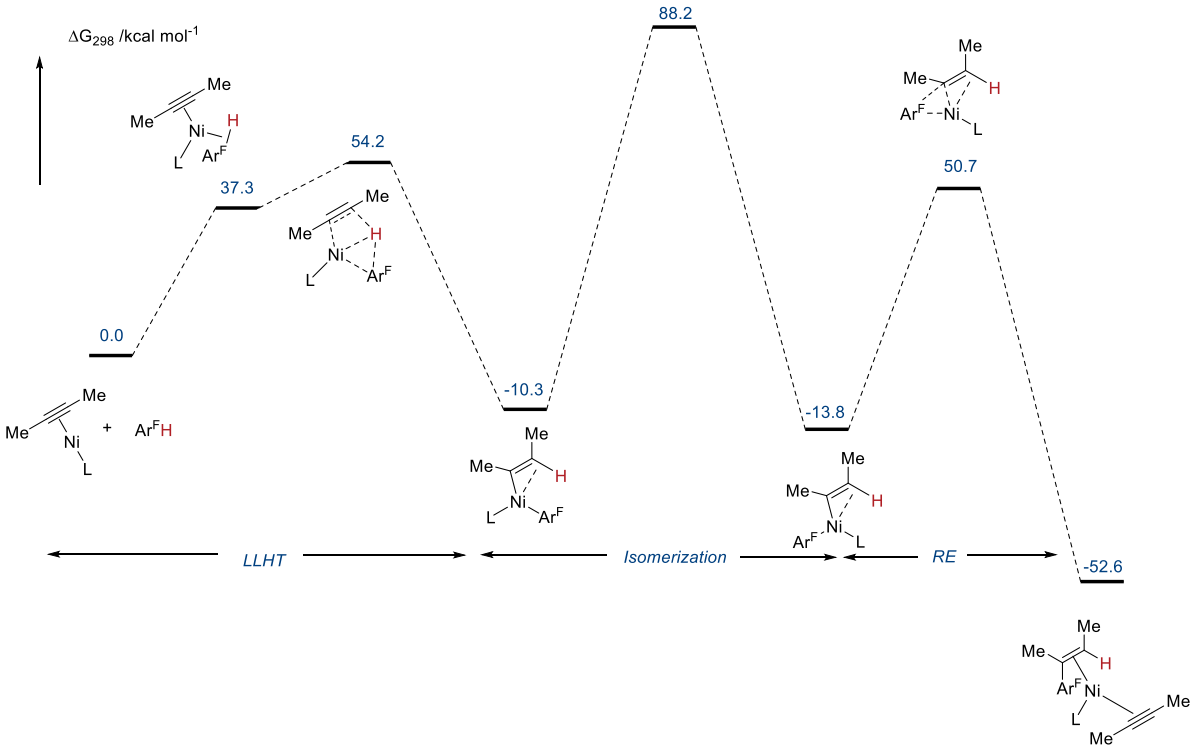

Scheme 1-11 Computed C–H activation via LLHT.

In 2017, detailed mechanistic investigations were conducted by the Montgomery group to elucidate the complexity of nickel catalyzed hydroarylation via C–H functionalization reactions.[38] Multiple competing reaction pathways as well as key parameters for reactivity and selectivity determination have been identified *in silico* and confirmed experimentally. The authors identified that the commonly employed Ni(0) pre-catalyst, bis(cyclooctadiene)nickel(0) can be problematic as the COD-mediated LLHT pathways ultimately resulted in the formation of π-allyl complexes which significantly inhibited catalysis. Though alleviated temperature was helpful for bypassing such thermodynamic traps, the use of 1,5-hexadiene as a stabilizing ligand disfavored LLHT at room temperature and allowed for superior reactivities at milder conditions. DFT calculation suggested the feasible LLHT C–H bond cleavage was followed by an alkyne facilitated isomerization which positioned the nickel for rate-determining reductive elimination. This

proposed catalytic cycle will be further discussed in **Chapter 2** to differentiate ligand-controlled reaction pathways between alkynes and alkenes.

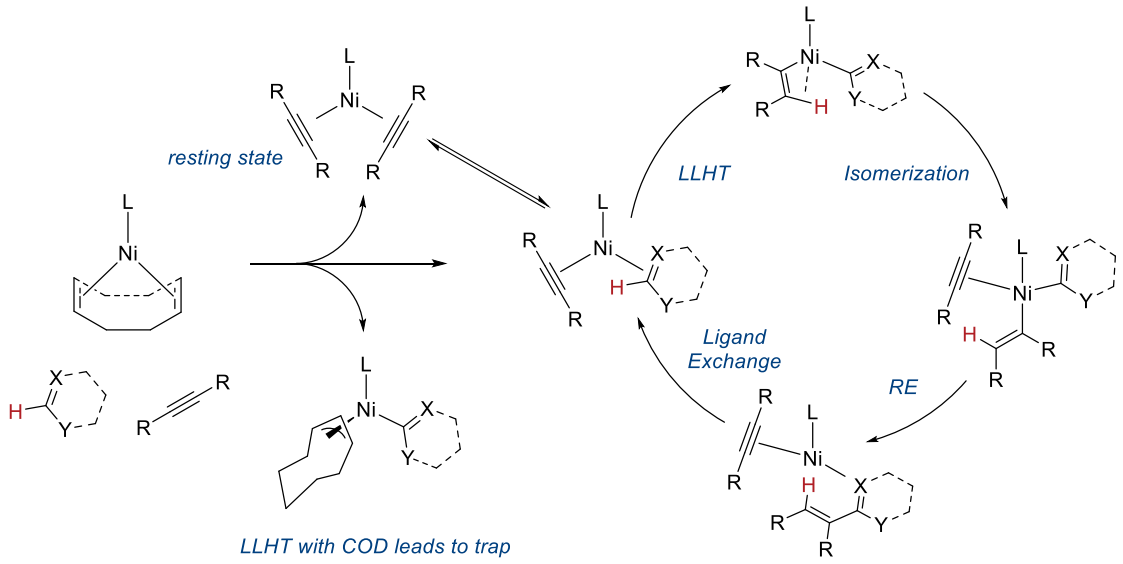

Scheme 1-12 The map of nickel catalyzed C–H alkenylation.

Chapter 2 Enantioselective Heteroaromatic C–H Functionalization via Ligand-to-Ligand Hydrogen Transfer (LLHT)

2.1 Introduction

Heteroaromatic rings are common motifs in natural products and FDA approved pharmaceuticals.[39] Direct functionalization of heteroaromatic C–H bonds has the potential to streamline the synthesis of complex molecules by avoiding the need for pre-functionalization steps.[40] Despite their prevalence, aromatic C–H bonds are relatively inert and often similar in reactivity, rendering their selective functionalization challenging, especially in intermolecular, non-directed processes.[41] Over the past several decades, enormous advances have been made in the field of selective C–H functionalization through the exploration of transition metal catalysis. These newly developed methods offer orthogonal opportunities to existing strategies for the synthesis of natural products, functional materials as well as exploration of structure-activity relationships by avoiding the pre-installation of functionalities required for traditional cross-couplings.[42] Selective transformation of heteroaromatic C–H bonds, however, typically rely on the use of directing groups and second- or third-row transition metal catalysts.[43] Towards this end, functionalizing heteroarenes that lack directing groups using earth abundant transition metals remains underdeveloped.[3, 6b, 44]

This chapter will be focusing on the development of enantioselective heteroaromatic C–H functionalization via nickel catalysis, which can be carried out under mild conditions using Ni(0) catalysts with *N*-heterocyclic carbene (NHC) ligands in the absence of Lewis acid co-catalysts. A series of 1,5-hexadiene supported NHC nickel complexes were synthesized via an operationally

simple approach, resulting in improved functional group tolerance and heteroarene scope. Mechanistic investigations are consistent with a ligand-to-ligand hydrogen transfer (LLHT) pathway where the C–H bond activation precedes a rate-determining reductive elimination step.

2.2 Nickel Catalyzed C–H Functionalization via LLHT

Seminal contribution in the field of LLHT was made by Nakao and Hiyama in 2008 when they reported a selective C–H alkenylation between polyfluoroarenes and internal alkynes using nickel catalysis (**Scheme 2-1**, top).[45] In a separate work, kinetic isotope effect (KIE) was measured by the same groups in order to elucidate this C–H activation mechanism (**Scheme 2-1**, bottom).[7] The authors concluded the absence of KIE as well as other experimental evidences on a rapid, reversible oxidative addition of C–H bond, yielding a nickel hydride complex which they believed to observe spectroscopically. Ligand exchange between the coordinating phosphine with an alkyne was believed to be the rate determining step, due to strong binding affinity of the phosphine ligand. The authors also rationalized the outstanding regioselectivity based on the steric repulsion between bulkier alkyne substituent and the polyfluoroarene.

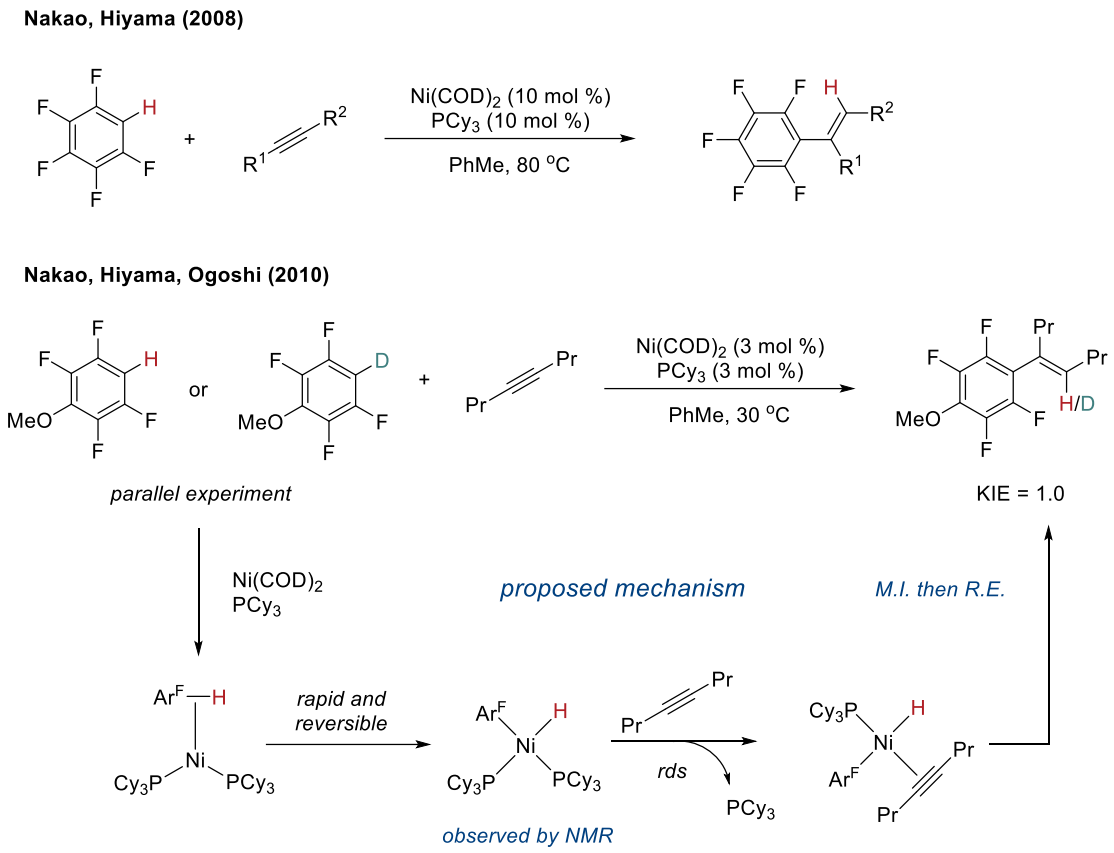

Scheme 2-1 Nickel catalyzed C–H alkenylation and its mechanistic studies.

DFT was introduced to describe the energy landscape of this transformation by Perutz, Eisenstein, and co-workers where they assessed the key C–H activation step whether via a formal nickel-hydride intermediate.[11] In this seminal paper, their data supported a concerted transfer mechanism, termed as ligand-to-ligand transfer (LLHT), as the preferred pathway for C–H bond cleavage.

Since the initial report of the LLHT mechanism, it has been generally accepted as the mode of C–H bond cleavage in hydrofunctionalizations of alkynes and alkenes by nickel catalysis. Attention then was focused on converting this conceptually novel pathway into enantioselective transformation.

2.3 Precedents for Nickel Catalyzed Asymmetric C–H Functionalization via LLHT

The campaign of developing enantioselective LLHT processes commenced with intramolecular asymmetric cyclization, as described by Ye[46], Cramer,[47,] Ackermann[48] and Shi[49] groups which were enabled by the design of novel ligand scaffolds (**Scheme 2-2**).

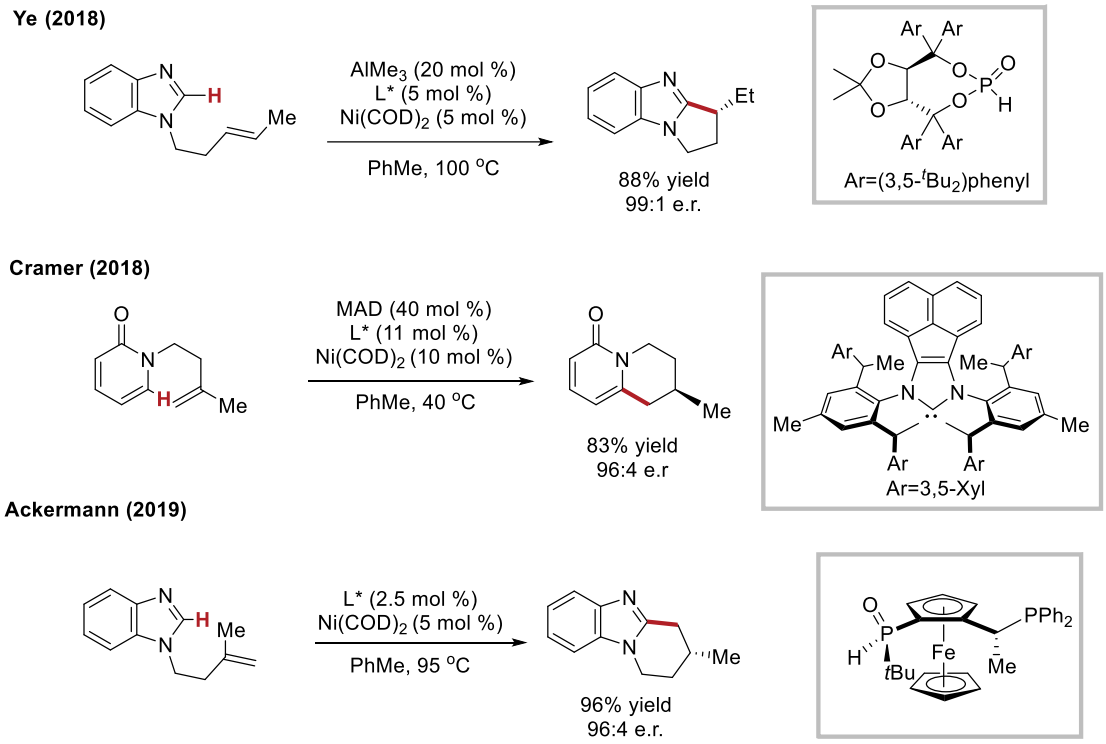

Scheme 2-2 Enantioselective cyclization via nickel catalyzed LLHT.

In 2018, the Ye group reported a Ni-Al bimetallic enantioselective C–H *exo*-selective cyclization of imidazole tethered alkenes promoted by secondary phosphine oxide (SPO) ligands.[46a] Shortly after, the Cramer group developed a modular synthesis of IPhEt ligand family, which was first reported by Galway and co-workers.[50] and successfully applied to the C–H functionalization of pyridones[47a, 47c], pyrroles and indoles.[47d] Independently, the Ackermann group discovered that the combination of nickel and JoSPOphos allowed for the asymmetric C–H functionalization of imidazole without the need of external Lewis acids, and they further illustrated this novel catalysis with a well-defined nickel(II)-JoSPOphos complex.[48a] Though benefiting from

higher reactivities due to closer proximity between C–H bonds and olefins, intramolecular transformations are inherently limited as a rigid scaffold, requiring the pre-installation of tethered alkenes to the heterocyclic starting materials. The tedious synthesis not only desecrates the conciseness of C–H functionalization, but also limits the substrate scope to *N*-heterocycles, excluding those that incapable of alkene installation.

Concurrent with this dissertation, Zhang, Shi and co-workers reported the intermolecular enantio- and regioselective nickel catalyzed C–H functionalization of pyridines with styrenes,[49c] demonstrating the unique selectivity of ANIPE-type ligands (**Scheme 2-3**, top).[51] It is worth highlighting that the bulky C_2-symmetric chiral NHC's aryl fragments demonstrated a strong π-π stacking interaction with trans-styrene, which was crucial for the high efficiency and enantiocontrol. Later in 2022, the Ye group demonstrated C2 selective pyridine C–H alkylation with 1,3-dienes via Ni-Al bimetallic catalysis (**Scheme 2-3**, bottom).[52] A wide range of pyridines, including those complex, pyridine-containing bioactive molecules were found compatible with this reaction. The regioselectivity switch from C4 to C2 C–H bonds was investigated computationally to identify a key 6-membered metalacyclic intermediate. Nevertheless, both protocols were limited to pyridine substrates, suffered from the use of strong Lewis acids as well as high reaction temperature, casting shadows on their functional group compatibilities.

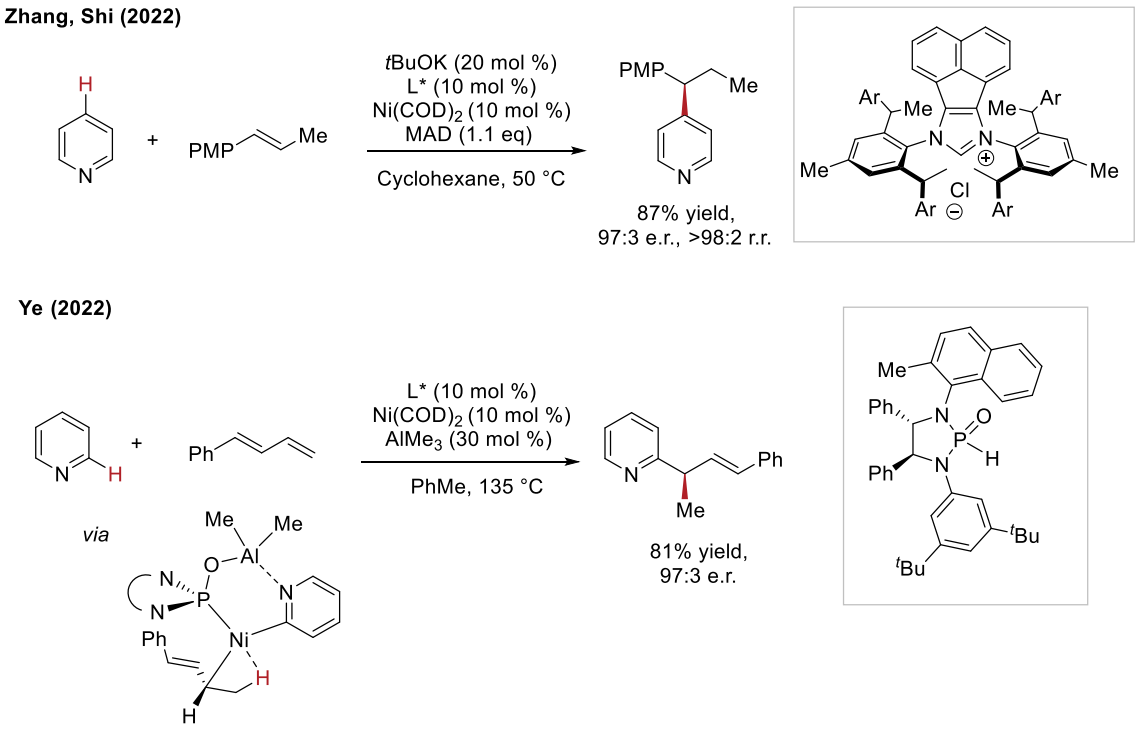

Scheme 2-3 Nickel catalyzed intermolecular enantioselective LLHT.

2.4 Developments Intermolecular Enantioselective Heteroaromatic C–H Functionalization

To mitigate the gap in the literature of intermolecular enantioselective C–H functionalization by developing a Lewis acid free nickel catalysis, we commenced our studies by examining the ligand-controlled reactivity between benzoxazole (**2-1**), which is an important core structure in different bioactive molecules,[53] with norbornene (**2-2**) (**Table 2-1**).

Table 2-1 Condition optimization

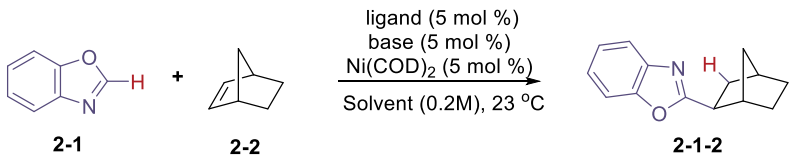

entry	ligand	base	solvent	% yield [a]	e.r.
1	**L1**	-	PhMe	32	42:58

2	**L2**	-	PhMe	<5	37:63
3	**L3-HBF$_4$**	KHMDS	PhMe	22	57:43
4	**L4-HBF$_4$**	KHMDS	PhMe	70	50:50
5	**L5-HBF$_4$**	KHMDS	PhMe	99	92:8
6	**L6-HBF$_4$**	KHMDS	PhMe	90	88:12
7	**L7-HCl**	KHMDS	PhMe	15	48:52
8	**L5-HBF$_4$**	KHMDS	Hexane	95	91:9
9	**L5-HBF$_4$**	KHMDS	$PhCF_3$	58	91:9
10	**L5-HBF$_4$**	KHMDS	THF	74	90:10
11	**L5-HBF$_4$**	KHMDS	Et_2O	61	91:9
12[b]	**L5-HBF$_4$**	KHMDS	PhMe	n.r.	-
13[c]	**L5-HBF$_4$**	KHMDS	PhMe	n.r.	-

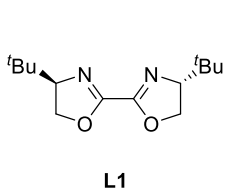

L1

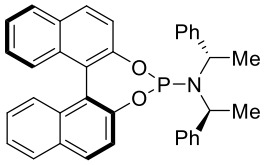

L2

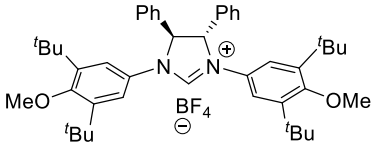

L3-HBF$_4$

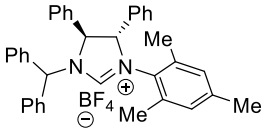

L4-HBF$_4$

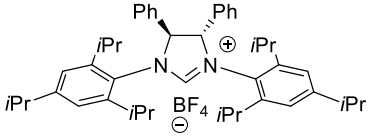

L5-HBF$_4$

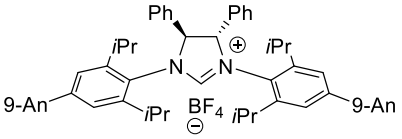

L6-HBF$_4$

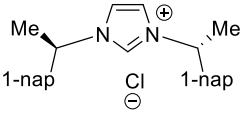

L7-HCl

Reactions were performed at 0.10 mmol scale and enantioselectivities were analyzed using SFC. n.r. : no reaction. [a] Yields were reported for isolated products. [b] at 4 °C. [c] No $Ni(COD)_2$.

Chiral *N*-donor ligands and phosphine ligands are widely applied in asymmetric nickel catalysis, but they failed to yield the desired alkylated product with good results (**Entries 1-2**). As

a sharp contrast, *N*-Heterocyclic Carbenes (NHCs) derived from commercially available chiral diamines provided appreciable enantio-induction while maintaining good reactivity (**Entries 3-7**). The structural activities relationship of chiral NHC ligands were further explored, and it became clear that the steric hinderance on the NHC arms played significant roles in enantioselectivity determination. When **L5**•HBF_4 was used as ligand with catalytic amount of potassium bis(trimethylsilyl)amide (KHMDS) as base for *in-situ* deprotonation, the desired product (**2-1-2**) was isolated with quantitative yield, and 92:8 enantiomeric ratio (e.r.). Attempts to further increase the steric hinderance to ^{t}Bu groups rendered the ligand synthesis inaccessible,[54] and efforts to extend the conjugation by placing ^{i}Pr with 9-anthracenyl yielded inferior results (**Entry 6**). It is also worth highlighting the level of enantiocontrol from chiral centers on the NHC backbone which is uncommon as compared to those possessing chirality within the *N*-substituent. Replacing the bulky 2,6-disubstituted aryl NHC arms with chiral amines in the absence of C2 backbone chirality led to diminished yield and enantioselectivity (**Entry 7**). Further evaluation of solvents demonstrated a good compatibility with aprotic, non-polar solvents although improvements of enantioselectivity were not observed (**Entries 8-11**). Lastly, performing the reaction at 4 °C completely shut down the reactivity, so did leave without the nickel pre-catalyst (**Entries 12-13**). Based on screening, *in-situ* preparation of an active chiral catalyst via the use of 5 mol % **L5**•HBF4, KHMDS, and $Ni(COD)_2$ (**Entry 5**) was brought forward to examine the substrate scope.

2.5 Synthesis of Ni(0) Pre-Catalysts

1,5-cyclooctadiene (COD) has been studied previously, demonstrating its inhibitory effect in nickel catalyzed C–H activation, leading to the formation of thermodynamically stable π-allyl

complexes, stalling the catalysis. Therefore, the development of accessible COD-free Ni(0) pre-catalysts would benefit nickel catalyzed C–H functionalization, enabling reactions that otherwise require high temperature to be performed at mild conditions. This feature would be especially advantageous in enantioselective control, favoring the kinetic product based on the energy difference of transition states.

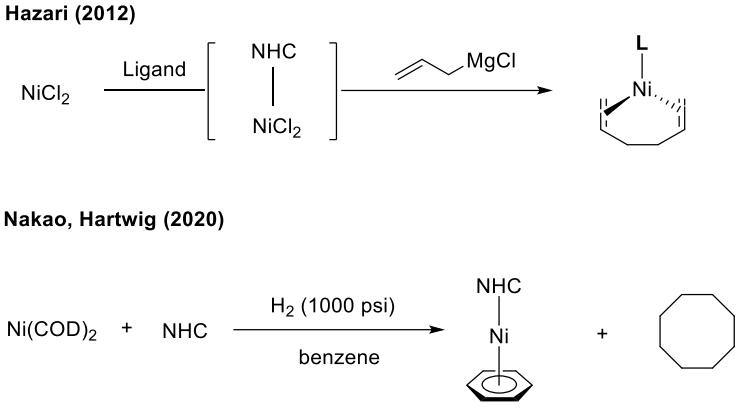

Scheme 2-4 Precedents for COD-free Ni(0) pre-catalyst synthesis.

The first synthesis of COD-free, 1,5-hexadiene supported Ni(0) pre-catalysts were reported by Hazari and co-workers (**Scheme 2-4**, top).[55] Reacting commercially available anhydrous $NiCl_2$ with ligand of choice, followed by treatment with allyl Grignard generated 1,5-heaxidiene supported Ni(0) pre-catalysts. This method allowed for the access of Ni(0) NHCs and phosphine complexes and has been applied in the context of olefin hydrogenation.

In 2020, Nakao and Hartwig groups reported the synthesis of [NHC–Ni(η^6-C_6H_6)] via hydrogenation of COD (**Scheme 2-4**, bottom).[56] The synthesized complexes have then been found as better catalyst precursors, enabling more reproducible catalysis for alkylation of benzene and its derivatives.

Nevertheless, these protocols can still be operationally challenging, as in Hazari's synthesis, the addition of Grignard reagents required additional cooling while in Nakao and Hartwig's synthesis, the operation of highly pressurized hydrogen reactor is less feasible in regular laboratory

settings. Inspired by work done by Wilke and co-workers on the synthesis of 'bis(olefin)nickel-ligand complexes'[57] as well as Belderrain and Nicasio's nickel bis-styrene complex,[58] it was anticipated that ligand exchange from COD to 1,5-hexadiene followed by trapping with free NHC ligands would allow facile access to a variety of sterically demanding NHC nickel complexes at room temperature with a simple glovebox setup. Using this approach, 1,5-hexadiene supported nickel complexes bearing IMes, IPr^{Me}, IPr^{*OMe} as well as the optimal ligand for the enantioselective transformation described above (**L5** in **Table 2-1**) were all successfully synthesized (see **Chapter 8** for details), the latter's structure was unambiguously confirmed using X-ray crystallography (**Scheme 2-5**). We envision this protocol can be further extended to the synthesis of dimethylvinyl silyl ether and other allyl ether supported nickel precatalysts.[59]

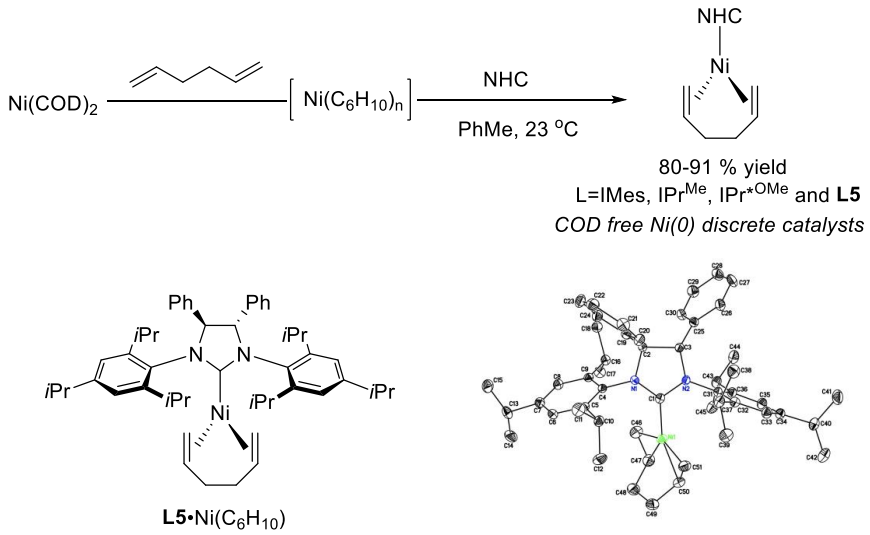

Scheme 2-5 Synthesis of NHC nickel complexes stabilized with 1,5-hexadiene.

2.6 Exploration of Reaction Scope

2.6.1 Heteroaromatic Scope

We were glad to find that the developed C–H functionalization process is tolerant of electron-neutral and electron-rich benzoxazoles substituted at various positions (**2-1, 2-3 – 2-7**) to give the alkylation products with good yields and enantioselectivities. Selective functionalization of benzofurans was also observed for C2 C–H bonds leaving functional groups such as boronic esters intact (**2-8 – 2-10**). LLHT products were not observed when using 5-bromobenzofuran as substrate (**2-11**), which could be attributed to the facile activation of C(sp^2)–Br bond in the presence of low-valent nickel catalyst. Benzimidazoles previously studied by Ackermann[48a] and Ye[46a] for enantioselective cyclization were also reactive in the intermolecular system. We showed that norbornene (nbe) reacted with *N*-Me and *N*-Ph benzimidazoles (**2-12, 2-13**) to yield the C–H functionalization products with moderate enantioselectivity at 60 °C (*vide infra*). Interestingly, the C5-alkylated 1,2,4-triazole was exclusively obtained with high regio- and enantioselectivity despite the more hindered environment (**2-14**). Other nitrogen containing heteroaromatic rings including caffeine (**2-15**) and 3-methylquinazolin-4(3*H*)-one (**2-16**) also underwent efficient couplings to give the desired product in good yields and 90:10 and 87:13 e.r. respectively. All of alkylation products were obtained as a single, exocyclic diastereomer originating from steric biases.

Table 2-2 Enantioselective heteroaromatic C–H functionalization scope

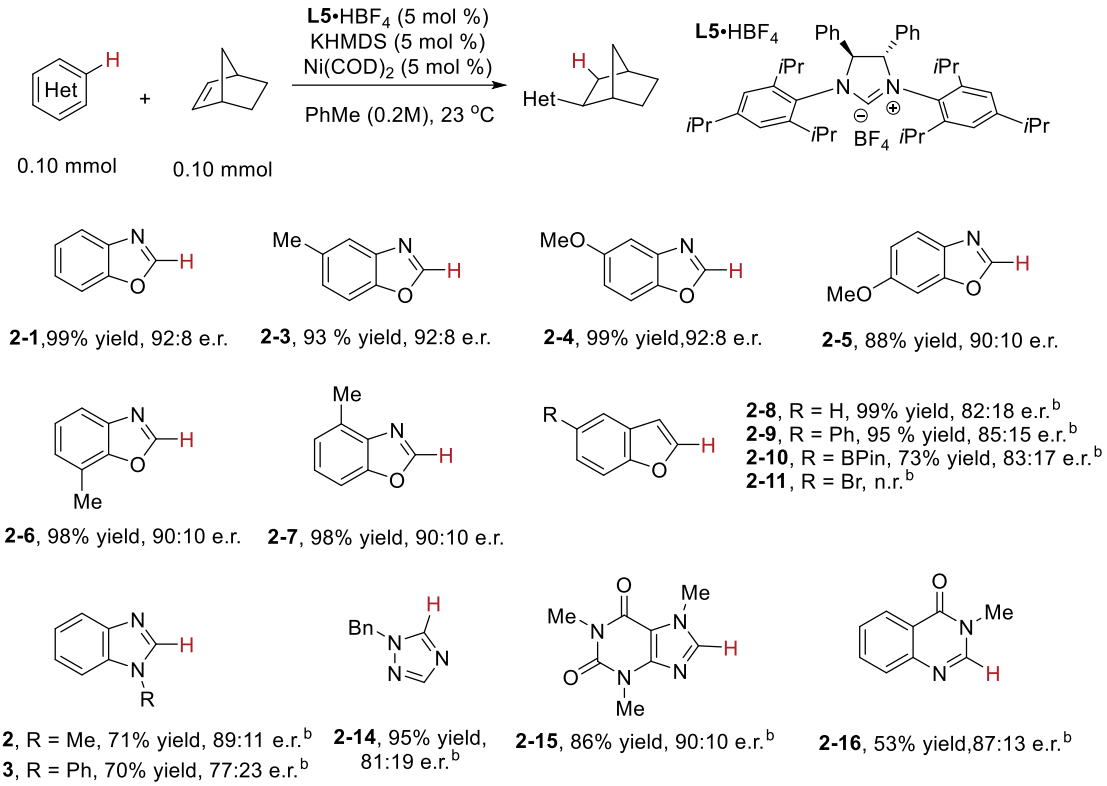

[a] Reactions were performed at 0.10 mmol scale and yields were reported for isolated products. [b] Reaction was carried out at 60 °C.

When examining benzoxazoles bearing electron-withdrawing substituents, however, the desired alkylation products were not obtained using the standard protocol described above. We postulated that the increased acidity of benzoxazole's C-2 C–H bond could lead to deleterious side reactions with 1,5-cyclooctadiene (COD) from the nickel pre-catalyst, resulting in unproductive off-cycle intermediates. The diminished reactivity of benzoxazoles bearing electron-withdrawing groups has similarly been observed by Ong and co-workers in their study of hydroarylation of cyclic dienes.[60] The inhibitory effect of COD in C–H activations was previously described by our laboratory in the development of alkyne hydroarylation reactions involving LLHT pathways.[38, 61] This feature originates from the participation of COD in a competing LLHT C–H activation that results in a stable off-cycle π-allyl complex that minimizes the concentration of the active catalyst

for productive catalysis. This side reaction was prevented by employing 1,5-hexadiene supported nickel pre-catalysts[55] leading to a more efficient alkyne hydroarylation at reduced temperatures.

Table 2-3 Broaden the scope with a pre-synthesized 1,5-hexadiene catalyst.

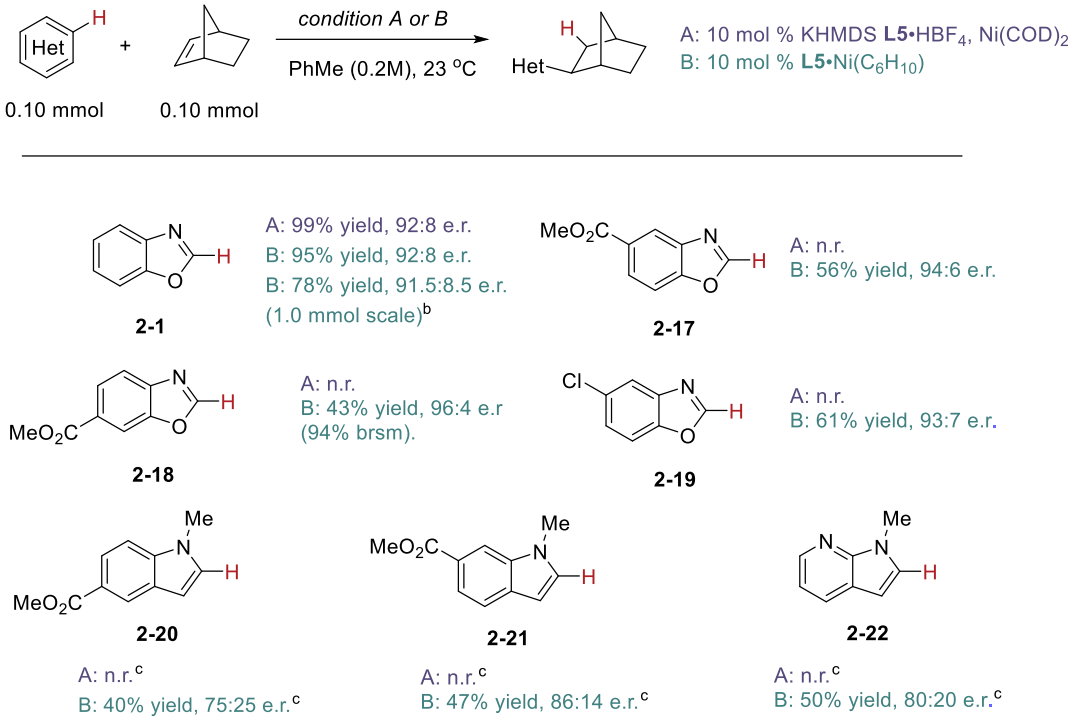

[a] Reactions were performed at 0.10 mmol scale unless noted. Yields were reported for isolated products. [b] Reaction was carried out with 2.5 mol % catalyst at 0.4M in PhMe. [c] Reaction was carried out using 2.0 equiv. nbe at 60 °C.

With the previously described 1,5-hexadiene supported novel catalyst **L5**-Ni(C_6H_{10}) in hand (**Section 2.5**), we first tested its reactivity using benzoxazole (**2-1**), and comparable results were obtained **(Table 2-3)**. Moreover, the synthesis of enantioenriched alkylation products could be carried out using as low as 2.5 mol % **L5**-Ni(C_6H_{10}) at 1.0 mmol scale without diminished enantioselectivity. We employed this catalyst with previously problematic substrates including those that feature electron-withdrawing substituents. While the *in-situ*-generated chiral catalyst at 10 mol % loading gave no reaction, **2-17** and **2-18** underwent alkylation smoothly to give desired

products using the discrete nickel catalyst **L5**-Ni(C_6H_{10}), where excellent enantioselectivities and clean reaction profiles were observed. Most surprisingly, products arising from chemoselective C–H functionalization were observed as the sole product with 93:7 e.r. in the presence of competing C–Cl bonds, which are susceptible to facile activation with low-valent nickel catalysts (**2-19**). The corresponding bromide substrate **2-11** (**Table 2-2**) was unreactive under condition B with defined pre-catalyst L5•Ni(C_6H_{10}). Lastly, substituted indoles and azaindoles could also be included into the scope simply by raising the reaction temperature to 60 °C (**2-20 – 2-22**), thus demonstrating the broad functional group compatibility of this Lewis acid free approach to C2 alkylated heteroarenes.

2.6.2 Styrene Scope

Enantioenriched 1,1-diaryl ethanes, which are recognized as valuable units in active pharmaceutical ingredients, are challenging structural motifs to access.[62] We hypothesized that this newly developed enantioselective hydroarylation strategy could enable access to enantioenriched 1,1-diaryl ethanes and allow for a rapid build-up of molecular complexity. As outlined in **Table 2-4**, an initial screen of several chiral NHCs that showed activity in the above studies revealed that ortho-substitution on the *N,N*-diaryl imidazolium scaffold had a large effect on reactivity and enantioselectivity. Though **L5**•HBF_4 exhibited poor regioselectivity control (linear to branched), steric effects were important in the observed enantioselectivities. Changing the identity of the aryl groups on imidazolium in **L7**•HBF_4 improved regioselectivity, though enantioselectivity was diminished. Further decreasing the steric hinderance with mono-substituted *N,N*-diaryl imidazolium **L8**•HCl suppressed the formation of linear product while increased the yield of the branched product, albeit with negligible improvements in enantioselectivity. As modification of

the mono-substituted arene of the imidazolium did not give improved results (**L9**•HCl), we opted to explore the preliminary scope of this reaction with **L8**•HCl, which gave the best reactivity and regioselectivity. 1,1-diaryl product **2-1-23** was formed in 80% yield and 66:34 e.r. when reacting benzoxazole (**2-1**) with styrene (**2-23**). This method could be applied to 1- and 2-vinyl naphthalenes (**2-24**, **2-25**), accessing exclusively the branched product with moderate control of enantioselectivity. Excellent regioselectivity for the benzylic position was observed with trans-β-methylstyrene (**2-26**), albeit modest yield and enantioselectivity. While the combination of regioselectivity and enantioselectivity of hydroarylations of simple styrenes falls short of the levels needed for synthetic application in its current form, the insights provided into the role of NHC structure in modulating the reaction outcome will be useful in guiding further study.

Table 2-4 Asymmetric alkylation with styrene and its derivatives

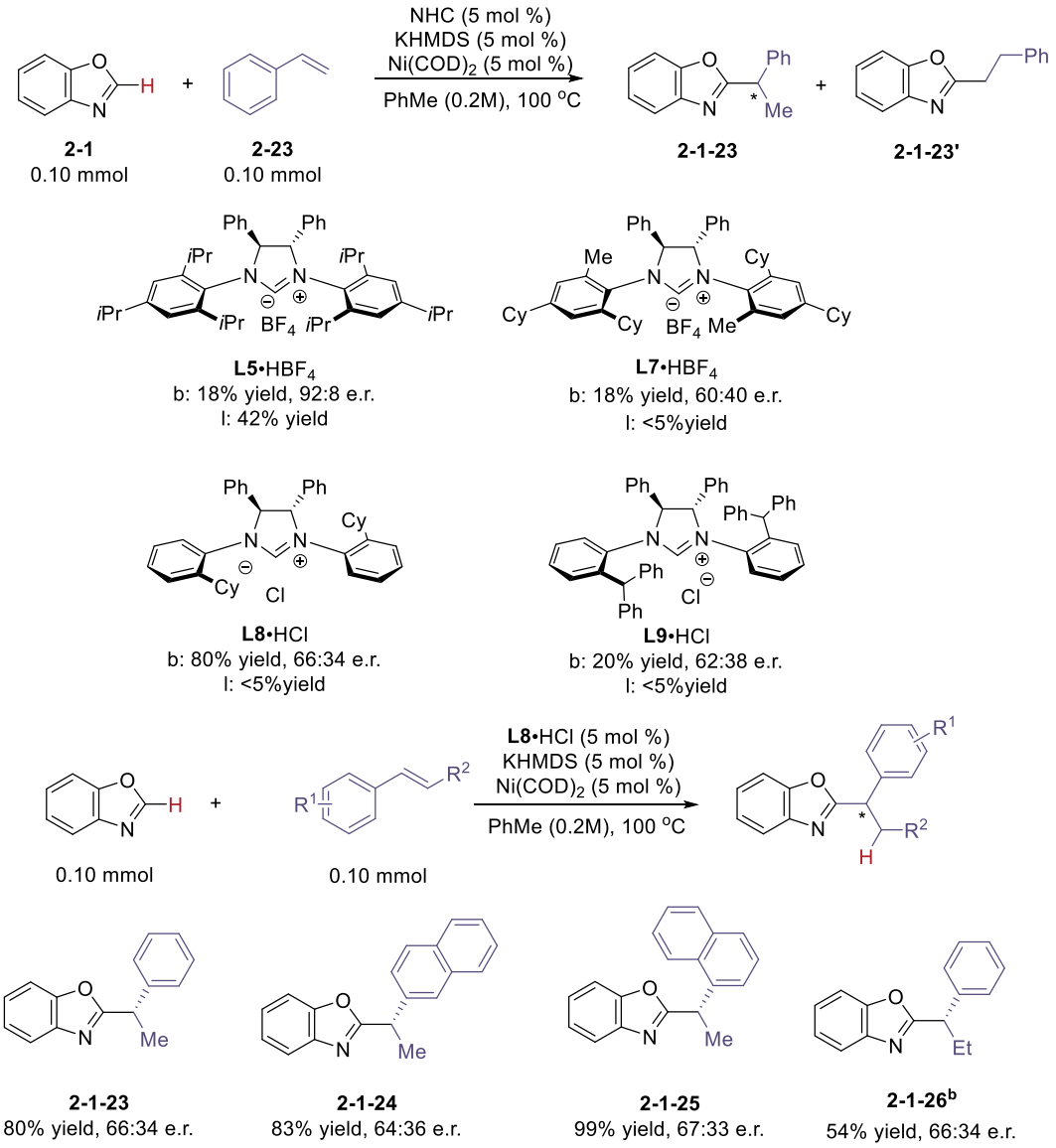

[a] Reactions were performed at 0.10 mmol scale and yields were reported for isolated products. [b] with 2 eq alkene.

2.6.3 Unsuccessful Alkenes

Various attempts have been made to explore the reaction scope outside activated alkenes (**Table 2-5**). Despites being successfully applied in transition metal catalyzed alkene

functionalization; structures listed below were unable to produce desired LLHT products. Only unreacted starting materials were observed based on GCMS analysis.

Table 2-5 Unsuccessful alkenes

2-1

unsuccessful substrates

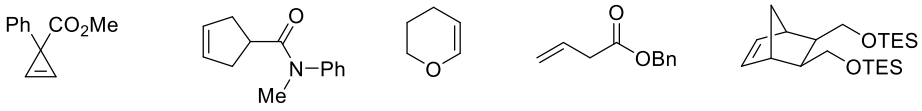

2-27 **2-28** **2-29** **2-30** **2-31**

2.7 Mechanistic Investigation via Reaction Progress Kinetic Analysis (RPKA)

2.7.1 Kinetic Isotope Effect (KIE)

Based on previous nickel-catalyzed C(sp^2)–H functionalization studies, we hypothesized that this reaction operates through a ligand-to-ligand hydrogen transfer (LLHT) mechanism where a concerted oxidative addition, migratory insertion bypasses the formation of a discrete nickel-hydride intermediate.[11] C–H functionalization that proceed through LLHT often exhibit a fast, reversible C–H activation and rate-determining reductive elimination.[38] To probe this characteristic, we conducted parallel KIE experiments with deuterium-labelled 5-phenylbenzofuran (**2-9-D**) at 50 °C. The absence of kinetic isotope effect (KIE=1.0) suggests that C–H activation is not involved in the rate-determining step, as expected in the LLHT mechanism (see **Chapter 8** for details).

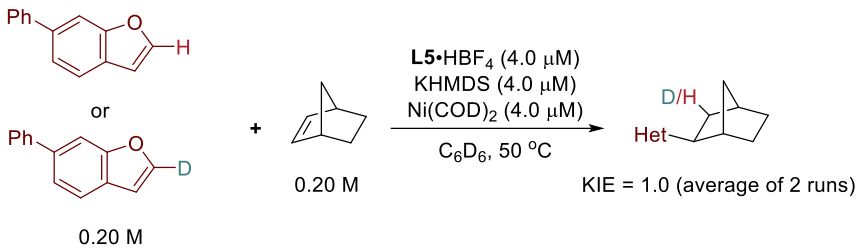

Scheme 2-6 KIE experiments.

2.7.2 'Same Excess' and 'Different Excess' Experiments

"Same excess" experiments were performed by maintaining the absolute concentration difference between nbe and arene to gain initial insights about the reaction progression.[63] As shown in **Scheme 2-7**, the overlay of three kinetic profiles indicates that neither catalyst deactivation nor product inhibition were occurring (see **Chapter 8** for details).. Next, varying the concentration of each component, the rate of the reaction was determined to be first order in arene and catalyst, and inverse first order in nbe which indicates a nbe dissociation before rate-determining step (**Scheme 2-8**).

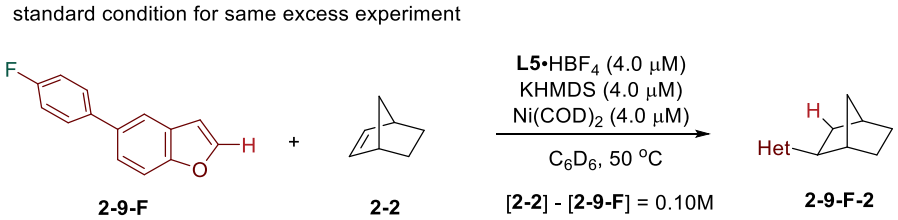

.

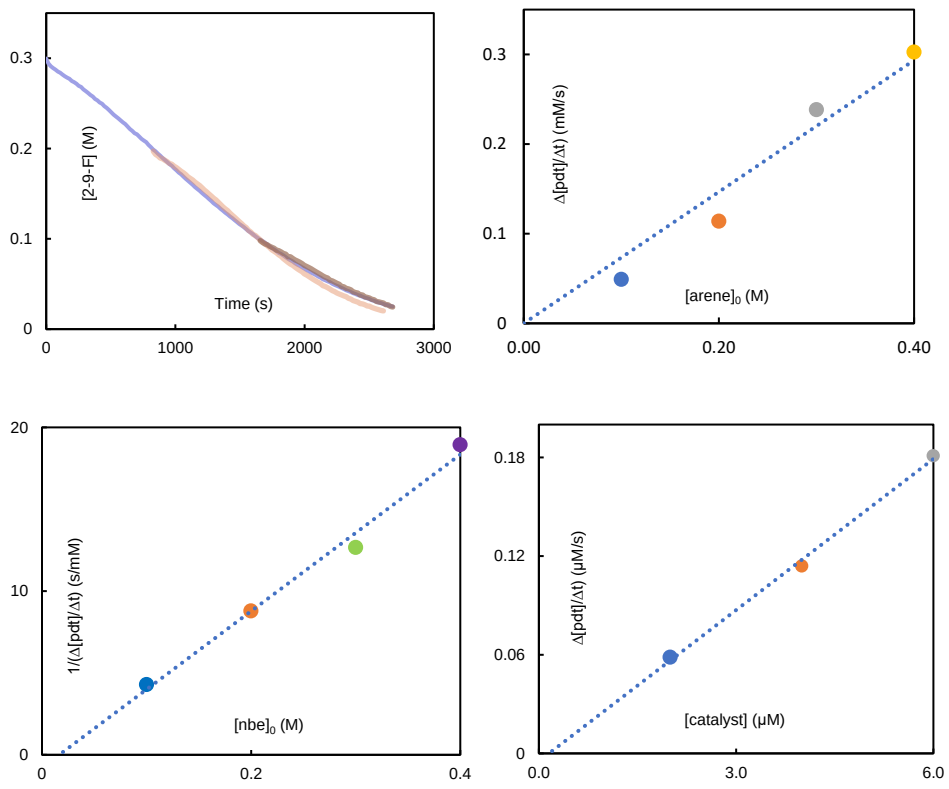

Scheme 2-7 Same excess and differenet excess experiments.

2.7.3 Proposed Mechanism

Based on the above observations and by drawing analogy with previous mechanistic studies,[11, 48b, 61, 64] we propose the following mechanism for the enantioselective C–H alkylation of heteroarenes (**Scheme 2-8**). The catalytic cycle is initiated by ligand exchange between nbe and heteroarene to form intermediate **II**, which then undergoes reversible ligand-to-ligand hydrogen transfer (LLHT),[65] resulting in the generation of aryl-bound Ni(II) species **III**. Previous studies by Hartwig and others have shown that the isomerization of **III** to a T-shaped intermediate **IV** precedes reductive elimination.[64, 66] From intermediate **IV**, rate-determining reductive elimination

delivers **V**, which, upon a fast ligand exchange with nbe, regenerates the catalyst, which is in good agreement with the result from "same excess" experiments that show no product inhibition.

The inverse first-order dependence in nbe is consistent with the dissociation of nbe in the **I** to **II** conversion, and the order analysis additionally indicates that nbe does not reassociate with the nickel center in the conversion of from intermediate **III** to **IV**. This absence of re-association of alkene has also been observed by Hartwig and co-workers in their studies of anti-Markovnikov hydroarylation reactions.[64] In contrast, previous studies by our group described a zero-order dependence in alkyne in the hydroarylation of alkynes, which was attributed to association of the alkyne to the nickel center prior to reductive elimination through a mechanism that otherwise patterns that described for nbe hydroarylation.[38]

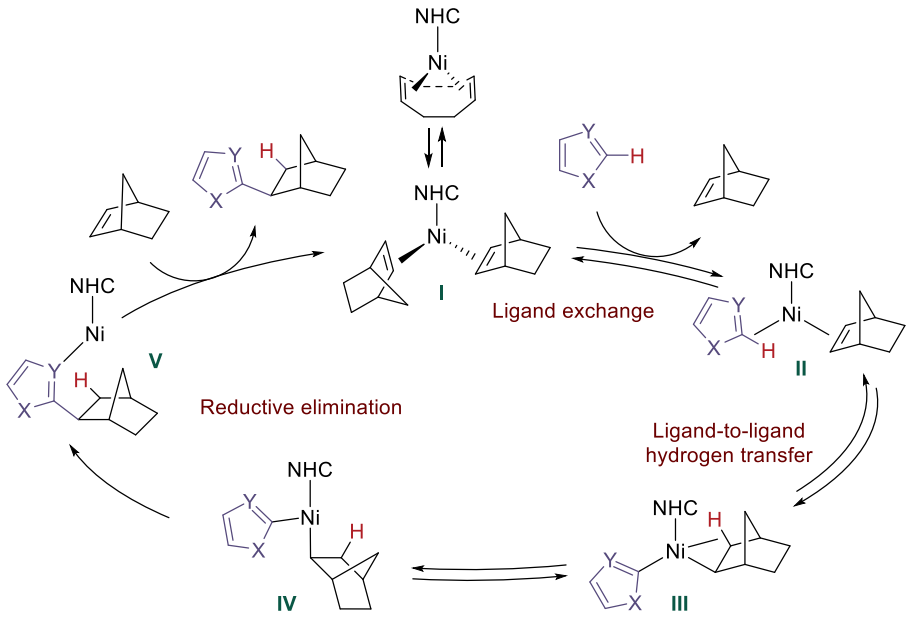

Scheme 2-8 Proposed Mechanism.

2.8 Conclusion

In conclusion, a strategy for the intermolecular enantioselective hydroarylation of alkenes using a nickel-catalyzed ligand-to-ligand hydrogen transfer approach has been developed.[23] The strategy involves an operationally simple approach using structurally well-defined NHC Ni(0) complexes that incorporate 1,5-hexadiene as ligand to improve reactivities. The method was applied to the enantioselective C–H functionalization under mild conditions with a wide heteroarene scope. This method was further examined with simple styrene derivatives, delivering 1,1-diaryl ethanes in good yields and modest enantioselectivities. The identification of a well-defined, sterically demanding C2-symmetric chiral NHC complex allows for intermolecular alkylation of a wider range of heteroarenes to occur without the need for Lewis acid additives. Mechanistic investigations are described by mapping the fundamental steps via kinetic profiles, which further support a LLHT pathway to activate the heteroaryl C–H bond and illustrate mechanistic differences that result from the nature of π-systems employed. This study provides important insights into the features that optimize catalyst performance in the enantioselective intermolecular functionalization of C(sp^2)–H bonds and explores a range of arenes and alkenes that participate in the transformation.

Chapter 3 Nickel Catalyzed C–H Alkenylation Polymerization via Ligand-to-Ligand Hydrogen Transfer

Special thanks to Siqi Li, Dr. Matt Hannigan, and Prof. Anne McNeil (UM), Dr. Junxiang Zhang and Prof. Seth Marder (CU Boulder), Prof. Colleen Scott (MSU), Prof Christine Luscombe (OIST) for their inputs.

3.1 Introduction

Direct arylation polymerization (DArP) has emerged as an effective strategy for accessing macromolecules from easily accessible, nonpreactivated monomers. Coupled with transition metal catalysis, DArP has seen broader application leveraging C–H bonds as latent nucleophiles, with one of the earliest regioselective synthesis of polythiophenes by McCullough using nickel catalysis. Despite recent advances in catalyst-transfer polymerization and other cross-coupling typed polymerization, few reports focus on the polycondesation of monomers that both free of pre-functionalization. Herein, we report the first example of nickel catalyzed C–H polymerization via a ligand-to-ligand hydrogen transfer (LLHT) mechanism to access defect-free cross-conjugated polymers under mild conditions. This unique C–H activation methodology is regioselective for the most acidic C–H bond and mechanistic excludes the formation of isomers from homocoupling.

Since the advent of transition metal catalyzed C–H functionalization, a myriad of methodologies has been applied to polymer science for the synthesis and modification of macromolecules.[40b, 42d, 67] Despite these advancements, there has been an increasing desire for developing earth abundant, first row transition metal as a more sustainable, cost-effective solution

which also stems from their fundamentally unique reactivities as compared to the noble metal catalyst.[68]

3.2 Design of Nickel Catalyzed C–H Alkenylation Polymerization

Though nickel has been one of the pivotal metal catalysts in today's polymer field,[69] it was first discovered by Ziegler and Holzkamp as a trace impurity which inhibited the polymerization by converting the ethylene monomer to 1-butene.[70] This nickel effect sparked a systematic investigation of 'possible substances having effects similar to nickel' and ultimately led to the discovery of Ziegler catalyst which was recognized with a Nobel Prize in 1963.[71] This 'poison' has also been successfully tamed by synthetic polymer chemists after extensive studies, with the remarkable contribution made by Yamamoto[72] and Lin[73] for poly(thiophene) synthesis via nickel catalysis. Later on McCullough and co-workers achieved regioregular synthesis of poly(3-alkylthiophene),[74] which has now been expanded to its own field, termed catalyst transfer polymerization, where nickel has been a major player.[69e, 75]

The past few decades have seen tremendous developments in the homogenous nickel catalysis for accessing small molecules of interest.[3, 6b, 28] In 2008, Nakao and Hiyama reported a chemoselective C–H alkenylation of polyfluoroarenes with exceptional regio- and stereoselectivities.[45] It was later discovered by Perutz and co-workers that, in the presence of alkenes and alkynes, nickel mediated C–H activation undergoes a concerted oxidative addition, migratory insertion pathway, bypassing the formation of nickel hydride intermediate.[11] Ligand-to-ligand hydrogen transfer (LLHT) has since then been identified as a prevalent mechanism in nickel catalyzed C–H functionalization including substitution,[9-10] cyclization,[46a, 47d, 48a] annulation,[76] ring expansion,[77] and enantioselective alkylation[49c, 52, 78]. We are especially intrigued by the concerted

mechanism which requires both coupling partners (arene and alkyne) binding to the nickel center preceding the C–H activation step.[6b] This highly regulated mechanism, if successfully applied in polymerization, could help avoiding structural defects.[79] Also, LLHT has been identified to chemo- and regioselectively activate the most acidic hydrogen, and transfer it preferentially to alkynes over alkenes, presumably due to the low kinetic barrier for alkyne binding, as well as the formation of a more thermodynamically stable C(sp2)–Ni bond.[4, 38] Therefore, these features are all advantageous for the synthesis of a defect-free, highly regulated polymer via nickel catalyzed LLHT manifold.

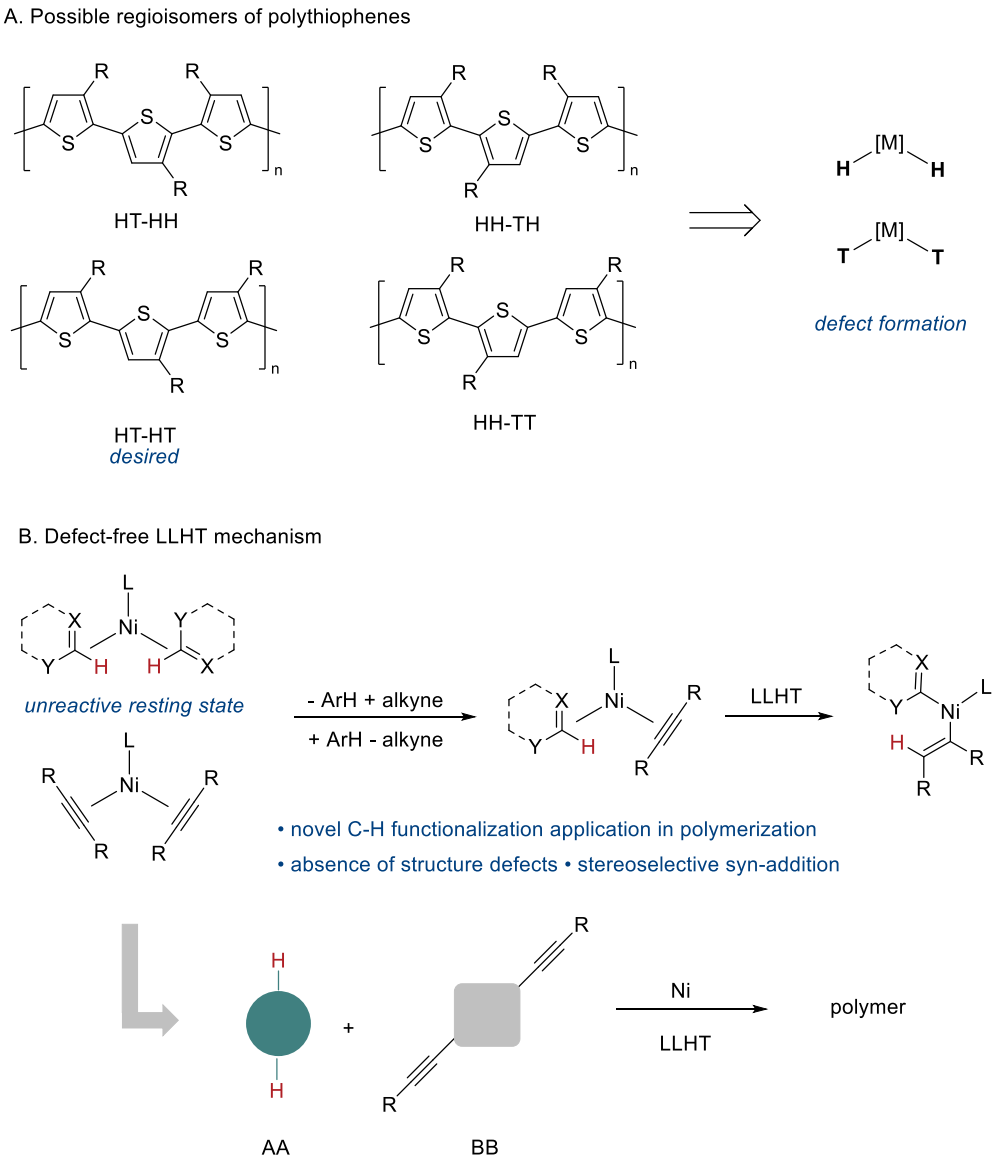

Scheme 3-1 Nickel catalyzed defect-free polymerization via LLHT

3.3 Optimization of Small Molecule System

To demonstrate the advantageous nickel catalyzed LLHT C–H alkenylation polymerization, we started our explorations by optimizing the small molecule system. The conditions originally reported for the alkyne hydroarylation were not suitable for this LLHT polymerization as an excess of the alkyne (1.5 to 4 eq) was necessary for high yields,[45] which

violates the stoichiometry requirement by Carothers equation. C–H alkenylation of 1,2,4,5-tetrafluorobenzene (**AA1**) with 4-octyne (**B1**) was chosen as model reaction condition examination. The desired C–H functionalization product was obtained using a 1,5-hexadiene supported nickel pre-catalyst, IMes-Ni(C_6H_{10}) at room temperature (**Table 3-1**).[78b]

Table 3-1 Optimization of small molecule system

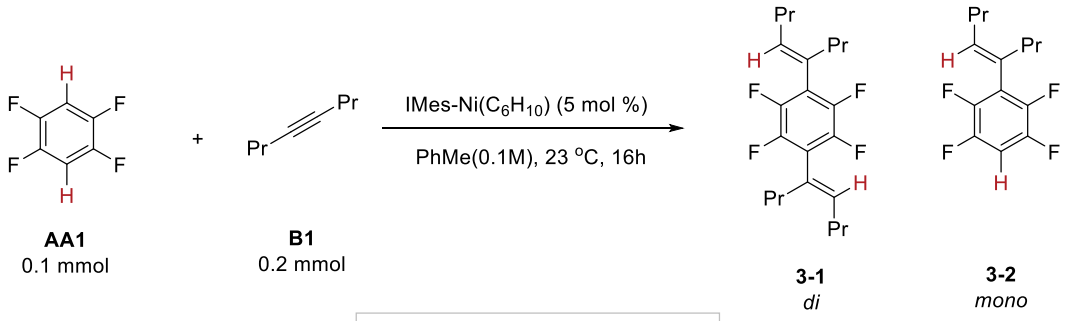

Entry	Deviation from above	% yield (NMR)	% di	% mono
1	None	70	0	70
2	IMes, $Ni(COD)_2$	0	–	–
3	IPr^{Me}, $Ni(COD)_2$	0	–	–
4	IPr^{*OMe}, $Ni(COD)_2$	0	–	–
5	PCy_3, $Ni(COD)_2$	0	–	–
6	0.5 M	21	5	16
7	10% [Ni]	62	36	26
8	10% [Ni] at 60 °C	98	58	40
9	10% [Ni], 0.2 M, at 60 °C	100	71	29

Standard reaction was performed with **AA1** (0.1 mmol), **B1** (0.2 mmol), IMes-Ni(C_6H_{10}) (5.0 μmol) in PhMe (1 mL) at 23 °C unless indicated otherwise. Yields were based on quantitative NMR analysis using CH_2Br_2 as an internal standard.

We have previously reported that this cyclooctadiene (COD) free nickel complex eliminates the COD competing reactivity with polyfluoroarenes, yielding the desired alkyne hydroarylation products under mild conditions (**Entry 1**).[61] On the contrary, the *in-situ* generated pre-catalyst from $Ni(COD)_2$, despite the proved catalytic efficiency in previous reports,[7, 80] failed to produce the desired product **3-1 & 3-2** (**Entries 2-5**) at 23 °C. Although increasing concentration to 0.5M led to the formation of desired, dialkenylated product **1**, it compromised the overall reactivity (**Entry 6**). Finally, running the reaction with 10 mol % catalyst loading produced overall better results with a 1:1 ratio between mono- and difunctionalized products (**Entry 7**). Further condition modifications revealed that higher concentration and elevated temperature promoted conversion to the desired product **3-1**, which was obtained in 71% yield based on quantitative NMR analysis (**Entry 9**).

Shown below is a typical crude NMR spectrum for reaction outcome determination. Although both the mono- and difunctionalized polyfluoroarenes exhibit the vinyl proton at 5.51 ppm as a triplet, the unfunctionalized aryl proton from **3-2** is characteristic at 6.91 as a multiplet. Thus, the molar quantity of **3-2** was determined to be 0.0255 mmol (0.51/2), and by extracting equal molar from the vinyl proton integration, 3-1 was determined to be 0.036 mmol [(1.95-0.51)/2].

Scheme 3-2 Crude reaction analysis

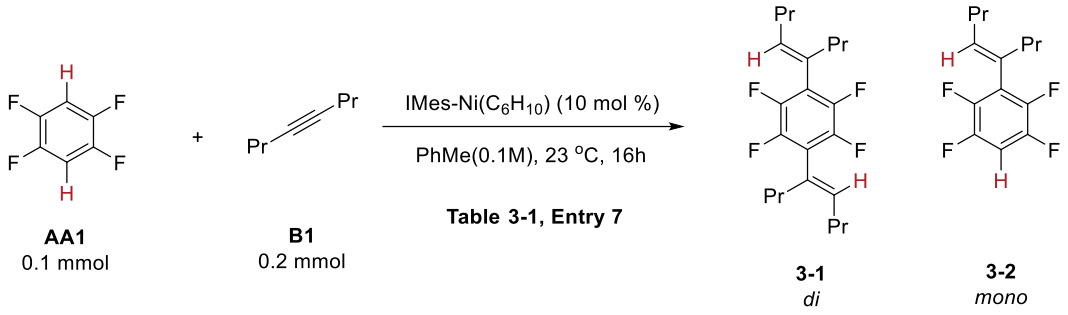

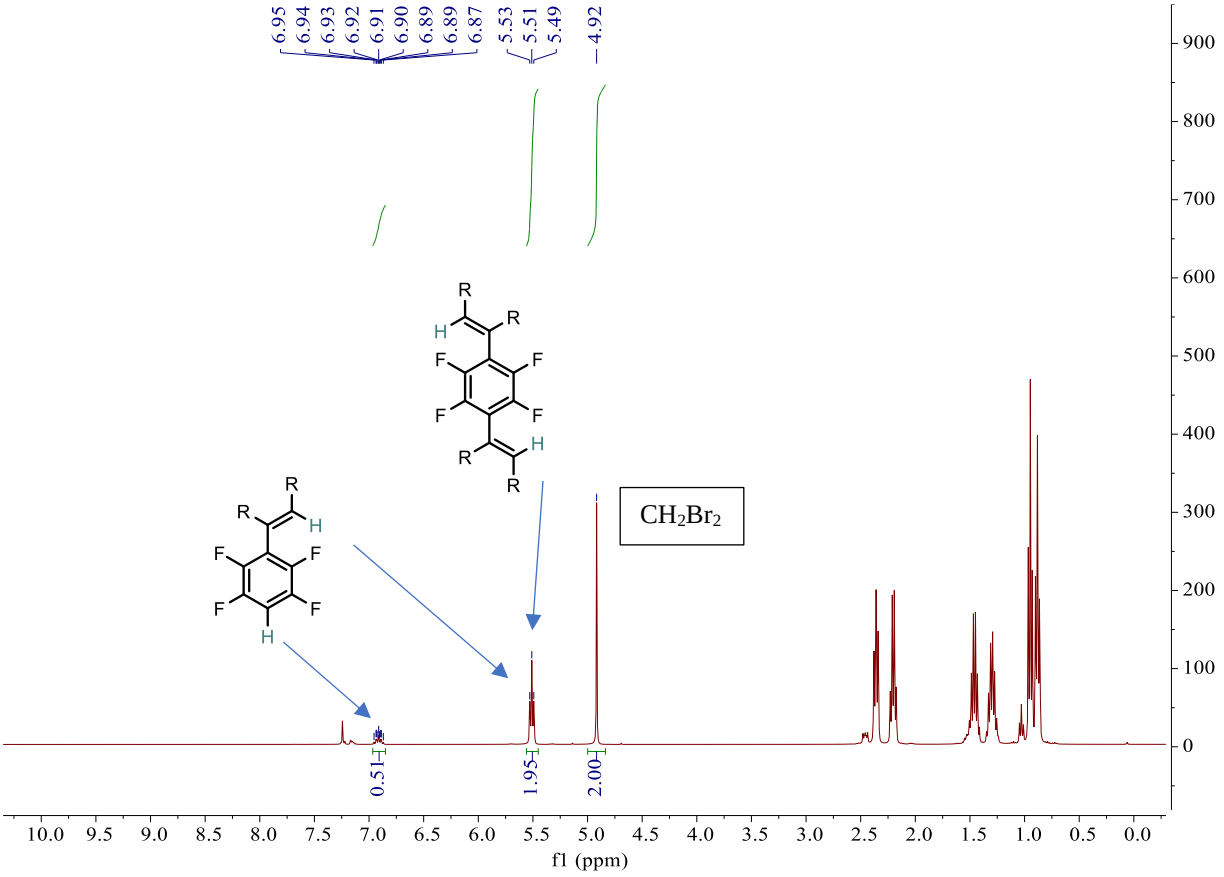

Preliminary structure activity relationship studies were sequentially conducted based on the optimal condition to examine the effects of alkyne identities on the reactivity. To our delight, switching from 4-octyne (**B1**) to trimethylsilyl (TMS) capped internal alkyne **B2**, **B3**, the desired difunctionalized products were formed exclusively in a stereoselective manner, paving the way for application in polymerization. We rationalize this superior reactivity based on previous work from

us[38] and Hartwig[64] that reductive elimination being the rate-determining step in LLHT typed C–H functionalization. Thus, the sterics from TMS group aided this slow step in the catalytic cycle, increasing the overall rate of the C–H alkenylation and in turn leading to full conversion to the difunctionalized products (**3-3 & 3-4**). It is also worthwhile to highlight the high stereoselectivity, which has been observed by Nakao and Hiyama in their alkyne hydroarylation work.[45] It is now believed that the LLHT C–H activation adopts the most energetic favored transition state where the sterically hindered ligand (IMes in this case) positions nickel away from the sterically demanding site on the substrate (α–C to TMS) and the migratory insertion results in exclusively syn-addition to the alkyne. Additional thermodynamic stability for this regioselectivity can also be attributed to the β-Si effect which we will not further discuss under this context.[81] With the monomer designing principle as well as the optimal reaction condition in hand, we then moved on to explore the polymerization with bisalkynes (**BB**), which can be easily accessed by Sonogashira coupling between TMS acetylene and aryl dibromides (see **Chapter 8** for details).

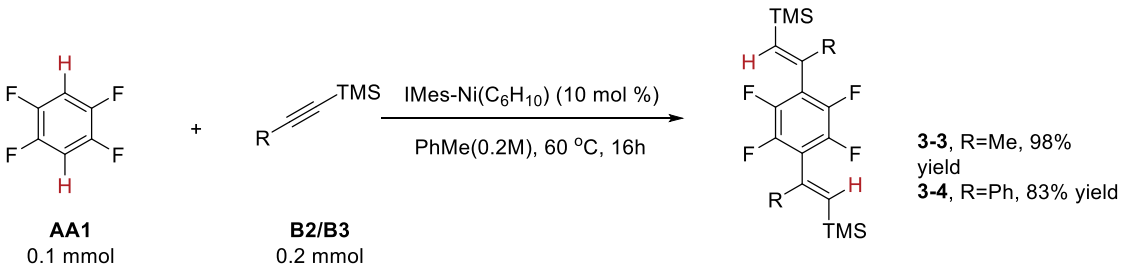

Scheme 3-3 Improved reactivities with TMS alkyne.

3.4 Polymerization Attempts

Table 3-2 Optimization of polymerization

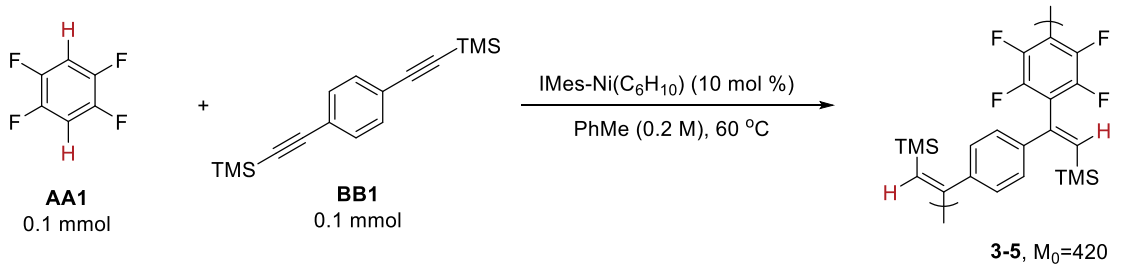

entry	Deviations from above	% yield (NMR)	M_n	DP	$Đ$
1	no	92	6100	14.5	2.45
2	IMes, $Ni(COD)_2$	77	6600	15.8	3.66
3	IPr^{Me}-Ni(C_6H_{10})	89	7200	17.2	2.32
4	$IPr*^{OMe}$-Ni(C_6H_{10})	n.r.	–	–	–
5	5 mol % [Ni]	86	4200	9.9	1.76
6	2.5 mol % [Ni]	n.r..	–	–	–
7	15 mol % [Ni]	96	5100	12.1	2.05
8	1.0 M in PhMe	99	4200	9.9	1.67

Standard reaction was performed with **AA1** (0.1 mmol), **BB1** (0.1 mmol), IMes-Ni(C_6H_{10}) (10.0 μmol) in PhMe (0.5 mL) at 60 °C unless indicated otherwise. Yields were based on quantitative NMR analysis using CH_2Br_2 as an internal standard. The resulting polymer was subjected to SEC analysis.

By coupling **AA1** (0.1 mmol) and **BB1** (0.1 mmol) at 60 °C, we were pleased to observe the desired polymer **3-5** in 92% yield with M_n=6100 under previously developed optimal condition (**Table 3-2**). Further screening reaction parameters including ligand combination (**Entries 2-4**), catalyst loading (**Entries 5-7**), and concentration (**Entry 8**), did not introduce substantial improvements, indicating the small molecule system we screened based on was generalizing enough to develop polymerization scope.

Two polyfluoroarenes were selected as bifunctional AA typed monomer, 1,2,4,5-tetrafluorobenzene (**AA1**) and 2,2′,3,3′,5,5′,6,6′-octafluorobiphenyl (**AA2**) and were tested in parallel in the polymerization with bisalkynes (**Table 3-3**). Although slightly lower yield and higher polymer dispersity index (*Đ*) were observed by switching from **AA1** to **AA2** when reacting with 1,4-bis((trimethylsilyl)ethynyl)benzene (**BB1**), higher average molecular weight (M_n) and degree of polymerization (DP) were achieved. Introducing an aliphatic side chain, a common strategy for increasing polymer solubility[82] to enable the synthesis of higher molecular weight polymer did not produce better results (**Entries 3-4, 9-10**). In fact, after the 16h reaction time, all polymerization attempts with **AA1** and **AA2** resulted in homogeneous mixtures, and resulted polymers are also well solubilized in $CDCl_3$ for examination of stereo-regularity. Since the biphenyl scaffold in polyfluoroarene resulted in higher DP, we were curious to see whether such effect was also true with the bisalkyne coupling partner (**BB3**). And indeed, we obtained the highest molecular weight polymer with a DP over 20. Further efforts for screening alkynes that bear common monomer structure (**BB4** and **BB5**) failed to offer better results. Instead of having a benzene linker, directly tethering the bisalkyne on the same silicon atom completely shuts down the reactivity (**BB6**), possibly due to the overwhelmingly hindered steric environment. Poly(thiophene), a typical π-conjugated conducting polymer, has found great applications in OLEDs.[83] Though this reported methodology generated polymers in a cross-conjugated manner, we were still intrigued by the possible electronic properties of thiophene by integrating it into the repeating unit. Polymerization using **AA2** with 2,5-bis((trimethylsilyl)ethynyl)thiophene (**BB7**) and 5,5'-bis((trimethylsilyl)ethynyl)-2,2'-bithiophene (**BB8**) both led to the formation of desired polymers in high yields and DP around 10 (**Entries 14 & 16**).

Table 3-3 Polymerization scope

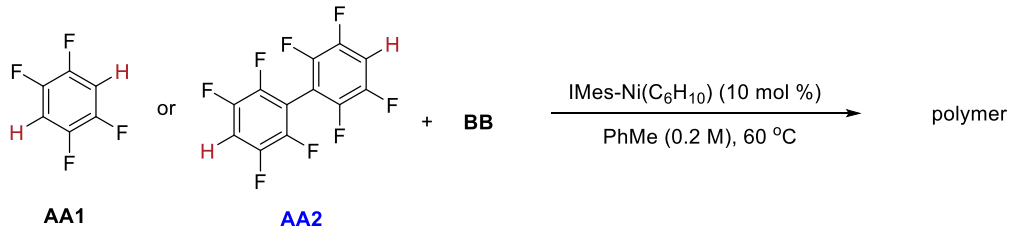

AA1 AA2

Entry[a]	AA	BB	% yield (NMR)	M_n	DP	$Đ$
1	AA1	BB1	92	6100	14.5	2.45
2	**AA2**	BB1	74	10000	17.7	3.30
3	AA1	BB2	85	7800	11.6	2.14
4	**AA2**	BB2	99	4700	5.7	1.87
5	AA1	BB3	38	3700	9.3	1.82
6	**AA2**	BB3	86	13000	20.3	2.64
7	AA1	BB4	100	6300	8.6	1.86
8	**AA2**	BB4	100	7100	8.1	1.90
9	AA1	BB5	90	7800	12.4	2.88
10	**AA2**	BB5	99	5300	6.7	2.42
11	AA1	BB6	n.r.	–	–	–
12	**AA2**	BB6	n.r.	–	–	–
13[b]	AA1	BB7	100	4600	10.9	2.16
14[b]	**AA2**	BB7	95	6100	10.7	2.37
15[b]	AA1	BB8	20	2200	4.3	1.25
16[b]	**AA2**	BB8	87	8000	12.2	2.08

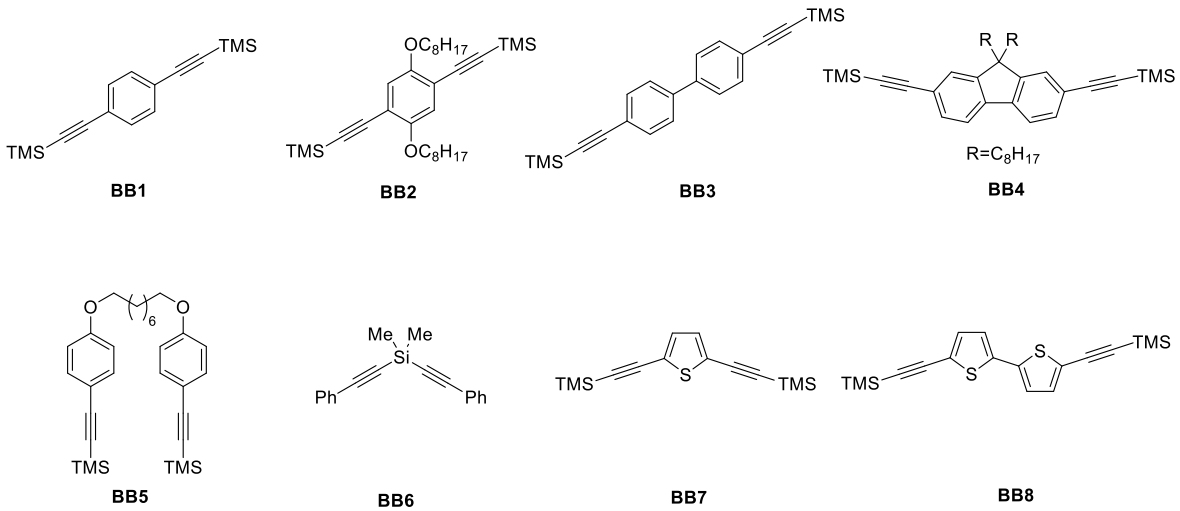

[a] Standard reaction was performed with **AA** (0.1 mmol), **BB** (0.1 mmol), IMes-Ni(C_6H_{10}) (10.0 μmol) in PhMe (0.5 mL) at 60 °C unless indicated otherwise. Yields were based on quantitative NMR analysis using CH_2Br_2 as an internal standard. The resulting polymer was subjected to SEC analysis. [b] IPr^{Me}-Ni(C_6H_{10}) (10.0 μmol) was used as the catalyst and the reaction was run at 100 °C.

3.5 Further Explorations of High Molecular Weight Polymer Synthesis

Inspired by the developed polymer scope, we would like to further understand the synthesis of high molecular weight polymer between monomers **AA2** and **BB3**. Different silyl substituents were evaluated and changing from TMS to larger silyl groups decreased the hydroarylation reactivity (**Entries 2-4**). Concentration has also been proved to have significant effects when studying the small molecule system. Similarly, by increasing the concentration to 0.5 M (**Entry 6**), the desired polymer **3-10** was successfully synthesized with a high yield and molecular weight (M_n >17kDa).

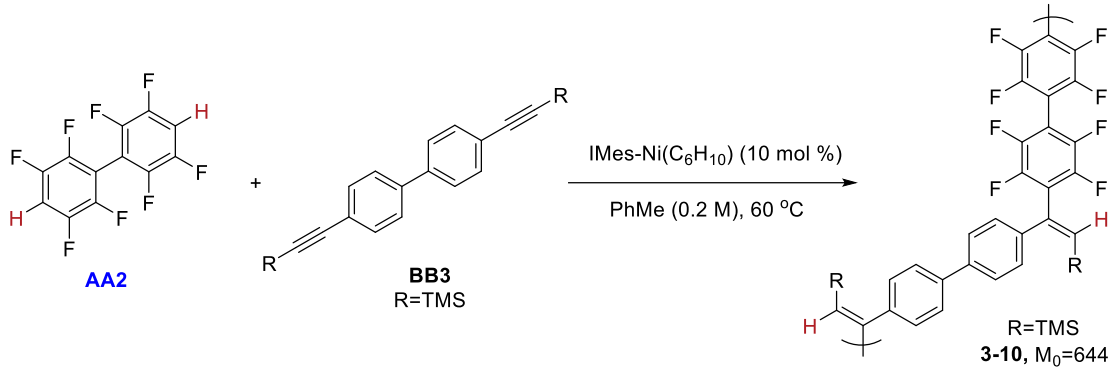

entry	Deviations from above	% yield	M_n	DP	$Đ$
1	none	86	13000	20.3	2.64
2	R=Si(^{t}Bu)Me$_2$ (**BB9**)	27	900	1.3	1.21
3	R=SiEt$_3$ (**BB10**)	52	4600	6.4	1.74
4	R=Si^{i}Pr$_3$ (**BB11**)	n.r.	-	-	-
5	0.1 M in PhMe	100	10200	15.8	2.17
6	0.5 M in PhMe	94	17000	26.4	3.14

Standard reaction was performed with **AA2** (0.1 mmol), **BB** (0.1 mmol), IMes-Ni(C_6H_{10}) (10.0 μmol) in PhMe (0.5 mL) at 60 °C unless indicated otherwise. Isolated yields were reported, and the resulting polymer was subjected to SEC analysis.

3.6 Conclusion

In summary, this chapter describes a nickel catalyzed C–H alkenylation polymerization via novel LLHT mechanism, demonstrating another successful application of small molecule system in polymer synthesis. Compared with other known methods, LLHT is unique for its highly regulated C–H activation step, avoiding possible generation of structure defects. Different internal TMS alkynes have been successfully used as coupling partners in this hydroarylation polymerization with excellent stereocontrol. Preliminary studies have been carried out to understand the steric effect on the reaction outcome and current efforts of our group are focusing on developing synthetic strategies towards conjugated polymer by substrate control.

Chapter 4 Investigations into Mechanism and Origin of Regioselectivity in the Nickel/Iridium Catalyzed α-Arylation of Benzamides

The following content is associated with these publications:

1) Rand, A. W.; Chen, M.; Montgomery, J. "Investigations into Mechanism and Origin of Regioselectivity in the Metallaphotoredox-Catalyzed α-Arylation of *N*-Alkylbenzamides" *Chem. Sci.* **2022**, *13*, 10566-10573
2) Rand, A. W.; Yin, H.; Xu, Liang, Giacoboni, J.; Martin-Montero, R.; Romano, C.; Montgomery, J.; Martin, R. "A Dual Catalytic Platform for Enabling sp3 α-C-H Arylation and Alkylation of Benzamides" *ACS Catal*. **2020**, *10*, 4671-4676.

Part of the results in this Chapter are obtained in collaboration with Dr. Alex Rand, and specific contributions are highlighted during discussion in respective sections.

4.1 Introduction

Nitrogen is ubiquitous in nature.[84] Amines have been found in core structures of natural products,[85] pharmaceuticals,[86] agrochemicals,[87] and synthetic polymers,[88] contributing to various fields of organic chemistry and biology. Taking active pharmaceutical ingredients (APIs) as an example,[89] analogs of nitrogen-based heterocycles occupy an exclusive position as a valuable source of therapeutic agents in medicinal chemistry, with more than 75% drugs approved by the FDA containing these motifs (**Scheme 4-1**).[90] Therefore, tremendous efforts have been made for enabling convenient accesses to wider chemical spaces of amine functionality, which come down to either *de novo* construction of the target molecule or structure modification of existing amine

derivatives.[91] In this vein, C–H functionalization through photoredox has emerged as a versatile strategy to derivatize readily available amines starting materials under mild conditions.[28, 92]

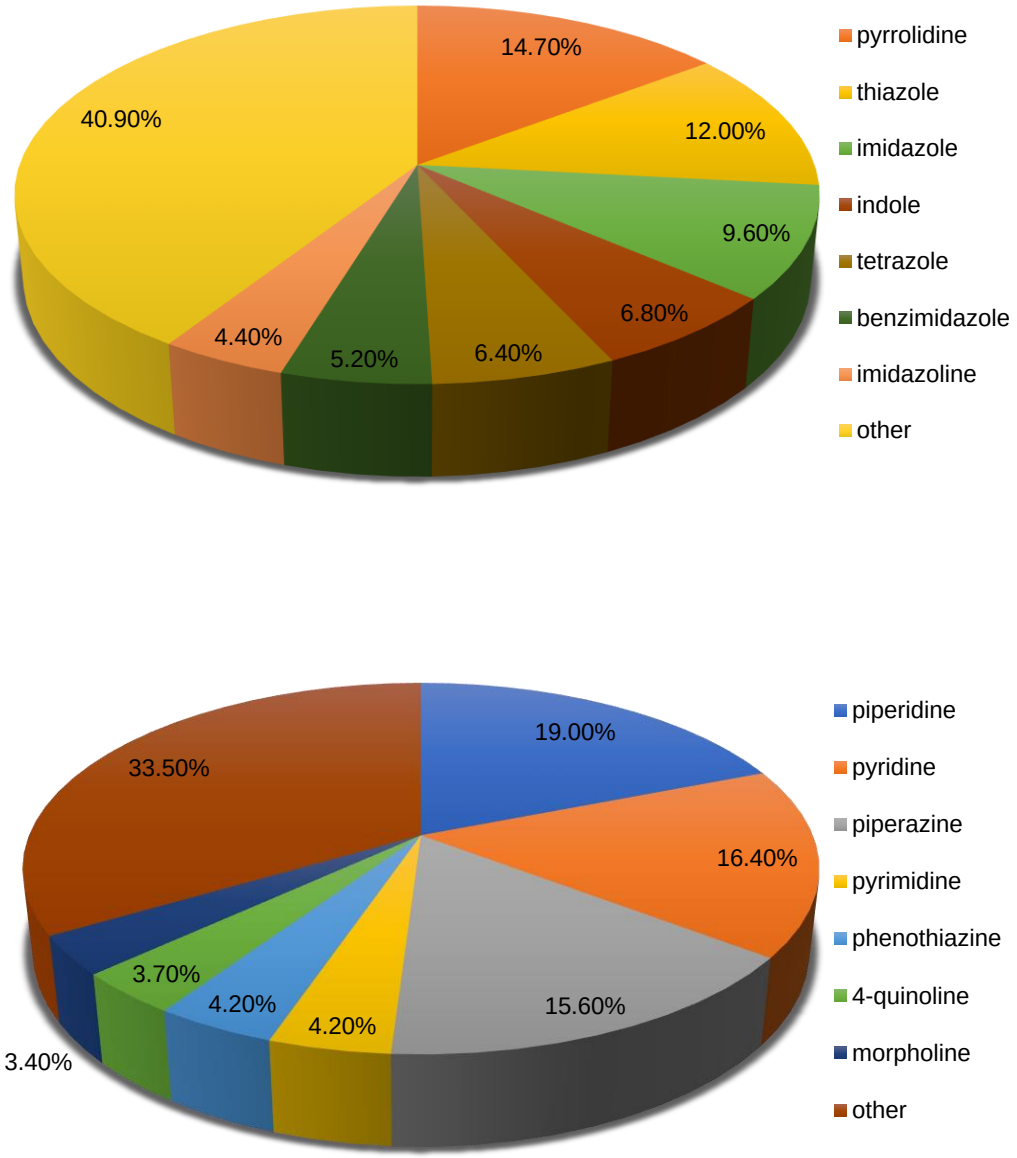

Scheme 4-1 Distribution of five- (left) and six-membered (right) nitrogen heterocycles in U.S. FDA approved pharmaceuticals.

Early precedents of amine C–H functionalization can be dated back to 19th century with the advent of Hofmann-Löffler-Freytag (HLF) reaction,[23] sparing the use of Cl_2 or Br_2 which inevitable led to a statistical mixtures of products.[93] The HLF reaction was elegantly designed to undergo a light-promoted 6-membered, chair-like transition state, exclusively installing functionalities at the δ-position of aliphatic secondary amines via 1,5-HAT process (**Scheme 4-2**, top).[94] Despite these early advances, application of photoredox C–H functionalization methodologies has been long hampered by their harsh reaction conditions until recently.[95] The past few decades have witnessed the renaissance of photoredox catalysis with the concomitant development of organo-photoredox catalysts exhibiting high oxidation potential, empowering transformations under mild conditions.[96]

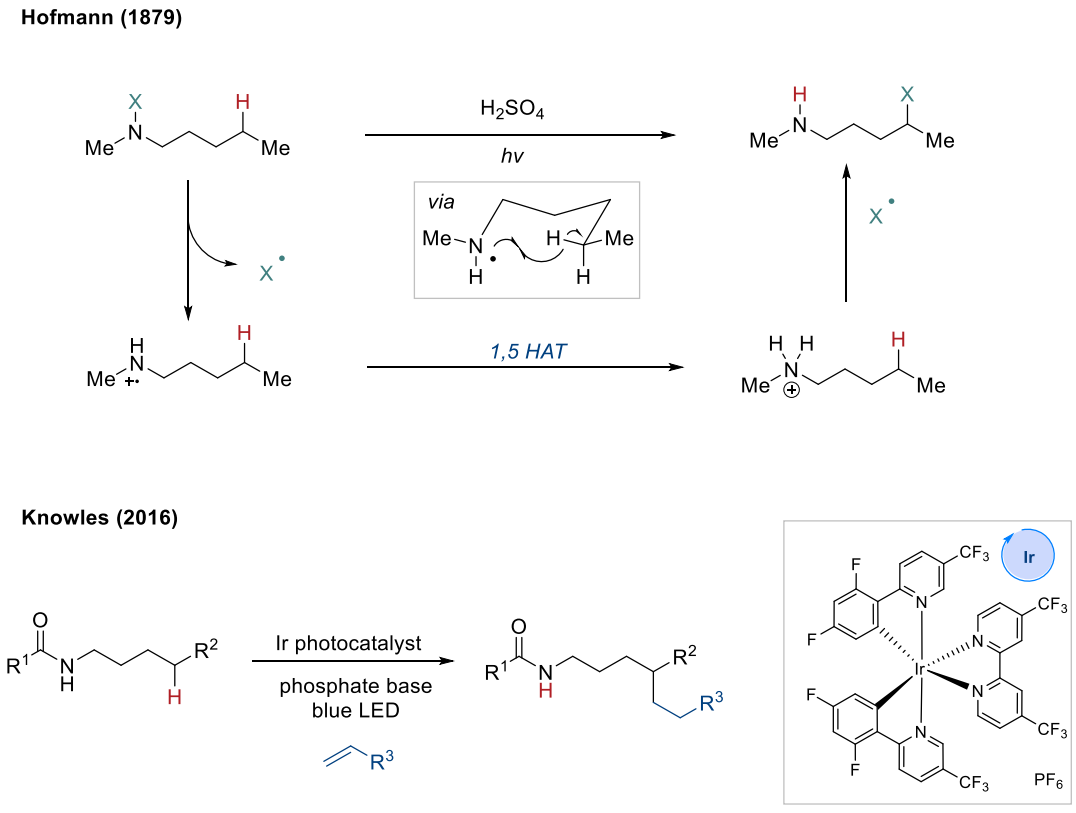

Scheme 4-2 HLF reaction and its application in metallaphotoredox via PCET. (X = Cl, Br).

The seminal contribution to the field was made by the Knowles group where they developed amide homolysis protocols using an excited-state iridium photocatalyst and a weak phosphate base, via a novel proton-coupled electron transfer (PCET) process (**Scheme 4-2**, bottom).[97] Despite the high bond-dissociation energy (BDE) of amide N–H bond,[98] the cooperation of photocatalyst and base circumvented the oxidative pre-functionalization of amide starting materials.[99] The generated of amidyl radicals from simple, unfunctionalized amides was coupled with various Michael acceptors, giving rise to distal C–H functionalization products. Given the prevalence of amides in pharmaceuticals and natural products,[100] the authors envisioned that the reported methodology would find wide application in late-stage functionalization towards the construction of complex molecules.[101]

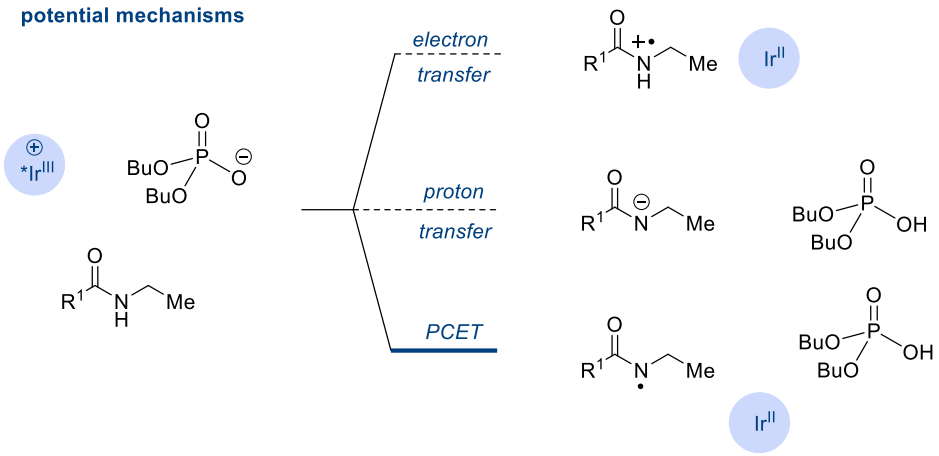

Scheme 4-3 Possible N–H bond activation mechanisms.

In terms of the N–H activation pathways, the direct electron transfer between amide substrates and photocatalyst was first excluded as the starting material did not quench the excited state of the Ir catalyst. Secondly, proton transfer between phosphate and amide was also deemed unfavorable, based on the endothermic nature of this deprotonation event. The sluggish acid base reactivity also did not match the rapid decay of excited photocatalyst, rendering the sequential electron transfer inaccessible. Lastly, based on evidence from Stern-Volmer assays where the

correlation of luminescence with both amide and phosphate concentration was observed, Knowles and co-workers believed that PCET was the operating N–H activation pathway (**Scheme 4-3**).

More recently, Rovis and co-workers examined the idea of merging carbon centered radicals generated from a formal HLF process with nickel catalysis (**Scheme 4-4**, top).[102] Towards this aim, several trifluoroacetamide-tethered frameworks were employed under metallaphotoredox conditions. The high oxidation potential of the activated iridium (Ir) photocatalyst was the key to success, enabling the generation of N centered radicals which would otherwise rely on the homolysis of N–Cl/Br bonds. These developments revived the interest in generating carbon centerer radicals via amidyl radicals and coupling it with nickel catalysis to enable a broader scope.

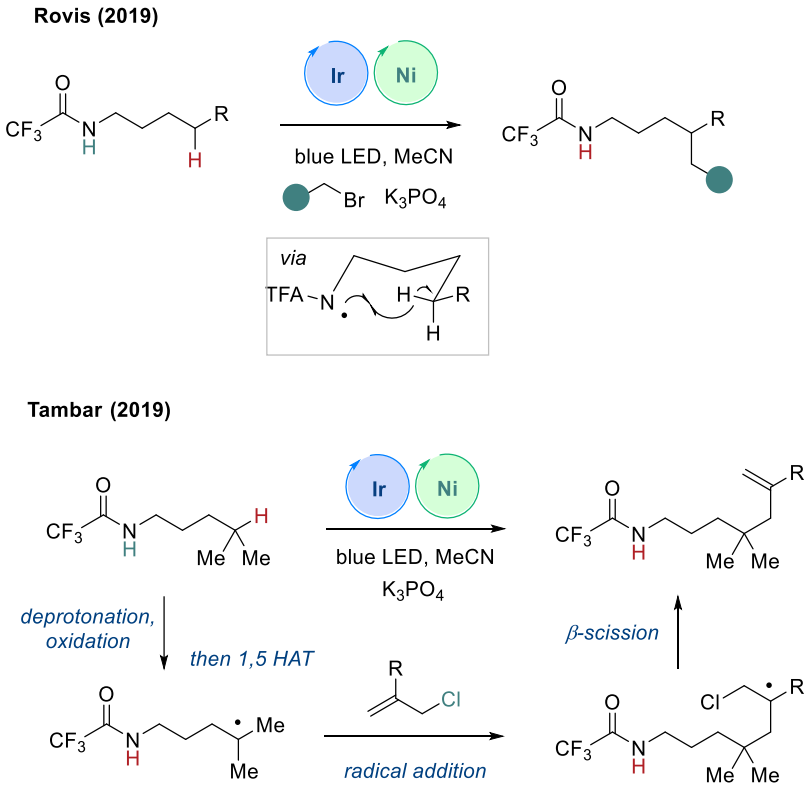

Scheme 4-4 Distal allylation of trifluoracetamides using metallaphotoredox catalysis.

Also in 2019, Tambar and co-workers exploited the distal functionalization with allyl chlorides with metallaphotoredox catalysis (**Scheme 4-4**, bottom).[103] Following the similar

pathway as proposed by the Rovis group,[102] where the acidified N–H bond underwent deprotonation / oxidation followed by 1,5 HAT to generate a carbon centered radical. Subsequent trapping with allyl chloride took place regioselectively, and eventually β-scission produced the C–H allylation product. It is worthwhile to point out that the desired product was still obtained in the absence of nickel catalysis in the control experiment, albeit the lower yield (48% vs 76%) indicating more complicated roles that metal catalysts could play. Unfortunately, it is not uncommon that during discoveries of metallaphotoredox catalysis, mechanistic investigations are often falling behind as compared to the method developments.[104] These gaps intrinsically brought difficulties not only for new reactivity explorations but also made it harder to understand the divergent outcomes from similar reaction manifolds with small deviations. Based on these reasons, there has been a growing interest in deconvoluting mechanisms of metallaphotoredox reactions.[104c] This chapter will be focusing on answering questions: 1) C–H or N–H activation, 2) the nature of HAT reagent, 3) the exact reaction pathway, and 4) roles that nickel catalyst play.

In 2020, Montgomery and Martin groups collaboratively reported a metallaphotoredox-catalyzed α-arylation and alkylation of *N*-alkylbenzamides using aryl and alkyl bromides (**Scheme 4-5**).[105] The unique site-selectivity was highlighted through the orthogonal α- and δ-functionalization of a common starting material using either this protocol or conditions developed by Knowles.[97] This method was also rendered asymmetric through the use of a chiral bioxazoline (BiOx) ligand, which allowed for high enantio-induction when the reaction was conducted at low temperatures.

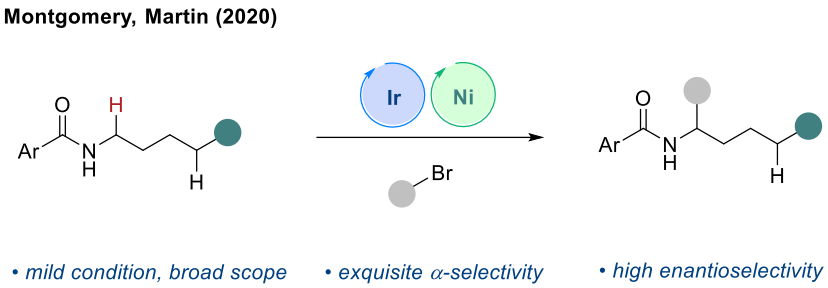

Scheme 4-5 Site-selective C(sp3)–H functionalization of amides.

Although the original project target was remote functionalization, we quickly discovered that proximal arylation was obtained instead. The initially conceived mechanistic hypothesis was the proton coupled electron transfer (PCET) between the photocatalyst, *N*-alkylbenzamides and K_3PO_4 to afford a nitrogen centered radical, followed by 1,5 HAT to yield a distal carbon centered radical.[97] The capture of such radical was followed by a series of β-hydride elimination and reinsertion as the chainwalking event to the most stable, proximal position α to the nitrogen (*vide infra*). Reductive elimination from Ni^{III} led to the observed α-functionalized product. To complete the catalytic cycle, electron transfer took place between nickel and iridium photocatalyst, yielding a cationic Ir species, which could then undergo the photoexcitation (**Scheme 4-6**).

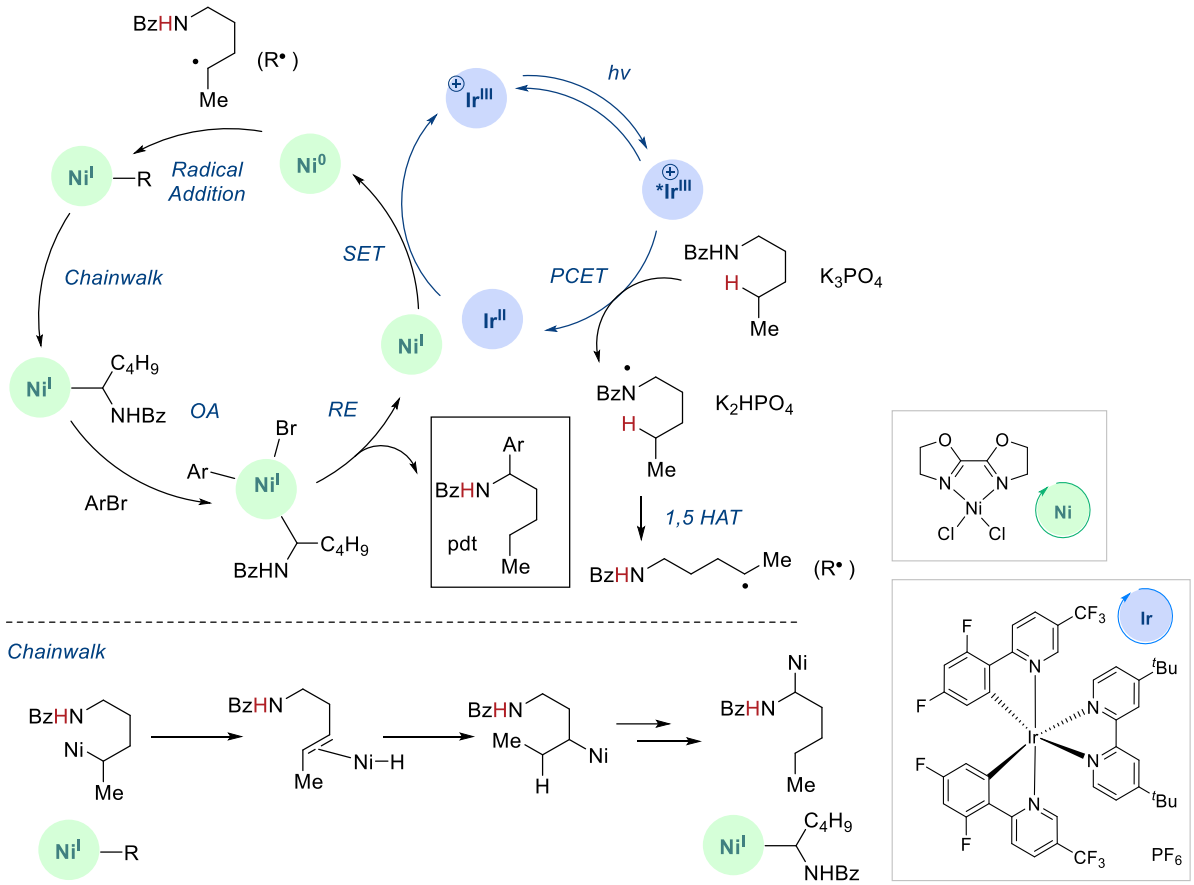

Scheme 4-6 Originally proposed mechanism.

4.2 Mechanistic Investigation

In order to probe whether 1,5 HAT / chainwalking was a viable pathway, different benzamides were tested. It is striking to notice *N*-alkylbenzamides substrates (**4-1**, **4-3**) which lack distal C–H bonds were still suitable substrates in this reaction, resulting in the phenylated products in moderate yields (**Scheme 4-7**, top). Furthermore, the necessity of free N–H bond was challenged as the use of DMAc in solvent quantity still yielded the desired C–H functionalization product (**4-5**). Lastly, the 1,5 HAT process was disapproved by treating the pre-synthesized potassium salt (**4-6**) under the standard reaction condition and the unfunctionalized *N*-alkylbenzamide was recovered quantitatively (**Scheme 4-7**, bottom). This observation suggested that the deprotonation of

benzamides was not involved in the catalytic cycle, and in fact, such deprotonation inhibited the productive pathway.

Scheme 4-7 1,5 HAT mechanism probe (by Dr. Alex Rand).

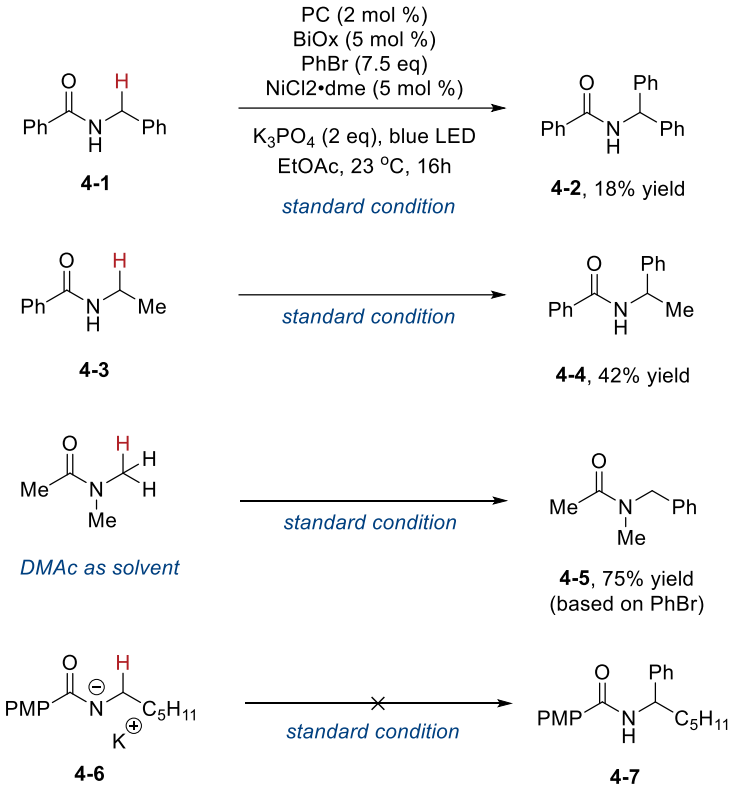

Reactions were carried out with 1.5 mmol PhBr, 0.20 mmol benzamide. Isolated yields were reported. PC refers to the photocatalyst, and its structure is shown in **Scheme 4-6**.

Additionally, several experimental observations disapproved the 1,5 HAT / chain walking mechanism. First, regioisomers or unsaturated benzamides were not observed in all reactions. Moreover, benzamide **4-8**, bearing a β-gem-dimethyl group which is uncapable of chain walking, still produced the arylated product in 6% yield, although the lower yield being attributed to the steric effect.

Scheme 4-8 Gem-dimethyl benzamide reactivity (by Dr. Alex Rand).

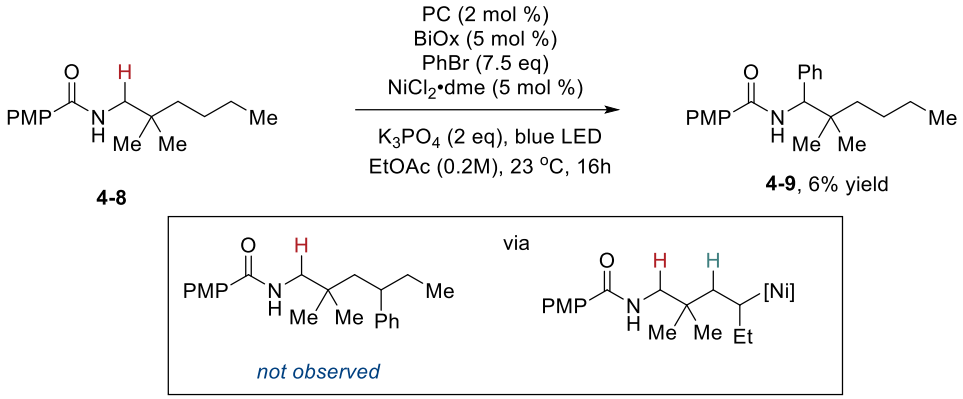

Reaction was carried out with 1.5 mmol PhBr, 0.20 mmol benzamide. Isolated yield was reported.

Stern-Volmer studies have then been performed to understand which reagent interacted with the excited photocatalyst under the reaction condition. The emission intensity (I) is the major readout from the fluorescence spectrophotometer, and concentration-dependent decrease of emission intensity (I_0/I) indicates the interaction between substances and excited photocatalysts which is termed as 'quenching'. Absences of quenching event with both benzamides and aryl bromides were not surprising as their redox potentials lie outside the range of PC ($E_{1/2}^{red}$ Ir(III*/II)=+1.21 V *vs.* SCE). Strong quenching from the nickel catalyst made us posit the electron transfer (ET) from Ir(III*) to Ni(II) would generate Ir(IV) and Ni(I), releasing a chloride anion. Recently, it has been reported that halide anions could be oxidized to form halide radicals, capable of abstracting weak C–H bonds.[106] We speculated that the bromide anion derived from PhBr could function as a potent HAT agent, as observed also by the Doyle group in their tetrabutylammonium bromide (TBAB) mediated cross coupling of acetals.[106b] This hypothesis was further confirmed by the Stern-Volmer quenching studies using an exogenous TBAB salt. Significant quenching of the photocatalyst (PC) indicated the intermolecular electron transfer between TBAB and PC at its excited state (**Scheme 4-9**).

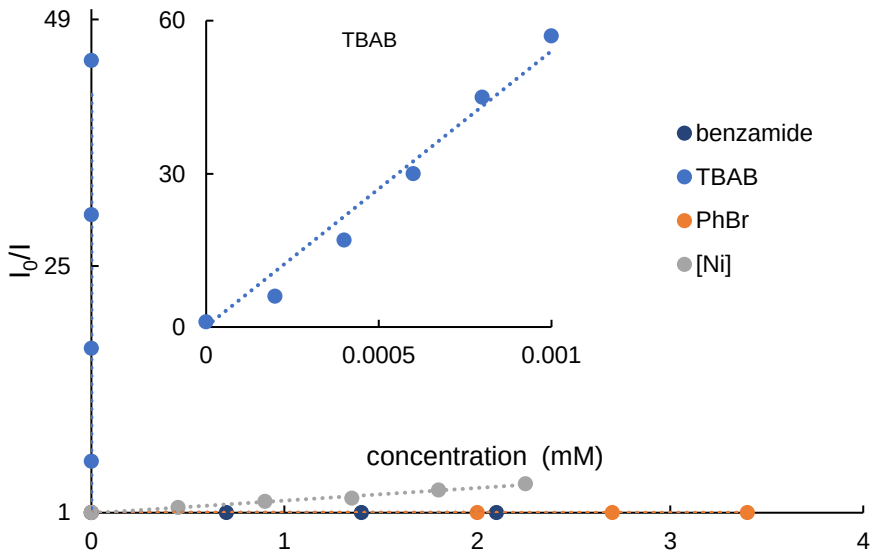

Scheme 4-9 Graphical representation of Io/I data collected in Stern-Volmer assays (by Dr. Alex Rand).

To validate the previous hypothesis that large excesses (7.5 eq) of PhBr were needed merely for the generation of enough HAT agents, second-round optimization was carried out using PhBr as a limiting reagent instead. The switch of stoichiometry, once successful, would find profound application when the aryl bromide coupling partners are more precious in the target molecule synthesis.

4.3 Improved Protocol Using TBAB as an Additive

The screening commenced with using only 1 eq PhBr and 2 eq benzamide (**4-10**) under otherwise standard reaction condition and sluggish reactivity was observed (**Entry 1**). When TBAB was used as an external bromide source, the yield was restored to 70% based on ^{1}H NMR analysis of crude reaction mixture (**Entry 2**). It is important to note that the quantity of available bromide anion in the beginning of reaction was also important as either using a sub-stoichiometry amount or TBAB (**Entry 3**) or using $NiBr_2$ pre-catalyst instead of $NiCl_2$ (**Entry 4**) both resulted

in lower yields. Lastly, the combination of $NiBr_2$ pre-catalyst and 1 eq TBAB improved the yield to 75%, supporting our hypothesis that bromide radical being the HAT agent (**Entry 5**).

Table 4-1 Evaluation of TBAB effects.

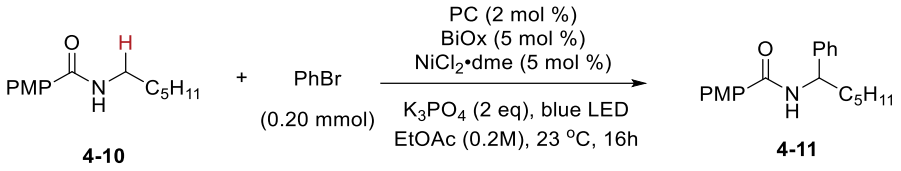

entry	Deviation from above	% yield [a]
1	NA	27
2	1 eq TBAB	70
3	10% TBAB	62
4	$NiBr_2$•dme, no TBAB	50
5	$NiBr_2$•dme, 1 eq TBAB	75

Reaction was carried out with 0.20 mmol PhBr, 0.40 mmol benzamide. [a] Yields were determined by ^1H NMR using dibromoethane as an internal standard. PC refers to the photocatalyst, and its structure is shown in **Scheme 4-6**.

In the seminal report by Montgomery, Martin, and co-workers, they also reported a $NiBr_2$ pre-catalyst with a bipyridine ligand combination for C(sp3)–H arylation of benzamides in parallel with the $NiCl_2$ pre-catalyst and BiOx. In the former case, similar stoichiometry was applied where aryl and primary alkyl bromide electrophiles were used as the limiting reagent. We were thus eager to explore whether this additive effect could also be beneficial across different nickel source and ligand scaffold combinations. Reacting 2 eq benzamide **4-12** with phenyl bromide under previously disclosed condition led to the desired product with 60% yield, while 1 eq TBAB offered a modest yield improvement (**Scheme 4-10**).

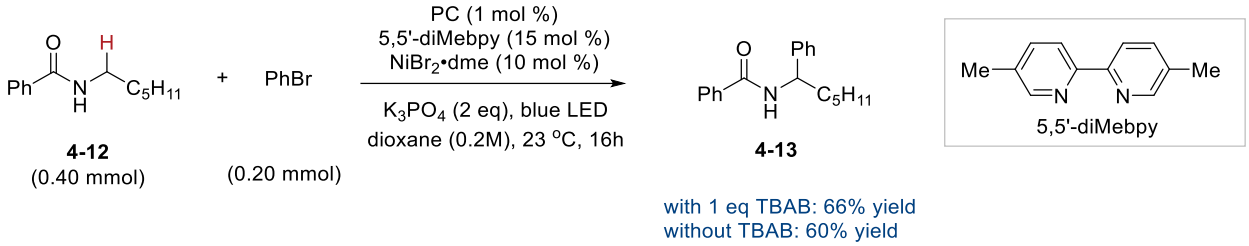

Scheme 4-10 Evaluation of TBAB effects.

Having observed better results when including TBAB, this method was applied to several previously low-yielding reactions.[105] Aryl bromides with ortho substituents typically lead to lower yields potentially due to steric reasons, but when including TBAB, the yield was increased from 33% using 7.5 eq of 2-bromotoluene to 41% when using the aryl bromide as the limiting reagent (**4-15**). Similarly, yields increased from 53% to 64% (**4-16**) when using electron-deficient aryl bromides such as 4-bromobenzotrifluoride. Different bromo benzoates were successfully employed as coupling partners, yielding the desired products also with substantial yield improvements. Lastly, benzamides that previously gave low yields benefitted from the inclusion of TBAB, which resulted in a drastic increase from 15% to 46% yield (**4-20**). These results show that including a HAT agent, such as TBAB, has a beneficial effect by improving reaction efficiency, which allows higher yields of the desired product with much lower excess of any reagent (**Table 4-2**).

Table 4-2 Improved yields using TBAB additive.

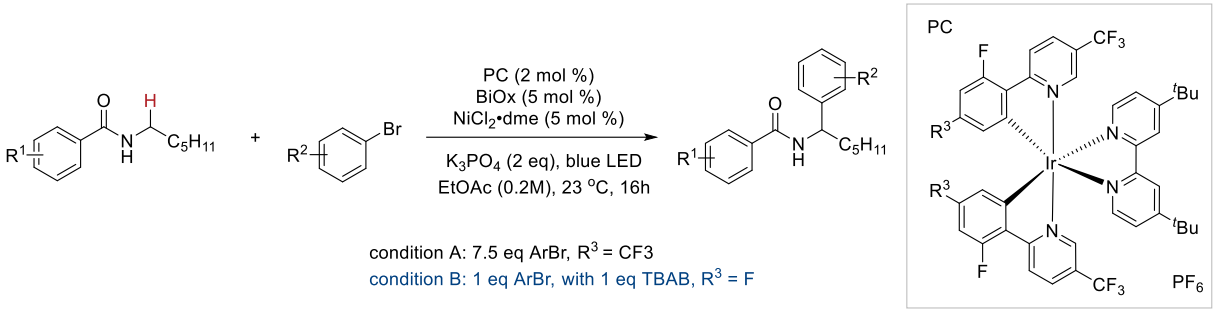

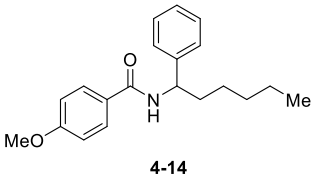

4-14

with condition A: 51% yield
with condition B: 66% yield

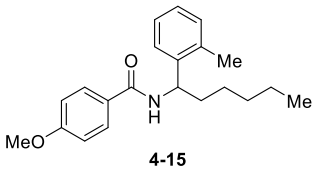

4-15

with condition A: 33% yield
with condition B: 41% yield

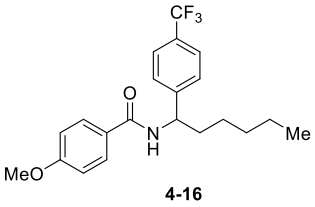

4-16

with condition A: 53% yield
with condition B: 64% yield

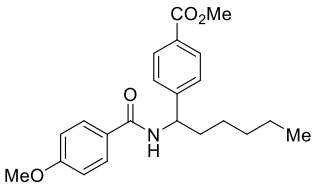

4-18

with condition A: 49% yield
with condition B: 67% yield

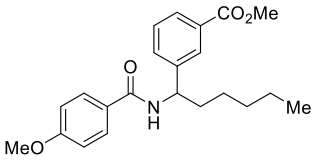

4-19

with condition A: 49% yield
with condition B: 59% yield

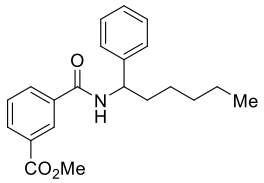

4-20

with condition A: 15% yield
with condition B: 46% yield

Reaction was carried out with 0.20 mmol ArBr, 0.40 mmol benzamide. Isolated yields were given.

4.4 Revised Mechanism

Guided by literature precedents on related systems, the proposed mechanism begins with the irradiation of photocatalyst (PC) to generate a photo-excited Ir(III*) species. Reduction of Ni(II) pre-catalyst would form Ir(IV) and Ni(I)Br (**A**) and a halide anion. Oxidation of surrounding anions (Cl^- or Br^-) to corresponding halide radical by Ir(IV) is thermodynamically feasible, and it has been previously proposed that the kinetic driving force for such redox event originates in a

favorable binding of halide anions to 3,3'-position of the bipyridine ligands. Building on recent investigations by Doyle, Molander and Huo, we posit the halide radical enacting as the HAT agent on benzamide to generate radical **E**. The balanced equation involves a base (K_3PO_4) sequestering process which happens off-cycle. It is in good correspondence with experimental observation that K_3PO_4, an insoluble base in EtOAc out-performed soluble phosphate base that has been utilized by Knowles and co-workers. After reduction of the Ni(II) species by the PC, radical capturing would take place for the generation of Ni(II) alkyl bromide intermediate (**B**). At this point, the further reduction from Ir(II) leads to the formation of Ni(I) alkyl species (**C**) and Ir(III). On the photoredox pathway, the Ir(III) can be irritated again to oxidize another equivalent of bromide anion to bromine radical for the continuation of the HAT process. For the C–C coupling cycle, the low-valent Ni(I) (**C**) undergoes oxidative addition with ArBr to Ni(III) (**D**) which would be poised for reductive elimination, releasing the C–H functionalization product, while generating the catalytically active Ni(I) bromide (**A**). For ease of understanding, the catalytic cycle was simplified as we believe with 1 eq TBAB as additive, bromide anion would be the dominant counterion for the nickel catalyst. Meanwhile, bromine radicals have also been shown as suitable HAT agent to abstract hydric C–H bonds such as those proximal to N in benzamides.

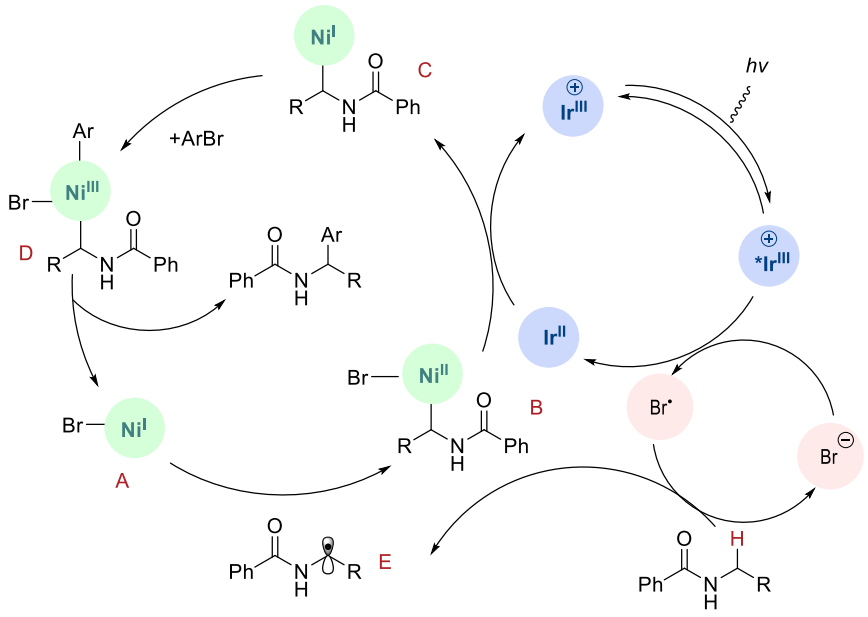

Scheme 4-11 Revised mechanism.

4.5 Conclusion

Through these studies, we observed the inclusion of TBAB leads to higher yields while lowering PhBr stoichiometry. Since exogenous Br^- is not necessary to produce the desired product, and the most likely HAT agent in the reaction after the initial catalytic cycle is bromine radical, we believe that the primary benefit of TBAB is to more efficiently generate them through oxidation of Br^- by PC, which serves to abstract the α C–H bonds of *N*-alkylbenzamides, during the initiation of the reaction when substrate-derived bromide concentration is low. When including TBAB in this reaction, the exogenous Br^- facilitates the formation of a higher concentration of Ir(III)–Br complex in solution, which more efficiently promotes oxidation of Br^- to bromine radical by Ir(III*). Because the oxidation of bromide is more favorable than chloride, bromine radical is expected to be the predominate HAT agent throughout the initial and subsequent catalytic cycles when TBAB is present at the beginning of the reaction.

Chapter 5 Nickel Catalyzed *N*-Heterocyclic C–H Functionalization Using Aldehydes as Coupling Reagents

The unpublished work described in this chapter was done in collaboration with Austin Ventura and Soumik Das, and their specific contributions were highlighted in discussion.

5.1 Introduction

Functionalization of sp3 C–H bonds allows organic chemists to 'escape from flatland', as compared to their sp2 and sp counterparts, enabling desired physical and chemical properties. Towards that regard, existing methodologies typically rely on pre-functionalized reagents (such as activated carboxylic acids, boronic esters, organozinc and organomagnesium) while the potentials of C–H bonds being latent nucleophile equivalents are generally neglected. Herein, we report the acylation of α-amino C(sp3)–H bonds using aldehydes as coupling reagents under a mild, redox-buffered condition with a broad substrate scope, representing an attractive approach for accessing α-amino ketones. A combination of experimental investigation and computational modelling reveals the primary mechanism to be plausibly radical based and further elucidates the origin of cross-selectivity.

Functionalization of C–H bonds, the most common bonds in organic molecules, has become a prominent strategy in the synthetic community, partially owing to the advantages for rapid buildups of molecular complexity without resorting to *de novo* synthesis.[42a, 107] The capabilities to couple otherwise inert building blocks, bypassing reductant synthetic handle installation, are appealing to chemists for streamlining the construction of target molecules.[39b, 89,

[108] However, the field of C–H functionalization still suffers from the challenging regio- and chemoselective controls, as well as those non-economic approaches relying on precious transition metals / ligand combination which inherently limits the development of new reaction manifolds.[2, 109]

5.2 Nickel Catalyzed C–H Functionalization via HAT

Our group has a long-standing interest in nickel (Ni) catalyzed C–C coupling reactions.[110] Aside from being highly earth-abundant, nickel has demonstrated complementary reactivity compared with second and third-row transition metals especially with respect to single electron transfer (SET).[3, 111] Seminal contribution by Doyle and MacMillan disclosed a metallaphotoredox catalyzed decarboxylative arylation using feedstock amino acid starting materials, enabling selective C(sp3)–C(sp2) cross coupling (**Scheme 5-1**).[30] The authors proposed a synergistic effect from photocatalyst and nickel where reductive quenching of the excited photocatalyst incurred the decarboxylative carbon centered radical formation, and nickel underwent SET and helped foraging the new C–C bond via reductive elimination. The successful application of carboxylic acids in transition metal catalyzed cross-coupling serves as an illustration of the tremendous scope expansion that is attainable by using this dual catalysis technology.

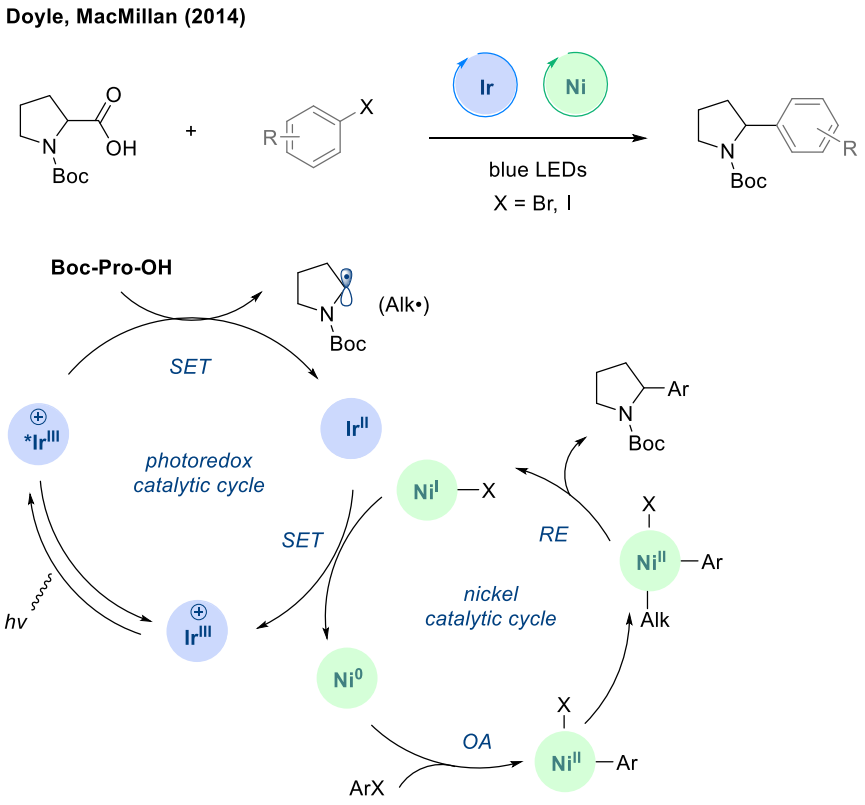

Scheme 5-1 Metallaphotoredox catalyzed decarboxylative cross-coupling.

The authors further demonstrated the utility of this dual catalysis strategy in C(sp3)–H functionalization with aryl halides. Analogous α-carbon centered radical was generated via a photo-oxidation, deprotonation sequence with aniline substrates. The conceived pathway was followed by a similar nickel mediated radical capture and reductive elimination, resulting in the C–H arylated products. Good yields with various *para*-substituted aryl bromides were shown (**5-1 - 5-3**), including a chemoselective C–Br coupling when 1-bromo-4-chlororbenzene was used as substrate (**Scheme 5-2**).

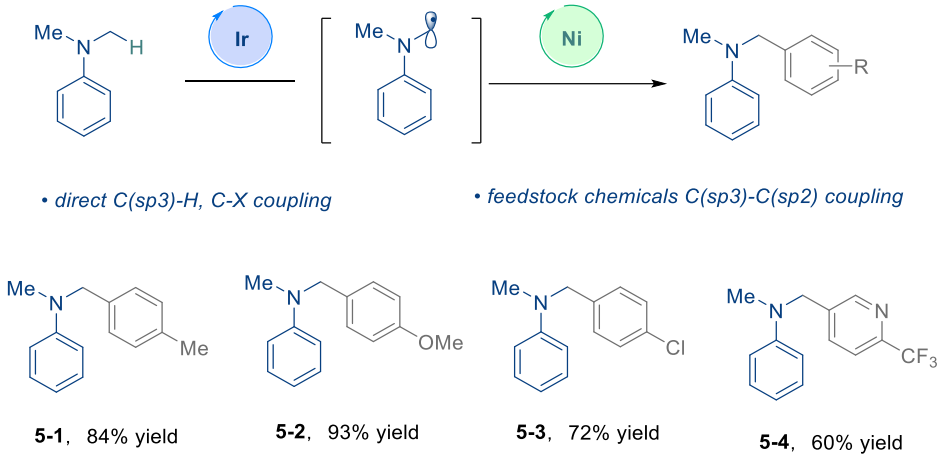

Scheme 5-2 Direct C(sp3)–H, C–X cross-coupling via photoredox-nickel catalysis.

This proof-of-concept study provided support for the idea that photocatalysts convert C(sp3)–H bonds to carbon centered radicals and nickel catalysis is leveraged to form C(sp3)–C bonds. Building on these efforts, the Doyle group developed a direct functionalization of C(sp^3)–H bonds of *N*-aryl amines by acyl electrophiles under a mild, metallaphotoredox condition (**Scheme 5-3**).[112] In the earlier precedent by the same group (**Scheme 5-2**), substrate scope was rather limited, and amines bearing β-hydrogen atoms were not tolerated. The successful employment of symmetric, activated acyl electrophiles enabled the synthesis of a variety of α-amino ketones from *N*-phenyl pyrrolidine. In events that the desired coupling involves complex acyl precursor, the authors figured out that instead of symmetric anhydrides, different activating groups for carboxylic acids could be applied to yield the desired ketone product (**5-6**). The use of 2-pyridylthioester[113] would offer better stability towards handling and its amenability in late-stage functionalization setting was successfully demonstrated.

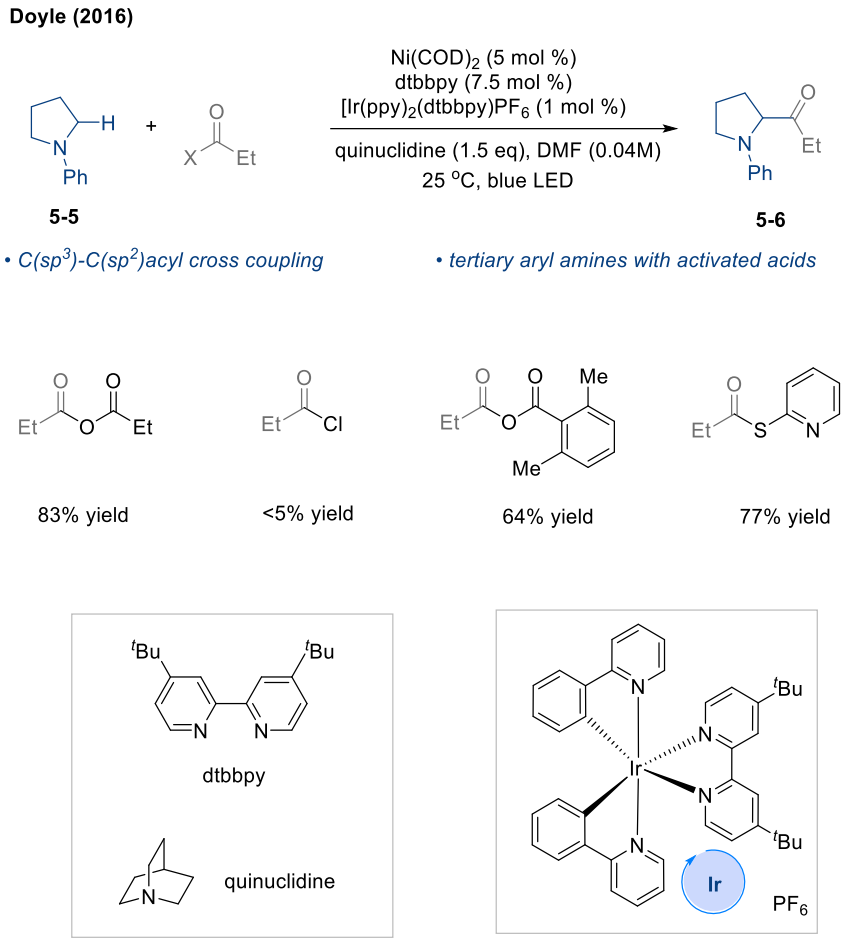

Scheme 5-3 C(sp3)–H acylation with different coupling partners via metallaphotoredox catalysis.

Following their report, the fields of photoredox and hydrogen atom transfer (HAT) have experienced rapid growth with broader scopes being demonstrated on *N*-heterocyclic C(sp3)–H functionalization with different coupling partners including halides,[31, 106a, 114] activated acids,[106c, 115] acrylates[116] ,azoliums[117].

More recently, MacMillan and co-workers further demonstrated the merger of nickel catalysis with decatungstate mediated HAT, enabling the late-stage C(sp^3)–H methylation of drug molecules (**Scheme 5-4**).[115] The direct introduction of methyl groups in a broad array of saturated heterocycles was believed to adopt a unique nickel-mediated radical sorting effect where the cross-selectivity for C(sp3)–C(sp3) bond formation benefited from the S_H2 reactivity .[118] In this case,

the stability of alkyl bounded nickel species are in reversed correlation with degree of substitution on carbon, presumably due to steric reasons. That being said, nickel catalyst is more prone to capture methyl radicals, resulting in a relatively low concentration of unbounded methyl radicals in solution. Meanwhile, the generated α-amino carbon centered radicals are formed in higher concentrations, leading to the hetero-coupled product.[119] It is important to note that the intermolecular reductive elimination happens in a S_H2 fashion, similar to the atom transfer catalysis observed in chemoenzymatic transformation.[120]

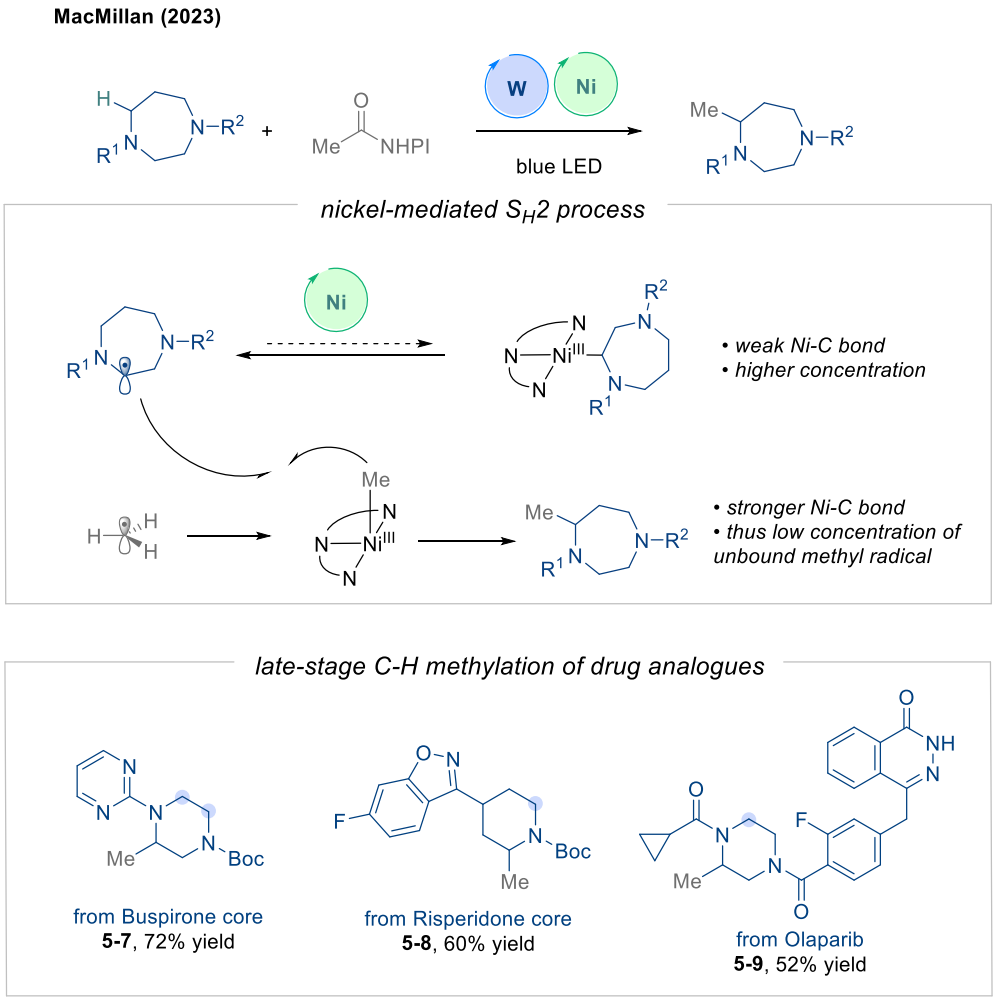

Scheme 5-4 Late-stage functionalization of drug molecules via radical sorting S_H2 pathway.

5.3 Peroxide-Mediated C–H Functionalization under Thermal Conditions

In parallel with the rapid development in the field of metallaphotoredox catalysis, concurrent efforts from Lei,[34, 121] Gong,[35] You[122] and others have focused on nickel catalyzed peroxide thermal activation leading to the functionalization of heterocyclic C(sp3)–H bonds.[123] Seminal contribution was made by Li and co-workers where they reported the cross-dehydrogenative coupling (CDC) between tetrahydroisoquinoline (**5-10**) and free indoles using copper catalysis while preserving the reactive N–H bonds (**Scheme 5-5**, top).[124] *tert*-Butyl hydroperoxide (TBHP) was applied as the HAT agent to abstract the relatively weak benzylic C–H bond.

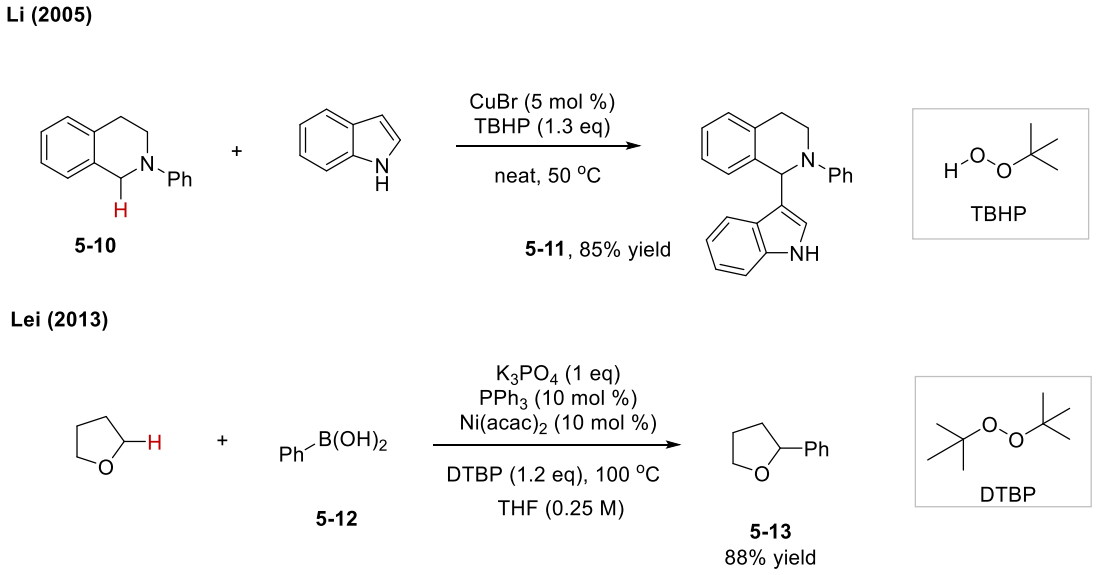

Scheme 5-5 Early precedents for peroxide-mediated C–H functionalization.

In 2013, the Lei group leveraged di-*tert*-butyl peroxide (DTBP) as a mild, stable organic peroxide, enacting as the HAT agent in the nickel catalyzed cyclic ether C–H functionalization (**Scheme 5-5**, bottom). This work represented the first nickel catalyzed oxidative arylation of C(sp3)–H arylation, although the cyclic ethers were used in solvent quantities. It is believed that DTBP played dual roles in this catalysis, SET with low-valent nickel catalyst to generate *tert*-

butoxy radical, which served as HAT agent, meanwhile, the *tert*-butoxide promoted transmetallation of boronic acids, leading to aryl bounded nickel species formation.

Recently, the Gong group reported a nickel catalyzed arylation of C(sp3)–H bonds with organohalides using DTBP as the HAT reagent (**Scheme 5-6**, top).[35] This protocol allowed for the arylation under mild, thermal conditions with a broad substrate scope including cyclic ethers, amines and even cyclohexane. Employing tetra-*n*-butylammonium iodide (TBAI) and pyridine as additives, desired α-arylation product (**5-16**) of Boc-pyrrolidine (**5-14**) was isolated with 80% yield. The transformation was also easily scaled up to a 10-gram scale, without significant decrease of yield. Mechanistic investigations were conducted to confirm that Zn was required as a stoichiometric reductant and could co-exist with the mild oxidant DTBP. Roles of nickel were also elucidated as an electron shuttle between the reductant and oxidant besides being the radical mediator which has also observed by MacMillan and co-workers.[115, 118e] Coincidentally, Stahl and co-workers separately developed a benzylic C(sp3)–H methylation strategy harvesting β-scission process of DTBP and applied it as a methylation reagent (**Scheme 5-6**, bottom).[37] Several experimental evidences supported their hypothesis. Firstly, the observed formation of acetone arguably came from the β-methyl scission of *tert*-butoxy radical. A pressure build-up was noticed within the reaction vial and the gaseous products were carefully analyzed to establish their identities. The formation of ethane was not surprising as the rapid generation of methyl radical led to inevitable formation of homodimers. The significant generation of methane, on the other hand, could indicate that methyl radical was not innocent in the HAT process. Moreover, the abstraction of weak C–H bonds by methyl radicals would be rendered both thermodynamically and kinetically (release of gas) favored.

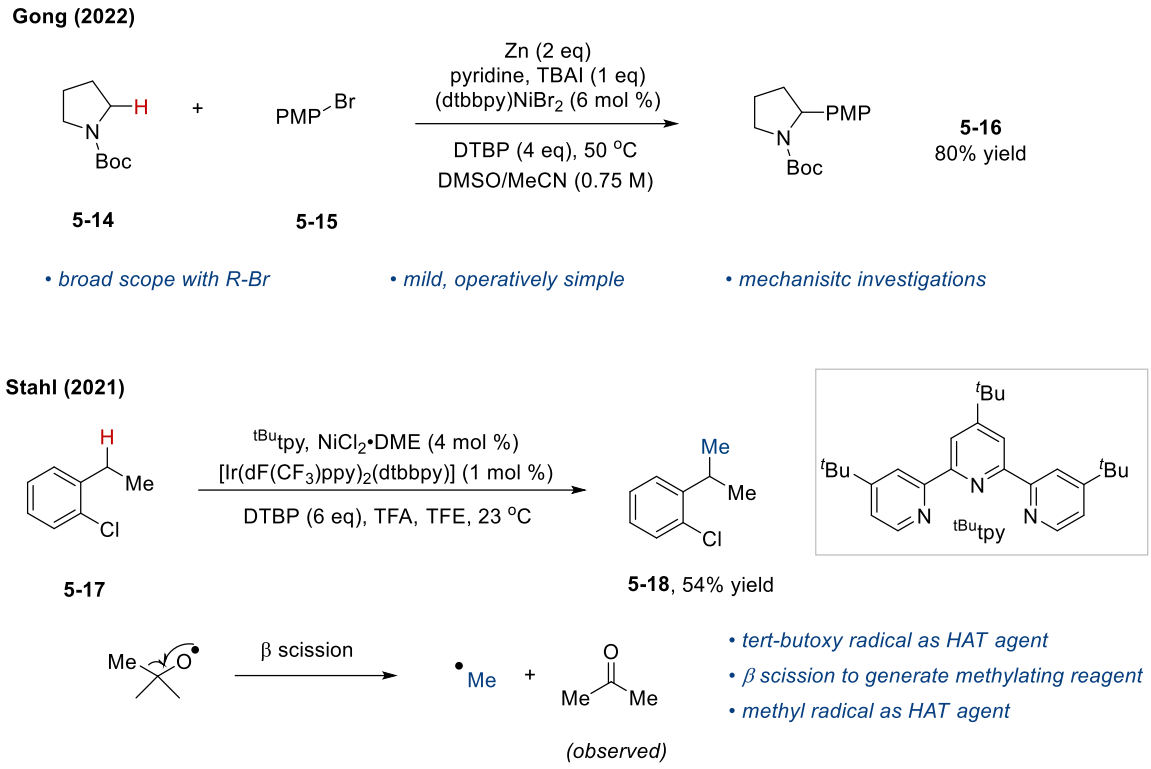

Scheme 5-6 DTBP-mediated C–H functionalization with nickel catalysis.

Nitrogen-containing heterocycles are prevalent in bio-active motifs, and the selective functionalization of their C(sp3)–H bonds allow for accessing greater chemical spaces which were rarely explored in traditional cross coupling reactions.[91, 124-125] In this vein, we became very interested in merging *N*-heterocyclic C(sp3)–H functionalization with aldehyde coupling based on our previous success[126] of employing aldehydes as feedstock building blocks.[127] We speculated that a different activation mode of aldehyde via HAT would incur a wider substrate scope and may lead to unique selectivity.[128] We were aware of the proposed dehydrogenative coupling could encounter several pitfalls including a) radical dimerization; b) radical degradation; c) formation of oxidized/reduced byproducts and d) formation of over-functionalized byproducts but were also eager to explore the combination of ligands and reagents to mitigate the side reaction while preserve the desired C–C coupling (**Scheme 5-7**).

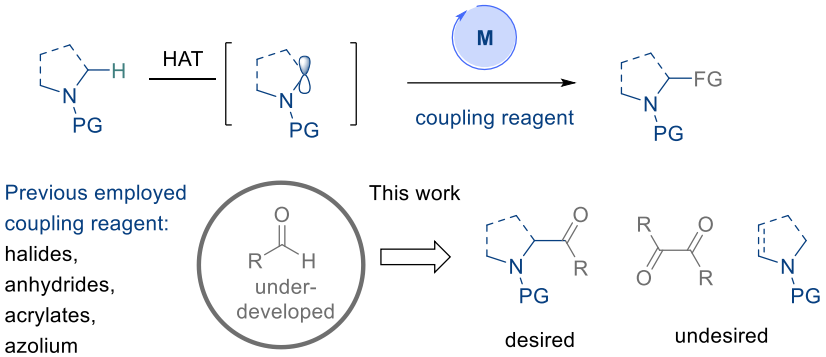

Scheme 5-7 Nickel catalyzed N-heterocyclic C–H functionalization using aldehydes as coupling reagents.

5.4 Development of Dehydrogenative Coupling between N-Heterocycles and Aldehydes

We commenced our experimental optimization from the coupling between benzaldehyde (**5-17**) and *N*-Boc pyrrolidine (**5-14**). To enable a rapid testing of wide range of ligands and high evaluation efficiency, both GCMS and NMR were applied for crude reaction mixture analysis, and the yield of desired product, **5-18**, was measured against an internal standard without isolation (**Table 5–1**). The initial optimization started from ligand screening, and it was aspiring to find that the desired acylated product (**5-18**) was obtained with simple bipyridine (L1, bpy), although at a low yield (27%). Further evaluation of electronic and steric on the bpy scaffold revealed that both electron-deficient and sterically hindered ligand tend to give lower yields (L2 - L5). And this observation was further supported by results obtained with bisquinoline (L6) and 1,10-phenanthroline (L7). Stepping out of the bpy scaffold, although bisoxazoline (L8) did not offer too much yield improvement, the use of bispyrazole pyridine (L9, bpp) significantly boosted the yield to 45%. Efforts were then directed to figure out whether this advantageous effect came from tridentate ligand scaffold or was unique to bpp. Switching to terpyridine (L12) and pyridine bisoxazoline (L13) both resulted in the formation of **5-18** in low yields. Unfortunately, further modifying the bpp structure based on electronics and sterics did not increase the reactivity (L10,

L11) and efforts resorting to ligands that have been applied to similar radical cross coupling ended in vain (L15, L16).[115] Nevertheless, other than *N*-donor ligands, phosphine and NHC ligands completely shut down the reactivity, empirically indicated that this reaction underwent SET pathway. Though the current yield is falling short from being synthetically useful, clean reaction profiles have been observed across the board, and the reminder of mass balances are unreacted starting materials **5-14**, **5-17** as observed on H NMR and DTBP can be tracked by GCMS.

Table 5-1 Ligand screening

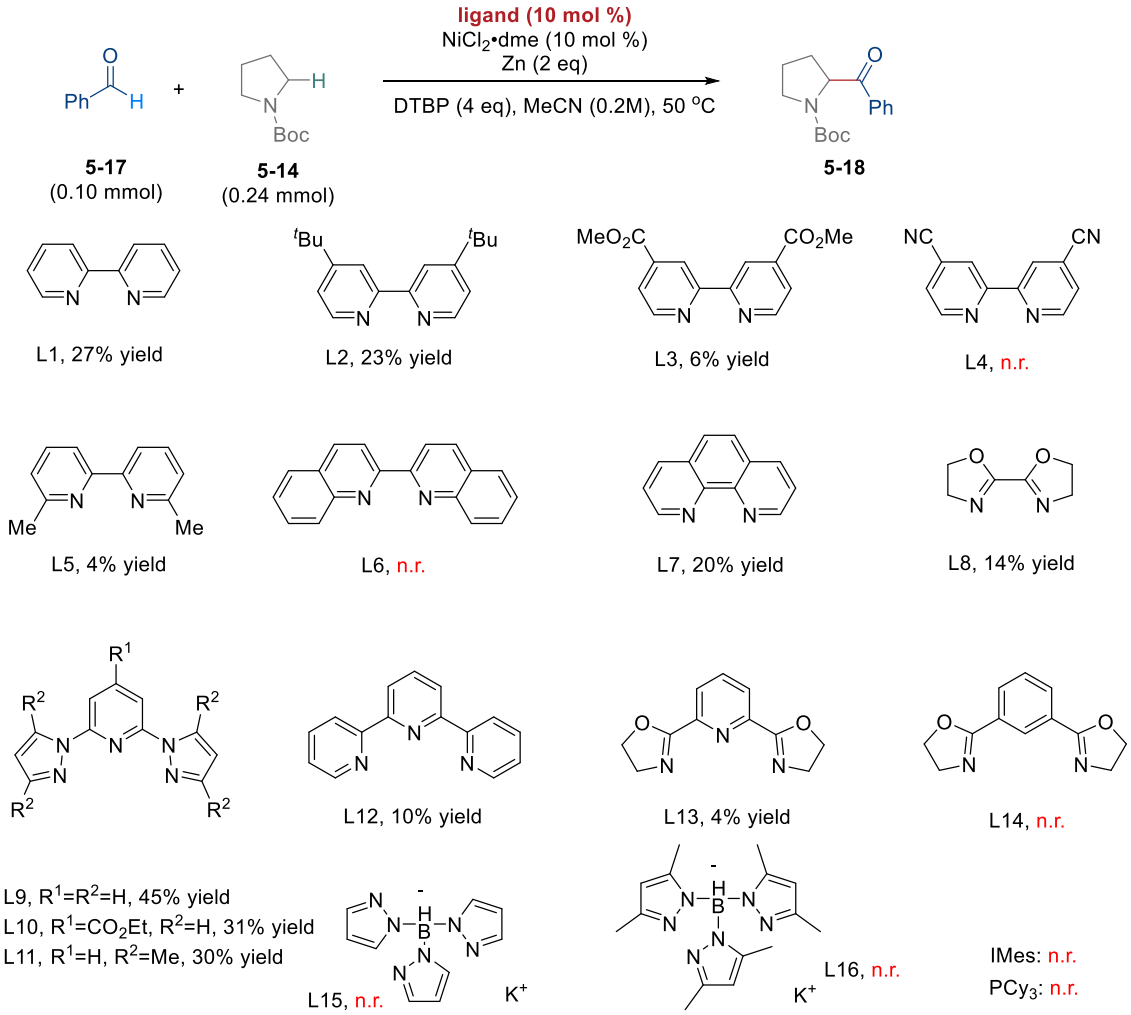

The reaction was performed with **5-17** (0.1 mmol, 1.0 eq), **5-14** (0.24 mmol, 2.4 eq), ligand (0.01 mmol, 0.1 eq), $NiCl_2$•dme (0.01 mmol, 0.1 eq), Zn (0.2 mmol, 2.0 eq) and DTBP (0.4 mmol, 4 eq) in MeCN (0.5

mL, 0.2 M) at 50 °C for 16h. Yield was determined by ^{1}H NMR using CH_2Br_2 as an internal standard or GCMS using tridecane as an internal standard. n.r. means no reaction.

Next, attention was turned to the identity of the reductant (**Table 5-2**). Control experiment was performed first to confirm the necessity of Zn (**Entry 1**). Switching to other commonly used reductants including Mn and tetrakis(dimethylamino)ethylene (TDAE) did not produce the desired product **5-18** (**Entries 2, 3**), demonstrating the unique role of Zn in this heterogeneous catalysis (**Entry 4**). Instead of normal Zn, the use of nano powder Zn increased the yield to 50%, which was rationalized based on the increased surface areas being beneficial for redox events (**Entry 5**). To reiterate the importance of stoichiometric reductant, nano powder Zn was examined in both catalytic and large excess (**Entries 6, 7**). Based on these results, 2 eq nano powder Zn was considered optimal and brought forward.

Table 5-2 Reductant screening

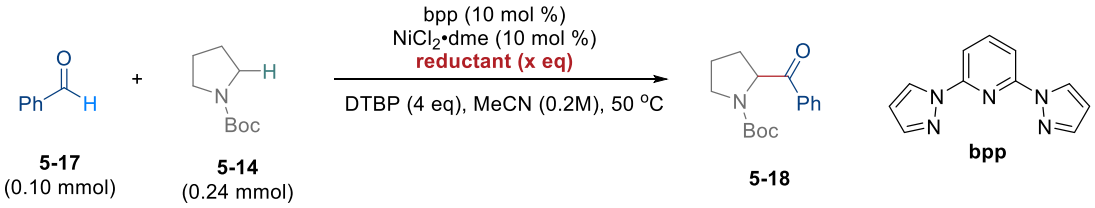

Entry	Reductant	x (eq)	% yield
1	No	NA	<5
2	Mn	2	0
3	TDAE	2	0
4	Normal Zn	2	45
5	Nano powder Zn	2	50
6	Nano powder Zn	0.2	14
7	Nano powder Zn	4	35

The reaction was performed with **5-17** (0.1 mmol, 1.0 eq), **5-14** (0.24 mmol, 2.4 eq), ligand (0.01 mmol, 0.1 eq), $NiCl_2$•dme (0.01 mmol, 0.1 eq), reductant and DTBP (0.4 mmol, 4 eq) in MeCN (0.5 mL, 0.2 M) at 50 °C for 16h. Yield was determined by ^{1}H NMR using CH_2Br_2 as an internal standard.

Different peroxides were then examined to evaluate their performances in promoting this oxidative coupling (**Table 5-3**). Hydrogen peroxides were found to be intolerant with the reaction scaffold, and it was first thought that after the SET with nickel catalysts, generation of nickel hydroxide could be prohibitive. Also, the possible generation of water as the HAT by product can also be problematic. The latter scenario can be easily examined by using water as an external additive which will be discussed in **Table 5-4**. Structure-activity relationship of peroxides were further examined using dicumyl peroxide (DCP) and *tert*-butylperoxy benzoate (TBPB), lower yields were obtained compared to DTBP (**Entries 3, 5, 6**). The use of carbonate-based peroxide *tert*-butylperoxy 2-ethylhexyl carbonate (TBEC) led to no reaction.

Table 5-3 Peroxide screening

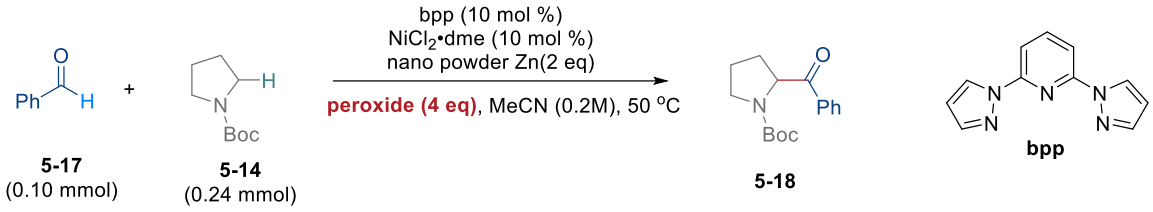

Entry	Peroxide	% yield
1	H_2O_2	0
2	^{t}BuOOH	0
3	DTBP	50
4	TBEC	0
5	DCP	35
6	TBPB	17

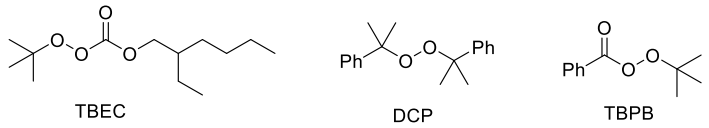

The reaction was performed with **5-17** (0.1 mmol, 1.0 eq), **5-14** (0.24 mmol, 2.4 eq), ligand (0.01 mmol, 0.1 eq), $NiCl_2$•dme (0.01 mmol, 0.1 eq), nano powder Zn (0.2 mmol, 2.0 eq) and peroxide (0.4 mmol, 4

eq) in MeCN (0.5 mL, 0.2 M) at 50 °C for 16h. Yield was determined by ^{1}H NMR using CH_2Br_2 as an internal standard.

To further increase the yield of acylated product **5-18**, different additives were explored in the categories of Lewis acid and base, Brønsted acid and base. LiCl has been used before to activate the heterogeneous reductant surface, though a lower yield was observed when it being used as an additive (**Entry 2**). We hypothesized that the oxidation byproduct of Zn is $Zn(O^tBu)_2$, unfortunately, the use of such Zn-based Lewis acid / Brønsted base additive did not increase the yield (**Entries 3-5**). It was encouraging to see that adding the reduction byproduct of DTBP, *tert*-butanol in the beginning of the reaction, resulted in a similar yield (**Entry 6**). Along with this line, effects of different Brønsted acid / hydrogen bond donating additives were then carefully examined. Drastic yield increase was observed when isopropanol, hexafluoroisopropanol and water were used as additive at 2 eq (**Entries 7-9**), where water championed amongst leading to the formation of desired product with 67% yield. It was also not surprising that further increasing the acidity of hydrogen bond donating additives to TFA completely shut down this reaction, as stoichiometric use of strong organic acid would lead to the deprotection of **5-14** at elevated temperature (*not shown in table*). Due to the prevalence of nitrogen-containing heterocycles in small molecule drugs, we were eager to explore the possibility of using water as a co-solvent for this acylation chemistry, with the outset that future applying it in building DNA-encoded library. It was very pleasing to see that despite MeCN and water being immiscible, the desired nickel catalyzed C–H functionalization still yielded the desired product **5-18**, with 29% yield.

Table 5-4 Additive screening

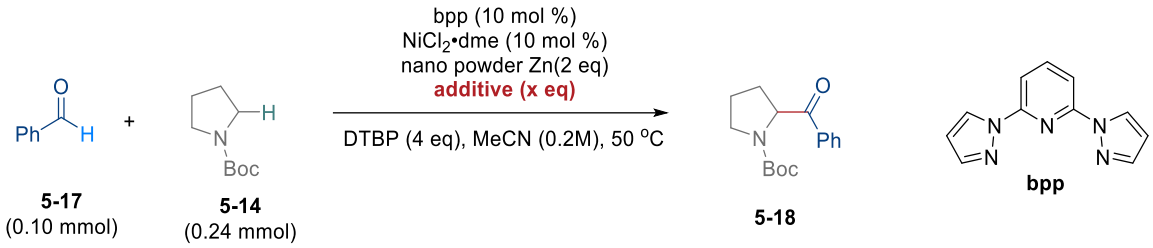

5-17 (0.10 mmol) + **5-14** (0.24 mmol) → **5-18**

Entry	Additive	x (eq)	% yield
1	No	NA	50
2	LiCl	0.2	29
3	$Zn(OTf)_2$	0.2	15
4	$Zn(O^tBu)_2$	0.2	25
5	$ZnCl_2$	1	24
6	^{t}BuOH	2	48
7	IPA	2	60
8	HFIP	2	64
9	H_2O	2	67
10	H_2O	56	29

The reaction was performed with **5-17** (0.1 mmol, 1.0 eq), **5-14** (0.24 mmol, 2.4 eq), ligand (0.01 mmol, 0.1 eq), $NiCl_2$•dme (0.01 mmol, 0.1 eq), nano powder Zn (0.2 mmol, 2.0 eq), additive (x eq), and DTBP (0.4 mmol, 4 eq) in MeCN (0.5 mL, 0.2 M) at 50 °C for 16h. Yield was determined by ^{1}H NMR using CH_2Br_2 as an internal standard.

Lastly, deviations from the standard reaction parameter were made to test their impacts on the reaction, including catalyst loading (**Entry 2**), DTBP loading (**Entry 3**) and concentration (**Entry 4**). Reaction time was also evaluated to establish the optimal condition (**Entry 6**). It is worth highlighting that comparable results were obtained when running the reaction in dark, excluding the possibility of peroxide photo-activation pathway (**Entry 7**).

Table 5-5 Condition optimization

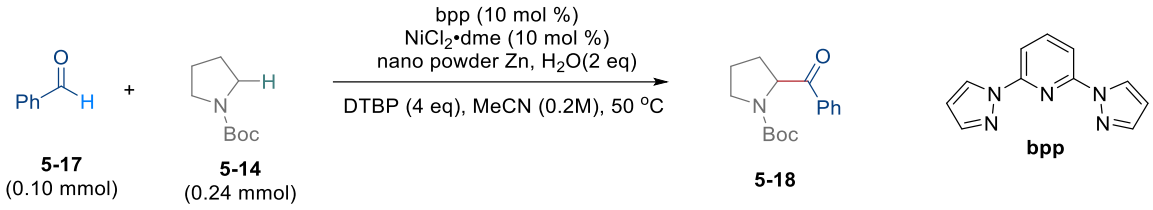

Entry	Deviation from above	% yield
1	No	67
2	5% Ni, bpp	37
3	6 eq DTBP	45
4	0.4M	52
5	1 eq $ZnCl_2$	24
6	2h instead of 16h	31
7	In dark	64

The reaction was performed with **5-17** (0.1 mmol, 1.0 eq), **5-14** (0.24 mmol, 2.4 eq), ligand (0.01 mmol, 0.1 eq), $NiCl_2$•dme (0.01 mmol, 0.1 eq), nano powder Zn (0.2 mmol, 2.0 eq), H_2O (2 eq), and DTBP (0.4 mmol, 4 eq) in MeCN (0.5 mL, 0.2 M) at 50 °C for 16h. Yield was determined by ^1H NMR using CH_2Br_2 as an internal standard.

The optimal condition was decided based on these extensive screenings, involving the use of 10 mol % $NiCl_2$•dme as pre-catalyst, bpp as ligand, 2 eq nano powder Zn and H_2O in MeCN at 0.2M and the aldehyde scope was first explored. This transformation tolerated different electronic environments on benzaldehydes, while electron withdrawing groups generally led to lower yields (**Table 5-6**). It was aspiring to find that functional groups that were facile for activation with nickel catalysis under reductive conditions underwent chemoselective C–H functionalization, enabling orthogonal reactivities at a later stage (**5-20**, **5-21** and **5-25**). Of note, by analyzing crude reaction profiles, remainders of mass balances turned out to be unreacted starting materials (aldehyde and **5-14**), and good mass recovery was demonstrated with the synthesis of **5-21** (93% brsm). The synthetic utility was proved with a successful 1.0 mmol scale synthesis of **5-18** with a 54% isolated yield. Heteroaryl aldehydes were also compatible with this dehydrogenative coupling (**5-26** - **5-**

29), and though electron-rich heterocycles gave lower yields, the absence of Minisici-type byproducts and clean reaction profile was worth highlighting. Further expanding the scope with the aliphatic aldehydes, both cyclopropanecarboxaldehyde (**5-30**) and hydrocinnamaldehyde (**5-31**) smoothly yielded the ketone product, the former with the ring intact and latter could be carried out with a 1:1 ratio of aldehyde and pyrrolidine. We envisioned that the potential of switching either coupling partner as the limiting reagent would better help medicinal chemists applying this methodology at a later stage or in a complex setting. Along with this line, aldehyde that derives from ricinoleic acid was well tolerated, leading to the formation with the desired coupling product **5-32** with a 55% yield.

Table 5-6 Aldehyde scope

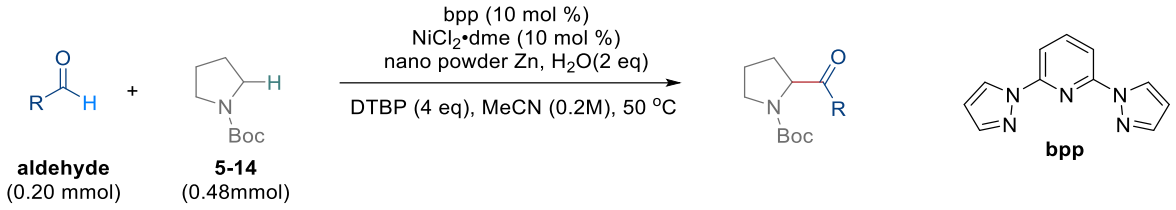

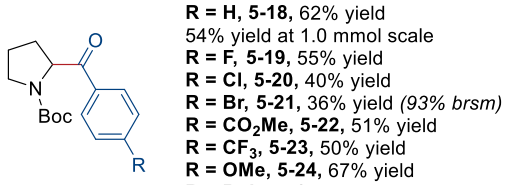

R = H, 5-18, 62% yield
54% yield at 1.0 mmol scale
R = F, 5-19, 55% yield
R = Cl, 5-20, 40% yield
R = Br, 5-21, 36% yield *(93% brsm)*
R = CO_2Me, 5-22, 51% yield
R = CF_3, 5-23, 50% yield
R = OMe, 5-24, 67% yield
R = Bpin, 5-25, 38% yield

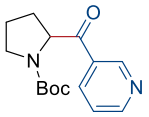

5-26, 42% yield

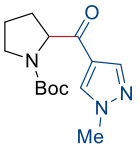

5-27, 48% yield

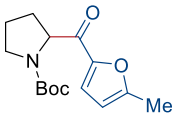

5-28, 33% yield

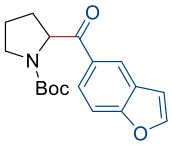

5-29, 27% yield

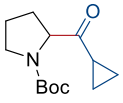

5-30, 56% yield

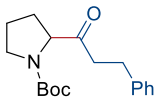

5-31, 70% yield
50% yield (1:1)

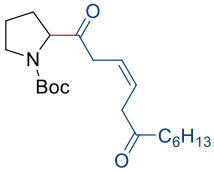

5-32, 55% yield
from ricinoleic acid

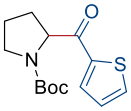

5-33, n.r.

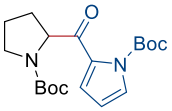

5-34, n.r.
unsuccessful results

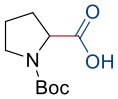

5-35, n.r.

A broad scope of amine coupling partners has also been developed (**Table 5-7**). Amino acid Boc-Pro-OMe was successfully converted to the corresponding acylated product (**5-36**) with 77% yield. Different protecting groups were well tolerated, including CBz, Ac, and Bz (**5-37 – 5-39**). Piperidine, one of the most prevalent motifs of pharmaceutical ingredient cores,[90, 129] was successfully applied to the dehydrogenative coupling (**5-40**), together with a regioselective C–H functionalization using Boc-morpholine (**5-41**). Orthogonal functionalization of multiple heteroatoms of similar reactivity has been long sought after in organic synthesis,[108b] and we took advantage of Ts as a deactivating protecting group to enable a regioselective activation of C–H bonds proximal to the Boc protected nitrogen of the piperazine. Such substrate-controlled regioselectivity has also been observed by Nicewicz and co-workers.[116] The desired acylation was also observed in acyclic systems, with simple building blocks such as *tert*-butyl *N*,*N*-dimethylcarbamate (**5-43**) and tetramethyl urea (**5-44**). Benzamides, which have been studied extensively under metallaphotoredox C–H functionalization regimes, also underwent the acylation reaction with a modest yield, providing orthogonal functionalization strategies to secondary amides (**5-45**). Benzylic C–H bonds were also successful candidates for aldehyde coupling and the desired product (**5-46**) was obtained without condition optimization, indicating a potentially broader scope outside the protected amines.

Table 5-7 Amine scope

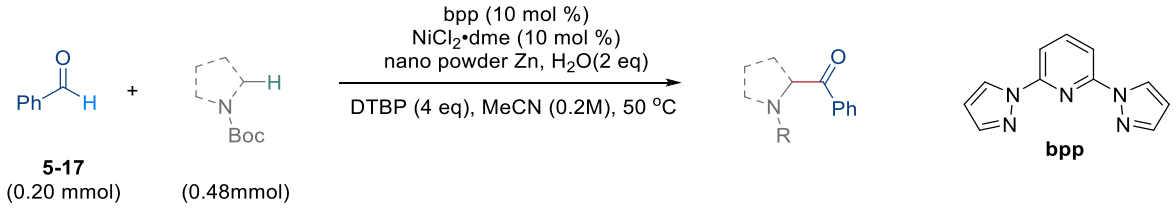

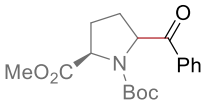

5-36, 77% yield
d.r. 1.1:1

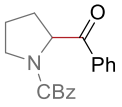

5-37, 37% yield

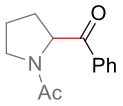

5-38, 66% yield

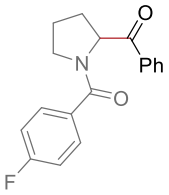

5-39, 62% yield

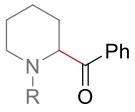

R = Boc, 5-40, 46% yield
R = Cy, Ts, n.r.

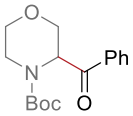

5-41, 49% yield

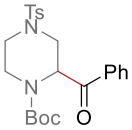

5-42, 46% yield

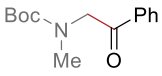

5-43, 51% yield

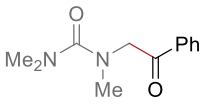

5-44, 41% yield

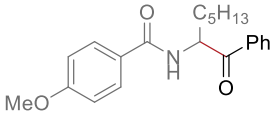

5-45, 40% yield

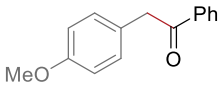

5-46, 22% yield

5.5 Mechanistic Investigations

To provide deeper insights about the catalytic cycle, mechanistic investigations have been performed experimentally as well as computationally. A series of radical trapping experiments were carried out to probe the proposed nickel catalyzed radical-radical cross coupling pathway (*vide infra*). Benzyl acrylate was selected as an electron deficient alkene for the Giese reaction[130] wherein the α-amino radical addition product was isolated in 30% yield (**Scheme 5-8A**). Swapping the radical scavenger to diphenyl diselenide, which has been used as a trapping agent for acyl radicals,[131] afforded the acyl-selenide product in 15% yield based on GCMS analysis. These experiments indicated that both carbon-centered radicals were involved in the transformation though the use of TEMPO as an additive completely shut down the reaction.

To further understand roles that Zn and DTBP played in this transformation, several control experiments have been conducted. In the absence of either nickel catalyst or Zn, trace decomposition of DTBP could be observed at 50 °C over 16h. Moreover, we were able to correlate

the stoichiometry of Zn and product yield based on GC analysis, indicating that Zn played a crucial role in the catalytic cycle rather than merely being a redox buffer reagent (**Scheme 5-8B**). Three potential HAT reagents were studied independently a) chlorine radicals (via oxidation of chloride from pre-catalyst); *tert*-butoxy radicals (via decomposition of DTBP); and c) methyl radicals (via β-scission of *tert*-butoxy radicals). Additions of different tetrabutylammonium halides salts, which has been shown in promoting HAT processes in metallaphotoredox reactions[106b, 106c] all led to inferior results, suggesting that chlorine radicals may not be the HAT reagent in this reaction. (**Scheme 5-8C**) Moreover, the trace acetone generation in this reaction also excluded the possibility of methyl radicals being the major HAT reagent (see **Chapter 8** for details).

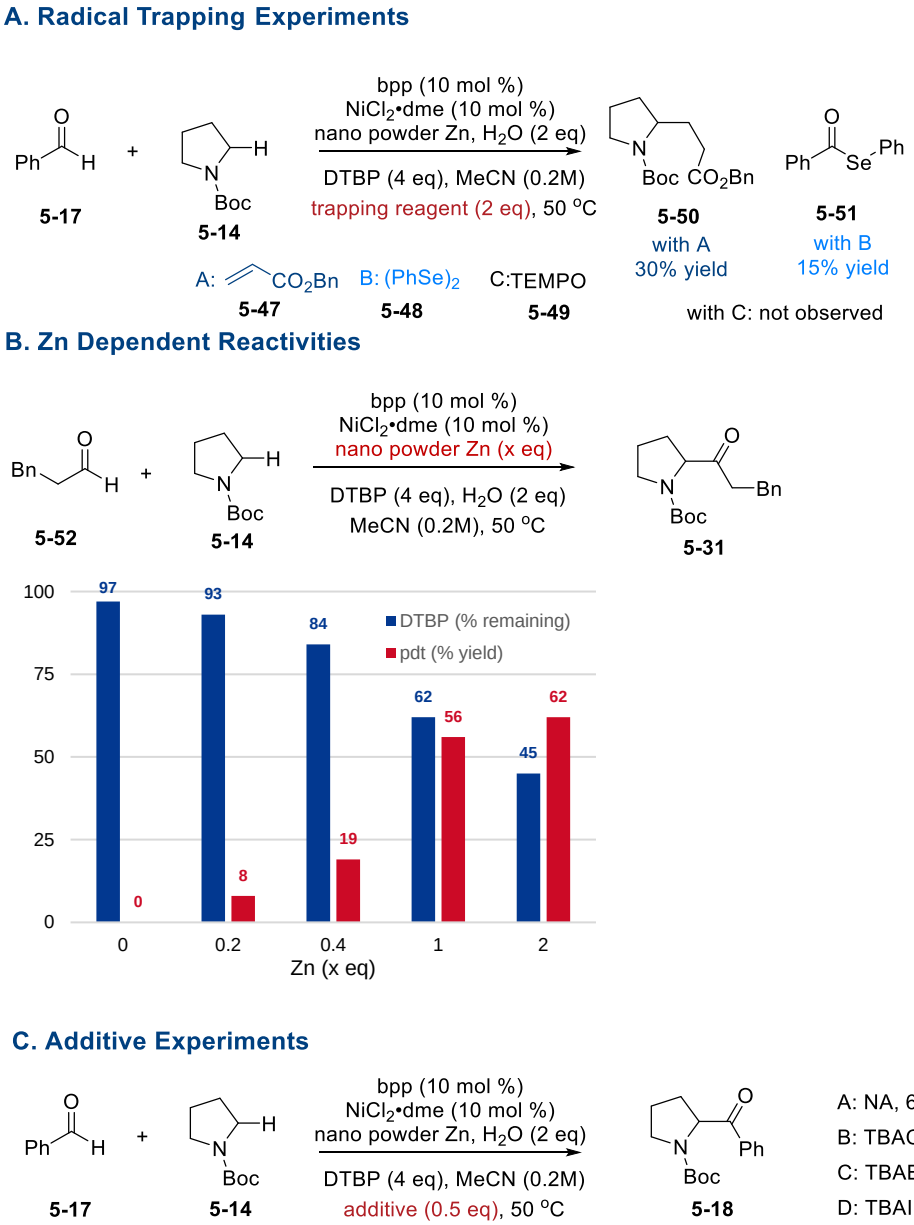

Scheme 5-8 Mechanistic investigations (A&B by Austin Ventura).

With the aforementioned experimental observations in hand, a plausible Ni^{I}/Ni^{III} redox cycle has been proposed as an operative pathway for catalytic conversion (**Scheme 5-9**). Quantum chemical path simulations revealed a feasible pathway to convert the pre-catalyst to the $Ni^{I}(O^{t}Bu)$(bpp) species (**A**), which could be further converted to a thermodynamically stable $Ni^{II}(O^{t}Bu)_2$(bpp) intermediate **B** by decomposing DTBP, generating a *tert*-butoxy radical. A plausible reversed reduction from Zn could potentially circulate the nickel catalyst between I and

II oxidation state, which would help build up concentration of *tert*-butoxy radical. From there, **B** can possibly undergo addition with either acyl radical (**1R**) or α-amino radical (**2R**), that are generated independently from off-cycle HAT processes governed by the accumulated *tert*-butoxy radicals. However, the addition with **1R** was found to be favorable by 13.8 kcal/mol compared to the alternative α-amino radical (**2R**) addition (see supporting information of related publications for details). Such energetic differences gave rise to the high cross selectivity, as the trapping of **B** with **1R** lowers the concentration of acyl radical in solution,[119a, 132] kinetically prohibiting the addition of second equivalent of **1R**. Similar phenomenon has also been observed by MacMillan and co-workers in their radical sorting pathway.[115, 118e] Following the formation of intermediate **C**, Zn based SET occurred to transform the Ni^{III} species to Ni^{II} intermediate **D** that captured the α-amino radical to generate Ni^{III} hetero-adduct (**E**) that underwent reductive elimination to produce the desired cross-coupled product, while regenerating the nickel complex

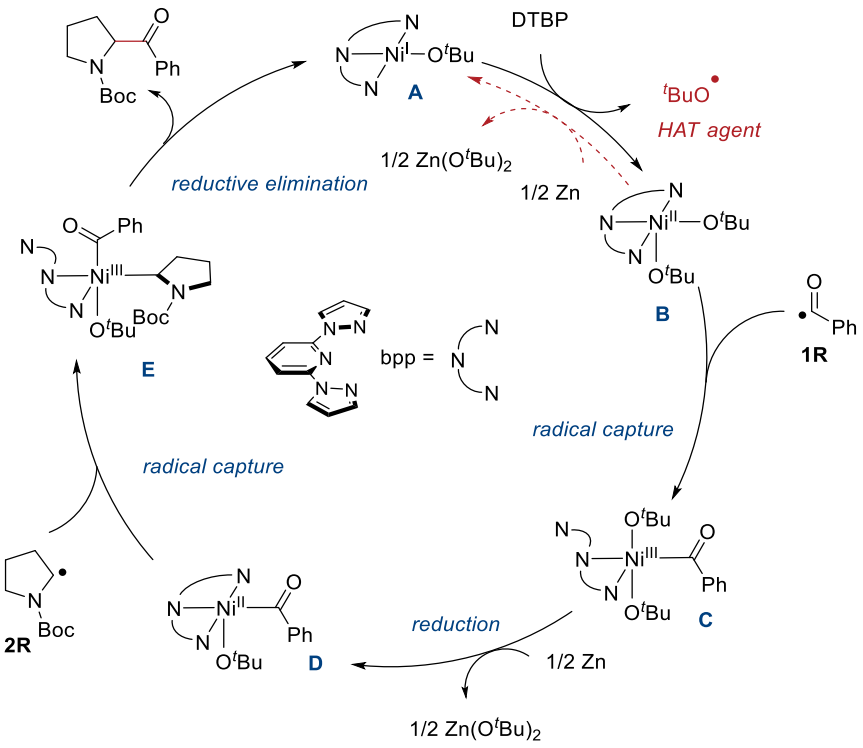

Scheme 5-9 Proposed mechanism.

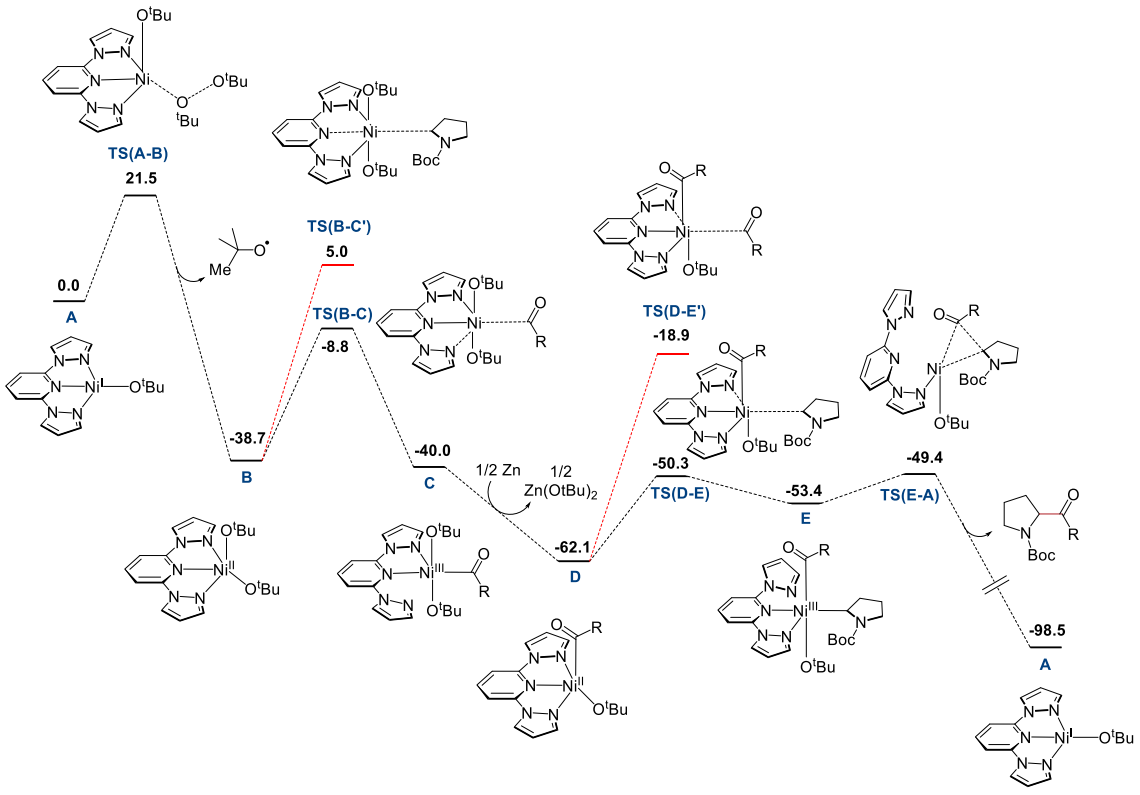

Scheme 5-10 Calculated energy diagram (by Soumik Das).

5.6 Conclusion

In summary, we report a method for nickel-catalyzed N-heterocycle C(sp3)–H functionalization using aldehydes as coupling reagents. We have demonstrated a highly cross selective dehydrogenative coupling with a broad scope of aldehydes and N-heterocycles. A unique combination of peroxide and reductant has been shown to be crucial for reaction success, with mechanistic investigations confirming a radical relay pathway. We hope to offer a convenient strategy for exploring a broader chemical space via late-stage C(sp3)–H acylation, expediating target molecule synthesis without resorting to *de novo* construction.

Chapter 6 Further Developments of Nickel Catalyzed Cross Coupling via Peroxide-Mediated HAT Processes

6.1 Introduction

As stated in **Chapter 5**, we have established the acylation of α-amino C(sp3)–H bonds using aldehydes as coupling reagents under a mild, redox-buffered condition with a broad substrate scope. The successful development of this conceptually novel transformation relies on nickel being a versatile transition metal catalyst for SET processes as well as the unique combination of DTBP and Zn, which *in-situ* generates the HAT agent in a controlled manner. Other than the developed broad substrate scope, the synthetic utility of this developed methodology is worth further highlighting.

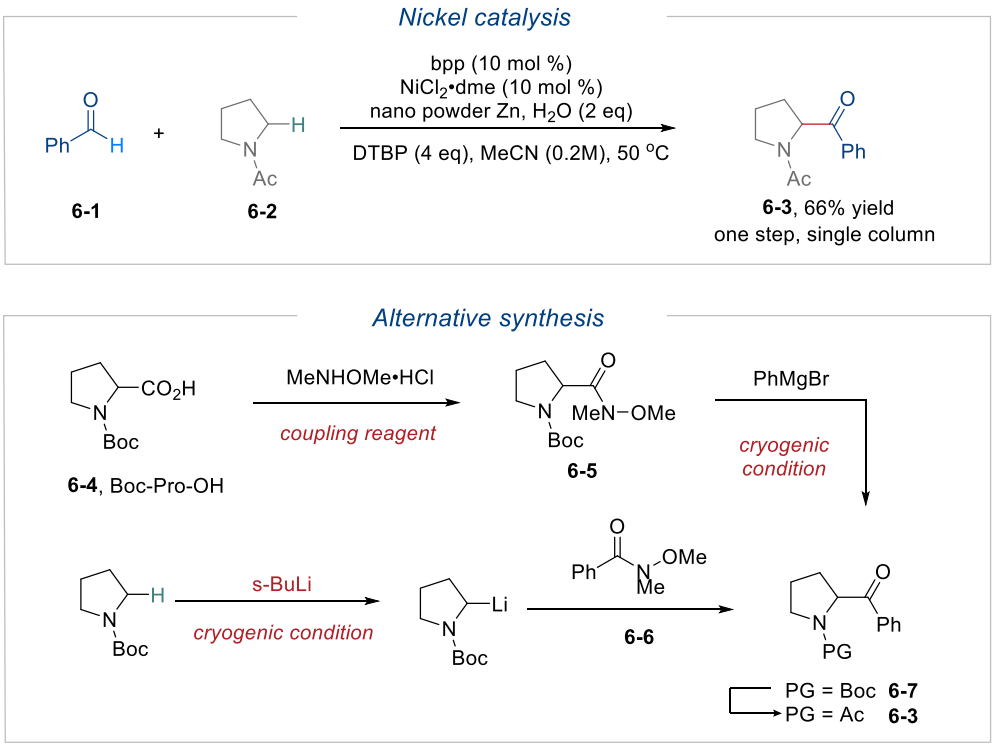

Scheme 6-1 Synthetic advantages

Take the synthesis of **6-3** as an example (*vide supra*), we have previously documented the nickel catalysis within one step, via a single column to obtain the desired coupling product with 66% yield (**Scheme 6-1**). It should also be noted that all reagents used in the transformation meet the requirements of the standard Schlenk technique. In cases where gloveboxes are easily accessible, the complete setup of the reaction at takes less than one hour (including glovebox pump in sequence). On the contrary, despite its simple appearance, accessing **6-3** would require a tedious synthetic route using traditional functional group interconversion strategies. Starting from commercially available Boc-Pro-OH (**6-4**), stoichiometric amount of coupling reagent is required to install the Weinreb amide and the consequent Grignard addition under cryogenic condition needs to be performed with extra care. The resulted phenyl ketone (**6-7**) can also be accessed from Boc-pyrrolidine via α-lithiation followed by coupling with benzamide **6-6**. However, this process is practically challenging due to the use of pyrophoric reagent, *s*-BuLi. On top of aforementioned multi-step synthesis, protecting group manipulation is inevitable as acetyl group (Ac) is labile towards nucleophilic addition. The extra step-counts, plus time and efforts coming with them, contradict the conciseness of nickel catalysis.

Besides the synthetic advancements, there are still unsolved mechanistic questions, that once answered, can be extremely helpful for deepening our understanding of the reaction pathway. This chapter will be focused on digging further into this redox-buffered nickel catalysis via experimental and computational investigations to better aid new catalysis developments.

6.2 In-Situ Oxidative Coupling Between Alcohols and Amines

In the early stages of the reaction development, the detailed mechanism for product formation was unclear. It was once thought that an electrophilic pyrrolidine bound Ni(III) species

(**III**) underwent a migratory insertion pathway generating intermediate **IV**. β-H elimination was followed by reductive elimination, releasing the desired acylated product, *tert*-butanol as by product, while regenerating the catalyst (**Scheme 6-2**).

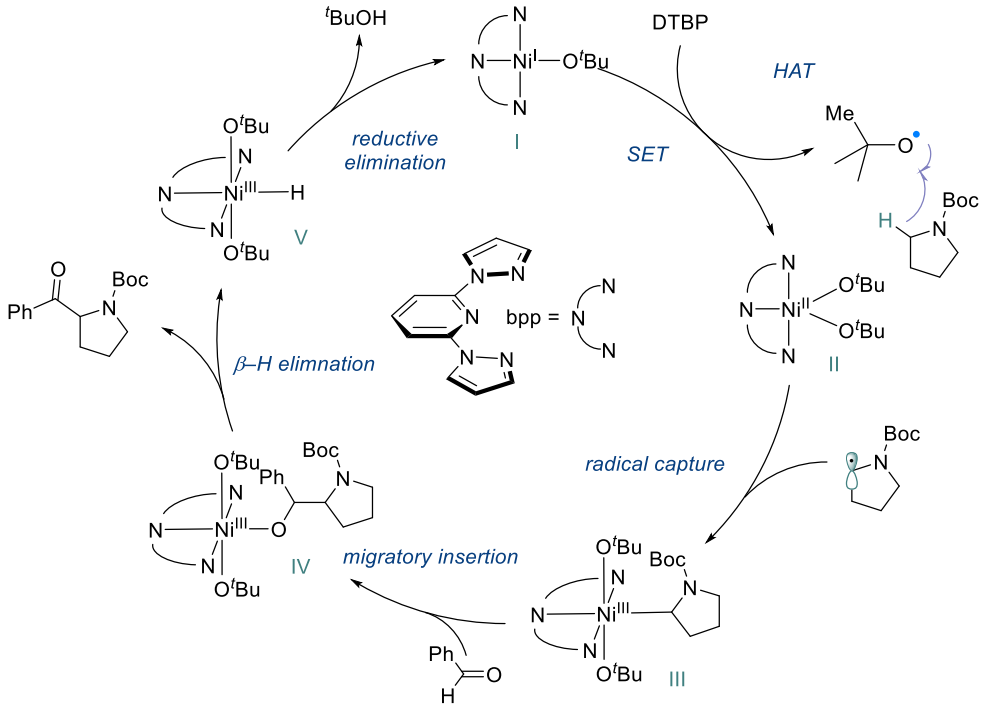

Scheme 6-2 Originally proposed mechanism

It was then hypothesized that Zn served as a redox buffer, preventing the accumulation of $Ni^{III}(O^tBu)_3$ (**III-1**) which could otherwise be a dead end for the nickel catalyst due to the prohibitive O–O bond reductive elimination (**Scheme 6-3**). The controlled regeneration of low-valent, active nickel species was first reported by Stahl and co-workers in their copper catalyzed C–H functionalization manifolds.[36]

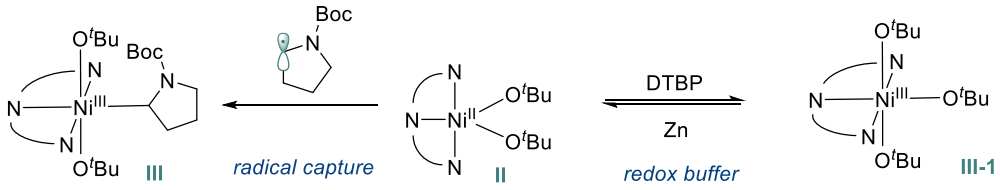

Scheme 6-3 Zn as a redox buffer

It now has become clear that the further oxidation of Ni^{II} turns out to be thermodynamically less feasible compared to radical capture with acyl radicals based on DFT calculations (see **chapter 5** for details). But we were eager to explore the viability of such a redox-buffer pathway experimentally during the initial reaction development period.

In 2019, the Weix group reported a reductive cross electrophile coupling between aldehydes and aryl bromides.[133] A similar migratory insertion step was proposed, followed by a Zn intercepted reduction led to the formation of hindered diarylmethanol (**Scheme 6-4**, top).

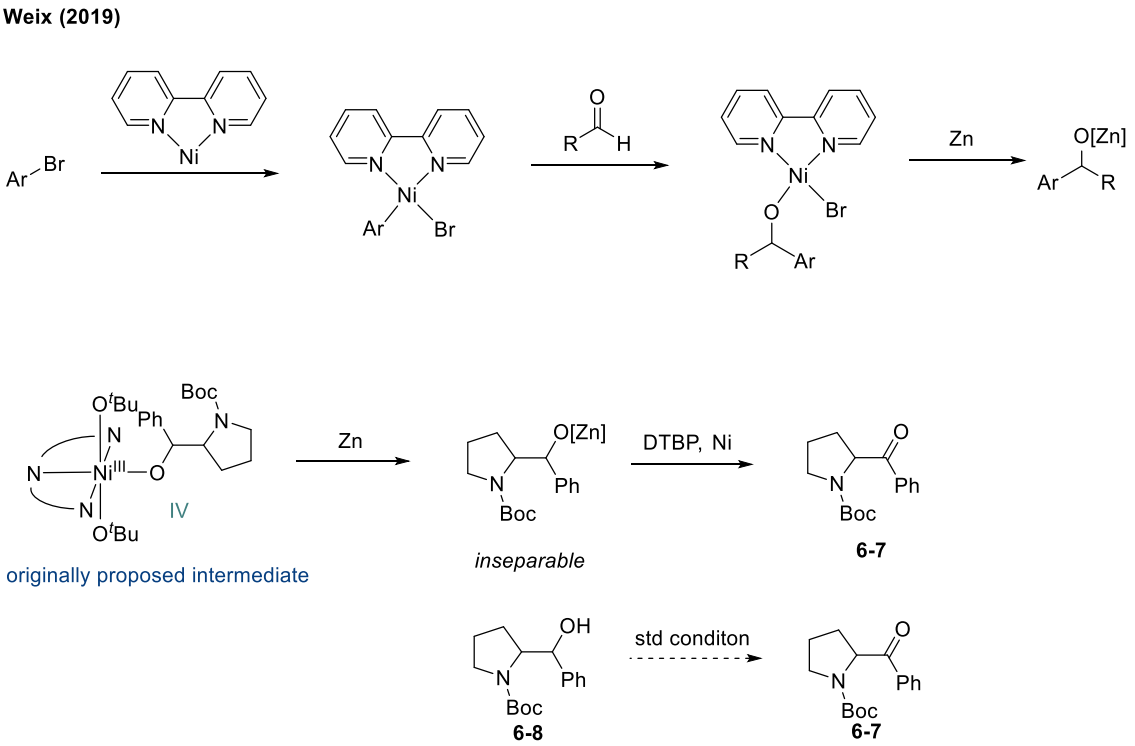

Scheme 6-4 Possible intermediacy of nickel alkoxide

If the reaction followed the original proposed pathway, reduction from intermediate **IV** could similarly take place, resulting in the reduced form of the C–C coupling product (**6-8**). Though we were not able to observe such alcohol formation, this fact could not exclude the possibility that the reaction condition was oxidizing enough to efficiently convert the alcohol (**6-8**) to the ketone product (**6-7**). In order to probe this hypothesis, alcohol **6-8** was independently

synthesized (**Scheme 6-5**). As depicted in **Section 6.1**, accessing α-amino ketone **6-7** was rather tedious: CDI promoted amide coupling was followed by phenylation using Grignard reagent. Reduction using sodium borohydride led to the formation of desired alcohol **6-8** with a 40% isolated yield.

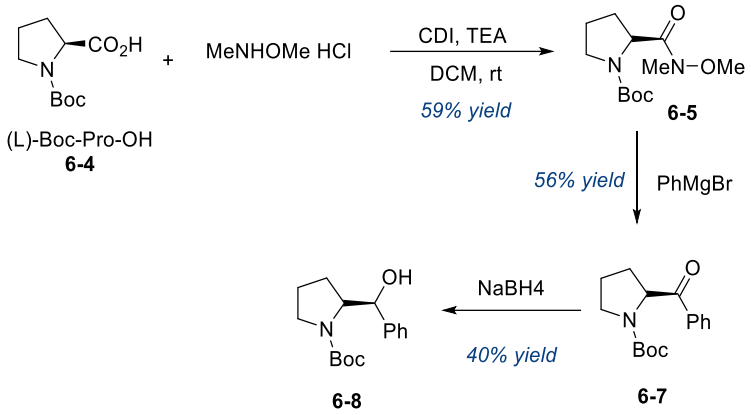

Scheme 6-5 Independent synthesis of alcohol 6-8

With the potential alcohol intermediate in hand, it was subsequently subjected to the standard reaction condition. Aside from 63% unreacted **6-8**, ketone **6-7** was observed in 36% yield based on crude NMR analysis, indicating the oxidation capability of the nickel DTBP combination at 50 °C.

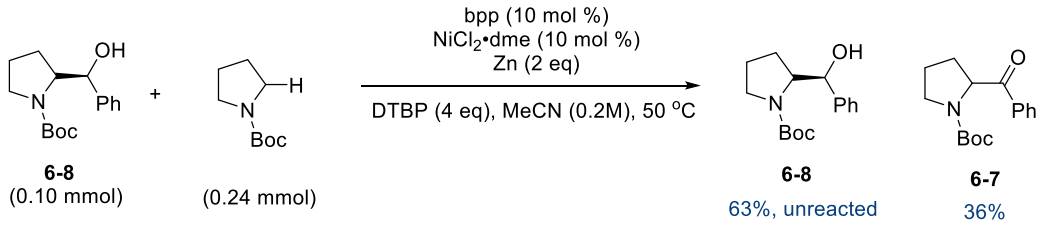

Scheme 6-6 Resubjecting alcohol intermediate

Although DFT calculation has later confirmed that the mechanism adopts a HAT pathway for aldehyde C–H activation, we are still inspired by the versatilities of alcohol oxidation under the standard reaction condition. If a primary alcohol can be used as the aldehyde precursor via *in-situ* oxidation, successive cross coupling with different protected amines can incur an even wider

substrate scope. The proposed transformation is conceptually novel as argued by Cernak and co-workers, complex molecules with distinct property profiles can be discovered within the nickel catalysis regime, depending on combination of starting material matrix, bond connection, and reaction condition.[134] Amines and alcohols are both common organic feedstock but have been rarely explored in the cross nucleophile C–C coupling setting.[135] Practically, aldehydes are often synthesized by alcohol oxidation and suffer from decomposition to carboxylic acids in air.[136] In this regard, alcohols represent widely accessible building blocks as well as a more stable precursor to aldehydes, saving efforts of fresh distillation before every single use.

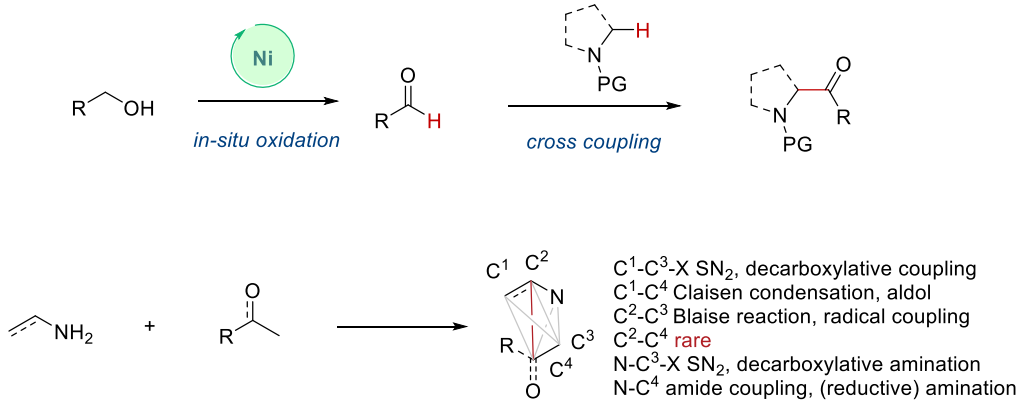

Scheme 6-7 Coupling map between amines and alcohols.

With the outset of developing the tandem oxidative coupling between amine and alcohol, control experiments were first performed to evaluate the necessity of each reaction component. It was intriguing to find that by omitting Boc-pyrrolidine (**6-10**) from the reaction, the desired oxidation was not observed (**Scheme 6-8**, top). Although the role of pyrrolidine in benzyl alcohol oxidation is unclear, previously developed C–H functionalization condition led to desired oxidative coupling product (**6-7**) in 31% yield.

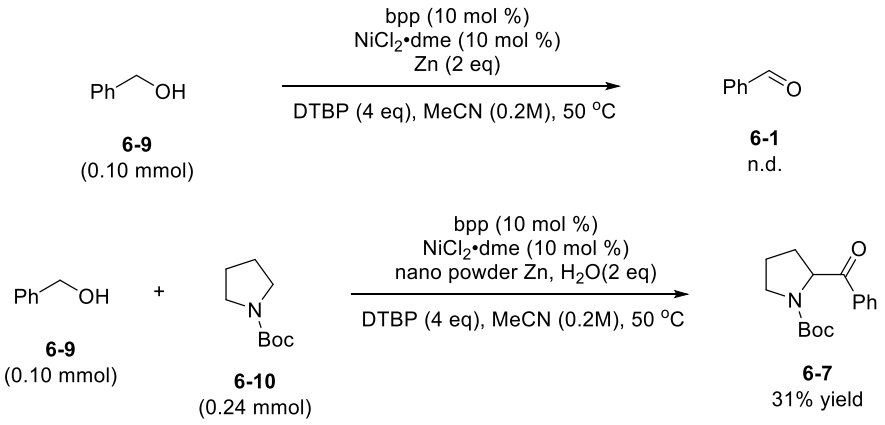

Scheme 6-8 Initial condition screening

Encouraged by this success, we next turned our attention to condition optimization by ligand, additive and stoichiometry screenings (**Table 6-1**). Recently, Newman and co-workers reported an intermolecular coupling of primary alcohols with aryl triflates via nickel catalysis. The authors successfully detected the intermediacy of aldehydes, which were responsible for the carbonyl Heck C–C bond formation.[137] Inspired by the two electron oxidation with phosphine ligand, we attempted a dual ligand scaffold for consecutive promoting alcohol oxidation and aldehyde coupling. However, this strategy did not work out as we hoped: the use of a phosphine ligand (dppf) and bpp unfortunately failed to yield the desired coupling product (**Entry 2**). We further explored this dual ligand manifold with bpy and BiOx, both of which produced inferior results (**Entries 3-4**). Copper catalyst has been shown to efficiently decomposing peroxides to oxygen centered radicals and have thus been tested as an additive, though neglectable improvements were observed (**Entries 5-6**).[124, 138] In the preliminary exploration, we overlooked that copper co-catalyst would compete with nickel for ligand binding, and thus these reactions may offer better results when suitable ligands are fed in sufficient amounts. Thus, a revisit of these reactions has been scheduled. Meanwhile, raising the temperature as well as changing Zn equivalents seem not to play a major role in the reaction result (**Entries 7-10**). Lastly, the

stoichiometry of DTBP was proved vital, as lowering it from 4 to 2 eq led to a significant yield drop (**Entry 11**). Increasing DTBP to 6 eq, on the other hand, did not seem to benefit the reaction outcome (**Entry 12**). Recently, Stahl and co-workers reported a *N*-hydroxyphthalimide (NHPI) mediated benzylic C–H oxidation via HAT and SET.[139] However, when NHPI was used as an additive, no reaction was observed (**Entry 13**). We attributed the failure of the desired C–C coupling to DTBP incapable of converting NHPI to its reactive form: phthalimide-*N*-oxyl (PINO) radical but NHPI instead triggered some deleterious pathway. If that was the case, electro-chemistry promoted nickel catalyzed dehydrogenative coupling could be utilized and NHPI would replace DTBP as a catalytic HAT agent. Further research exploration with collaboration opportunities would greatly benefit this development process.

Table 6-1 Condition optimization

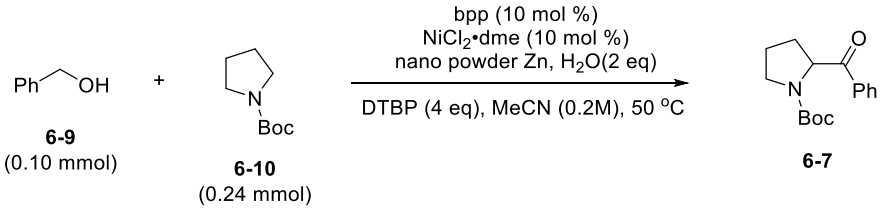

Entry	Deviation	% yield
1	NA	31
2	With 10% dppf	<5
3	With 10% bpy	17
4	With 10% BiOx	<5
5	With 10% CuBr	27
6	With 10% $Cu(MeCN)_4PF_6$	29
7	At 65 °C	30
8	At 80 °C	26
9	1 eq Zn	23
10	4 eq Zn	25

11	2 eq DTBP	17
12	6 eq DTBP	32
13	With 0.5 eq NHPI	n.r.

6.3 Carbon Centered Radical Interception with Michael Acceptors

As discussed in **Chapter 5**, a series of radical trapping experiments were carried out to probe the proposed nickel catalyzed radical-radical cross coupling pathway (*vide infra*). Benzyl acrylate was selected as an electron deficient alkene for the Giese reaction,[130] wherein the α-amino radical addition product (**6-11**) was isolated in 30% yield (**Scheme 6-9**). Swapping the radical scavenger to diphenyl diselenide, which has been used as a trapping agent for acyl radicals,[131] afforded the acyl-selenide product (**6-12**) in 15% yield based on GCMS analysis. Though these experiments served as direct evidence that both carbon-centered radicals were involved in the transformation, it was still intriguing to point out the unique trapping selectivity between acyl and pyrrolidine radicals. It also needs to be highlighted that when either trapping agent was used, the dehydrogenative coupling product **6-7** was not observed. The use of TEMPO as an additive completely inhibits the reaction, which has also been observed in other nickel catalysis.[140]

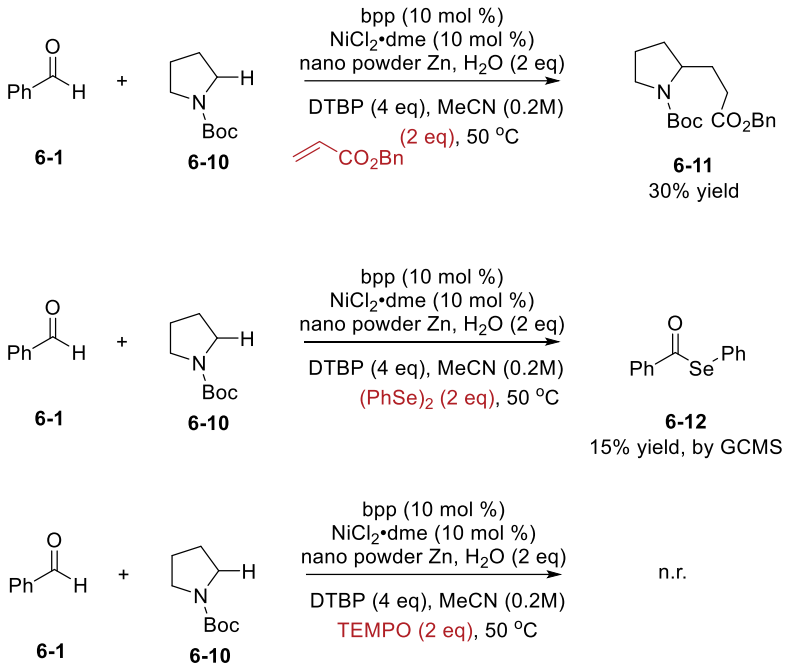

Scheme 6-9 Radical trapping experiments

Taking a step back to summarize previously discovered pyrrolidine C–H functionalization, numerous methodologies have been developed to installation of a C(sp2) functionality of *N*-heterocycles, though carboxylation and esterification remain challenging (**Scheme 6-10**).[141] Moreover, the construction of a saturated carbon linker has been rarely exploited in the transition metal catalysis setting, partly due to the challenging C(sp3)–C(sp3) reductive elimination.[142] With the success of nickel catalyzed C(sp3)–H acylation, we aim at achieving exhaustive access to all degrees of oxidation products by choosing different coupling partners. This section will be describing our efforts to install the least oxidized carbon side chain using Michael acceptor as the coupling reagent.

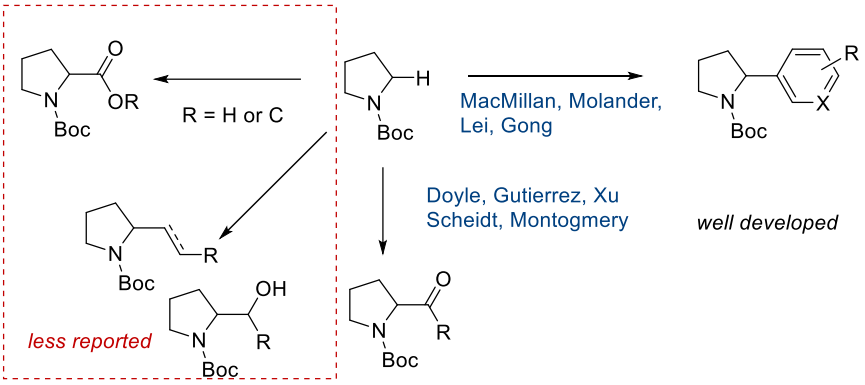

Scheme 6-10 α-C–H functionalization of pyrrolidine, a wide chemical space

Seminal contribution in this area was made by the Nicewicz group in 2018, when they reported the C–H alkylation of carbamate-protected secondary amines using an organic acridinium photocatalyst (**Scheme 6-11**).[143] Once irritated with 455 nm LEDs, this highly oxidizing photocatalyst leads to the formation of amine radical cation, which upon deprotonation, resulting in an open-shell carbon centered radical. A variety of Michael acceptors have been applied to elaborate α-functionalization products under mild condition.

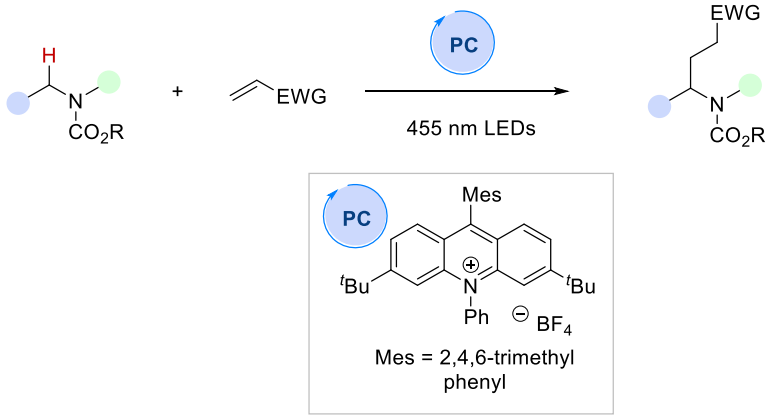

Scheme 6-11 Organophotoredox C–H alkylation with Michael acceptors

We believe the development of an operational simple nickel catalysis leveraging DTBP as a HAT agent under thermal condition would become a complementary strategy to the reported organophotoredox catalysis (**Scheme 6-12**). With this in mind, we began the reaction optimization by analyzing the radical trapping experiment. Other than 30% desired trapping product **6-11**,

unreacted starting materials (**6-10 & 6-1**) were observed based on crude NMR. However, the reminder mass balance of benzyl acrylate was mainly the polymerization byproduct. It was not surprising that DTBP, a commonly used radical initiator promoted acrylate polymerization.[144] Unfortunately, the presence of polymer byproducts complicated the crude NMR, making it impossible to calculate the reaction yield based on quantitative proton analysis. In the meantime, similar R_f of the product (**6-11**) and bpp on the TLC plate rendered a clean separation challenging. These all call for a better choice of substrate for the model system before commencing condition optimization. Before switching to a more polar Michael acceptor, efforts were made to simplify the reaction condition, starting with figuring out whether aldehyde **6-1** was necessary for the successful generation of pyrrolidine coupling product. It was to our surprise that, when conducting the trapping experiment under otherwise identical conditions without benzaldehyde, the desired alkylated pyrrolidine **6-11** was not obtained. Though similar observations were made in **Section 6.2**, that by omitting pyrrolidine, oxidation of benzyl alcohol was not feasible (**Scheme 6-8**), it is still unclear why a seemingly irrelevant component has such drastic effects on the reactivity. Given the limitation of preliminary reaction development, efforts to further dig into mechanistic investigation will be discussed in the next **Section 6.4**.

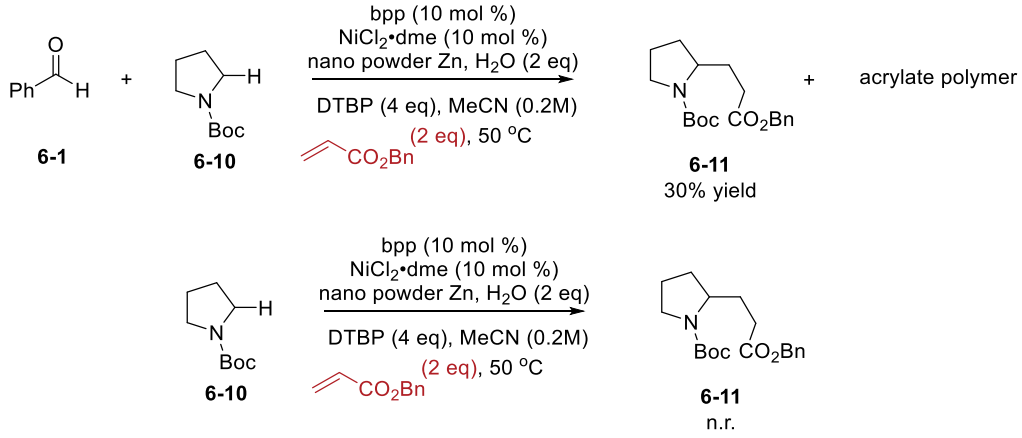

Scheme 6-12 Reactivities with Michael acceptors

Moving forward, we would like to explore different Michael acceptors with the hope of figuring out one that simplifies the reactivity analysis process, which would have a huge benefit when it comes to condition optimization. Different vinyl ketones, acrylates and acrylamides are possible candidates for this coupling reaction. We anticipate that the fluorine tag will enable crude F NMR analysis while not significantly affecting the reactivity (**Scheme 6-13**).

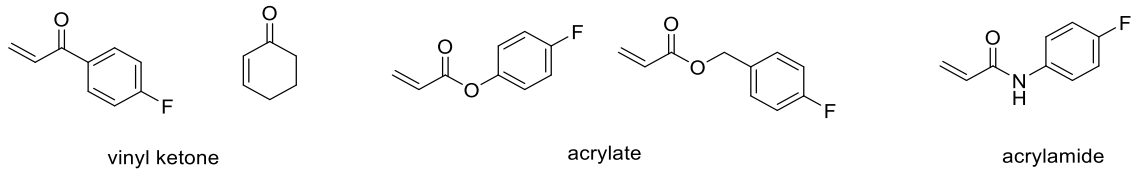

Scheme 6-13 Michael acceptors screening

In terms of condition optimization, there are several aspects we would like to especially focus on. First, though the role that aldehyde plays in the transformation is unknown, it can be treated as an additive. Thus, the screening of different aldehydes, or substrates which have similar BDEs would be helpful for verifying whether the reactivity is unique to this substrate combination, and this would in turn help elucidating how aldehyde is involved in the cross coupling between pyrrolidine and acrylate. Secondly, as the previous optimal condition was developed for the aldehyde coupling, it would not be surprising to discover a better ligand combination that promotes the acrylate coupling. In fact, a careful tune of parameters such as temperature and concentration can also be crucial for forming C–H alkylation product (**6-11**) and suppressing polymerization byproducts. A clean reaction profile will be beneficial in reaction efficiency and future substrate scope exploration.

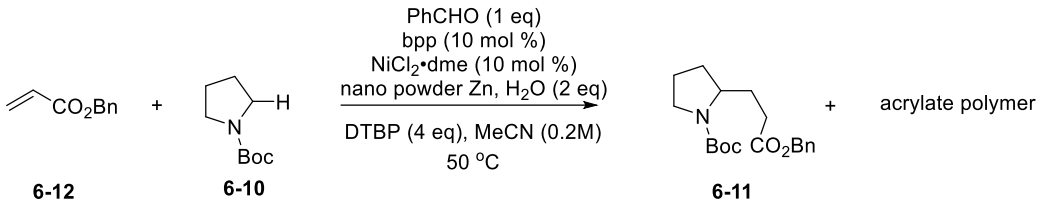

Scheme 6-14 Revisiting condition optimization

6.4 Entrances, Traps, and Rate-Controlling Factors in Nickel Catalyzed Dehydrogenative Coupling

In order to gain further mechanistic insights, we would like to understand the nickel catalyzed C–H functionalization from both macro and micro perspectives. The efforts to deconvolute reaction pathway should cover both the reaction progress, referred to as macro, as well as micro, detailed fundamental organometallic steps. These investigations in the long run would complement each other, in best case scenarios, the stoichiometric synthesis of an off-cycle intermediate would account for the stalled reactivity, or the identification of the reaction initiation period may suggest a propagation of reactive intermediates.

Our macro mechanistic studies start with the reaction progress kinetic analysis (RPKA). RPKA employs *in-situ* measurements of complex catalytic reaction behavior to obtain a comprehensive reaction picture.[63, 145] It is usually conducted under conditions that are similar to the developed transformation and thus most resembles the real reaction. Practically, minimal numbers of experiments are required to establish a reliable correlation, thus allowing deeper understanding of a specific reaction pathway in limited amount of time, especially helpful during the preliminary discovery stage. We choose to monitor the reaction progress using GCMS analysis based on several reasons: a) each reaction component (other than Zn) shows up with a distinct signal on the GC trace, allowing for tracking; b) calibration curves are easily established, with high

accuracy based on instrument's auto integration feature, reducing human errors; c) high response factors for most monitored substances lower the error margin; d) insignificant byproduct formation was observed during most reactions and a rough correlation between starting material consumption and product formation can be established.

The first monitored reaction progression was the kinetic isotope effect (KIE) study. The deuterated benzaldehyde suffers from challenging isolation due to its relatively low boiling point and is also prone to oxidation. Thus, we synthesized deuterated *para*-methyoxybenzaldehyde by quenching lithiated *para*-methoxybromobenzene with DMF-d_7, and the resulted **6-13-d** is more stable in air and can be easily purified by column. Take the reaction monitoring with *para*-methyoxybenzaldehyde (**6-13**) as an example: small amounts of aliquot were sent to GCMS at 20-minute intervals to determine the starting material consumption. Shown in **Scheme 6-15** is a typical GCMS trace at 0 time point.

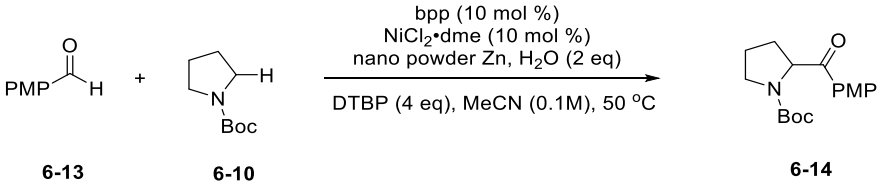

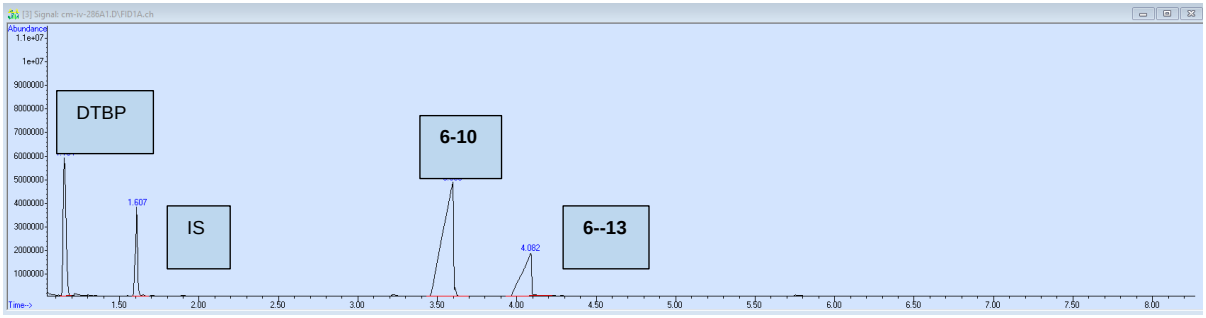

Scheme 6-15 Reaction progress via GCMS analysis. IS abbreviates for internal standard (tridecane).

The parallel KIE experiments were repeated in duplicate to minimize systematic error and the conversion of starting material was plotted at early time point (~10% conversion). The KIE was calculated to be 1.7 by extracting the slope of the reaction progress graph (**Scheme 6-16**).

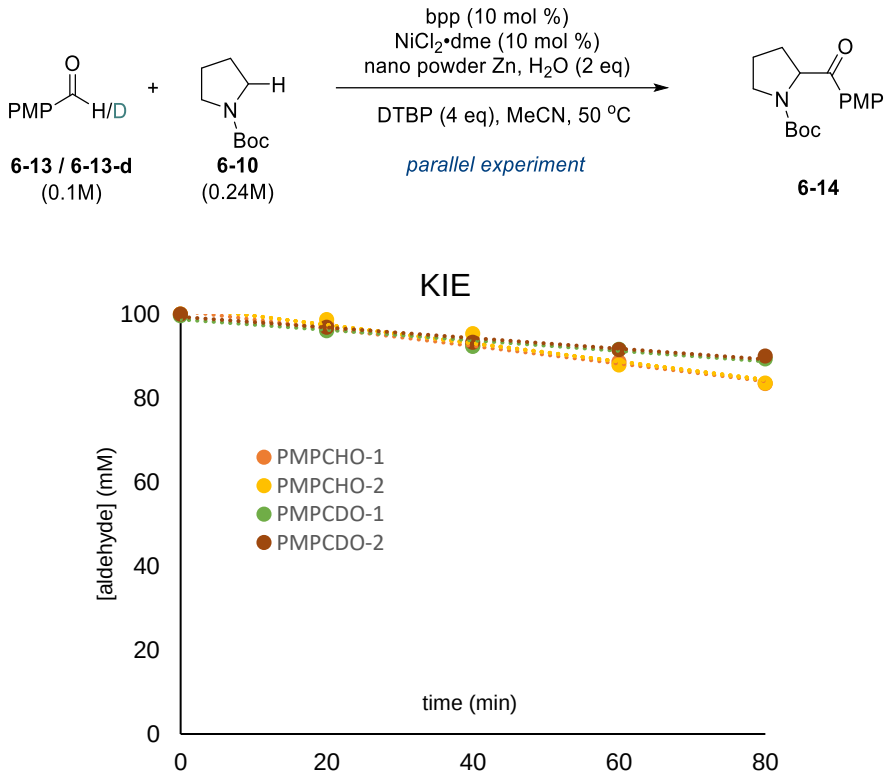

Scheme 6-16 Parallel KIE experiments

On the other hand, this dehydrogenative scaffold poses challenges for obtaining the competing KIE. As one would expect, **6-13** and **6-13-d** have identical GC retention time and yield the same product **6-14**, due to the functionalization of acyl C–H bond. Efforts to deconvolute the ratio of **6-13** and **6-13-d** in unknown mixture based on m/z abundance are far from trivial, different factors have to be considered including which pair of signals to monitor, sample concentration etc. To overcome this problem, and possibly shine light on the commonly encountered KIE challenge in studying dehydrogenative coupling, we came up with a new NMR strategy for product analysis. In this case, deuterated *para*-methyoxybenzaldehyde (**6-13-d**) and *para*-ethoxybenzaldehyde (**6-15**) are used as competing starting materials which are believed to have similar reactivity towards the nickel catalysis (**Scheme 6-17**). The deutero-substrate is marked with the 4-methoxy while the proteo-aldehyde can be identified through its 4-ethoxy signal. The reaction was let run for 40 minutes (based on RPKA in the parallel system, around 10% conversion) before quenching. Crude

NMR analysis was followed by careful column isolation, in this case one can both isolate the starting materials and the products. We focus on product **6-14** and **6-16** for good reasons: first, R_f of this mixture outlies the other component (aldehydes, bpp, and unreacted **6-10**); second, if rate needs to be calculated based on starting material consumption, complete recovery of both aldehyde is required to enable accurate analysis for KIE {([**6-13-d**]$_0$-[**6-13-d**])/([**6-15**]$_0$-[**6-15**])}. On the contrary, KIE can also be calculated by the product distribution ([**6-16**]/[**6-14**]) and systematic errors (column separation, loss during transfer, NMR analysis etc.), if any, impact both products and would not affect the overall ratio. Lastly, it is believed that as long as detecting error (e.g. NMR baseline noise) can be minimized, calculation from product generation is more accurate than starting material consumption. As highlighted in the spectrum snapshot of the isolated **6-16**, **6-14** mixture, methylene CH_2 from the ethoxy group and methyl CH_3 from the methoxy group have been identified to account for their respective ratio against CH_2Br_2 internal standard and the competing KIE is determined to be 3.3 [(0.26*3)/(0.12*2)] (**Scheme 6-17**, bottom).

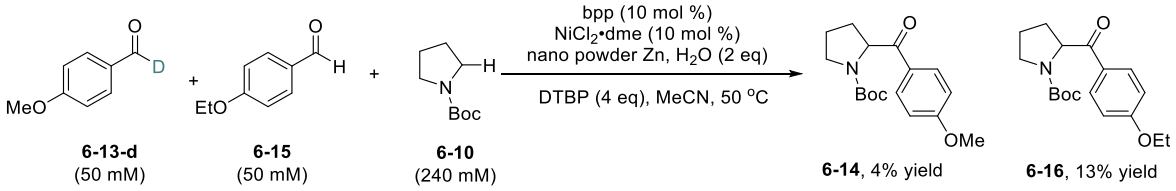

Scheme 6-17 Competing KIE experiment. The complicated signals are due to rotamer presences.

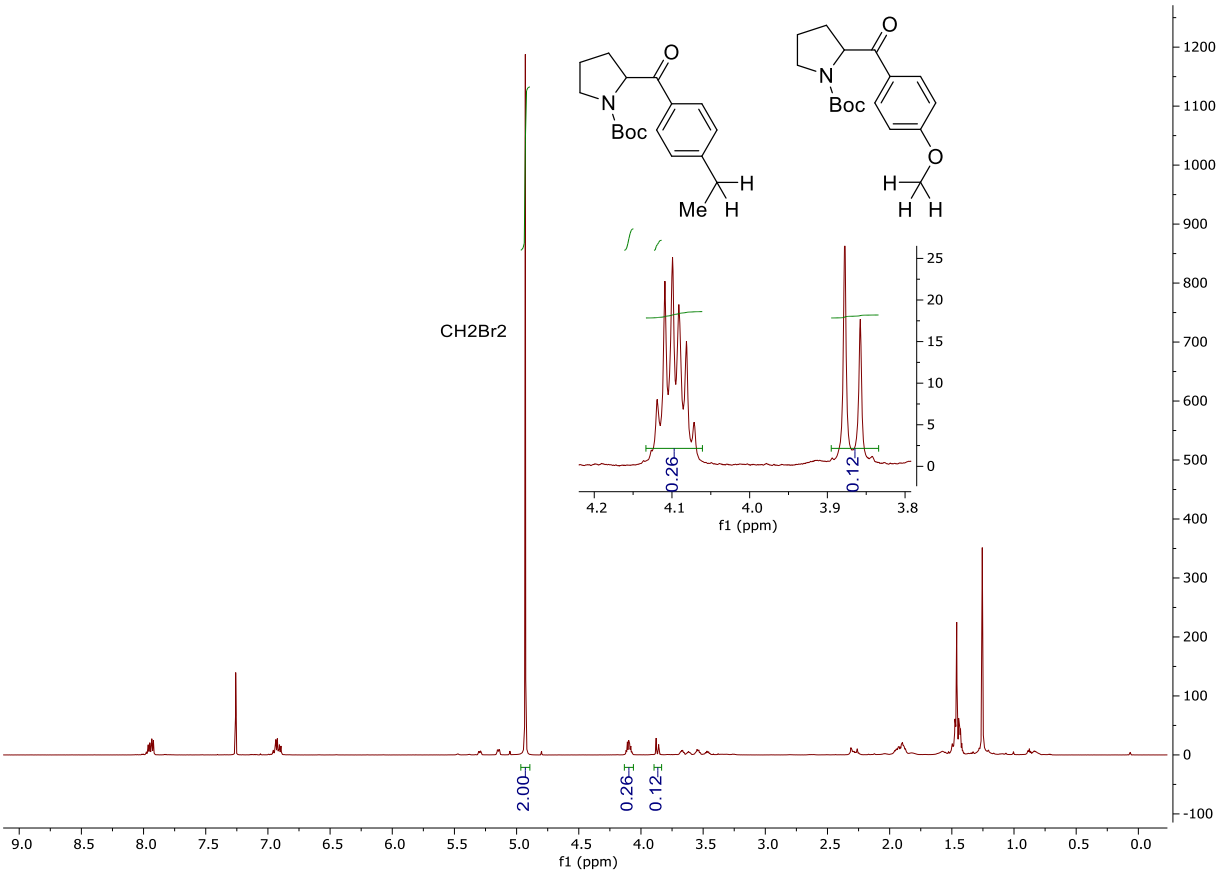

To further solidify the NMR competing KIE experiment and provide future guidance for similar circumstances in follow-up investigations, we will conduct control experiments to verify the rate difference does not originate in the starting material preferences (methoxy vs ethoxy). Running a competing experiment between proteo-substrates (**6-13** and **6-15**) following the same procedure would be helpful to determine an innate product distribution between **6-14** and **6-16**, as a correlation factor for previously disclosed competing KIE.

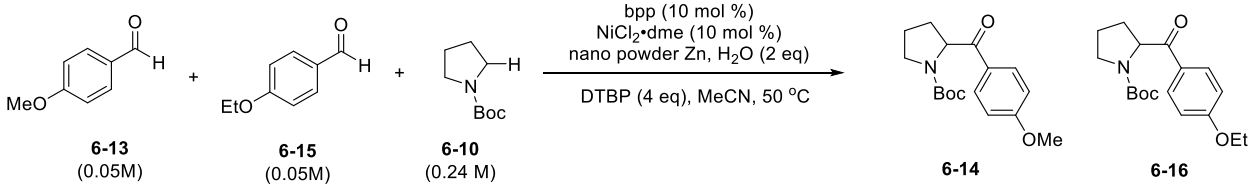

6-13 (0.05M) + **6-15** (0.05M) + **6-10** (0.24 M) → **6-14** + **6-16**

Scheme 6-18 Competing experiments between proteo-substrates.

Both GCMS and NMR analysis have been developed as powerful tools for RPKA analysis of the nickel catalyzed C–H functionalization. To better understand the kinetic properties of this transformation, we expect to conduct 'different excess' experiments to determine the rate order of each component;[63] 'same excess' experiments[145] to determine whether catalyst deactivation or product inhibition is relevant in the reaction process. Although the kinetic profile for 'same excess' experiment was not yet obtained, an end point experiment was conducted, and a similar yield was obtained (**Scheme 6-19**). This observation partially excludes the equilibrium hypothesis being responsible for the stalled reactivity.

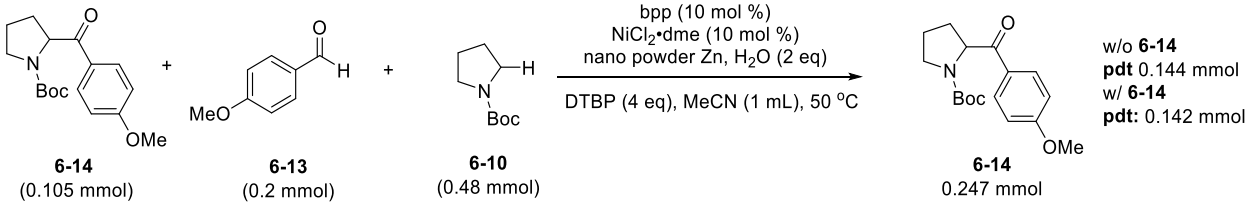

Scheme 6-19 Product inhibition experiment

Other than kinetic experiments, efforts have been made to understand the fundamental steps involved in the catalytic cycle from a micro perspective. Previous DFT calculations have identified a thermodynamically stable (bpp)$Ni^{II}(O^tBu)_2$ intermediate, which can possibly be synthesized and isolated independently. Recently, Sevov and co-workers reported an electroreductive C(sp3)–C(sp2) coupling by controlling nickel redox states via dynamic ligand exchange (**Scheme 6-20**, top).[146] This seminal work documented an identical Ni-bpp scaffold promoting C(sp3)–C(sp2) cross coupling which is aspiring to what we are trying to explore. Moreover, the authors disclosed the synthesis of the catalytically relevant (bpp)$NiBr_2$ species (**Scheme 6-20**, bottom) which sets the starting point for our organometallic exploration.

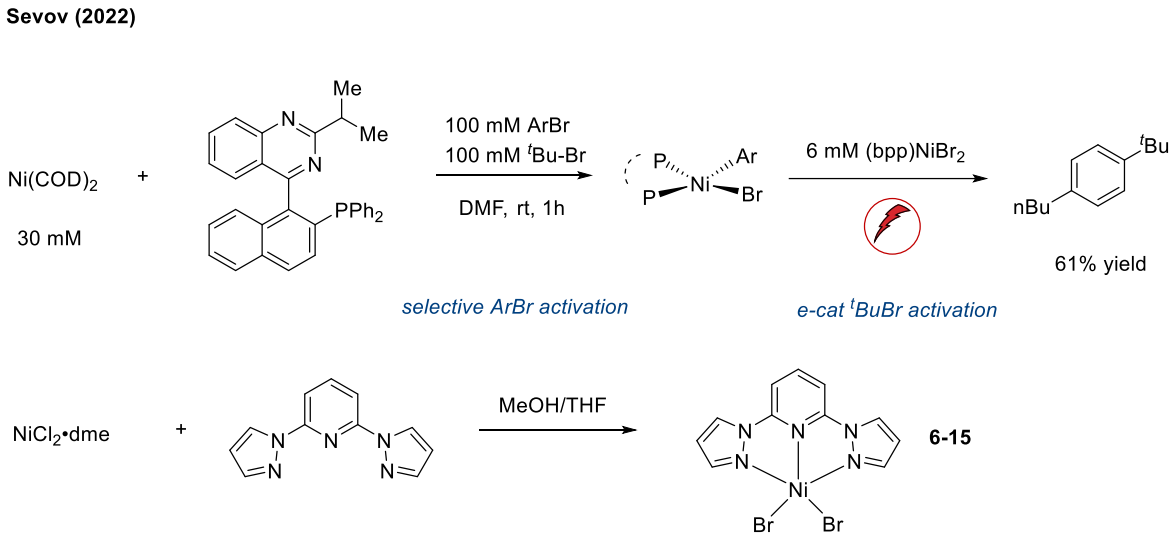

Scheme 6-20 Electroreductive C–C coupling and nickel catalyst synthesis.

Following the known procedure, the complex **6-15** was successfully isolated via bench synthesis as a green solid. Though we were not able to perform NMR analysis on this paramagnetic compound (also noted by Sevov *et al.*), it successfully replaces the nickel pre-catalyst leading to the desired C–C coupling product with 53% yield (**Scheme 6-21**).

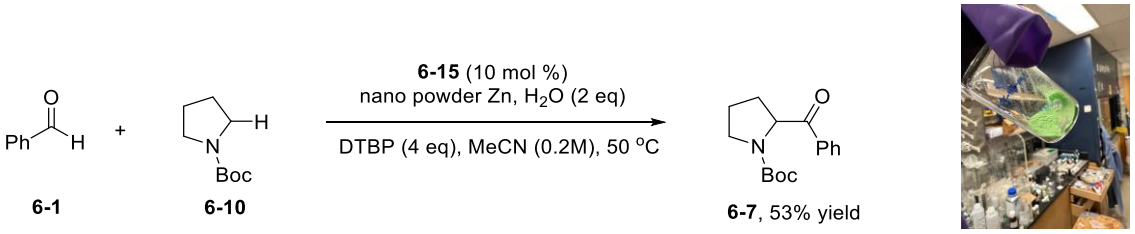

Scheme 6-21 Complex **6-15** (right) as pre-catalyst

Next, we turned our attention to the synthesis of (bpp)$Ni^{II}(O^tBu)_2$. Initial attempts for anionic ligand exchange with KO^tBu resulted in a yellow slurry and efforts for isolating nickel complexes from this mixture ended in vain. Fortunately, we were able to derive the intermediate from the standard catalytic condition by treating **6-15** with DTBP in the presence of reductant. An instant color change was observed once suspending the (bpp)$Ni^{II}Br_2$ in MeCN with Zn. It should also be noted that $NiBr_2$ pre-catalysts are insoluble in MeCN (**Scheme 6-22**, bottom) and Zn may

be beneficial for the solubilization by promoting the reduction to a low-valent nickel species (purple). After initial stirring for about 1 minute, DTBP was added dropwisely, and the solution turned colorless after the precipitate was allowed to settle down. Though these observations are not conclusive, the colorless solution matches our expectation for metal *tert*-butoxides, and sequential work up in the glovebox after overnight (16h) stirring at room temperature led to a pale green solid after isolation. The suspected (bpp)$Ni^{II}(O^tBu)_2$ is paramagnetic and was proven catalytically relevant by resubjecting it to the catalysis shown in **Scheme 6-21**. A similar 50% yield was obtained. Future endeavors will be focusing on fully characterizing structure **6-16** and exploring it in catalysis.

Scheme 6-22 Synthesis of (bpp)$Ni^{II}(OtBu)_2$.

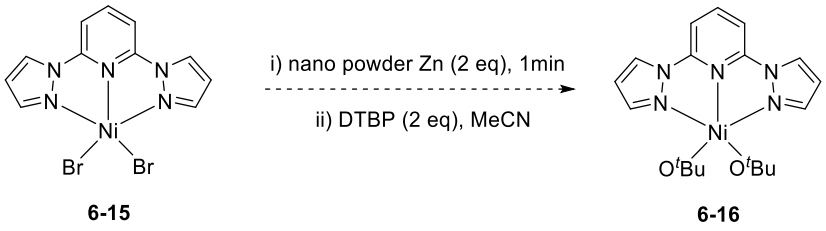

6-15 **6-16**

Middle left: addition of MeCN, middle center: addition of DTBP, middle right: isolated nickel complex. Bottom ligand from left to right: phen, dtbbpy, bpp, bpy, tpy.

With possible opportunities for collaboration inside and outside the department of chemistry here at Michigan, we would like to develop reliable synthesis and characterization of relevant nickel complexes and monitor their redox potential. Understanding the redox events for theses isolable nickel intermediates via organometallic synthesis would be extremely helpful for optimizing our nickel catalysis development, figuring out catalyst resting states as well as those energetic demanding steps in the catalytic cycle. Though seminal contributions have been made by Sanford,[118d, 147] Diao,[148] Weix[149] and others[111, 150] in understanding the behavior of open-shell nickel species, the field is still haunted by unanswered questions, especially under this unique redox-buffered manifold. We hope to leverage this nickel catalysis as a platform to elucidate the entrances, traps, and rate-controlling factors in nickel catalyzed C–C coupling, especially those involving SET and heterogeneous redox event. We expect the mechanistic investigation approach described here can serve as guidance for exploring similar catalysis scaffold, and the knowledge acquired in this process has great promise in directing future reaction design.

Chapter 7 Conclusion

As described by Nobel laureate David Macmillan in his lecture, catalysis is a process that 'makes existing reactions easier, faster and allows new chemical reactions to happen'. The coupling between easily accessible building blocks to forage new C–C bonds via nickel catalysis represents an attractive field in synthetic organic chemistry due to the versatilities of different C–H functionalization scaffolds. Contrary to myriad of reported methodologies, efforts towards understanding the reaction mechanism are unfortunately falling behind, partially owing to the perplexing nature of nickel mediated C–H activation pathway.

As described in this dissertation, research developments are based on mechanistic investigations and further experiments are designed to verify the theoretical hypothesis. These insights, on the other hand, have in turn fueled additional reaction discoveries and have been applied to delineate synthetic applications. In this vein, the first report of intermolecular enantioselective C–H functionalization has been described based on a conceptually novel LLHT mechanism. Being a kinetically feasible process, LLHT has been applied to polymer synthesis to offer a high degree of polymerization with good regio- and stereoselectivity under mild conditions using easily accessible monomers. Standing out from other transition metals, nickel undergoes facile SET to odd oxidation state, and this unique reactivity has been further highlighted in the photo and thermal C–H functionalization via HAT, enabling the coupling of feedstock chemicals.

Future efforts are focusing on the expansion of the peroxide mediated C–H functionalization via reaction screening, kinetic analysis, organometallic exploration, and quantum chemical simulations with exciting collaboration opportunities.

Chapter 8 Experimental Section

8.1 General Considerations

All reagents were obtained from commercial sources and used as received unless otherwise noted. Solvents were purified under nitrogen using a solvent purification system (Innovative Technology, Inc. Model #SPS400-3 and PS-400-3). IMes free carbene, IPr^{Me}·HCl, **L5**·HBF_4 were synthesized from known procedures[54, 151] 2,6-di(1H-pyrazol-1-yl)pyridine (bpp) was synthesized from known procedure[54, 151] and stored in an inert atmosphere glovebox. $Ni(COD)_2$ (Strem Chemicals, Inc.) nano powder Zn (40-60 nm average particle size, Sigma, 578002-5G), and other ligands (Sigma Aldrich and Strem), bases (Sigma Aldrich and Oakwood) were also stored in the glovebox. Ethyl acetate (Sigma-Aldrich, 99.8% anhydrous) was distilled over CaH_2 (Sigma-Aldrich) and then freeze, pumped, thawed three times before storing under N_2. Aryl bromides (Oakwood) were dried in a high vacuum or distilled over CaH_2 prior to use. K_3PO_4 (Strem, anhydrous) was finely ground and then heated under vacuum at 100 ºC overnight before transferring to a glove box.

Analytical thin layer chromatography (TLC) was performed on Kieselgel 60 F254 (250 μm silica gel) glass plates and compounds were visualized with UV light (254nm) and potassium permanganate or ceric ammonium molybdate stains. Flash column chromatography was performed using SiliaFlash® P60 (230 – 400 mesh) silica gel. Eluent mixtures are reported as v/v percentages of the minor constituent in the major constituent. All compounds purified by column chromatography were sufficiently pure for use in further experiments unless otherwise indicated. NMR spectra were collected on Varian vnmrs 500, Varian vnmrs 600, and Varian vnmrs 700 instruments. The proton signal of the residual, non-deuterated solvent (δ 7.26 for $CHCl_3$) was used

as the internal reference for ^{1}H NMR spectra. ^{13}C NMR spectra were completely heterodecoupled and measured on the abovementioned instruments. ^{19}F NMR spectra were measured on Varian vnmrs 600 instrument. ESI-HRMS were recorded using an Agilent 6230 TOF HPLC-MS.

Chiral separations were conducted with either supercritical fluid chromatography (SFC) analysis on a Waters Investigator SFC using a Waters 2998 photodiode array detector or an Agilent Infinity 1260. Samples were run on analytical chiral columns using an isopropanol/CO_2 gradient (SFC) or isopropanol/hexane (HPLC). Optical rotations were measured at room temperature on a Jasco P-2000 polarimeter.

Polymer molecular weight was analyzed by dissolving respective sample in THF (1mg/mL) and passed through a 0.2 μm PTFE filter prior to analysis. A 50 μL injection volume was allowed to pass through a Shimadzu GPC with UV-vis and RI detection with 3 columns connected in series: a Waters Styragel HT-4 (7.8 x 300 mm, 10 μm particles), a Waters Styragel HT-3 (7.8 x 300 mm, 10 μm particles), and a 100 Å PSS GRAM (8 x 300 mm, 10 μm particles). Molecular weights were calculated relative to polystyrene standards using UV-vis detection at 254 nm with a flow rate of 1 mL/min.

GCMS analysis was carried out on a HP 6980 Series GC system with HP-5MS column (30 m x 0.250 mm x 0.25 μm). GCFID analysis was carried out on a HP 6980N Series GC system with a HP-5 column (30 m x 0.32 mm x 0.25 μm).

8.2 Experimental Details for Chapter 2

8.2.1 Synthesis and Characterization of Discrete Nickel Complexes

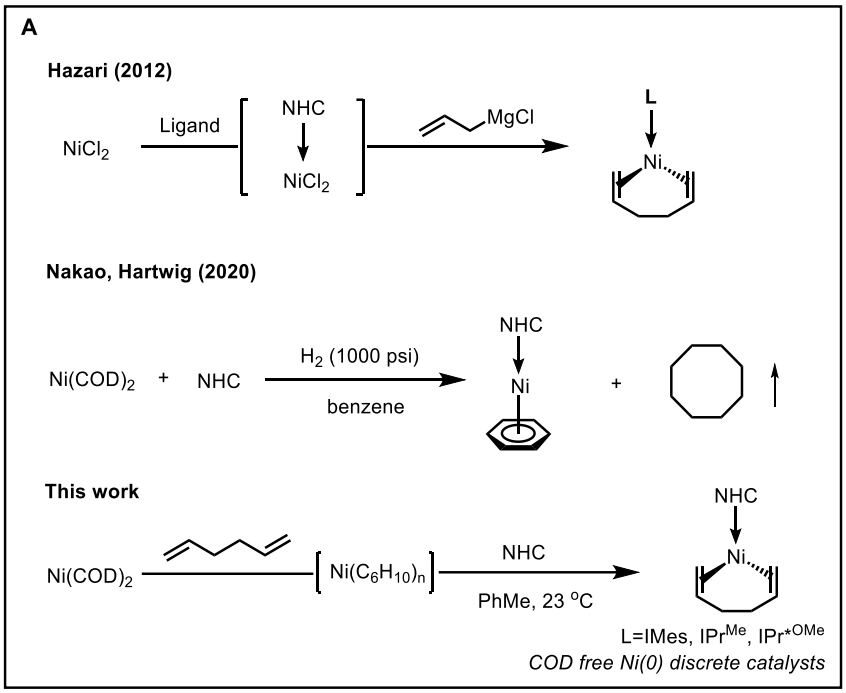

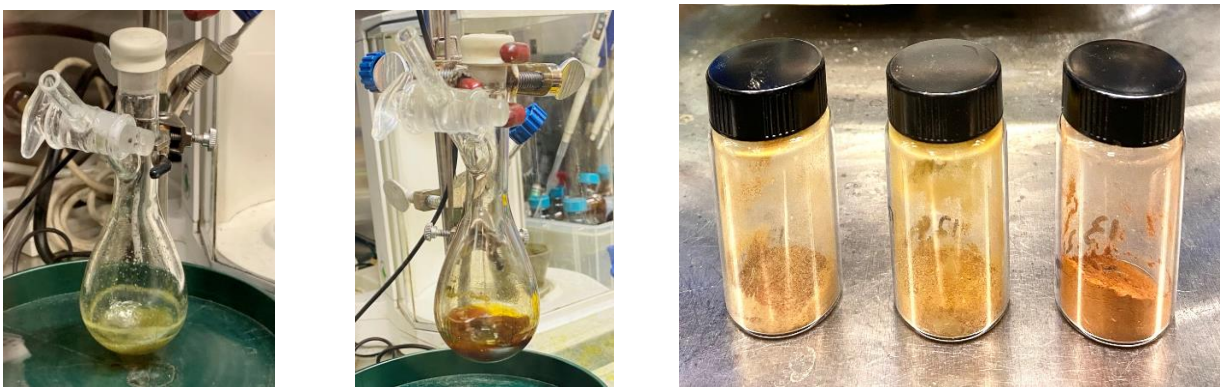

Literature precedent for COD-free Ni(0) complex synthesis. IMes-Ni(C_6H_{10}), IPrMe-Ni(C_6H_{10}), IPr*OMe-Ni(C_6H_{10}) (from left to right).

General Procedure for the synthesis of NHC-Ni(C_6H_{10}) complexes: NHC-Ni(C_6H_{10}) complexes were prepared based on modified literature procedures.[51b, 57] Inside a glove box, an oven-dried Schlenk flask was charged with $Ni(COD)_2$ (1.0 equiv) and a stir bar. Toluene and 1,5-

hexadiene (4.0 equiv) were sequentially added to this flask and capped with a septum. After 30 min rigorous stirring, all volatiles were removed by vacuum followed by re-addition of toluene and 1,5-hexadiene (4.0 equiv), and the addition – stirring – evaporation were repeated three times in total. To the same flask, a solution of the NHC free carbene (0.95 equiv) and 1,5-hexadiene (4.0 equiv) in toluene was added. A significant color change from dark green to orange or brown was immediately observed, and the reaction was allowed to stir for 16 h, and all the volatiles were removed under reduced pressure. The resulting residue was extracted with pentane and filtered through celite. Pentane was removed by vacuum to give the NHC-Ni(C_6H_{10}) complex. Further purification by recrystallization was carried out when necessary to upgrade catalyst purity.

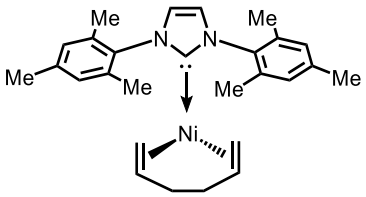

IMes-Ni(C_6H_{10}) (S1) The general procedure was followed using Ni(COD)$_2$ (275 mg, 1.00 mmol), toluene (2.00 mL*3), 1,5-hexadiene (0.470 mL*3) and IMes free carbene (289 mg, 0.950 mmol). 367 mg IMes-Ni(C_6H_{10}) was isolated in 82% yield as a yellow solid, and its NMR spectral data matched the previous report.2a

^{1}H NMR (700 MHz, C_6D_6) δ 6.73 (s, 4H), 6.35 (s, 2H), 4.13 (s, 2H), 2.79 (d, J =9.0 Hz, 2H), 2.58 (s, 2H), 2.35 (d, J =13.1 Hz, 2H), 2.18 (s, 12H), 2.06 (s, 6H), 1.48 (s, 2H).

^{13}C NMR (176 MHz, C_6D_6) δ 204.0, 137.7, 137.5, 135.2, 128.7, 121.1, 75.3, 53.1, 35.8, 20.6, 17.9.

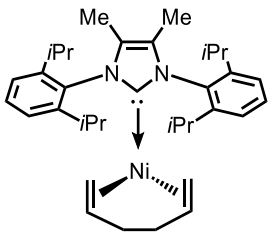

IPr^{Me}-Ni(C_6H_{10}) (**S2**)The general procedure was followed using Ni(COD)$_2$ (257 mg, 0.934 mmol), toluene (2.00 mL*3), 1,5-hexadiene (0.440 mL*3) and IPr^{Me} free carbene (370 mg, 0.887 mmol). 472 mg IPr^{Me} -Ni(C_6H_{10}) was isolated in 91% yield as a yellow solid.

^{1}H NMR (700 MHz, C_6D_6) δ 7.16 (t, *J* =7.7 Hz, 2H), 7.07 (d, *J* =7.7 Hz, 4H), 4.04 (s, 2H), 3.16 (s, 4H), 2.58 (s, 2H), 2.48 – 2.34 (m, 2H), 2.05 (s, 2H), 1.63 (s, 6H), 1.55 – 1.44 (m, 2H), 1.31 (d, *J* =6.9 Hz, 12H), 1.04 (d, *J* =6.9 Hz, 12H).

^{13}C NMR (176 MHz, C_6D_6) δ 202.5, 146.2, 136.3, 128.8, 125.0, 123.7, 76.4, 54.2, 35.8, 30.5, 28.1, 24.3, 23.5.

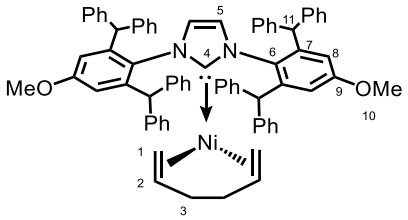

IPr^{*OMe}-Ni(C_6H_{10}) (**S3**) The general procedure was followed using Ni(COD)$_2$ (66.0 mg, 0.240 mmol), toluene (1.00 mL*3), 1,5-hexadiene (0.110 mL*3) and IPr^{*OMe} free carbene (from Strem) (220 mg). 173 mg IPr*^{OMe}-Ni(C_6H_{10}) was isolated in 80% yield as an orange solid. NMR assignments were confirmed by HSQC and HMBC analysis.

^{1}H NMR (700 MHz, C_6D_6) δ 7.36 (d, *J* =7.7 Hz, 8H), 7.03 (t, *J* =7.6 Hz, 9H), 6.94 (d, *J* =7.4 Hz, 11H), 6.85 (t, *J* =7.5 Hz, 9H), 6.80 (d, *J* =7.4 Hz, 5H), 6.73 (s, 4H), 6.21 (s, 4H), 5.33 (s, 2H), 4.62 (d, *J* =11.6 Hz, 2H), 3.14 (d, *J* =9.1 Hz, 2H), 2.96 (s, 6H), 2.90 (d, *J* =11.9 Hz, 2H), 2.75 (d, *J* =13.4 Hz, 2H), 2.03 (s, 2H).

^{13}C NMR (176 MHz, C_6D_6) δ 202.6 (C4), 158.8 (C9), 144.2, 144.0, 143.4 (C7), 133.3 (C6), 130.0, 129.4, 129.0, 128.23, 128.16, 126.5, 126.2, 122.0 (C5), 114.9 (C8), 77.9 (C2), 54.9 (C1), 54.1 (C10), 51.9 (C11), 36.6 (C3).

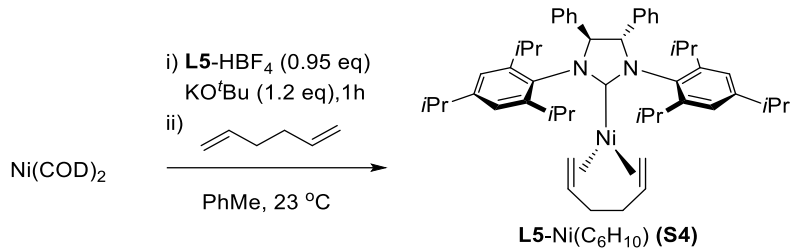

L5-Ni(C_6H_{10}) **(S4)**

L5-Ni(C_6H_{10}) (**S4**) Following the procedure developed by Belderrain and Nicasio with modification[58]: in a nitrogen-filled glove box, Ni(COD)$_2$ (82.5 mg, 0.300 mmol, 1.0 equiv), **L5**•HBF_4 (214 mg, 0.285 mmol, 0.95 equiv), KO^{t}Bu (40.4 mg, 0.36 mmol, 1.2 equiv) and toluene (2.00 mL) were charged to a Schlenk flask equipped with a magnetic stirring bar. The reaction mixture was allowed to stir at rt for 1 h. 1,5-hexadiene (0.690 mL, 3.00 mmol, 10.0 equiv) was added dropwise, and stirring was continued for 16 h. The resulting reaction mixture was concentrated under vacuum and extracted with pentane and filtered through a pad of celite. All volatiles were then removed to give the title compound **L5**-Ni(C_6H_{10}) as a yellow solid in 83% yield (215 mg). Single crystals for x-ray analysis were grown from a saturated pentane solution at -35 °C.

^{1}H NMR (700 MHz, C_6D_6) δ 7.34 – 7.28 (m, 4H), 6.95 – 6.89 (m, 4H), 6.88 (s, 4H), 5.66 (s, 2H), 4.08 (s, 1H), 4.01 (s, 1H), 3.87 (q, *J* =6.8 Hz, 2H), 3.50 – 3.41 (m, 2H), 2.93 (s, 1H), 2.65 (pd, *J* =6.9, 2.4 Hz, 2H), 2.55 (d, *J* =14.5 Hz, 2H), 2.25 (s, 1H), 2.03 (d, *J* =2.4 Hz, 1H), 1.91 (d, *J* =12.9 Hz, 1H), 1.71 (d, *J* =6.5 Hz, 6H), 1.58 (d, *J* =6.7 Hz, 6H), 1.23 (d, *J* =6.8 Hz, 6H), 1.07 (d, *J* =6.9 Hz, 12H), 0.53 (d, *J* =6.7 Hz, 6H).

^{13}C NMR (176 MHz, C_6D_6) δ 229.8, 148.8, 148.1, 145.6, 139.6, 135.2, 128.7, 128.4, 122.0, 121.8, 89.3, 77.8, 77.5, 76.4, 54.9, 54.4, 36.9, 34.4, 30.5, 29.0, 28.2, 26.5, 26.0, 24.4, 24.0, 23.7.

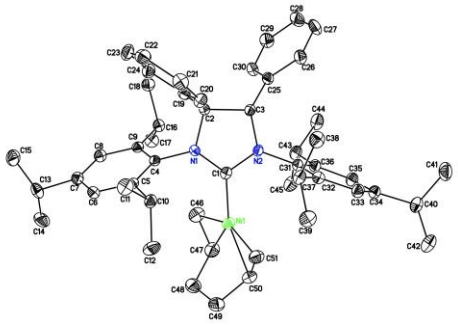

Empirical formula	$C_{51}H_{68}N_2Ni$
Formula weight	767.78
Temperature	85(2) K
Wavelength	1.54184 A
Crystal system, space group	Orthorhombic, P2(1)2(1)2(1)
Unit cell dimensions	a = 13.73143(9) A alpha = 90 deg. b = 15.55817(11) A beta = 90 deg. c = 21.10855(12) A gamma = 90 deg.
Volume	4509.55(5) A^3
Z, Calculated density	4, 1.131 Mg/m^3
Absorption coefficient	0.864 mm^-1
F(000)	1664
Crystal size	0.220 x 0.040 x 0.040 mm
Theta range for data collection	3.529 to 69.472 deg

Limiting indices	-16<=h<=16, -18<=k<=18, -25<=l<=25
Reflections collected / unique	69209 / 8403 [R(int) = 0.0649]
Completeness to theta	67.684 100.0 %
Absorption correction	Semi-empirical from equivalents
Max. and min. transmission	1.00000 and 0.61303
Refinement method	Full-matrix least-squares on F^2
Data / restraints / parameters	8403 / 0 / 539
Goodness-of-fit on F^2	1.026
Final R indices [I>2sigma(I)]	R1 = 0.0308, wR2 = 0.0818
R indices (all data)	R1 = 0.0316, wR2 = 0.0827
Absolute structure parameter	-0.001(9)
Extinction coefficient	n/a
Largest diff. peak and hole	0.287 and -0.326 e.A^-3

8.2.2 Synthesis of Starting Materials

General procedure for the synthesis of substituted benzoxazoles.

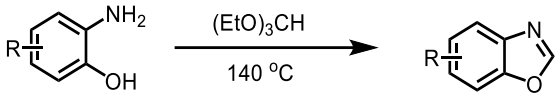

Substituted benzoxazoles were prepared according to a literature procedure.[152] A mixture of substituted 2-amino phenol and triethyl orthoformate (0.5M) was heated at 140 °C for 16 h. Upon completion, as determined by TLC, triethyl orthoformate was removed under vacuum and the residue was purified by flash chromatography to afford the title compound.

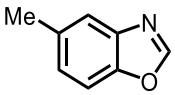

5-methylbenzo[d]oxazole (2-3). The title compound was synthesized according to the general procedure using 2-amino-4-methylphenol (492 mg, 4.00 mmol) and purified by column chromatography eluting with ethyl acetate/hexane (0 to 10/90) to afford the desired product (378 mg, 71% yield). ^{1}H NMR (400 MHz, $CDCl_3$) δ 8.05 (s, 1H), 7.60 – 7.53 (m, 1H), 7.45 (d, *J* =8.3 Hz, 1H), 7.21 – 7.13 (m, 1H), 2.47 (s, 3H). ^{1}H NMR spectral data matched the previous report. [153]

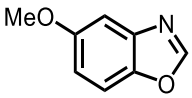

5-methoxybenzo[d]oxazole (2-4). The title compound was synthesized according to the general procedure using 2-amino-4-methoxyphenol (280 mg, 2.00 mmol) and purified by column chromatography eluting with ethyl acetate/hexane (0 to 10/90) to afford the desired product (224 mg, 75% yield). ^{1}H NMR (400 MHz, $CDCl_3$) δ 8.08 (s, 1H), 7.47 (d, *J* =9.0 Hz, 1H), 7.25 (d, *J* =3.5 Hz, 1H), 6.99 – 6.93 (m, 1H), 3.83 (s, 3H). ^{1}H NMR spectral data matched the previous report. [154]

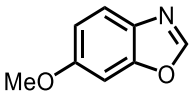

6-methoxybenzo[d]oxazole (2-5). The title compound was synthesized according to the general procedure using 2-amino-5-methoxyphenol (250 mg, 1.80 mmol) and purified by column chromatography eluting with ethyl acetate/hexane (0 to 10/90) to afford the desired product (189 mg, 71% yield). ^{1}H NMR (700 MHz, $CDCl_3$) δ 7.89 (s, 1H), 7.51 (d, *J* =8.7 Hz, 1H), 6.92 (d, *J* =2.4 Hz, 1H), 6.82 (dd, *J* =8.8, 2.4 Hz, 1H), 3.67 (s, 3H). ^{1}H NMR spectral data matched the previous report. [154]

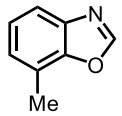

7-methylbenzo[d]oxazole (2-6). The title compound was synthesized according to the general procedure using 2-amino-6-methylphenol (246 mg, 2.00 mmol) and purified by column chromatography eluting with ethyl acetate/hexane (0 to 10/90) to afford the desired product (123 mg, 46% yield). ^{1}H NMR (700 MHz, $CDCl_3$) δ 8.08 (d, *J* =3.5 Hz, 1H), 7.61 (d, *J* =7.9 Hz, 1H), 7.25 (t, *J* =7.6 Hz, 1H), 7.17 (d, *J* =7.4 Hz, 1H), 2.54 (s, 3H). ^{1}H NMR spectral data matched the previous report. [154]

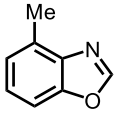

4-methylbenzo[d]oxazole (2-7). The title compound was synthesized according to the general procedure using 2-amino-6-methylphenol (492 mg, 4.00 mmol) and purified by column chromatography eluting with ethyl acetate/hexane (0 to 10/90) to afford the desired product (123 mg, 23% yield). ^{1}H NMR (400 MHz, $CDCl_3$) δ 8.02 (s, 1H), 7.34 (d, *J* =8.2 Hz, 1H), 7.21 (t, *J* =7.8 Hz, 1H), 7.10 (dt, *J* =7.4, 1.0 Hz, 1H), 2.60 (s, 3H). ^{1}H NMR spectral data matched the previous report. [153]

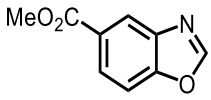

methyl benzo[d]oxazole-5-carboxylate (2-17). The title compound was synthesized according to the general procedure using methyl 3-amino-4-hydroxybenzoate (501 mg, 3.00 mmol) and purified by column chromatography eluting with ethyl acetate/hexane (0 to 10/90) to afford the desired product (352 mg, 66% yield). ^{1}H NMR (700 MHz, $CDCl_3$) δ 8.50 (d, *J* =1.6 Hz, 1H), 8.17 (s, 1H),

8.15 (dd, *J* =8.6, 1.6 Hz, 1H), 7.63 (dd, *J* =8.6, 0.7 Hz, 1H), 3.97 (s, 3H). ^{1}H NMR spectral data matched the previous report. [155]

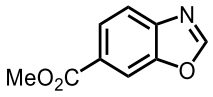

methyl benzo[d]oxazole-6-carboxylate (2-18). The title compound was synthesized according to the general procedure using methyl 4-amino-3-hydroxybenzoate (501 mg, 3.00 mmol) and purified by column chromatography eluting with ethyl acetate/hexane (0 to 10/90) to afford the desired product (473 mg, 89% yield). ^{1}H NMR (700 MHz, $CDCl_3$) δ 8.30 (s, 1H), 8.23 (s, 1H), 8.11 (d, *J* =8.3 Hz, 1H), 7.83 (d, *J* =8.3 Hz, 1H), 3.97 (s, 3H). ^{13}C NMR (176 MHz, $CDCl_3$) δ 166.5, 154.9, 143.9, 127.9, 126.3, 120.3, 112.8, 52.5. **HRMS (ESI+):** m/z: calculated for $C_9H_7NO_3$ $[M + H]^+$: 178.0498; found: 178.0499

General procedure for the synthesis of substituted benzofurans

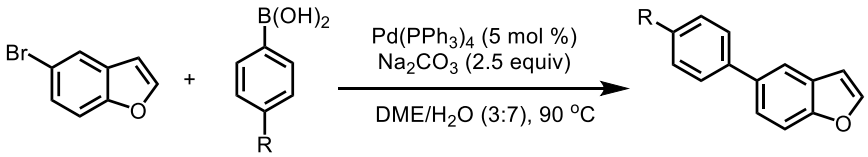

Substituted benzofurans were prepared according to literature with slight modifications.[156] Sodium carbonate (2.50 equiv), boronic acid (1.25 equiv) and a stir bar were charged to an oven-dried 100 mL Schlenk flask. The flask was brought into glovebox to add palladium tetrakis and then capped with a septum. Outside glovebox, DME/H_2O (3:7) was added to the Schlenk flask to dissolve the mixture followed by addition of 5-bromobenzofuran (1.00 equiv). The flask was placed in a pre-heated oil bath and allowed to stir at 90 °C. Upon completion, as determined by TLC, the reaction was cooled down and extracted with ethyl acetate, washed with brine, and dried with sodium

sulfate. All volatiles were removed under vacuum and the residue was purified by flash chromatography eluting with hexanes/ethyl acetate to afford the title compound.

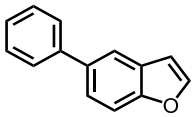

5-phenylbenzofuran (2-9). The title compound was synthesized according to the general procedure using 5-bromobenzofuran (394 mg, 2.00 mmol), phenyl boronic acid, (300 mg, 2.50 mmol), palladium tetrakis (116 mg, 0.10 mmol), sodium carbonate (530 mg, 5.00 mmol) and 3.0 mL DME, 7.0 mL H_2O. After purification with column chromatography eluting with pure hexane, the desired product was obtained (350 mg, 90% yield). ^{1}H NMR (700 MHz, $CDCl_3$) δ 7.79 (d, *J* =1.8 Hz, 1H), 7.66 (d, *J* =2.2 Hz, 1H), 7.62 (dd, *J* =8.1, 1.3 Hz, 2H), 7.56 (d, *J* =8.5 Hz, 1H), 7.53 (dd, *J* =8.5, 1.9 Hz, 1H), 7.45 (t, *J* =7.7 Hz, 2H), 7.36 – 7.33 (m, 1H), 6.83 – 6.81 (m, 1H). ^{1}H NMR spectral data matched the previous report.[157]

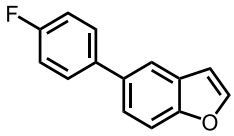

5-(4-fluorophenyl)benzofuran (2-9-F). The title compound was synthesized according to the general procedure using 5-bromobenzofuran (394 mg, 2.00 mmol), (4-fluorophenyl)boronic acid, (350 mg, 2.50 mmol), palladium tetrakis (116 mg, 0.10 mmol), sodium carbonate (530 mg, 5.00 mmol) and 3.0 mL DME, 7.0 mL H_2O. After purification with column chromatography eluting with pure hexane, the desired product was obtained (335 mg, 79% yield). ^{1}H NMR (600 MHz, $CDCl_3$) δ 7.79 (d, *J* =1.9 Hz, 1H), 7.72 (d, *J* =2.2 Hz, 1H), 7.65 – 7.59 (m, 3H), 7.52 (dd, *J* =8.5, 1.9 Hz, 1H), 7.21 (t, *J* =8.7 Hz, 2H), 6.85 (d, *J* =2.1 Hz, 1H). ^{19}F NMR (564 MHz, $CDCl_3$) δ -116.16. ^{1}H NMR spectral data matched the previous report.[158]

Preparation of 5-phenylbenzofuran-2-d (2-9-D)

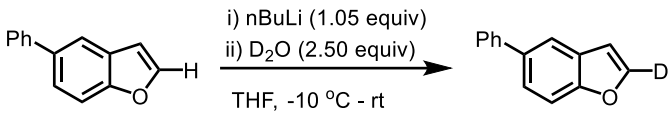

An oven-dried 100 mL round bottom flask was charged with 5-phenylbenzofuran (1.00 equiv) and a stir bar. The flask was evacuated and refilled with nitrogen three times before addition of dry THF. The reaction mixture was cooled down to -10 °C with an ice/salt bath and remained at this temperature during the addition of nBuLi (1.05 equiv, 2.5M in hexane). The resulting mixture was allowed to stir at -10 °C for 30 min followed by carefully slow addition of D_2O (2.50 equiv) and let warm up to room temperature. After another 30 min, the reaction mixture was quenched with water, extracted with ethyl acetate, washed with brine and dried with sodium sulfate. All volatiles were removed under vacuum and the residue was purified by flash chromatography eluting with hexanes to afford the title compound (320 mg, 82% yield). ^{1}H NMR (700 MHz, $CDCl_3$) δ 7.80 (d, *J* =1.7 Hz, 1H), 7.62 (dd, *J* =7.3, 1.0 Hz, 2H), 7.58 – 7.56 (m, 1H), 7.53 (dd, *J* =8.5, 1.7 Hz, 1H), 7.45 (t, *J* =7.6 Hz, 2H), 7.35 (t, *J* =7.4 Hz, 1H), 6.82 (s, 1H). ^{13}C NMR (176 MHz, $CDCl_3$) δ 154.5, 145.3 (t, *J* =30.9 Hz), 141.7, 136.5, 128.7, 127.9, 127.5, 126.9, 124.0, 119.7, 111.5, 106.6. **HRMS (EI+):** calculated for $C_{14}H_9DO$ $[M]^+$: 195.0794; found: 195.0794.

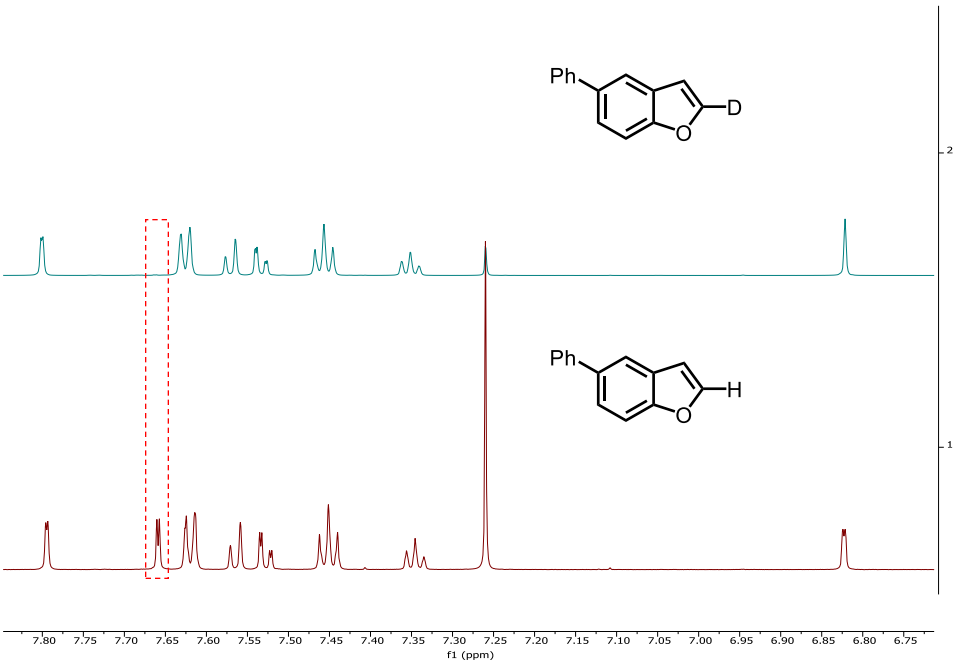

General preparation of N-alkylated heterocycles

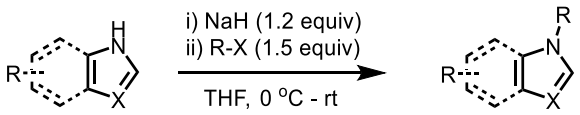

An oven-dried 100 mL round bottom flask was charged with NaH (1.2 equiv) and a stir bar. The flask was evacuated and refilled with nitrogen three times before addition of dry THF. The reaction mixture was cooled down to 0 °C with an ice bath and remained at this temperature during the addition of N-heterocycle (1.0 equiv) in THF. The resulting mixture was allowed to stir at 0 °C for 30 min followed by carefully slow addition of alkylating reagent R–X (1.5 equiv) and let warm up to room temperature. Upon completion, as indicated by TLC, the reaction mixture was quenched with water, extracted with ethyl acetate, washed with brine and dried with sodium sulfate. All volatiles were removed under vacuum and the residue was purified by flash chromatography to afford the title compound.

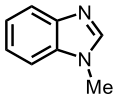

1-methyl-1H-benzo[d]imidazole (2-12). The title compound was synthesized according to the general procedure using 1H-benzo[d]imidazole (590 mg, 5.00 mmol), NaH (144 mg, 6.00 mmol), iodomethane (780 mg, 7.50 mmol). After purification with column chromatography eluting with MeOH/DCM (0 – 10/90), the desired product was obtained (456 mg, 3.50 mmol). ^{1}H NMR (700 MHz, $CDCl_3$) δ 7.32 (dd, *J* =10.0, 7.2 Hz, 1H), 7.14 (d, *J* =10.3 Hz, 1H), 6.72 (dtd, *J* =22.1, 9.8, 8.7, 5.0 Hz, 2H), 6.64 (dd, *J* =10.1, 7.4 Hz, 1H), 2.90 (s, 3H). ^{1}H NMR spectral data matched the previous report.[159]

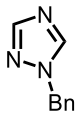

1-benzyl-1H-1,2,4-triazole (2-14). The title compound was synthesized according to the general procedure using 1H-1,2,4-triazole (345 mg, 5.00 mmol), NaH (144 mg, 6.00 mmol), benzyl bromide (940 mg, 7.50 mmol). After purification with column chromatography eluting with ethyl acetate/hexane (0 – 15/85), the desired product was obtained (440 mg, 2.8 mmol, 55% yield). ^{1}H NMR (400 MHz, $CDCl_3$) δ 7.91 (s, 1H), 7.69 (s, 1H), 7.07 (t, *J* =7.3 Hz, 3H), 7.00 (d, *J* =7.6 Hz, 2H), 5.09 (s, 2H). ^{1}H NMR spectral data matched the previous report.[160]

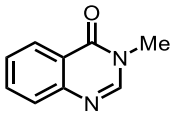

3-methylquinazolin-4(3H)-one (2-16). The title compound was synthesized according to the general procedure using quinazolin-4(3H)-one (438 mg, 3.00 mmol), NaH (89.0 mg, 3.60 mmol), methyl iodide (639 mg, 4.50 mmol). After purification with column chromatography eluting with

ethyl acetate/hexane (0 – 15/85), the desired product was obtained (208 mg, 43% yield). ^{1}H NMR (400 MHz, $CDCl_3$) δ 8.31 (dd, *J* =8.0, 1.5 Hz, 1H), 8.09 (s, 1H), 7.77 (ddd, *J* =8.5, 6.9, 1.5 Hz, 1H), 7.71 (d, *J* =7.6 Hz, 1H), 7.51 (ddd, *J* =8.1, 6.9, 1.3 Hz, 1H), 3.62 (s, 3H). ^{1}H NMR spectral data matched the previous report.[161]

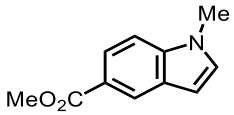

methyl 1-methyl-1H-indole-5-carboxylate (2-20). The title compound was synthesized according to the general procedure using methyl 1H-indole-5-carboxylate (526 mg, 3.00 mmol), NaH (96.0 mg, 3.60 mmol), methyl iodide (639 mg, 4.50 mmol). After purification with column chromatography eluting with ethyl acetate/hexane (0 – 15/85), the desired product was obtained (480 mg, 85% yield). ^{1}H NMR (400 MHz, $CDCl_3$) δ 8.38 (dd, *J* =1.7, 0.7 Hz, 1H), 7.91 (dd, *J* =8.7, 1.7 Hz, 1H), 7.34 – 7.29 (m, 1H), 7.10 (d, *J* =3.2 Hz, 1H), 6.57 (dd, *J* =3.2, 0.9 Hz, 1H), 3.91 (s, 3H), 3.81 (s, 3H). ^{1}H NMR spectral data matched the previous report.[162]

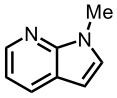

1-methyl-1H-pyrrolo[2,3-b]pyridine (2-22). The title compound was synthesized according to the general procedure using 1H-pyrrolo[2,3-b]pyridine (236 mg, 2.00 mmol), NaH (58.0 mg, 2.40 mmol), methyl iodide (426 mg, 3.00 mmol). After purification with column chromatography eluting with ethyl acetate/hexane (0 – 15/85), the desired product was obtained (119 mg, 45% yield). ^{1}H NMR (600 MHz, $CDCl_3$) δ 8.32 (dd, *J* =4.7, 1.6 Hz, 1H), 7.84 (dd, *J* =7.8, 1.5 Hz, 1H), 7.09 (d, *J* =3.5 Hz, 1H), 6.99 (dd, *J* =7.8, 4.7 Hz, 1H), 6.39 (d, *J* =3.5 Hz, 1H), 3.81 (s, 3H). ^{1}H NMR spectral data matched the previous report.[163]

8.2.3 Intermolecular C–H Functionalization via Nickel Catalysis

General Procedure A: Intermolecular C–H Functionalization with achiral nickel complexes

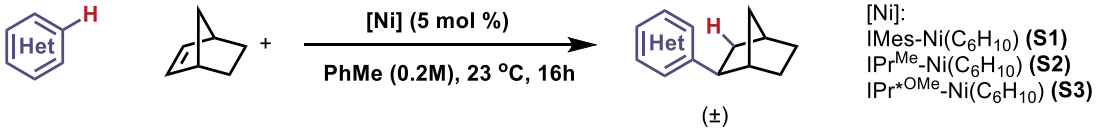

The 1,5-hexadiene-supported NHC nickel complex (5.0 μmmol, 0.050 equiv) was weighed in an oven-dried 1 dram vial charged with a stir bar in an inert atmosphere glovebox and dissolved in 0.300 mL toluene. To a separate vial, arene starting material (0.10 mmol, 1.0 equiv) was added, followed by addition of 0.200 mL norbornene (0.10 mmol, 1.0 equiv) stock solution (0.5M in toluene). This solution was transferred to the previous vial using a micropipette and the reaction vial was capped and brought outside the glovebox to a stir plate. After 16 h, the reaction mixture was quenched with 2 mL dichloromethane and run through a silica gel plug with 2 mL ethyl acetate. The solvent was removed, and the crude reaction mixture was purified by silica gel chromatography.

General Procedure B: Asymmetric functionalization with in-situ generated chiral nickel complex.

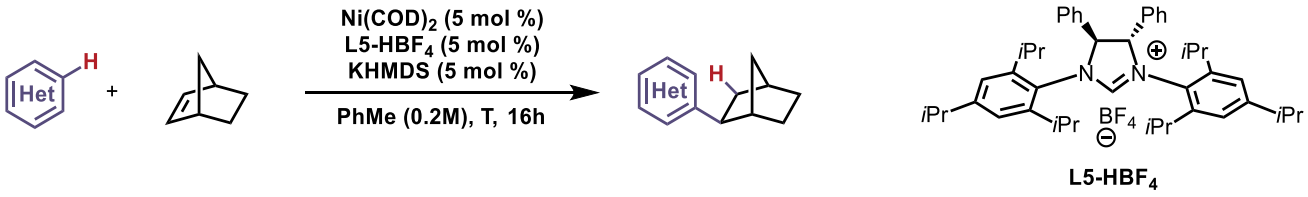

To an oven-dried 1 dram vial equipped with a Teflon-coated magnetic stir bar in a N_2 filled glovebox was added **L5**•HBF_4 (3.6 mg, 5.0 μmmol, 0.050 equiv), KHMDS (1.0 mg, 5.0 μmmol, 0.050 equiv), $Ni(COD)_2$ (1.4 mg, 5.0 μmmol, 0.050 equiv) and 0.100 mL toluene. The mixture

was stirred for 10 min before adding a solution of arene starting material (0.10 mmol, 1.0 equiv) and norbornene (0.10 mmol, 1.0 equiv) in 0.400 mL toluene. The vial was sealed with a Teflon cap before removing from the glovebox and stirred for 16 h. The reaction mixture was quenched with 2 mL dichloromethane and run through a silica gel plug with 2 mL ethyl acetate. The solvent was removed, and the crude reaction mixture was purified by silica gel chromatography.

General Procedure C: Asymmetric functionalization with well-defined chiral nickel complex

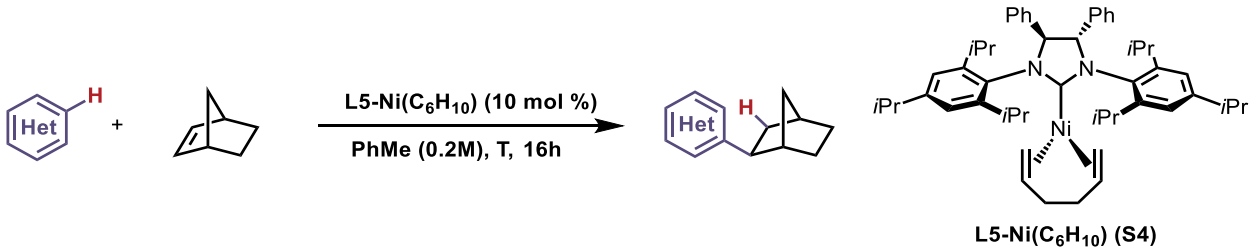

To an oven-dried 1 dram vial equipped with a Teflon-coated magnetic stir bar in a N_2 filled glovebox was added **L5**-Ni(C_6H_{10}) (7.6 mg, 10 μmmol, 0.050 equiv) and a solution of arene starting material (0.10 mmol, 1.0 equiv) and norbornene (1.0 or 2.0 equiv) in 0.500 mL toluene. The vial was sealed with a Teflon cap before removing from the glovebox and stirred for 16 h. The reaction mixture was quenched with 2 mL dichloromethane and run through a silica gel plug with 2 mL ethyl acetate. The solvent was removed, and the crude reaction mixture was purified by silica gel chromatography.

*Please note that the absolute configuration was determined only for the compound **2-8-2** and **2-1-26**. The absolute configuration for other nbe or styrene products were inferred by analogy with **2-8-2** and **2-1-26** respectively. (See Section **8.2.5** for details)*

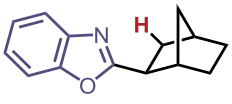

(±)

exo-2-(bicyclo[2.2.1]heptan-2-yl)benzo[d]oxazole (2-1-2) This compound was prepared by following general procedure A using benzo[d]oxazole (11.9 mg, 0.10 mmol), 0.200 mL norbornene (0.10 mmol) stock solution (0.5M in toluene) and IPr^{Me}-Ni(C_6H_{10}) (2.8 mg, 5.0 μmmol). Purification by column chromatography eluting with ethyl acetate / hexane (0 – 10/90) afforded the desired product as a yellow liquid (21.2 mg, 99% yield).

^{1}H NMR (700 MHz, $CDCl_3$) δ 7.69 – 7.63 (m, 1H), 7.48 – 7.43 (m, 1H), 7.30 – 7.24 (m, 2H), 2.98 (dd, *J* =9.2, 5.2 Hz, 1H), 2.68 (d, *J* =4.2 Hz, 1H), 2.42 (d, *J* =4.4 Hz, 1H), 2.20 – 2.14 (m, 1H), 1.76 (ddd, *J* =12.1, 9.0, 2.4 Hz, 1H), 1.66 – 1.62 (m, 2H), 1.60 (tq, *J* =12.0, 3.7 Hz, 1H), 1.41 (tt, *J* =11.9, 2.7 Hz, 1H), 1.30 (dddd, *J* =11.7, 9.4, 4.4, 2.2 Hz, 1H), 1.26 (dd, *J* =9.8, 1.9 Hz, 1H). ^{13}C NMR (176 MHz, $CDCl_3$) δ 170.5, 150.9, 141.3, 124.3, 123.9, 119.5, 110.2, 42.0, 41.6, 36.4, 36.3, 35.4, 29.6, 28.8. These spectra matched the report in literature.[164] **HRMS (ESI+):** m/z: calculated for $C_{14}H_{15}NO$ $[M + H]^+$: 214.1227; found: 214.1229

SFC: OJ-H 0.2% IPA, 3 mL/min

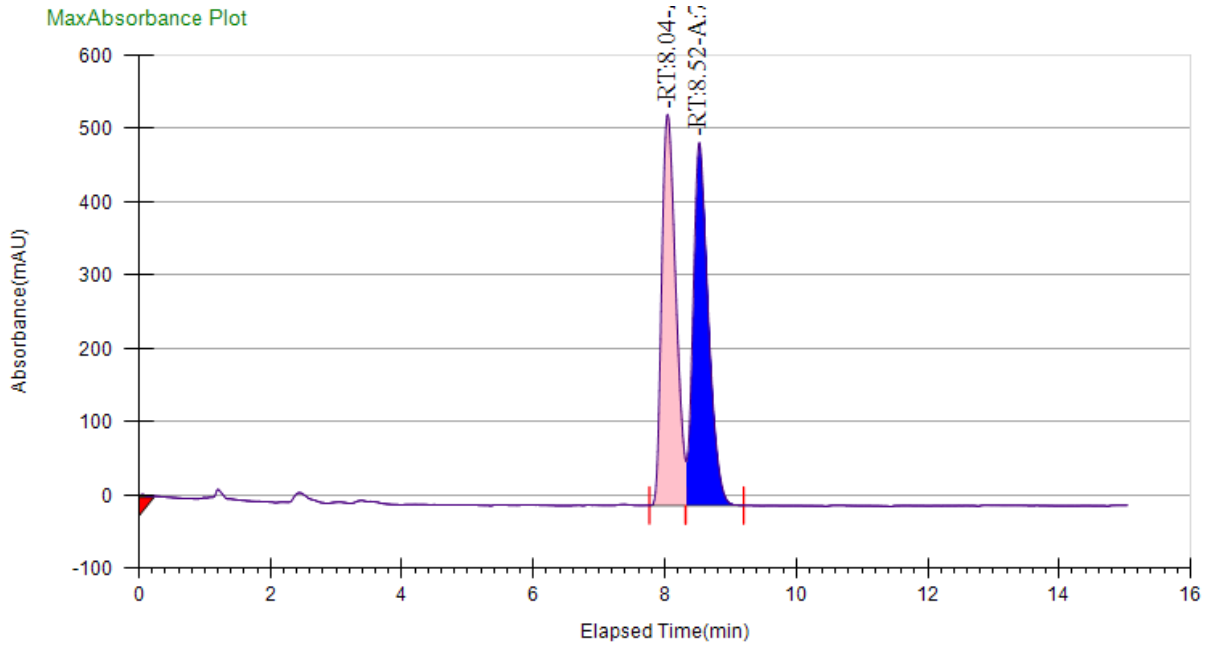

Peak Information

Peak No	% Area	Area	Ret. Time	Height	Cap. Factor
1	49.8735	7837.8536	8.04 min	534.0241	0
2	50.1265	7877.5988	8.52 min	495.3048	0

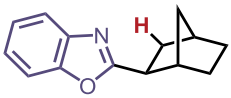

2-((1S,2S,4R)-bicyclo[2.2.1]heptan-2-yl)benzo[d]oxazole (2-1-2) This compound was prepared by following general procedure B using benzo[d]oxazole (11.9 mg, 0.10 mmol), 0.200 mL norbornene (0.10 mmol) stock solution (0.5M in toluene), **L5**-HBF_4 (3.6 mg, 5.0 μmmol), KHMDS (1.0 mg, 5.0 μmmol) and $Ni(COD)_2$ (1.4 mg 5.0 μmmol). Purification by column chromatography eluting with ethyl acetate / hexane (0 – 10/90) afforded the desired product as a yellow liquid (21.2 mg, 99% yield). $[\alpha]_D^{23}$ = +4.5 (c = 0.69, $CHCl_3$)

^{1}H NMR (700 MHz, $CDCl_3$) δ 7.70 – 7.64 (m, 1H), 7.49 – 7.44 (m, 1H), 7.31 – 7.25 (m, 2H), 2.99 (dd, *J* =9.1, 5.2 Hz, 1H), 2.68 (d, *J* =4.2 Hz, 1H), 2.43 (s, 1H), 2.21 – 2.14 (m, 1H), 1.80 – 1.73

(m, 1H), 1.70 – 1.64 (m, 2H), 1.61 (dt, *J* =7.6, 3.8 Hz, 1H), 1.47 – 1.39 (m, 1H), 1.32 (dt, *J* =10.8, 5.4 Hz, 1H), 1.26 (d, *J* =10.6 Hz, 1H).

SFC: OJ-H 0.2% IPA, 3 mL/min

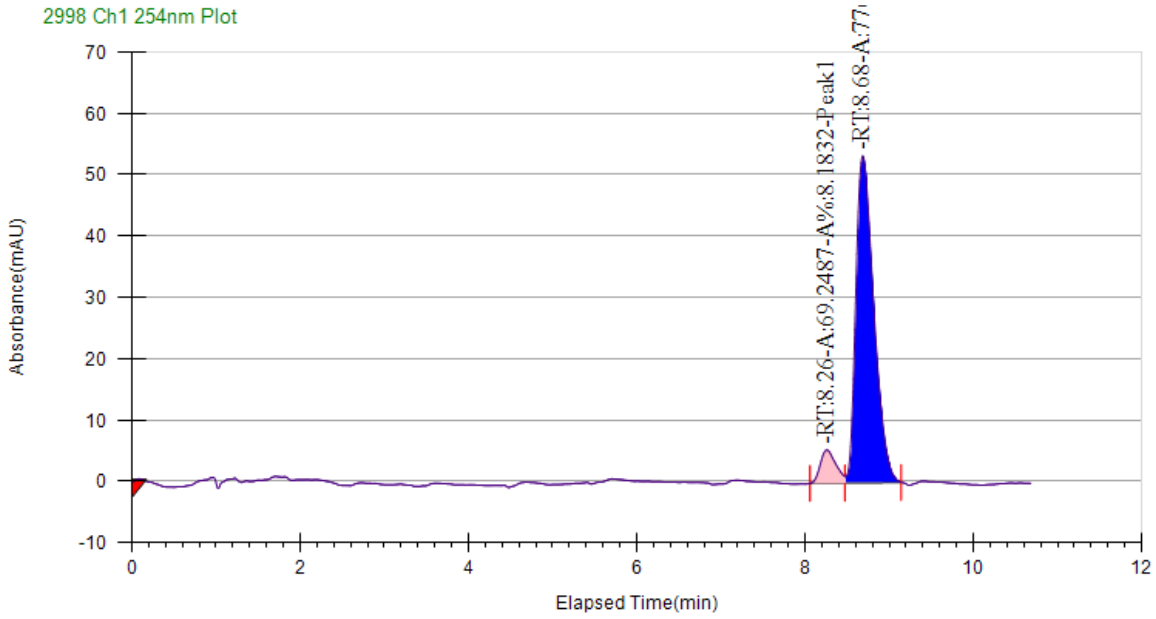

Peak Information

Peak No	% Area	Area	Ret. Time	Height	Cap. Factor
1	8.1832	69.2487	8.26 min	5.4176	0
2	91.8168	776.9824	8.68 min	53.3497	0

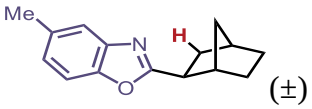

(±)

exo-2-(bicyclo[2.2.1]heptan-2-yl)-5-methylbenzo[d]oxazole (2-3-2) This compound was prepared by following general procedure A using 5-methylbenzo[d]oxazole (13.3 mg, 0.10 mmol), 0.200 mL norbornene (0.10 mmol) stock solution (0.5M in toluene) and IPr^{Me}-Ni(C_6H_{10}) (2.8 mg, 5.0 μmmol). Purification by column chromatography eluting with ethyl acetate / hexane (0 – 10/90) afforded the desired product as a colorless liquid (18.4 mg, 81% yield). ^{1}H NMR (700 MHz,

$CDCl_3$) δ 7.44 (d, *J* =1.6 Hz, 1H), 7.32 (d, *J* =8.2 Hz, 1H), 7.08 (dd, *J* =8.2, 1.7 Hz, 1H), 2.97 (dd, *J* =9.2, 5.2 Hz, 1H), 2.67 (d, *J* =4.2 Hz, 1H), 2.44 (s, 3H), 2.42 (t, *J* =4.4 Hz, 1H), 2.16 (dtd, *J* =12.5, 4.7, 3.1 Hz, 1H), 1.75 (ddd, *J* =12.0, 9.0, 2.4 Hz, 1H), 1.68 – 1.62 (m, 2H), 1.62 – 1.57 (m, 1H), 1.41 (ddq, *J* =11.7, 8.7, 2.5 Hz, 1H), 1.30 (dddd, *J* =11.7, 9.4, 4.3, 2.1 Hz, 1H), 1.25 (ddd, *J* =10.0, 2.6, 1.4 Hz, 1H). ^{13}C NMR (176 MHz, $CDCl_3$) δ 170.6, 149.1, 141.5, 133.7, 125.3, 119.5, 109.6, 42.0, 41.6, 36.4, 36.3, 35.4, 29.6, 28.8, 21.4. **HRMS (ESI+):** m/z: calculated for $C_{15}H_{17}NO$ $[M + H]^+$: 228.1383; found: 228.1389

SFC: OJ-H 0-1% MeOH, 3 mL/min

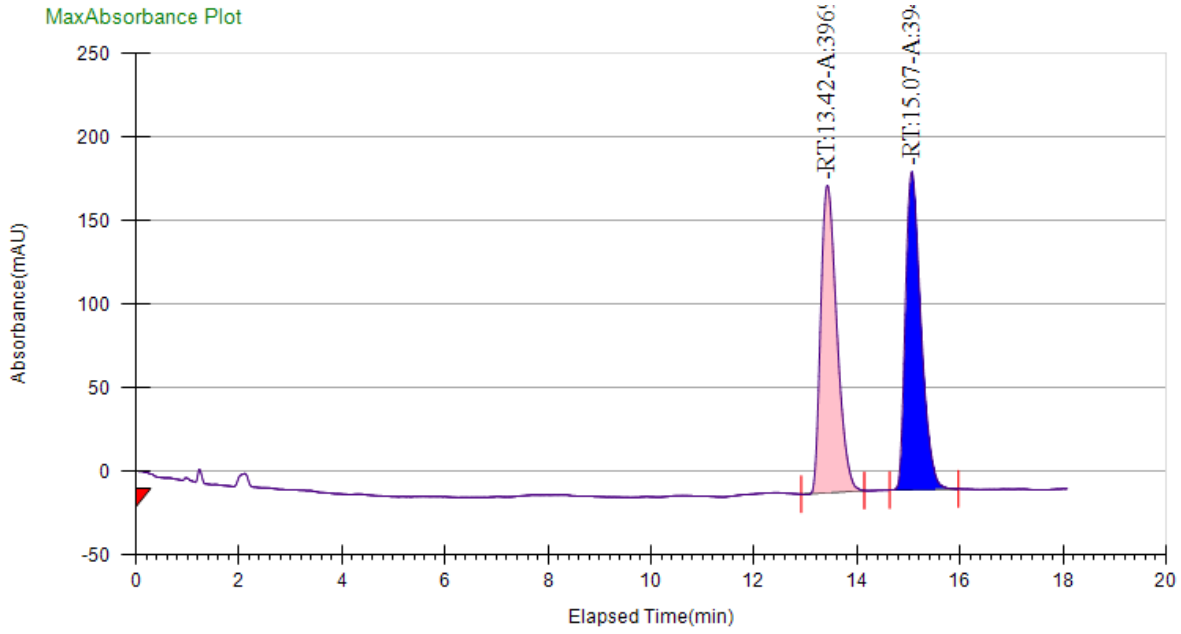

Peak Information

Peak No	% Area	Area	Ret. Time	Height	Cap. Factor
1	50.1275	3969.7526	13.42 min	183.8679	13423.8
2	49.8725	3949.5642	15.07 min	190.0496	15065.45

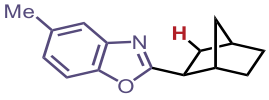

2-((1S,2S,4R)-bicyclo[2.2.1]heptan-2-yl)-5-methylbenzo[d]oxazole (2-3-2) This compound was prepared by following general procedure B using 5-methylbenzo[d]oxazole (13.3 mg, 0.10 mmol), 0.200 mL norbornene (0.10 mmol) stock solution (0.5M in toluene), **L5**-HBF_4 (3.6 mg, 5.0 μmmol), KHMDS (1.0 mg, 5.0 μmmol) and $Ni(COD)_2$ (1.4 mg, 5.0 μmmol). Purification by column chromatography eluting with ethyl acetate / hexane (0 – 10/90) afforded the desired product as a colorless liquid (21.1 mg, 93% yield). $[\alpha]_D^{23}$ = +10.5 (c = 0.31, $CHCl_3$)

^{1}H NMR (400 MHz, $CDCl_3$) δ 7.45 – 7.41 (m, 1H), 7.31 (d, *J* =8.3 Hz, 1H), 7.06 (dd, *J* =8.3, 1.7 Hz, 1H), 2.99 – 2.92 (m, 1H), 2.65 (d, *J* =3.2 Hz, 1H), 2.43 (s, 3H), 2.40 (d, *J* =4.1 Hz, 1H), 2.14 (dtd, *J* =12.4, 4.9, 2.8 Hz, 1H), 1.74 (ddd, *J* =12.1, 9.1, 2.4 Hz, 1H), 1.66 – 1.63 (m, 1H), 1.61 (q, *J* =1.8 Hz, 1H), 1.60 – 1.53 (m, 1H), 1.41 (dd, *J* =12.0, 2.7 Hz, 1H), 1.30 (dt, *J* =7.1, 2.2 Hz, 1H), 1.26 – 1.23 (m, 1H).

SFC: OJ-H 0-1% MeOH, 3 mL/min

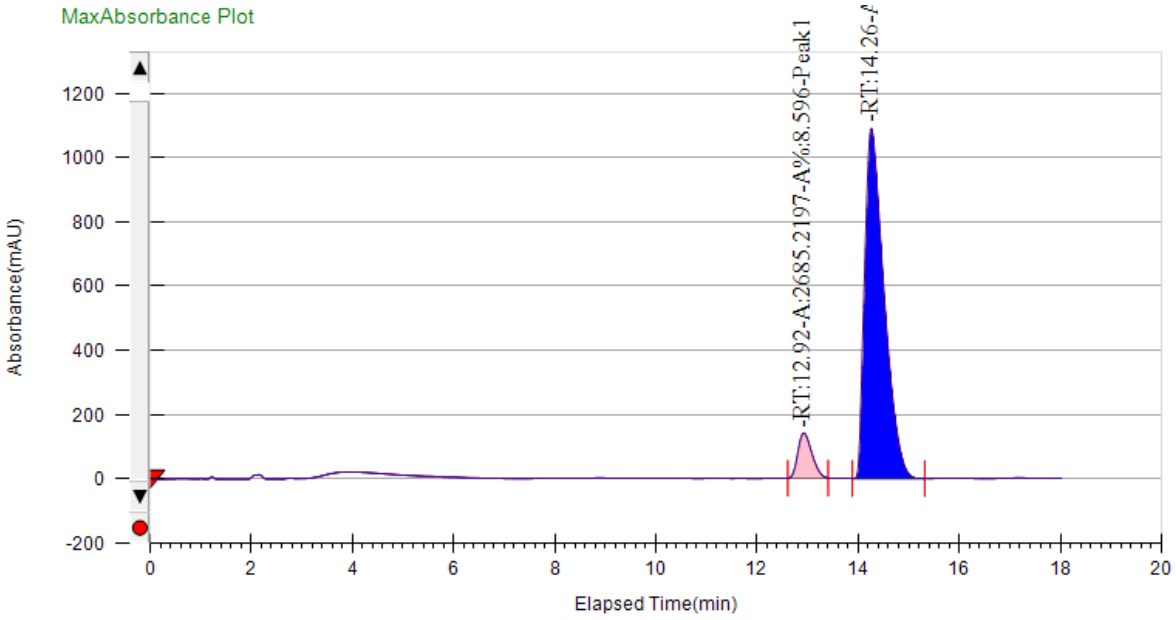

Peak Information

Peak No	% Area	Area	Ret. Time	Height	Cap. Factor
1	8.596	2685.2197	12.92 min	140.4607	12923.8167
2	91.404	28552.9061	14.26 min	1088.2162	14257.1167

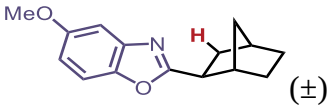

(±)

exo-2-(bicyclo[2.2.1]heptan-2-yl)-5-methoxylbenzo[d]oxazole (2-4-2) This compound was prepared by following general procedure A using 5-methoxybenzo[d]oxazole (14.9 mg, 0.10 mmol), 0.200 mL norbornene (0.10 mmol) stock solution (0.5M in toluene) and IPr^{Me}-Ni(C_6H_{10}) (2.8 mg, 5.0 μmmol). Purification by column chromatography eluting with ethyl acetate / hexane (0 – 10/90) afforded the desired product as a colorless liquid (18.4 mg, 76% yield). ^{1}H NMR (500 MHz, $CDCl_3$) δ 7.33 (d, *J* =8.8 Hz, 1H), 7.17 (d, *J* =2.6 Hz, 1H), 6.86 (dd, *J* =8.8, 2.5 Hz, 1H), 3.83 (s, 3H), 2.95 (dd, *J* =9.2, 5.2 Hz, 1H), 2.66 (d, *J* =4.1 Hz, 1H), 2.41 (d, *J* =4.4 Hz, 1H), 2.15 (dtd, *J* =12.5, 4.7, 2.9 Hz, 1H), 1.75 (ddd, *J* =12.0, 9.0, 2.4 Hz, 1H), 1.69 – 1.56 (m, 3H), 1.44 – 1.37 (m, 1H), 1.33 – 1.28 (m, 1H), 1.27 – 1.24 (m, 1H). ^{13}C NMR (126 MHz, $CDCl_3$) δ 171.4, 156.9, 145.5, 142.1, 112.6, 110.3, 102.8, 55.9, 42.1, 41.7, 36.4, 36.3, 35.4, 29.6, 28.8. **HRMS (ESI+):** m/z: calculated for $C_{15}H_{17}NO_2$ $[M + H]^+$: 244.1332; found: 244.1336

SFC: OJ-H 0-1% MeOH, 3 mL/min

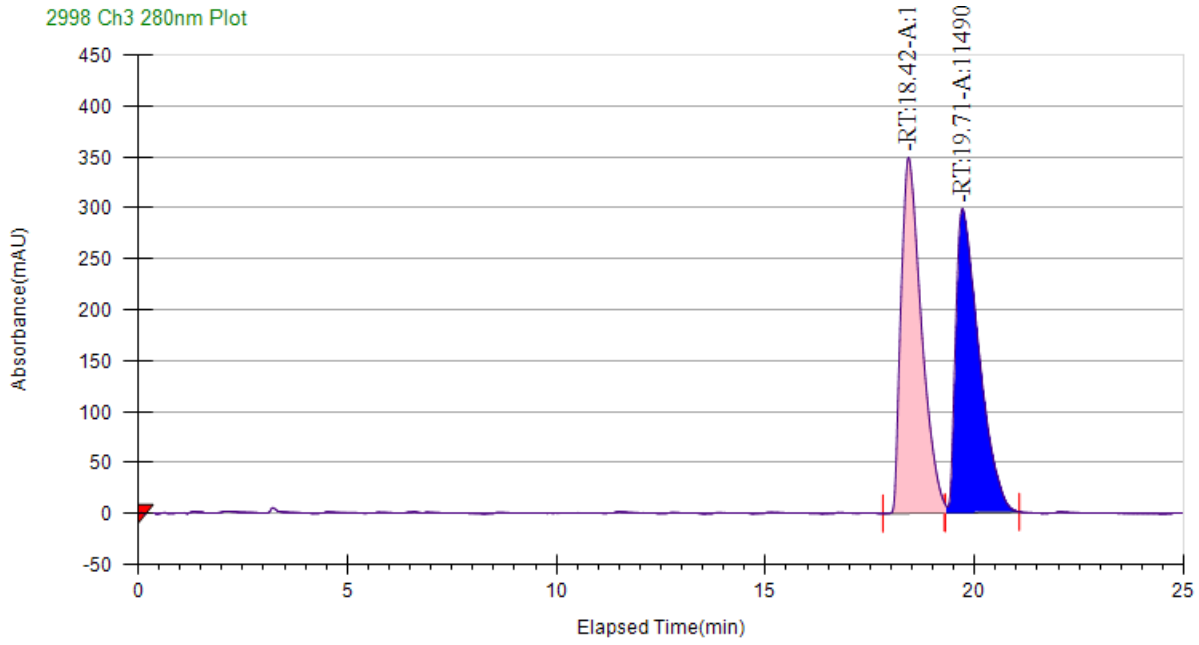

Peak Information

Peak No	% Area	Area	Ret. Time	Height	Cap. Factor
1	50.5796	11759.9467	18.42 min	348.9187	18415.6667
2	49.4204	11490.4224	19.71 min	298.1871	19707.3333

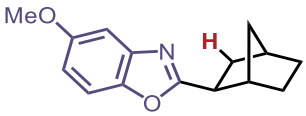

2-((1S,2S,4R)-bicyclo[2.2.1]heptan-2-yl)-5-methoxybenzo[d]oxazole (2-4-2) This compound was prepared by following general procedure B using 5-methoxybenzo[d]oxazole (14.9 mg, 0.10 mmol 1.0 equiv), 0.200 mL norbornene (0.10 mmol, 1.0 equiv) stock solution (0.5M in toluene), **L5**-HBF_4 (3.6 mg, 5.0 μmmol), KHMDS (1.0 mg, 5.0 μmmol) and $Ni(COD)_2$ (1.4 mg, 5.0 μmmol). Purification by column chromatography eluting with ethyl acetate / hexane (0 – 10/90) afforded the desired product as a colorless liquid (24.2 mg, 99% yield). $[\alpha]_D^{23}$ = +7.9 (c = 0.54, $CHCl_3$)

^1H NMR (700 MHz, $CDCl_3$) δ 7.33 (d, *J* =8.8 Hz, 1H), 7.17 (d, *J* =2.5 Hz, 1H), 6.86 (dd, *J* =8.8, 2.4 Hz, 1H), 3.82 (s, 3H), 2.95 (dd, *J* =9.2, 5.3 Hz, 1H), 2.66 (d, *J* =4.2 Hz, 1H), 2.41 (t, *J* =4.4 Hz, 1H), 2.18 – 2.12 (m, 1H), 1.74 (ddd, *J* =12.3, 9.1, 2.4 Hz, 1H), 1.65 (dd, *J* =10.4, 6.5 Hz, 2H),

1.60 (dt, *J* =11.9, 3.9 Hz, 1H), 1.40 (tt, *J* =11.6, 2.9 Hz, 1H), 1.32 – 1.28 (m, 1H), 1.25 (d, *J* =7.5 Hz, 1H).

SFC: OJ-H 0-1% MeOH, 3 mL/min

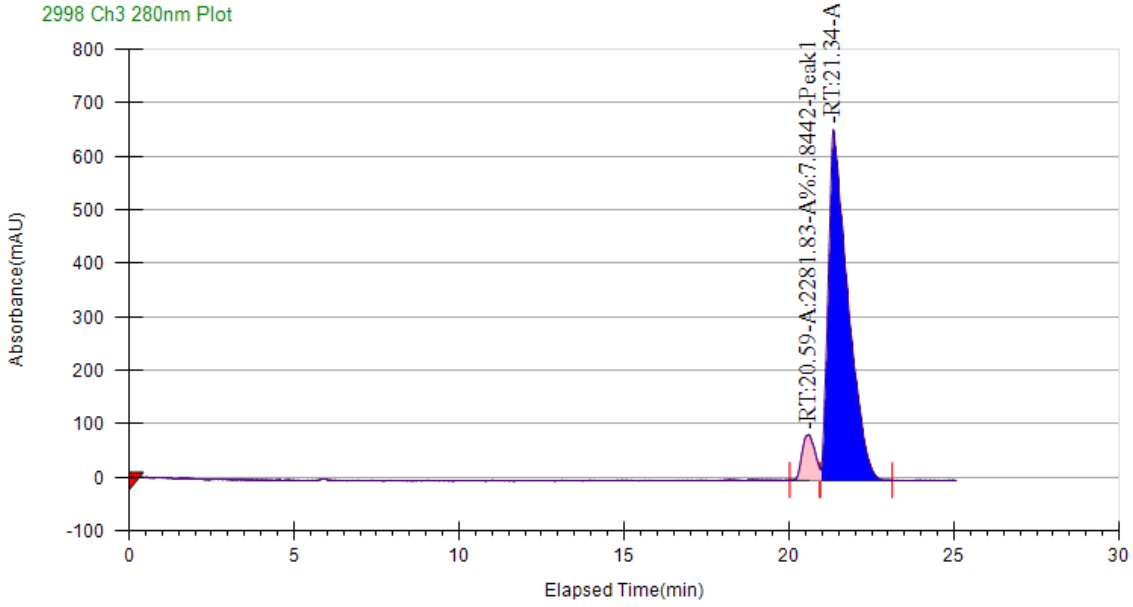

Peak Information

Peak No	% Area	Area	Ret. Time	Height	Cap. Factor
1	7.8442	2281.83	20.59 min	84.7418	20590.6667
2	92.1558	26807.5794	21.34 min	655.0791	21340.6667

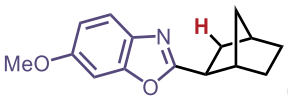

(±)

exo-2-(bicyclo[2.2.1]heptan-2-yl)-6-methoxybenzo[d]oxazole (2-5-2) This compound was prepared by following general procedure A using 6-methoxybenzo[d]oxazole (14.9 mg, 0.10 mmol), 0.200 mL norbornene (0.10 mmol) stock solution (0.5M in toluene) and IPr^{Me}-Ni(C_6H_{10}) (2.8 mg, 5.0 μmmol). Purification by column chromatography eluting with ethyl acetate / hexane (0 – 10/90) afforded the desired product as a brown solid (21.2 mg, 87% yield) ^{1}H NMR (700 MHz, $CDCl_3$) δ 7.52 (d, *J* =8.7 Hz, 1H), 7.00 (d, *J* =2.4 Hz, 1H), 6.88 (dd, *J* =8.7, 2.4 Hz, 1H),

3.83 (s, 3H), 2.94 (dd, *J* =8.9, 5.2 Hz, 1H), 2.65 (d, *J* =4.2 Hz, 1H), 2.43 – 2.40 (m, 1H), 2.18 – 2.11 (m, 1H), 1.78 – 1.72 (m, 1H), 1.68 – 1.58 (m, 3H), 1.40 (dddd, *J* =11.4, 8.8, 3.9, 2.3 Hz, 1H), 1.30 (tdd, *J* =9.5, 4.3, 2.3 Hz, 1H), 1.25 (ddq, *J* =9.8, 3.0, 1.6 Hz, 1H). ^{13}C NMR (176 MHz, $CDCl_3$) δ 169.6, 157.6, 151.7, 135.0, 119.4, 111.8, 95.4, 55.9, 42.0, 41.5, 36.4, 36.2, 35.4, 29.5, 28.8. **HRMS (ESI+):** m/z: calculated for $C_{15}H_{17}NO_2$ $[M + H]^+$: 244.1332; found: 244.1339

SFC: OJ-H 2% IPA, 3 mL/min

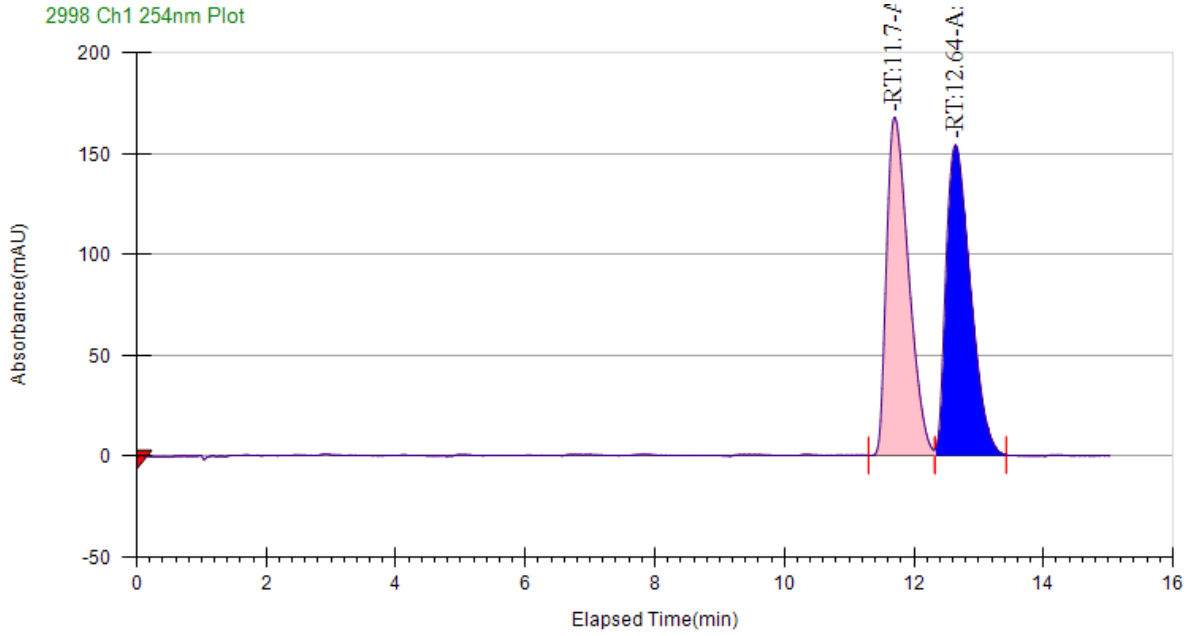

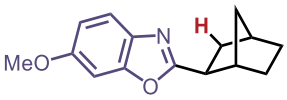

2-((1S,2S,4R)-bicyclo[2.2.1]heptan-2-yl)-6-methoxybenzo[d]oxazole (2-5-2) This compound was prepared by following general procedure B using 6-methoxybenzo[d]oxazole (14.9 mg, 0.10 mmol), 0.200 mL norbornene (0.10 mmol) stock solution (0.5M in toluene), **L5**-HBF_4 (3.6 mg, 5.0 μmmol), KHMDS (1.0 mg, 5.0 μmmol) and $Ni(COD)_2$ (1.4 mg, 5.0 μmmol). Purification by column chromatography eluting with ethyl acetate / hexane (0 – 10/90) afforded the desired product as a brown solid (21.5 mg, 88% yield). $[\alpha]_D^{23}$ = -2.8 (c = 0.92, $CHCl_3$)

^{1}H NMR (700 MHz, $CDCl_3$) δ 7.52 (d, *J* =8.7 Hz, 1H), 7.00 (d, *J* =2.4 Hz, 1H), 6.88 (dd, *J* =8.7, 2.4 Hz, 1H), 3.83 (s, 3H), 2.94 (dd, *J* =8.9, 5.2 Hz, 1H), 2.65 (d, *J* =4.2 Hz, 1H), 2.41 (t, *J* =4.5 Hz, 1H), 2.14 (dtd, *J* =12.5, 4.7, 3.1 Hz, 1H), 1.74 (ddd, *J* =12.1, 9.0, 2.4 Hz, 1H), 1.68 – 1.58 (m, 3H), 1.42 – 1.35 (m, 1H), 1.31 – 1.26 (m, 1H), 1.25 (ddd, *J* =9.9, 2.6, 1.4 Hz, 1H).

SFC: OJ-H 2% IPA, 3 mL/min

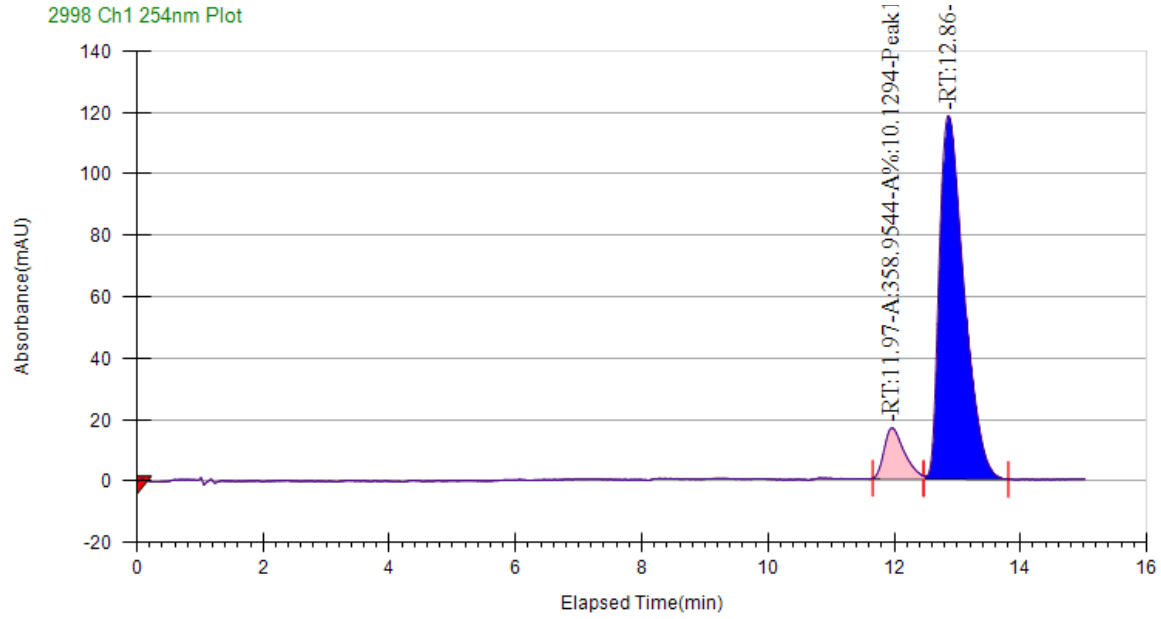

Peak Information

Peak No	% Area	Area	Ret. Time	Height	Cap. Factor
1	10.1294	358.9544	11.97 min	16.4014	11965.6667
2	89.8706	3184.7243	12.86 min	118.3547	12857.3333

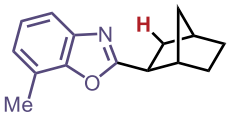

(±)

exo-2-(bicyclo[2.2.1]heptan-2-yl)-7-methylbenzo[d]oxazole (2-6-2) This compound was prepared by following general procedure A using 7-methylbenzo[d]oxazole (13.3 mg, 0.10 mmol), 0.200 mL norbornene (0.10 mmol) stock solution (0.5M in toluene) and IPr^{Me}-Ni(C_6H_{10}) (2.8 mg, 5.0 μmmol). Purification by column chromatography eluting with ethyl acetate / hexane (0 – 10/90)

afforded the desired product as a brown liquid (15.1 mg, 67% yield) ^{1}H NMR (700 MHz, $CDCl_3$) δ 7.49 (d, *J* =7.9 Hz, 1H), 7.17 (t, *J* =7.6 Hz, 1H), 7.07 (d, *J* =7.4 Hz, 1H), 2.99 (dd, *J* =9.1, 5.2 Hz, 1H), 2.69 (d, *J* =4.2 Hz, 1H), 2.51 (s, 3H), 2.43 (d, *J* =4.5 Hz, 1H), 2.19 (dq, *J* =12.6, 4.2 Hz, 1H), 1.76 (ddd, *J* =12.2, 9.0, 2.3 Hz, 1H), 1.69 – 1.65 (m, 2H), 1.61 (ddq, *J* =12.2, 8.1, 3.6 Hz, 1H), 1.43 (tt, *J* =11.8, 2.9 Hz, 1H), 1.36 – 1.29 (m, 1H), 1.27 – 1.24 (m, 1H). ^{13}C NMR (126 MHz, Chloroform-d) δ 170.2, 150.0, 140.8, 125.3, 123.8, 120.8, 116.8, 42.1, 41.6, 36.4, 36.3, 35.4, 29.6, 28.8, 15.2. **HRMS (ESI+):** m/z: calculated for $C_{15}H_{17}NO$ $[M + H]^+$: 228.1383; found: 228.1384

SFC: OD-H 0-10% IPA, 3 mL/min

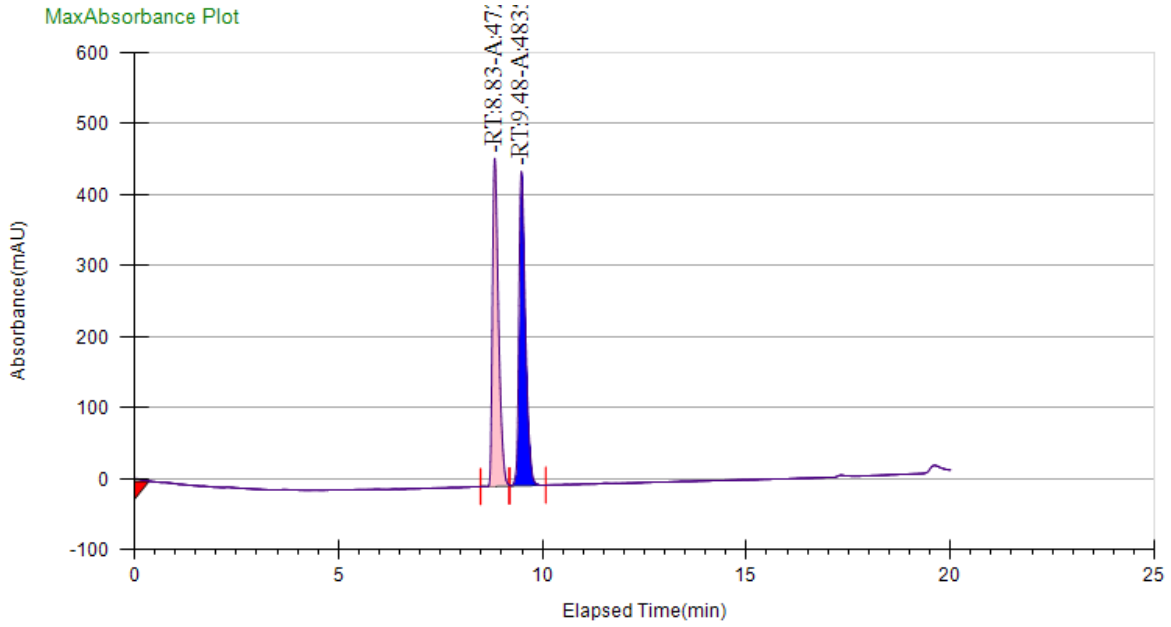

Peak Information

Peak No	% Area	Area	Ret. Time	Height	Cap. Factor
1	49.42	4724.8578	8.83 min	462.0975	0
2	50.58	4835.7544	9.48 min	442.6492	0

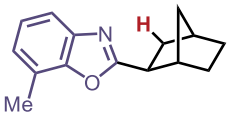

2-((1S,2S,4R)-bicyclo[2.2.1]heptan-2-yl)-7-methylbenzo[d]oxazole (2-6-2) This compound was prepared by following general procedure B using 7-methylbenzo[d]oxazole (13.3 mg, 0.10 mmol), 0.200 mL norbornene (0.10 mmol) stock solution (0.5M in toluene), **L5**-HBF_4 (3.6 mg, 5.0 μmmol), KHMDS (1.0 mg, 5.0 μmmol) and $Ni(COD)_2$ (1.4 mg, 5.0 μmmol). Purification by column chromatography eluting with ethyl acetate / hexane (0 – 10/90) afforded the desired product as a brown liquid (22.2 mg, 98% yield). $[\alpha]_D^{23}$ = -7.8 (c = 0.75, $CHCl_3$)

^{1}H NMR (700 MHz, $CDCl_3$) δ 7.28 (d, *J* =8.1 Hz, 1H), 7.15 (t, *J* =7.8 Hz, 1H), 7.07 (d, *J* =7.4 Hz, 1H), 3.01 (dd, *J* =9.2, 5.3 Hz, 1H), 2.66 (d, *J* =4.1 Hz, 1H), 2.59 (s, 3H), 2.43 (t, *J* =4.5 Hz, 1H), 2.20 – 2.15 (m, 1H), 1.75 (ddd, *J* =11.9, 9.0, 2.4 Hz, 1H), 1.69 (d, *J* =9.9 Hz, 1H), 1.63 (ddt, *J* =23.5, 11.9, 4.2 Hz, 2H), 1.42 (td, *J* =8.8, 8.4, 2.9 Hz, 1H), 1.31 (tdd, *J* =11.3, 4.1, 2.2 Hz, 1H), 1.26 (dd, *J* =9.9, 1.9 Hz, 1H).

SFC: OD-H 0-10% IPA, 3 mL/min

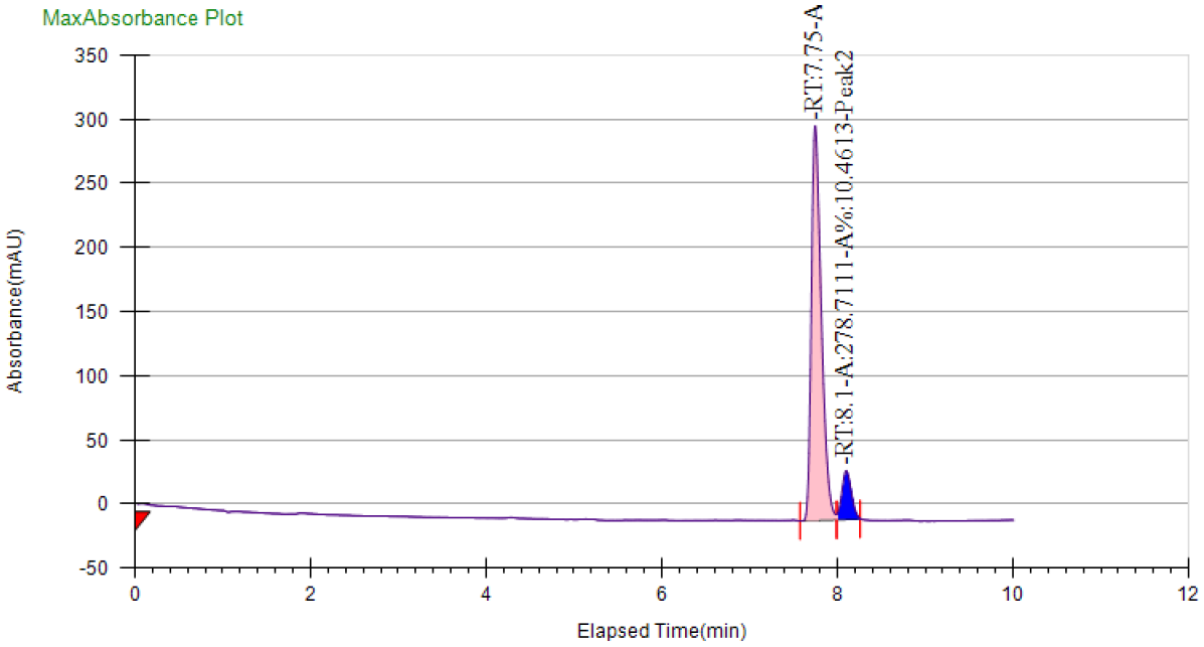

Peak Information

Peak No	% Area	Area	Ret. Time	Height	Cap. Factor
1	89.5387	2385.4875	7.75 min	307.8253	0
2	10.4613	278.7111	8.1 min	38.1135	0

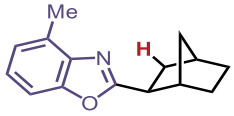

(±)

exo-2-(bicyclo[2.2.1]heptan-2-yl)-4-methylbenzo[d]oxazole (2-7-2) This compound was prepared by following general procedure A using 4-methylbenzo[d]oxazole (13.3 mg, 0.10 mmol), 0.200 mL norbornene (0.10 mmol) stock solution (0.5M in toluene) and IPr^{Me}-Ni(C_6H_{10}) (2.8 mg, 5.0 μmmol). Purification by column chromatography eluting with ethyl acetate / hexane (0 – 10/90) afforded the desired product as a colorless liquid (19.2 mg, 85% yield) ^{1}H NMR (700 MHz, $CDCl_3$) δ 7.28 (d, *J* =8.1 Hz, 1H), 7.15 (t, *J* =7.8 Hz, 1H), 7.07 (d, *J* =7.4 Hz, 1H), 3.01 (dd, *J* =9.2, 5.3 Hz, 1H), 2.66 (d, *J* =4.1 Hz, 1H), 2.59 (s, 3H), 2.43 (t, *J* =4.4 Hz, 1H), 2.20 – 2.15 (m, 1H), 1.75 (ddd, *J* =11.9, 9.0, 2.4 Hz, 1H), 1.69 (dt, *J* =9.9, 2.1 Hz, 1H), 1.68 – 1.63 (m, 1H), 1.60 (ddd, *J* =12.2, 8.0, 3.8 Hz, 1H), 1.42 (td, *J* =11.7, 11.0, 2.9 Hz, 1H), 1.33 – 1.29 (m, 1H), 1.26 (dt, *J* =9.9, 2.0 Hz, 1H). ^{13}C NMR (176 MHz, $CDCl_3$) δ 169.5, 150.6, 140.6, 129.9, 124.5, 123.9, 107.5, 42.2, 41.7, 36.5, 36.3, 35.5, 29.7, 28.7, 16.5. **HRMS (ESI+):** m/z: calculated for $C_{15}H_{17}NO$ $[M + H]^+$: 228.1383; found: 228.1390

SFC: OD-H 0-10% IPA, 3 mL/min

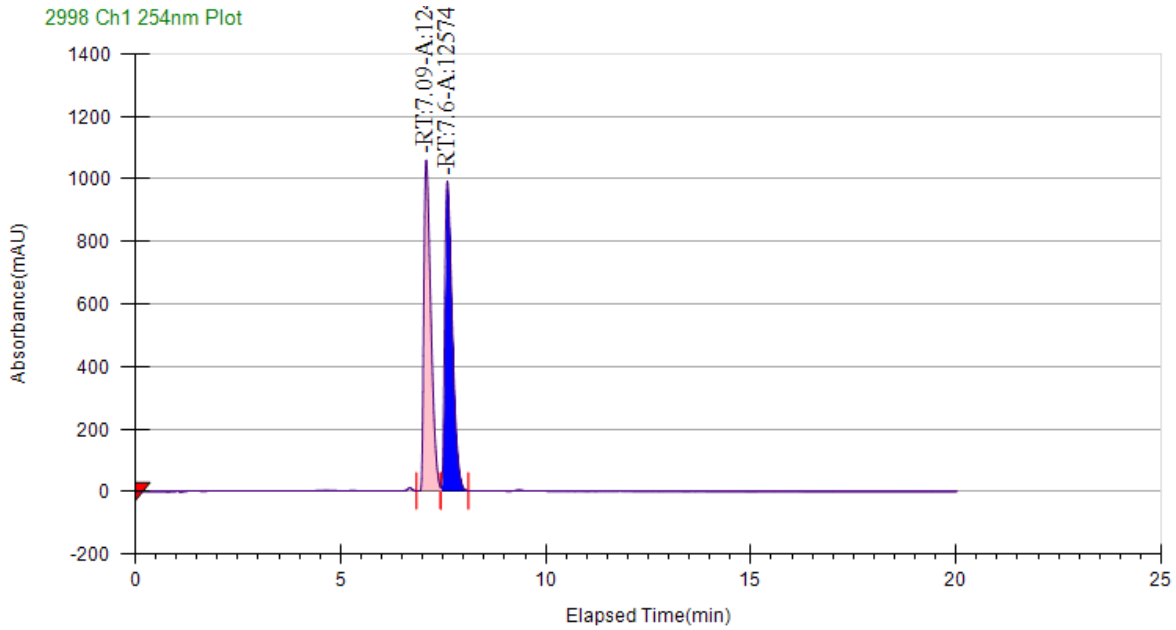

Peak Information

Peak No	% Area	Area	Ret. Time	Height	Cap. Factor
1	49.6744	12411.8078	7.09 min	1058.4315	0
2	50.3256	12574.5001	7.6 min	991.3019	0

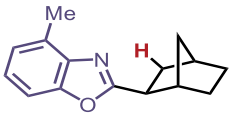

2-((1S,2S,4R)-bicyclo[2.2.1]heptan-2-yl)-4-methylbenzo[d]oxazole (2-7-2) This compound was prepared by following general procedure B using 4-methylbenzo[d]oxazole (13.3 mg, 0.10 mmol), 0.200 mL norbornene (0.10 mmol) stock solution (0.5M in toluene), **L5**-HBF_4 (3.6 mg, 5.0 μmmol), KHMDS (1.0 mg, 5.0 μmmol) and $Ni(COD)_2$ (1.4 mg, 5.0 μmmol). Purification by column chromatography eluting with ethyl acetate / hexane (0 – 10/90) afforded the desired product as a colorless liquid (18.4 mg, 81% yield). $[\alpha]_D^{23}$ = +2.1 (c = 0.50, $CHCl_3$)

^{1}H NMR (500 MHz, $CDCl_3$) δ 7.29 (d, *J* =3.8 Hz, 1H), 7.19 – 7.13 (m, 1H), 7.07 (d, *J* =9.6 Hz, 1H), 3.01 (dt, *J* =9.1, 4.4 Hz, 1H), 2.66 (s, 1H), 2.59 (s, 3H), 2.43 (d, *J* =4.3 Hz, 1H), 2.17 (dtd, *J* =12.5, 4.8, 2.9 Hz, 1H), 1.79 – 1.74 (m, 1H), 1.69 (ddt, *J* =11.6, 7.0, 3.1 Hz, 1H), 1.62 (qd, *J*

=12.0, 6.3 Hz, 2H), 1.42 (ddq, *J* =10.3, 7.3, 2.9, 2.0 Hz, 1H), 1.32 (dp, *J* =6.8, 2.4 Hz, 1H), 1.28 – 1.22 (m, 1H).

SFC: OD-H 0-10% IPA, 3 mL/min

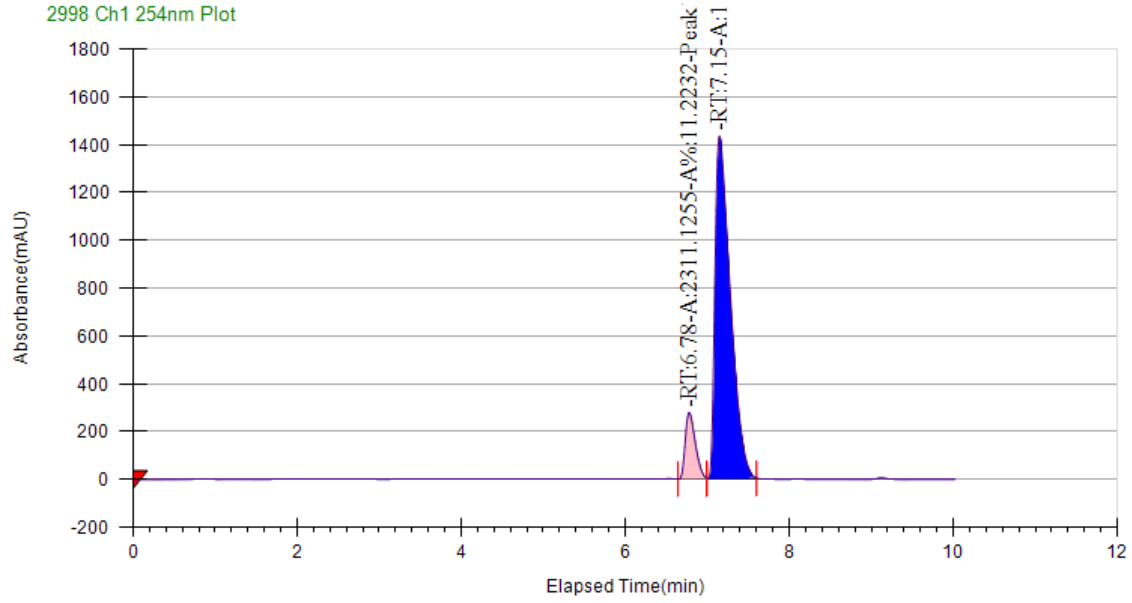

Peak Information

Peak No	% Area	Area	Ret. Time	Height	Cap. Factor
1	11.2232	2311.1255	6.78 min	277.5109	0
2	88.7768	18281.2688	7.15 min	1432.4114	0

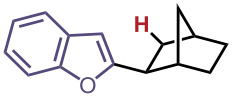

(±)

exo-2-(bicyclo[2.2.1]heptan-2-yl)benzofuran (2-8-2) This compound was prepared by following general procedure A using benzofuran (11.8 mg, 0.10 mmol), 0.200 mL norbornene (0.10 mmol) stock solution (0.5M in toluene) and IPr^{*OMe}-Ni(C_6H_{10}) (5.4 mg, 5.0 μmmol) at 60 °C. Purification by column chromatography eluting with hexane afforded the desired product as a colorless liquid (18.6 mg, 88% yield) ^1H NMR (700 MHz, $CDCl_3$) δ 7.48 (dd, *J* =7.7, 1.4 Hz, 1H), 7.41 (dd, *J* =8.0, 0.9 Hz, 1H), 7.20 (td, *J* =7.6, 1.5 Hz, 1H), 7.17 (td, *J* =7.3, 1.2 Hz, 1H), 6.34 (s, 1H), 2.87

(dd, *J* =9.0, 5.4 Hz, 1H), 2.53 (d, *J* =4.1 Hz, 1H), 2.38 (d, *J* =4.4 Hz, 1H), 1.79 (dddd, *J* =12.4, 5.4, 4.2, 2.9 Hz, 1H), 1.74 (ddd, *J* =12.2, 8.9, 2.3 Hz, 1H), 1.64 (tt, *J* =10.9, 4.1 Hz, 1H), 1.59 (dddd, *J* =16.4, 12.0, 5.1, 3.0 Hz, 1H), 1.55 (ddd, *J* =7.9, 4.0, 2.0 Hz, 1H), 1.40 (ddq, *J* =13.1, 8.4, 2.5 Hz, 1H), 1.30 (dddd, *J* =11.6, 9.6, 4.1, 2.2 Hz, 1H), 1.23 – 1.20 (m, 1H). ^{13}C NMR (176 MHz, $CDCl_3$) δ 163.7, 154.6, 128.9, 123.0, 122.3, 120.2, 110.7, 100.5, 41.9, 41.5, 36.3, 36.2, 29.6, 28.9. These spectra matched the report in literature.[165] **HRMS (APCI+):** calculated for $C_{15}H_{16}O$ [M + H]$^+$: 213.1374; found: 213.1373

SFC: OJ-H 0-1% MeOH, 3.0 mL/min

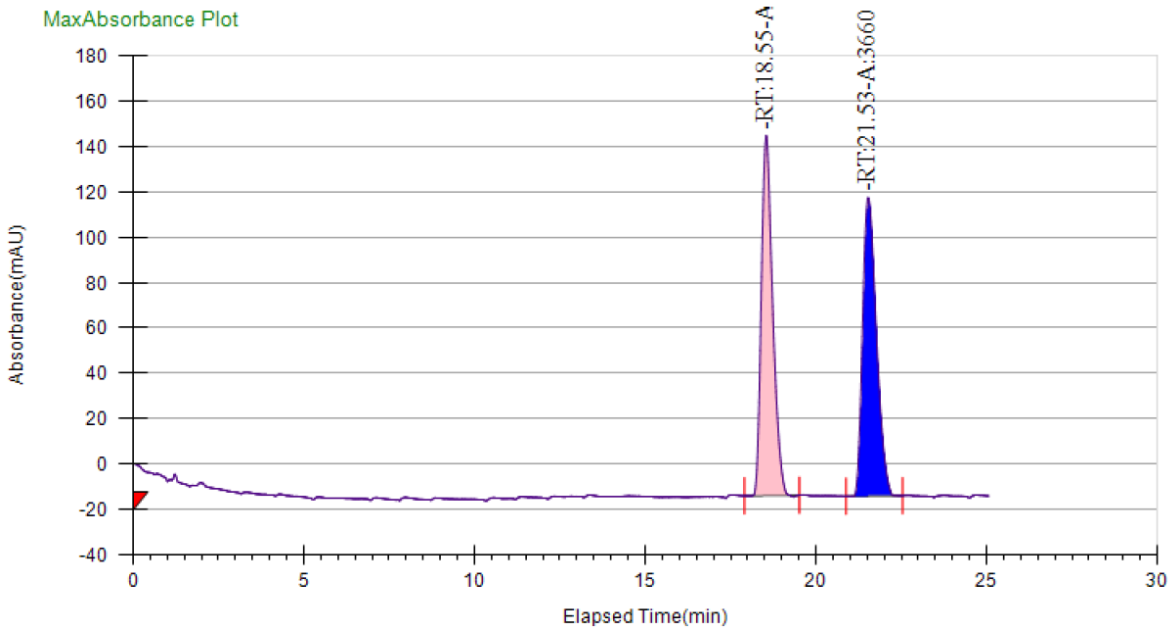

Peak Information

Peak No	% Area	Area	Ret. Time	Height	Cap. Factor
1	49.796	3630.8872	18.55 min	158.5989	18548.7167
2	50.204	3660.6312	21.53 min	131.5225	21532.0167

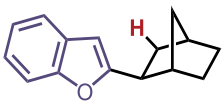

2-((1S,2S,4R)-bicyclo[2.2.1]heptan-2-yl)benzofuran (2-8-2) This compound was prepared by following general procedure B using benzofuran (11.8 mg, 0.10 mmol), 0.200 mL norbornene (0.10 mmol) stock solution (0.5M in toluene), **L5**-HBF_4 (3.6 mg, 5.0 μmmol), KHMDS (1.0 mg, 5.0 μmmol) and $Ni(COD)_2$ (1.4 mg, 5.0 μmmol) at 60 °C. Purification by column chromatography eluting with hexane afforded the desired product as a colorless liquid (21.1 mg, 99% yield). $[\alpha]_D^{24}$ = +4.9 (c = 0.25, $CHCl_3$)

^{1}H NMR (700 MHz, $CDCl_3$) δ 7.47 (dd, *J* =7.4, 1.5 Hz, 1H), 7.42 – 7.39 (m, 1H), 7.18 (dtd, *J* =20.9, 7.3, 1.3 Hz, 2H), 6.34 (s, 1H), 2.86 (dd, *J* =9.0, 5.5 Hz, 1H), 2.52 (d, *J* =4.0 Hz, 1H), 2.39 – 2.35 (m, 1H), 1.78 (ddd, *J* =5.4, 4.2, 2.9 Hz, 1H), 1.73 (ddd, *J* =12.2, 8.9, 2.3 Hz, 1H), 1.68 – 1.57 (m, 2H), 1.54 (d, *J* =10.8 Hz, 1H), 1.40 (ddq, *J* =13.1, 8.5, 2.5 Hz, 1H), 1.30 (ddd, *J* =9.2, 4.1, 2.1 Hz, 1H), 1.26 (dd, *J* =11.7, 6.9 Hz, 1H), 1.22 – 1.19 (m, 1H).

SFC: OJ-H 0-1% MeOH, 3.0 mL/min

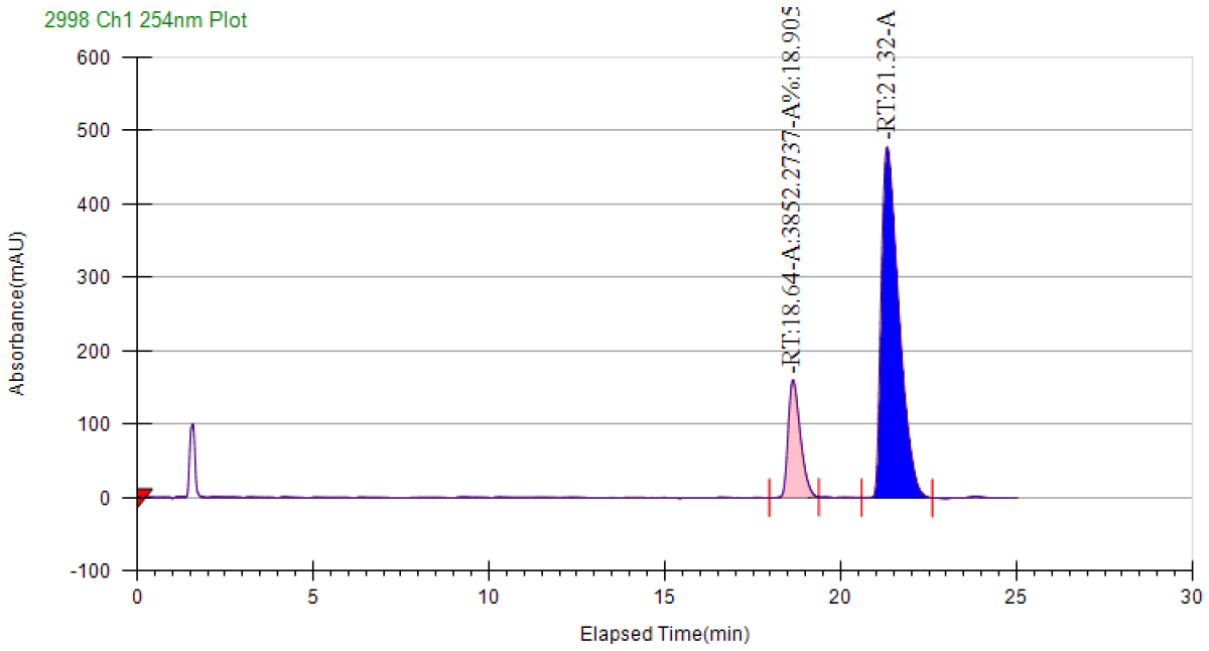

Peak Information

Peak No	% Area	Area	Ret. Time	Height	Cap. Factor
1	18.9051	3852.2737	18.64 min	160.0823	18640.6667
2	81.0949	16524.6273	21.32 min	478.5649	21315.6667

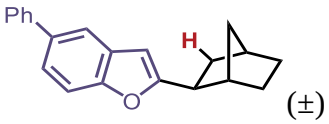

(±)

exo-2-(bicyclo[2.2.1]heptan-2-yl)-5-phenylbenzofuran (2-9-2) This compound was prepared by following general procedure A using 5-phenylbenzofuran (19.4 mg, 0.10 mmol), 0.200 mL norbornene (0.10 mmol) stock solution (0.5M in toluene) and IPr^{*OMe}-Ni(C_6H_{10}) (5.4 mg, 5.0 μmmol) at 60 °C. Purification by column chromatography eluting with hexane afforded the desired product as a white solid (28.5 mg, 99% yield) ^{1}H NMR (600 MHz, $CDCl_3$) δ 7.67 (d, *J* =1.8 Hz, 1H), 7.61 (dd, *J* =8.0, 1.5 Hz, 2H), 7.48 – 7.42 (m, 4H), 7.34 (t, *J* =7.4 Hz, 1H), 6.39 (s, 1H), 2.89

(dd, *J* =8.9, 5.4 Hz, 1H), 2.55 (d, *J* =4.1 Hz, 1H), 2.39 (d, *J* =4.3 Hz, 1H), 1.81 (dtd, *J* =12.3, 4.9, 2.9 Hz, 1H), 1.75 (ddd, *J* =12.2, 8.8, 2.3 Hz, 1H), 1.64 (dddd, *J* =21.6, 11.6, 7.6, 4.1 Hz, 2H), 1.59 – 1.55 (m, 1H), 1.41 (ddt, *J* =10.8, 8.2, 2.1 Hz, 1H), 1.31 (tdd, *J* =9.7, 4.9, 2.4 Hz, 1H), 1.23 (dt, *J* =9.9, 1.9 Hz, 1H). ^{13}C NMR (151 MHz, $CDCl_3$) δ 164.5, 154.3, 142.0, 136.1, 129.4, 128.7, 127.4, 126.7, 122.7, 118.8, 110.8, 100.8, 41.9, 41.6, 36.3, 36.2, 36.2, 29.6, 28.9. **HRMS (APCI+):** calculated for $C_{21}H_{20}O$ $[M + H]^+$: 289.1587; found: 289.1594

HPLC: IB 0.5% IPA, 1.0 mL/min

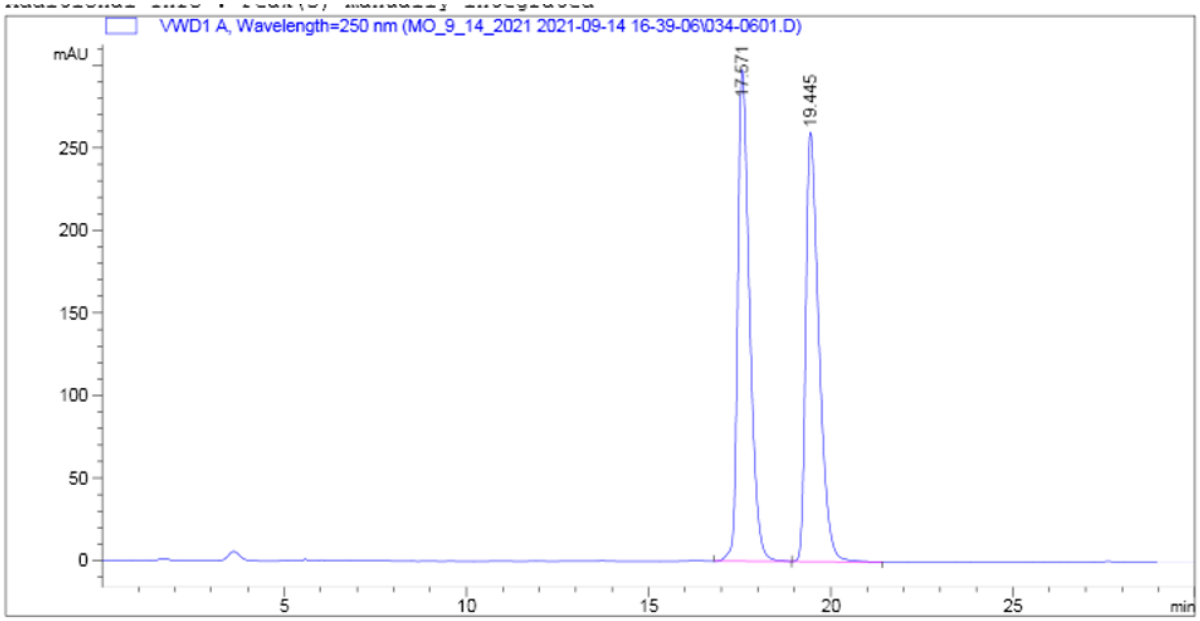

Signal 1: VWD1 A, Wavelength=250 nm

Peak #	RetTime [min]	Type	Width [min]	Area [mAU*s]	Height [mAU]	Area %
1	17.571	BB	0.3419	6713.98682	297.89890	50.7715
2	19.445	BB	0.3783	6509.93896	259.81998	49.2285

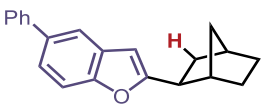

2-((1S,2S,4R)-bicyclo[2.2.1]heptan-2-yl)-5-phenylbenzofuran (2-9-2) This compound was prepared by following general procedure B using 5-phenylbenzofuran (19.4 mg, 0.10 mmol), 0.200

mL norbornene (0.10 mmol) stock solution (0.5M in toluene), **L5**-HBF_4 (3.6 mg, 5.0 μmmol), KHMDS (1.0 mg, 5.0 μmmol) and $Ni(COD)_2$ (1.4 mg, 5.0 μmmol) at 60 °C. Purification by column chromatography eluting with hexane afforded the desired product as a white solid (27.4 mg, 95% yield). $[\alpha]_D^{24}$ = +4.6 (c = 1.0, $CHCl_3$)

^{1}H NMR (500 MHz, $CDCl_3$) δ 7.68 (d, *J* =1.6 Hz, 1H), 7.62 (d, *J* =7.6 Hz, 2H), 7.46 (td, *J* =7.8, 7.2, 5.1 Hz, 4H), 7.35 (t, *J* =7.4 Hz, 1H), 6.40 (s, 1H), 2.90 (dd, *J* =8.8, 5.5 Hz, 1H), 2.56 (d, *J* =3.9 Hz, 1H), 2.40 (d, *J* =4.3 Hz, 1H), 1.86 – 1.79 (m, 1H), 1.76 (ddd, *J* =12.2, 8.9, 2.3 Hz, 1H), 1.65 (dddt, *J* =18.1, 11.2, 7.4, 3.9 Hz, 2H), 1.58 (dt, *J* =9.8, 1.9 Hz, 1H), 1.46 – 1.39 (m, 1H), 1.34 – 1.28 (m, 2H), 1.25 – 1.21 (m, 1H).

HPLC: IB 0.5% IPA, 1.0 mL/min

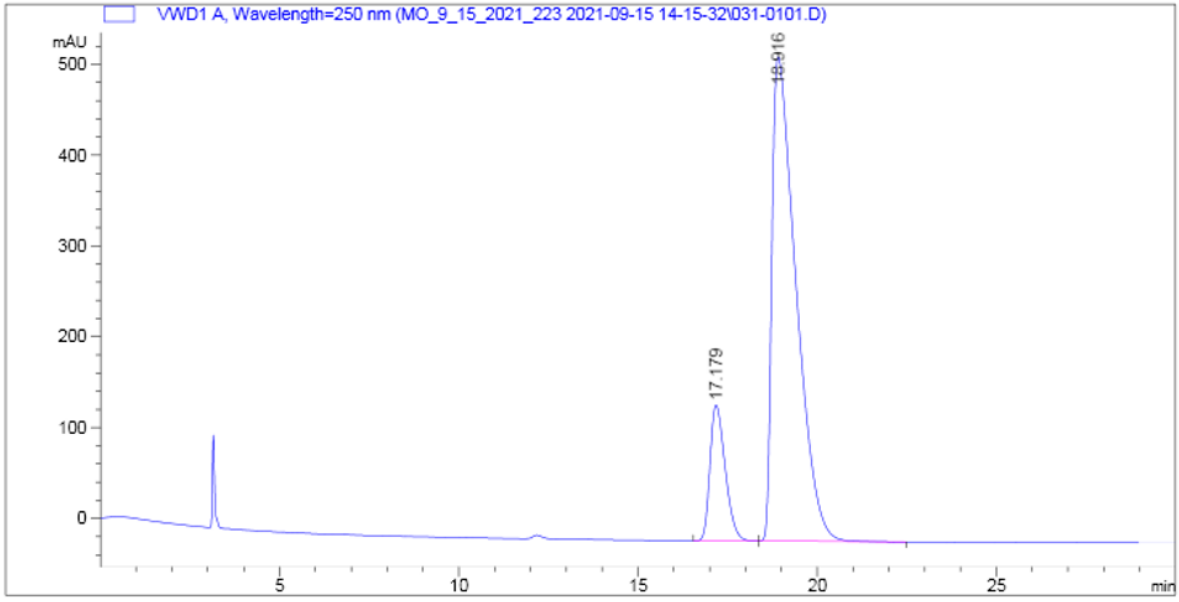

Signal 1: VWD1 A, Wavelength=250 nm

Peak #	RetTime [min]	Type	Width [min]	Area [mAU*s]	Height [mAU]	Area %
1	17.179	BB	0.4566	4414.43359	149.46901	15.1202
2	18.916	BB	0.7014	2.47813e4	533.03125	84.8798

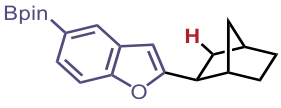

(±)

exo-2-(bicyclo[2.2.1]heptan-2-yl)-4,4,5,5-tetramethyl-1,3,2-dioxaborolane (2-10-2) This compound was prepared by following general procedure A using 2-(benzofuran-5-yl)-4,4,5,5-tetramethyl-1,3,2-dioxaborolane (24.4 mg, 0.10 mmol), 0.200 mL norbornene (0.10 mmol) stock solution (0.5M in toluene) and IPr^{*OMe}-Ni(C_6H_{10}) (5.4 mg, 5.0 μmmol) at 60 °C. Purification by column chromatography eluting with ethyl acetate / hexane (0 – 10/90) afforded the desired product as a white solid (31.4 mg, 93% yield) ^{1}H NMR (600 MHz, $CDCl_3$) δ 7.97 (s, 1H), 7.67 (dd, *J* =8.2, 1.2 Hz, 1H), 7.39 (d, *J* =8.2 Hz, 1H), 6.32 (s, 1H), 2.85 (dd, *J* =8.9, 5.4 Hz, 1H), 2.52 (d, *J* =4.0 Hz, 1H), 2.36 (d, *J* =4.3 Hz, 1H), 1.78 (dtd, *J* =12.4, 5.0, 3.0 Hz, 1H), 1.72 (ddd, *J* =12.2, 8.8, 2.3 Hz, 1H), 1.64 (ddd, *J* =11.8, 8.0, 3.7 Hz, 1H), 1.60 (ddd, *J* =11.4, 5.7, 3.4 Hz, 1H), 1.52 (dt, *J* =9.8, 2.0 Hz, 1H), 1.40 (d, *J* =9.6 Hz, 1H), 1.36 (s, 12H), 1.29 (ddd, *J* =11.7, 6.3, 3.9 Hz, 1H), 1.20 (dt, *J* =9.8, 1.9 Hz, 1H). ^{13}C NMR (151 MHz, $CDCl_3$) δ 163.7, 156.8, 129.8, 128.6, 127.5, 110.2, 100.6, 83.6, 41.9, 41.5, 36.3, 36.13, 36.11, 29.6, 28.9, 24.89, 24.87. **HRMS (APCI+):** calculated for $C_{21}H_{27}BO_3$ $[M + H]^+$: 339.2126; found: 339.2127

HPLC: IB 0.5% IPA, 1.0 mL/min

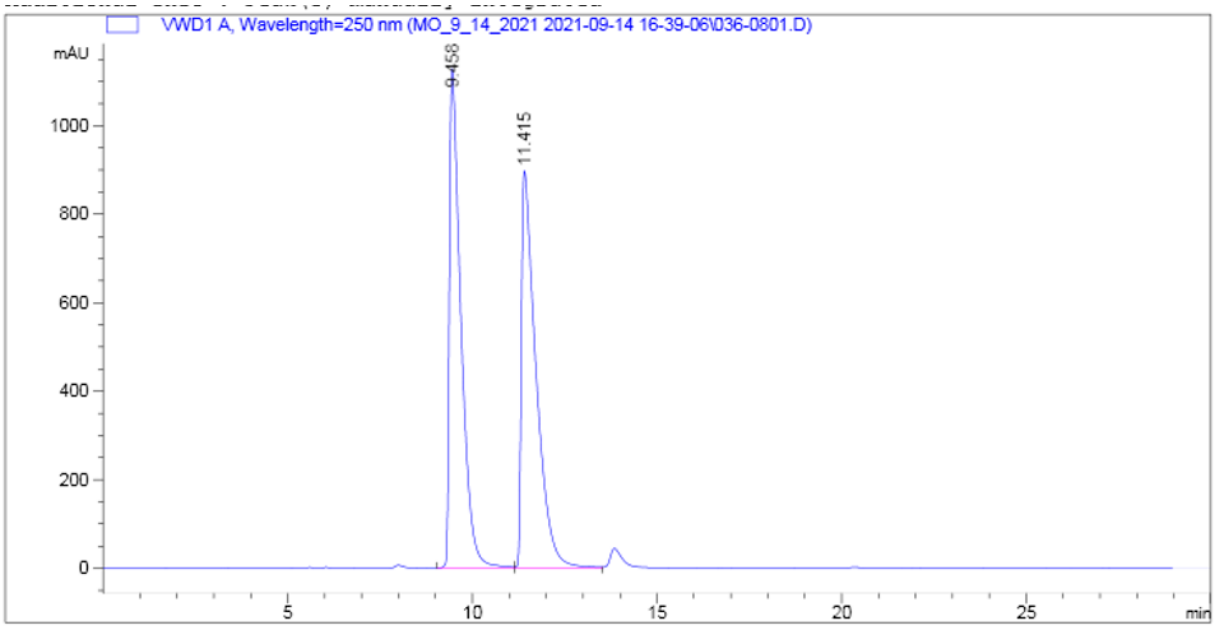

Signal 1: VWD1 A, Wavelength=250 nm

Peak #	RetTime [min]	Type	Width [min]	Area [mAU*s]	Height [mAU]	Area %
1	9.458	BV	0.3134	2.44205e4	1128.71814	49.8682
2	11.415	VV	0.3892	2.45496e4	897.38623	50.1318

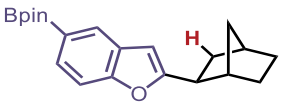

2-(2-((1S,2S,4R)-bicyclo[2.2.1]heptan-2-yl)benzofuran-5-yl)-4,4,5,5-tetramethyl-1,3,2-dioxaborolane (2-10-2) This compound was prepared by following general procedure D using 2-(benzofuran-5-yl)-4,4,5,5-tetramethyl-1,3,2-dioxaborolane (24.4 mg, 0.10 mmol), 0.200 mL norbornene (0.10 mmol) stock solution (0.5M in toluene), **L5**-HBF_4 (3.6 mg, 5.0 μmmol), KHMDS (1.0 mg, 5.0 μmmol) and $Ni(COD)_2$ (1.4 mg, 5.0 μmmol) at 60 °C. Purification by column chromatography eluting with ethyl acetate / hexane (0 – 10/90) afforded the desired product as a white solid (24.7 mg, 73% yield). $[\alpha]_D^{24}$ = +3.4 (c = 0.93, $CHCl_3$)

^{1}H NMR (500 MHz, $CDCl_3$) δ 7.97 (s, 1H), 7.67 (dd, *J* =8.2, 1.3 Hz, 1H), 7.39 (d, *J* =8.2 Hz, 1H), 6.31 (s, 1H), 2.85 (dd, *J* =8.9, 5.5 Hz, 1H), 2.52 (d, *J* =3.9 Hz, 1H), 2.36 (d, *J* =4.2 Hz, 1H), 1.81 – 1.76 (m, 1H), 1.72 (ddd, *J* =12.2, 8.8, 2.2 Hz, 1H), 1.64 (ddd, *J* =11.6, 7.8, 3.7 Hz,

1H), 1.61 – 1.58 (m, 1H), 1.52 (dt, *J* =9.8, 2.0 Hz, 1H), 1.40 (d, *J* =10.1 Hz, 1H), 1.36 (s, 12H), 1.29 (dt, *J* =9.1, 2.2 Hz, 1H), 1.20 (dt, *J* =9.9, 1.8 Hz, 1H).

HPLC: IB 0.5% IPA, 1.0 mL/min

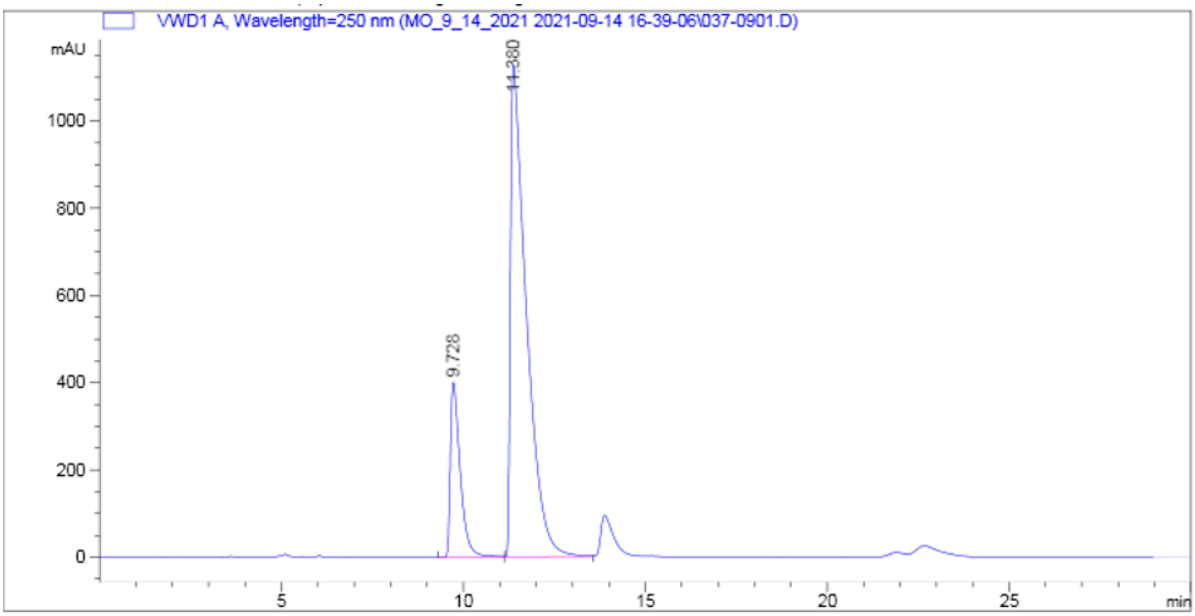

Signal 1: VWD1 A, Wavelength=250 nm

Peak #	RetTime [min]	Type	Width [min]	Area [mAU*s]	Height [mAU]	Area %
1	9.728	BV	0.2773	7495.75586	400.68835	18.0106
2	11.380	VV	0.4256	3.41228e4	1128.94373	81.9894

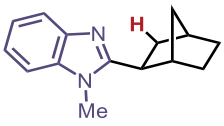

(±)

exo-2-(bicyclo[2.2.1]heptan-2-yl)-1-methyl-1*H*-benzo[d]imidazole (2-12-2) This compound was prepared by following general procedure A using 1-methyl-1*H*-benzo[d]imidazole (13.2 mg, 0.10 mmol), 0.200 mL norbornene (0.10 mmol) stock solution (0.5M in toluene) and IPr^{*OMe}-Ni(C_6H_{10}) (5.4 mg, 5.0 μmmol) at 60 °C. Purification by column chromatography eluting with methanol / DCM (0 – 10/90) afforded the desired product as a colorless liquid (22.5 mg, 99% yield). ^{1}H NMR (700 MHz, $CDCl_3$) δ 7.75 (dd, *J* =6.8, 1.7 Hz, 1H), 7.28 (dd, *J* =6.9, 1.8 Hz, 1H),

7.25 – 7.17 (m, 2H), 3.73 (s, 3H), 2.90 (dd, *J* =8.6, 4.8 Hz, 1H), 2.54 (d, *J* =4.1 Hz, 1H), 2.45 (d, *J* =4.4 Hz, 1H), 2.33 (dtd, *J* =12.3, 4.7, 3.0 Hz, 1H), 1.78 (dt, *J* =9.8, 2.0 Hz, 1H), 1.73 (ddd, *J* =11.8, 8.9, 2.4 Hz, 1H), 1.71 – 1.67 (m, 1H), 1.65 (dtd, *J* =12.2, 8.4, 7.7, 4.1 Hz, 2H), 1.46 – 1.41 (m, 1H), 1.34 (dddd, *J* =11.6, 9.5, 4.1, 2.2 Hz, 1H), 1.24 (dd, *J* =9.9, 1.1 Hz, 1H). ^{13}C NMR (176 MHz, $CDCl_3$) δ 158.6, 142.3, 136.2, 121.9, 121.5, 119.3, 108.7, 41.8, 39.9, 36.4, 36.1, 35.6, 29.8, 29.7, 29.1. **HRMS (ESI+):** m/z: calculated for $C_{15}H_{18}N_2$ $[M + H]^+$: 227.1543; found: 227.1549

HPLC: AD-H 1% IPA, 1.0 mL/min

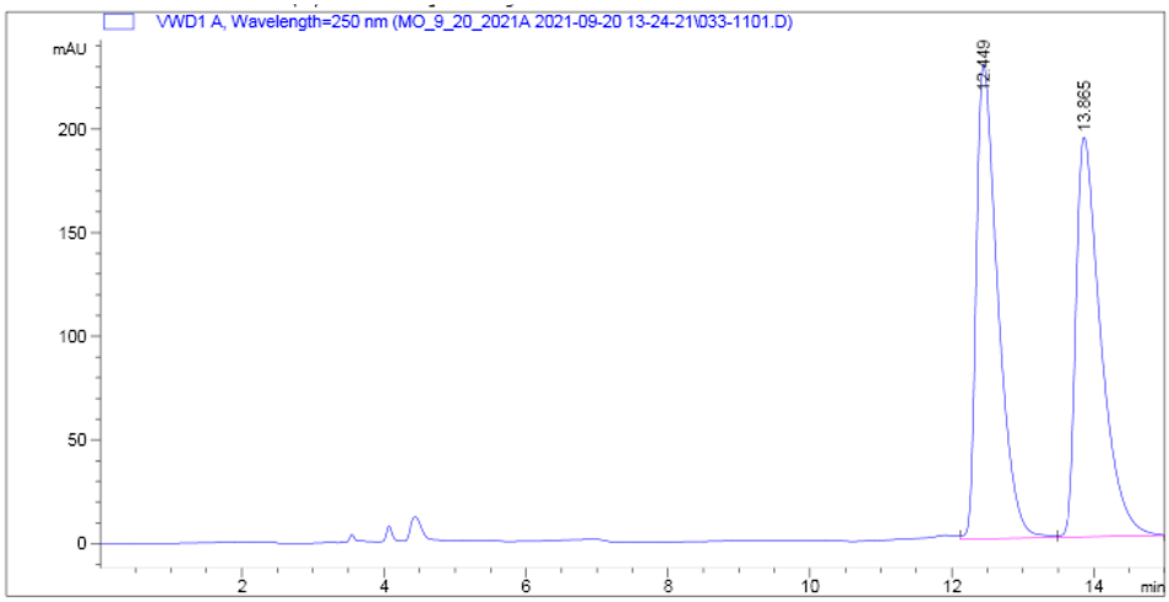

Signal 1: VWD1 A, Wavelength=250 nm

Peak #	RetTime [min]	Type	Width [min]	Area [mAU*s]	Height [mAU]	Area %
1	12.449	VV	0.3174	4842.91504	229.29883	50.7262
2	13.865	VBA	0.3622	4704.25977	193.12926	49.2738

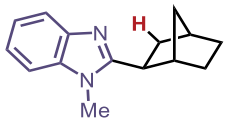

2-((1S,2S,4R)-bicyclo[2.2.1]heptan-2-yl)-1-methyl-1*H*-benzo[d]imidazole (2-12-2) This compound was prepared by following general procedure B using 1-methyl-1*H*-benzo[d]imidazole (13.2 mg, 0.10 mmol), 0.200 mL norbornene (0.10 mmol) stock solution (0.5M in toluene), **L5-**

HBF_4 (3.6 mg, 5.0 μmmol), KHMDS (1.0 mg, 5.0 μmmol) and $Ni(COD)_2$ (1.4 mg, 5.0 μmmol) at 60 °C. Purification by column chromatography eluting with methanol / DCM (0 – 10/90) afforded the desired product as a colorless liquid (16.0 mg, 71% yield). $[\alpha]_D^{24}$ = +2.6 (c = 0.50, $CHCl_3$)

^{1}H NMR (700 MHz, Chloroform-d) δ 7.75 (dd, *J* =6.7, 1.8 Hz, 1H), 7.28 (dd, *J* =6.8, 2.1 Hz, 1H), 7.24 – 7.22 (m, 1H), 7.22 – 7.20 (m, 1H), 3.72 (s, 3H), 2.89 (dd, *J* =9.0, 5.1 Hz, 1H), 2.54 (d, *J* =4.1 Hz, 1H), 2.45 (t, *J* =4.4 Hz, 1H), 2.33 (dtd, *J* =12.3, 4.7, 3.0 Hz, 1H), 1.78 (dt, *J* =9.9, 2.0 Hz, 1H), 1.73 (ddd, *J* =11.8, 8.9, 2.4 Hz, 1H), 1.68 (dt, *J* =11.2, 4.1 Hz, 1H), 1.63 (ddt, *J* =12.1, 8.1, 3.5 Hz, 1H), 1.43 (ddt, *J* =14.4, 8.5, 2.6 Hz, 1H), 1.34 (dddd, *J* =11.5, 9.4, 4.2, 2.2 Hz, 1H), 1.25 – 1.22 (m, 1H).

HPLC: AD-H 1% IPA, 1.0 mL/min

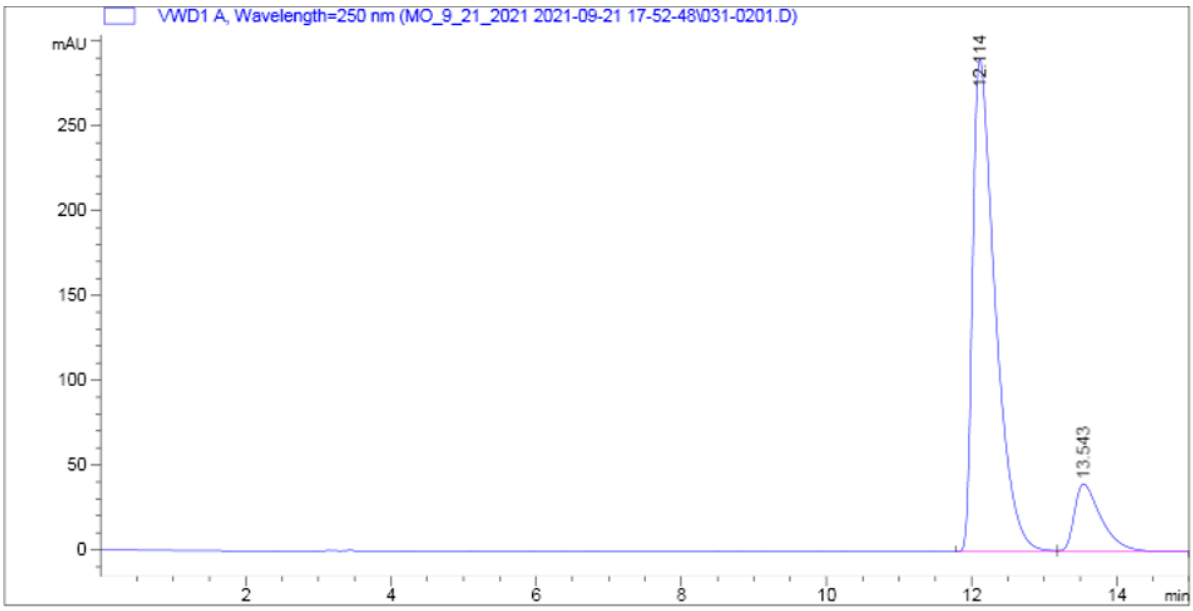

Signal 1: VWD1 A, Wavelength=250 nm

Peak #	RetTime [min]	Type	Width [min]	Area [mAU*s]	Height [mAU]	Area %
1	12.114	BV	0.3219	6240.22852	290.11194	85.8955
2	13.543	VBA	0.3815	1024.67712	39.91753	14.1045

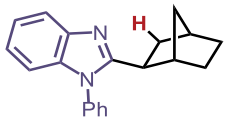

(±)

exo-2-(bicyclo[2.2.1]heptan-2-yl)-1-methyl-1*H*-benzo[d]imidazole (2-13-2) This compound was prepared by following general procedure A using 1-phenyl-1*H*-benzo[d]imidazole[166] (19.4 mg, 0.10 mmol), 0.200 mL norbornene (0.10 mmol) stock solution (0.5M in toluene) and IPr^{*OMe}-Ni(C_6H_{10}) (5.4 mg, 5.0 μmmol) at 60 °C. Purification by column chromatography eluting with methanol / DCM (0 – 10/90) afforded the desired product as an off-white solid (17.9 mg, 62% yield). ^{1}H NMR (700 MHz, $CDCl_3$) δ 7.81 (d, *J* =8.0 Hz, 1H), 7.58 (t, *J* =7.7 Hz, 2H), 7.52 (t, *J* =7.5 Hz, 1H), 7.37 (d, *J* =7.5 Hz, 2H), 7.26 – 7.23 (m, 1H), 7.17 (td, *J* =7.6, 7.1, 1.1 Hz, 1H), 7.06 (d, *J* =7.9 Hz, 1H), 2.79 – 2.75 (m, 1H), 2.46 (d, *J* =4.0 Hz, 1H), 2.40 – 2.37 (m, 1H), 2.20 (dtd, *J* =12.4, 4.9, 2.9 Hz, 1H), 1.97 (d, *J* =9.7 Hz, 1H), 1.56 – 1.47 (m, 3H), 1.25 – 1.22 (m, 1H), 1.16 (ddt, *J* =12.4, 7.9, 2.3 Hz, 1H), 1.07 (ddt, *J* =10.2, 7.5, 2.0 Hz, 1H). ^{13}C NMR (176 MHz, $CDCl_3$) δ 159.2, 142.4, 136.9, 136.3, 129.8, 128.7, 127.7, 122.4, 122.1, 119.2, 109.8, 42.7, 39.7, 37.0, 36.39, 36.35, 29.7, 28.7. **HRMS (ESI+):** m/z: calculated for $C_{20}H_{20}N_2$ $[M + H]^+$:289.1699; found: 289.1701

SFC: AD-H 0-30% IPA, 3.0 mL/min

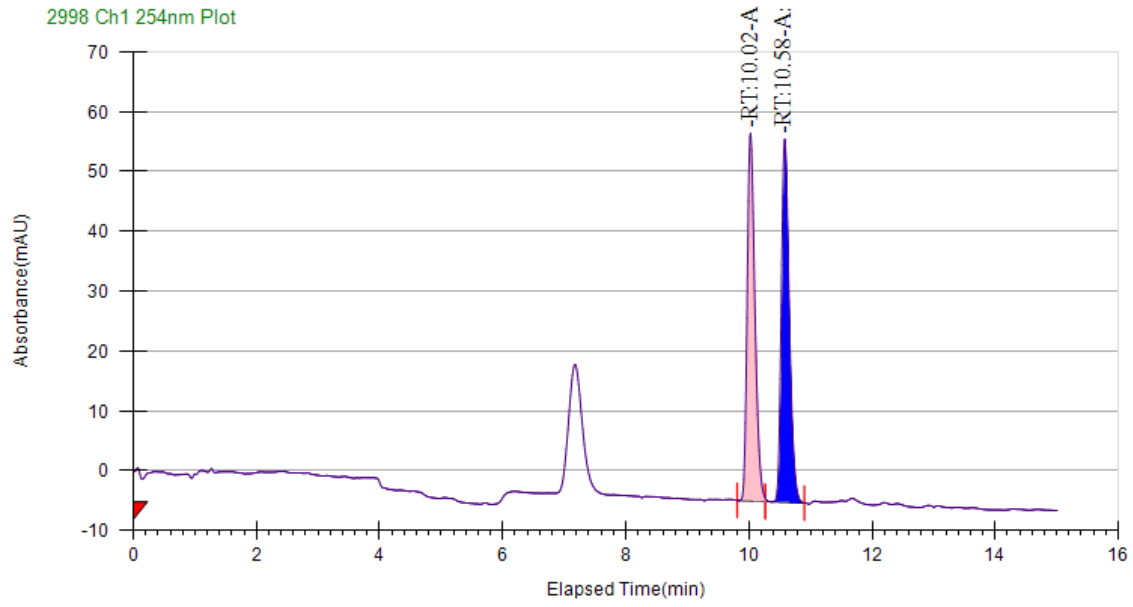

Peak Information

Peak No	% Area	Area	Ret. Time	Height	Cap. Factor
1	49.6104	525.0994	10.02 min	61.4863	10024
2	50.3896	533.3465	10.58 min	60.7765	10582.3333

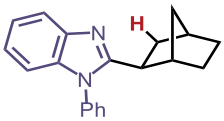

2-((1S,2S,4R)-bicyclo[2.2.1]heptan-2-yl)-1-phenyl-1*H*-benzo[d]imidazole (2-13-2) This compound was prepared by following general procedure D using 1-phenyl-1*H*-benzo[d]imidazole[166] (19.4 mg, 0.10 mmol), 0.200 mL norbornene (0.10 mmol) stock solution (0.5M in toluene), **L5**-HBF_4 (3.6 mg, 5.0 μmmol), KHMDS (1.0 mg, 5.0 μmmol) and $Ni(COD)_2$ (1.4 mg, 5.0 μmmol) at 60 °C. Purification by column chromatography eluting with methanol / DCM (0 – 10/90) afforded the desired product as an off-white solid (16.0 mg, 71% yield). $[\alpha]_D^{24}$ = +2.7 (c = 1.0, $CHCl_3$)

^{1}H NMR (600 MHz, $CDCl_3$) δ 7.81 (d, *J* =8.0 Hz, 1H), 7.58 (t, *J* =7.6 Hz, 2H), 7.52 (t, *J* =7.4 Hz, 1H), 7.37 (d, *J* =7.6 Hz, 2H), 7.27 – 7.22 (m, 1H), 7.17 (t, *J* =7.6 Hz, 1H), 7.06 (d, *J* =8.0 Hz, 1H), 2.77 (dd, *J* =9.1, 5.3 Hz, 1H), 2.46 (d, *J* =3.9 Hz, 1H), 2.39 (d, *J* =4.3 Hz, 1H), 2.20 (dtd, *J* =12.4, 4.8, 2.8 Hz, 1H), 1.97 (dt, *J* =9.9, 2.1 Hz, 1H), 1.56 – 1.46 (m, 3H), 1.23 (d, *J* =9.7 Hz, 1H), 1.16 (ddt, *J* =9.7, 4.6, 2.3 Hz, 1H), 1.09 – 1.04 (m, 1H).

SFC: AD-H 0-30% IPA, 3.0 mL/min

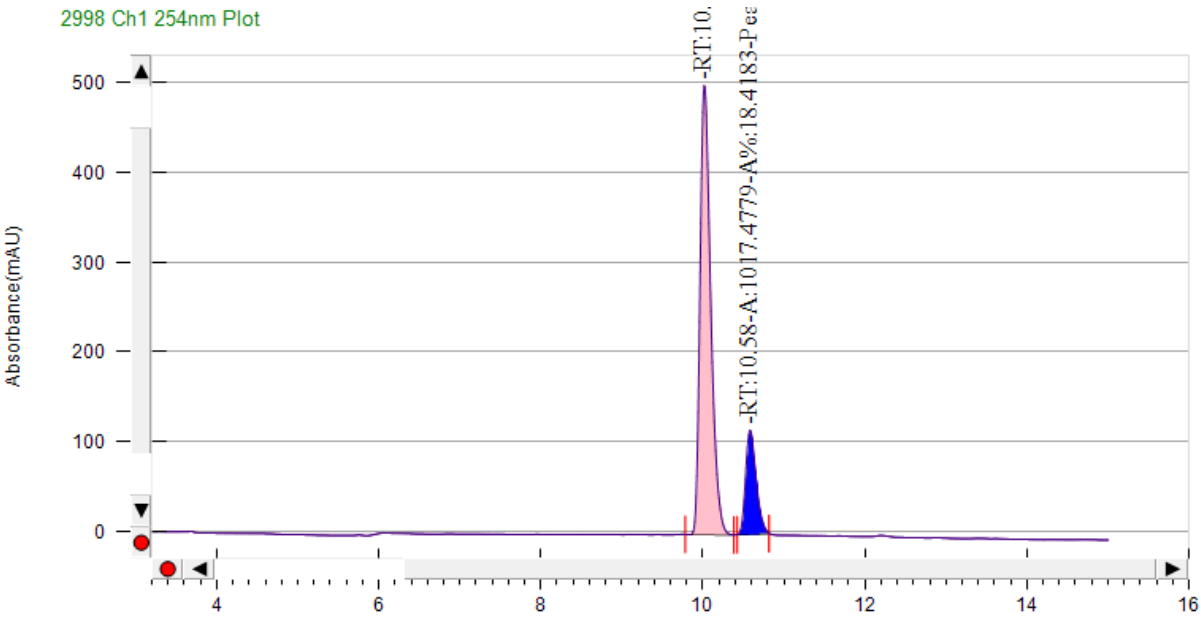

Peak Information

Peak No	% Area	Area	Ret. Time	Height	Cap. Factor
1	81.5817	4506.8014	10.02 min	499.7656	0
2	18.4183	1017.4779	10.58 min	115.8679	0

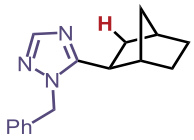

(±)

exo-1-benzyl-5-(bicyclo[2.2.1]heptan-2-yl)-1*H*-1,2,4-triazole (2-14-2) This compound was prepared by following general procedure A using 1-benzyl-1*H*-1,2,4-triazole (15.9 mg, 0.10 mmol), 0.200 mL norbornene (0.10 mmol) stock solution (0.5M in toluene) and IPr^{*OMe}-Ni(C_6H_{10}) (5.4 mg, 5.0 μmmol) at 60 °C. Purification by column chromatography eluting with methanol / DCM (0 – 10/90) afforded the desired product as a colorless liquid (16.4 mg, 65% yield). ^{1}H NMR (600 MHz, $CDCl_3$) δ 7.81 (s, 1H), 7.34 (t, *J* =7.3 Hz, 2H), 7.30 (d, *J* =7.0 Hz, 1H), 7.17 (d, *J* =7.3 Hz, 2H), 5.31 (s, 1H), 5.28 (d, *J* =15.7 Hz, 1H), 2.69 (dd, *J* =9.0, 5.1 Hz, 1H), 2.38 (d, *J* =4.1 Hz, 1H), 2.20 (d, *J* =3.5 Hz, 1H), 1.98 (dtd, *J* =12.0, 4.7, 2.3 Hz, 1H), 1.76 (dt, *J* =9.7, 2.1 Hz, 1H), 1.60 (dd, *J* =12.1, 9.2 Hz, 1H), 1.57 – 1.51 (m, 2H), 1.22 (dd, *J* =7.4, 2.3 Hz, 2H), 1.19 (dd, *J*

=9.9, 1.9 Hz, 1H). ^{13}C NMR (151 MHz, $CDCl_3$) δ 159.7, 150.1, 135.6, 128.9, 128.1, 127.2, 51.9, 42.1, 38.4, 36.7, 36.2, 36.1, 29.8, 28.7. **HRMS (ESI+):** m/z: calculated for $C_{19}H_{19}N_3$ $[M + H]^+$: 254.1652; found: 254.1648 The regiochemistry of **3m** is further clarified with HSQC and HMBC analysis.

SFC: IC 10% IPA, 3.0 mL/min

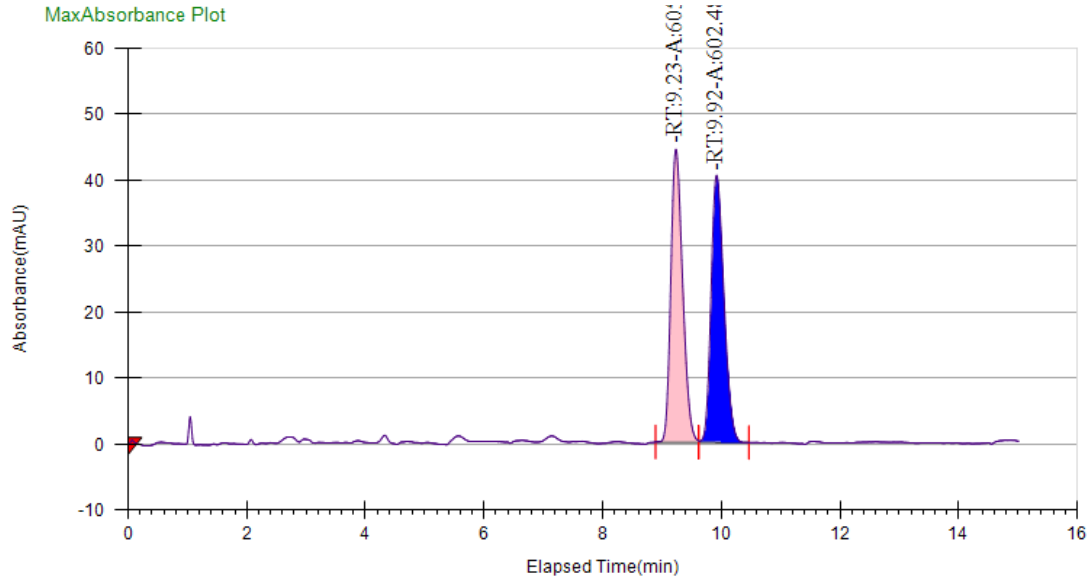

Peak Information

Peak No	% Area	Area	Ret. Time	Height	Cap. Factor
1	50.1176	605.3252	9.23 min	44.4323	9232.2
2	49.8824	602.4847	9.92 min	40.4998	9923.85

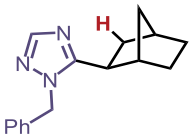

1-benzyl-5-((1S,2S,4R)-bicyclo[2.2.1]heptan-2-yl)-1*H*-1,2,4-triazole (2-14-2) This compound was prepared by following general procedure B using 1-benzyl-1*H*-1,2,4-triazole (15.9 mg, 0.10 mmol), 0.200 mL0.20 mL norbornene (0.10 mmol) stock solution (0.5M in toluene), **L5**-HBF_4 (3.6 mg, 5.0 μmmol), KHMDS (1.0 mg, 5.0 μmmol) and $Ni(COD)_2$ (1.4 mg, 5.0 μmmol) at 60 °C.

Purification by column chromatography eluting with methanol / DCM (0 – 10/90) afforded the desired product as a colorless liquid (24.1 mg, 95% yield). $[\alpha]_D^{24}$ = -1.6(c = 1.0, $CHCl_3$)

^{1}H NMR (700 MHz, $CDCl_3$) δ 7.80 (s, 1H), 7.33 (t, *J* =7.5 Hz, 2H), 7.29 (t, *J* =6.9 Hz, 1H), 7.16 (d, *J* =7.6 Hz, 2H), 5.30 (q, *J* =15.7 Hz, 2H), 2.69 (dd, *J* =9.0, 5.2 Hz, 1H), 2.37 (d, *J* =4.1 Hz, 1H), 2.22 – 2.18 (m, 1H), 1.97 (dq, *J* =12.1, 4.5 Hz, 1H), 1.77 – 1.73 (m, 1H), 1.59 (ddd, *J* =11.7, 8.8, 2.4 Hz, 1H), 1.54 (dd, *J* =8.6, 3.5 Hz, 2H), 1.22 (dd, *J* =7.8, 2.3 Hz, 2H), 1.19 – 1.16 (m, 1H).

SFC: IC 10% IPA, 3.0 mL/min

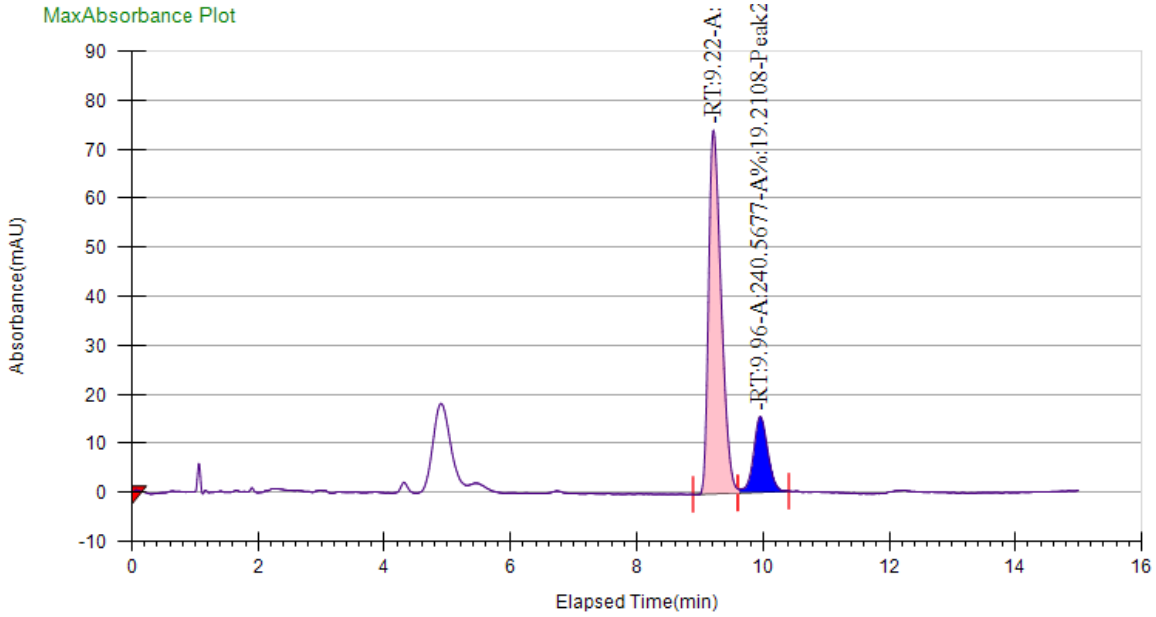

Peak Information

Peak No	% Area	Area	Ret. Time	Height	Cap. Factor
1	80.7892	1011.6848	9.22 min	74.133	0
2	19.2108	240.5677	9.96 min	15.4246	0

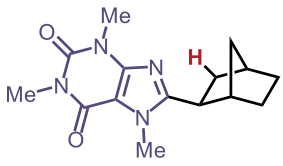

(±)

exo-8-(bicyclo[2.2.1]heptan-2-yl)-1,3,7-trimethyl-3,7-dihydro-1*H*-purine-2,6-dione (2-15-2)

This compound was prepared by following general procedure A using 1,3,7-trimethyl-3,7-dihydro-1*H*-purine-2,6-dione (19.4 mg, 0.10 mmol), 0.200 mL norbornene (0.10 mmol) stock solution (0.5M in toluene) and IPr^{*OMe}-Ni(C_6H_{10}) (5.4 mg, 5.0 μmmol) at 60 °C. Purification by column chromatography eluting with methanol / DCM (0 – 10/90) afforded the desired product as a white solid (28.5 mg, 99% yield). ^{1}H NMR (700 MHz, $CDCl_3$) δ 3.89 (s, 3H), 3.55 (s, 3H), 3.38 (s, 3H), 2.71 (dd, *J* =9.0, 5.2 Hz, 1H), 2.41 (d, *J* =4.2 Hz, 1H), 2.38 (d, *J* =3.8 Hz, 1H), 2.16 (dtd, *J* =12.2, 4.7, 2.7 Hz, 1H), 1.72 (dt, *J* =9.8, 2.0 Hz, 1H), 1.68 – 1.58 (m, 3H), 1.37 (ddd, *J* =10.6, 6.9, 2.5 Hz, 1H), 1.29 (tt, *J* =9.1, 2.0 Hz, 1H), 1.21 (dt, *J* =9.6, 1.9 Hz, 1H). ^{13}C NMR (176 MHz, $CDCl_3$) δ 157.8, 155.4, 151.7, 147.6, 107.5, 42.0, 39.1, 36.2, 36.0, 35.6, 31.5, 29.8, 29.6, 28.8, 27.8. **HRMS (ESI+):** m/z: calculated for $C_{15}H_{20}N_4O_2$ $[M + H]^+$: 289.1659; found: 289.1666.

SFC: AD-H 0-30% IPA, 3.0 mL/min

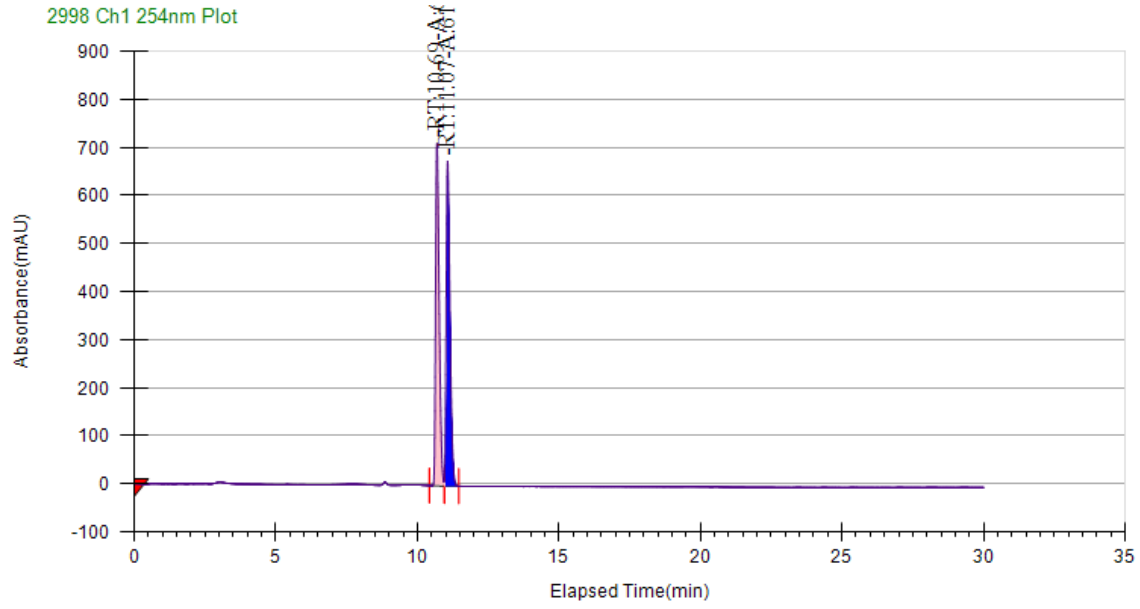

Peak Information

Peak No	% Area	Area	Ret. Time	Height	Cap. Factor
1	50.1184	6227.673	10.69 min	712.1068	10690.6667
2	49.8816	6198.2598	11.07 min	675.6294	11065.6667

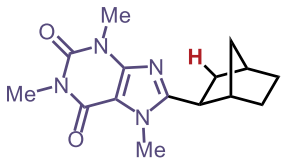

8-((1S,2S,4R)-bicyclo[2.2.1]heptan-2-yl)-1,3,7-trimethyl-3,7-dihydro-1*H*-purine-2,6-dione

(2-15-2) This compound was prepared by following general procedure B using 1,3,7-trimethyl-3,7-dihydro-1*H*-purine-2,6-dione (19.4 mg, 0.10 mmol), 0.200 mL norbornene (0.10 mmol) stock solution (0.5M in toluene), **L5**-HBF_4 (3.6 mg, 5.0 μmmol), KHMDS (1.0 mg, 5.0 μmmol) and $Ni(COD)_2$ (1.4 mg, 5.0 μmmol) at 60 °C. Purification by column chromatography eluting with methanol / DCM (0 – 10/90) afforded the desired product as a white solid (24.8 mg, 86% yield). $[\alpha]_D^{24}$ = -6.7 (c = 1.0, $CHCl_3$)

^{1}H NMR (600 MHz, $CDCl_3$) δ 3.89 (s, 3H), 3.55 (s, 3H), 3.38 (s, 3H), 2.71 (dd, *J* =9.0, 5.2 Hz, 1H), 2.41 (d, *J* =4.2 Hz, 1H), 2.38 (d, *J* =3.8 Hz, 1H), 2.15 (dtd, *J* =12.1, 4.6, 2.6 Hz, 1H), 1.75 – 1.69 (m, 1H), 1.64 (dddd, *J* =16.6, 12.7, 9.3, 3.1 Hz, 3H), 1.38 – 1.33 (m, 1H), 1.31 – 1.24 (m, 1H), 1.20 (ddd, *J* =9.9, 2.5, 1.4 Hz, 1H).

SFC: AD-H 0-30% IPA, 3.0 mL/min

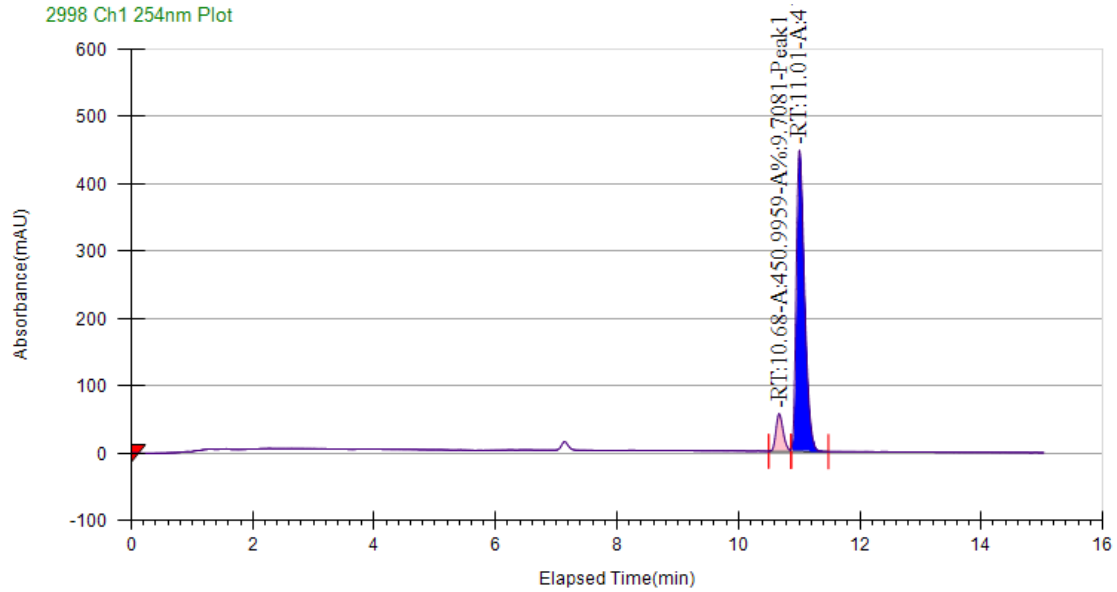

Peak Information

Peak No	% Area	Area	Ret. Time	Height	Cap. Factor
1	9.7081	450.9959	10.68 min	55.6396	10674
2	90.2919	4194.5863	11.01 min	447.4019	11007.3333

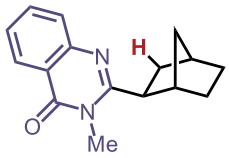

(±)

exo-2-(bicyclo[2.2.1]heptan-2-yl)-3-methylquinazolin-4(3*H*)-one (2-16-2) This compound was prepared by following general procedure A using 3-methylquinazolin-4(3*H*)-one (16.0 mg, 0.10 mmol 1), 0.200 mL norbornene (0.10 mmol) stock solution (0.5M in toluene) and IPr^{*OMe}-$Ni(C_6H_{10})$ (5.4 mg, 5.0 μmmol) at 60 °C. Purification by column chromatography eluting with methanol / DCM (0 – 10/90) afforded the desired product as a colorless liquid (16.1 mg, 63% yield). ^{1}H NMR (600 MHz, $CDCl_3$) δ 8.25 (dd, *J* =8.1, 1.6 Hz, 1H), 7.69 (ddd, *J* =8.5, 7.0, 1.6 Hz, 1H), 7.64 (dd, *J* =8.2, 1.4 Hz, 1H), 7.41 (ddd, *J* =8.1, 7.0, 1.3 Hz, 1H), 3.65 (s, 3H), 2.84 (dd, *J* =8.9, 5.4 Hz, 1H), 2.59 (d, *J* =3.8 Hz, 1H), 2.41 (d, *J* =4.3 Hz, 1H), 2.32 – 2.27 (m, 1H), 1.76 (dt, *J* =9.8, 2.0 Hz, 1H), 1.71 – 1.67 (m, 1H), 1.66 – 1.62 (m, 2H), 1.42 – 1.38 (m, 1H), 1.34 (dt, *J* =9.0, 2.0 Hz, 1H), 1.22 (ddd, *J* =9.7, 2.6, 1.4 Hz, 1H). ^{13}C NMR (151 MHz, $CDCl_3$) δ 163.1, 158.9, 147.1, 133.8, 127.3, 126.6, 126.1, 120.0, 45.9, 41.7, 36.4, 36.0, 35.5, 30.4, 29.8, 29.1. **HRMS (ESI+):** m/z: calculated for $C_{16}H_{18}N_2O$ $[M + H]^+$: 255.1491; found: 255.1493.

HPLC: IA 1% IPA, 1.0 mL/min

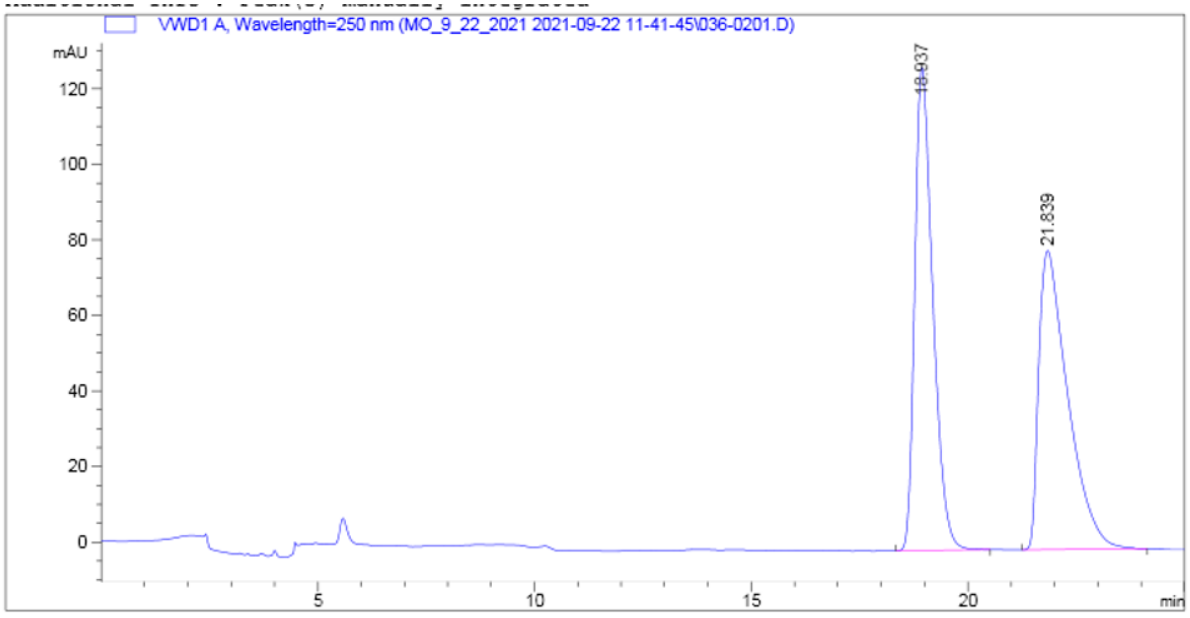

Signal 1: VWD1 A, Wavelength=250 nm

Peak #	RetTime [min]	Type	Width [min]	Area [mAU*s]	Height [mAU]	Area %
1	18.937	BB	0.4372	3692.70996	127.76348	50.0153
2	21.839	BB	0.6832	3690.45166	79.11037	49.9847

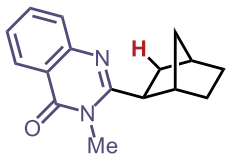

2-((1S,2S,4R)-bicyclo[2.2.1]heptan-2-yl)-3-methylquinazolin-4(3*H*)-one (2-16-2) This compound was prepared by following general procedure B using 3-methylquinazolin-4(3*H*)-one (16.0 mg, 0.10 mmol), 0.200 mL norbornene (0.10 mmol) stock solution (0.5M in toluene), **L5**-HBF_4 (3.6 mg, 5.0 μmmol), KHMDS (1.0 mg, 5.0 μmmol) and $Ni(COD)_2$ (1.4 mg, 5.0 μmmol) at 60 °C. Purification by column chromatography eluting with methanol / DCM (0 – 10/90) afforded the desired product as a colorless liquid (13.4 mg, 53% yield). $[\alpha]_D^{24}$ = +6.6 (c = 0.87, $CHCl_3$) ^{1}H NMR (700 MHz, $CDCl_3$) δ 8.24 (d, *J* =8.0 Hz, 1H), 7.69 (t, *J* =7.6 Hz, 1H), 7.64 (d, *J* =8.1 Hz, 1H), 7.41 (t, *J* =7.5 Hz, 1H), 3.64 (s, 3H), 2.83 (dd, *J* =8.8, 5.5 Hz, 1H), 2.59 (d, *J* =3.8 Hz,

1H), 2.41 (d, *J* =4.3 Hz, 1H), 2.28 (ddt, *J* =9.6, 4.9, 2.4 Hz, 1H), 1.76 (dd, *J* =9.7, 2.0 Hz, 1H), 1.64 (ddd, *J* =12.0, 8.7, 2.6 Hz, 3H), 1.42 – 1.37 (m, 1H), 1.35 – 1.32 (m, 1H), 1.24 – 1.21 (m, 1H).

HPLC: IA 1% IPA, 1.0 mL/min

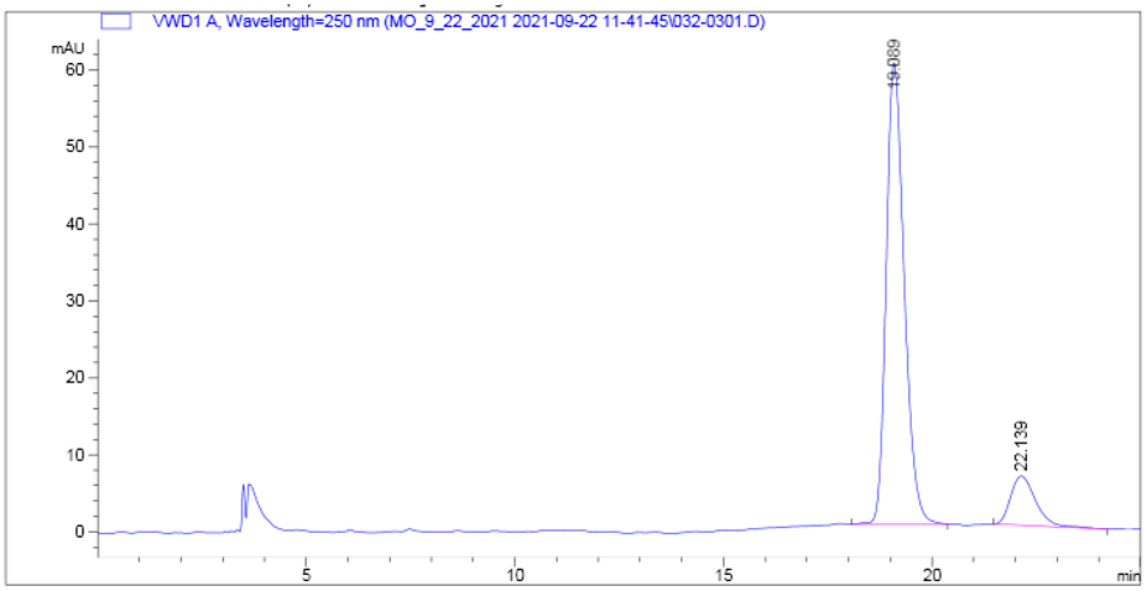

Signal 1: VWD1 A, Wavelength=250 nm

Peak #	RetTime [min]	Type	Width [min]	Area [mAU*s]	Height [mAU]	Area %
1	19.089	BB	0.4608	1796.77539	59.92706	87.0931
2	22.139	BB	0.6421	266.27670	6.36441	12.9069

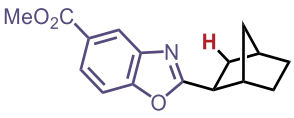

(±)

exo-2-(bicyclo[2.2.1]heptan-2-yl)methyl benzo[d]oxazole-5-carboxylate (2-17-2) This compound was prepared by following general procedure A using methyl benzo[d]oxazole-5-carboxylate (17.7 mg, 0.10 mmol), 0.200 mL norbornene (0.10 mmol) stock solution (0.5M in toluene) and IPr^{Me}-Ni(C_6H_{10}) (2.8 mg, 5.0 μmmol). Purification by column chromatography eluting with ethyl acetate / hexane (0 – 10/90) afforded the desired product as a colorless liquid (19.6 mg, 72% yield) ^{1}H NMR (600 MHz, $CDCl_3$) δ 8.35 (d, *J* =1.6 Hz, 1H), 8.03 (dd, *J* =8.5, 1.7

Hz, 1H), 7.48 (d, *J* =8.5 Hz, 1H), 3.93 (s, 3H), 2.99 (dd, *J* =9.1, 5.2 Hz, 1H), 2.68 (d, *J* =4.2 Hz, 1H), 2.43 (d, *J* =4.4 Hz, 1H), 2.16 (dtd, *J* =12.5, 4.8, 3.1 Hz, 1H), 1.77 (ddd, *J* =12.1, 9.0, 2.4 Hz, 1H), 1.68 (dd, *J* =7.3, 4.9 Hz, 1H), 1.66 – 1.62 (m, 2H), 1.62 – 1.57 (m, 1H), 1.42 (ddq, *J* =11.4, 8.6, 2.5 Hz, 1H), 1.32 (dtd, *J* =9.4, 5.0, 4.5, 2.6 Hz, 1H), 1.28 – 1.26 (m, 1H). ^{13}C NMR (151 MHz, $CDCl_3$) δ 171.9, 166.9, 153.9, 141.4, 126.5, 126.4, 121.6, 110.0, 52.2, 42.1, 41.6, 36.4, 36.3, 35.4, 29.6, 28.7. **HRMS (ESI+):** m/z: calculated for $C_{16}H_{17}NO_3$ $[M + H]^+$: 272.1281; found: 272.1286

HPLC: OJ-H 1% IPA, 1.0 mL/min

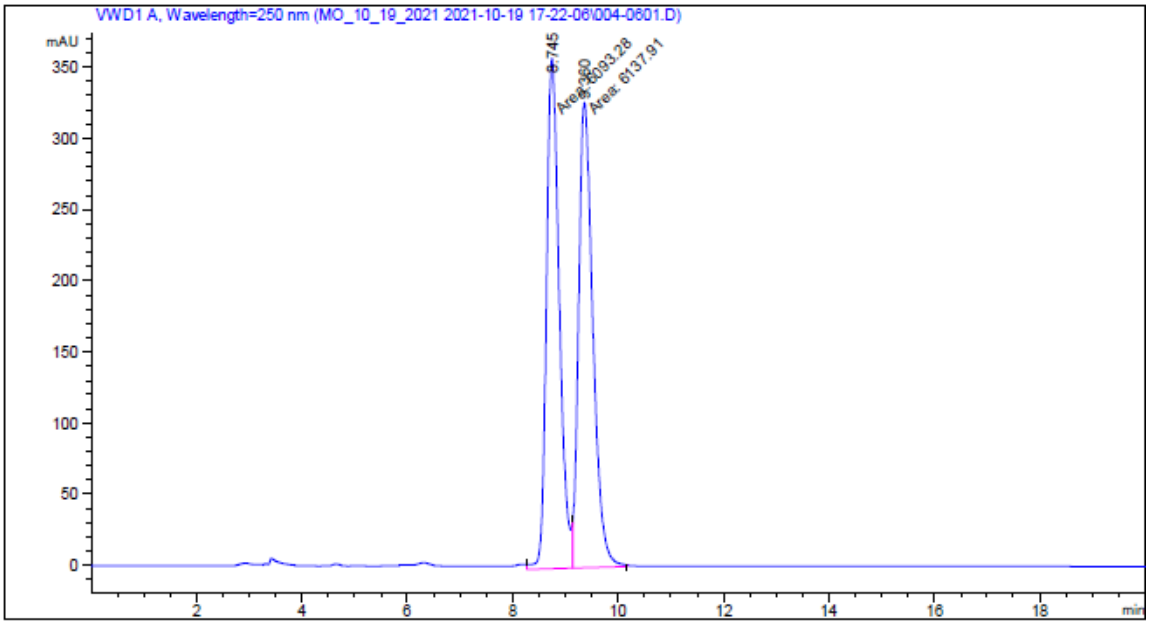

Signal 1: VWD1 A, Wavelength=250 nm

Peak #	RetTime [min]	Type	Width [min]	Area [mAU*s]	Height [mAU]	Area %
1	8.745	MF	0.2834	6093.28076	358.40262	49.8175
2	9.360	FM	0.3130	6137.91260	326.87424	50.1825

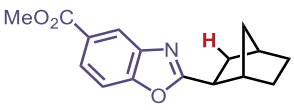

2-(bicyclo[2.2.1]heptan-2-yl)methyl benzo[d]oxazole-5-carboxylate (2-17-2) This compound was prepared by following general procedure C using methyl benzo[d]oxazole-5-carboxylate (17.7

mg, 0.10 mmol), 0.200 mL norbornene (0.10 mmol) stock solution (0.5M in toluene), **L5-Ni(C_6H_{10})** (7.7 mg, 10 μmmol). Purification by column chromatography eluting with ethyl acetate / hexane (0 – 10/90) afforded the desired product as a colorless liquid (15.3 mg, 56% yield). $[\alpha]_D^{23}$ = +4.9 (c = 0.74, $CHCl_3$)

^{1}H NMR (700 MHz, $CDCl_3$) δ 8.35 (s, 1H), 8.04 (d, *J* =8.5 Hz, 1H), 7.49 (d, *J* =8.5 Hz, 1H), 3.94 (s, 3H), 3.00 (dd, *J* =9.2, 5.3 Hz, 1H), 2.69 (d, *J* =4.2 Hz, 1H), 2.44 (d, *J* =4.4 Hz, 1H), 2.19 – 2.14 (m, 1H), 1.78 (ddd, *J* =12.1, 9.1, 2.4 Hz, 1H), 1.69 (dt, *J* =12.3, 4.4 Hz, 1H), 1.65 (dd, *J* =11.5, 3.1 Hz, 1H), 1.61 (dq, *J* =8.1, 4.0 Hz, 1H), 1.42 (ddd, *J* =11.7, 7.3, 4.3 Hz, 1H), 1.35 – 1.30 (m, 1H), 1.28 (d, *J* =10.0 Hz, 1H).

HPLC: OJ-H 1% IPA, 1.0 mL/min

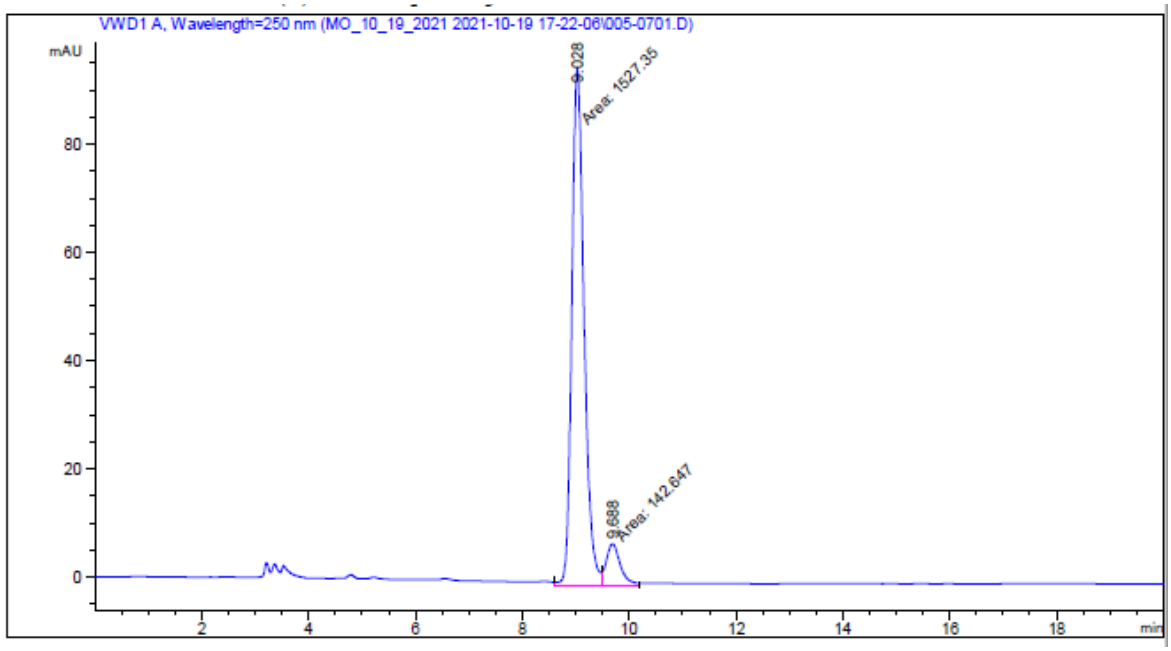

Signal 1: VWD1 A, Wavelength=250 nm

Peak #	RetTime [min]	Type	Width [min]	Area [mAU*s]	Height [mAU]	Area %
1	9.028	MF	0.2662	1527.34888	95.64279	91.4583
2	9.688	FM	0.3067	142.64662	7.75095	8.5417

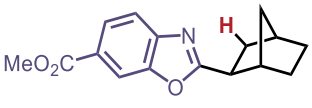

(±)

exo-methyl 2-bicyclo[2.2.1]heptan-2-yl)benzo[d]oxazole-6-carboxylate (2-18-2) This compound was prepared by following general procedure A using methyl benzo[*d*]oxazole-6-carboxylate (17.7 mg, 0.1 mmol), 0.200 mL norbornene (0.10 mmol) stock solution (0.5M in toluene) and IMes-Ni(C_6H_{10}) (2.3 mg, 5.0 μmmol). Purification by column chromatography eluting with ethyl acetate / hexane (0 – 10/90) afforded the desired product as a colorless liquid (21.5 mg, 79% yield) ^{1}H NMR (700 MHz, $CDCl_3$) δ 8.15 (d, *J* =1.0 Hz, 1H), 8.02 (dd, *J* =8.3, 1.5 Hz, 1H), 7.67 (d, *J* =8.3 Hz, 1H), 3.94 (s, 3H), 3.01 (dd, *J* =9.5, 4.3 Hz, 1H), 2.69 (d, *J* =4.2 Hz, 1H), 2.43 (d, *J* =4.5 Hz, 1H), 2.16 (ddd, *J* =12.5, 8.1, 5.1 Hz, 1H), 1.78 (ddd, *J* =12.1, 9.0, 2.4 Hz, 1H), 1.70 – 1.66 (m, 1H), 1.64 (dd, *J* =10.0, 1.9 Hz, 1H), 1.63 – 1.58 (m, 1H), 1.45 – 1.40 (m, 1H), 1.32 (dddd, *J* =11.7, 9.3, 4.4, 2.2 Hz, 1H), 1.28 (dd, *J* =10.0, 1.1 Hz, 1H). ^{13}C NMR (176 MHz, $CDCl_3$) δ 173.4, 166.8, 150.5, 145.3, 126.5, 125.8, 119.1, 111.9, 52.3, 42.1, 41.7, 36.5, 36.3, 35.4, 29.6, 28.7. **HRMS (ESI+):** m/z: calculated for $C_{16}H_{17}NO_3$ $[M + H]^+$: 272.1281; found: 272.1282

SFC: AS-H 5% IPA, 3.0 mL/min

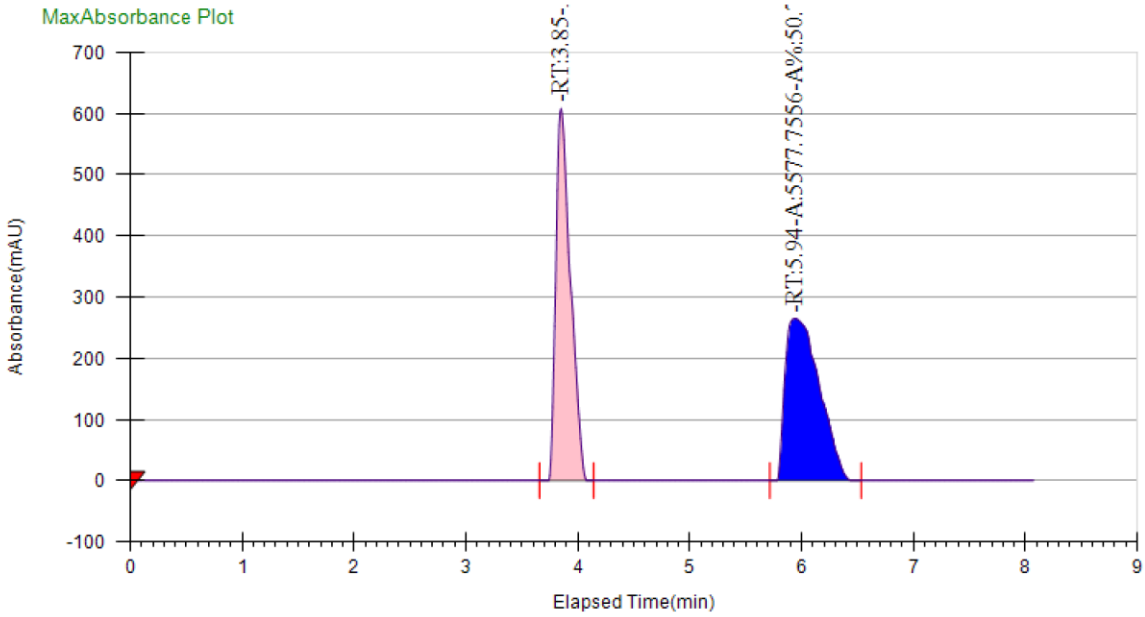

Peak Information

Peak No	% Area	Area	Ret. Time	Height	Cap. Factor
1	49.2498	5412.8632	3.85 min	608.3302	3848.95
2	50.7502	5577.7556	5.94 min	265.0042	5940.5833

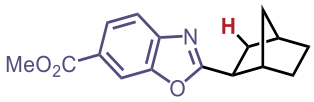

methyl 2-((1S,2S,4R)-bicyclo[2.2.1]heptan-2-yl)benzo[d]oxazole-6-carboxylate (2-18-2) This compound was prepared by following general procedure C using methyl benzo[d]oxazole-6-carboxylate (17.7 mg, 0.10 mmol), 0.200 mL norbornene (0.10 mmol) stock solution (0.5M in toluene), **L5**-Ni(C_6H_{10}) (7.7 mg, 10 μmmol). Purification by column chromatography eluting with ethyl acetate / hexane (0 – 10/90) afforded the desired product as a colorless liquid (10.9 mg, 40% yield). $[\alpha]_D^{23}$ = -4.8 (c = 0.36, $CHCl_3$)

^{1}H NMR (700 MHz, $CDCl_3$) δ 8.16 (d, *J* =1.5 Hz, 1H), 8.03 (dd, *J* =8.3, 1.5 Hz, 1H), 7.68 (d, *J* =8.3 Hz, 1H), 3.95 (s, 3H), 3.02 (dd, *J* =9.0, 5.4 Hz, 1H), 2.70 (d, *J* =4.2 Hz, 1H), 2.46 – 2.43 (m, 1H), 2.17 (dtd, *J* =12.6, 4.8, 3.2 Hz, 1H), 1.79 (ddd, *J* =12.1, 9.1, 2.4 Hz, 1H), 1.71 – 1.67 (m,

1H), 1.66 – 1.64 (m, 1H), 1.63 (s, 1H), 1.46 – 1.41 (m, 1H), 1.34 (ddd, *J* =9.6, 4.4, 2.4 Hz, 1H), 1.29 (ddt, *J* =10.0, 2.6, 1.5 Hz, 1H).

SFC: AS-H 5% IPA, 3.0 mL/min

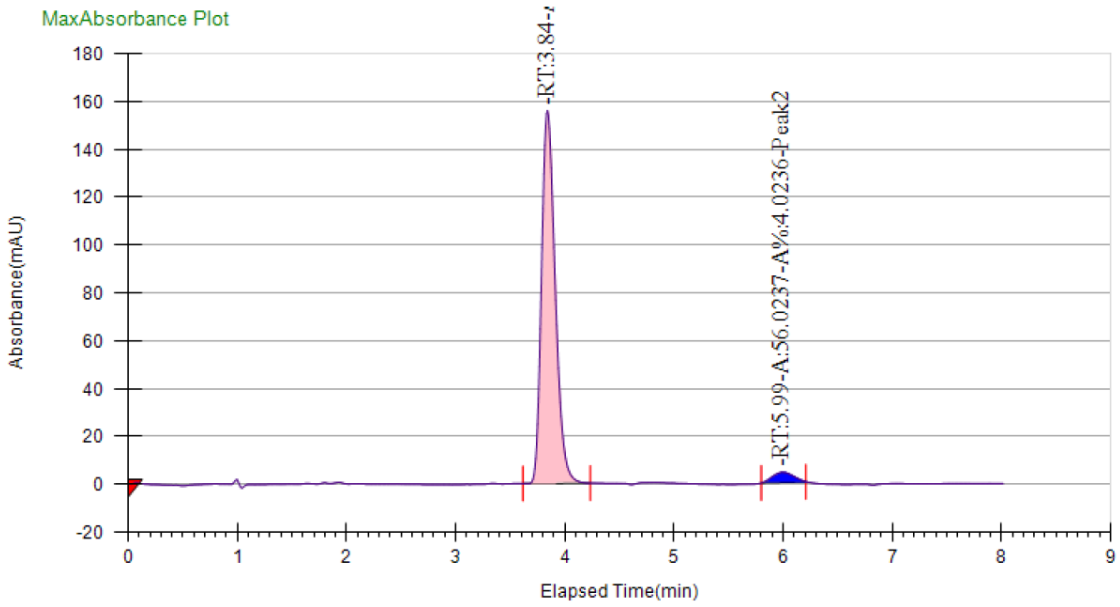

Peak Information

Peak No	% Area	Area	Ret. Time	Height	Cap. Factor
1	95.9764	1336.3497	3.84 min	155.7445	0
2	4.0236	56.0237	5.99 min	4.2322	0

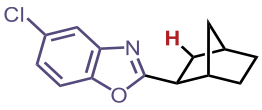

(±)

exo-2-((1S,2S,4R)-bicyclo[2.2.1]heptan-2-yl)-5-chlorobenzo[d]oxazole (2-19-2) This compound was prepared by following general procedure A using 5-chlorobenzo[d]oxazole (15.3 mg, 0.10 mmol), 0.200 mL norbornene (0.10 mmol) stock solution (0.5M in toluene) and IMes-Ni(C_6H_{10}) (4.5 mg, 10 μmmol). Purification by column chromatography eluting with ethyl acetate / hexane (0 – 10/90) afforded the desired product as a colorless liquid (21.7 mg, 88% yield) ^{1}H NMR (700 MHz, $CDCl_3$) δ 7.63 (d, *J* =2.1 Hz, 1H), 7.37 (d, *J* =8.6 Hz, 1H), 7.24 (dd, *J* =8.6, 2.1

Hz, 1H), 2.99 – 2.95 (m, 1H), 2.66 (d, *J* =4.2 Hz, 1H), 2.43 (t, *J* =4.4 Hz, 1H), 2.14 (ddt, *J* =12.6, 4.7, 2.4 Hz, 1H), 1.76 (ddd, *J* =12.1, 9.1, 2.4 Hz, 1H), 1.69 – 1.59 (m, 3H), 1.43 – 1.39 (m, 1H), 1.31 (dddd, *J* =9.3, 7.2, 4.5, 2.1 Hz, 1H), 1.28 – 1.25 (m, 1H). ^{13}C NMR (176 MHz, $CDCl_3$) δ 172.0, 149.4, 142.5, 129.4, 124.6, 119.6, 110.9, 42.1, 41.6, 36.4, 36.3, 35.4, 29.6, 28.7. **HRMS (ESI+):** m/z: calculated for $C_{14}H_{14}ClNO$ $[M + H]^+$: 248.0837; found: 248.0842

HPLC: OJ-H 0.5% IPA, 1.0 mL/min

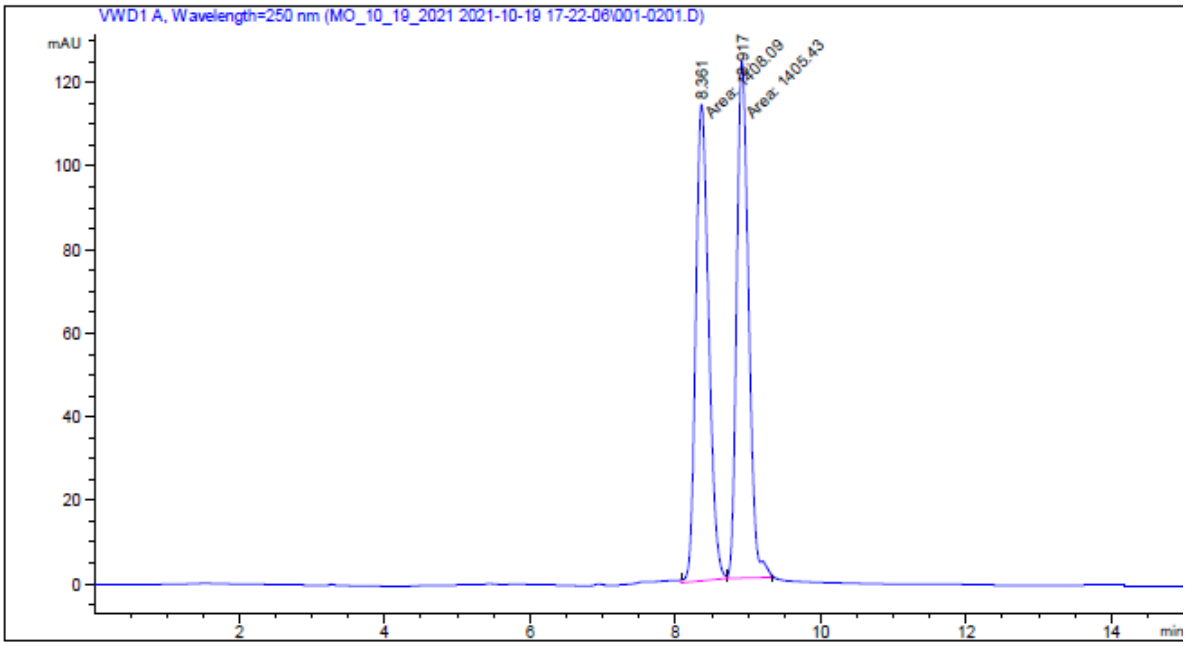

Signal 1: VWD1 A, Wavelength=250 nm

Peak #	RetTime [min]	Type	Width [min]	Area [mAU*s]	Height [mAU]	Area %
1	8.361	MM	0.2059	1408.08618	113.95872	50.0472
2	8.917	MM	0.1894	1405.43127	123.69727	49.9528

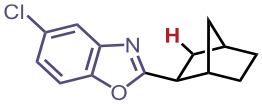

2-((1S,2S,4R)-bicyclo[2.2.1]heptan-2-yl)-5-chlorobenzo[d]oxazole (2-19-2)

This compound was prepared by following general procedure C using 5-chlorobenzo[d]oxazole (15.3 mg, 0.10 mmol), 0.200 mL norbornene (0.10 mmol) stock solution (0.5M in toluene), **L5-**

Ni(C_6H_{10}) (7.7 mg, 10 μmmol). Purification by column chromatography eluting with ethyl acetate / hexane (0 – 10/90) afforded the desired product as a colorless liquid (15.0 mg, 61% yield). $[\alpha]_D^{23}$ = +2.4 (c = 0.75, $CHCl_3$)

^{1}H NMR (600 MHz, $CDCl_3$) δ 7.63 (d, *J* =2.1 Hz, 1H), 7.37 (d, *J* =8.5 Hz, 1H), 7.25 (dd, *J* =8.6, 2.1 Hz, 1H), 2.97 (dd, *J* =9.2, 5.2 Hz, 1H), 2.67 (d, *J* =4.2 Hz, 1H), 2.43 (t, *J* =4.3 Hz, 1H), 2.14 (ddt, *J* =12.5, 4.7, 2.4 Hz, 1H), 1.76 (ddd, *J* =12.1, 9.1, 2.4 Hz, 1H), 1.70 – 1.64 (m, 1H), 1.64 – 1.62 (m, 1H), 1.61 (dd, *J* =7.0, 3.1 Hz, 1H), 1.42 (ddq, *J* =11.4, 8.5, 2.5 Hz, 1H), 1.32 (ddd, *J* =9.1, 4.1, 2.1 Hz, 1H), 1.27 (dq, *J* =10.3, 1.9 Hz, 1H).

HPLC: OJ-H 0.5% IPA, 1.0 mL/min

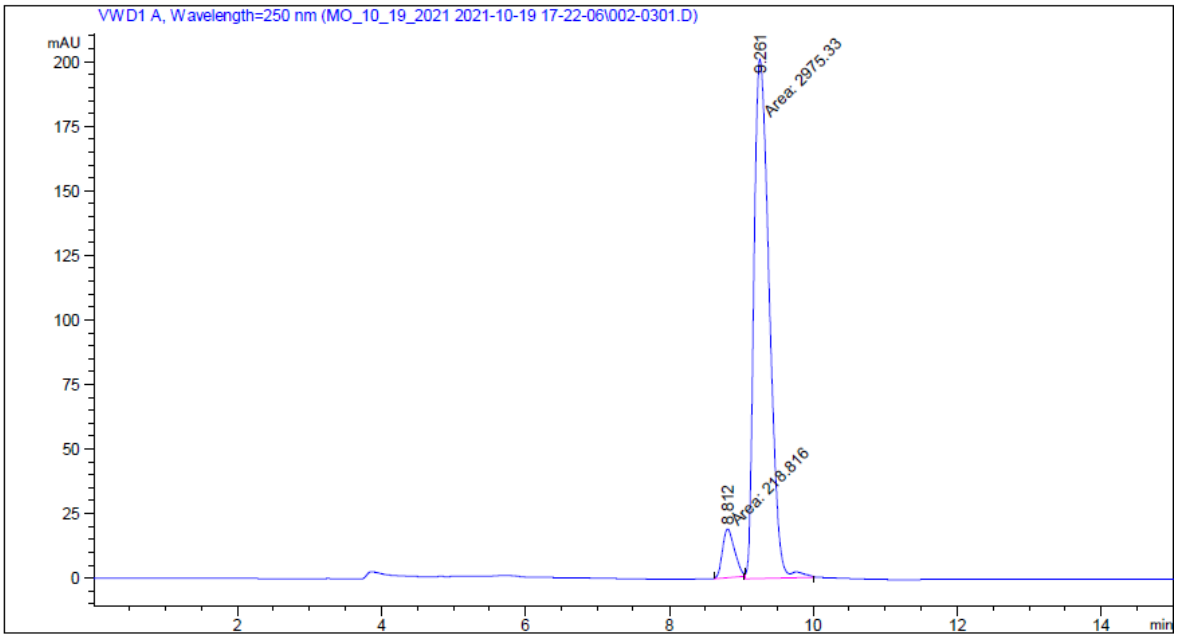

Signal 1: VWD1 A, Wavelength=250 nm

Peak #	RetTime [min]	Type	Width [min]	Area [mAU*s]	Height [mAU]	Area %
1	8.812	MM	0.1934	218.81644	18.85947	6.8505
2	9.261	MM	0.2467	2975.32959	201.02385	93.1495

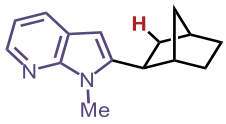

(±)

exo-2-(bicyclo[2.2.1]heptan-2-yl)-1-methyl-1*H*-pyrrolo[2,3-*b*]pyridine (2-22-2) This compound was prepared by following general procedure A using 1-methyl-1*H*-pyrrolo[2,3-*b*]pyridine (13.2 mg, 0.10 mmol), 0.400 mL norbornene (0.20 mmol) stock solution (0.5M in toluene) and IPr^{*OMe}-Ni(C_6H_{10}) (5.4 mg, 5.0 μmmol) at 100 °C. Purification by column chromatography eluting with ethyl acetate / hexane (0 – 10/90) afforded the desired product as a colorless liquid (16.0 mg, 71% yield). ^{1}H NMR (600 MHz, $CDCl_3$) δ 8.23 (dd, *J* =4.8, 1.6 Hz, 1H), 7.78 (dd, *J* =7.7, 1.6 Hz, 1H), 6.99 (dd, *J* =7.7, 4.7 Hz, 1H), 6.16 (d, *J* =1.0 Hz, 1H), 3.80 (s, 3H), 2.86 (dd, *J* =8.8, 5.4 Hz, 1H), 2.45 (d, *J* =4.0 Hz, 1H), 2.41 – 2.38 (m, 1H), 1.80 (ddd, *J* =11.4, 8.8, 2.3 Hz, 1H), 1.76 – 1.73 (m, 1H), 1.68 (ddd, *J* =15.8, 7.8, 4.1 Hz, 1H), 1.63 (ddd, *J* =11.5, 4.0, 2.9 Hz, 1H), 1.60 (dq, *J* =9.7, 2.3 Hz, 1H), 1.43 (tt, *J* =10.7, 2.9 Hz, 1H), 1.33 (dddd, *J* =11.7, 9.7, 4.0, 2.2 Hz, 1H), 1.24 – 1.21 (m, 1H). ^{13}C NMR (151 MHz, $CDCl_3$) δ 148.8, 146.9, 141.4, 127.2, 120.4, 115.4, 94.9, 41.7, 39.8, 37.3, 36.6, 36.0, 29.9, 28.9, 28.2. **HRMS (ESI+):** m/z: calculated for $C_{15}H_{18}N_2$ $[M + H]^+$: 227.1543; found: 227.1548

HPLC: AD-H 1% IPA, 1.0 mL/min

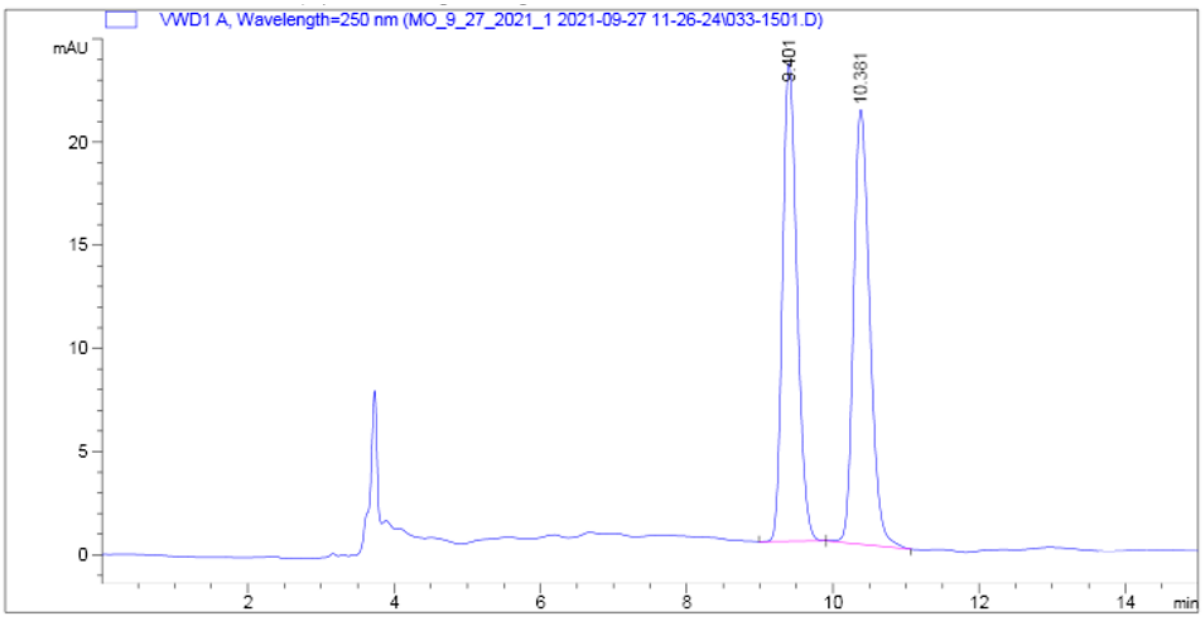

Signal 1: VWD1 A, Wavelength=250 nm

Peak #	RetTime [min]	Type	Width [min]	Area [mAU*s]	Height [mAU]	Area %
1	9.401	BB	0.2132	317.99963	23.16196	49.4847
2	10.381	BB	0.2388	324.62207	21.06830	50.5153

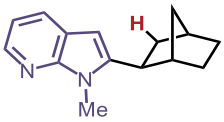

2-((1S,2S,4R)-bicyclo[2.2.1]heptan-2-yl)-1-methyl-1*H*-pyrrolo[2,3-*b*]pyridine (2-22-2) This compound was prepared by following general procedure C using 1-methyl-1*H*-pyrrolo[2,3-*b*]pyridine (13.2 mg, 0.10 mmol), 0.400 mL norbornene (0.20 mmol) stock solution (0.5M in toluene), **L5**-Ni(C_6H_{10}) (7.7 mg, 10 μmmol) at 60 °C. Purification by column chromatography eluting with ethyl acetate / hexane (0 – 10/90) afforded the desired product as a colorless liquid (11.3 mg, 50% yield). $[\alpha]_D^{24}$ = +7.1 (c = 0.78, $CHCl_3$)

^{1}H NMR (700 MHz, Chloroform-*d*) δ 8.23 (dd, *J* =4.7, 1.6 Hz, 1H), 7.78 (dd, *J* =7.7, 1.6 Hz, 1H), 6.99 (dd, *J* =7.7, 4.7 Hz, 1H), 6.16 (d, *J* =1.0 Hz, 1H), 3.80 (s, 3H), 2.86 (dd, *J* =8.9, 5.4 Hz, 1H), 2.45 (d, *J* =4.1 Hz, 1H), 2.41 (d, *J* =4.3 Hz, 1H), 1.80 (ddd, *J* =11.5, 8.8, 2.3 Hz, 1H), 1.74 (dtd,

J =8.2, 4.2, 2.1 Hz, 1H), 1.71 – 1.64 (m, 2H), 1.60 (dt, *J* =9.8, 2.0 Hz, 1H), 1.43 (ddt, *J* =11.2, 8.8, 2.5 Hz, 1H), 1.33 (dddd, *J* =11.7, 9.5, 4.2, 2.1 Hz, 1H), 1.23 (ddt, *J* =8.3, 2.5, 1.5 Hz, 1H).

HPLC: AD-H 1% IPA, 1.0 mL/min

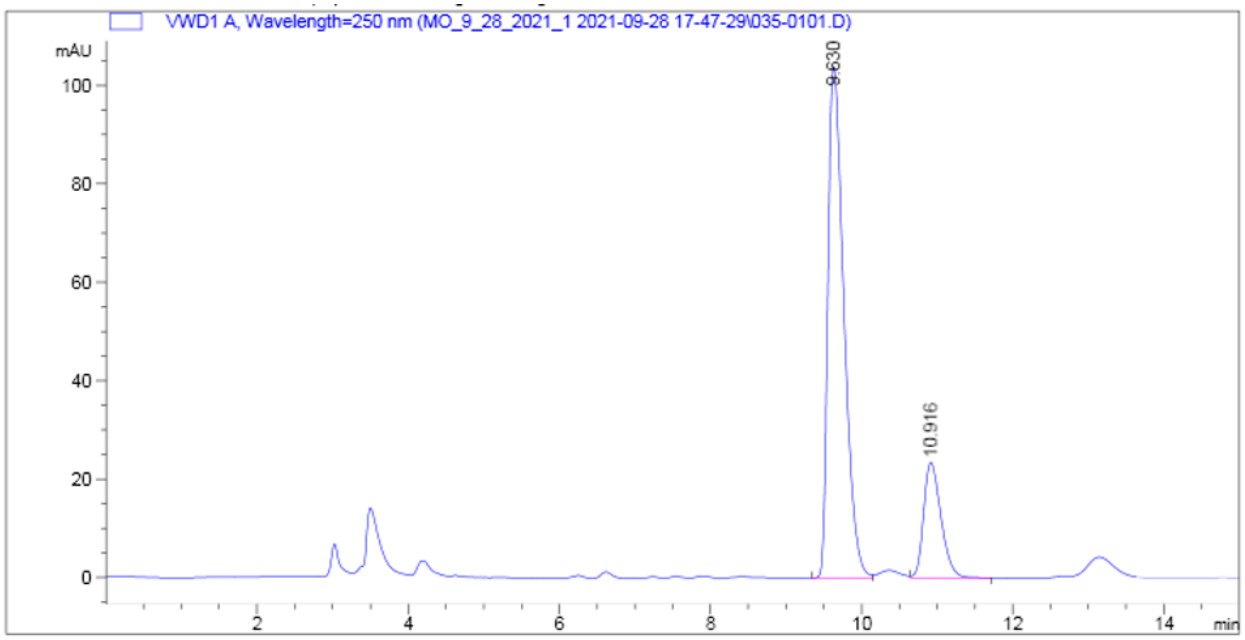

Signal 1: VWD1 A, Wavelength=250 nm

Peak #	RetTime [min]	Type	Width [min]	Area [mAU*s]	Height [mAU]	Area %
1	9.630	BV	0.2263	1515.28601	103.82971	80.2955
2	10.916	VB	0.2454	371.85120	23.40131	19.7045

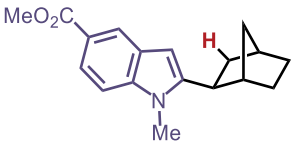

(±)

exo methyl 2-(bicyclo[2.2.1]heptan-2-yl)-1-methyl-1*H*-indole-5-carboxylate (2-20-2) This compound was prepared by following general procedure A using methyl 1-methyl-1*H*-indole-5-carboxylate (18.9 mg, 0.10 mmol), 0.400 mL norbornene (0.20 mmol) stock solution (0.5M in toluene) and IPr^{*OMe}-Ni(C_6H_{10}) (5.4 mg, 5.0 μmmol) at 100 °C. Purification by column chromatography eluting with ethyl acetate / hexane (0 – 10/90) afforded the desired product as a colorless liquid (20.3 mg, 72% yield). ^{1}H NMR (700 MHz, $CDCl_3$) δ 8.31 (d, *J* =1.6 Hz, 1H), 7.88

(dd, *J* =8.6, 1.7 Hz, 1H), 7.28 (d, *J* =4.0 Hz, 1H), 6.32 (s, 1H), 3.94 (s, 3H), 3.71 (s, 3H), 2.83 (dd, *J* =8.9, 5.4 Hz, 1H), 2.45 (d, *J* =4.1 Hz, 1H), 2.42 (d, *J* =4.3 Hz, 1H), 1.82 (ddd, *J* =11.4, 8.8, 2.3 Hz, 1H), 1.77 – 1.73 (m, 1H), 1.72 – 1.67 (m, 1H), 1.67 – 1.64 (m, 1H), 1.63 – 1.62 (m, 1H), 1.44 (tt, *J* =11.2, 2.6 Hz, 1H), 1.34 (dddd, *J* =11.6, 9.5, 4.2, 2.1 Hz, 1H), 1.25 (dt, *J* =9.9, 1.9 Hz, 1H). ^{13}C NMR (176 MHz, $CDCl_3$) δ 168.4, 147.8, 140.1, 127.2, 122.8, 122.1, 121.1, 108.2, 98.5, 51.7, 41.8, 39.7, 37.6, 36.6, 36.0, 30.0, 29.9, 28.9. **HRMS (ESI+):** m/z: calculated for $C_{18}H_{21}NO_2$ [M + H]$^+$: 284.1645; found: 284.1647

HPLC: IA 1% IPA, 1.0 mL/min

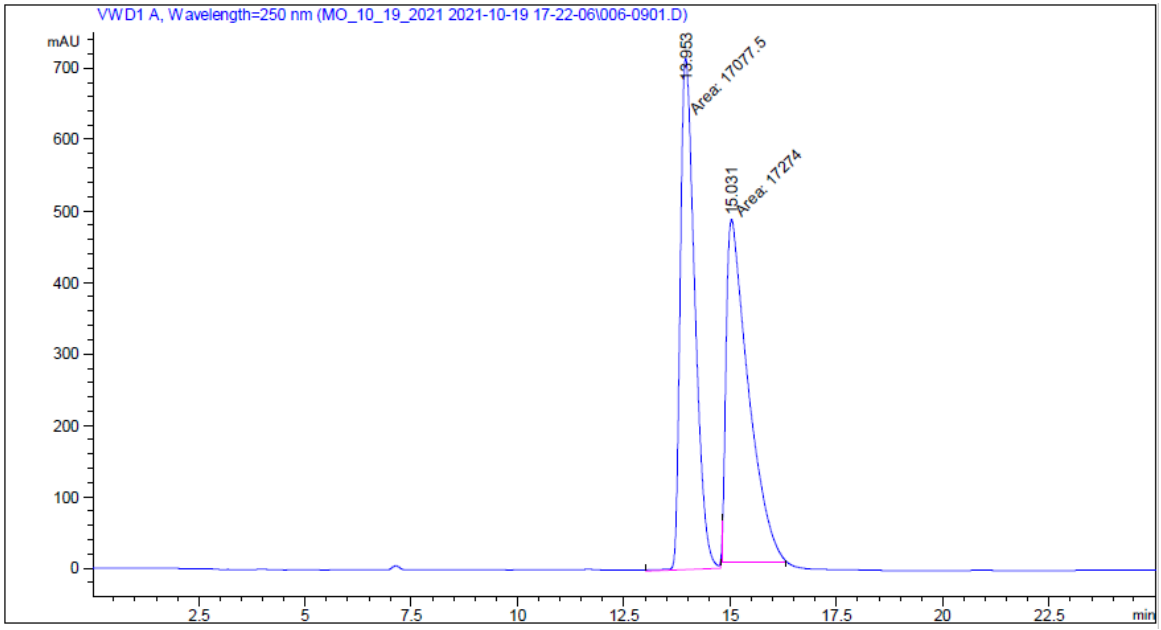

Signal 1: VWD1 A, Wavelength=250 nm

Peak #	RetTime [min]	Type	Width [min]	Area [mAU*s]	Height [mAU]	Area %
1	13.953	MM	0.3975	1.70775e4	716.09229	49.7140
2	15.031	MM	0.6007	1.72740e4	479.30368	50.2860

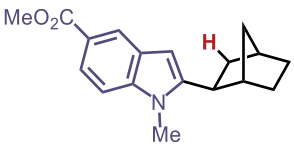

Methyl 2-((1S,2S,4R)-bicyclo[2.2.1]heptan-2-yl)-1-methyl-1*H*-indole-5-carboxylate (2-20-2)

This compound was prepared by following general procedure C using methyl 1-methyl-1*H*-indole-5-carboxylate (18.9 mg, 0.10 mmol), 0.400 mL norbornene (0.20 mmol) stock solution (0.5M in toluene), **L5**-Ni(C_6H_{10}) (7.7 mg, 10 μmmol) at 60 °C. Purification by column chromatography eluting with ethyl acetate / hexane (0 – 10/90) afforded the desired product as a colorless liquid (11.4 mg, 40% yield). $[\alpha]_D^{24}$ = +4.2 (c = 0.80, $CHCl_3$)

^{1}H NMR (700 MHz, $CDCl_3$) δ 8.05 – 8.01 (m, 1H), 7.76 (dd, *J* =8.3, 1.4 Hz, 1H), 7.52 (dd, *J* =8.3, 0.6 Hz, 1H), 6.27 (s, 1H), 3.94 (s, 3H), 3.74 (s, 3H), 2.84 (dd, *J* =8.9, 5.3 Hz, 1H), 2.45 (d, *J* =4.1 Hz, 1H), 2.41 (t, *J* =4.3 Hz, 1H), 1.81 (ddd, *J* =11.6, 8.9, 2.3 Hz, 1H), 1.75 – 1.72 (m, 1H), 1.71 – 1.67 (m, 1H), 1.66 – 1.62 (m, 2H), 1.42 (ddq, *J* =11.1, 8.5, 2.5 Hz, 1H), 1.33 (dddd, *J* =11.7, 9.5, 4.2, 2.1 Hz, 1H), 1.25 – 1.23 (m, 1H).

HPLC: IA 1% IPA, 1.0 mL/min

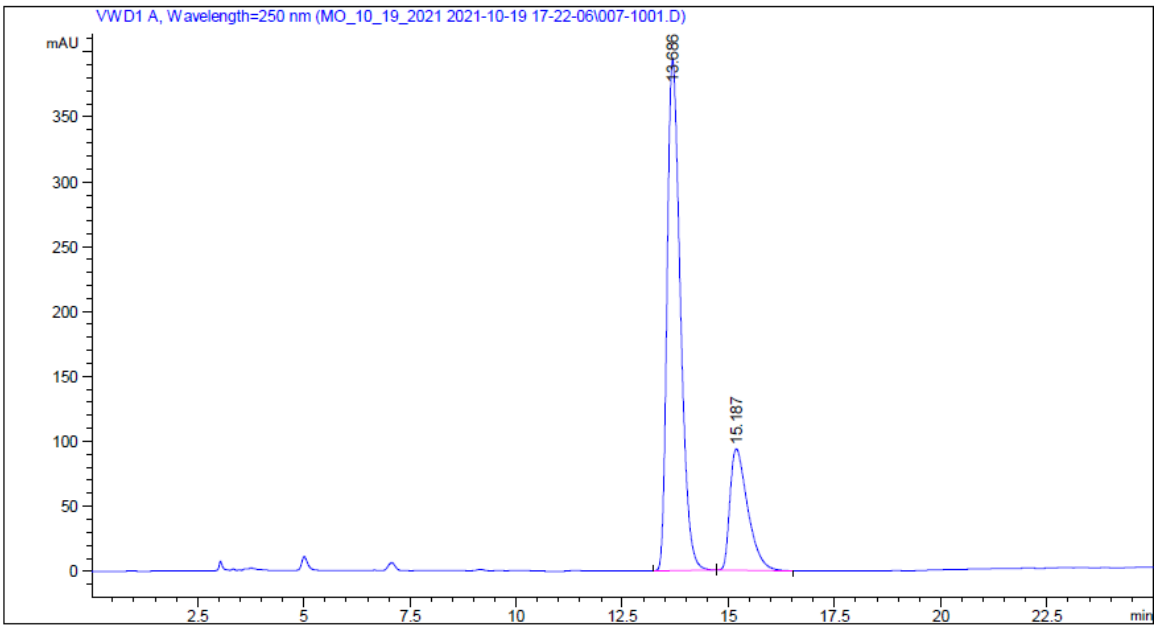

Signal 1: VWD1 A, Wavelength=250 nm

Peak #	RetTime [min]	Type	Width [min]	Area [mAU*s]	Height [mAU]	Area %
1	13.686	BB	0.3362	8549.49121	393.85849	75.8436
2	15.187	BB	0.4425	2723.03760	93.58473	24.1564

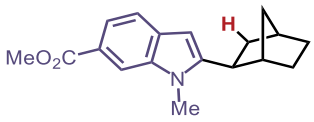

(±)

exo methyl 2-(bicyclo[2.2.1]heptan-2-yl)-1-methyl-1*H*-indole-6-carboxylate (2-21-2) This compound was prepared by following general procedure A using methyl 1-methyl-1*H*-indole-6-carboxylate (18.9 mg, 0.10 mmol), 0.400 mL norbornene (0.20 mmol) stock solution (0.5M in toluene) and IPr^{*OMe}-Ni(C_6H_{10}) (5.4 mg, 5.0 μmmol) at 100 °C. Purification by column chromatography eluting with ethyl acetate / hexane (0 – 10/90) afforded the desired product as a colorless liquid (24.9 mg, 88% yield). ^{1}H NMR (700 MHz, $CDCl_3$) δ 8.03 (s, 1H), 7.76 (dd, *J* =8.2, 1.4 Hz, 1H), 7.52 (d, *J* =8.2 Hz, 1H), 6.27 (s, 1H), 3.94 (s, 3H), 3.73 (s, 3H), 2.84 (dd, *J* =8.9, 5.3 Hz, 1H), 2.45 (d, *J* =4.1 Hz, 1H), 2.40 (d, *J* =4.4 Hz, 1H), 1.81 (ddd, *J* =11.6, 8.8, 2.3 Hz, 1H), 1.75 – 1.71 (m, 1H), 1.71 – 1.66 (m, 1H), 1.65 – 1.62 (m, 1H), 1.61 (dt, *J* =9.7, 1.8 Hz, 1H), 1.42 (ddq, *J* =11.1, 8.6, 2.5 Hz, 1H), 1.33 (dddd, *J* =11.6, 9.5, 4.2, 2.1 Hz, 1H), 1.24 (ddd, *J* =9.8, 2.4, 1.4 Hz, 1H). ^{13}C NMR (176 MHz, $CDCl_3$) δ 168.5, 150.1, 136.9, 131.5, 121.9, 120.4, 119.2, 111.0, 97.7, 51.9, 41.8, 39.9, 37.6, 36.6, 36.1, 29.90, 29.89, 28.9. **HRMS (ESI+):** m/z: calculated for $C_{18}H_{21}NO_2$ $[M + H]^+$: 284.1645; found: 284.1649

SFC: OJ-H 5% IPA, 3.0 mL/min

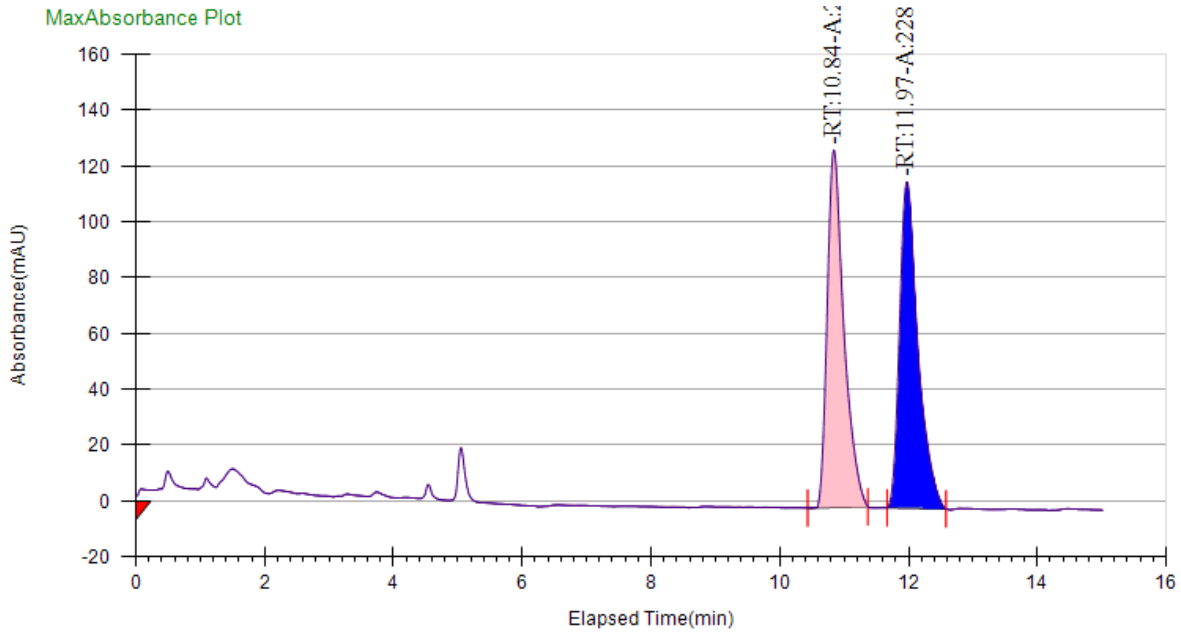

Peak Information

Peak No	% Area	Area	Ret. Time	Height	Cap. Factor
1	49.9569	2281.813	10.84 min	128.1009	0
2	50.0431	2285.7469	11.97 min	116.952	0

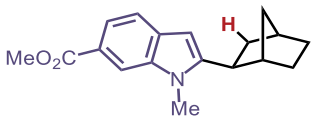

Methyl 2-((1S,2S,4R)-bicyclo[2.2.1]heptan-2-yl)-1-methyl-1*H*-indole-6-carboxylate (2-21-2)

This compound was prepared by following general procedure C using 1-methyl-1*H*-indole-6-carboxylate (18.9 mg, 0.10 mmol), 0.400 mL norbornene (0.20 mmol) stock solution (0.5M in toluene), **L5**-Ni(C_6H_{10}) (7.7 mg, 10 μmmol) at 60 °C. Purification by column chromatography eluting with ethyl acetate / hexane (0 – 10/90) afforded the desired product as a colorless liquid (13.3 mg, 47% yield). $[\alpha]_D^{24}$ = +10.8 (c = 0.80, $CHCl_3$)

^{1}H NMR (600 MHz, $CDCl_3$) δ 8.04 – 8.02 (m, 1H), 7.76 (dd, *J* =8.3, 1.4 Hz, 1H), 7.52 (d, *J* =8.3 Hz, 1H), 6.27 (s, 1H), 3.94 (s, 3H), 3.74 (s, 3H), 2.84 (dd, *J* =8.9, 5.3 Hz, 1H), 2.45 (d, *J* =4.0 Hz, 1H), 2.40 (d, *J* =4.4 Hz, 1H), 1.81 (ddd, *J* =11.5, 8.8, 2.3 Hz, 1H), 1.74 (ddd, *J* =9.1, 4.6, 2.3 Hz,

1H), 1.71 – 1.66 (m, 1H), 1.64 – 1.60 (m, 2H), 1.42 (tt, *J* =10.9, 2.8 Hz, 1H), 1.33 (ddq, *J* =11.5, 7.5, 2.3 Hz, 1H), 1.26 – 1.23 (m, 1H).

SFC: OJ-H 5% IPA, 3.0 mL/min

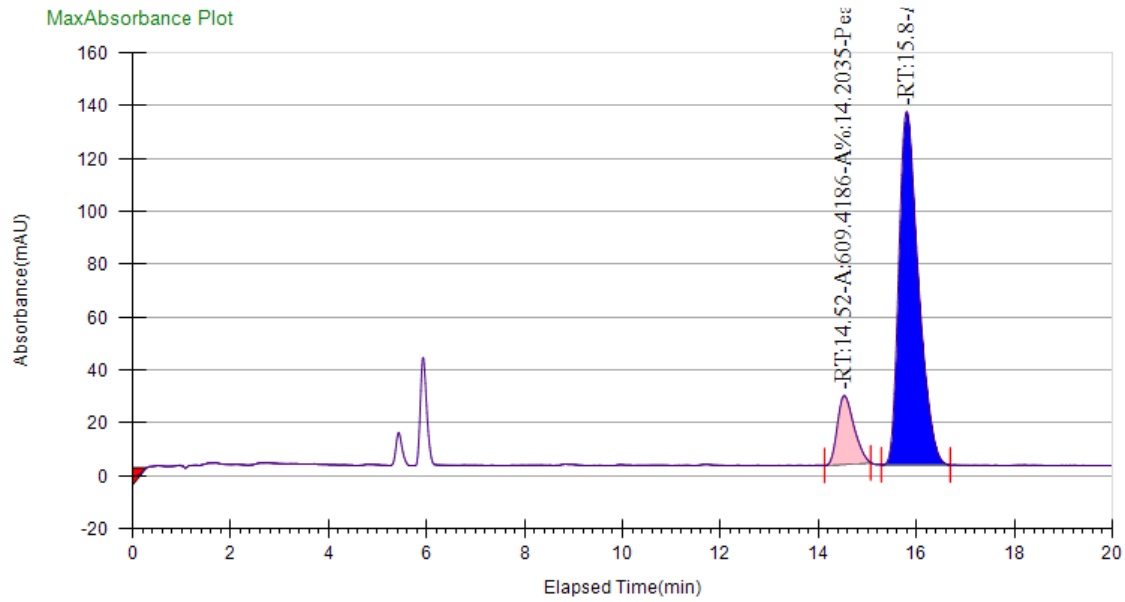

Peak Information

Peak No	% Area	Area	Ret. Time	Height	Cap. Factor
1	14.2035	609.4186	14.52 min	25.946	0
2	85.7965	3681.2186	15.8 min	133.6304	0

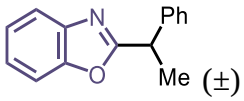

(±)

2-(1-phenylethyl)benzo[d]oxazole (2-1-23) This compound was prepared by following general procedure A using benzo[d]oxazole (11.9 mg, 0.10 mmol), styrene (10.4 mg, 0.10 mmol) and IMes-Ni(C_6H_{10}) (2.3 mg, 5.0 μmmol) at 100 °C. Purification by column chromatography eluting with ethyl acetate / hexane (0 – 10/90) afforded the desired product as a brown liquid (22.3 mg, 100% yield). ^{1}H NMR (700 MHz, $CDCl_3$) δ 7.72 (d, *J* = 8.4 Hz, 1H), 7.44 (d, *J* = 7.4 Hz, 1H), 7.37 (d, *J* = 7.5 Hz, 2H), 7.34 (t, *J* = 7.5 Hz, 2H), 7.28 (dq, *J* = 17.5, 5.9, 4.7 Hz, 3H), 4.42 (q, *J* =

7.2 Hz, 1H), 1.84 (d, *J* = 7.2 Hz, 3H). ^{13}C NMR (176 MHz, $CDCl_3$) δ 168.8, 150.9, 141.2, 141.2, 128.8, 127.5, 127.3, 124.7, 124.1, 119.9, 110.5, 40.2, 19.8. The NMR spectra matched previous report. [167]

SFC OJ-H 0-2% IPA, 3.0 mL/min

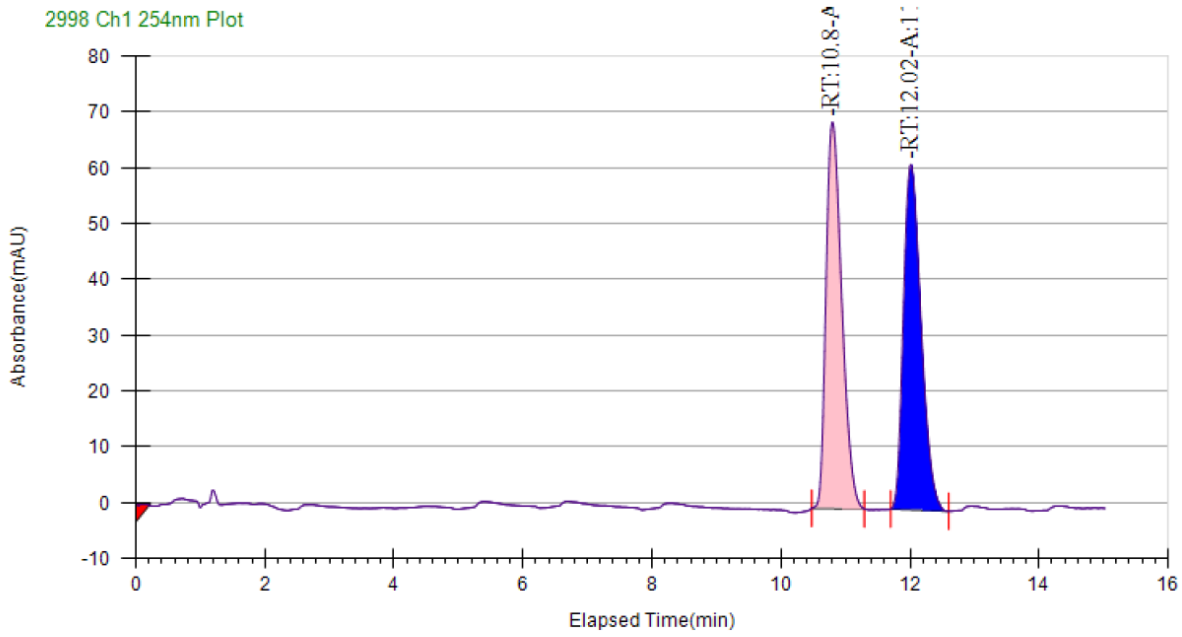

Peak Information

Peak No	% Area	Area	Ret. Time	Height	Cap. Factor
1	49.9749	1161.9986	10.8 min	69.2312	10799
2	50.0251	1163.1666	12.02 min	61.8645	12015.6667

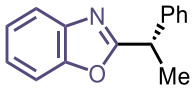

(S)-2-(1-phenylethyl)benzo[d]oxazole (2-1-23) This compound was prepared by following general procedure B using benzo[d]oxazole (11.9 mg, 0.10 mmol), styrene (10.4 mg, 0.10 mmol), **L8**-HBF_4 (3.2 mg, 5.0 μmmol), KHMDS (1.0 mg, 5.0 μmmol) and $Ni(COD)_2$ (1.4 mg, 5.0 μmmol).

Purification by column chromatography eluting with ethyl acetate / hexane (0 – 10/90) afforded the desired product as a brown liquid (17.8 mg, 80% yield). $[\alpha]_D^{25}$ = -6.2 (c = 0.53, $CHCl_3$)

^1H NMR (500 MHz, $CDCl_3$) δ 7.76 – 7.71 (m, 1H), 7.46 (m, 1H), 7.41 – 7.27 (m, 7H).

SFC OJ-H 0-2% IPA, 3.0 mL/min

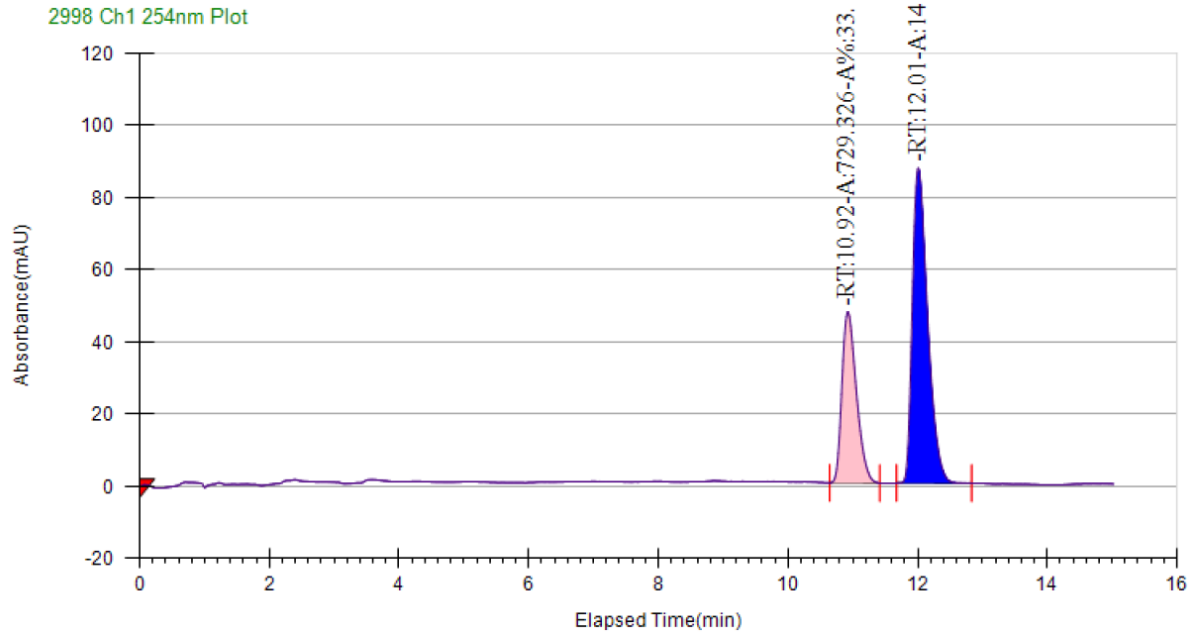

Peak Information

Peak No	% Area	Area	Ret. Time	Height	Cap. Factor
1	33.9501	729.326	10.92 min	47.4804	10924
2	66.0499	1418.9003	12.01 min	87.4089	12007.3333

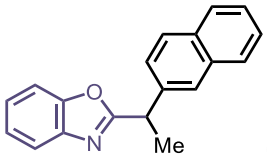

(±)

2-(1-(naphthalen-2-yl)ethyl)benzo[d]oxazole (2-1-24) This compound was prepared by following general procedure A using benzo[d]oxazole (11.9 mg, 0.10 mmol), 2-vinylnaphthalene (15.4 mg, 0.10 mmol) and IMes-Ni(C_6H_{10}) (2.3 mg, 5.0 μmmol) at 100 °C. Purification by column

chromatography eluting with ethyl acetate / hexane (0 – 10/90) afforded the desired product as a brown solid (20.0 mg, 73% yield). ^{1}H NMR (700 MHz, $CDCl_3$): δ 7.82 (m, 4H), 7.74 (d, *J* = 7.7 Hz, 1H), 7.50 (d, *J* = 8.6 Hz, 1H), 7.45 (dt, *J* = 13.1, 7.5 Hz, 3H), 7.30 (dddd, *J* = 16.7, 9.0, 6.8, 3.7 Hz, 2H), 4.60 (q, *J* = 7.2 Hz, 1H), 1.93 (d, *J* = 7.2 Hz, 3H). ^{13}C NMR (176 MHz, $CDCl_3$) δ 168.7, 150.9, 141.2, 138.6, 133.5, 132.6, 128.6, 127.8, 127.6, 126.2, 126.1, 125.9, 125.6, 124.7, 124.1, 119.9, 110.5, 40.3, 19.8. The NMR spectra matched previous report.[168]

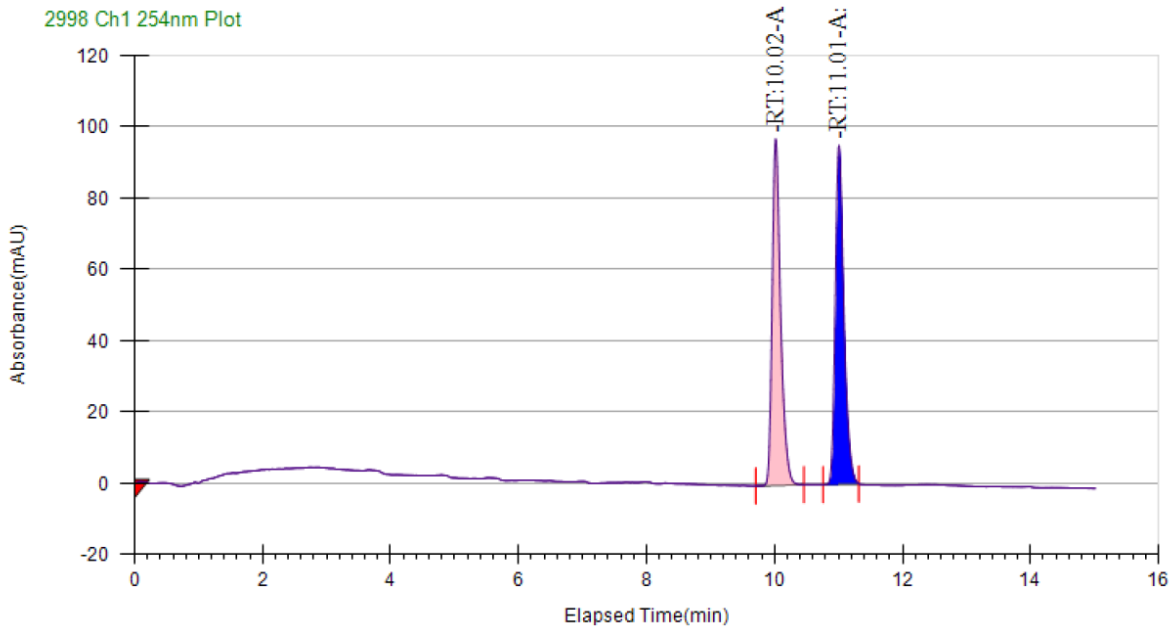

Peak Information

Peak No	% Area	Area	Ret. Time	Height	Cap. Factor
1	50.0556	878.6391	10.02 min	97.2566	0
2	49.9444	876.6888	11.01 min	95.1708	0

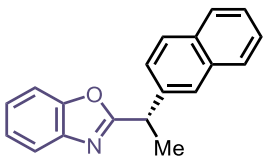

(S)-2-(1-(naphthalen-2-yl)ethyl)benzo[d]oxazole (2-1-24) This compound was prepared by following general procedure B using benzo[d]oxazole (11.9 mg, 0.10 mmol), styrene (10.4 mg, 0.10 mmol), **L8**-HBF_4 (3.2 mg, 5.0 μmmol), KHMDS (1.0 mg, 5.0 μmmol) and $Ni(COD)_2$ (1.4

mg, 5.0 μmmol). Purification by column chromatography eluting with ethyl acetate / hexane (0 – 10/90) afforded the desired product as a brown solid (22.7 mg, 83% yield). $[\alpha]_D^{24}$ = -13.4 (c = 1.0, $CHCl_3$)

^{1}H NMR (700 MHz, $CDCl_3$) δ 7.82 (d, *J* = 7.4 Hz, 4H), 7.75 (d, *J* = 7.7 Hz, 1H), 7.47 (ddd, *J* = 20.8, 16.6, 8.0 Hz, 4H), 7.30 (dt, *J* = 18.9, 7.4 Hz, 2H), 4.60 (q, *J* = 7.2 Hz, 1H), 1.93 (d, *J* = 7.2 Hz, 3H).

SFC OD-H 0-30% IPA, 3.0 mL/min

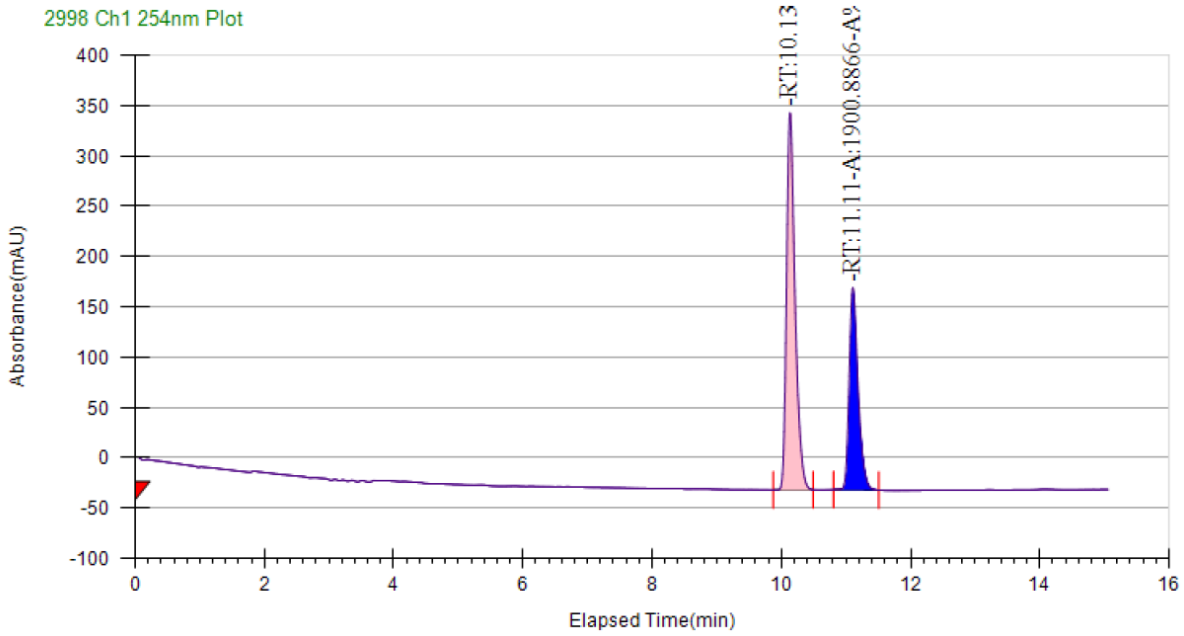

Peak Information

Peak No	% Area	Area	Ret. Time	Height	Cap. Factor
1	64.004	3379.9475	10.13 min	374.6694	10132.3333
2	35.996	1900.8866	11.11 min	200.92	11107.3333

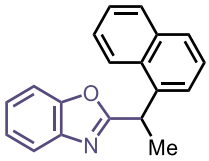

(±)

2-(1-(naphthalen-1-yl)ethyl)benzo[d]oxazole (2-1-25) This compound was prepared by following general procedure A using benzo[d]oxazole (11.9 mg, 0.10 mmol), 1-vinylnaphthalene (15.4 mg, 0.10 mmol) and IMes-Ni(C_6H_{10}) (2.3 mg, 5.0 μmmol) at 100 °C. Purification by column chromatography eluting with ethyl acetate / hexane (0 – 10/90) afforded the desired product as a colorless liquid (27.0 mg, 98% yield). ^{1}H NMR (700 MHz, $CDCl_3$): δ 8.22 (d, *J* = 8.5 Hz, 1H), 7.89 (d, *J* = 8.1 Hz, 1H), 7.80 (t, *J* = 4.8 Hz, 1H), 7.75 (d, *J* = 7.8 Hz, 1H), 7.59 – 7.53 (m, 1H), 7.50 (t, *J* = 7.5 Hz, 1H), 7.45 (d, *J* = 4.8 Hz, 2H), 7.41 (d, *J* = 7.9 Hz, 1H), 7.31 (t, *J* = 7.5 Hz, 1H), 7.28 (t, *J* = 7.9 Hz, 1H), 5.24 (q, *J* = 7.2 Hz, 1H), 1.99 (d, *J* = 7.2, 3H). ^{13}C NMR (176 MHz, $CDCl_3$) δ 169.0, 150.9, 141.2, 137.2, 134.0, 131.1, 129.0, 128.0, 126.5, 125.7, 125.6, 124.73, 124.68, 124.1, 123.0, 119.9, 110.5, 36.0, 19.5. The NMR spectra matched previous report.[167]

SFC OJ-H 0-30% IPA, 3.0 mL/min

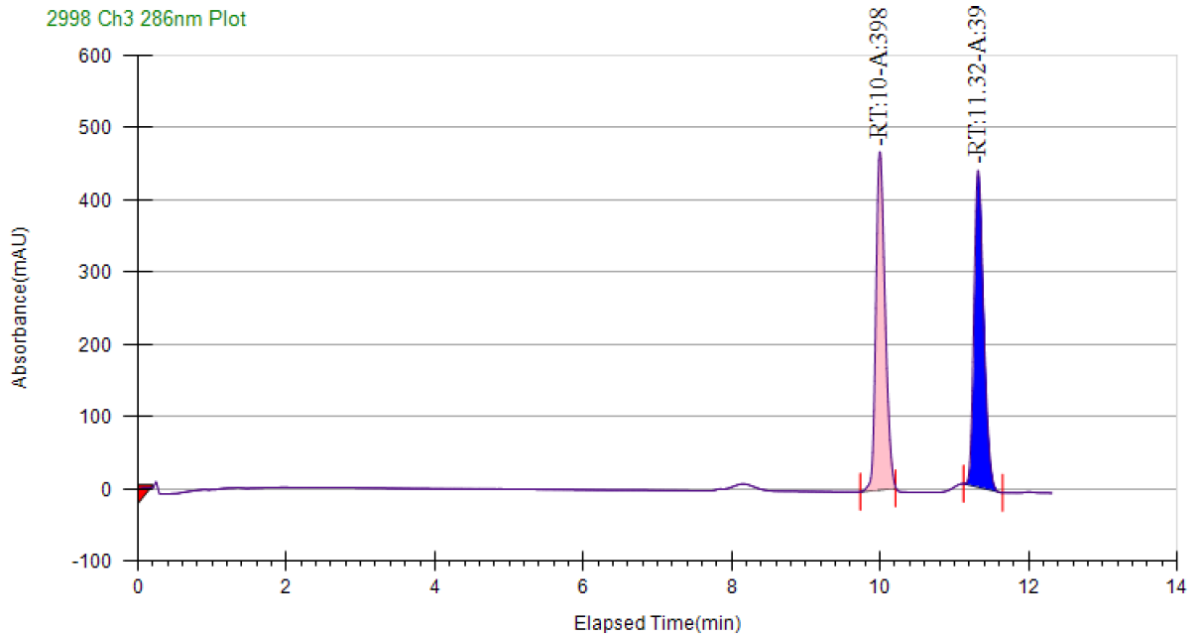

Peak Information

Peak No	% Area	Area	Ret. Time	Height	Cap. Factor
1	50.2817	3981.247	10 min	468.1115	9999
2	49.7183	3936.6372	11.32 min	438.1936	11315.6667

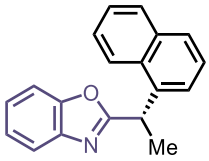

(S)-2-(1-(naphthalen-1-yl)ethyl)benzo[d]oxazole (2-1-25) This compound was prepared by following general procedure B using benzo[d]oxazole (11.9 mg, 0.10 mmol), styrene (10.4 mg, 0.10 mmol), **L8**-HBF_4 (3.2 mg, 5.0 μmmol), KHMDS (1.0 mg, 5.0 μmmol) and $Ni(COD)_2$ (1.4 mg, 5.0 μmmol). Purification by column chromatography eluting with ethyl acetate / hexane (0 – 10/90) afforded the desired product as a colorless liquid (27.2 mg, 99% yield). $[\alpha]_D^{24}$ = -33.9 (c = 0.90, $CHCl_3$)

^1H NMR (700 MHz, $CDCl_3$) δ 8.22 (d, *J* = 8.5 Hz, 1H), 7.89 (d, *J* = 8.1 Hz, 1H), 7.80 (t, *J* = 4.8 Hz, 1H), 7.76 (d, *J* = 7.8 Hz, 1H), 7.55 (d, *J* = 8.5 Hz, 1H), 7.50 (t, *J* = 7.4 Hz, 1H), 7.45 (d, *J* = 4.8 Hz, 2H), 7.41 (d, *J* = 8.0 Hz, 1H), 7.31 (t, *J* = 7.5 Hz, 1H), 7.28 (t, *J* = 7.6 Hz, 1H).

SFC OD-H 0-30% IPA, 3.0 mL/min

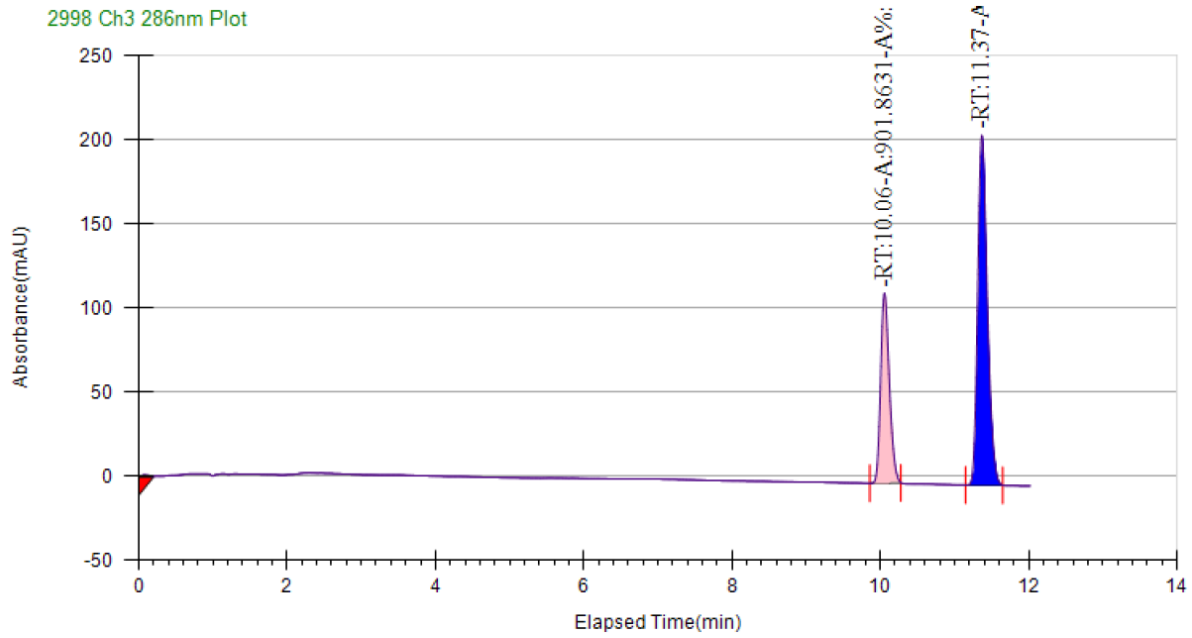

Peak Information

Peak No	% Area	Area	Ret. Time	Height	Cap. Factor
1	32.8785	901.8631	10.06 min	112.9668	10057.3333
2	67.1215	1841.1554	11.37 min	207.9823	11365.6667

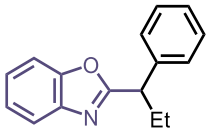

(±)

2-(1-phenylpropyl)benzo[d]oxazole (2-1-26) This compound was prepared by following general procedure A using benzo[d]oxazole (11.9 mg, 0.10 mmol), trans-β-methylstyrene (11.8 mg, 0.10 mmol) IMes-Ni(C_6H_{10}) (2.3 mg, 5.0 μmmol) at 100 °C. Purification by column chromatography eluting with ethyl acetate / hexane (0 – 10/90) afforded the desired product as a colorless solid (7.8 mg, 33% yield).

^{1}H NMR (700 MHz, $CDCl_3$) δ 7.71 (dd, J = 6.8, 2.1 Hz, 1H), 7.45 (dd, *J* = 7.0, 2.0 Hz, 1H), 7.39 (d, *J* = 7.3 Hz, 2H), 7.33 (t, *J* = 7.6 Hz, 2H), 7.29 (ddd, *J* = 7.2, 5.2, 1.6 Hz, 2H), 7.26 (t, *J* = 3.7 Hz, 1H), 4.13 (t, *J* = 7.8 Hz, 1H), 2.42 (dp, *J* = 14.8, 7.5 Hz, 1H), 2.15 (dp, *J* = 14.8, 7.4 Hz, 1H),

0.99 (t, *J* = 7.4 Hz, 3H). ^{13}C NMR (176 MHz, $CDCl_3$) δ 168.1, 150.8, 141.2, 139.8, 128.7, 128.0, 127.3, 124.6, 124.1, 119.8, 110.5, 47.9, 27.6, 12.3. The NMR spectra matched previous report.[169]

HPLC OD-H 0% IPA, 0.3 mL/min

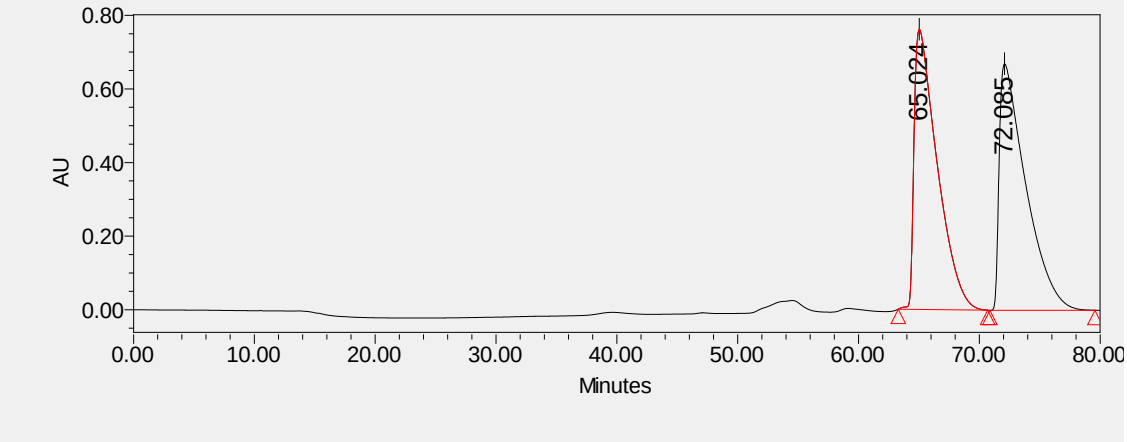

	Retention Time	Area	% Area	Height
1	65.024	101157889	49.80	761156
2	72.085	101960059	50.20	669903

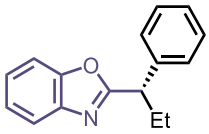

(S)-2-(1-(naphthalen-1-yl)ethyl)benzo[d]oxazole (2-1-26) This compound was prepared by following general procedure B using benzo[d]oxazole (11.9 mg, 0.10 mmol), trans-β-methylstyrene (23.6 mg, 0.20 mmol) **L8**-HBF_4 (3.2 mg, 5.0 μmmol), KHMDS (1.0 mg, 5.0 μmmol) and $Ni(COD)_2$ (1.4 mg, 5.0 μmmol). Purification by column chromatography eluting with ethyl acetate / hexane (0 – 10/90) afforded the desired product as a colorless liquid (12.8 mg, 54% yield). ^{1}H NMR (400 MHz, $CDCl_3$) δ 7.70 (dt, *J* = 7.0, 3.1 Hz, 1H), 7.44 (dt, *J* = 5.9, 3.0 Hz, 1H), 7.38 (d, *J* = 6.9 Hz, 2H), 7.35 – 7.22 (m, 5H), 4.12 (t, *J* = 7.8, 1H), 2.40 (dp, *J* = 14.6, 7.5 Hz, 1H), 2.13 (dp, *J* = 14.6, 7.7, 1H), 0.97 (t, *J* = 7.4 Hz. 3H). $[\alpha]_D^{24}$ = -18.5 (c = 0.15, MeOH). The absolute configuration was determined by comparison with report from Nieddu and co-workers.[170]

HPLC OD-H 0% IPA, 0.3 mL/min

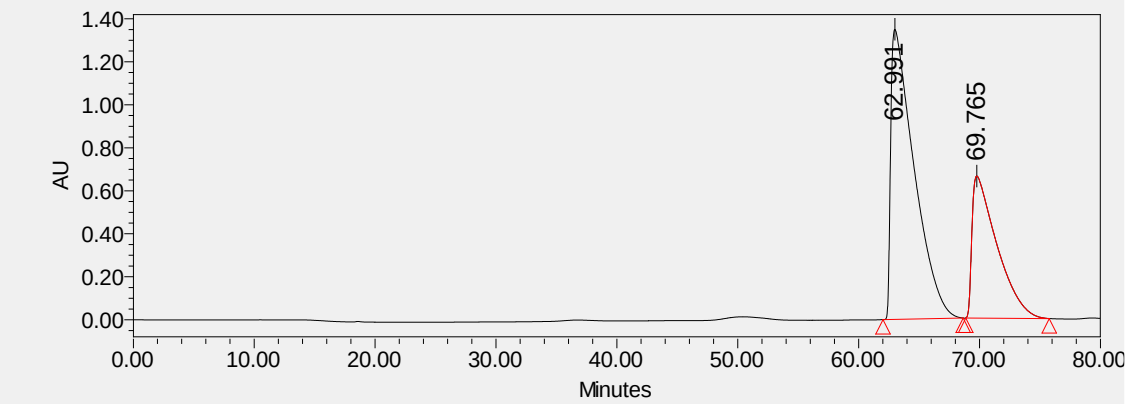

Retention Time	Area	% Area	Height
62.991	180946842	65.67	1349036
69.765	94572975	34.33	660690

8.2.4 Scale-Up Synthesis of 2-1-2

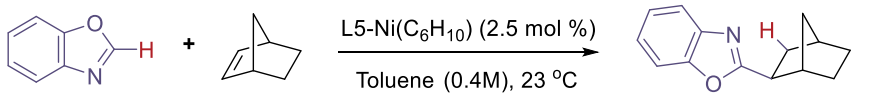

1.0 mmol 1.0 mmol 78% yield, 91.5:8.5 e.r.

Inside a N_2 filled glovebox, an oven-dried 1 dram vial equipped with a Teflon-coated magnetic stir bar was charged with **L5**-Ni(C_6H_{10}) (19.2 mg, 25 μmmol, 0.025 equiv). The vial was sealed with a Teflon cap before removing it from the glovebox. A solution of benzoxazole (119 mg, 1.0 mmol, 1.0 equiv) and norbornene (94 mg, 1.0 mmol, 1.0 equiv) in 2.5 mL toluene was added to the vial which was left stirring rigorously on a stir plate for 16 h. The reaction mixture was quenched with 2 mL dichloromethane and run through a silica gel plug with 2 mL ethyl acetate. The solvent was removed, and the crude reaction mixture was purified by silica gel chromatography yielding a yellow liquid (168mg, 78% yield, 91.5:8.5 e.r.).

8.2.5 Determination of Absolute Configuration for 2-8-2

The preparation of 2-((1*R*,2*R*,4*S*)-bicyclo[2.2.1]heptan-2-yl)benzofuran has been reported by Hartwig and co-workers.[165] Following their procedure, it was synthesized using iridium-catalyzed intermolecular asymmetric hydroheteroarylation of norbornene and the enantiomers were separated using SFC. The major enantiomer has a retention time of 18.32 min (*vide infra*). The same SFC separation method has been used for the racemic and chiral samples prepared using the nickel catalysis described in this work. As shown in the spectra, the signals displayed good accordance of retention time within the detection error, indicating the major enantiomer synthesized in this work had a (1*S*,2*S*,4*R*)-configuration.

Hartwig 2013

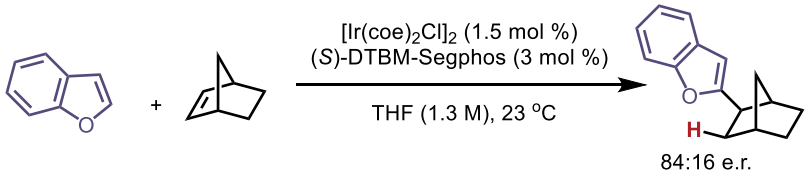

SFC: OJ-H 0-1% MeOH, 3.0 mL/min

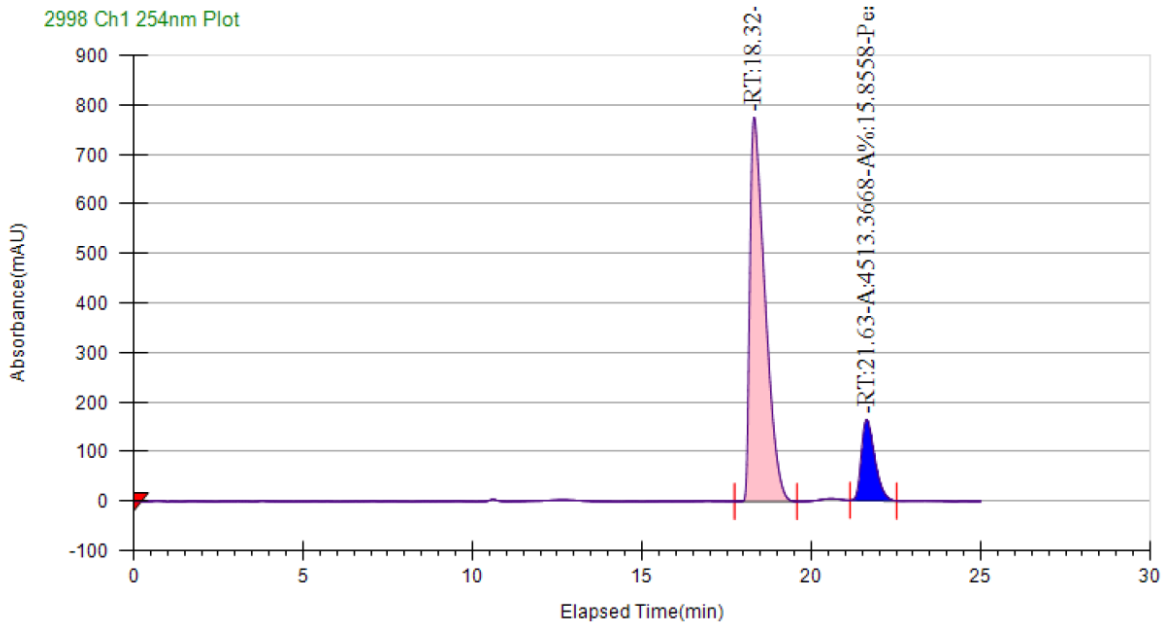

Peak Information

Peak No	% Area	Area	Ret. Time	Height	Cap. Factor
1	84.1442	23951.6429	18.32 min	775.2374	0
2	15.8558	4513.3668	21.63 min	163.1483	0

SFC: OJ-H 0-1% MeOH, 3.0 mL/min

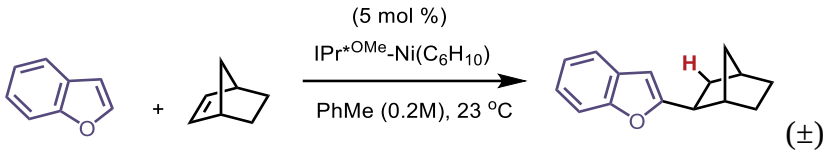

SFC: OJ-H 0-1% MeOH, 3.0 mL/min

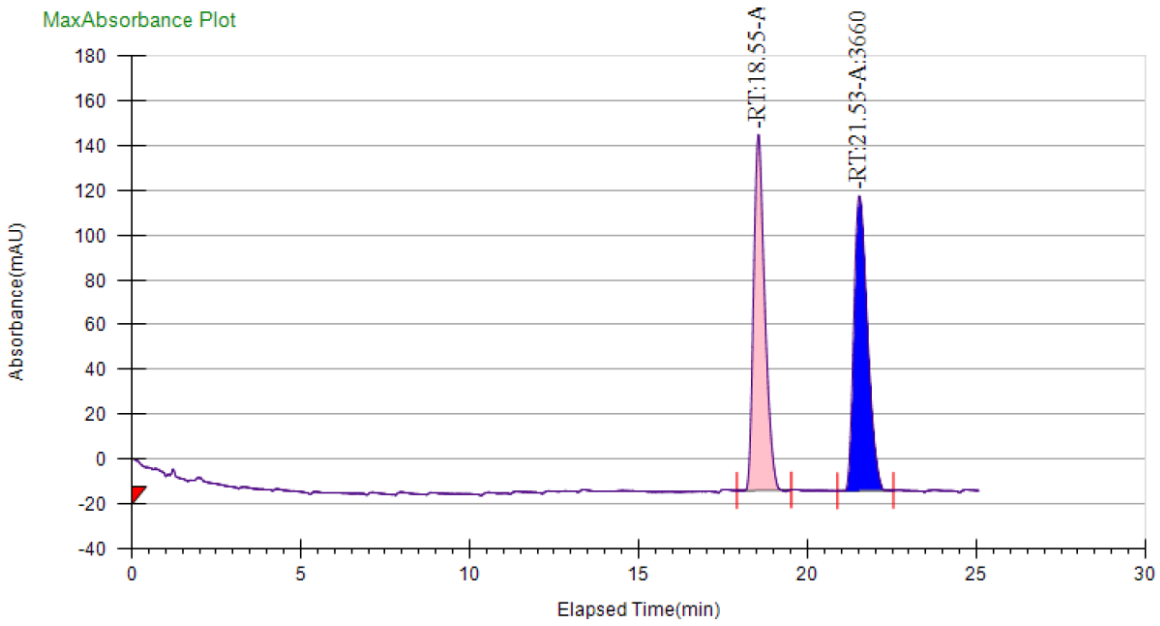

Peak Information

Peak No	% Area	Area	Ret. Time	Height	Cap. Factor
1	49.796	3630.8872	18.55 min	158.5989	18548.7167
2	50.204	3660.6312	21.53 min	131.5225	21532.0167

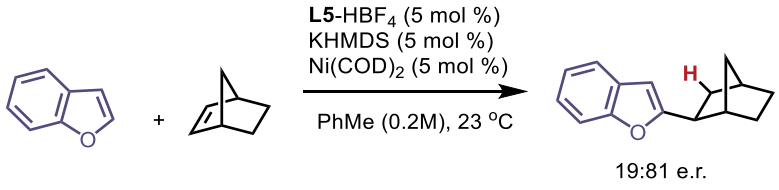

(this work)

SFC: OJ-H 0-1% MeOH, 3.0 mL/min

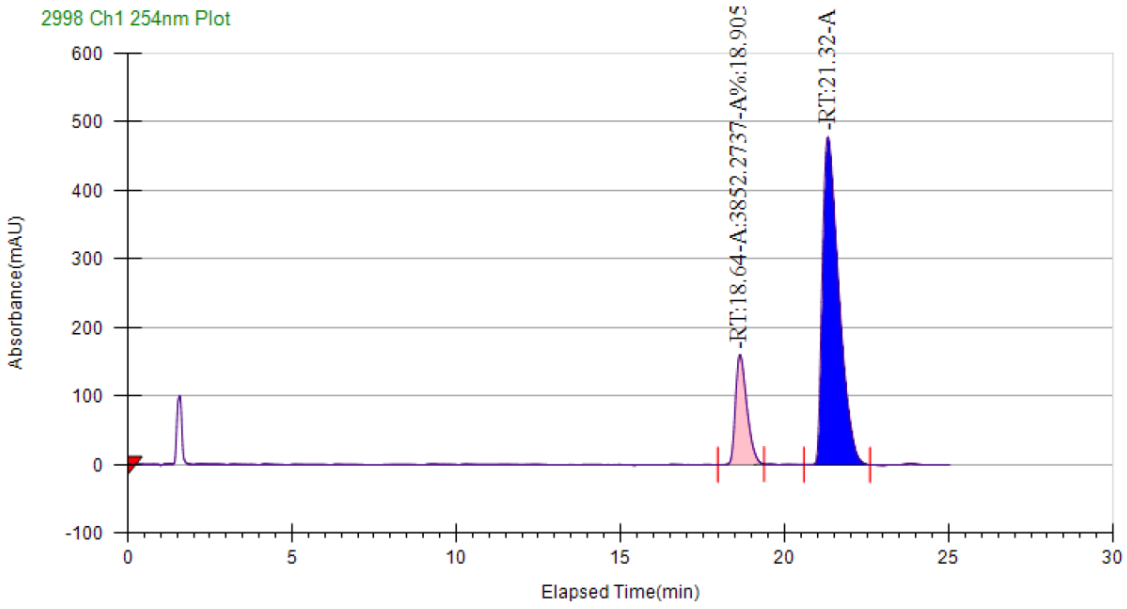

Peak Information

Peak No	% Area	Area	Ret. Time	Height	Cap. Factor
1	18.9051	3852.2737	18.64 min	160.0823	18640.6667
2	81.0949	16524.6273	21.32 min	478.5649	21315.6667

8.2.6 Mechanistic Investigations

Technical details: All reactions were monitored in real time by ^{1}H or ^{19}F NMR using screw-cap NMR tubes with septa caps. All reactions were homogenous and did not require stirring. Automated data collection was used so that there was a fixed time interval of 36 or 18 seconds between each run (for ^{1}H and ^{19}F NMR respectively). For ^{1}H NMR, each run was done with 4 scans and a relaxation delay of 5 seconds which was sufficient for accurate integration of starting material and product. For ^{19}F NMR, each run was done with 2 scans and a relaxation delay of 5 seconds. Kinetic experiments were run at 50 °C with 2 mol % catalyst loading as compared to 60 °C, 5 mol % catalyst loading for other benzofuran substrates, in order to measure enough early time points.

General Procedure A (standard reaction condition for reaction order determination): Inside glovebox, to an oven-dried 1 dram vial equipped with a Teflon-coated magnetic stir bar in a N_2 filled glovebox was added **L5**•HBF_4 (3.6 mg, 5.0 μmmol), KHMDS (1.0 mg, 5.0 μmmol), $Ni(COD)_2$ (1.4 mg, 5.0 μmmol) and 0.500 mL C_6D_6. The solution was allowed to stir at room temperature for 30 min. In a separate vial, a solution of 5-(4-fluorophenyl)benzofuran **2-9-F** (0.10 mmol) and norbornene (0.10 mmol) in 0.300 mL C_6D_6 was combined with 0.200 mL of the catalyst solution. This mixture was transferred to a screw-cap NMR tube and capped to bring out from glove box. The NMR tube was then carefully transferred to the NMR instrument which has been properly shimmed and pre-set at 50 °C. Equilibration time represents the time between finishing preparing the NMR sample and beginning of data acquisition.

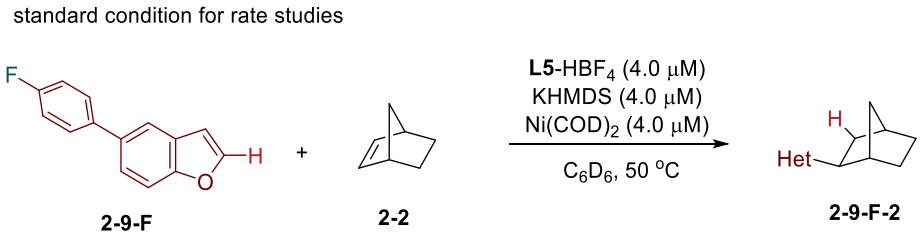

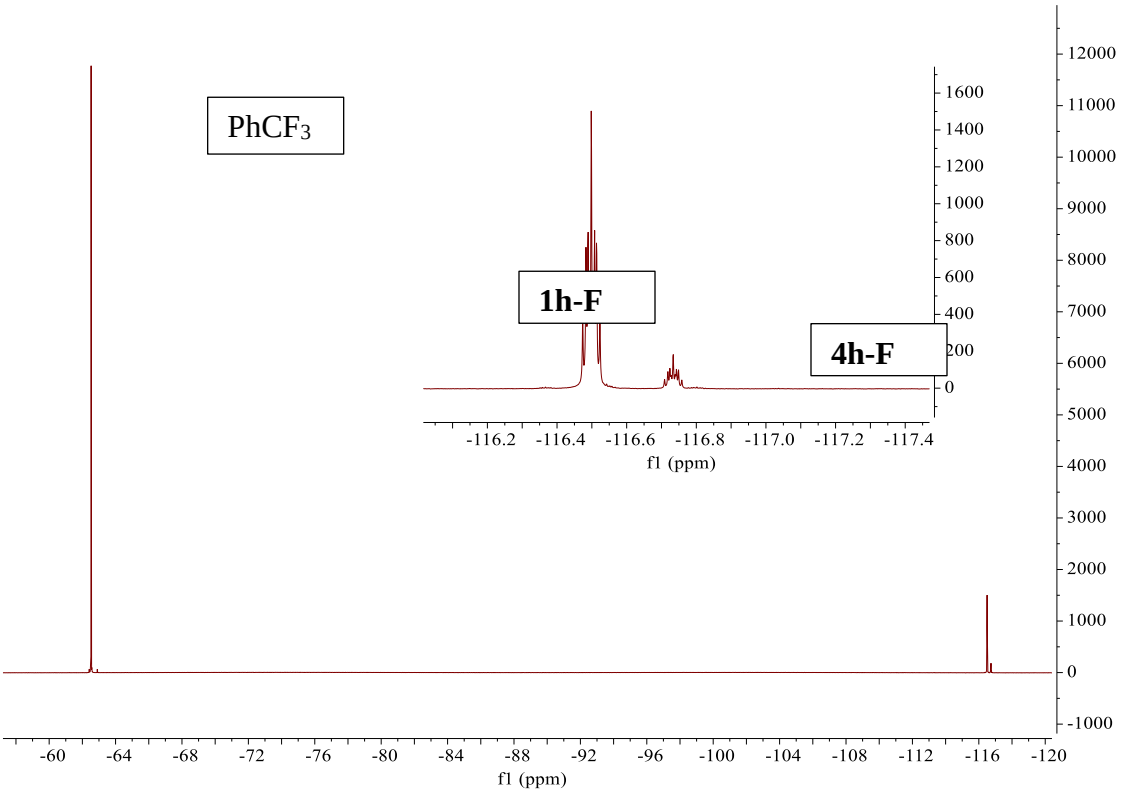

Example of ^{19}F NMR monitored reaction progress kinetic analysis.

Determination of the reaction order in the concentration of arene by initial rates.

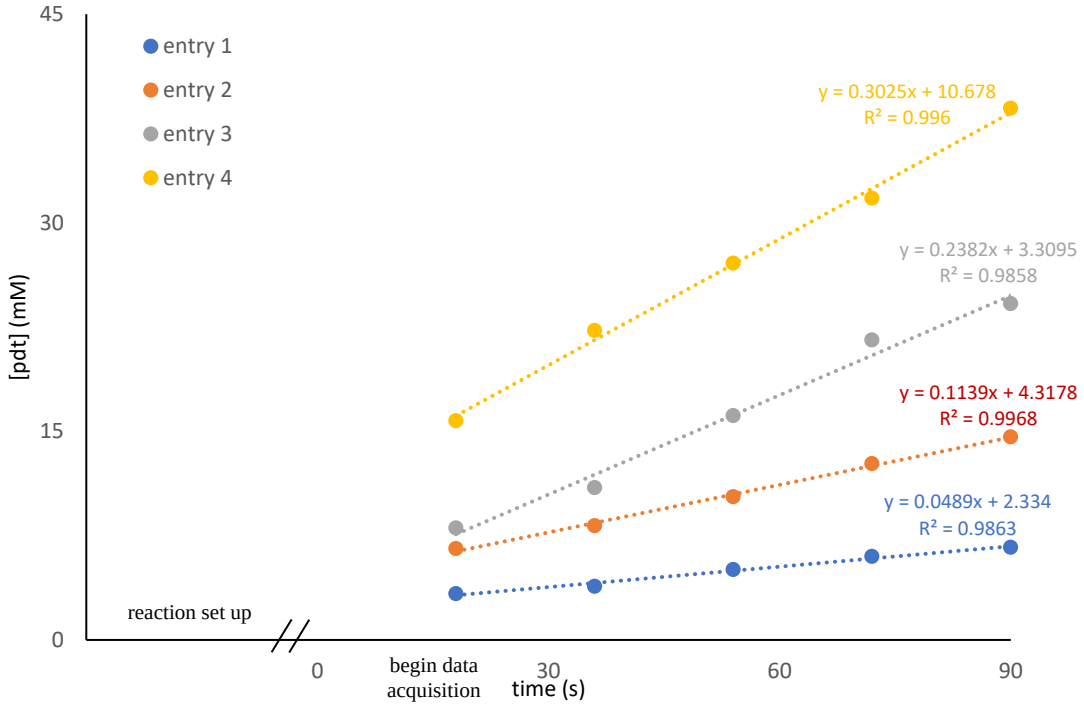

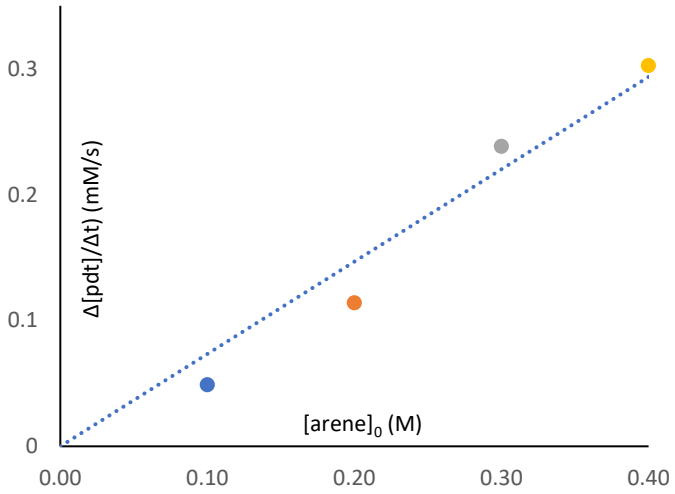

Entry	[5-(4-fluorophenyl)benzofuran]$_0$ (M)	Initial rate (mM/s)
1	**0.10**	**0.0489**
2	**0.20**	**0.1139**
3	**0.30**	**0.2382**
4	**0.40**	**0.3025**

Determination of the reaction order in the concentration of nbe by initial rates.

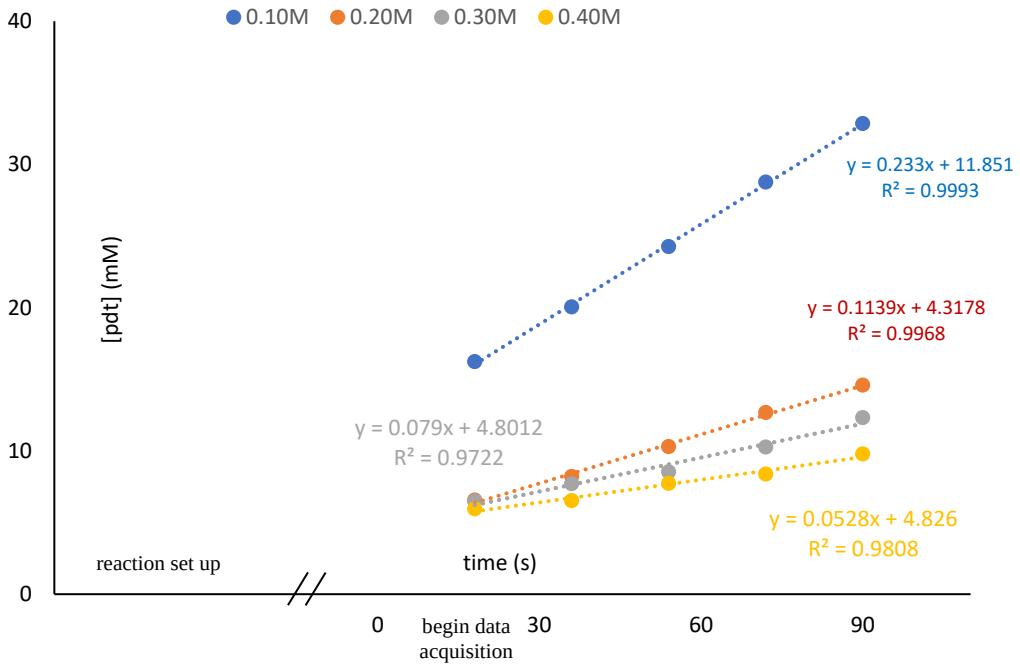

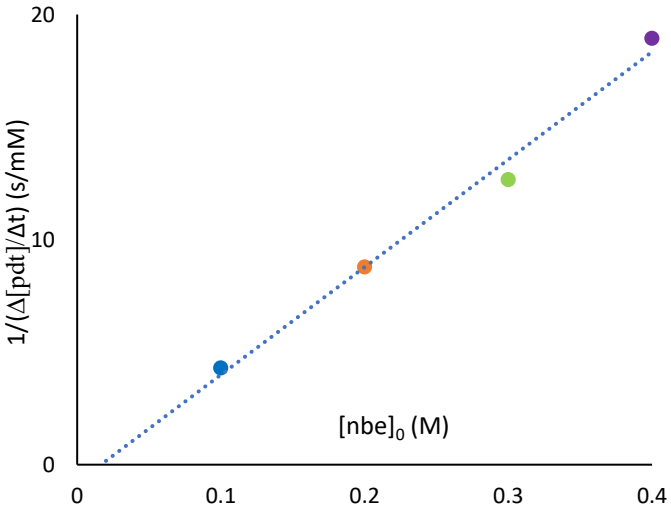

Entry	$[nbe]_0$ (M)	Initial rate k (mM/s)	1/k (s/mM)
1	**0.10**	**0.2330**	**4.29**
2	**0.20**	**0.1139**	**8.78**
3	**0.30**	**0.0790**	**12.66**
4	**0.40**	**0.0528**	**18.94**

Determination of the reaction order in the concentration of catalyst by initial rates.

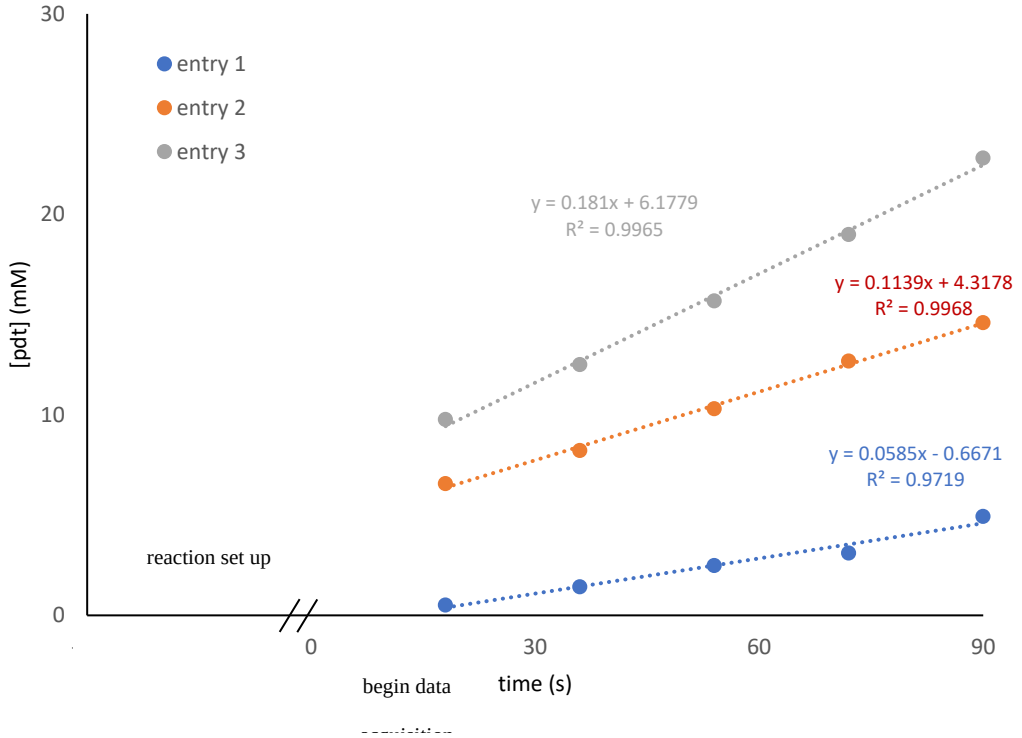

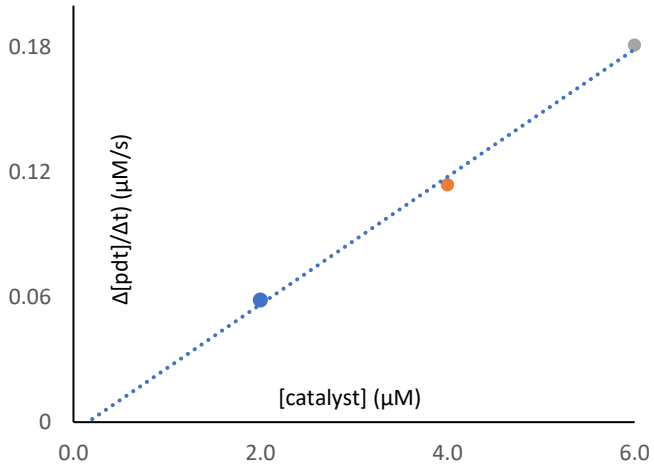

Entry	[catalyst]$_0$ (μM)	Initial rate (mM/s)
1	**2.0**	**0.0585**
2	**4.0**	**0.1139**
3	**6.0**	**0.1810**

Same Excess Experiments

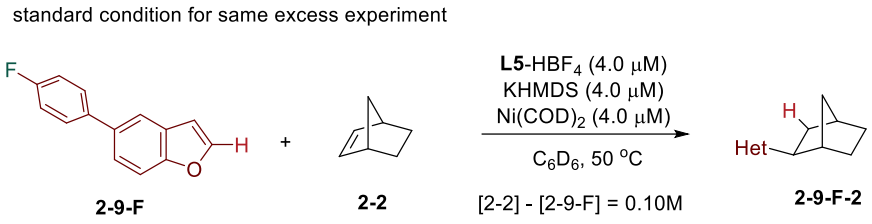

General procedure A was followed, and the initial concentrations of reagents are shown below.

Reaction time has been adjusted for overlap.

Entry	[arene]$_0$ (M)	[nbe]$_0$ (M)	[catalyst]$_0$ (μM)	[arene]$_0$ - [nbe]$_0$ (M)
1	0.10	0.20	4.0	-0.10
2	0.20	0.30	4.0	-0.10
3	0.30	0.40	4.0	-0.10

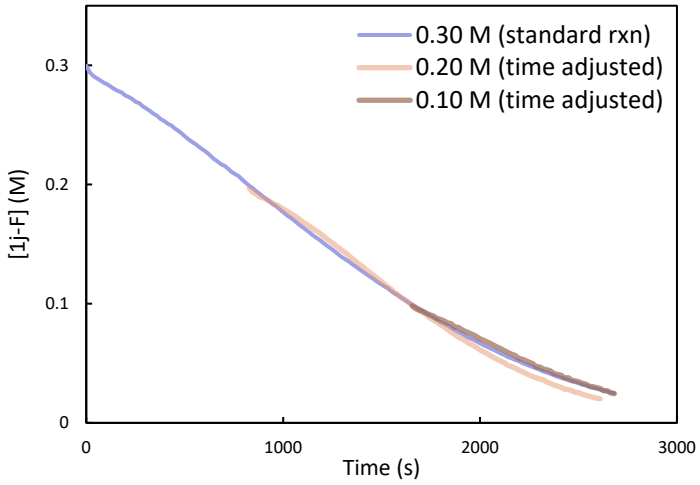

Measurement of the kinetic isotope effect for enantioselective Ni catalysis

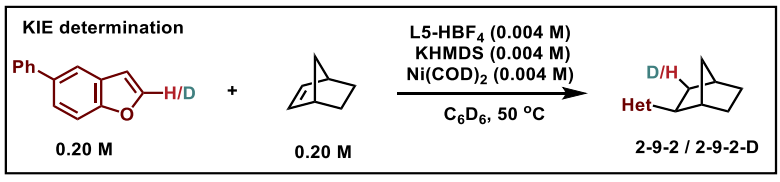

General Procedure B (KIE determination): Inside glovebox, to an oven-dried 1 dram vial equipped with a Teflon-coated magnetic stir bar in a N_2 filled glovebox was added **L5**•HBF_4 (3.6 mg, 5.0 μmmol), KHMDS (1.0 mg, 5.0 μmmol), $Ni(COD)_2$ (1.4 mg, 5.0 μmmol) and 0.500 mL C_6D_6. The solution was allowed to stir at room temperature for 30 min. In a separate vial, a solution of 5-phenylbenzofuran or 5-phenylbenzofuran-2-d (0.10 mmol), norbornene (0.10 mmol) and mesitylene (13 μmmol) in 0.300 mL C_6D_6 was combined with 0.200 mL of the catalyst solution. This mixture was transferred to a screw-cap NMR tube and capped to bring out from glove box. The NMR tube was then carefully transferred to the NMR instrument which has been properly shimmed and pre-set at 50 °C. KIE was determined to be 1.0 based on early time points in 4 parallel experiments.

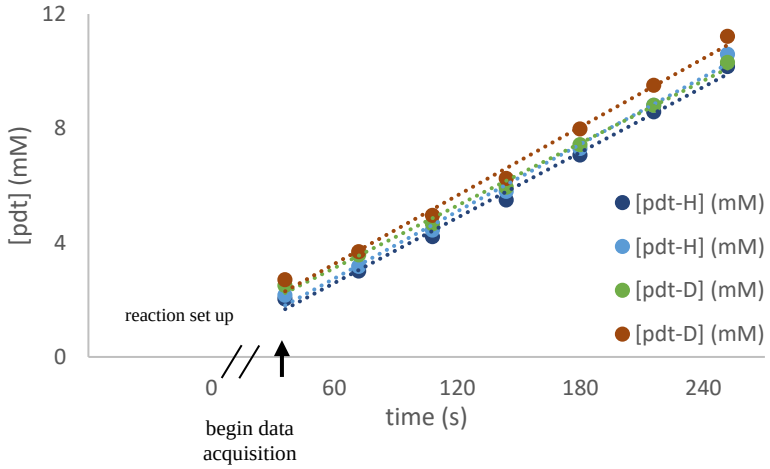

8.3 Experimental Details for Chapter 3

8.3.1 General Procedure for Small Molecule System

IMes-Ni(C_6H_{10}) (5.0 μmmol, 0.050 equiv) was weighed in an oven-dried 1dram vial charged with a stir bar in an inert atmosphere glovebox. To a separate vial, arene starting material **AA1** (15 mg, 0.10 mmol, 1.0 equiv) and 4-octyne (22 mg, 0.20 mmol, 2.0 equiv) was added, followed by addition of toluene. This solution was transferred to the previous vial using a micropipette and the reaction vial was capped and brought outside the glovebox to a stir plate. After 16 h, the reaction mixture was quenched with 2 mL dichloromethane and run through a silica gel plug with 2 mL ethylacetate. The solvent was removed, and the crude reaction mixture was analyzed by NMR using CH_2Br_2 as an internal standard to determine product ratio.

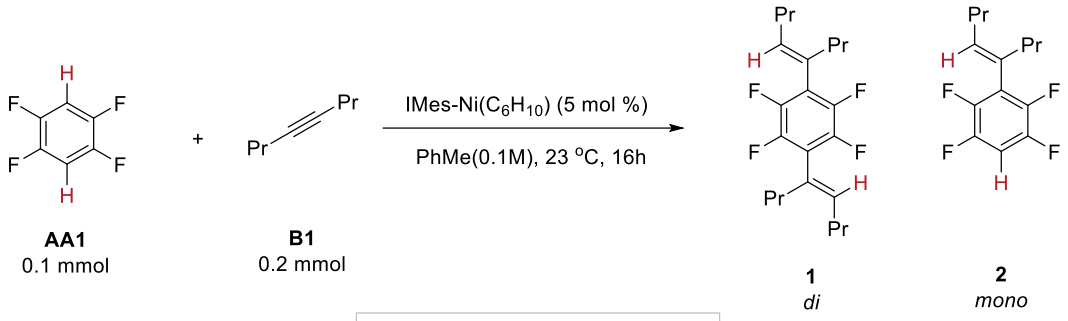

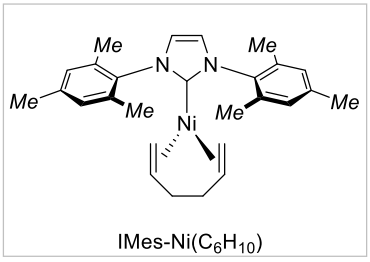

Entry	Deviation from above	% yield (NMR)	% di	% mono
1	None	70	0	70
2	IMes, $Ni(COD)_2$	0	–	–
3	IPr^{Me}, $Ni(COD)_2$	0	–	–

4	IPr*^{OMe}, Ni(COD)$_2$	0	–	–
5	PCy$_3$, Ni(COD)$_2$	0	–	–
6	0.5 M	21	5	16
7	10% [Ni]	62	36	26
8	10% [Ni] at 60 °C	98	58	40
9	10% [Ni], 0.2 M, at 60 °C	100	71	29

Example of NMR yield determination (entry 7):

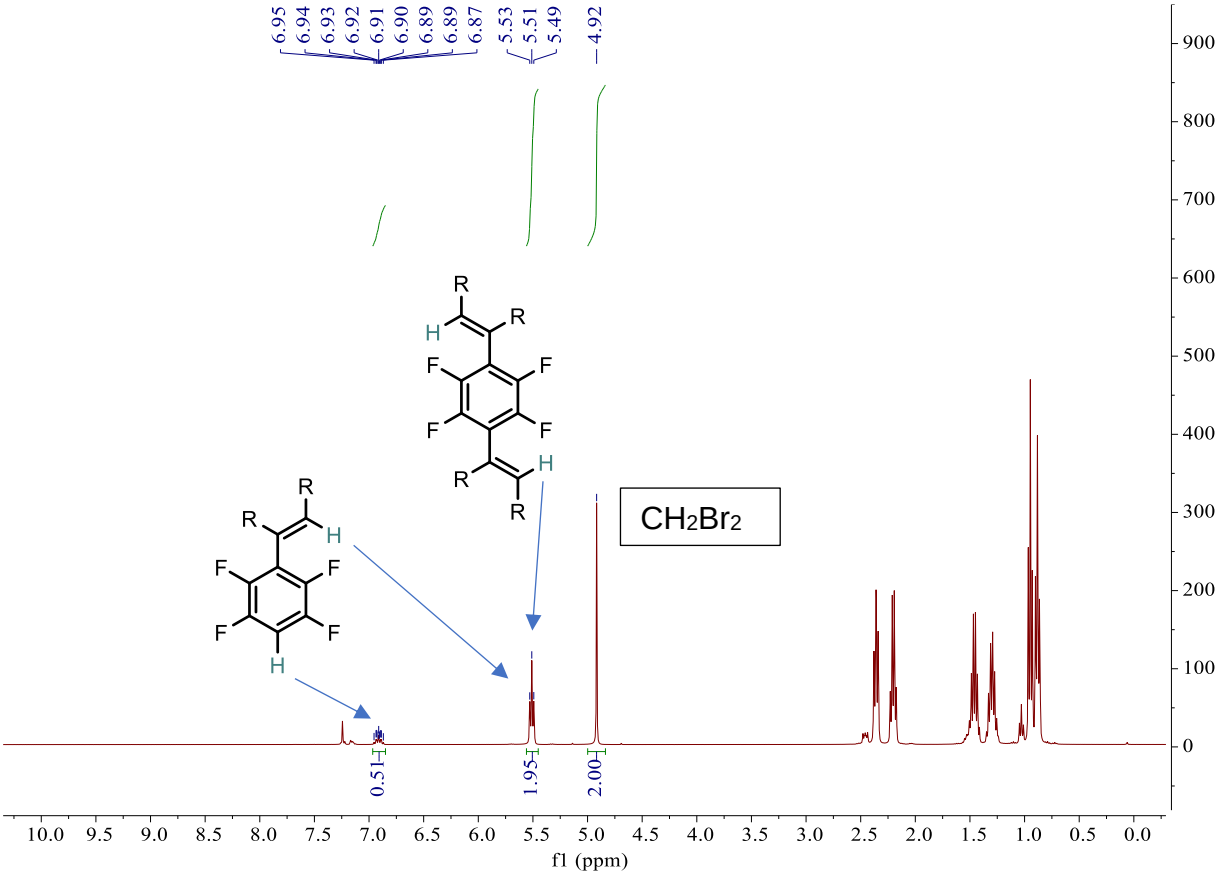

8.3.2 Synthesis of BB Monomers

Other then commercially available BB6, synthesis of bis-alkyne monomers followed reports in the literature with modifications.

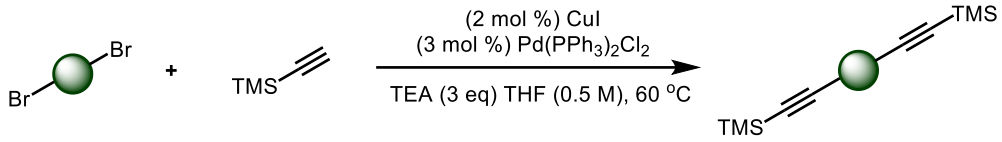

To an oven-dried flask charged with a magnetic stir bar, add 105 mg $Pd(PPh_3)Cl_2$ (0.15 mmol, 0.03 eq), 19 mg CuI (0.10 mmol, 0.02 eq) and corresponding bromides (5.0 mmol, 1.0 eq), if solid. The flask was evaluated, backfilled with nitrogen three times before addition of 10 mL THF and 1.4 mL TEA (10 mmol, 2.0 eq). Trimethylsilylacetylene (15 mmol, 3.0 eq) was added dropwise via a syringe and the flask was placed in a pre-heated oil bath at 60 °C for 16h. Upon finished as indicated by TLC, the reaction was quenched with 10 mL saturated aqueous solution of NH_4Cl and extracted with EtOAc. The combined organic phases were further washed with brine, dried over Na_2SO_4, concentrated at reduced pressure. The residue was purified by chromatography using hexane and EtOAc as eluent. Recrystallization was performed if necessary, using pentane and DCM as solvent.

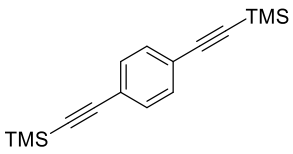

BB1

BB1 was synthesized according to the general procedure at 8.5 mmol scale with 1,4-dibromobenzene and ethynyltrimethylsilane, purification by chromatography resulted in the title compound 1.43 g, 63% yield. ^{1}H NMR (400 MHz, Chloroform-d) δ 7.37 (s, 4H), 0.23 (s, 18H).

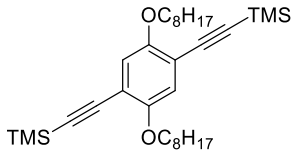

BB2

BB2 was synthesized according to the general procedure at 1.0 mmol scale with 1,4-dibromo-2,5-bis(octyloxy)benzene and ethynyltrimethylsilane, purification by chromatography resulted in the title compound 200 mg, 74% yield. ^{1}H NMR (400 MHz, Chloroform-*d*) δ 7.06 (s, 2H), 3.92 (t, *J* = 6.5 Hz, 4H), 1.78 (p, *J* = 6.6 Hz, 4H), 1.51 – 1.41 (m, 4H), 1.30 (dt, *J* = 17.1, 5.6 Hz, 17H), 0.91 – 0.83 (m, 6H).

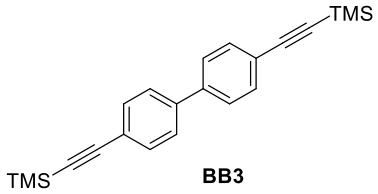

BB3

BB3 was synthesized according to the general procedure at 5.0 mmol scale with . 4,4'-dibromo-1,1'-biphenyl and ethynyltrimethylsilane, purification by chromatography resulted in the title compound 1.1 g, 63% yield ^{1}H NMR (700 MHz, Chloroform-*d*) δ 7.52 (s, 8H), 0.26 (s, 18H).

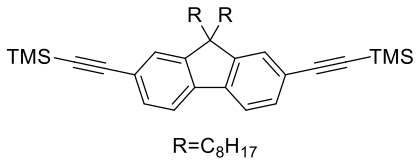

BB4

BB4 was synthesized according to the general procedure at 2.0 mmol scale with . 2,7-dibromo-9,9-dioctyl-9H-fluorene and ethynyltrimethylsilane, purification by chromatography resulted in the title compound 900 mg, 77% yield ^{1}H NMR (700 MHz, Chloroform-*d*) δ 7.52 (s, 8H), 0.26 (s, 18H). ^{1}H NMR (400 MHz, Chloroform-d) δ 7.57 (d, J = 7.6 Hz, 2H), 7.48 – 7.39 (m, 4H), 1.99 – 1.86 (m, 4H), 1.27 – 0.96 (m, 21H), 0.82 (t, J = 6.7 Hz, 6H), 0.53 (s, 4H), 0.28 (s, 18H).

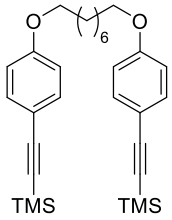

BB5

BB5 was synthesized according to the general procedure at 0.95 mmol scale with . 1,8-bis(4-iodophenoxy)octane and ethynyltrimethylsilane, purification by chromatography resulted in the title compound 360 mg, 77% yield ^{1}H NMR (400 MHz, Chloroform-d) δ 7.37 (d, J = 8.3 Hz, 4H), 6.78 (d, J = 8.4 Hz, 4H), 3.92 (t, J = 6.5 Hz, 4H), 1.75 (p, J = 6.7 Hz, 4H), 1.47 – 1.30 (m, 8H), 0.22 (s, 17H).

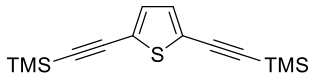

BB7

BB7 was synthesized according to the general procedure at 5.0 mmol scale with . 2,5-dibromothiophene and ethynyltrimethylsilane, purification by chromatography resulted in the title compound 400 mg, 29% yield ^{1}H NMR (401 MHz, Chloroform-d) δ 7.04 (s, 2H), 0.24 (s, 18H).

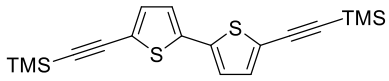

BB8

BB8 was synthesized according to the general procedure at 5.0 mmol scale with . 5,5'-dibromo-2,2'-bithiophene and ethynyltrimethylsilane, purification by chromatography resulted in the title compound 684 mg, 38% yield ^{1}H NMR (600 MHz, Chloroform-d) δ 7.11 (d, J = 3.8 Hz, 2H), 6.99 (d, J = 3.8 Hz, 2H), 0.25 (s, 18H).

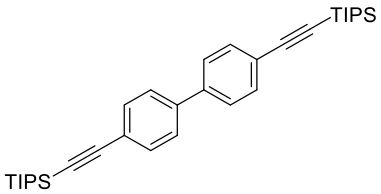

BB9

BB9 was synthesized according to the general procedure at 2.0 mmol scale with . 4,4'-dibromo-1,1'-biphenyl and ethynyltriisopropylsilane, purification by chromatography resulted in the title compound 375 mg, 37% yield ^{1}H NMR (700 MHz, Chloroform-d) δ 7.57 – 7.51 (m, 8H), 1.16 (s, 42H).

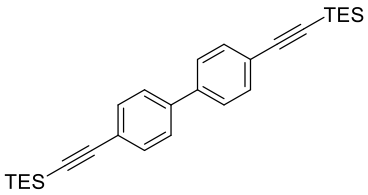

BB10

BB10 was synthesized according to the general procedure at 2.0 mmol scale with . 4,4'-dibromo-1,1'-biphenyl and triethyl(ethynyl)silane, purification by chromatography resulted in the title compound 617 mg, 72% yield ^{1}H NMR (700 MHz, Chloroform-d) δ 7.58 – 7.51 (m, 8H), 1.10 (t, J = 7.9 Hz, 18H), 0.72 (q, J = 7.9 Hz, 12H).

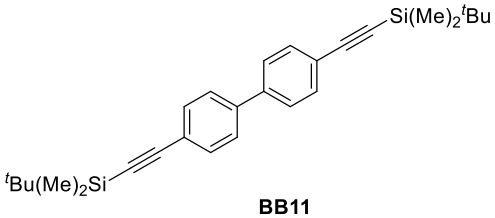

BB11

BB11 was synthesized according to the general procedure at 2.0 mmol scale with . 4,4'-dibromo-1,1'-biphenyl and triethyl(ethynyl)silane, purification by chromatography resulted in the title compound 466 mg, 54% yield ^{1}H NMR (700 MHz, Chloroform-d) δ 7.52 (s, 8H), 1.01 (s, 18H), 0.20 (s, 12H).

8.3.3 Polymerization Attempts

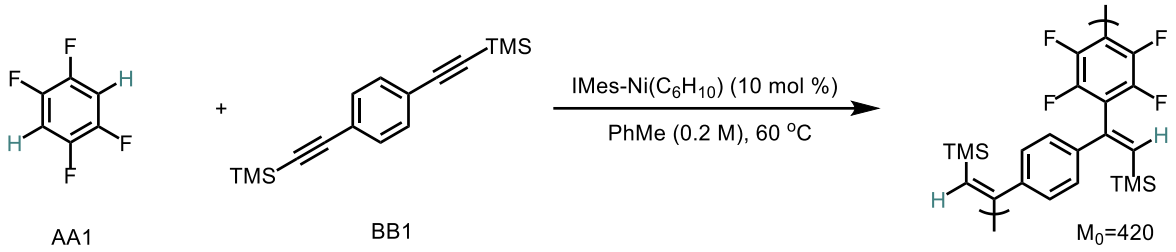

IMes-Ni(C_6H_{10}) (10 μmmol, 0.10 equiv) was weighed in an oven-dried 1dram vial charged with a stir bar in an inert atmosphere glovebox. To a separate vial, arene starting material **AA1** (15 mg, 0.10 mmol, 1.0 equiv) and **BB1** (27 mg, 0.10 mmol, 1.0 equiv) was added, followed by addition of 0.5 mL toluene. This solution was transferred to the previous vial using a micropipette and the reaction vial was capped and brought outside the glovebox to a stir plate pre-heated at 60 °C. After 16 h, the reaction mixture was quenched with 2 mL dichloromethane. The solvent was removed, and the crude reaction mixture was analyzed by NMR using CH_2Br_2 as an internal standard to determine the yield. 1mg/mL (ca.) solution of crude mixture in THF was prepared for GPC analysis.

See NMR spectra attached to the end of this dissertation.

GPC data is not included with this dissertation.

8.4 Experimental Details for Chapter 4

8.4.1 General Procedures for the α-Arylation of Benzamides

To an oven-dried 1 dram vial equipped with a Teflon-coated magnetic stir bar in a N_2 filled glovebox was added [Ir(dF(CF_3)ppy)$_2$(4,4'-di-*t*-buBpy)]PF_6 (PC1) (4.4 mg, 0.004 mmol, 0.02 equiv), $NiCl_2$•DME (2.2 mg, 0.01 mmol, 0.05 equiv), bisoxazoline (BiOx) (1.4 mg, 0.01 mmol, 0.05 equiv), K_3PO_4 (85 mg, 0.4 mmol, 2.0 equiv), and benzamide (0.4 mmol, 2.0 equiv) were combined and suspended in 1.0 mL of dry, degassed EtOAc at rt. The mixture was stirred for 10 minutes before adding aryl bromide (0.2 mmol, 1.0 equiv). The vial was sealed with a Teflon cap before removing it from the glovebox. The reaction was stirred at 900 rpm for 16 h in a recrystallization dish filled with water (for cooling) and irradiated with a 34 W blue LED lamp placed 1 cm away. Upon completion, the reaction mixture was quenched with 1 mL EtOAc and run through a silica gel plug with 5 mL EtOAc. The solvent was removed by rotary evaporation and the crude reaction mixture was purified by silica gel chromatography.

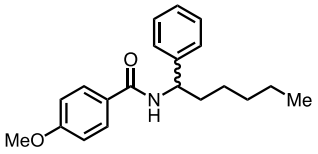

2d

4-methoxy-*N*-(1-phenylhexyl)benzamide (**4-11**)

The general procedure for the α-arylation of benzamides was followed using **4-10** (96 mg, 0.400 mmol, 2.00 equiv), PC1 (4.4 mg, 0.004 mmol, 0.02 equiv), $NiCl_2$•DME (2.2 mg, 0.010 mmol, 0.05 equiv), BiOx (1.4 mg, 0.010 mmol, 0.05 equiv), K_3PO_4 (85 mg, 0.400 mmol, 2.00 equiv), TBAB (64 mg, 0.200 mmol, 1.00 equiv), and bromobenzene (20.8 uL, 0.200 mmol, 1 equiv) in 1.0 mL EtOAc. Analysis by GCFID using tridecane as an internal standard showed 73% yield of the

desired product. Purification by silica gel chromatography (70:30 hexanes/EtOAc) gave the title compound as a white solid.

Rf: 0.35 (70:30 hexanes/EtOAc)

^{1}H NMR (500 MHz, Chloroform-*d*) δ 7.73 (d, *J* = 8.5 Hz, 2H), 7.49 – 7.14 (m, 5H), 6.91 (d, *J* = 8.6 Hz, 2H), 6.21 (d, *J* = 8.1 Hz, 1H), 5.15 (q, *J* = 7.6 Hz, 1H), 3.84 (s, 3H), 2.01 – 1.76 (m, 2H), 1.50 – 1.20 (m, 6H), 0.86 (t, *J* = 6.8 Hz, 3H).

^{13}C NMR (126 MHz, Chloroform-*d*) δ 166.27, 162.28, 142.74, 128.83 (two overlapping peaks), 127.46, 127.12, 126.78, 113.87, 55.58, 53.96, 36.45, 31.75, 26.13, 22.65, 14.16.

HRMS: (ESI) (m/z): [M+H] calculated for $C_{20}H_{25}NO_2$, 312.1963, found 312.1994.

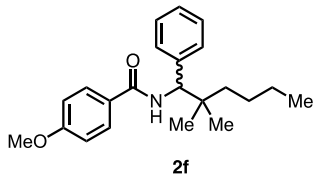

2f

N-(2,2-dimethyl-1-phenylhexyl)-4-methoxybenzamide (**4-9**)

The general procedure for the α-arylation of benzamides was followed **4-8** (50 mg, 0.200 mmol, 1.00 equiv), PC1 (4.5 mg, 0.004 mmol, 0.02 equiv), $NiCl_2$•DME (2.2 mg, 0.010 mmol, 0.05 equiv), BiOx (1.4 mg, 0.010 mmol, 0.05 equiv), K_3PO_4 (85 mg, 0.400 mmol, 2.00 equiv), and bromobenzene (156 uL, 1.500 mmol, 7.50 equiv) in 1 mL EtOAc. Purification by silica gel chromatography (90:10 to 70:30 hexanes/EtOAc) gave the title compound as a white solid (3.8 mg, 0.011 mmol, 6% yield) and recovered **1f** (38.6 mg, 0.154 mmol, 77% recovery).

Rf: 0.25 (70:30 hexanes/EtOAc)

^{1}H NMR (700 MHz, Chloroform-*d*) δ 7.75 – 7.68 (m, 2H), 7.42 (d, *J* = 8.3 Hz, 1H), 7.32 – 7.18 (m, 5H), 6.93 (d, *J* = 8.5 Hz, 2H), 6.63 (d, *J* = 8.4 Hz, 1H), 6.59 (d, *J* = 9.1 Hz, 1H), 5.05 (d, *J* = 9.1 Hz, 1H), 3.84 (s, 3H), 3.72 (s, 1H), 1.37 – 1.22 (m, 4H), 1.00 – 0.85 (m, 9H).

^{13}C NMR (176 MHz, Chloroform-*d*) δ 166.21, 162.23, 140.30, 131.14, 128.73, 128.40, 127.94, 127.47, 127.12, 113.93, 113.56, 60.85, 55.56, 55.45, 41.14, 39.62, 37.55, 29.85, 26.23, 26.20, 24.22, 23.89, 23.68, 14.28.

HRMS: (ESI) (m/z): [M+H] calculated for $C_{22}H_{29}NO_2$, 340.2276, found 340.2329.

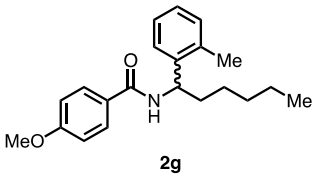

2g

4-methoxy-*N*-(1-(*o*-tolyl)hexyl)benzamide (**4-15**)

The general procedure for the α-arylation of benzamides was followed using **4-10** (94 mg, 0.400 mmol, 2.00 equiv), PC1 (4.4 mg, 0.004 mmol, 0.02 equiv), $NiCl_2$•DME (2.2 mg, 0.010 mmol, 0.05 equiv), BiOx (1.4 mg, 0.010 mmol, 0.05 equiv), K_3PO_4 (85 mg, 0.400 mmol, 2.00 equiv), and 2-methylbromobenzene1 (24 uL, 0.200 mmol, 1.00 equiv) in 1 mL EtOAc. Analysis by ^{1}H NMR using dibromomethane as an internal standard showed 54% yield of the desired product. Purification by silica gel chromatography (90:10 to 80:20 hexanes/EtOAc) gave the title compound as a white solid.

Rf: 0.40 (70:30 hexanes/EtOAc)

^{1}H NMR (400 MHz, Chloroform-*d*) δ 7.70 (d, *J* = 9.0 Hz, 2H), 7.28 (d, *J* = 7.4 Hz, 2H), 7.23 – 7.10 (m, 3H), 6.88 (d, *J* = 8.8 Hz, 2H), 6.17 (d, *J* = 8.1 Hz, 1H), 5.36 (q, *J* = 7.6 Hz, 1H), 3.81 (s, 3H), 2.43 (s, 3H), 1.84 (tdd, *J* = 15.3, 11.3, 5.7 Hz, 1H), 1.28 (p, *J* = 11.8 Hz, 6H), 0.84 (t, 6.6 Hz, 3H).

^{13}C NMR (100 MHz, Chloroform-*d*) δ 166.12, 162.24, 140.89, 136.44, 130.89, 128.79, 127.26, 127.03, 126.40, 125.04, 113.84, 55.54, 50.03, 36.20, 31.84, 26.20, 22.67, 19.63, 14.18.

HRMS: (ESI) (m/z): [M+H] calculated for $C_{21}H_{27}NO_2$, 326.2120, found 326.2125.

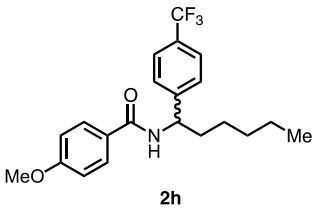

2h

4-methoxy-*N*-(1-(4-(trifluoromethyl)phenyl)hexyl)benzamide (**4-16**)

The general procedure for the α-arylation of benzamides was followed using **4-10** (94 mg, 0.400 mmol, 2.00 equiv), PC1 (4.4 mg, 0.004 mmol, 0.02 equiv), $NiCl_2$•DME (2.2 mg, 0.010 mmol, 0.05 equiv), BiOx (1.4 mg, 0.010 mmol, 0.05 equiv), K_3PO_4 (85 mg, 0.400 mmol, 2.00 equiv), and 4-bromobenzotrifluoride (28 uL, 0.200 mmol, 1.00 equiv) in 1 mL EtOAc. Analysis by ^{1}H NMR using dibromomethane as an internal standard showed 71% yield of the desired product. Purification by silica gel chromatography (90:10 to 80:20 hexanes/EtOAc) gave the title compound as a white solid.

Rf: 0.40 (70:30 hexanes/EtOAc)

^{1}H NMR (500 MHz, Chloroform-*d*) δ 7.85 (d, *J* = 8.0 Hz, 2H), 7.77 – 7.57 (m, 2H), 7.28 (q, *J* = 4.5 Hz, 1H), 6.45 (d, *J* = 7.9 Hz, 1H), 5.15 (q, *J* = 7.7 Hz, 1H), 2.04 – 1.82 (m, 2H), 1.44 – 1.14 (m, 8H), 0.86 (t, *J* = 6.7 Hz, 3H).

^{13}C NMR (126 MHz, Chloroform-*d*) δ 165.58, 142.14, 138.09, 133.41, 133.15, 128.93, 128.23, 127.71, 127.54, 126.76, 125.71 (q, *J* = 3.6 Hz), 123.78 (q, *J* = 272.3 Hz), 54.40, 36.26, 31.68, 26.13, 22.63, 14.13.

^{19}F NMR (377 MHz, Chloroform-*d*) δ -63.03.

HRMS: (ESI) (m/z): [M+H] calculated for $C_{21}H_{24}F_3NO_2$, 380.1837, found 380.1893.

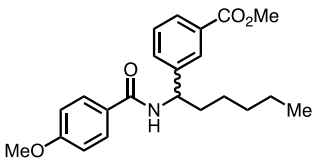

2i

methyl 3-(1-(4-methoxybenzamido)hexyl)benzoate (**4-19**)

The general procedure for the α-arylation of benzamides was followed using **1d** (94 mg, 0.400 mmol, 2.00 equiv), PC1 (4.4 mg, 0.004 mmol, 0.02 equiv), $NiCl_2$•DME (2.2 mg, 0.010 mmol, 0.05 equiv), BiOx (1.4 mg, 0.010 mmol, 0.05 equiv), K_3PO_4 (85 mg, 0.400 mmol, 2.00 equiv), and methyl-3-bromobenzoate (43 mg, 0.2 mmol, 1.00 equiv) in 1 mL EtOAc. Analysis by ^{1}H NMR using dibromomethane as an internal standard showed 59% yield of the desired product. Purification by silica gel chromatography (100% hexanes to 80:20 hexanes/EtOAc) gave the title compound as a white solid.

Rf: 0.20 (2.5:97.5 acetone/DCM)

^{1}H NMR (700 MHz, Chloroform-*d*) δ 8.02 (s, 1H), 7.91 (d, *J* = 7.8 Hz, 1H), 7.79 – 7.65 (m, 2H), 7.54 (d, *J* = 7.8 Hz, 1H), 7.38 (t, *J* = 7.7 Hz, 1H), 6.88 (d, *J* = 8.8 Hz, 2H), 6.45 (d, *J* = 7.9 Hz, 1H), 5.16 (q, *J* = 7.5 Hz, 1H), 3.89 (s, 3H), 3.82 (s, 3H), 1.95 – 1.81 (m, 2H), 1.45 – 1.22 (m, 6H), 0.84 (t, *J* = 6.8 Hz, 3H).

^{13}C NMR (176 MHz, Chloroform-*d*) δ 167.12, 166.41, 162.31, 143.49, 131.83, 130.62, 128.88, 128.79, 128.59, 127.44, 126.80, 55.51, 53.78, 52.24, 36.46, 31.63, 29.39, 26.11, 22.59, 14.10.

HRMS: (ESI) (m/z): [M+H] calculated for $C_{22}H_{27}NO_4$, 370.2018, found 370.1994.

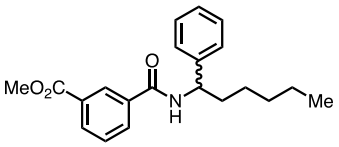

2j

methyl 3-((1-phenylhexyl)carbamoyl)benzoate (**4-20**)

The general procedure for the α-arylation of benzamides was followed using **benzamide** (106 mg, 0.400 mmol, 2.00 equiv), PC1 (4.4 mg, 0.004 mmol, 0.02 equiv), $NiCl_2$•DME (2.2 mg, 0.010 mmol, 0.05 equiv), BiOx (1.4 mg, 0.010 mmol, 0.05 equiv), K_3PO_4 (85 mg, 0.400 mmol, 2.00 equiv), and bromobenzene (21 uL, 0.200 mmol, 1.00 equiv) in 1 mL EtOAc/DMAc (9:1). Analysis by ^{1}H NMR using dibromomethane as an internal standard showed 58% yield of the desired product. Purification by silica gel chromatography (70:30 hexanes/EtOAc) gave the title compound as a white solid.

Rf: 0.35 (80:20 hexanes/EtOAc)

^{1}H NMR (400 MHz, Chloroform-*d*) δ 8.35 (s, 1H), 8.14 (d, *J* = 7.6 Hz, 1H), 8.03 (d, *J* = 7.8 Hz, 1H), 7.51 (t, *J* = 7.8 Hz, 1H), 7.40 – 7.30 (m, 5H), 7.28 (d, *J* = 3.1 Hz, 1H), 6.44 (d, *J* = 8.2 Hz, 2H), 5.17 (q, *J* = 7.6 Hz, 2H), 3.93 (s, 3H), 1.93 (dq, *J* = 16.4, 9.4, 7.1 Hz, 2H), 1.33 (m, 6H), 0.86 (t, *J* = 6.7 Hz, 3H).

^{13}C NMR (176 MHz, Chloroform-*d*) δ 166.55, 165.69, 142.26, 135.08, 132.52, 132.14, 130.54, 129.08, 128.91, 127.66, 127.48, 126.84, 54.30, 52.57, 36.26, 31.71, 26.16, 22.65, 14.17.

HRMS: (ESI) (m/z): [M+H] calculated for $C_{21}H_{25}NO_3$, 340.1912, found 340.1913.

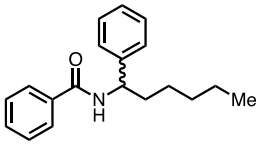

2k

N-(1-phenylhexyl)benzamide (**4-13**)

The general procedure for the α-arylation of benzamides was followed using **4-12** (86 mg, 0.400 mmol, 2.00 equiv), PC1 (4.4 mg, 0.004 mmol, 0.02 equiv), $NiCl_2$•DME (2.2 mg, 0.010 mmol, 0.05 equiv), BiOx (1.4 mg, 0.010 mmol, 0.05 equiv), K_3PO_4 (85 mg, 0.400 mmol, 2.00 equiv), and bromobenzene (21 uL, 0.200 mmol, 1.00 equiv) in 1 mL EtOAc/DMAc (9:1). Purification by silica

gel chromatography (100% hexanes to 85:15 hexanes/EtOAc) gave the title compound as a white solid (37.1 mg, 0.132 mmol, 66% yield).

Rf: 0.60 (70:30 hexanes/EtOAc)

^{1}H NMR (500 MHz, Chloroform-*d*) δ 7.76 (d, *J* = 7.6 Hz, 2H), 7.48 (t, *J* = 7.5 Hz, 1H), 7.41 (t, *J* = 7.5 Hz, 2H), 7.38 – 7.31 (m, 5H), 7.27 (d, *J* = 8.0 Hz, 1H), 6.40 (d, *J* = 9.2 Hz, 1H), 5.16 (q, *J* = 7.7 Hz, 1H), 1.90 (ddt, *J* = 23.5, 16.9, 8.3 Hz, 2H), 1.33 (q, *J* = 19.6, 11.8 Hz, 6H), 0.86 (t, *J* = 6.3 Hz, 3H).

^{13}C NMR (126 MHz, Chloroform-*d*) δ 166.79, 142.56, 134.82, 131.53, 128.81, 128.65, 127.48, 127.03, 126.75, 54.06, 36.38, 31.71, 26.12, 22.63, 14.15.

8.4.2 Evaluation of TBAB Effects

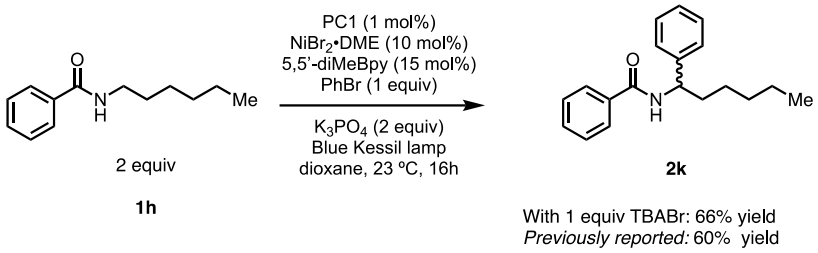

Discussion: Using conditions previously developed for the arylation of benzamides using a $NiBr_2$•DME/ 5,5'-diMeByp catalytic system, modest increases in yield were observed.

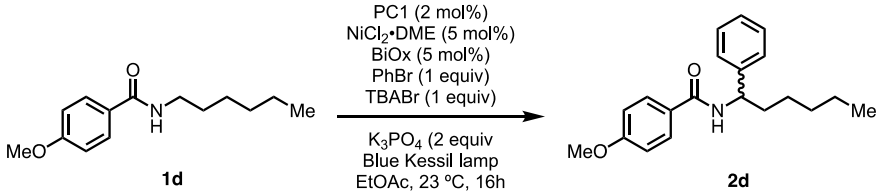

entry	Deviation from above	% yield [a]
1	none	70

2	10% TBAB	62
3	$NiBr_2$•dme, no TBAB	50
4	$NiBr_2$•dme, 1 eq TBAB	75

[a] Reaction was carried out with 0.20 mmol PhBr, 0.40 mmol benzamide. Yield is determined by ^1H NMR using dibromoethane as an internal standard.

8.5 Experimental Details for Chapter 5

8.5.1 Synthesis of Starting Materials

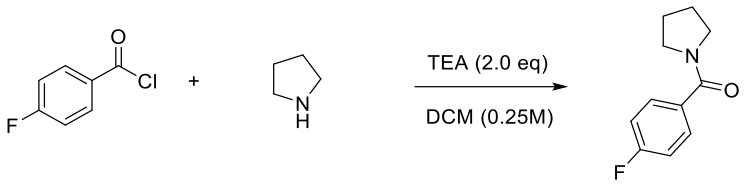

(4-fluorophenyl)(pyrrolidin-1-yl)methanone was synthesized according to literature.

Under N_2 atmosphere, to a round bottom flask with a stir bar, a sequential addition of 4-fluorobenzoyl chloride (0.79 g, 5.0 mmol, 1.0 eq), DCM (20 mL), pyrrolidine (0.36 g, 5.0 mmol, 1.0 eq) was followed by triethyl amine (1.0 g, 10 mmol, 2.0 eq). The mixture was washed with water, extracted with DCM and washed with brine. The organic layer was dried with Na_2SO_4, concentrated under reduced pressure. Further purification via recrystallization from DCM / pentane as a white solid (0.45 g, 47% yield) The spectra matched previous reports.[171]

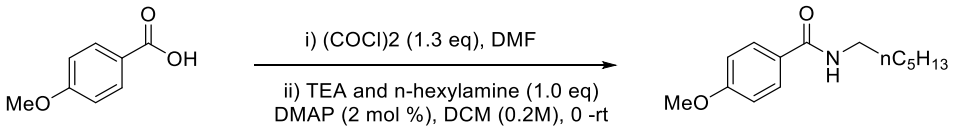

N-hexyl-4-methoxybenzamide was synthesized according to literature.

Under N_2 atmosphere, to a pre-stirred solution of 4-methoxybenzoic acid (0.6 g, 3.9 mmol, 1.0 eq) in DCM, added oxalyl chloride (0.43 mL, 5.1 mmol, 1.3 eq), DMF (3 drops), followed by triethyl amine (0.55 mL, 3.9 mmol, 1.0 eq), *n*-hexylamine (0.52 mL, 3.9 mmol, 1.0 eq) and DMAP (10 mg, 0.1 mmol, 0.02 eq). The reaction was quenched with water, extracted with DCM and washed with brine. The organic layer was dried with Na_2SO_4, concentrated under reduced pressure, and purified by column ethyl acetate / hexane(0 – 15/85), yielding the title compound as a white solid (0.87g, 94% yield). The spectra matched previous reports.[172]

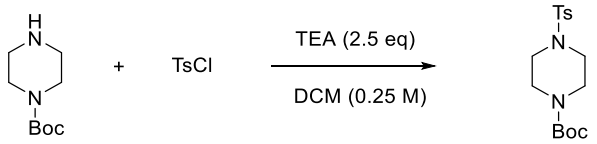

tert-butyl 4-tosylpiperazine-1-carboxylate was synthesized according to literature .

Under N_2 atmosphere, to a pre-stirred solution of *tert*-butyl piperazine-1-carboxylate (0.93 g, 5.0 mmol, 1.0 eq), 4-methylbenzenesulfonyl chloride (1.9 g, 10.0 mmol, 2.0 eq) in DCM, added triethyl amine (1.3 g, 12 mmol, 2.5 eq). The reaction was quenched with water, extracted with DCM and washed with brine. The organic layer was dried with Na_2SO_4, concentrated under reduced pressure and was purified by column ethyl acetate / hexane(0 – 15/85) as a white solid (0.45 g, 47% yield). The spectra matched previous reports.[173]

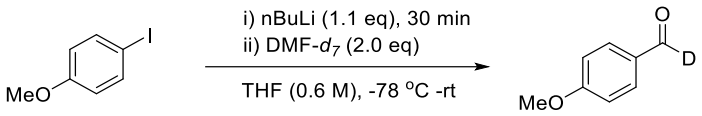

4-methoxybenzaladehyde-d_1 was synthesized according to the literature.

Under N_2 atmosphere at -78 °C, to a pre-stirred solution of 1-iodo-4-methoxybenzene (1.47g, 6.28 mmol, 1.0 eq) in THF, slowly added nBuLi (4.3 mL, 1.6 M in THF, 1.1 eq). The solution was kept stirring at the same temperature for 30 min before the slow addition of DMF-d_7 (1.1 mL, 12.6 mmol, 2.0 eq). The reaction was allowed to warm up to room temperature over a further 30 min. The reaction mixture was quenched with sat NH_4Cl solution (30 mL) and H_2SO_4 (1 drop), extracted with EtOAc, washed with brine. The organic layer was dried with Na_2SO_4, concentrated under reduced pressure, and was purified by column ethyl acetate / hexane(0 – 10/90) as an amber oil (0.60 g, 70% yield). The spectra matched previous reports.

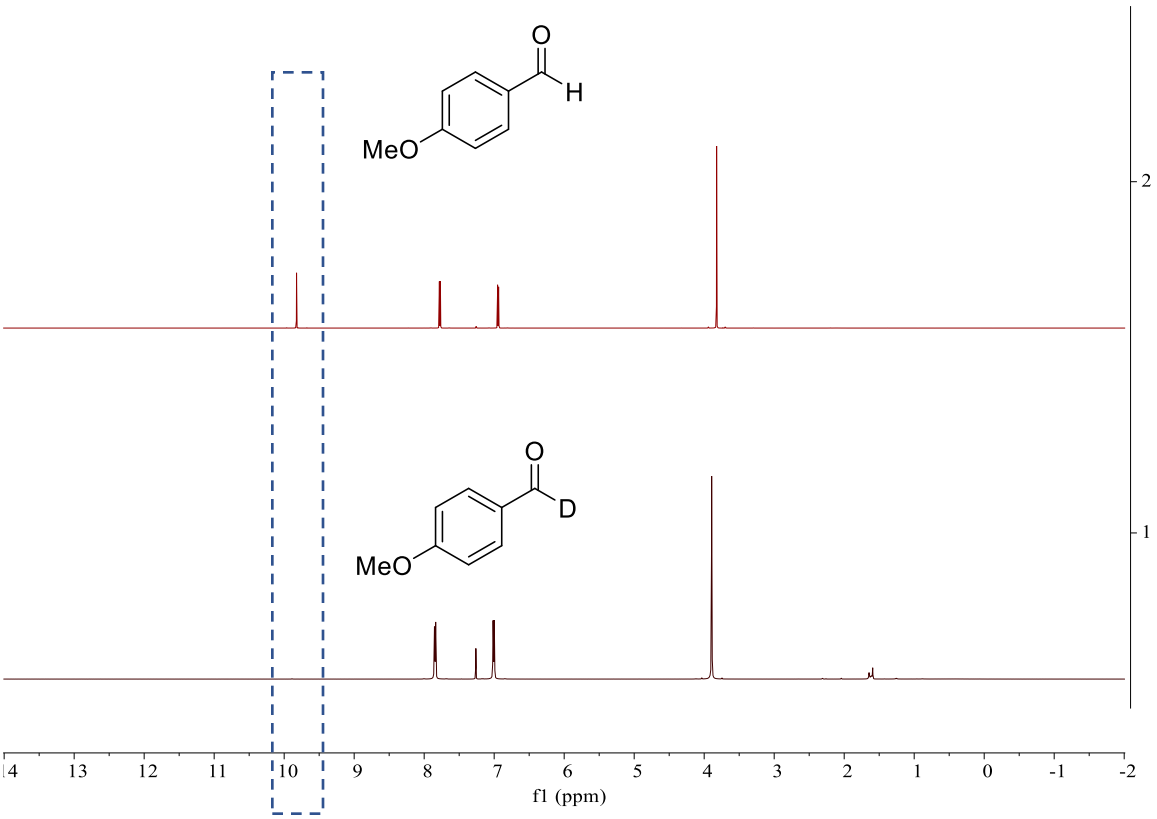

8.5.2 General Procedure and Experimental Setup

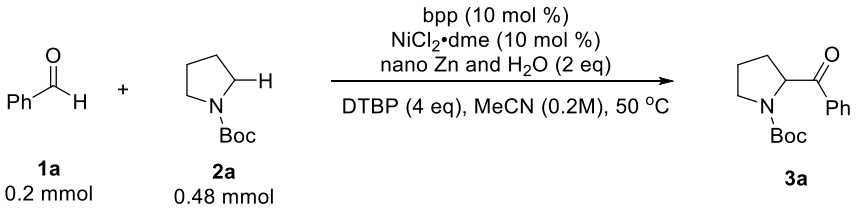

To an oven-dried 1 dram vial charged with a stir bar in an inert atmosphere glovebox (GB), weighed nano powder Zn (26 mg, 0.40 mmol, 2.0 eq), bpp (4.2 mg, 0.02 mmol, 0.1 eq), $NiCl_2$•dme (4.4 mg, 0.02 mmol, 0.1 eq). The vial was capped and brought outside the GB.

To a separate vial outside GB, benzaldehyde (21 mg, 0.20 mmol, 1.0 eq), *N*-Boc-pyrrolidine (82 mg, 0.48 mmol, 2.4 eq) and water (3.6 mg, 0.40 mmol, 2.0 eq) was added via micro-pipette. The starting materials were dissolved with MeCN (1.0 mL) before addition of DTBP (112 mg, 0.8

mmol, 4.0 eq). This solution was transferred to the previous vial via syringe and the needle hole was sealed with high-vac grease and parafilm. The vial was let stir at 800 rpm at 50 °C for 16h behind a safety blast shield before being quenched with 2 mL DCM. The solution was passed through syringe filter and concentrated under reduced pressure. The crude reaction mixture was analyzed by NMR using CH_2Br_2 as an internal standard to determine products ratio if necessary. Purification via chromatography yielded the title compound.

Caution! Although control experiments showed that Zn alone would not decompose DTBP at 50 °C, all reaction vials were placed on the heating plate behind a blast shield, which could also be helpful in situation where pressure builds up (potential formation of gas via β-methyl scission of *tert*-butoxyl radicals) although we have never observed in all experiments.

Please note that the proton, carbon, and fluorine spectra could all present rotameric signals and were all labelled and integrated to the best as we can.

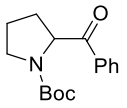

3a

tert-butyl 2-benzoylpyrrolidine-1-carboxylate (**5-18**) was prepared according to the general procedure with benzaldehyde **5-17** (21 mg, 0.2 mmol, 1.0 eq), *N*-Boc-pyrrolidine **5-14** (82 mg, 0.48 mmol, 2.4 eq). After purification with column chromatography eluting with ethyl acetate / hexane (0 – 10/90), the desired product was obtained as a colorless oil (34.0 mg, 62% yield).

^{1}H NMR (700 MHz, Chloroform-d) δ 7.96 (dd, *J* = 25.3, 7.7 Hz, 2H), 7.56 (dt, *J* = 24.4, 7.4 Hz, 1H), 7.46 (dt, *J* = 22.8, 7.6 Hz, 2H), 5.33 (dd, *J* = 9.4, 2.9 Hz, 0.4H), 5.19 (dd, *J* = 9.0, 3.6 Hz, 0.6H), 3.71 – 3.60 (m, 1H), 3.51 (ddt, J = 55.3, 11.7, 7.1 Hz, 1H), 2.36 – 2.24 (m, 1H), 1.92 (m, 3H), 1.46 (s, 5H), 1.25 (s, 5H).

^{13}C NMR (176 MHz, $CDCl_3$) δ 198.9, 198.4, 154.4, 153.8, 135.3, 135.1, 133.18, 133.15, 128.7, 128.6, 128.5, 128.2 , 79.8, 79.6, 61.3, 61.1, 46.8, 46.6, 30.9, 29.8, 28.5, 28.2, 24.2, 23.5.

The spectra matched previous reports.[174]

HRMS (ESI+): m/z: calculated for $C_{16}H_{21}NO_3$ [M + Na]+: 298.1413; found: 298.1412

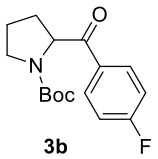

3b

tert-butyl 2-(4-fluorobenzoyl)pyrrolidine-1-carboxylate (**5-19**) was prepared according to the general procedure with 4-fluorobenzaldehyde (25 mg, 0.2 mmol, 1.0 eq), *N*-Boc-pyrrolidine **5-14** (82 mg, 0.48 mmol, 2.4 eq). After purification with column chromatography eluting with ethyl acetate / hexane (0 – 10/90), the desired product was obtained as a colorless oil (32.2 mg, 55% yield).

^{1}H NMR (700 MHz, Chloroform-*d*) δ 8.00 (dt, *J* = 21.3, 6.8 Hz, 2H), 7.14 (dt, *J* = 23.5, 8.4 Hz, 2H), 5.28 (dd, *J* = 9.2, 3.5 Hz, 0.5H), 5.14 (dd, *J* = 9.2, 3.8 Hz, 0.6H), 3.70 – 3.60 (m, 1H), 3.57 – 3.46 (m, 1H), 2.36 – 2.26 (m, 1H), 1.97 – 1.88 (m, 3H), 1.46 (s, 6H), 1.25 (s, 5H).

^{13}C NMR (176 MHz, Chloroform-*d*) δ 197.4, 197.0, 166.5 (d, *J* = 4.4 Hz), 165.1 (d, *J* = 4.6 Hz), 154.5, 153.7, 131.6 (d, *J* = 3.1 Hz), 131.5 (d, *J* = 3.0 Hz), 131.2 (d, *J* = 9.3 Hz), 130.8 (d, *J* = 9.3 Hz), 115.8 (dd, *J* = 27.1, 21.9 Hz), 79.8, 79.7, 61.2, 60.9, 46.8, 46.6, 30.9, 29.8, 28.5, 28.2, 24.2, 23.6.

^{19}F NMR (471 MHz, Chloroform-*d*) δ -104.77 (p, *J* = 7.3, 6.8 Hz), -105.00 (t, *J* = 7.7 Hz).

The spectra matched previous reports.[175]

HRMS (ESI+): m/z: calculated for $C_{16}H_{20}FNO_3$ [M + Na]+: 316.1319; found: 316.1329.

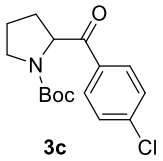

3c

tert-butyl 2-(4-chlorobenzoyl)pyrrolidine-1-carboxylate (**5-20**) was prepared according to the general procedure with 4-chlorobenzaldehyde (28 mg, 0.2 mmol, 1.0 eq), *N*-Boc-pyrrolidine **5-14** (82 mg, 0.48 mmol, 2.4 eq). After purification with column chromatography eluting with ethyl acetate / hexane (0 – 10/90), the desired product was obtained as a colorless oil (24.6 mg, 40% yield).

^{1}H NMR (500 MHz, Chloroform-*d*) δ 7.85 (dd, *J* = 14.7, 8.6 Hz, 2H), 7.38 (dd, *J* = 16.8, 8.6 Hz, 2H), 5.20 (dd, *J* = 9.2, 3.5 Hz, 0.4H), 5.07 (dd, *J* = 9.1, 3.8 Hz, 0.5H), 3.58 (m, 1H), 3.51 – 3.39 (m, 1H), 2.29 – 2.17 (m, 1H), 1.93 – 1.81 (m, 3H), 1.39 (s, 6H), 1.19 (s, 4H).

^{13}C NMR (126 MHz, Chloroform-*d*) δ 197.8, 197.4, 154.5, 153.7, 139.7, 139.6, 133.6, 133.5, 129.9, 129.6, 129.1, 128.9, 109.4, 108.0, 79.9, 79.8, 61.3, 61.0, 46.8, 46.6, 30.8, 29.8, 28.51, 28.48, 24.2, 23.6.

HRMS (ESI+): m/z: calculated for $C_{16}H_{20}ClNO_3$ [M + Na]+: 332.1024; found: 332.1022.

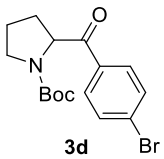

3d

tert-butyl 2-(4-bromobenzoyl)pyrrolidine-1-carboxylate (**5-21**) was prepared according to the general procedure with 4-bromobenzaldehyde (37 mg, 0.2 mmol, 1.0 eq), *N*-Boc-pyrrolidine **5-14** (82 mg, 0.48 mmol, 2.4 eq). After purification with column chromatography eluting with ethyl acetate / hexane (0 – 10/90), the desired product was obtained as a colorless oil (25.8 mg, 36% yield).

^{1}H NMR (500 MHz, Chloroform-*d*) δ 7.77 (dd, *J* = 14.6, 8.6 Hz, 2H), 7.54 (dd, *J* = 16.9, 8.6 Hz, 2H), 5.19 (dd, *J* = 9.2, 3.6 Hz, 0.4H), 5.06 (dd, *J* = 9.0, 3.9 Hz, 0.6H), 3.63 – 3.52 (m, 1H), 3.44 (m, 1H), 2.30 – 2.16 (m, 1H), 1.90 – 1.81 (m, 3H), 1.40 (s, 6H), 1.19 (s, 5H).

^{13}C NMR (126 MHz, Chloroform-*d*) δ 198.0, 197.7, 154.5, 153.7, 142.4, 141.5, 134.0, 133.9, 132.1, 131.9, 130.0, 129.7, 128.44, 128.37, 109.4, 108.0, 79.9, 79.8, 61.3, 61.0, 46.8, 46.6, 30.8, 29.8, 28.5, 28.2, 24.2, 23.6.

HRMS (ESI+): m/z: calculated for $C_{16}H_{20}BrNO_3$ [M + Na]+: 376.0519; found: 376.0516.

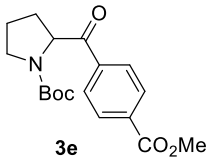

3e

tert-butyl 2-(4-(methoxycarbonyl)benzoyl)pyrrolidine-1-carboxylate (**5-22**) was prepared according to the general procedure with methyl 4-formylbenzoate (33 mg, 0.2 mmol, 1.0 eq), *N*-Boc-pyrrolidine **5-14** (82 mg, 0.48 mmol, 2.4 eq). After purification with column chromatography eluting with ethyl acetate / hexane (0 – 10/90), the desired product was obtained as a colorless oil (33.9 mg, 51% yield).

^{1}H NMR (700 MHz, Chloroform-*d*) δ 8.12 (dd, *J* = 22.5, 8.5 Hz, 2H), 8.01 (dd, *J* = 21.1, 7.7 Hz, 2H), 5.31 (dt, *J* = 7.1, 3.7 Hz, 0.5H), 5.18 (dd, *J* = 9.4, 3.7 Hz, 0.6H), 3.95 (m, 3H), 3.66 (m, 1H), 3.58 – 3.46 (m, 1H), 2.32 (m, 1H), 1.99 – 1.88 (m, 3H), 1.46 (s, 4H), 1.25 (s, 6H).

^{13}C NMR (176 MHz, Chloroform-*d*) δ 198.6, 198.2, 166.2, 166.1, 154.4, 153.6, 138.6, 138.5, 134.0, 133.9, 129.9, 129.8, 128.4, 128.1, 80.0, 79.8, 61.5, 61.3, 52.5, 52.4, 46.8, 46.6, 30.7, 29.7, 28.5, 28.2, 24.2, 23.6.

HRMS (ESI+): m/z: calculated for $C_{18}H_{23}NO_5$ [M + Na]+: 356.1468; found: 356.1471

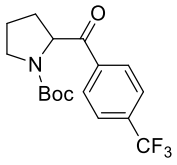

3f

tert-butyl 2-(4-(trifluoromethyl)benzoyl)pyrrolidine-1-carboxylate (**5-23**) was prepared according to the general procedure with 4-(trifluoromethyl)benzaldehyde (35 mg, 0.2 mmol, 1.0 eq), *N*-Boc-pyrrolidine **5-14** (82 mg, 0.48 mmol, 2.4 eq). After purification with column chromatography eluting with ethyl acetate / hexane (0 – 10/90), the desired product was obtained as a colorless oil (35.0 mg, 50% yield).

^{1}H NMR (500 MHz, Chloroform-d) δ 8.07 (dd, *J* = 15.9, 8.1 Hz, 2H), 7.74 (dd, *J* = 17.2, 8.2 Hz, 2H), 5.30 (dd, *J* = 9.1, 3.7 Hz, 0.4H), 5.17 (dd, *J* = 9.1, 4.0 Hz, 0.6H), 3.73 – 3.61 (m, 1H), 3.58 – 3.46 (m, 1H), 2.37 – 2.25 (m, 1H), 1.99 – 1.88 (m, 3H), 1.46 (s, 5H), 1.26 (s, 5H).

^{13}C NMR (126 MHz, Chloroform-d) δ 197.1, 197.0, 153.4, 152.6, 137.03, 136.98, 133.48 (dd, *J* = 32.7, 16.4 Hz), 127.8, 127.5, 124.8 (q, *J* = 3.8), 124.65 (q, *J* = 3.7 Hz)f, 79.0, 78.9, 60.6, 60.2, 45.8, 45.6, 29.7, 28.6, 27.4, 27.2, 23.3, 22.5.

^{19}F NMR (564 MHz, Chloroform-d) δ -63.20.

HRMS (ESI+): m/z: calculated for $C_{17}H_{20}F_3NO_3$ [M + Na]+: 366.1287; found: 366.1283

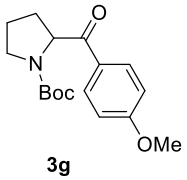

3g

tert-butyl 2-(4-methoxybenzoyl)pyrrolidine-1-carboxylate (**5-24**) was prepared according to the general procedure with 4-methoxybenzaldehyde (27 mg, 0.2 mmol, 1.0 eq), *N*-Boc-pyrrolidine **5-14** (82 mg, 0.48 mmol, 2.4 eq). After purification with column chromatography eluting with ethyl

acetate / hexane (0 – 10/90), the desired product was obtained as a colorless oil (41.2 mg, 67% yield).

^{1}H NMR (500 MHz, Chloroform-*d*) δ 7.94 (dd, *J* = 14.0, 8.9 Hz, 2H), 6.92 (dd, *J* = 15.6, 8.9 Hz, 2H), 5.29 (dd, *J* = 9.2, 2.8 Hz, 0.4H), 5.14 (dd, *J* = 8.8, 3.8 Hz, 0.6H), 3.85 (d, *J* = 10.4 Hz, 3H), 3.69 – 3.57 (m, 1H), 3.55 – 3.45 (m, 1H), 2.33 – 2.22 (m, 1H), 1.96 – 1.86 (m, 3H), 1.45 (s, 5H), 1.24 (s, 5H).

^{13}C NMR (126 MHz, Chloroform-*d*) δ 197.4, 196.8, 163.5, 154.5, 153.9, 130.8, 130.5, 128.2, 128.0, 113.9, 113.8, 79.6, 79.5, 61.0, 60.8, 55.48, 55.46, 46.8, 46.6, 31.0, 30.0, 28.50, 28.46, 28.4, 28.2, 24.2, 23.6.

The spectra matched previous reports.[176]

HRMS (ESI+): m/z: calculated for $C_{17}H_{23}NO_4$ [M + Na]+: 328.1519; found: 328.1519

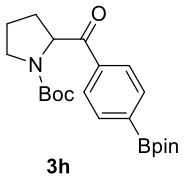

3h

tert-butyl 2-(4-(4,4,5,5-tetramethyl-1,3,2-dioxaborolan-2-yl)benzoyl)pyrrolidine-1-carboxylate (**5-25**) was prepared according to the general procedure with 4-(4,4,5,5-tetramethyl-1,3,2-dioxaborolan-2-yl)benzaldehyde (46 mg, 0.2 mmol, 1.0 eq), *N*-Boc-pyrrolidine **5-14** (82 mg, 0.48 mmol, 2.4 eq). After purification with column chromatography eluting with ethyl acetate / hexane (0 – 10/90), the desired product was obtained as a colorless oil (30.5 mg, 38% yield).

^{1}H NMR (500 MHz, Chloroform-d) δ 7.97 – 7.77 (m, 4H), 5.34 (dd, J = 9.3, 3.2 Hz, 0.4H), 5.20 (dd, J = 9.0, 3.6 Hz, 0.6H), 3.72 – 3.59 (m, 1H), 3.58 – 3.45 (m, 1H), 2.35 – 2.25 (m, 1H), 1.95 – 1.85 (m, 3H), 1.47 (s, 6H), 1.36 (d, J = 3.5 Hz, 9H), 1.26 (s, 6H).

^{13}C NMR (126 MHz, Chloroform-d) δ 199.2, 198.6, 154.5, 153.8, 137.2, 137.0, 135.0, 134.9, 127.5, 127.2, 115.9, 84.3, 84.2, 79.8, 79.7, 61.4, 61.3, 46.8, 46.6, 29.8, 29.7, 28.5, 28.2, 24.91, 24.88, 24.1, 23.6.

HRMS (ESI+): m/z: calculated for $C_{22}H_{32}BNO_5$ [M + Na]+: 424.2266; found: 424.2267

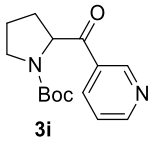

3i

tert-butyl 2-nicotinoylpyrrolidine-1-carboxylate (**5-26**) was prepared according to the general procedure with nicotinaldehyde (21 mg, 0.2 mmol, 1.0 eq), *N*-Boc-pyrrolidine **5-14** (82 mg, 0.48 mmol, 2.4 eq). After purification with column chromatography eluting with ethyl acetate / hexane (0 – 10/90), the desired product was obtained as a colorless oil (23.1 mg, 42% yield).

^{1}H NMR (500 MHz, Chloroform-*d*) δ 9.19 (d, *J* = 8.0 Hz, 1H), 8.79 (dd, *J* = 18.9, 4.3 Hz, 1H), 8.26 (dd, *J* = 18.2, 7.9 Hz, 1H), 7.43 (ddd, *J* = 17.8, 8.0, 4.9 Hz, 1H), 5.27 (dd, *J* = 9.2, 3.7 Hz, 0.5H), 5.15 (dd, *J* = 8.8, 3.8 Hz, 0.5H), 3.65 (m, 1H), 3.59 – 3.44 (m, 1H), 2.34 (m, 1H), 1.95 (m, 3H), 1.46 (s, 5H), 1.26 (s, 4H).

^{13}C NMR (126 MHz, Chloroform-*d*) δ 198.1, 197.7, 154.5 153.7, 153.6, 149.7, 149.5, 136.0, 135.6, 130.7, 130.6, 123.8, 123.7, 80.1, 80.0, 61.6, 61.3, 46.8, 46.7, 30.7, 29.6, 28.5, 28.2, 24.3, 23.6.

HRMS (ESI+): m/z: calculated for $C_{15}H_{20}N_2O_3$ [M + H]+: 277.1546; found: 277.1550

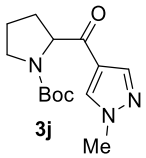

3j

tert-butyl 2-(1-methyl-1H-pyrazole-4-carbonyl)pyrrolidine-1-carboxylate (**5-27**) was prepared according to the general procedure with 1-methyl-1H-pyrazole-4-carbaldehyde (22 mg, 0.2 mmol, 1.0 eq), *N*-Boc-pyrrolidine **5-14** (82 mg, 0.48 mmol, 2.4 eq). After purification with column

chromatography eluting with ethyl acetate / DCM (0 – 10/90), the desired product was obtained as a colorless oil (26.9 mg, 48% yield).

^{1}H NMR (500 MHz, Chloroform-*d*) δ 7.94 – 7.86 (m, 2H), 4.84 (dd, *J* = 8.9, 3.6 Hz, 0.4H), 4.65 (dd, *J* = 8.4, 4.6 Hz, 0.6H), 3.93 (d, *J* = 14.9 Hz, 3H), 3.64 – 3.54 (m, 2H), 2.32 – 2.19 (m, 1H), 1.98 – 1.84 (m, 3H), 1.44 (s, 4H), 1.27 (s, 6H).

^{13}C NMR (126 MHz, Chloroform-*d*) δ 193.8, 193.2, 154.5, 154.0, 140.4, 133.0, 132.4, 121.6, 121.2, 80.0, 79.8, 63.7, 62.8, 46.9, 46.8, 39.4, 39.3, 31.2, 30.1, 28.5, 28.2, 24.4, 23.8.

HRMS (ESI+): m/z: calculated for $C_{14}H_{21}N_3O_3$ [M + Na]+: 302.1475; found: 302.1474

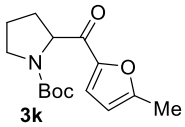

3k

tert-butyl 2-(5-methylfuran-2-carbonyl)pyrrolidine-1-carboxylate (**5-28**) was prepared according to the general procedure with 5-methylfuran-3-carbaldehyde (22 mg, 0.2 mmol, 1.0 eq), *N*-Boc-pyrrolidine **5-14** (82 mg, 0.48 mmol, 2.4 eq). After purification with column chromatography eluting with ethyl acetate / hexane (0 – 10/90), the desired product was obtained as a colorless oil (18.4 mg, 33% yield).

^{1}H NMR (500 MHz, Chloroform-*d*) δ 7.16 (dd, *J* = 20.5, 3.5 Hz, 1H), 6.15 (dd, *J* = 11.5, 3.5 Hz, 1H), 5.03 (dd, *J* = 8.7, 3.6 Hz, 0.4H), 4.84 (dd, *J* = 8.5, 4.5 Hz, 0.6H), 3.67 – 3.51 (m, 2H), 2.39 (d, *J* = 15.8 Hz, 3H), 2.32 – 2.20 (m, 1H), 2.02 – 1.88 (m, 3H), 1.45 (s, 5H), 1.27 (s, 5H).

^{13}C NMR (126 MHz, Chloroform-*d*) δ 187.9, 187.3, 158.0, 153.8, 119.9, 119.5, 109.0, 108.9, 79.8, 79.7, 61.6, 60.9, 47.0, 46.7, 31.3, 30.2, 28.5, 28.2, 24.3, 23.8, 14.1.

HRMS (ESI+): m/z: calculated for $C_{15}H_{21}NO_4$ [M + Na]+: 302.1363; found: 302.1362

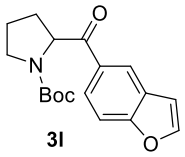

3l

tert-butyl 2-(benzofuran-5-carbonyl)pyrrolidine-1-carboxylate (**5-29**) was prepared according to the general procedure with benzofuran-5-carbaldehyde (30 mg, 0.2 mmol, 1.0 eq), *N*-Boc-pyrrolidine **5-14** (82 mg, 0.48 mmol, 2.4 eq). After purification with column chromatography eluting with ethyl acetate / hexane (0 – 10/90), the desired product was obtained as a colorless oil (16.8 mg, 21% yield).

^{1}H NMR (500 MHz, Chloroform-*d*) δ 8.28 (dd, *J* = 21.4, 1.8 Hz, 1H), 7.98 (ddd, *J* = 10.8, 8.7, 1.8 Hz, 1H), 7.70 (dd, *J* = 15.6, 2.2 Hz, 1H), 7.56 (dd, *J* = 17.1, 8.7 Hz, 1H), 6.90 – 6.83 (m, 1H), 5.42 (dd, *J* = 8.6, 2.2 Hz, 0.4H), 5.28 (dd, *J* = 8.9, 3.6 Hz, 0.6H), 3.74 – 3.63 (m, 1H), 3.60 – 3.47 (m, 1H), 2.40 – 2.28 (m, 1H), 1.95 (m, 3H), 1.47 (s, 4H), 1.26 (s, 5H).

^{13}C NMR (126 MHz, Chloroform-*d*) δ 198.3, 198.1, 157.6, 157.5, 154.5, 153.9, 146.5, 146.3, 130.7, 130.6, 127.63, 127.55, 125.3, 124.9, 122.8, 122.4, 111.7, 111.6, 107.30, 107.29, 79.7, 79.6, 61.4, 61.1, 46.9, 46.7, 31.1, 30.1, 28.5, 28.2, 24.2, 23.6.

HRMS (ESI+): m/z: calculated for $C_{18}H_{21}NO_4$ [M + Na]+: 338.1363; found: 338.1364

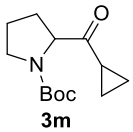

3m

tert-butyl 2-(cyclopropanecarbonyl)pyrrolidine-1-carboxylate (**5-30**) was prepared according to the general procedure with cyclopropanecarbaldehyde (14 mg, 0.2 mmol, 1.0 eq), *N*-Boc-pyrrolidine **5-14** (82 mg, 0.48 mmol, 2.4 eq). After purification with column chromatography eluting with ethyl acetate / hexane (0 – 10/90), the desired product was obtained as a colorless oil (26.8 mg, 56% yield).

^{1}H NMR (700 MHz, Chloroform-*d*) δ 4.48 (dd, *J* = 9.0, 4.3 Hz, 0.3H), 4.26 (dd, *J* = 8.7, 5.8 Hz, 0.6H), 3.62 – 3.41 (m, 2H), 2.27 – 2.14 (m, 1H), 1.98 – 1.85 (m, 3H), 1.45 (s, 4H), 1.40 (d, *J* = 2.1 Hz, 5H), 1.11 – 0.99 (m, 2H), 0.94 – 0.85 (m, 2H).

^{13}C NMR (176 MHz, Chloroform-*d*) δ 210.3, 209.5, 154.5, 154.1, 80.0, 79.6, 66.1, 65.4, 46.84, 46.79, 30.4, 29.0, 28.4, 28.3, 24.3, 23.8, 17.2, 16.0.

HRMS (ESI+): m/z: calculated for $C_{13}H_{21}NO_3$ [M + Na]+: 262.1413; found: 262.1412

These spectra matched previous reports.[176]

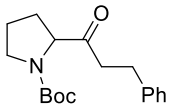

3n

tert-butyl 2-(3-phenylpropanoyl)pyrrolidine-1-carboxylate (**5-31**) was prepared according to the general procedure with 3-phenylpropanal (27 mg, 0.2 mmol, 1.0 eq), *N*-Boc-pyrrolidine **5-14** (82 mg, 0.48 mmol, 2.4 eq). After purification with column chromatography eluting with ethyl acetate / hexane (0 – 10/90), the desired product was obtained as a colorless oil (42.6 mg, 70% yield).

^{1}H NMR (700 MHz, Chloroform-*d*) δ 7.26 (q, *J* = 8.7, 8.1 Hz, 2H), 7.18 (d, *J* = 7.6 Hz, 3H), 4.33 (dd, *J* = 9.0, 4.7 Hz, 0.4H), 4.21 (dd, *J* = 8.7, 5.5 Hz, 0.6H), 3.54 – 3.47 (m, 1H), 3.46 – 3.38 (m, 1H), 2.91 (q, *J* = 7.7 Hz, 2H), 2.75 (m, 2H), 2.07 (m, 1H), 1.80 (m, 2H), 1.67 (m, 1H), 1.46 (s, 4H), 1.38 (s, 6H).

^{13}C NMR (176 MHz, Chloroform-*d*) δ 209.2, 209.1, 154.6,153.9, 141.3, 141.1, 128.5, 128.40, 128.36, 126.2, 126.0, 80., 79.81, 65.3, 64.8, 46.9, 46.7, 40.8, 40.1, 29.7, 29.4, 28.5, 28.4, 28.3, 24.3, 23.7.

The spectra matched previous reports.[176]

HRMS (ESI+): m/z: calculated for $C_{18}H_{25}NO_3$ [M + Na]+: 326.1726; found: 326.1716

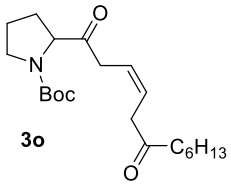

3o

tert-butyl (*Z*)-2-(12-oxooctadec-9-enoyl)pyrrolidine-1-carboxylate (**5-32**) was prepared according to the general procedure with (Z)-12-oxooctadec-9-enal (56 mg, 0.2 mmol, 1.0 eq), *N*-Boc-pyrrolidine **5-14** (82 mg, 0.48 mmol, 2.4 eq). After purification with column chromatography eluting with ethyl acetate / hexane (0 – 10/90), the desired product was obtained as a colorless oil (36.7 mg, 41% yield).

^{1}H NMR (500 MHz, $CDCl_3$) δ 5.60 – 5.49 (m, 2H), 4.21 (dd, *J* = 8.7, 5.0 Hz, 1H), 3.48 (m, 2H), 3.14 (d, *J* = 6.4 Hz, 2H), 2.42 (m, 4H), 2.22 – 2.06 (m, 1H), 2.00 (m, 2H), 1.82 (m, 3H), 1.56 (m, 4H), 1.42 (d, *J* = 26.9 Hz, 9H), 1.27 (m, 14H), 0.87 (t, *J* = 6.7 Hz, 3H).

^{13}C NMR (126 MHz, $CDCl_3$) δ 210.2, 210.2, 209.4, 209.3, 154.6, 154.0, 133.6, 133.5, 121.0, 121.0, 80.1, 79.7, 65.3, 64.7, 46.9, 46.8, 42.4, 41.7, 39.3, 38.3, 31.6, 30.0, 29.7, 29.33, 29.30, 29.19, 29.17, 29.10, 28.97, 28.90, 28.85, 28.5, 28.4, 27.5, 24.4, 23.8, 23.7, 23.3, 23.2, 22.5, 14.1.

HRMS (ESI+): m/z: calculated for $C_{27}H_{47}NO_4$ [M + Na]+: 472.3397; found 472.3400

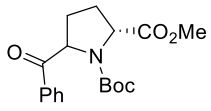

3p

1-(*tert*-butyl) 2-methyl (2*R*)-5-benzoylpyrrolidine-1,2-dicarboxylate (**5-36**) was prepared according to the general procedure with benzaldehyde **5-17** (21 mg, 0.2 mmol, 1.0 eq), 1-(*tert*-butyl) 2-methyl (*R*)-pyrrolidine-1,2-dicarboxylate (110 mg, 0.48 mmol, 2.4 eq). The d.r. ratio (1.14:1) was determined by crude ^{1}H NMR using CH_2Br_2 as the internal standard. After purification with column chromatography eluting with ethyl acetate / hexane (0 – 15/85), the desired product was obtained as a colorless oil (51.0 mg, 77% yield).

The major diasteromer:

^{1}H NMR (700 MHz, Chloroform-*d*) δ 7.97 (dd, *J* = 24.5, 7.6 Hz, 2H), 7.58 (dt, *J* = 23.2, 7.3 Hz, 1H), 7.47 (dt, *J* = 22.1, 7.6 Hz, 2H), 5.55 (d, *J* = 9.6 Hz, 0.5H), 5.45 (d, *J* = 9.6 Hz, 0.5H), 4.67 (d, *J* = 9.2 Hz, 0.5H), 4.56 (d, *J* = 9.2 Hz, 0.5H), 3.76 (d, *J* = 3.8 Hz, 3H), 2.48 – 2.26 (m, 2H), 2.01 – 1.89 (m, 2H), 1.41 (s, 5H), 1.27 (s, 5H).

^{13}C NMR (176 MHz, Chloroform-*d*) δ 198.2, 197.8, 173.6, 173.4, 153.5, 134.9, 134.7, 133.41, 133.40, 128.8, 128.7, 128.6, 128.2, 80.6, 80.5, 61.5, 61.4, 59.7, 59.5, 52.3, 52.1, 28.80, 28.77, 28.2, 28.1, 27.9, 27.8.

HRMS (ESI+): m/z: calculated for $C_{18}H_{23}NO_5$ [M + Na]+: 356.1468; found: 356.1464

The minor diasteromer:

^{1}H NMR (500 MHz, Chloroform-*d*) δ 8.10 – 7.99 (m, 2H), 7.56 (dd, *J* = 14.7, 7.4 Hz, 1H), 7.51 – 7.44 (m, 2H), 5.38 (dd, *J* = 8.4, 4.7 Hz, 0.5H), 5.19 (t, *J* = 7.6 Hz, 0.5H), 4.53 (dd, *J* = 7.4, 5.2 Hz, 0.5H), 4.40 (t, *J* = 7.2 Hz, 0.5H), 3.80 (d, *J* = 4.8 Hz, 3H), 2.38 – 2.23 (m, 2H), 2.21 – 2.06 (m, 2H), 1.43 (s, 6H), 1.26 (s, 4H).

^{13}C NMR (126 MHz, Chloroform-*d*) δ 197.1, 196.9, 172.4, 172.2, 153.7, 153.6, 135.5, 135.4, 133.2, 133.1, 128.7, 128.6, 128.5, 128.3, 81.0, 80.7, 62.6, 61.8, 60.3, 59.8, 52.3, 52.1, 30.1, 29.4, 29.1, 28.7, 28.3, 28.1.

HRMS (ESI+): m/z: calculated for $C_{18}H_{23}NO_5$ [M + Na]+: 356.1468; found: 356.1461

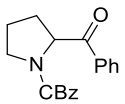

3q

2-benzoyl *N*-CBz pyrrolidine (**5-37**) was prepared according to the general procedure with benzaldehyde **5-17** (11 mg, 0.1 mmol, 1.0 eq), *N*-CBz pyrrolidine (45 mg, 0.24 mmol, 2.4 eq).

After purification with column chromatography eluting with ethyl acetate / hexane (0 – 10/90), the desired product was obtained as a colorless liquid (11.6 mg, 37% yield).

^{1}H NMR (500 MHz, Chloroform-*d*) δ 8.03 – 7.98 (m, 1H), 7.93 – 7.87 (m, 1H), 7.61 – 7.54 (m, 1H), 7.51 – 7.44 (m, 2H), 7.40 – 7.29 (m, 3H), 7.19 – 7.16 (m, 1H), 7.11 (dd, *J* = 7.4, 2.1 Hz, 1H), 5.39 (dd, *J* = 9.1, 3.0 Hz, 0.5H), 5.31 (dd, *J* = 9.1, 3.2 Hz, 0.5H), 5.22 – 5.09 (m, 0.5H), 5.08 – 4.98 (m, 0.5H), 3.74 (dddd, *J* = 15.8, 10.6, 7.5, 5.0 Hz, 1H), 3.67 – 3.55 (m, 1H), 2.39 – 2.28 (m, 1H), 1.96 (dddd, *J* = 10.9, 7.8, 4.8, 2.4 Hz, 3H).

^{13}C NMR (126 MHz, Chloroform-*d*) δ 198.3, 198.0, 154.9, 154.3, 136.9, 136.5, 135.0, 134.9, 133.4, 133.3, 128.71, 128.68, 128.6, 128.5, 128.4, 128.2, 128.0, 127.9, 127.7, 127.6, 67.0, 66.9, 61.6, 61.2, 47.2, 46.7, 30.9, 29.9, 24.2, 23.4.

These spectra matched previous reports.[174]

HRMS (ESI+): m/z: calculated for $C_{19}H_{17}NO_2$ [M + Na]+: 332.1257; found: 332.1257

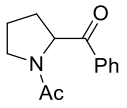

3r

1-(2-benzoylpyrrolidin-1-yl)ethan-1-one (**5-38**) was prepared according to the general procedure with benzaldehyde **5-17** (21 mg, 0.2 mmol, 1.0 eq), 1-(pyrrolidin-1-yl)ethan-1-one (54 mg, 0.48 mmol, 2.4 eq). After purification with column chromatography eluting with ethyl acetate / hexane (0 – 10/90), the desired product was obtained as a colorless liquid (28.5 mg, 66% yield).

^{1}H NMR (500 MHz, Chloroform-*d*) δ 8.02 – 7.97 (m, 2H), 7.66 – 7.54 (m, 1H), 7.54 – 7.44 (m, 2H), 5.52 (dd, *J* = 9.1, 3.6 Hz, 0.8H), 5.33 (dd, *J* = 9.4, 3.0 Hz, 0.2H), 3.76 (ddd, *J* = 9.6, 7.8, 4.6 Hz, 1H), 3.59 (dt, *J* = 9.8, 7.4 Hz, 1H), 2.29 (dtd, *J* = 12.6, 9.1, 7.2 Hz, 1H), 2.13 (s, 3H), 2.08 – 1.93 (m, 3H).

^{13}C NMR (126 MHz, Chloroform-*d*) δ 197.8, 197.0, 169.5, 169.0, 135.1, 134.1, 134.0, 133.3, 129.0, 128.64, 128.57, 128.4, 63.0, 60.9, 48.0, 46.7, 31.7, 29.4, 24.7, 22.6, 22.5, 22.2.

These spectra matched previous reports.[177]

HRMS (ESI+): m/z: calculated for $C_{13}H_{15}NO_2$ [M + Na]+: 240.0995; found: 240.0995

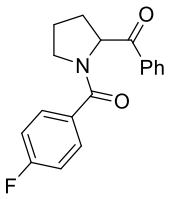

3s

(2-benzoylpyrrolidin-1-yl)(4-fluorophenyl)methanone (**5-39**) was prepared according to the general procedure with benzaldehyde **5-17** (21 mg, 0.2 mmol, 1.0 eq), (4-fluorophenyl)(pyrrolidin-1-yl)methanone (93 mg, 0.48 mmol, 2.4 eq). After purification with column chromatography eluting with methanol / DCM (0 – 10/90), the desired product was obtained as a white solid (37.0 mg, 62% yield).

^{1}H NMR (500 MHz, Chloroform-*d*) δ 8.05 (d, *J* = 7.6 Hz, 2H), 7.64 (dd, *J* = 8.5, 5.5 Hz, 2H), 7.59 (t, *J* = 7.4 Hz, 1H), 7.49 (t, *J* = 7.6 Hz, 2H), 7.09 (t, *J* = 8.6 Hz, 2H), 5.70 (dd, *J* = 8.7, 5.0 Hz, 1H), 3.74 (dt, *J* = 10.3, 6.6 Hz, 1H), 3.63 (dt, *J* = 10.1, 6.1 Hz, 1H), 2.41 (ddd, *J* = 12.5, 8.6, 6.0 Hz, 1H), 2.10 – 2.03 (m, 1H), 1.99 (dt, *J* = 10.7, 5.0 Hz, 2H).

^{13}C NMR (126 MHz, Chloroform-*d*) δ 197.6, 168.3, 164.7, 133.4, 129.7 (d, *J* = 8.5 Hz), 128.7 (d, *J* = 17.4 Hz), 115.3 (d, *J* = 21.7 Hz), 61.5, 50.2, 29.5, 25.5.

^{19}F NMR (564 MHz, Chloroform-*d*) δ -109.86 (tt, *J* = 9.2, 5.4 Hz), -110.56 (tt, *J* = 9.2, 5.3 Hz).

HRMS (ESI+): m/z: calculated for $C_{14}H_{18}FNO_2$ [M + Na]+: 320.1057; found: 320.1052

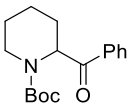

3t

tert-butyl 2-benzoylpiperidine-1-carboxylate (**5-40**) was prepared according to the general procedure with benzaldehyde **5-17** (21 mg, 0.2 mmol, 1.0 eq), 1-(*tert*-butyl) tert-butyl piperidine-1-carboxylate (89 mg, 0.48 mmol, 2.4 eq). After purification with column chromatography eluting with ethyl acetate / hexane (0 – 10/90), the desired product was obtained as a colorless oil (26.6 mg, 46% yield).

^{1}H NMR (500 MHz, Chloroform-*d*) δ 7.91 (br, 2H), 7.54 (br, 1H), 7.44 (br, 2H), 5.72 – 5.43 (m, 1H), 4.07 – 3.86 (m, 1H), 3.27 – 3.10 (m, 1H), 2.18 – 2.00 (m, 1H), 1.93 – 1.47 (m, 5H), 1.37 (s, 9H).

^{13}C NMR (126 MHz, Chloroform-*d*) δ 201.1, 200.6, 155.9, 155.3, 135.9, 132.9, 128.55, 128.55, 128.3, 128.0, 80.4, 57.2, 56.1, 42.7, 41.9, 28.4, 26.4, 26.2, 25.1, 24.7, 20.0, 19.8.

HRMS (ESI+): m/z: calculated for $C_{17}H_{23}NO_3$ [M + Na]+: 312.1570; found: 312.1567

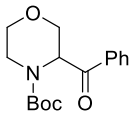

3u

tert-butyl 3-benzoylmorpholine-4-carboxylate (**5-41**) was prepared according to the general procedure with benzaldehyde **5-17** (21 mg, 0.2 mmol, 1.0 eq), tert-butyl morpholine-4-carboxylate (90 mg, 0.48 mmol, 2.4 eq). After purification with column chromatography eluting with ethyl acetate / hexane (0 – 10/90), the desired product was obtained as a colorless oil (28.3 mg, 49% yield).

^{1}H NMR (500 MHz, Chloroform-*d*) δ 8.01 – 7.79 (m, 2H), 7.61 – 7.53 (m, 1H), 7.50 – 7.42 (m, 2H), 5.44 – 5.20 (m, 1H), 4.26 (dd, *J* = 56.5, 12.1 Hz, 1H), 4.07 – 3.87 (m, 1H), 3.86 – 3.71 (m, 2H), 3.55 (dt, *J* = 44.0, 12.8 Hz, 2H), 1.48 (s, 6H), 1.37 (s, 3H).

^{13}C NMR (126 MHz, Chloroform-*d*) δ 198.3, 198.2, 155.9, 155.3, 134.7, 133.7, 133.2, 128.9, 128.8, 128.2, 127.9, 80.7, 80.5, 67.4, 67.0, 66.8, 66.7, 57.8, 56.6, 42.3, 41.1, 28.4.

HRMS (ESI+): m/z: calculated for $C_{16}H_{21}NO_4$ [M + Na]+: 314.1363; found: 314.1360

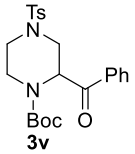

3v

tert-butyl 2-benzoyl-4-tosylpiperazine-1-carboxylate (**5-42**) was prepared according to the general procedure with benzaldehyde **5-17** (21 mg, 0.2 mmol, 1.0 eq), *tert*-butyl 4-tosylpiperazine-1-carboxylate (163 mg, 0.48 mmol, 2.4 eq). After purification with column chromatography eluting with ethyl acetate / hexane (0 – 10/90), the desired product was obtained as a colorless liquid (40.7 mg, 46% yield).

^{1}H NMR (500 MHz, Chloroform-*d*) δ 7.79 (d, *J* = 7.6 Hz, 2H), 7.55 (d, *J* = 8.3 Hz, 3H), 7.46 (t, *J* = 7.3 Hz, 2H), 7.27 (d, *J* = 8.7 Hz, 2H), 5.45 (br, 1H), 3.99 (br, 2H), 3.67 – 3.52 (m, 2H), 3.12 – 2.63 (m, 2H), 2.42 (s, 3H), 1.40 (br, 9H).

^{13}C NMR (126 MHz, Chloroform-*d*) δ 197.4, 144.0, 135.4, 133.2, 132.6, 129.8, 127.8, 81.2, 46.4, 45.5, 45.3, 29.7, 28.2, 21.6.

HRMS (ESI+): m/z: calculated for $C_{13}H_{15}NO_2$ [M + Na]+: 467.1611; found: 467.1609

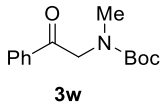

3w

tert-butyl methyl(2-oxo-2-phenylethyl)carbamate (**5-43**) was prepared according to the general procedure with benzaldehyde **5-17** (21 mg, 0.2 mmol, 1.0 eq), *tert*-butyl dimethylcarbamate (70 mg, 0.48 mmol, 2.4 eq). After purification with column chromatography eluting with ethyl acetate / hexane (0 – 10/90), the desired product was obtained as a colorless oil (25.6 mg, 51% yield).

^{1}H NMR (500 MHz, Chloroform-*d*) δ 7.96 – 7.90 (m, 2H), 7.58 (dd, *J* = 14.4, 7.3 Hz, 1H), 7.53 – 7.44 (m, 2H), 4.68 (s, 1H), 4.58 (s, 1H), 2.96 (d, *J* = 16.1 Hz, 3H), 1.49 (s, 5H), 1.38 (s, 4H).

^{13}C NMR (126 MHz, Chloroform-*d*) δ 195.2, 194.8, 156.3, 155.7, 133.52, 133.48, 129.17, 129.15, 128.8, 128.7, 127.89, 127.7, 80.1, 80.0, 55.7, 55.1, 35.7, 35.6, 28.4, 28.2.

These spectra matched previous reports.[178]

HRMS (ESI+): m/z: calculated for $C_{14}H_{19}NO_3$ [M + Na]+: 272.1357; found: 272.1360

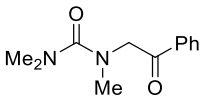

1,1,3-trimethyl-3-(2-oxo-2-phenylethyl)urea (**5-44**) was prepared according to the general procedure with benzaldehyde **5-17** (21 mg, 0.2 mmol, 1.0 eq), 1,1,3,3-tetramethylurea (56 mg, 0.48 mmol, 2.4 eq). After purification with column chromatography eluting with ethyl acetate / hexane (0 – 30/70), the desired product was obtained as a colorless oil (17.9 mg, 41% yield).

^{1}H NMR (600 MHz, Chloroform-*d*) δ 7.95 (d, *J* = 7.5 Hz, 2H), 7.58 (t, *J* = 7.4 Hz, 1H), 7.47 (t, *J* = 7.7 Hz, 2H), 4.65 (s, 2H), 2.96 (s, 3H), 2.85 (s, 6H).

^{13}C NMR (151 MHz, Chloroform-*d*) δ 195.7, 165.1, 135.4, 133.4, 128.7, 127.8, 56.4, 38.7, 38.4.

HRMS (ESI+): m/z: calculated for $C_{12}H_{16}N_2O_2$ [M + Na]+: 243.1104; found: 243.1103

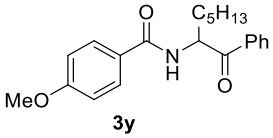

3y

4-methoxy-N-(1-oxo-1-phenylheptan-2-yl)benzamide (**5-45**) was prepared according to the general procedure with benzaldehyde **5-17** (21 mg, 0.2 mmol, 1.0 eq), *N*-hexyl-4-methoxybenzamide (113 mg, 0.48 mmol, 2.4 eq). After purification with column chromatography eluting with ethyl acetate / hexane (0 – 10/90), the desired product was obtained as a white solid (27.3 mg, 40% yield).

^{1}H NMR (500 MHz, Chloroform-*d*) δ 8.04 (d, *J* = 7.4 Hz, 2H), 7.83 (d, *J* = 8.8 Hz, 2H), 7.63 (t, *J* = 7.4 Hz, 1H), 7.52 (t, *J* = 7.7 Hz, 2H), 7.09 (d, *J* = 7.7 Hz, 1H), 6.95 (d, *J* = 8.8 Hz, 2H), 5.82 (td,

J = 7.4, 4.6 Hz, 1H), 3.86 (s, 3H), 2.06 (ddt, *J* = 15.1, 10.4, 5.1 Hz, 1H), 1.75 – 1.65 (m, 1H), 1.56 – 1.35 (m, 2H), 1.27 – 1.19 (m, 6H), 0.81 (t, *J* = 6.8 Hz, 3H).

^{13}C NMR (126 MHz, Chloroform-*d*) δ 199.5, 166.5, 162.4, 134.6, 133.9, 128.9, 128.8, 128.6, 126.5, 113.8, 113.7, 55.5, 54.2, 33.6, 31.6, 24.6, 22.4, 13.9.

m/z: calculated for $C_{21}H_{27}NO_3$ [M]+:341.1991; GCMS found: 341.2

Attempts to obtain the exact mass (HRMS) for the title compound with both EI and ESI source ended in failure, potentially due to the facile imine/enamine formation when sample being analyzed.

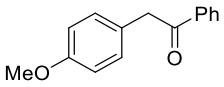

3z

2-(4-methoxyphenyl)-1-phenylethan-1-one (**5-46**) was prepared according to the general procedure with benzaldehyde **5-17** (21 mg, 0.2 mmol, 1.0 eq), 1-methoxy-4-methylbenzene (59 mg, 0.48 mmol, 2.4 eq). After purification with column chromatography eluting with ethyl acetate / hexane (0 – 5/95), the desired product was obtained as a white solid (9.8 mg, 22% yield).

^{1}H NMR (500 MHz, Chloroform-*d*) δ 7.94 (d, *J* = 7.0 Hz, 2H), 7.48 (t, *J* = 7.4 Hz, 1H), 7.38 (t, *J* = 7.7 Hz, 2H), 7.11 (d, *J* = 8.6 Hz, 2H), 6.79 (d, *J* = 8.6 Hz, 2H), 4.16 (s, 2H), 3.71 (s, 3H).

^{13}C NMR (126 MHz, Chloroform-*d*) δ 197.9, 158.6, 136.6, 133.1, 130.5, 128.6, 128.6, 126.5, 114.2, 55.3, 44.7.

These spectra matched previous reports.[179]

HRMS (ESI+): m/z: calculated for $C_{15}H_{14}NO_2$ [M + Na]+: 249.0886; found: 249.0881

8.5.3 Mechanistic Investigation

For radical trapping and Zn titration experiments, and DFT calculation please refer to publication SI for details.

KIE Experiments (Chapter 6.4)

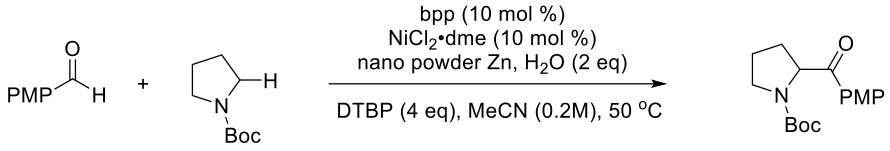

To an oven-dried 1dram vial charged with a stir bar in an inert atmosphere glovebox (GB), weighed nano powder Zn (26 mg, 0.40 mmol, 2.0 eq), bpp (4.2 mg, 0.02 mmol, 0.1 eq), $NiCl_2$•dme (4.4 mg, 0.02 mmol, 0.1 eq). The vial was capped and brought outside the GB.

To a separate vial outside GB, 4-methoxybenzaldehyde (27.2 mg, 0.20 mmol, 1.0 eq) or 4-methoxybenzaladehyde-d_1 (27.4 mg, 0.20 mmol, 1.0 eq), *N*-Boc-pyrrolidine (82 mg, 0.48 mmol, 2.4 eq), anisole (10.0 mg, 0.0925 mmol, 0.46 eq), and water (7.2 mg, 0.40 mmol, 2.0 eq) was added via micro-pipette. The starting materials were dissolved with MeCN (2.0 mL, 0.1 M) before addition of DTBP (112 mg, 0.8 mmol, 4.0 eq).

The stock solution was transferred via syringe to the previously sealed vial and the reaction was stirred at 800 rpm and 50 ºC under nitrogen. 100 uL aliquots were taken from the reaction at 20-minute intervals and were diluted and filtered through a celite pad and a syringe filter using 300 uL MeCN. The aliquots were measured up to 80 minutes and analyzed via GCMS against anisole as the internal standard.

KIE was determined to be 1.70 based on the experiments shown below.

GC-fid traces: auto-integration was adopted to ensure consistency between experiments

Example of 0 time point

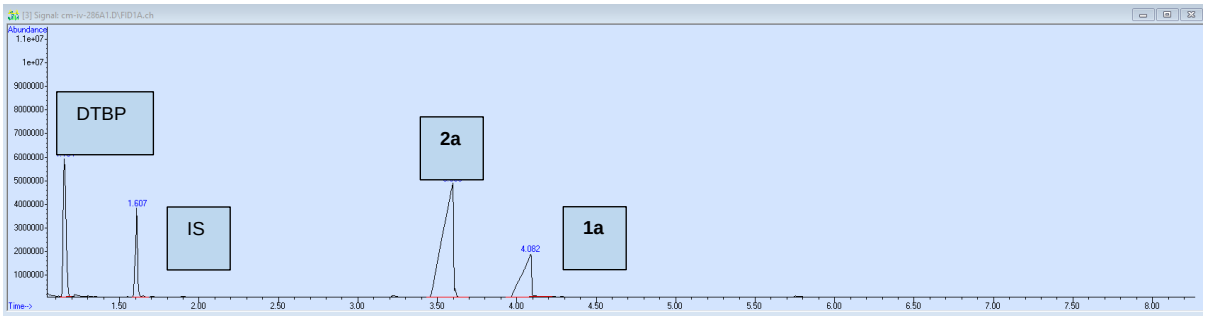

Example of reaction progress

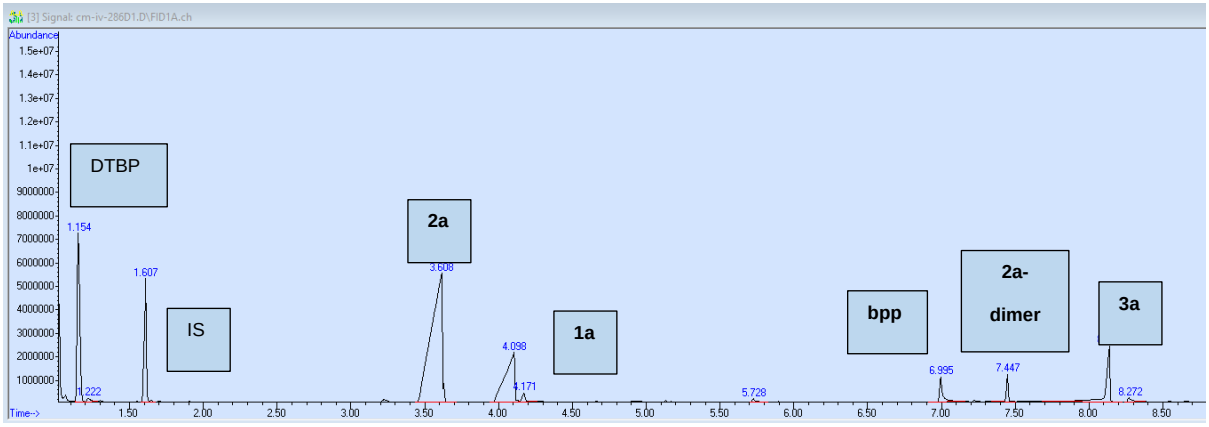

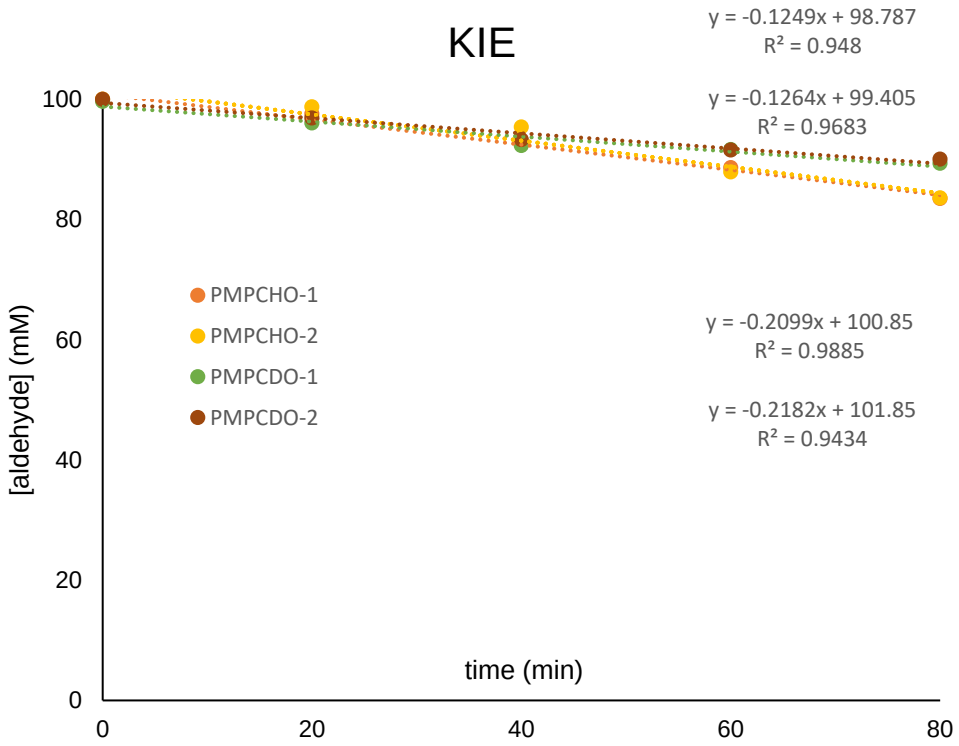

min	PMPCHO-1	PMPCHO-2	PMPCDO-1	PMPCDO-2
0	100	100	99.6350365	100
20	97.56453089	98.72604506	96.03840216	96.8826957
40	92.59389136	95.37774855	92.30426752	93.2846305
60	88.63398438	87.89002723	91.63780622	91.549758
80	83.47928309	83.59865902	89.34941944	90.0244382

8.6 NMR Spectra

8.6.1 Chapter 2

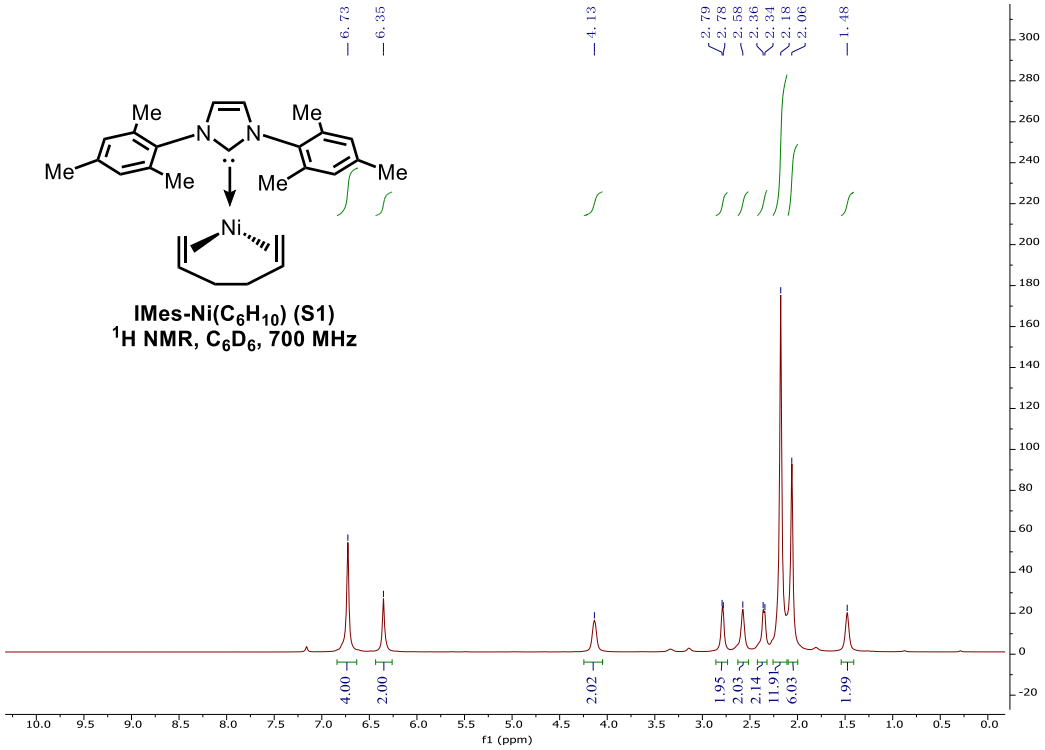

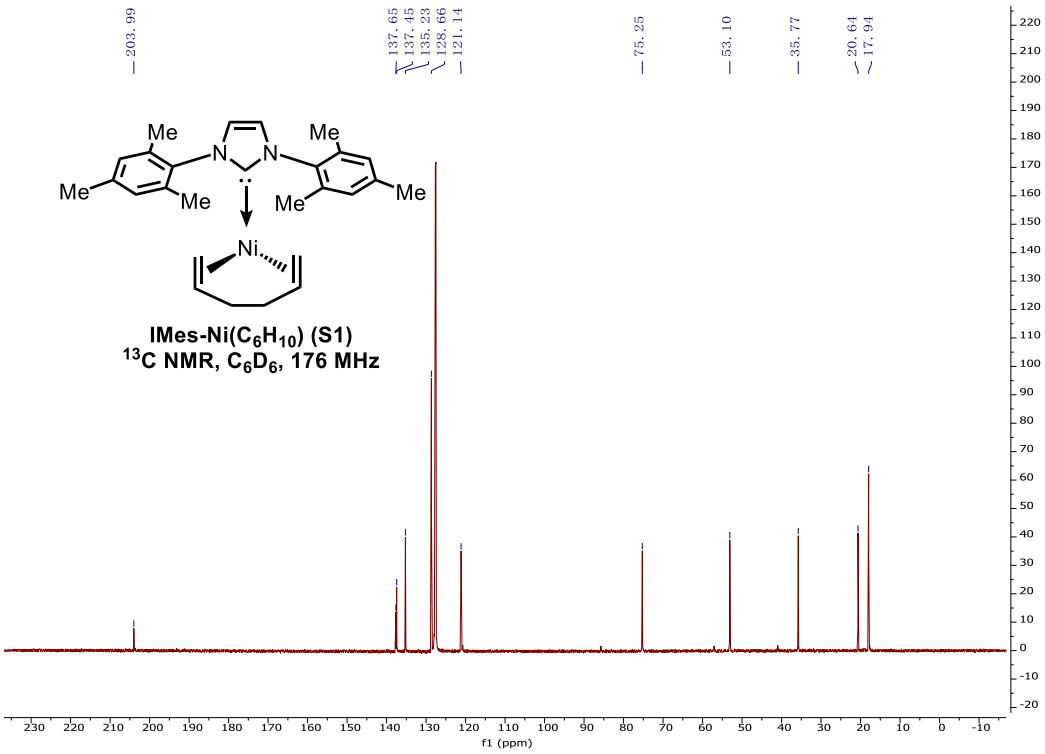

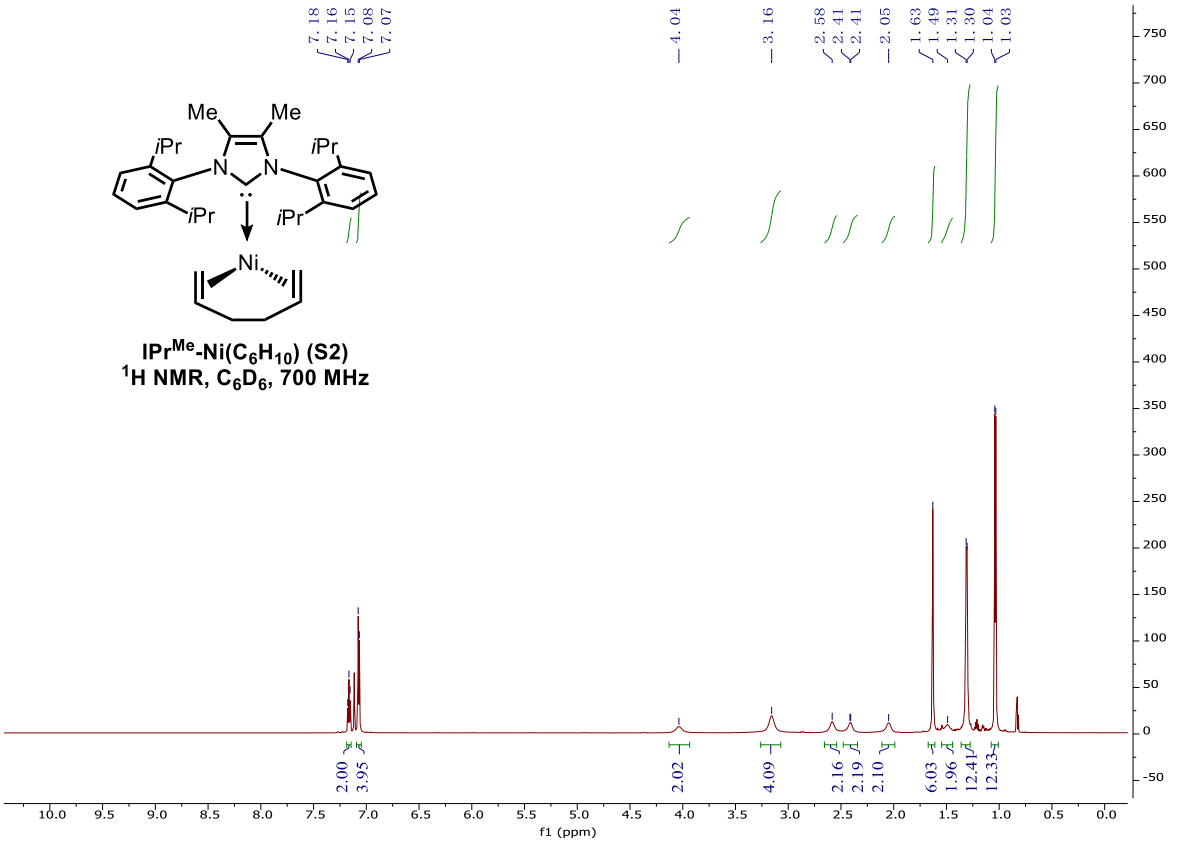

IPr^{Me}-Ni(C_6H_{10}) (S2)
^{1}H NMR, C_6D_6, 700 MHz

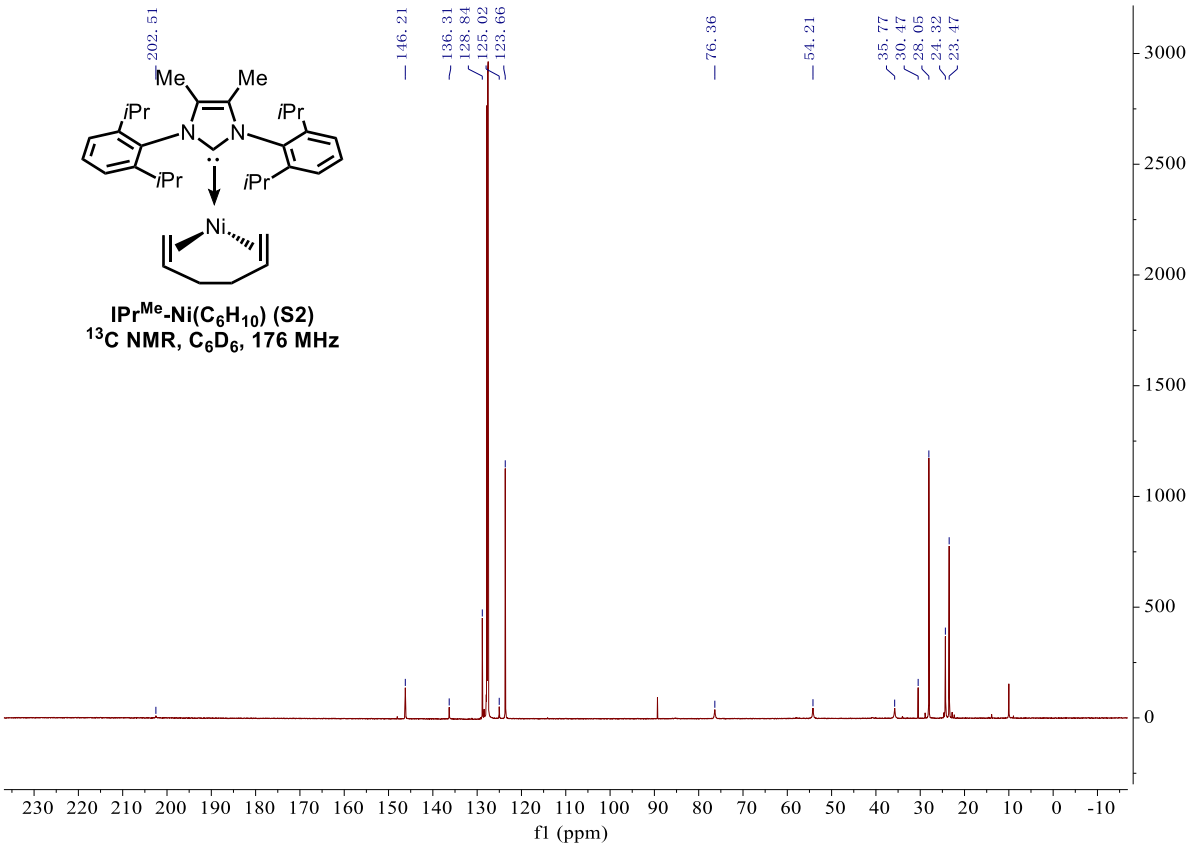

IPr^{Me}-Ni(C_6H_{10}) (S2)
^{13}C NMR, C_6D_6, 176 MHz

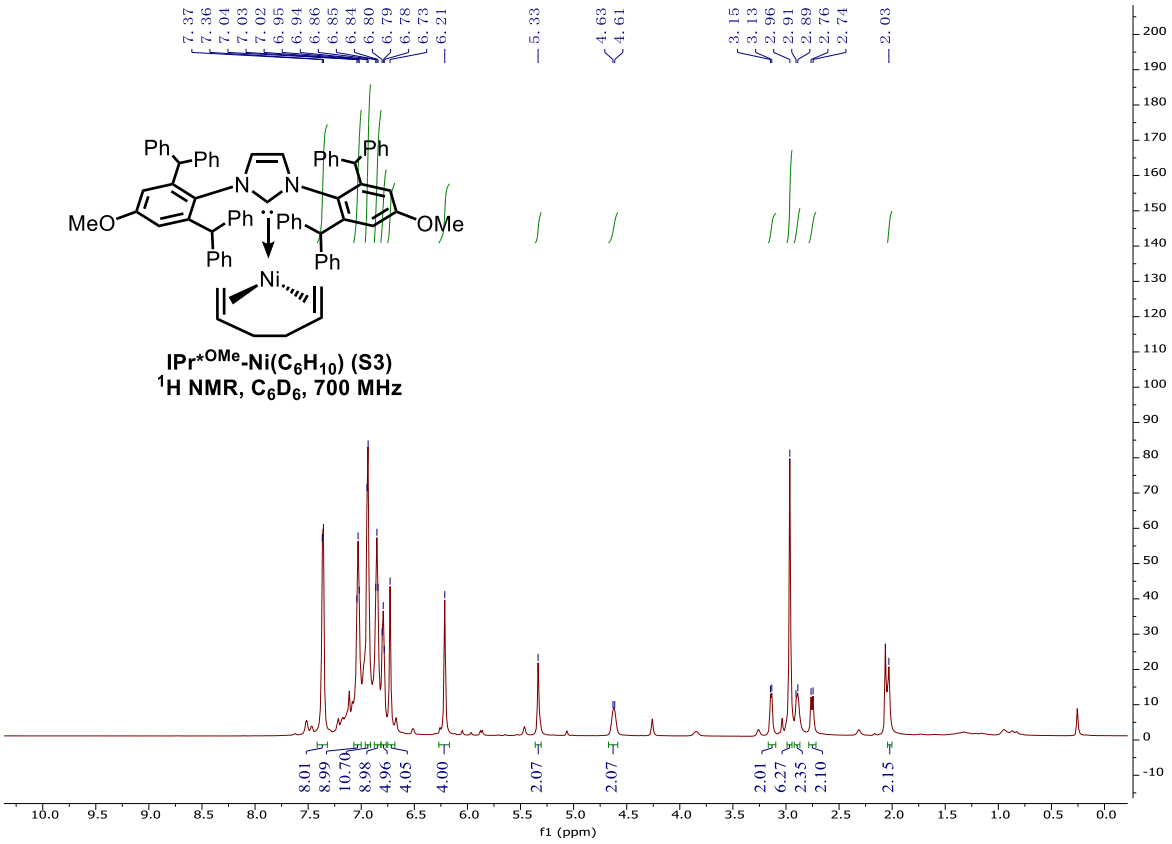

IPr*^{OMe}-Ni(C_6H_{10}) (S3)
^{1}H NMR, C_6D_6, 700 MHz

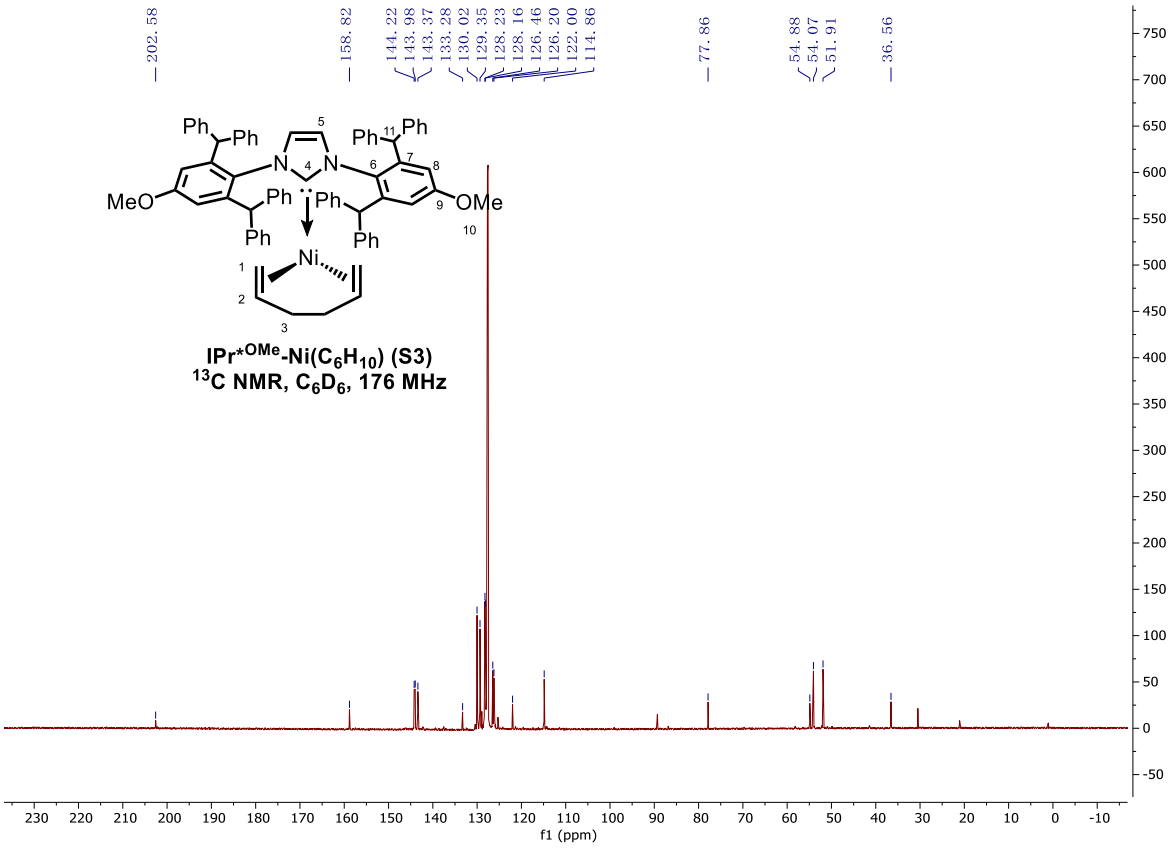

IPr*^{OMe}-Ni(C_6H_{10}) (S3)
^{13}C NMR, C_6D_6, 176 MHz

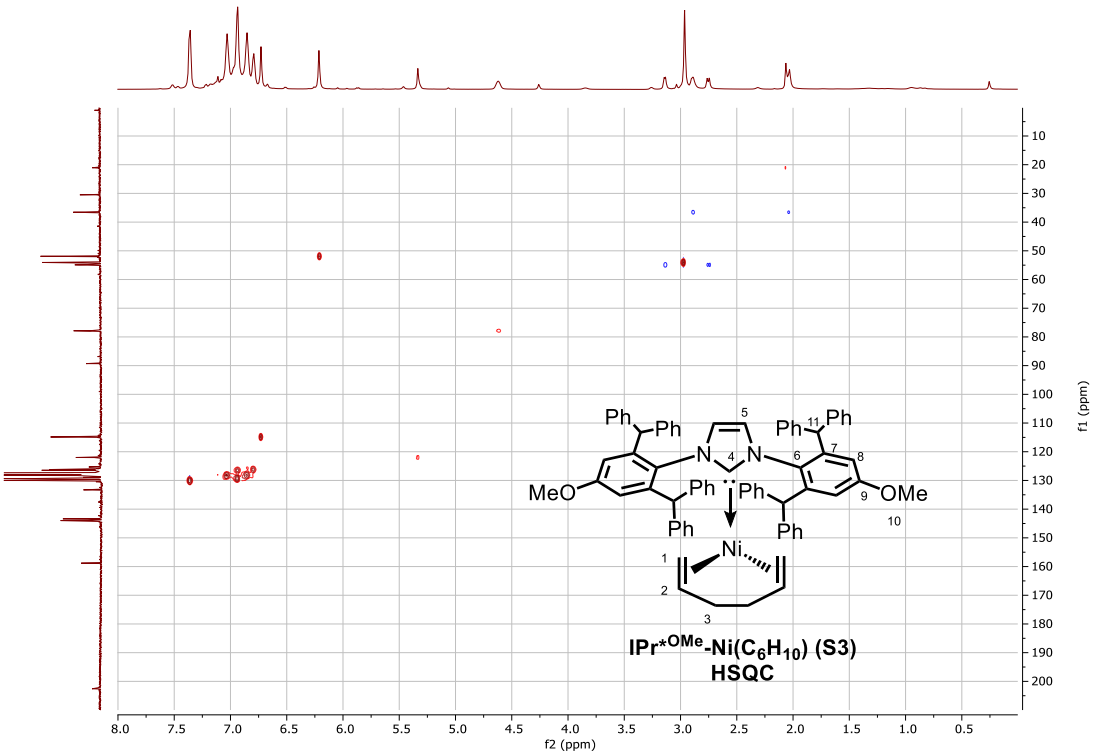

HSQC (above) HMBC (below)

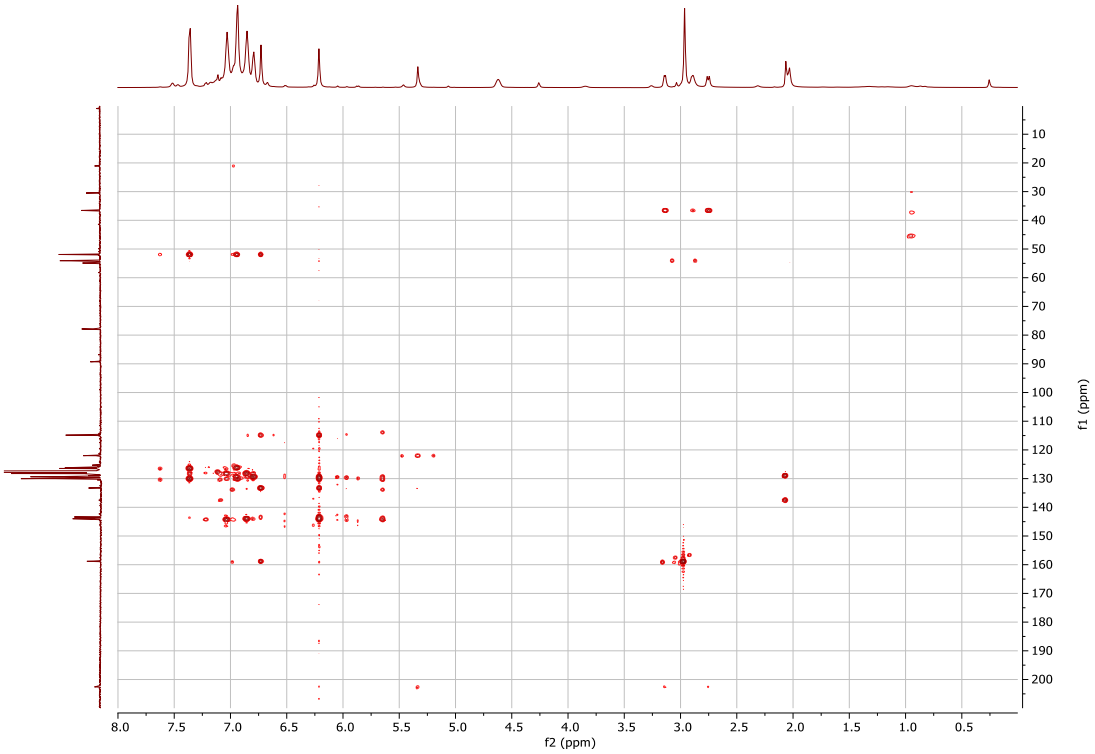

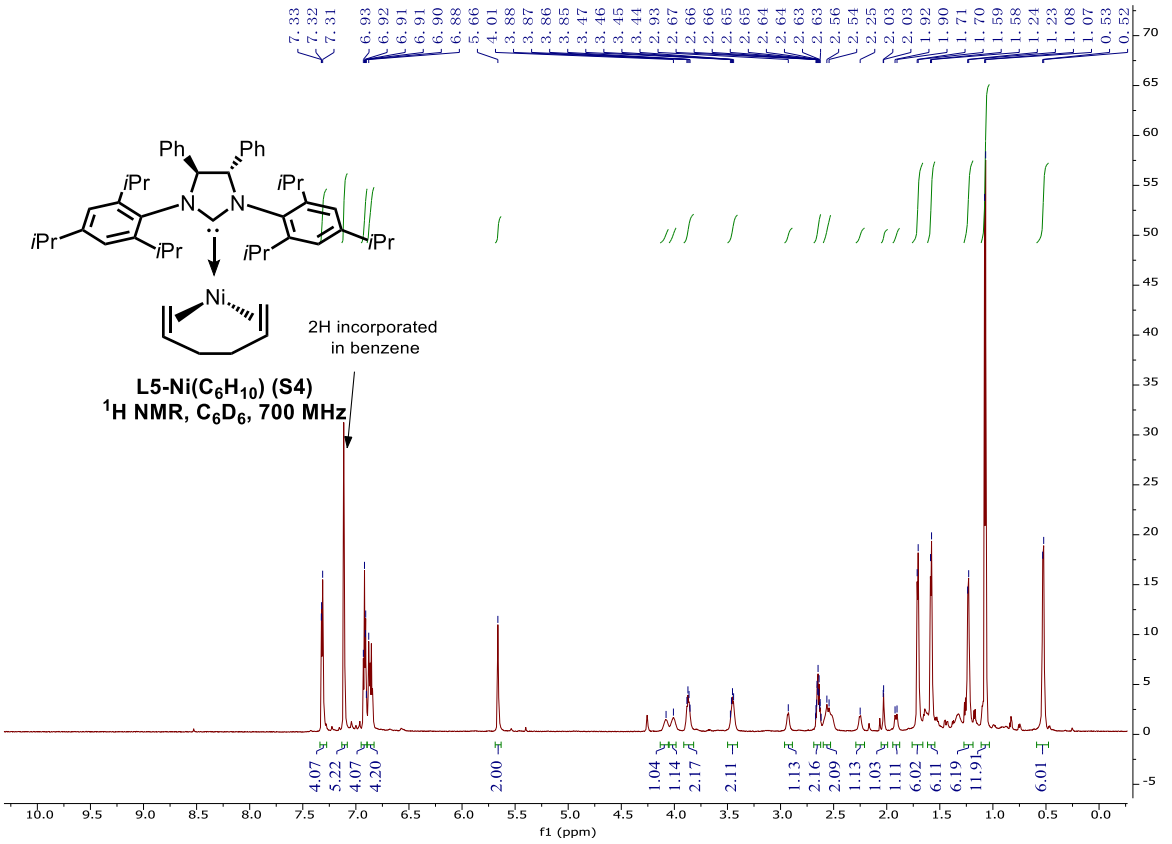
Ph
Ph
iPr
iPr
iPr
iPr
iPr
iPr
N
N
Ni
2H incorporated
in benzene
L5-Ni(C6H10) (S4)
1H NMR, C6D6, 700 MHz
f1 (ppm)

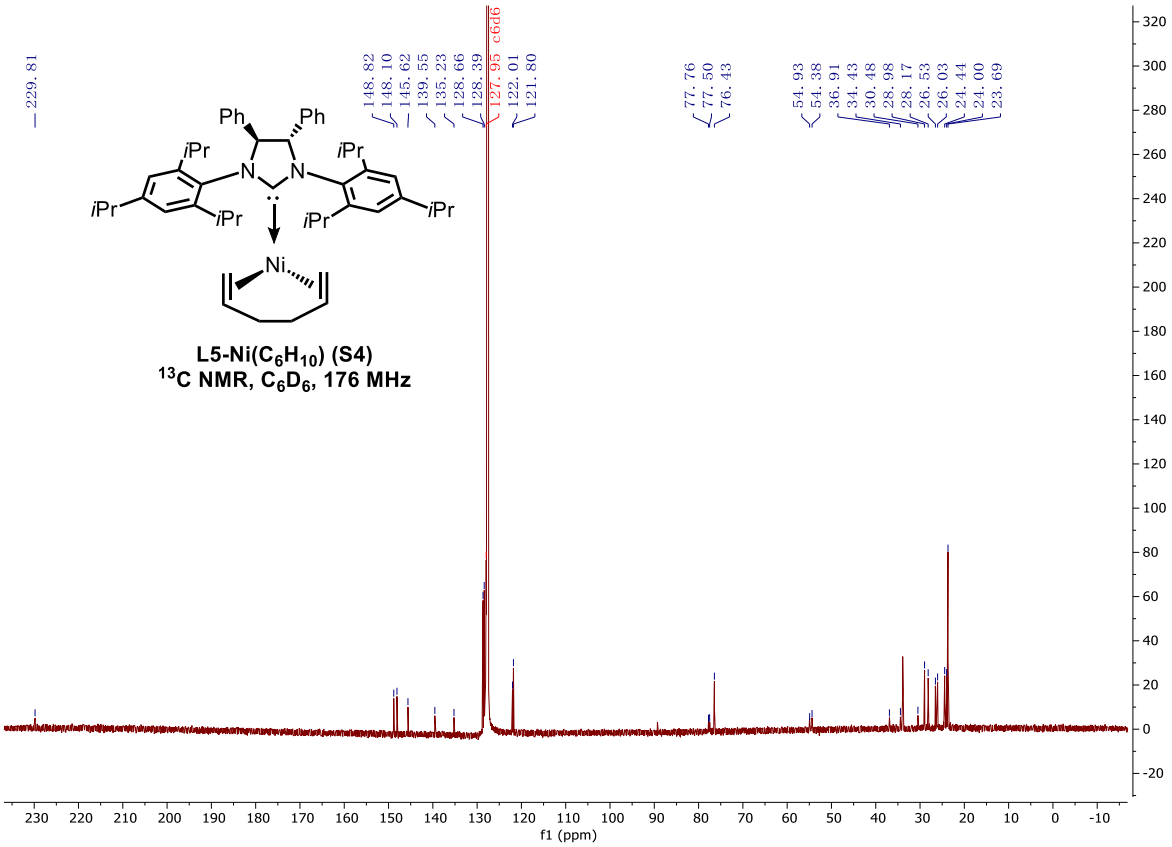
Ph
Ph
iPr
iPr
iPr
iPr
iPr
iPr
N
N
Ni
L5-Ni(C6H10) (S4)
13C NMR, C6D6, 176 MHz
f1 (ppm)

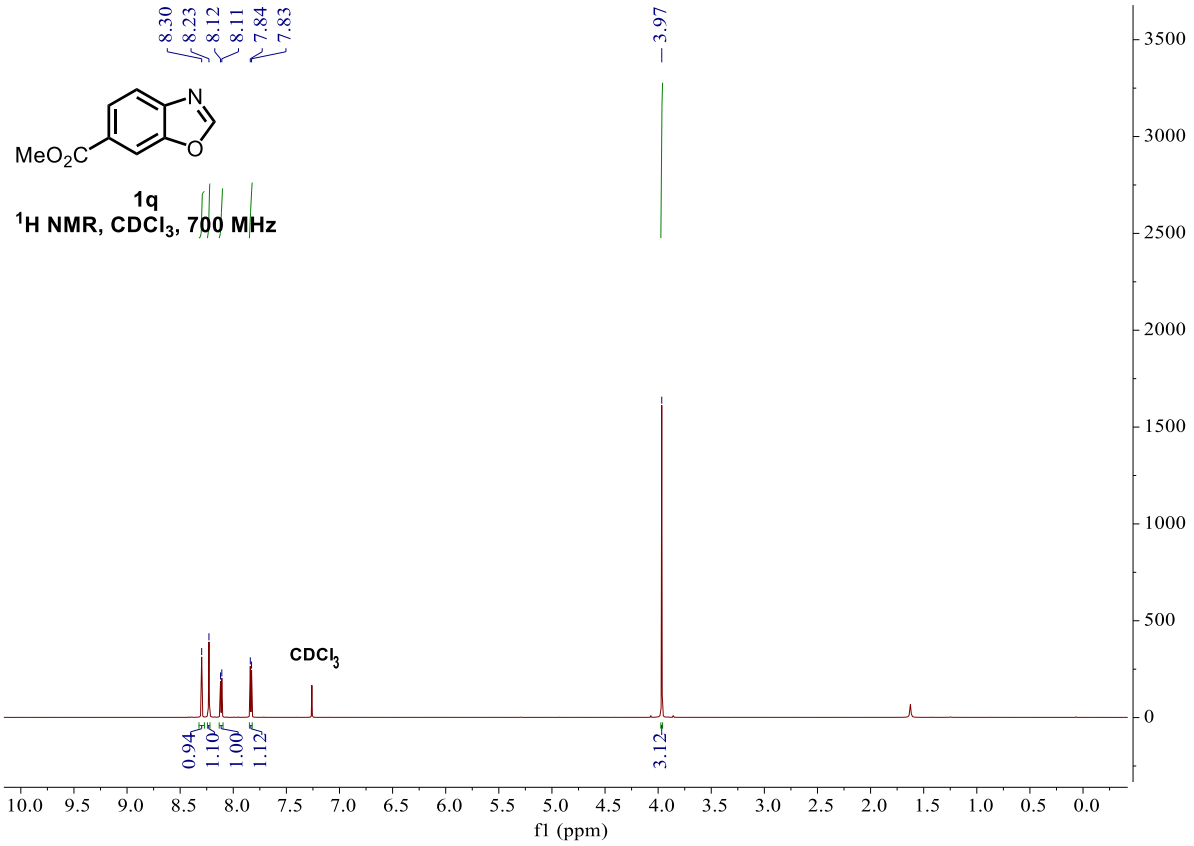
8.30
8.23
8.12
8.11
7.84
7.83
3.97
MeO2C
N
O
1q
1H NMR, CDCl3, 700 MHz
CDCl3
0.94
1.10
1.00
1.12
3.12
fl (ppm)

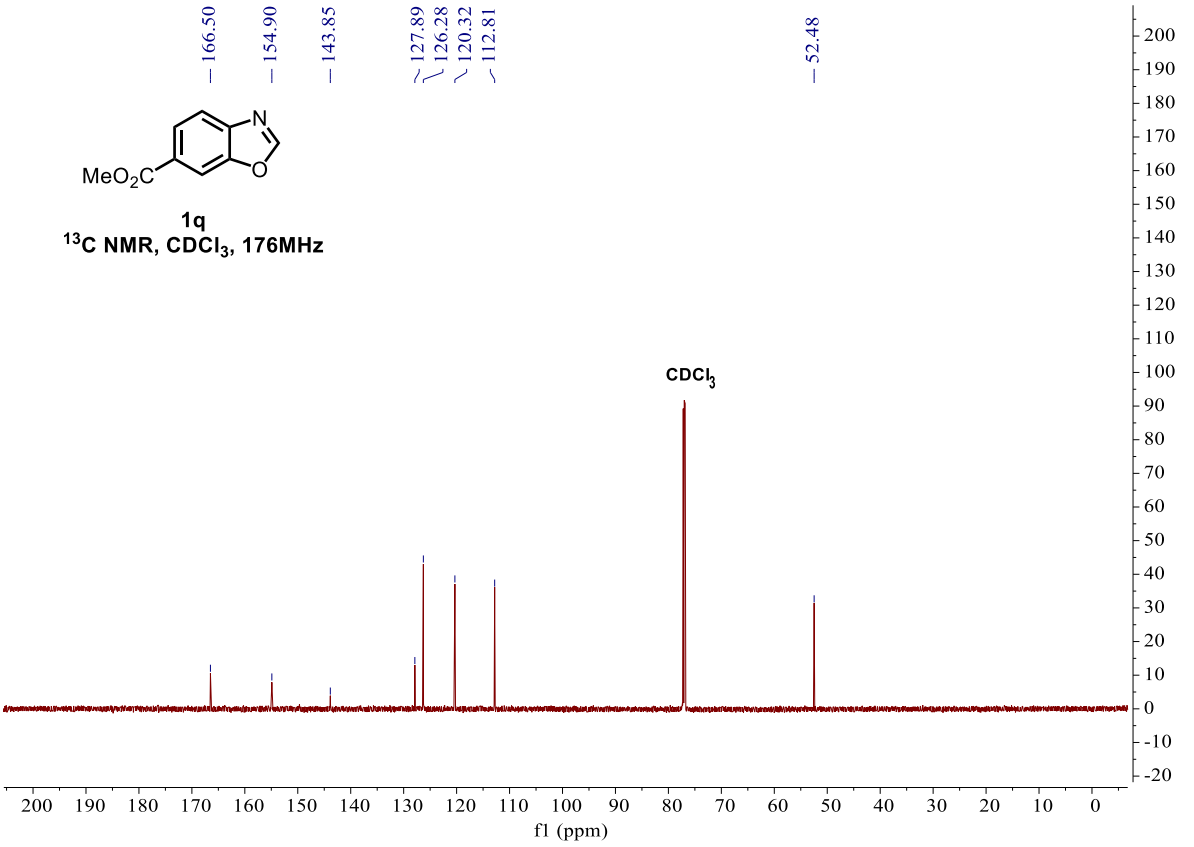
166.50
154.90
143.85
127.89
126.28
120.32
112.81
52.48
MeO2C
N
O
1q
13C NMR, CDCl3, 176MHz
CDCl3
fl (ppm)

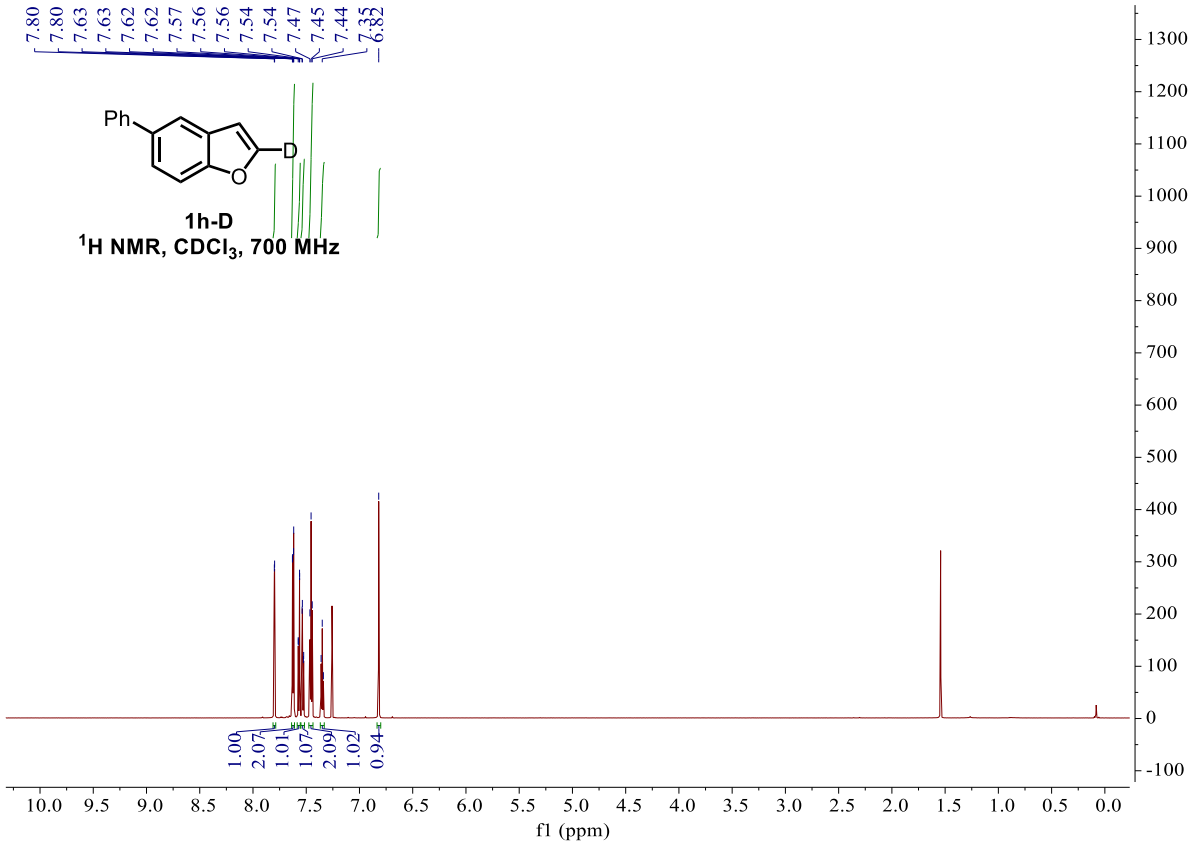
7.80
7.80
7.63
7.63
7.62
7.62
7.57
7.56
7.56
7.54
7.54
7.47
7.45
7.44
7.35
6.82
Ph
D
O
1h-D
1H NMR, CDCl3, 700 MHz
1.00
2.07
1.01
1.07
2.09
1.02
0.94
f1 (ppm)

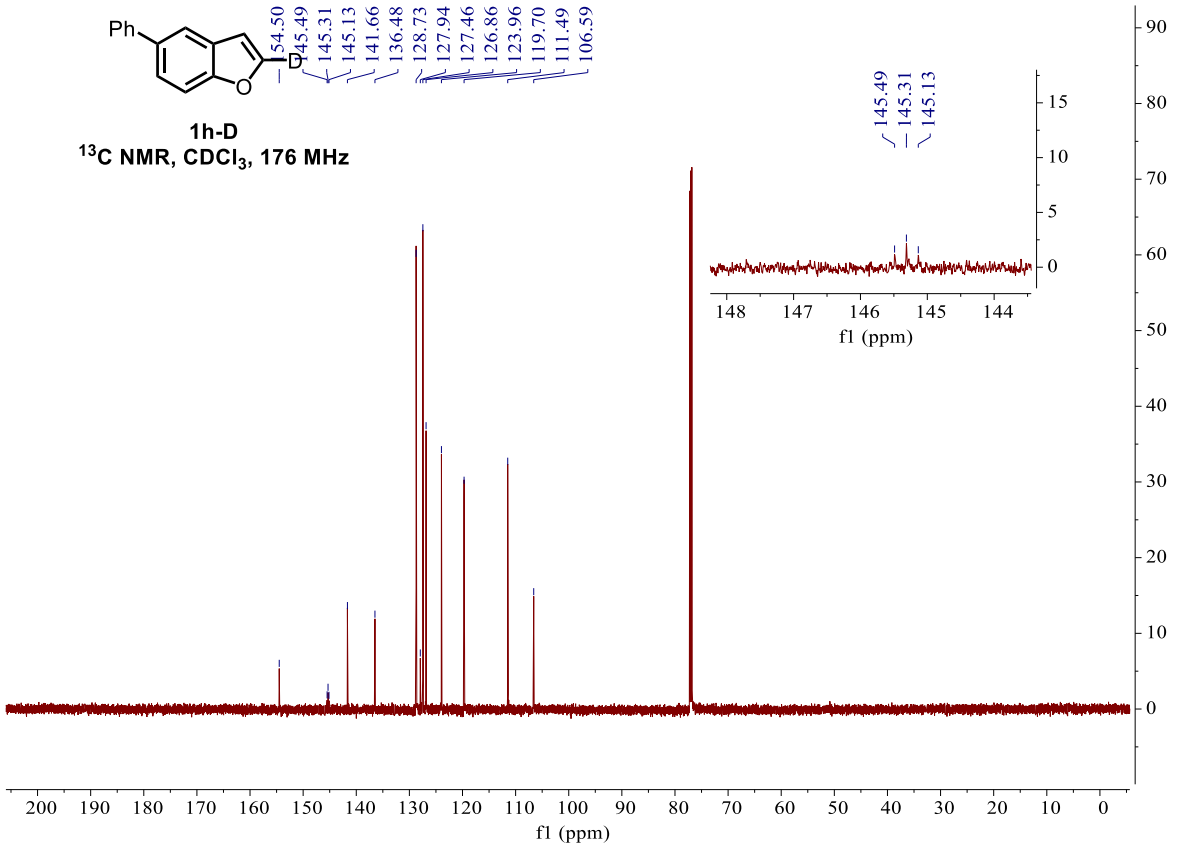
Ph
D
O
1h-D
13C NMR, CDCl3, 176 MHz
154.50
145.49
145.31
145.13
141.66
136.48
128.73
127.94
127.46
126.86
123.96
119.70
111.49
106.59
f1 (ppm)

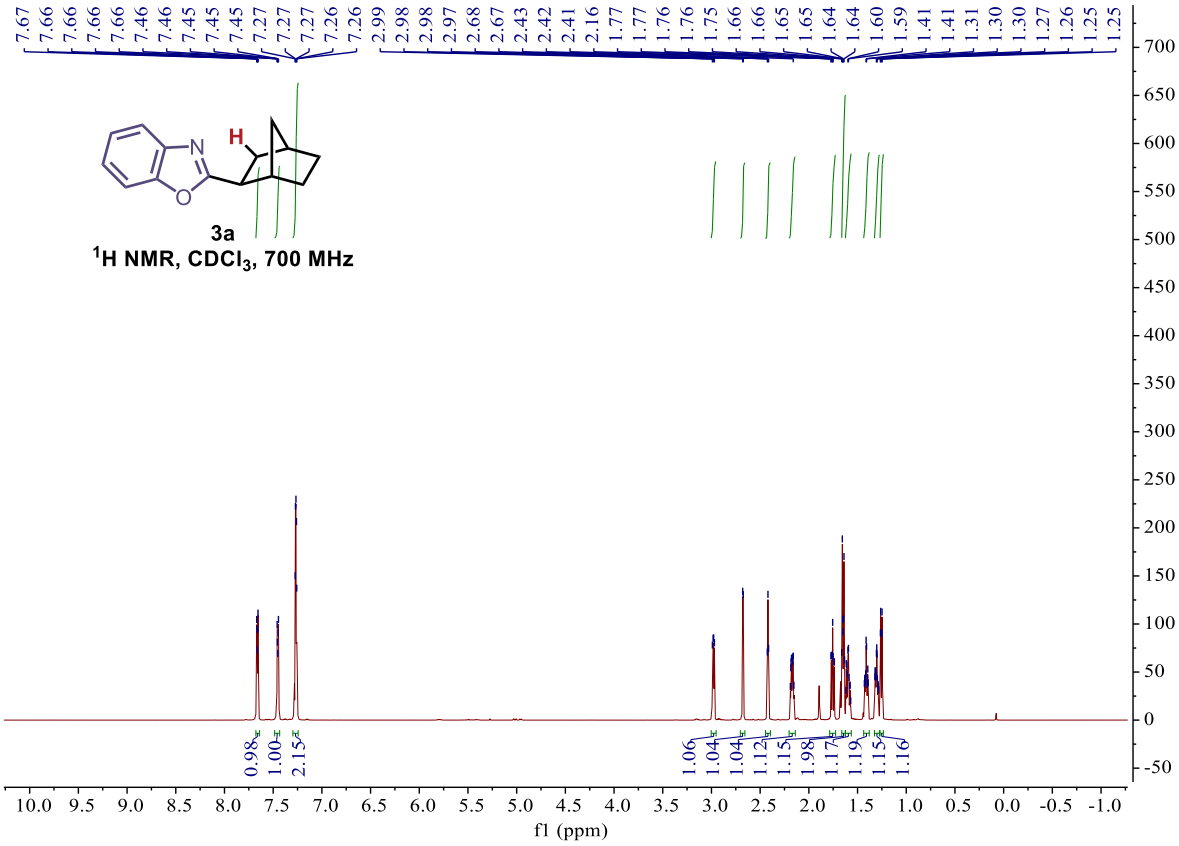

3a

^{1}H NMR, $CDCl_3$, 700 MHz

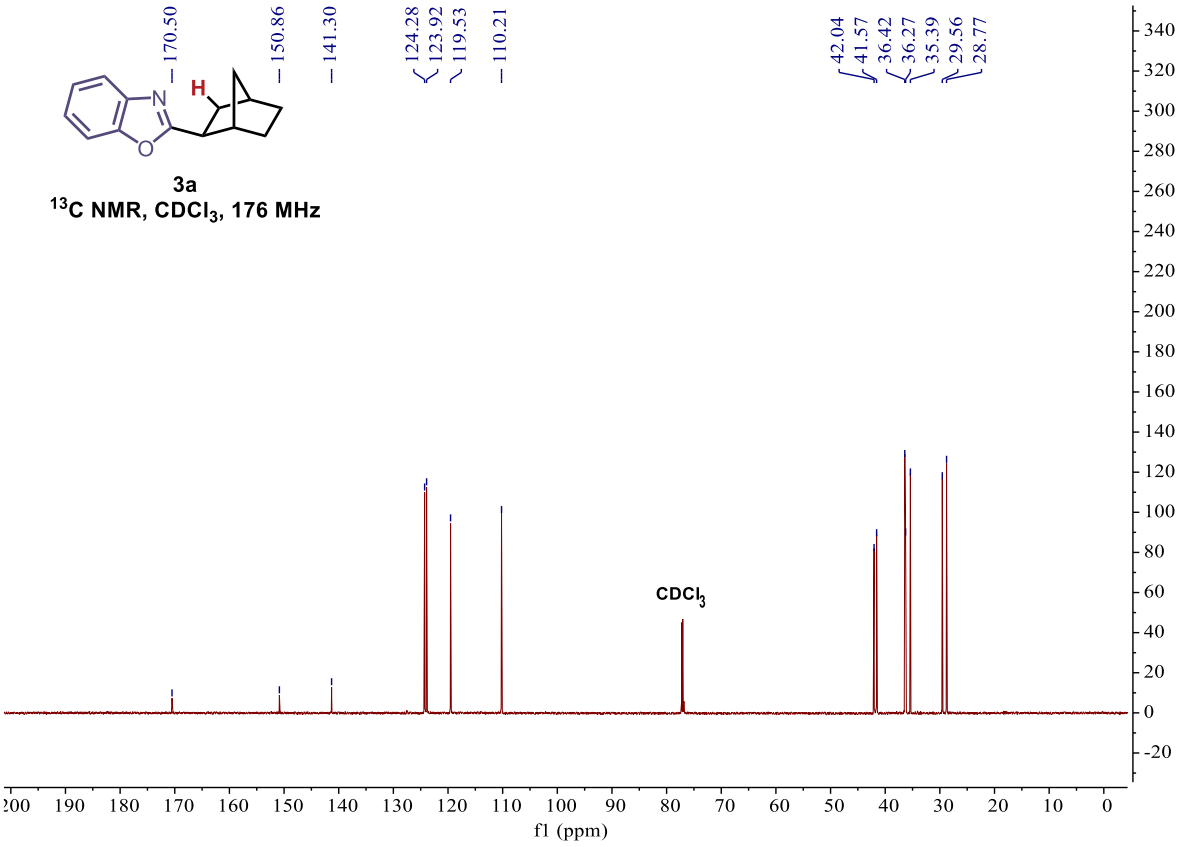

3a

^{13}C NMR, $CDCl_3$, 176 MHz

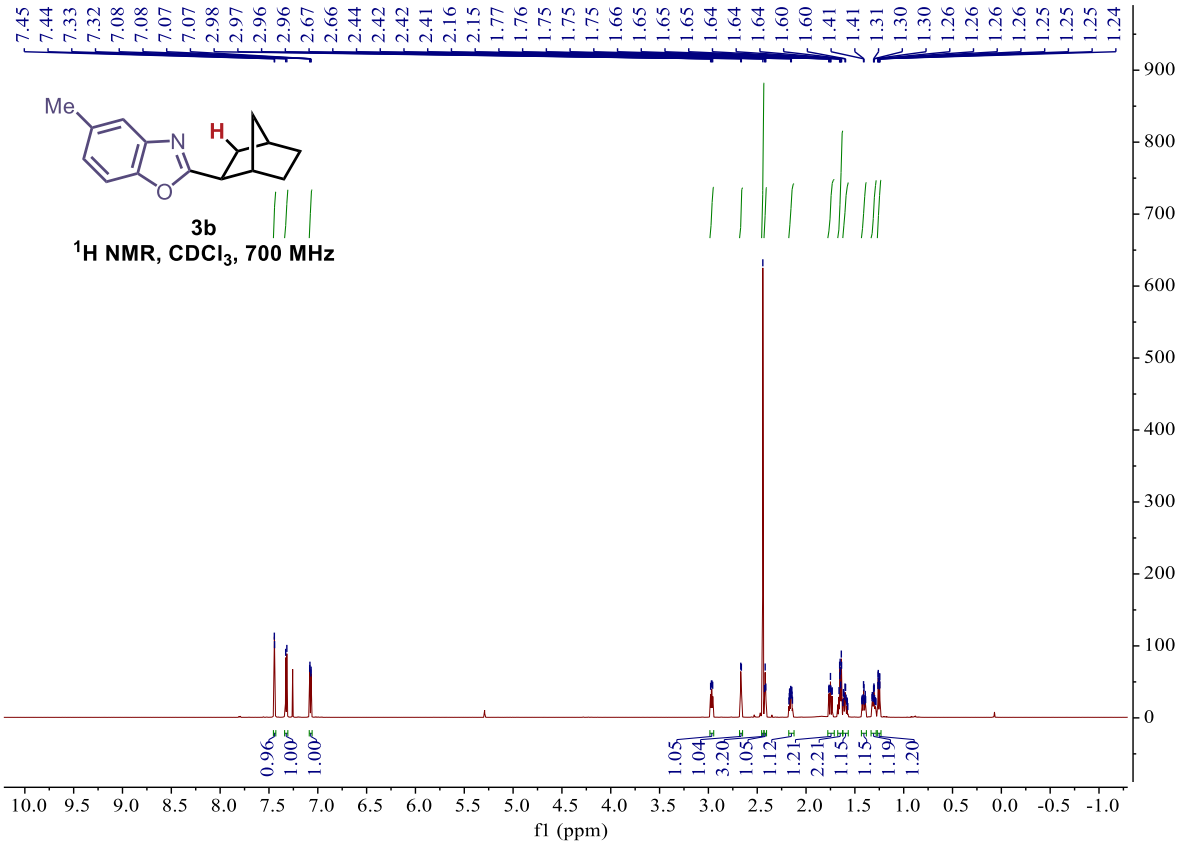
Me
N
O
H
3b
^{1}H NMR, $CDCl_3$, 700 MHz
fl (ppm)

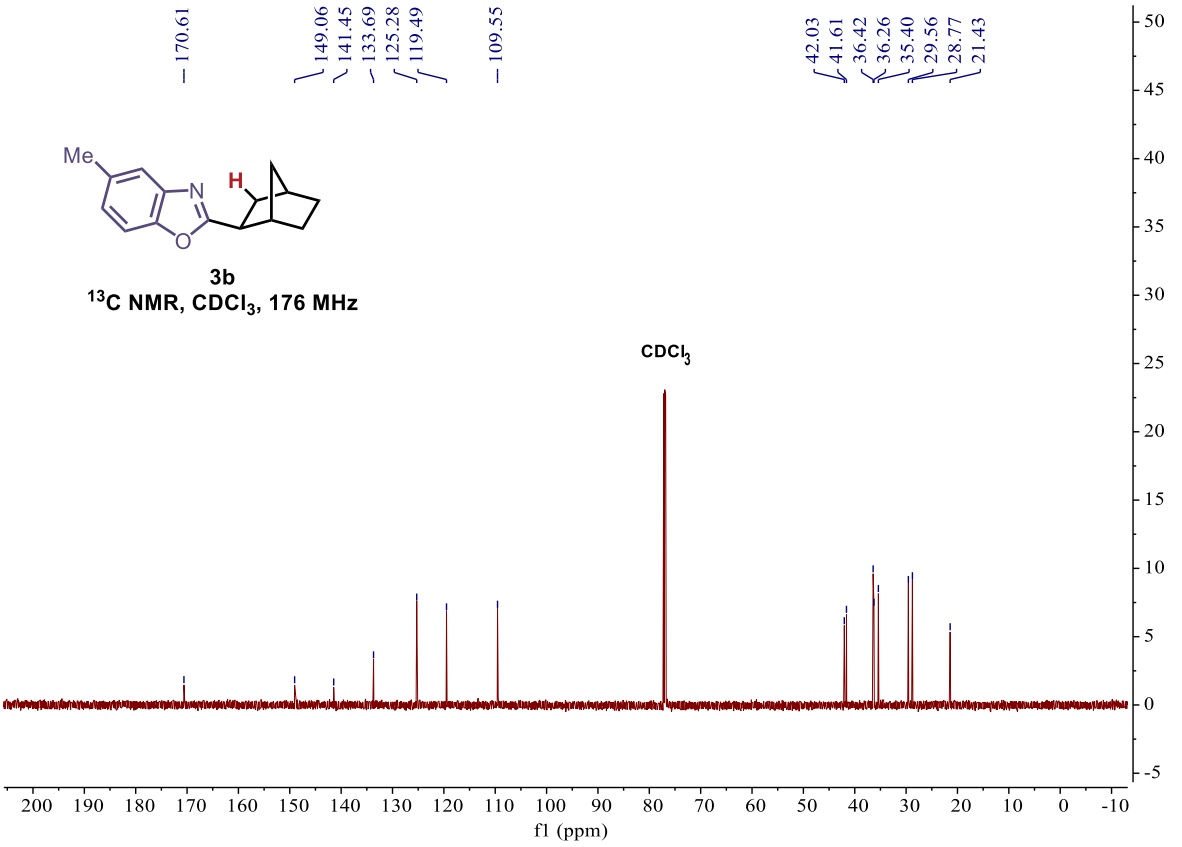
Me
N
O
H
3b
^{13}C NMR, $CDCl_3$, 176 MHz
$CDCl_3$
fl (ppm)

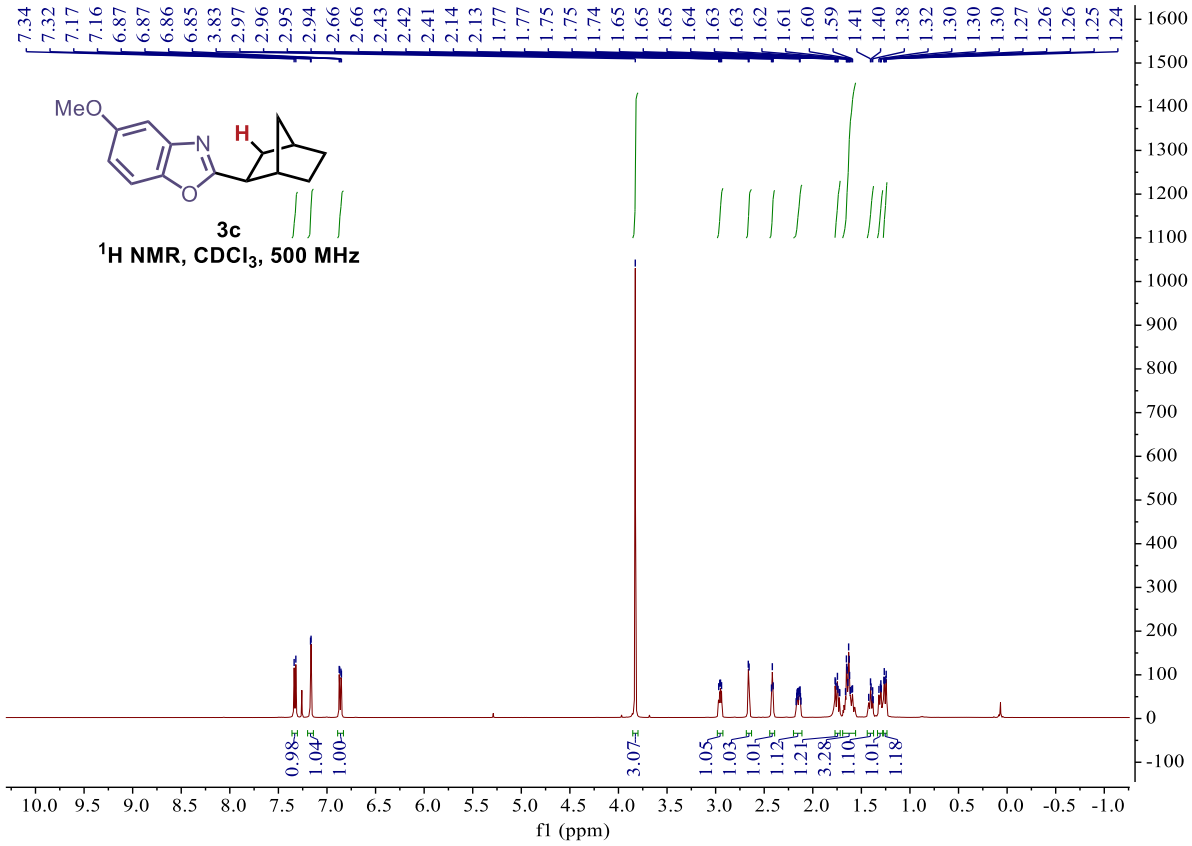
MeO
N
O
H
3c
^{1}H NMR, CDCl$_3$, 500 MHz
fl (ppm)

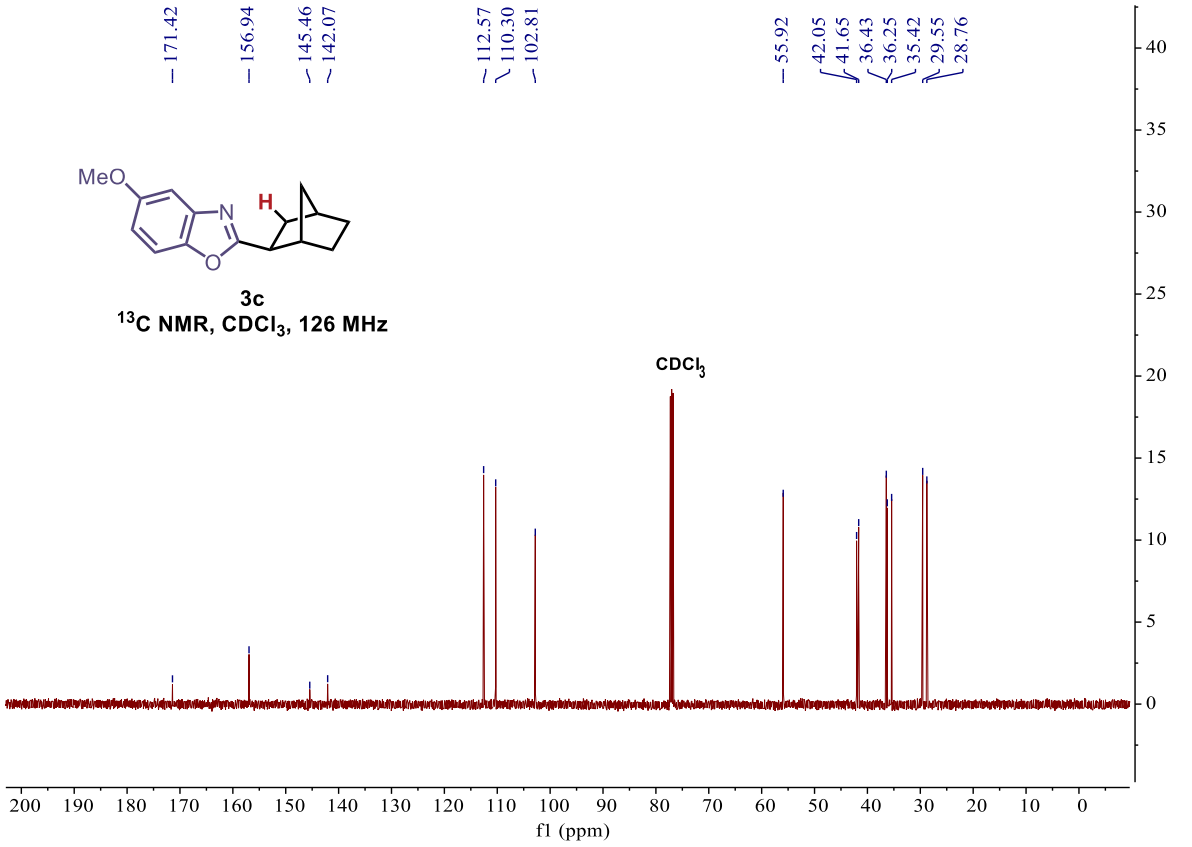
MeO
N
O
H
3c
^{13}C NMR, CDCl$_3$, 126 MHz
CDCl$_3$
fl (ppm)

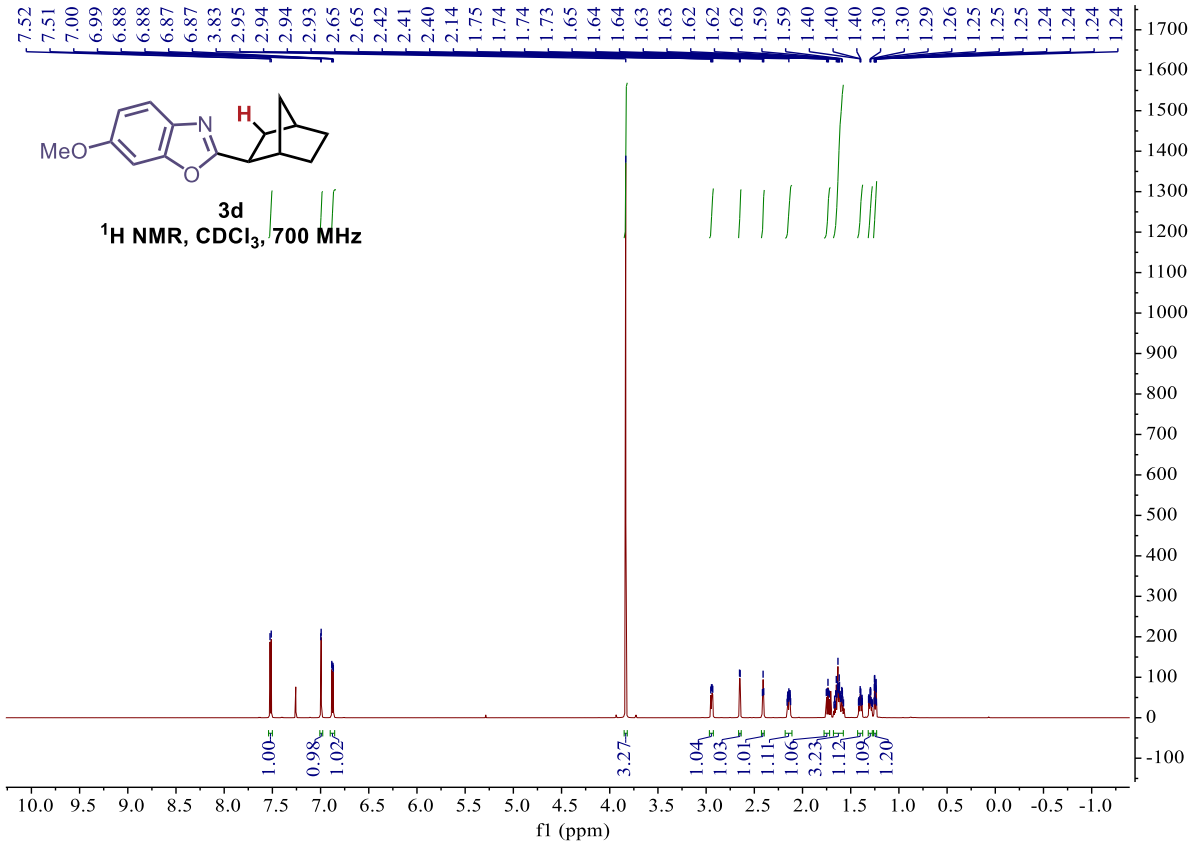
MeO
N
O
H
3d
^{1}H NMR, CDCl$_3$, 700 MHz
fl (ppm)

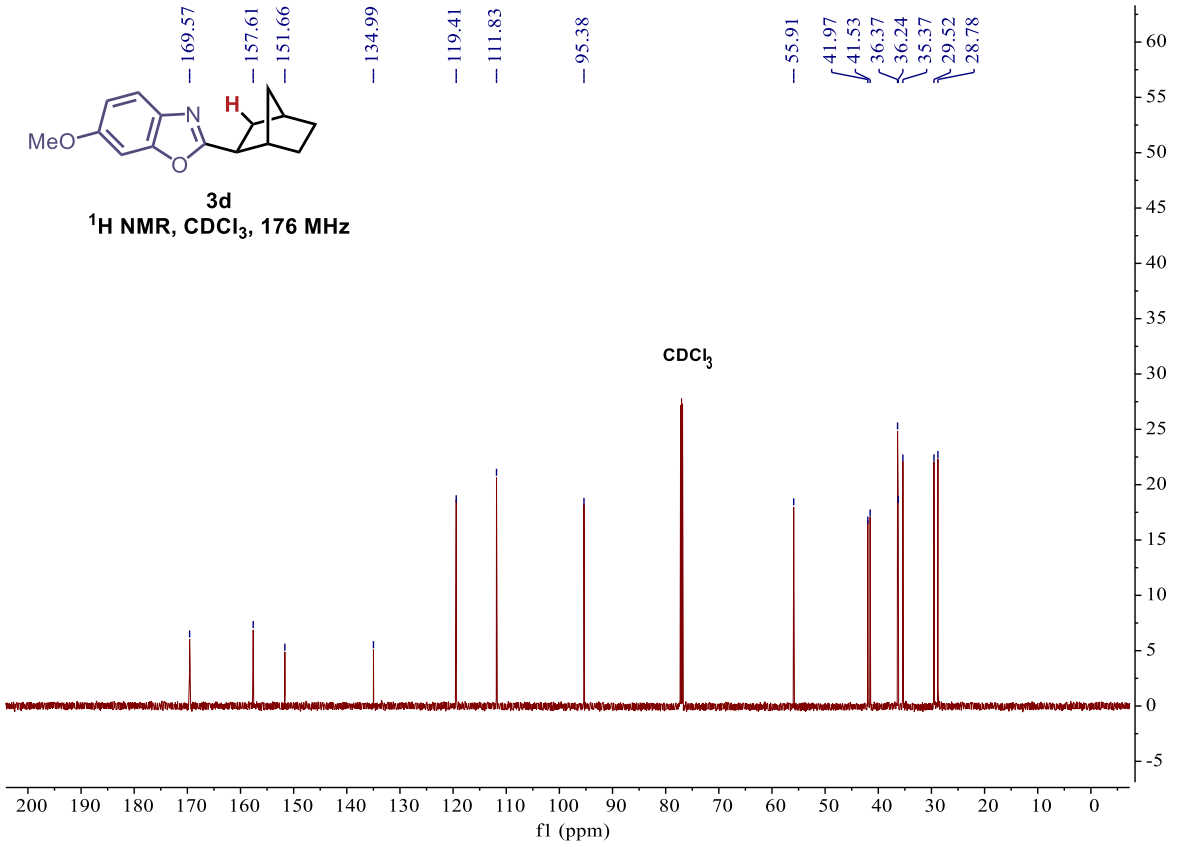
MeO
N
O
H
3d
^{1}H NMR, CDCl$_3$, 176 MHz
CDCl$_3$
fl (ppm)

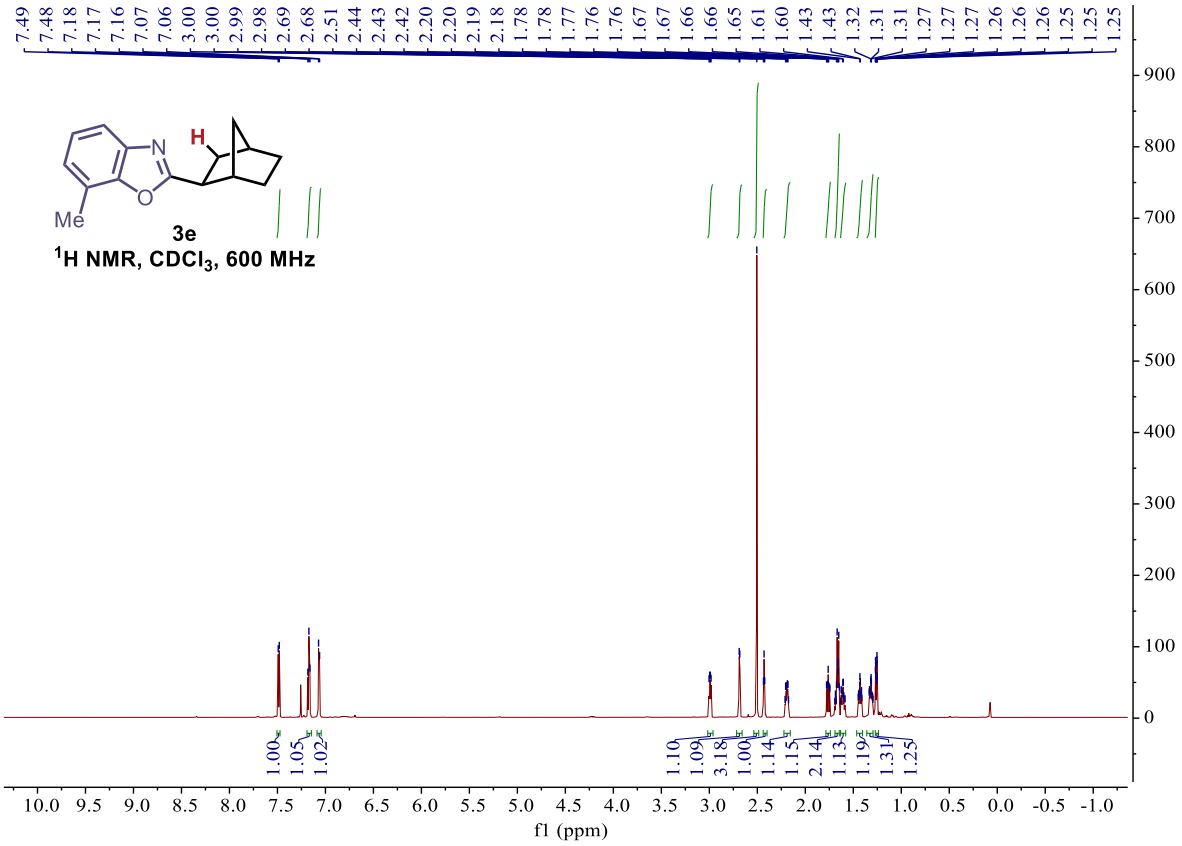
7.49 7.48 7.18 7.17 7.16 7.07 7.06 3.00 3.00 2.99 2.98 2.69 2.68 2.51 2.44 2.43 2.42 2.20 2.20 2.19 2.18 1.78 1.78 1.77 1.76 1.76 1.67 1.67 1.66 1.66 1.65 1.61 1.60 1.43 1.43 1.32 1.31 1.31 1.27 1.27 1.26 1.26 1.26 1.25 1.25 1.25
N
H
O
Me
3e
1H NMR, CDCl3, 600 MHz
1.00 1.05 1.02 1.10 1.09 3.18 1.00 1.14 1.15 2.14 1.13 1.19 1.31 1.25
f1 (ppm)

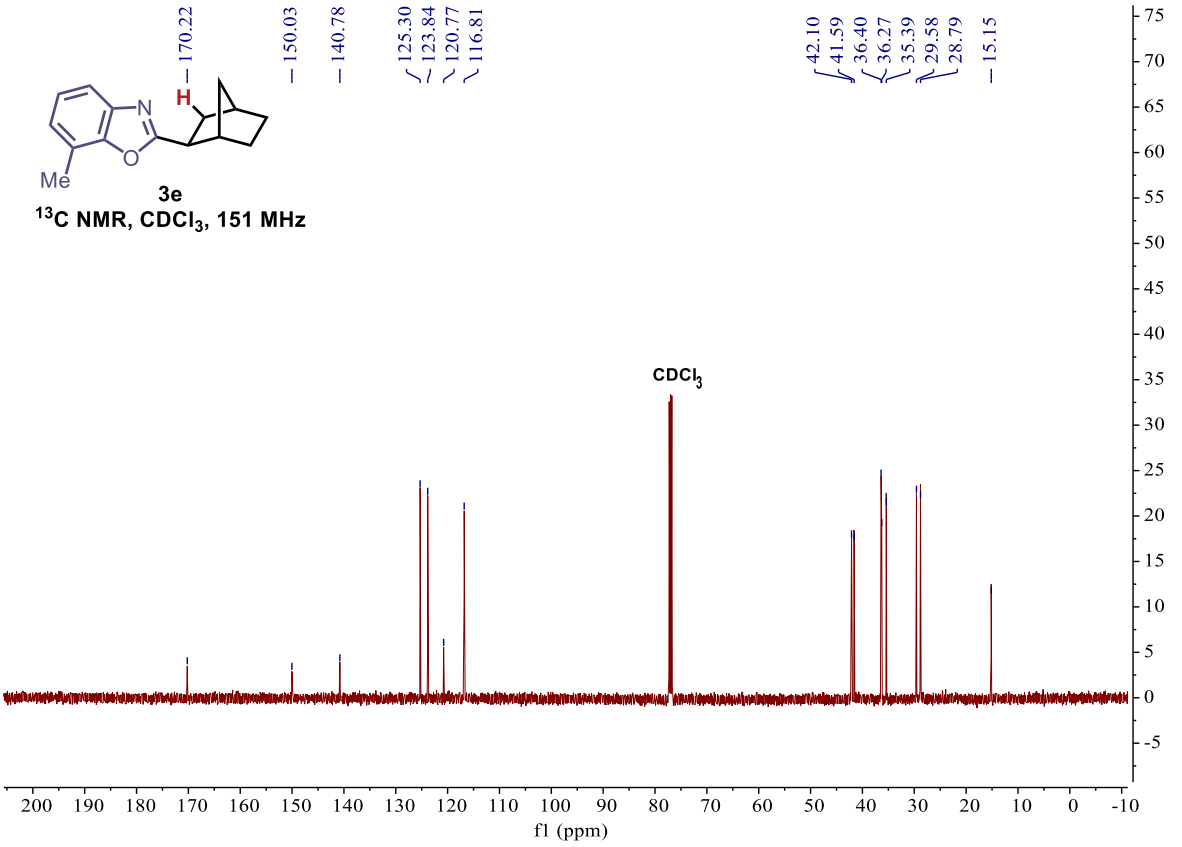
170.22 150.03 140.78 125.30 123.84 120.77 116.81 42.10 41.59 36.40 36.27 35.39 29.58 28.79 15.15
N
H
O
Me
3e
13C NMR, CDCl3, 151 MHz
CDCl3
f1 (ppm)

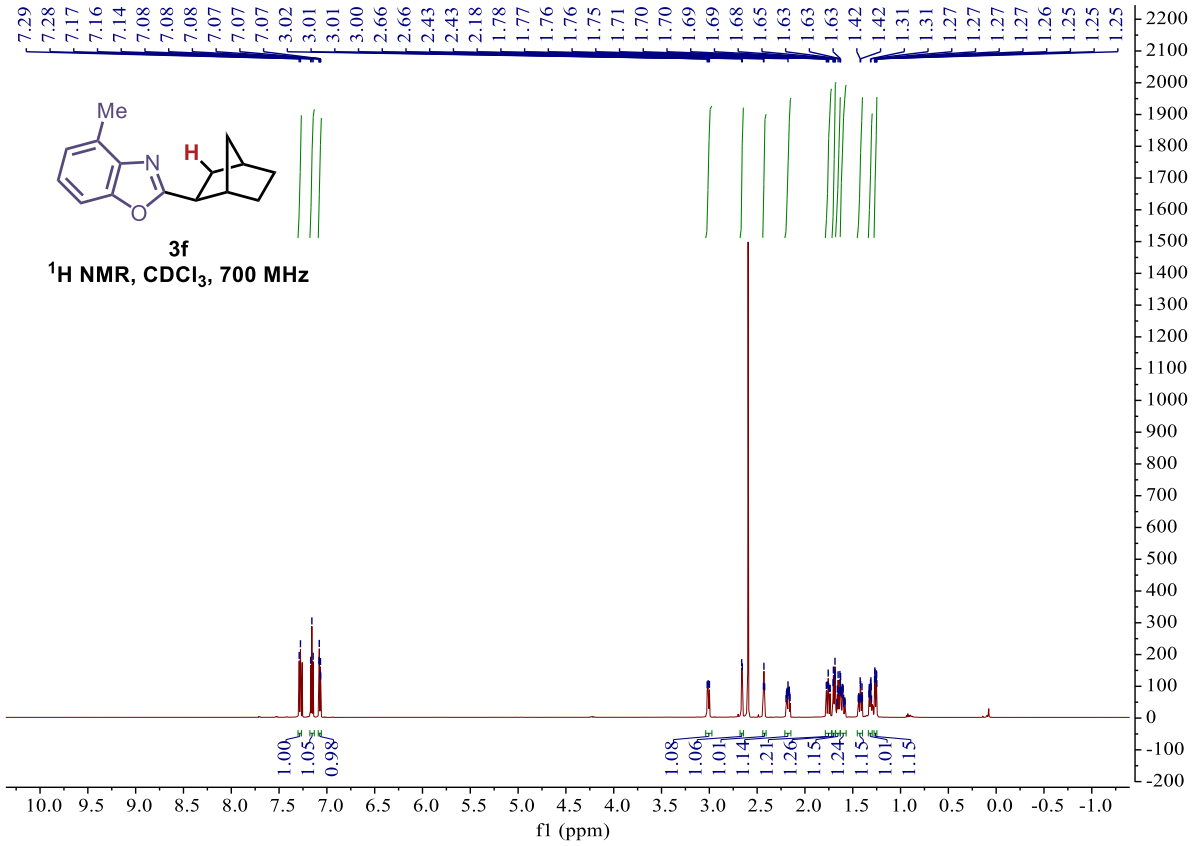
Me
H
N
O
3f
^{1}H NMR, $CDCl_3$, 700 MHz
fl (ppm)

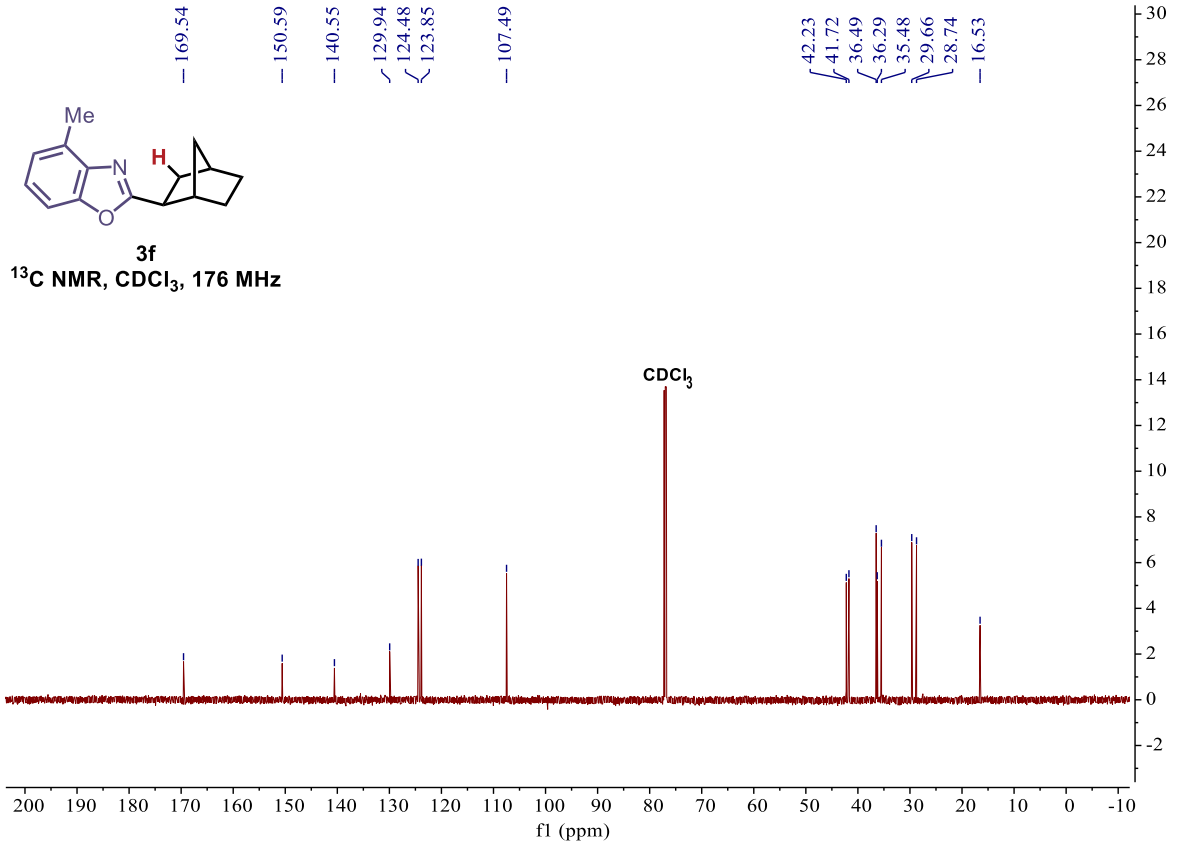
Me
H
N
O
3f
^{13}C NMR, $CDCl_3$, 176 MHz
$CDCl_3$
fl (ppm)

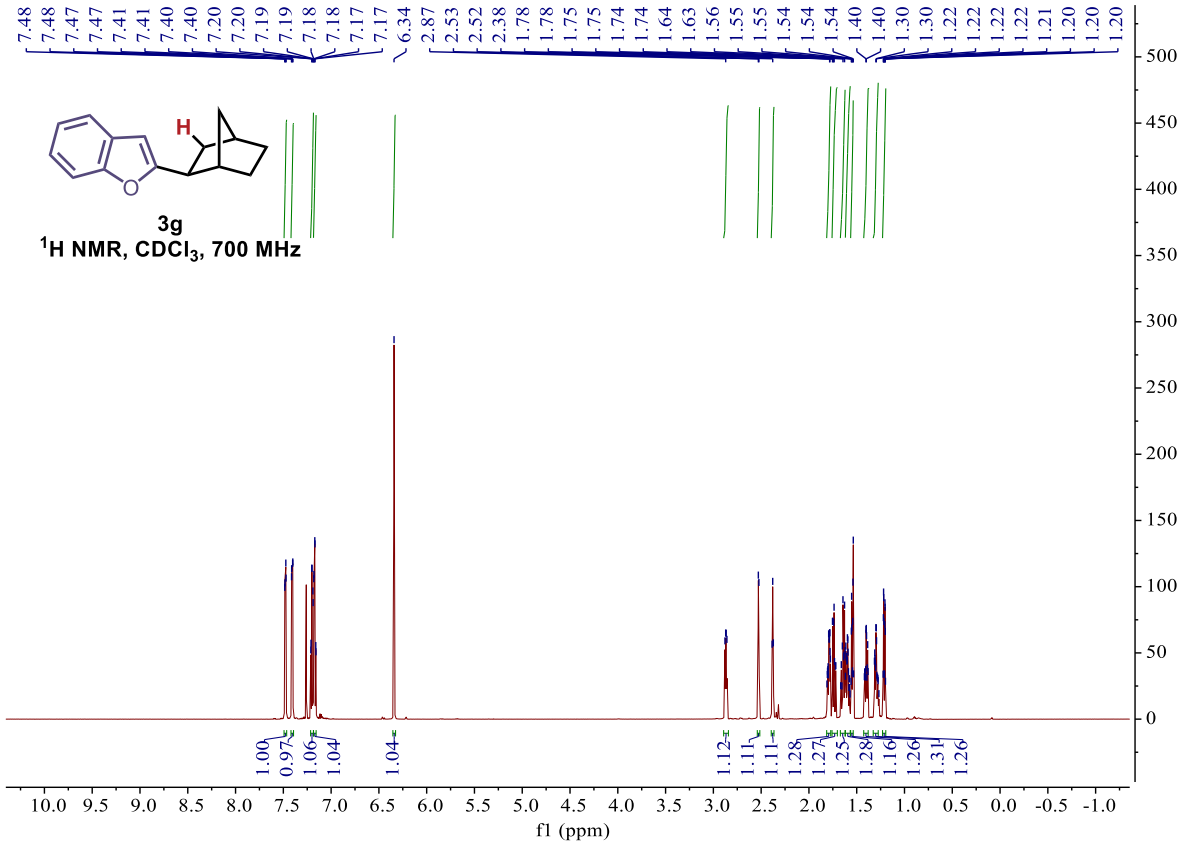
H
O
3g
^{1}H NMR, CDCl$_3$, 700 MHz
fl (ppm)

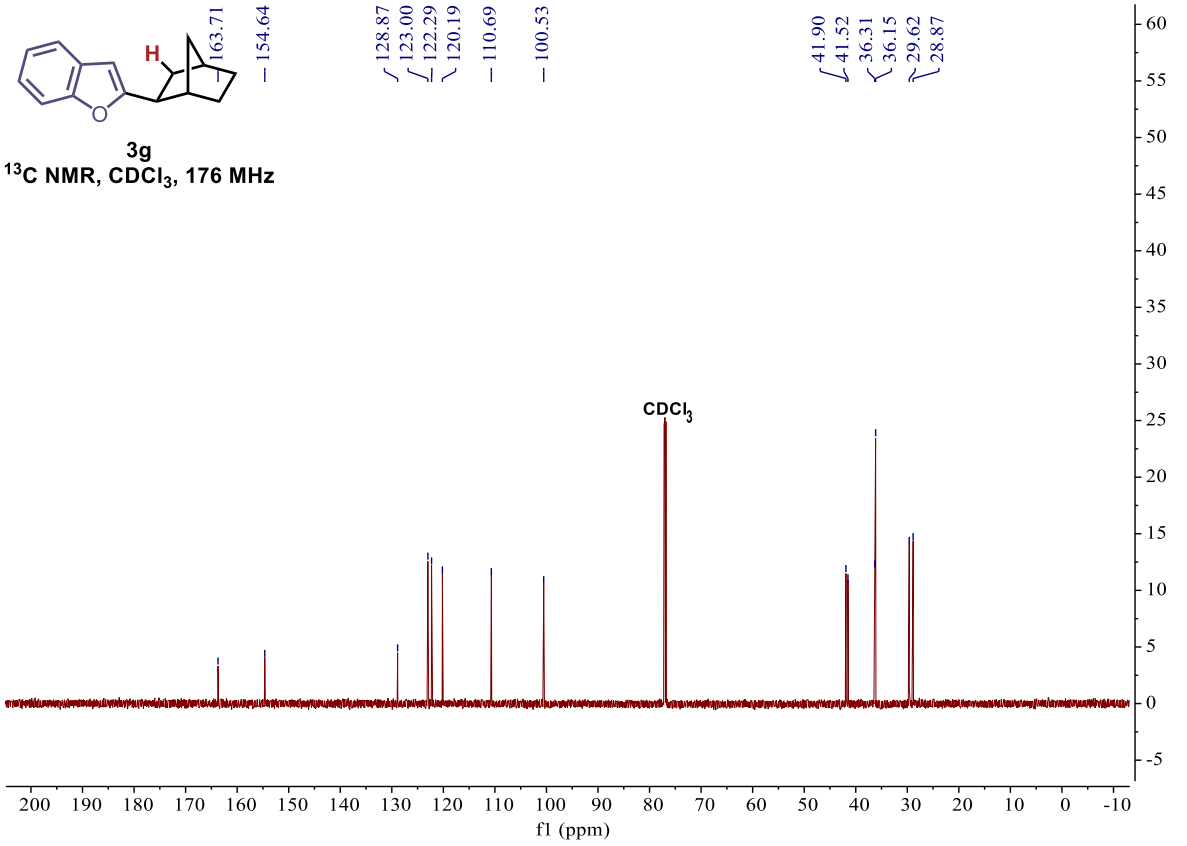
H
O
3g
^{13}C NMR, CDCl$_3$, 176 MHz
CDCl$_3$
fl (ppm)

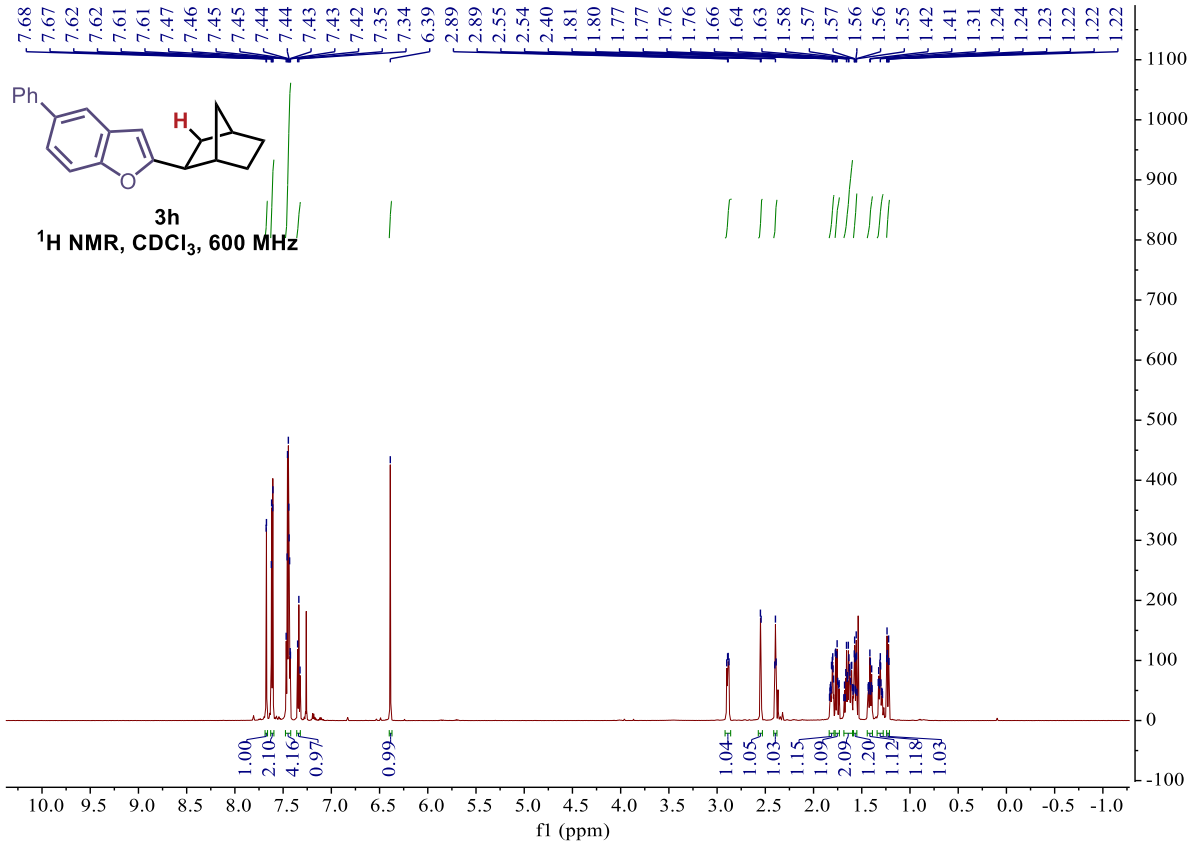

3h

^{1}H NMR, $CDCl_3$, 600 MHz

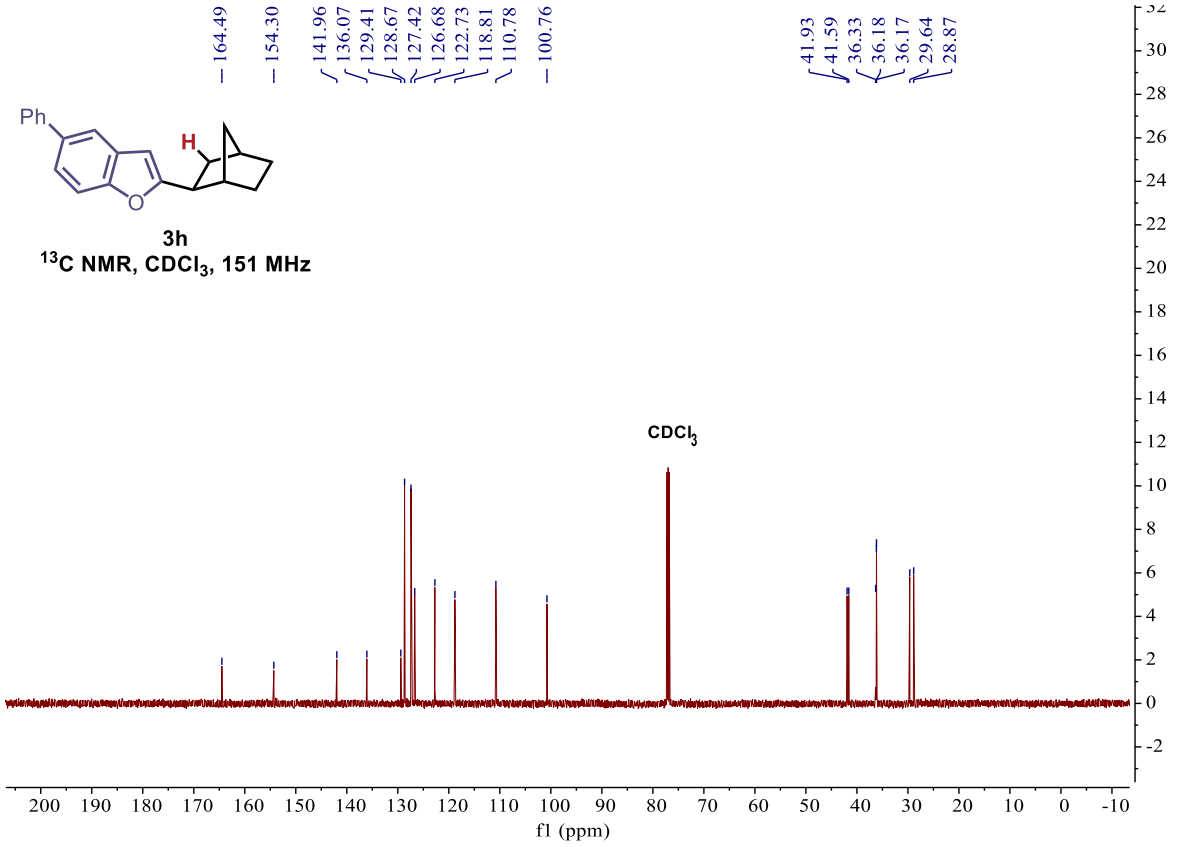

3h

^{13}C NMR, $CDCl_3$, 151 MHz

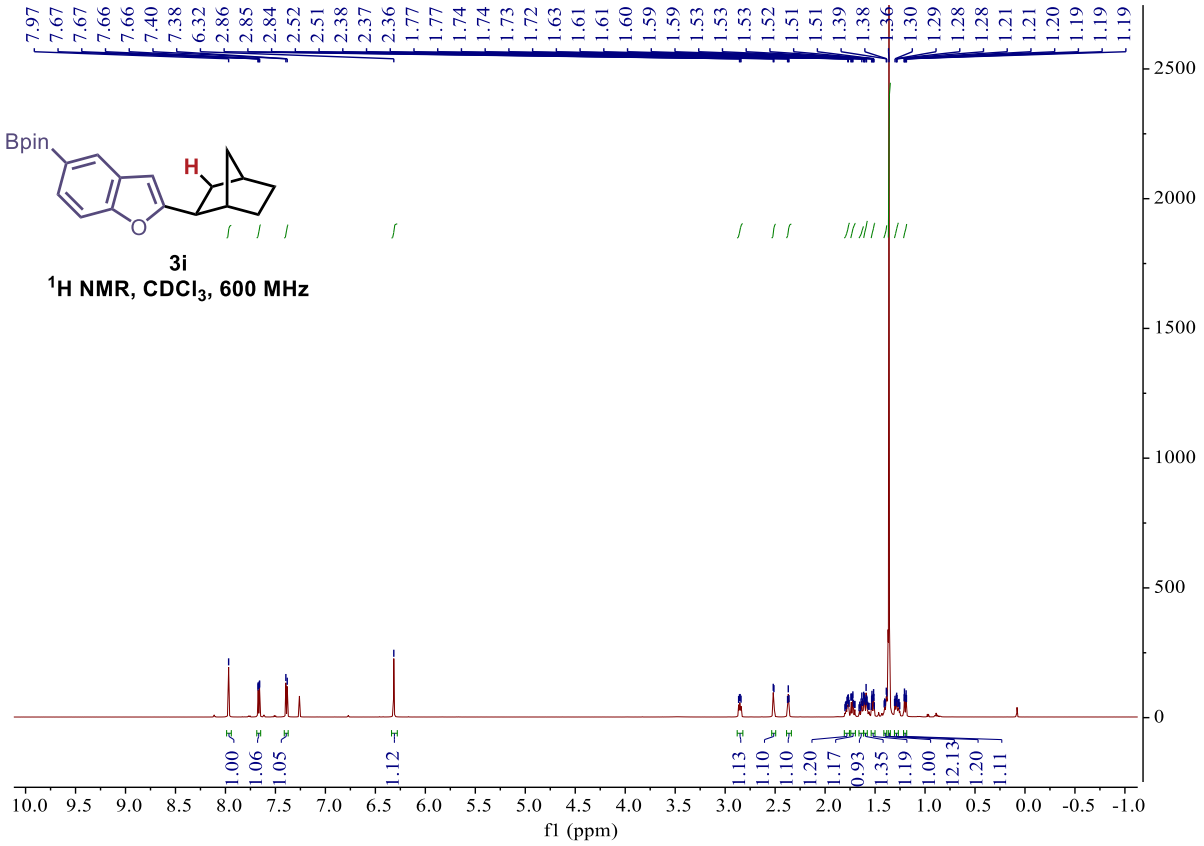

3i

^{1}H NMR, $CDCl_3$, 600 MHz

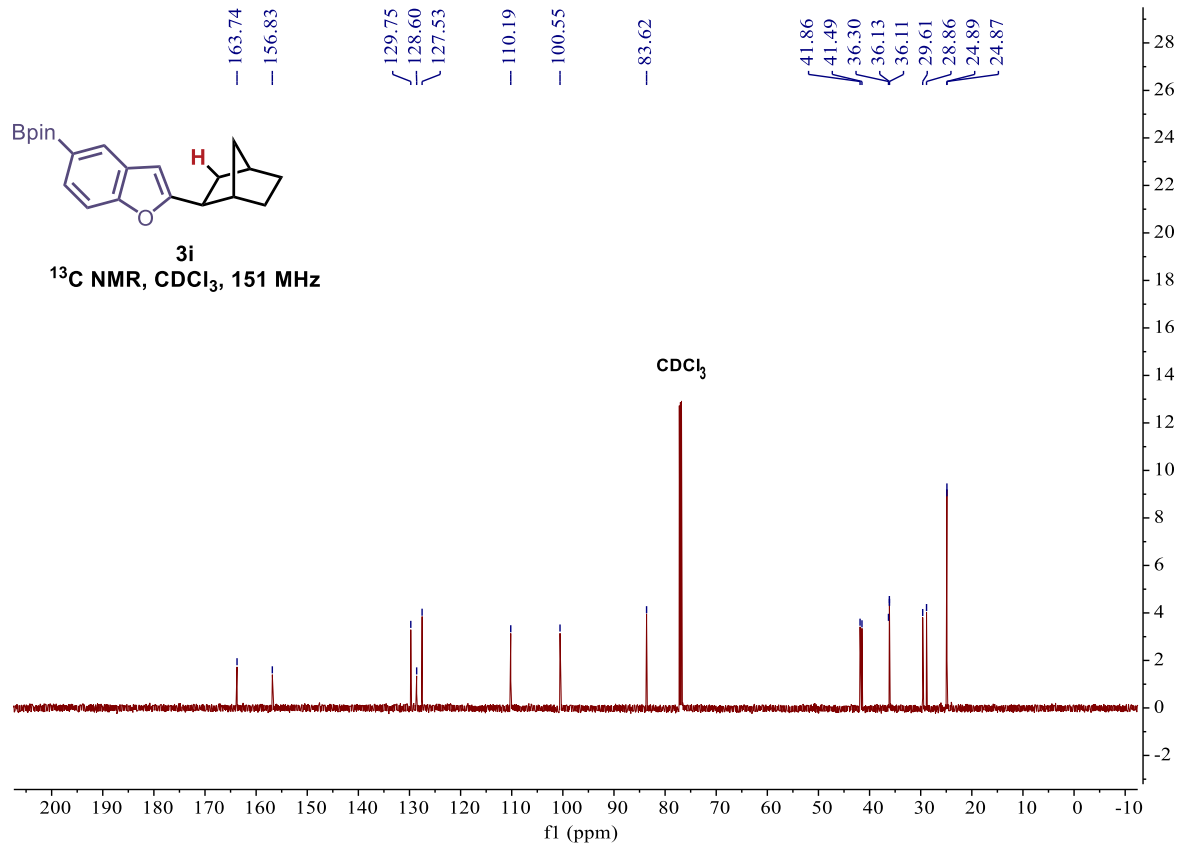

3i

^{13}C NMR, $CDCl_3$, 151 MHz

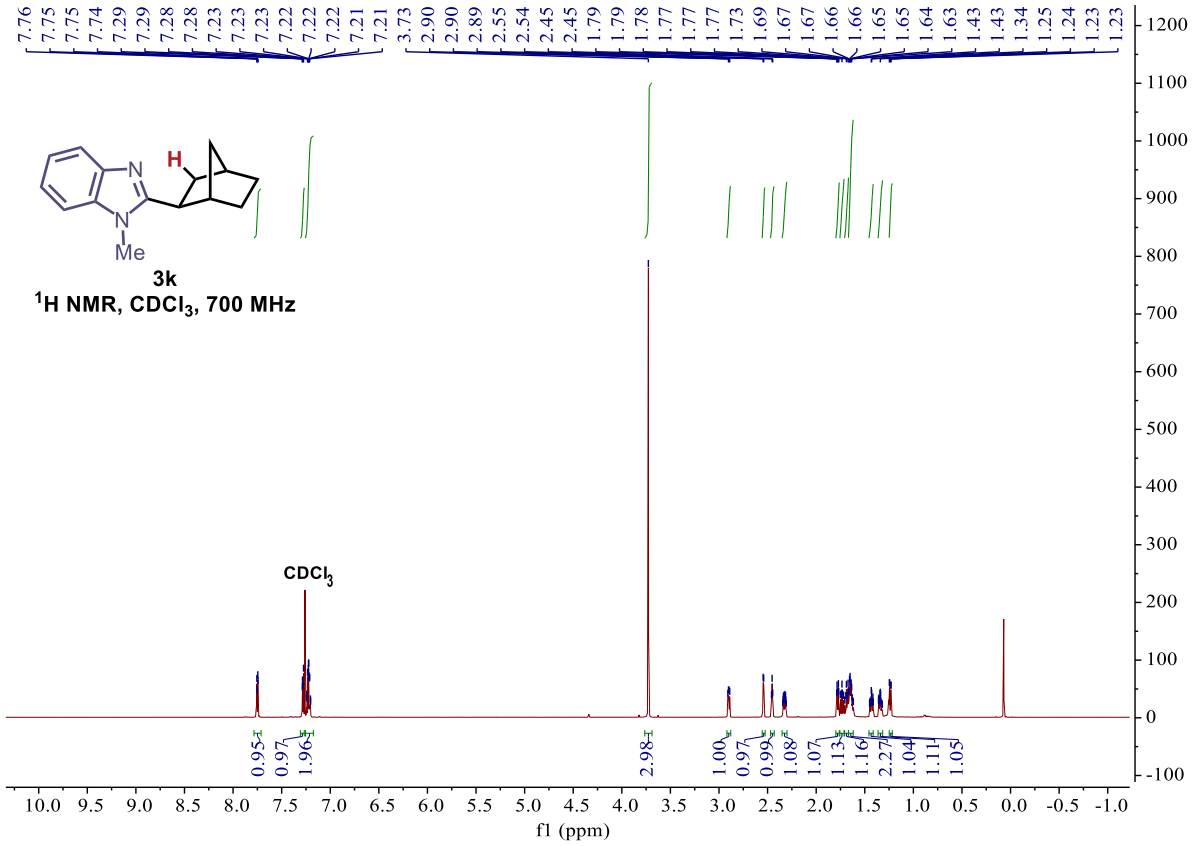
7.76 7.75 7.75 7.74 7.29 7.29 7.28 7.28 7.23 7.23 7.23 7.22 7.22 7.22 7.21 7.21 3.73 2.90 2.90 2.89 2.55 2.54 2.45 2.45 1.79 1.79 1.78 1.77 1.77 1.77 1.73 1.69 1.67 1.67 1.66 1.66 1.65 1.65 1.64 1.63 1.43 1.43 1.34 1.25 1.24 1.23 1.23
N
H
N
Me
3k
^{1}H NMR, $CDCl_3$, 700 MHz
$CDCl_3$
0.95 0.97 1.96 2.98 1.00 0.97 0.99 1.08 1.07 1.13 1.16 2.27 1.04 1.11 1.05
10.0 9.5 9.0 8.5 8.0 7.5 7.0 6.5 6.0 5.5 5.0 4.5 4.0 3.5 3.0 2.5 2.0 1.5 1.0 0.5 0.0 -0.5 -1.0
f1 (ppm)
1200 1100 1000 900 800 700 600 500 400 300 200 100 0 -100

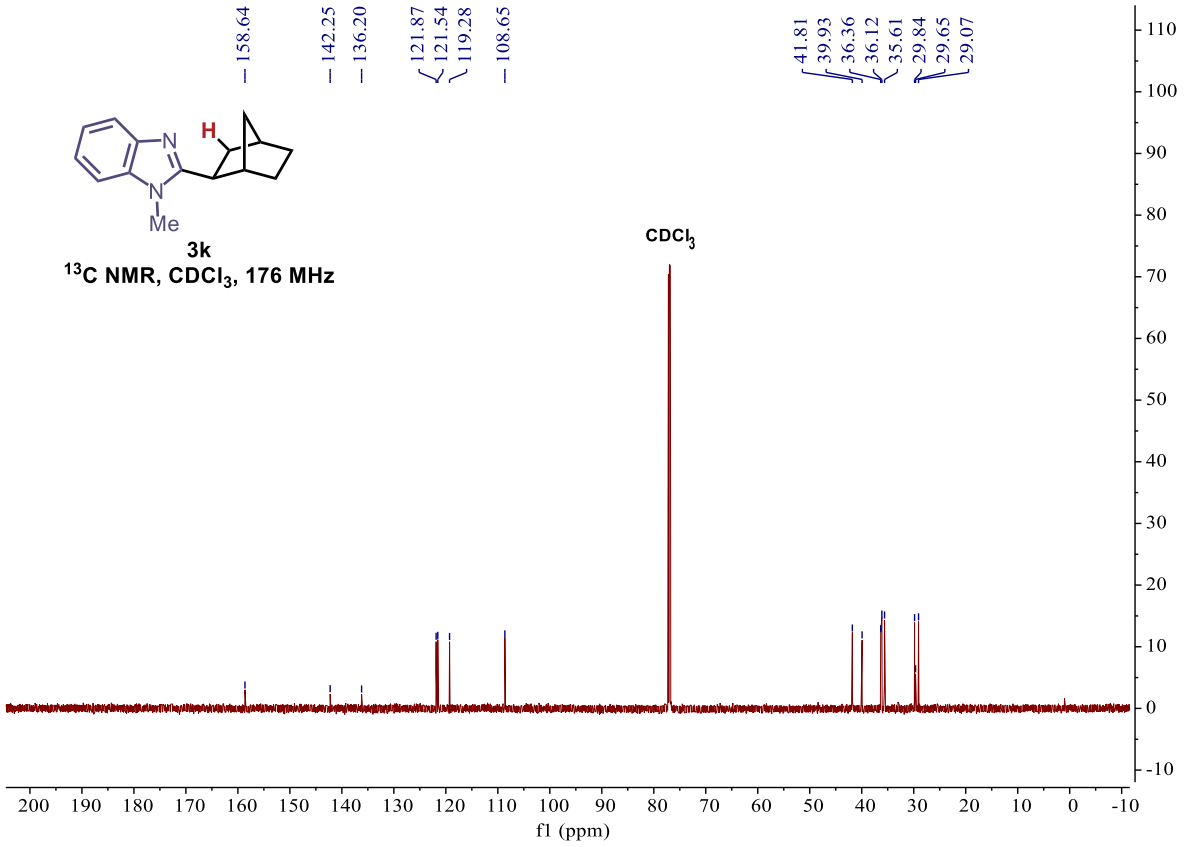
158.64 142.25 136.20 121.87 121.54 119.28 108.65
41.81 39.93 36.36 36.12 35.61 29.84 29.65 29.07
N
H
N
Me
3k
^{13}C NMR, $CDCl_3$, 176 MHz
$CDCl_3$
200 190 180 170 160 150 140 130 120 110 100 90 80 70 60 50 40 30 20 10 0 -10
f1 (ppm)
110 100 90 80 70 60 50 40 30 20 10 0 -10

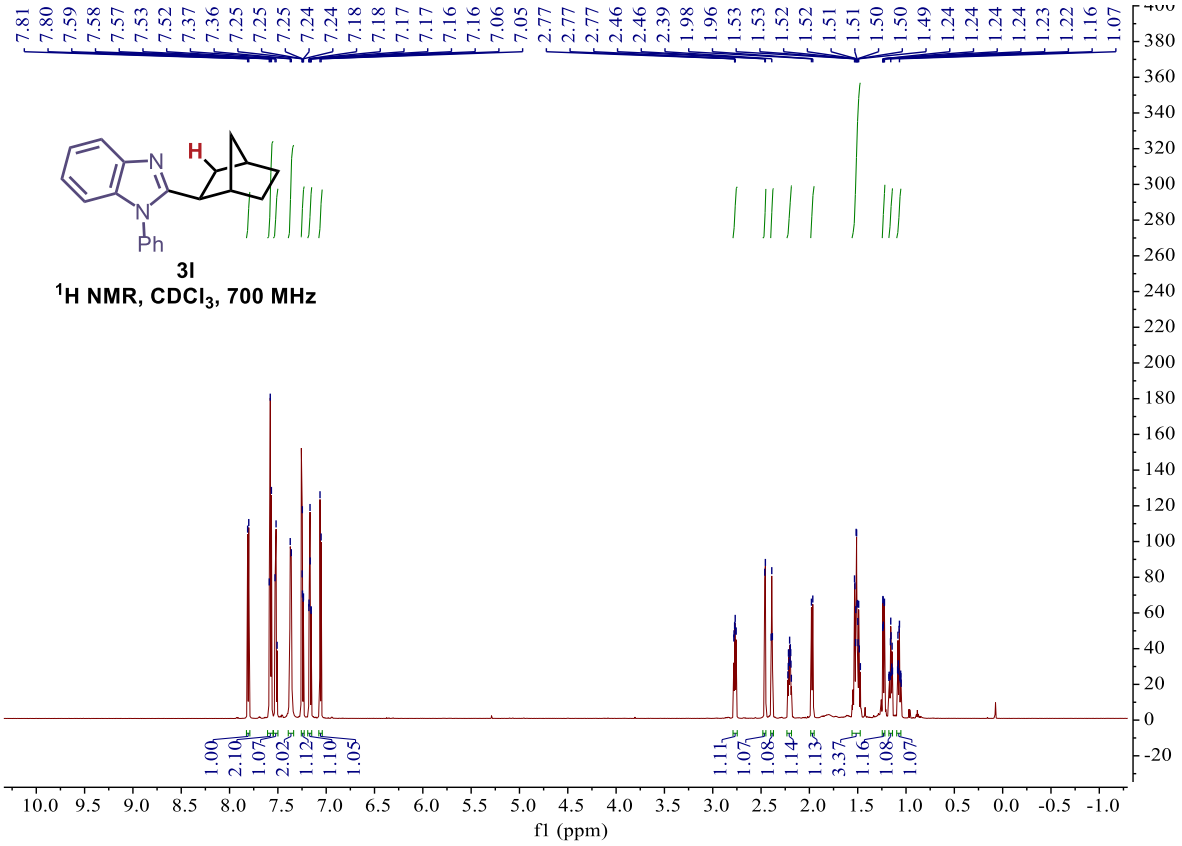

3l

^{1}H NMR, $CDCl_3$, 700 MHz

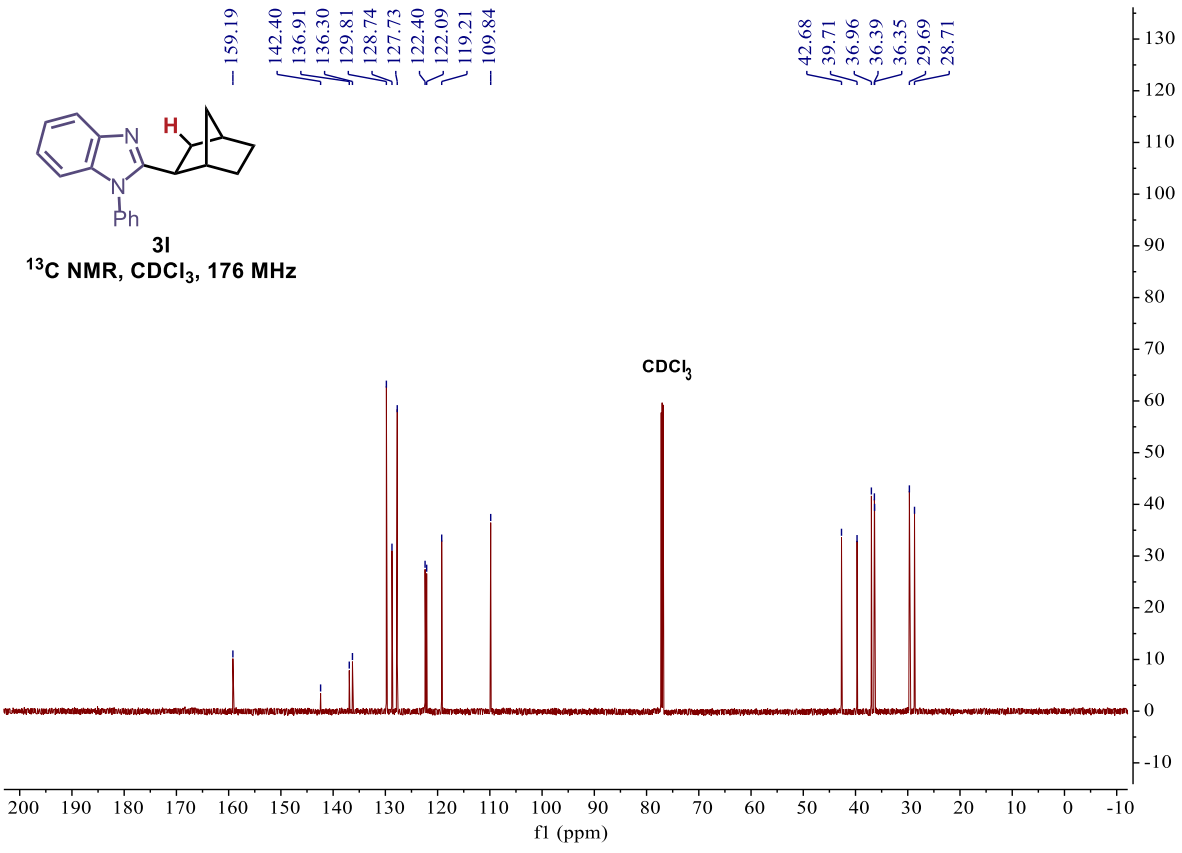

3l

^{13}C NMR, $CDCl_3$, 176 MHz

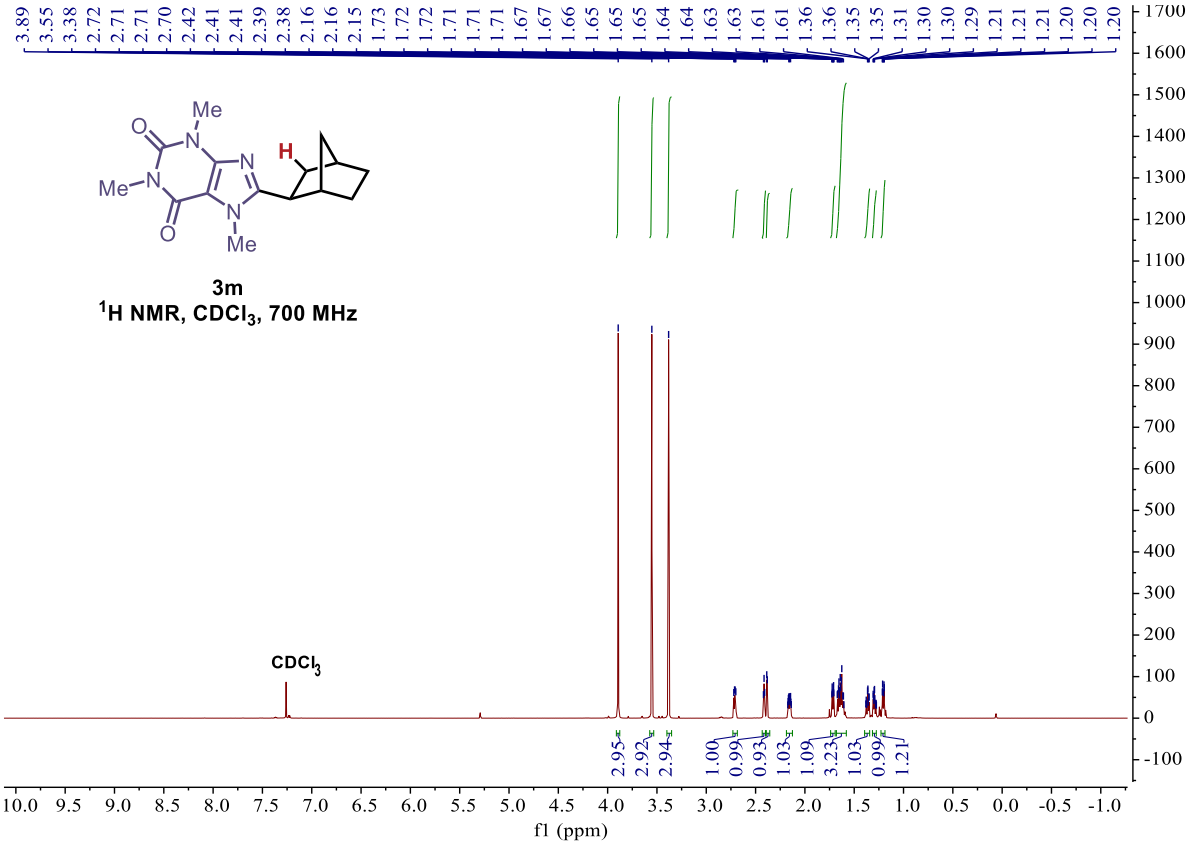

3m
^{1}H NMR, $CDCl_3$, 700 MHz

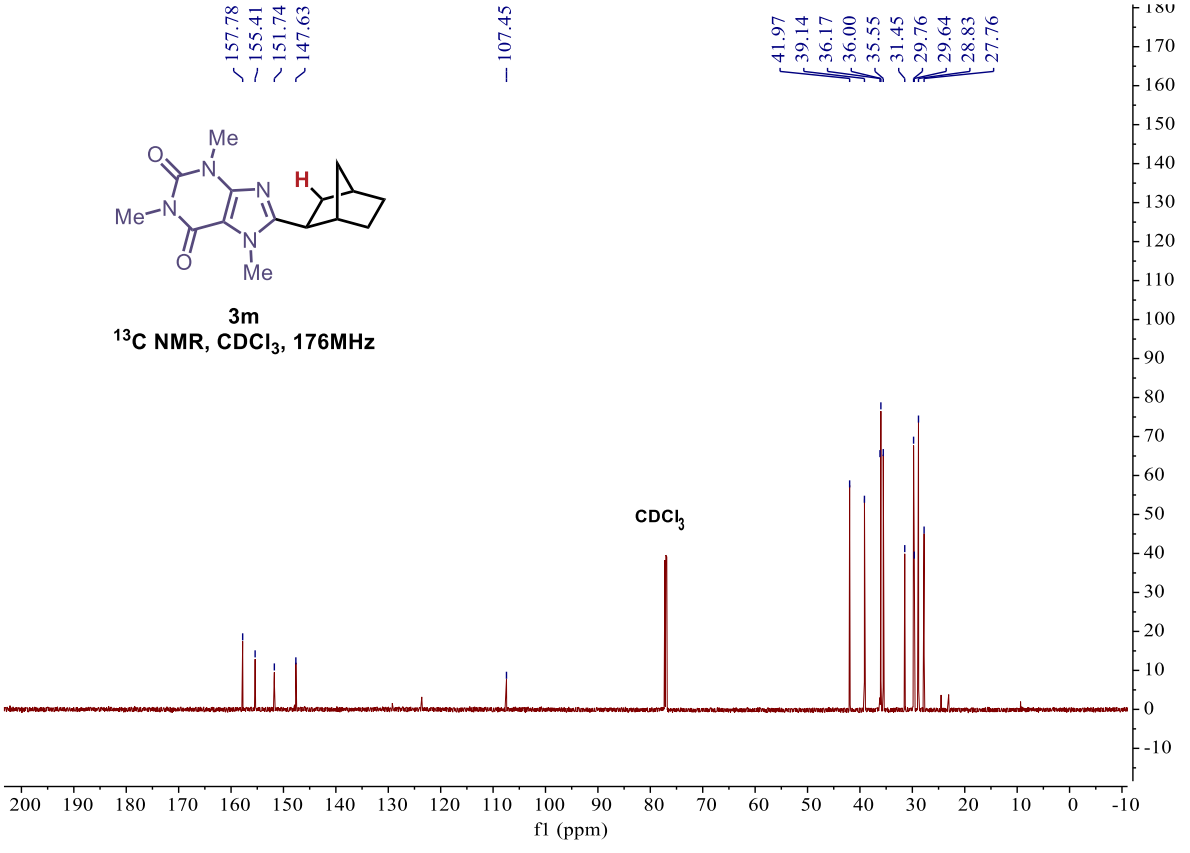

3m
^{13}C NMR, $CDCl_3$, 176MHz

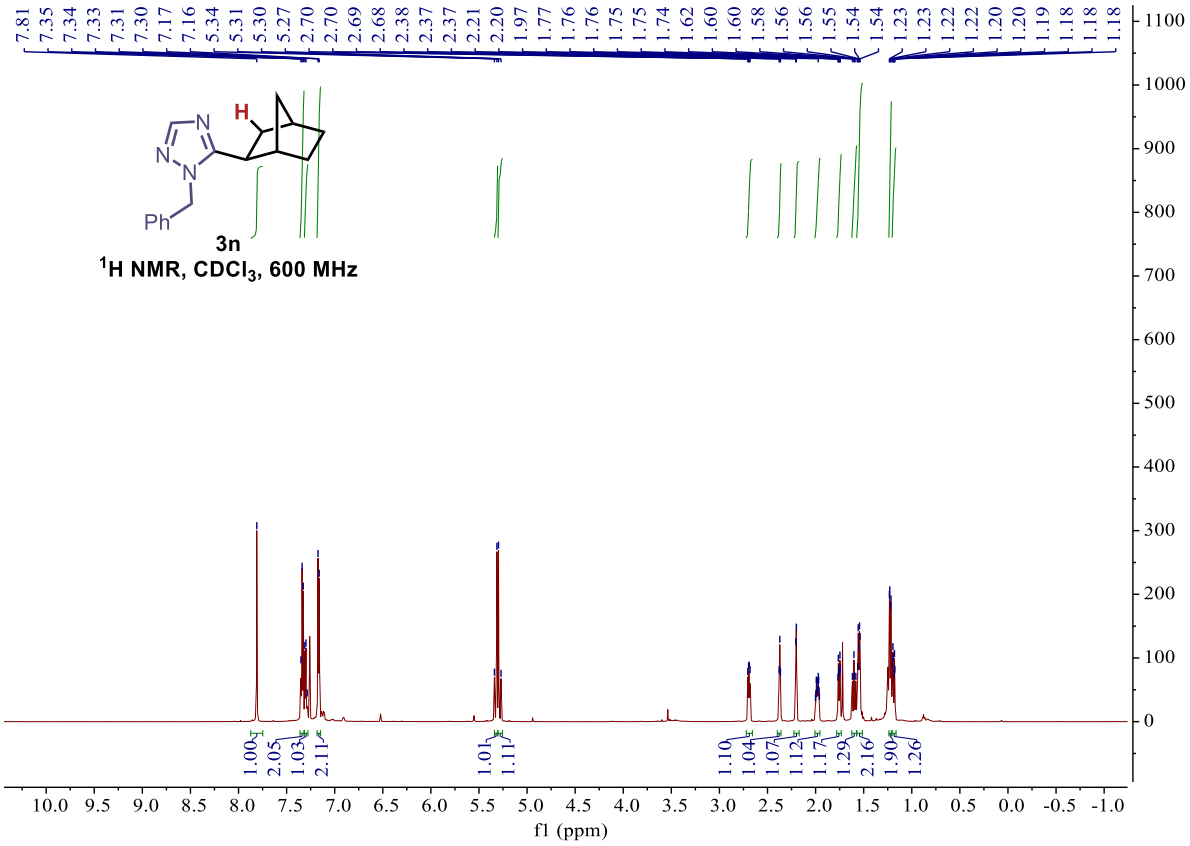

3n

^{1}H NMR, $CDCl_3$, 600 MHz

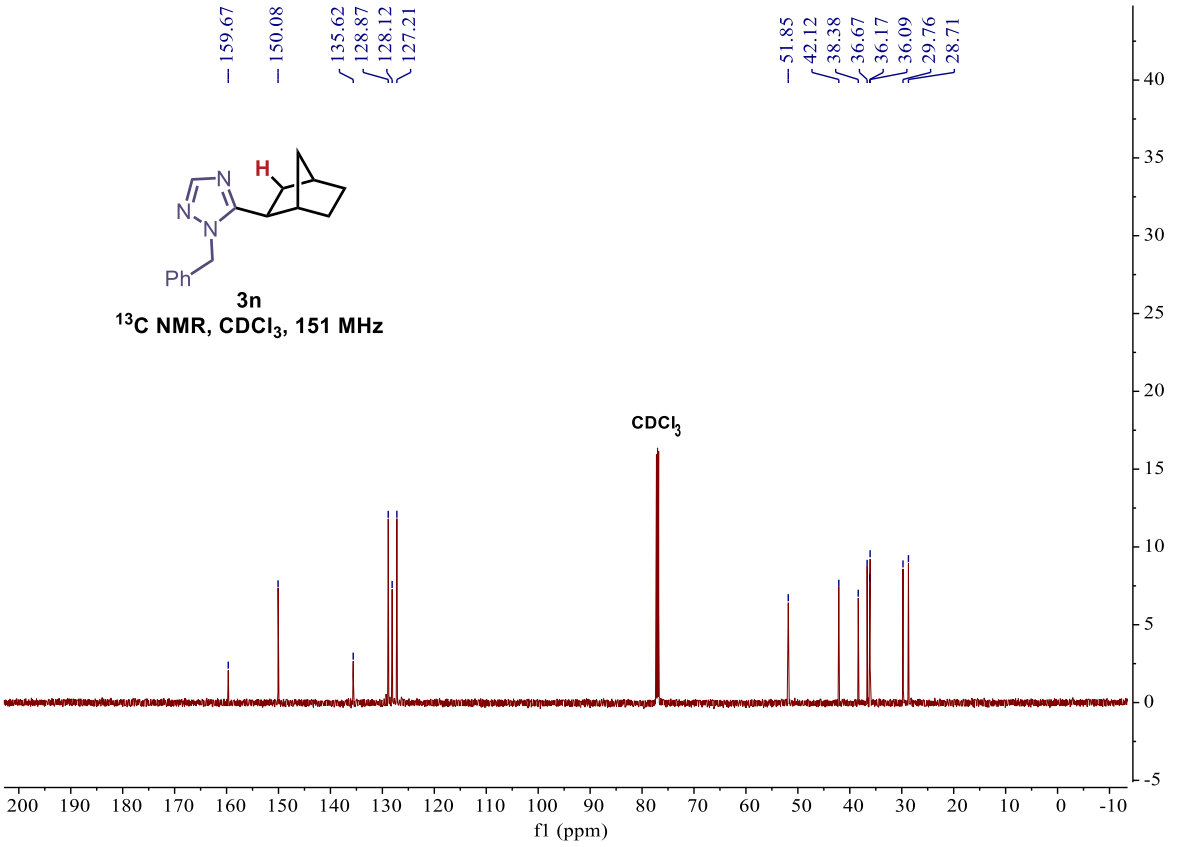

3n

^{13}C NMR, $CDCl_3$, 151 MHz

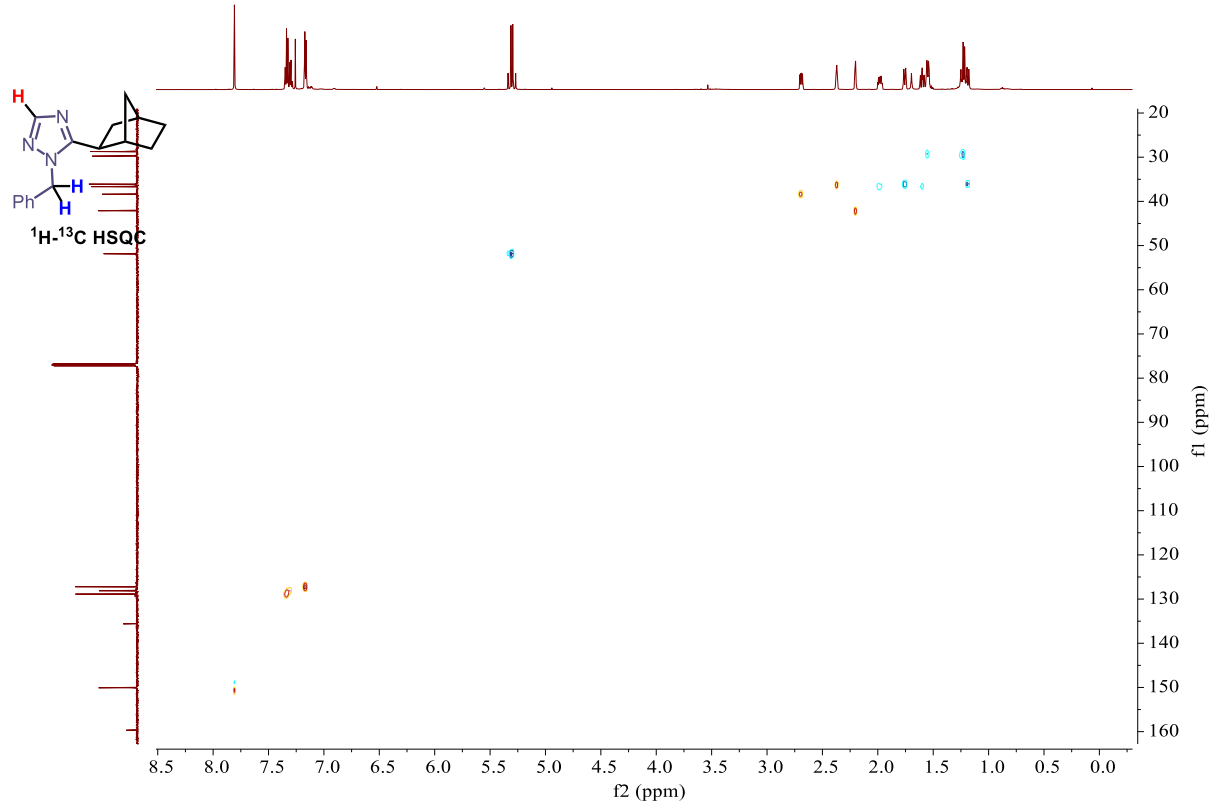
H
N
N
Ph
H
H
^{1}H-^{13}C HSQC
20
30
40
50
60
70
80
90
100
110
120
130
140
150
160
f1 (ppm)
8.5
8.0
7.5
7.0
6.5
6.0
5.5
5.0
4.5
4.0
3.5
3.0
2.5
2.0
1.5
1.0
0.5
0.0
f2 (ppm)

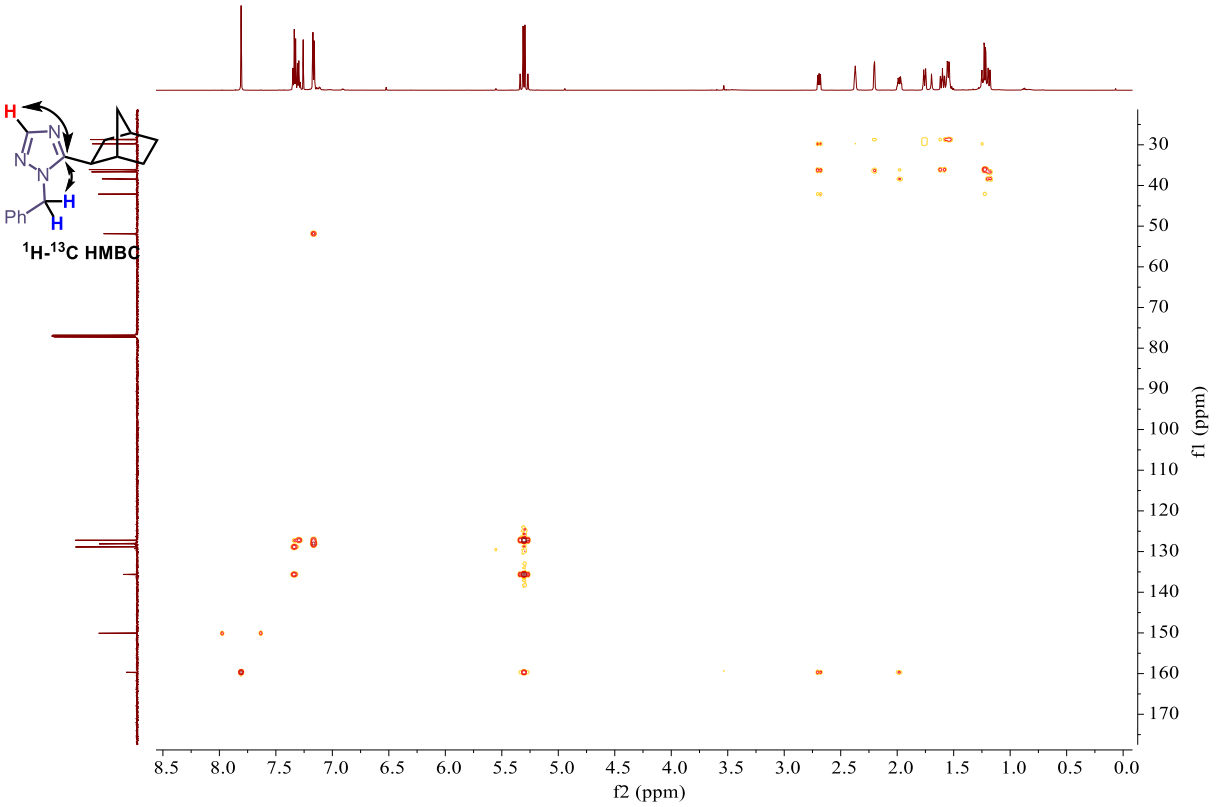
H
N
N
Ph
H
H
^{1}H-^{13}C HMBC
30
40
50
60
70
80
90
100
110
120
130
140
150
160
170
f1 (ppm)
8.5
8.0
7.5
7.0
6.5
6.0
5.5
5.0
4.5
4.0
3.5
3.0
2.5
2.0
1.5
1.0
0.5
0.0
f2 (ppm)

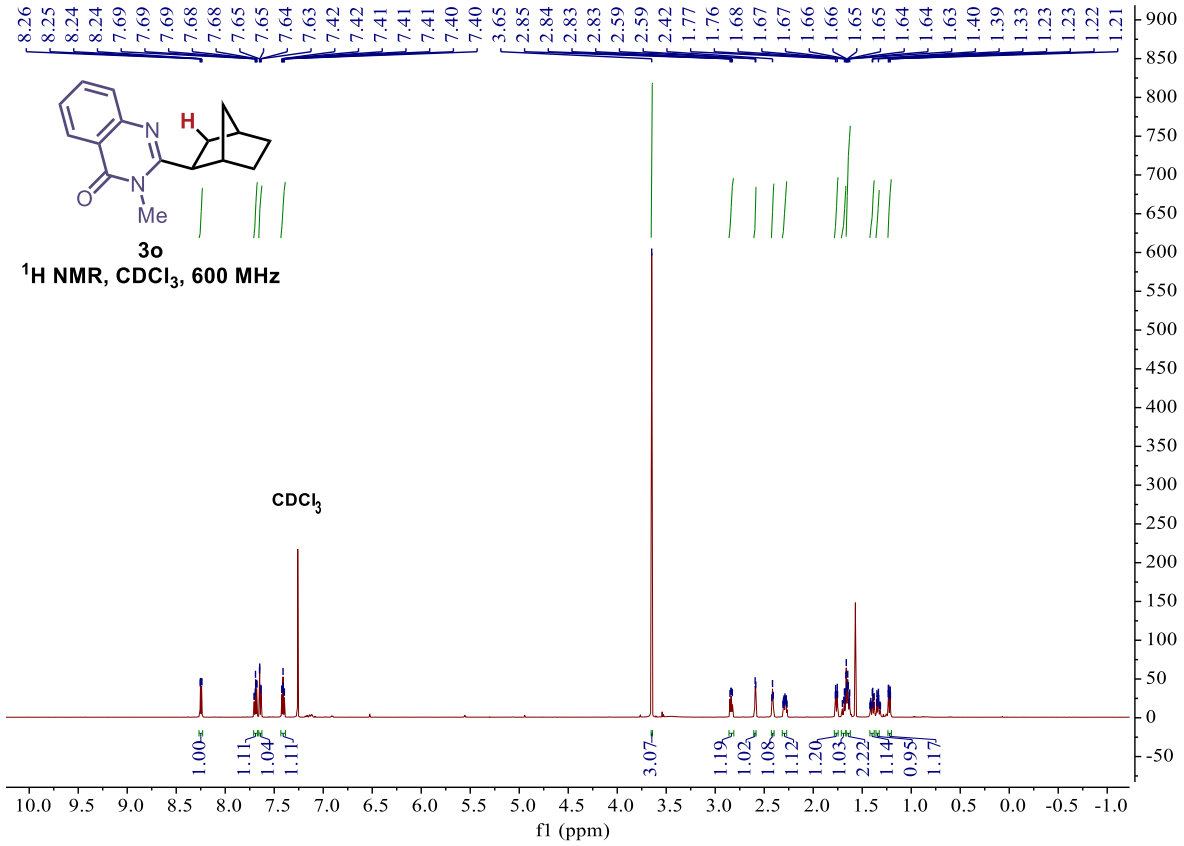
8.26 8.25 8.24 8.24 8.24 7.69 7.69 7.69 7.68 7.68 7.65 7.65 7.64 7.63 7.42 7.42 7.41 7.41 7.41 7.40 7.40
3.65 2.85 2.84 2.83 2.83 2.59 2.59 2.42 1.77 1.76 1.68 1.67 1.67 1.66 1.66 1.65 1.65 1.64 1.64 1.63 1.40 1.39 1.33 1.23 1.23 1.22 1.21
N
H
O
N
Me
3o
1H NMR, CDCl3, 600 MHz
CDCl3
1.00 1.11 1.04 1.11 3.07 1.19 1.02 1.08 1.12 1.20 1.03 2.22 1.14 0.95 1.17
f1 (ppm)

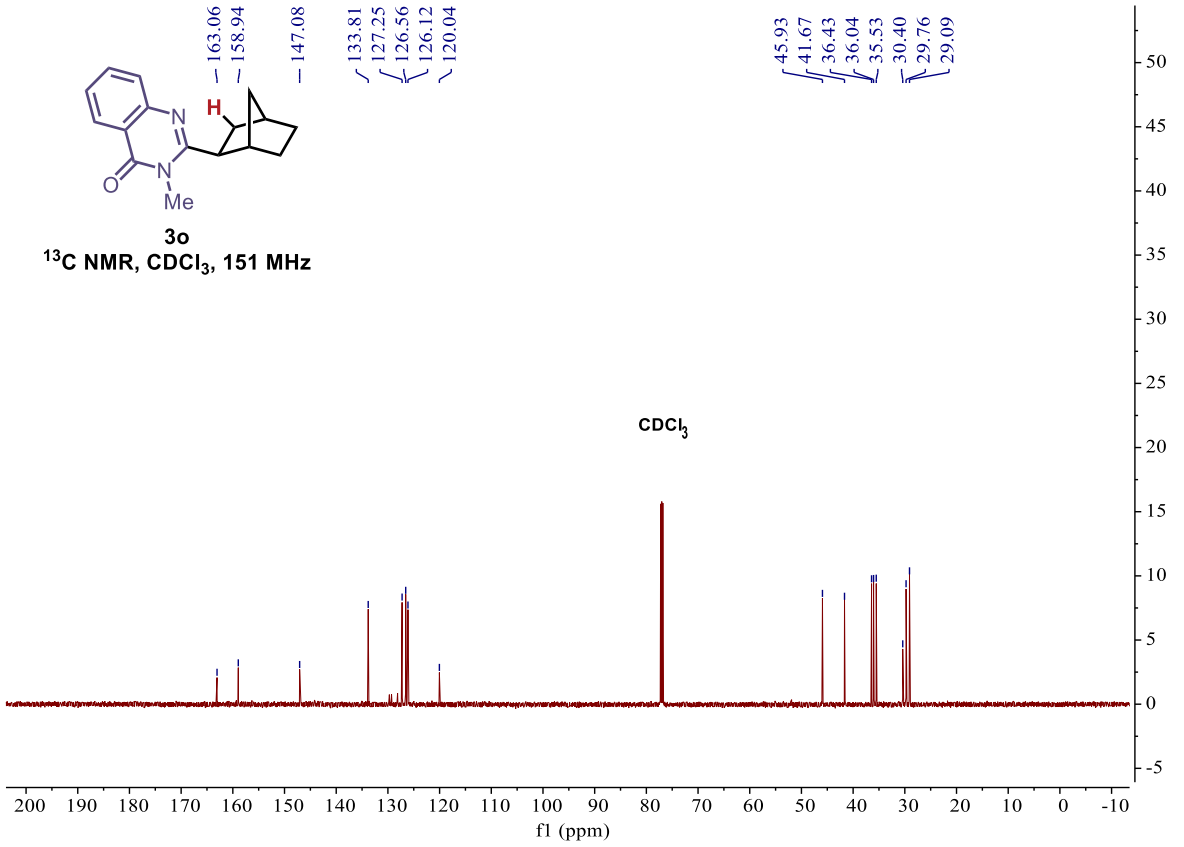
163.06 158.94 147.08 133.81 127.25 126.56 126.12 120.04
45.93 41.67 36.43 36.04 35.53 30.40 29.76 29.09
N
H
O
N
Me
3o
13C NMR, CDCl3, 151 MHz
CDCl3
f1 (ppm)

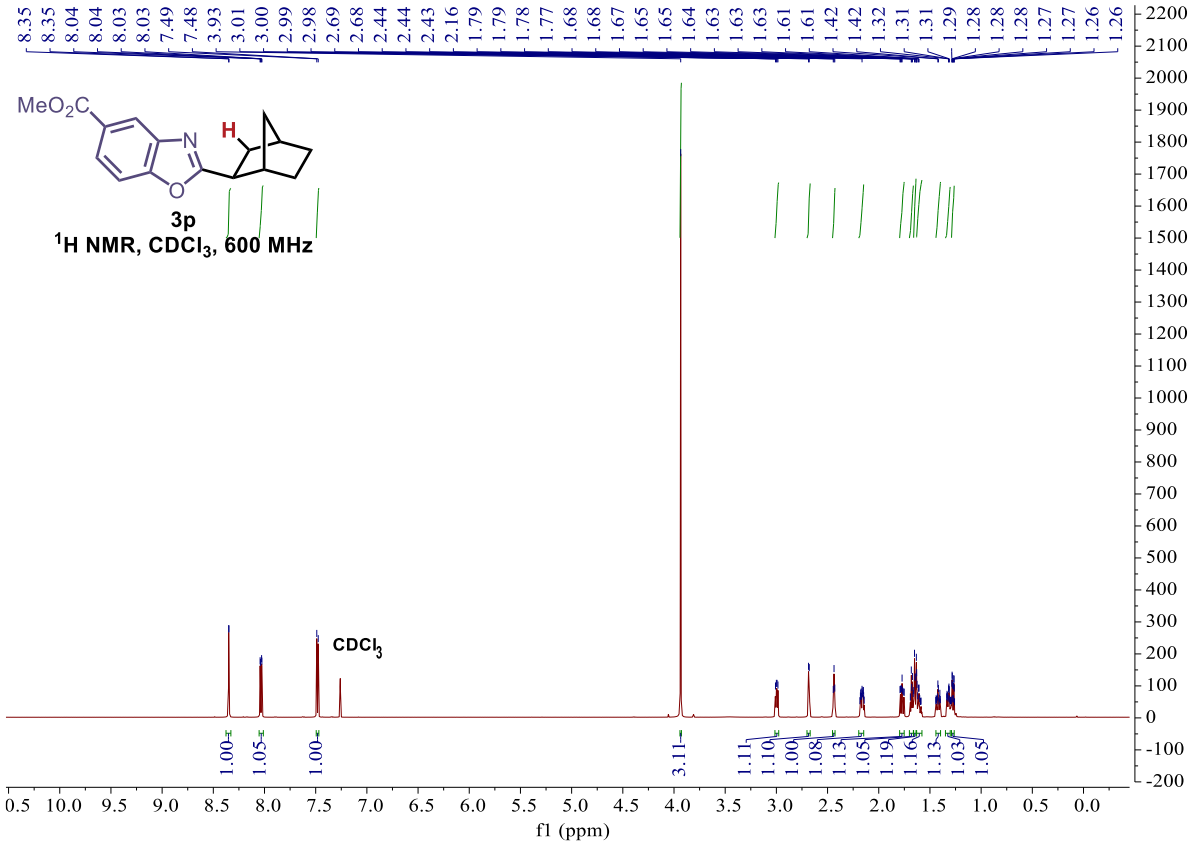
MeO2C
N
O
H
3p
1H NMR, CDCl3, 600 MHz
CDCl3
f1 (ppm)

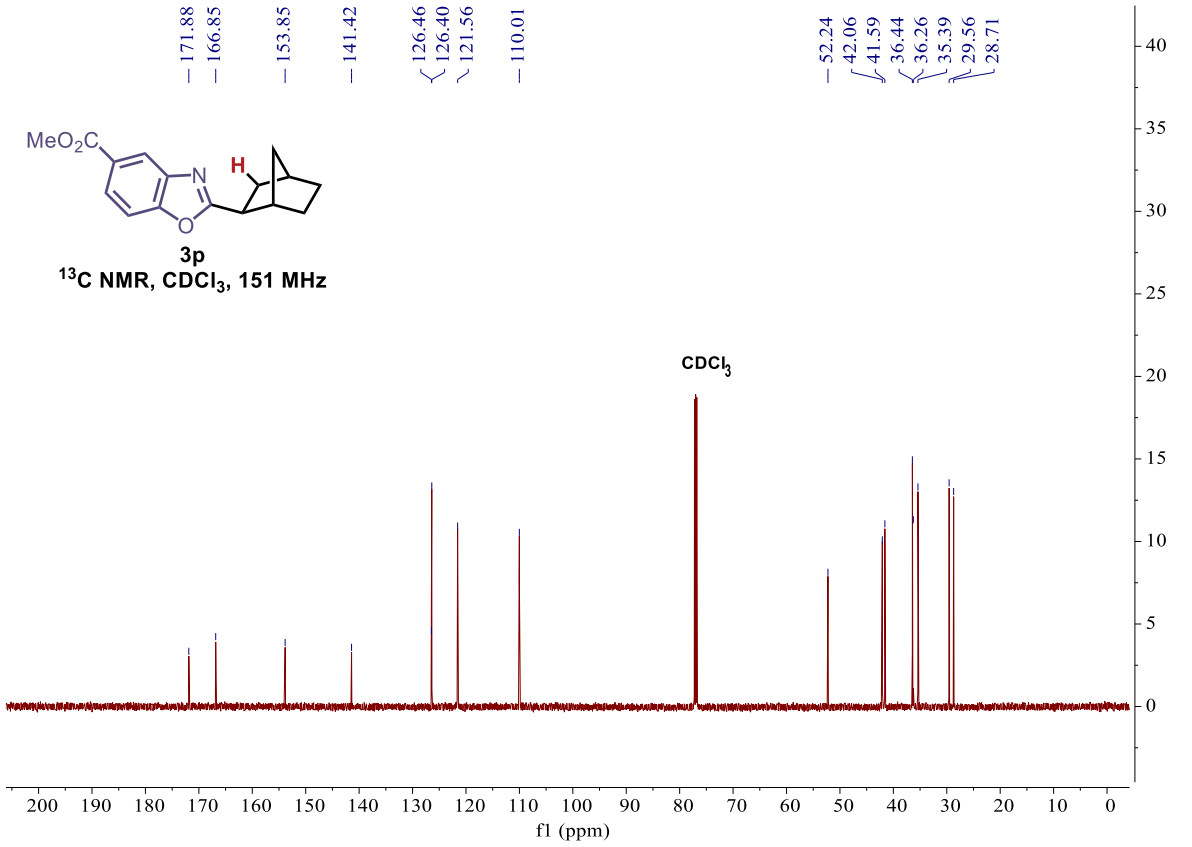
MeO2C
N
O
H
3p
13C NMR, CDCl3, 151 MHz
CDCl3
f1 (ppm)

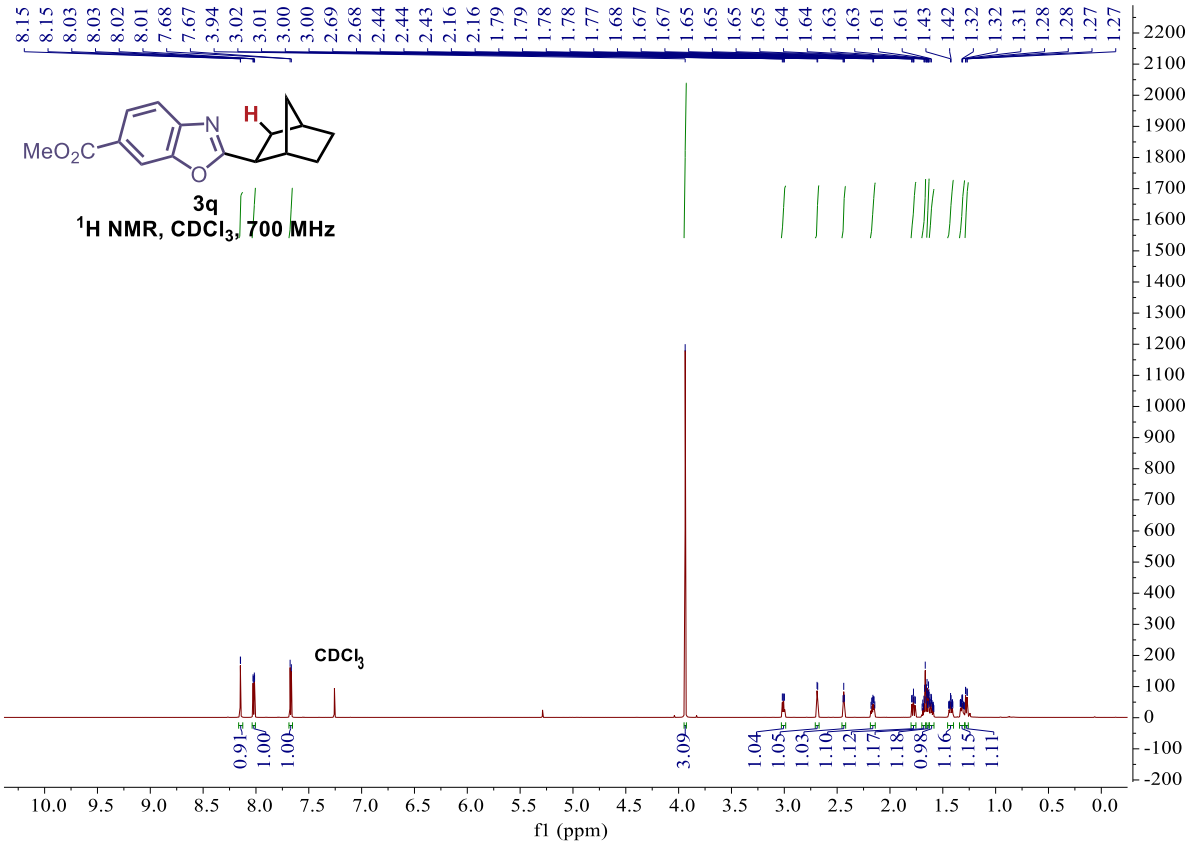
MeO2C
N
O
H
3q
1H NMR, CDCl3, 700 MHz
CDCl3
0.91
1.00
1.00
3.09
1.04
1.05
1.03
1.10
1.12
1.17
1.18
0.98
1.16
1.15
1.11
fl (ppm)

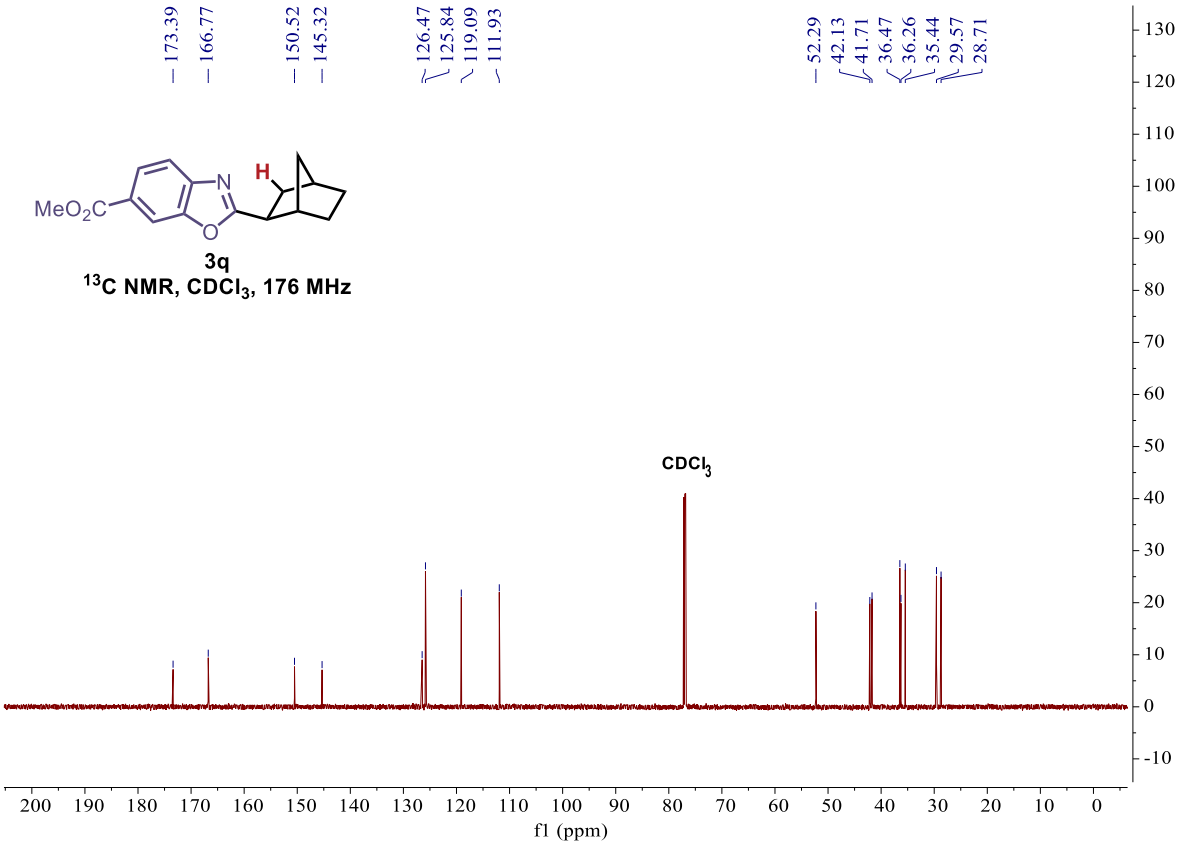
173.39
166.77
150.52
145.32
126.47
125.84
119.09
111.93
52.29
42.13
41.71
36.47
36.26
35.44
29.57
28.71
MeO2C
N
O
H
3q
13C NMR, CDCl3, 176 MHz
CDCl3
fl (ppm)

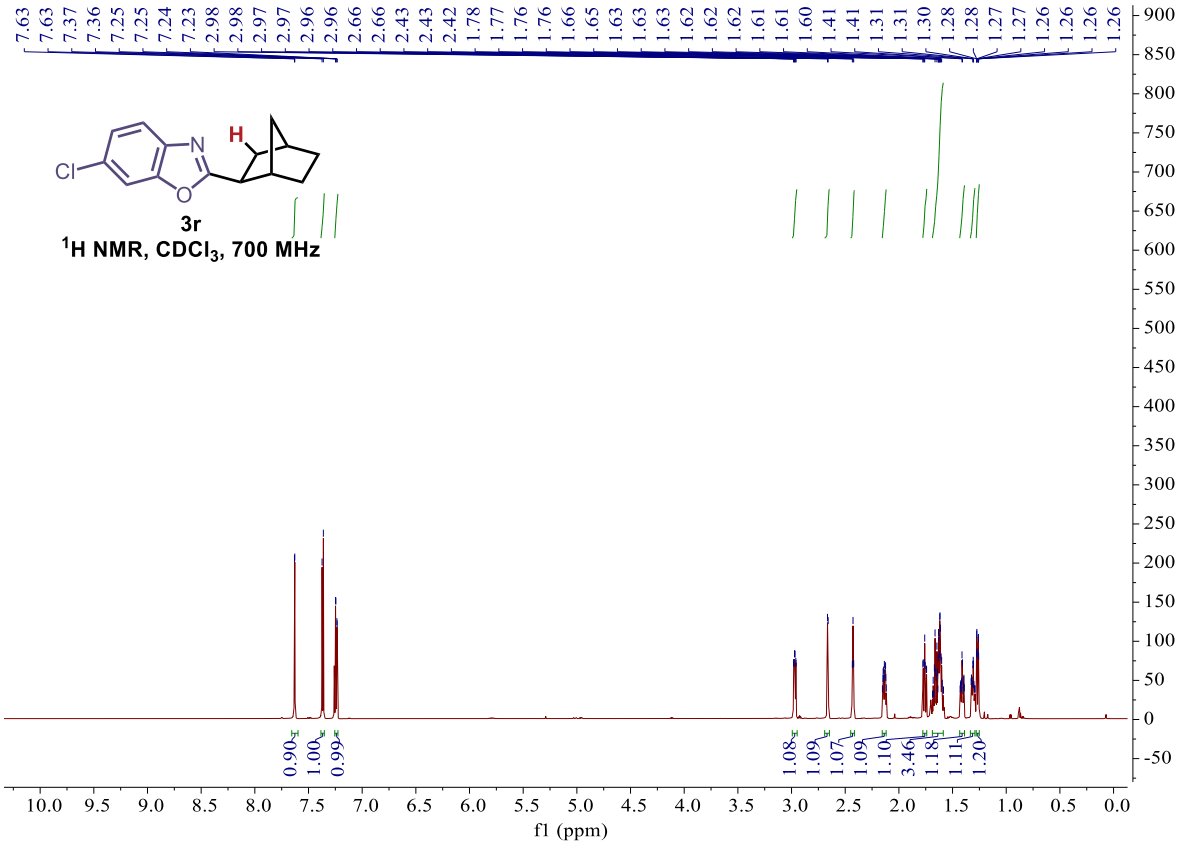
3r
^{1}H NMR, CDCl$_3$, 700 MHz
f1 (ppm)

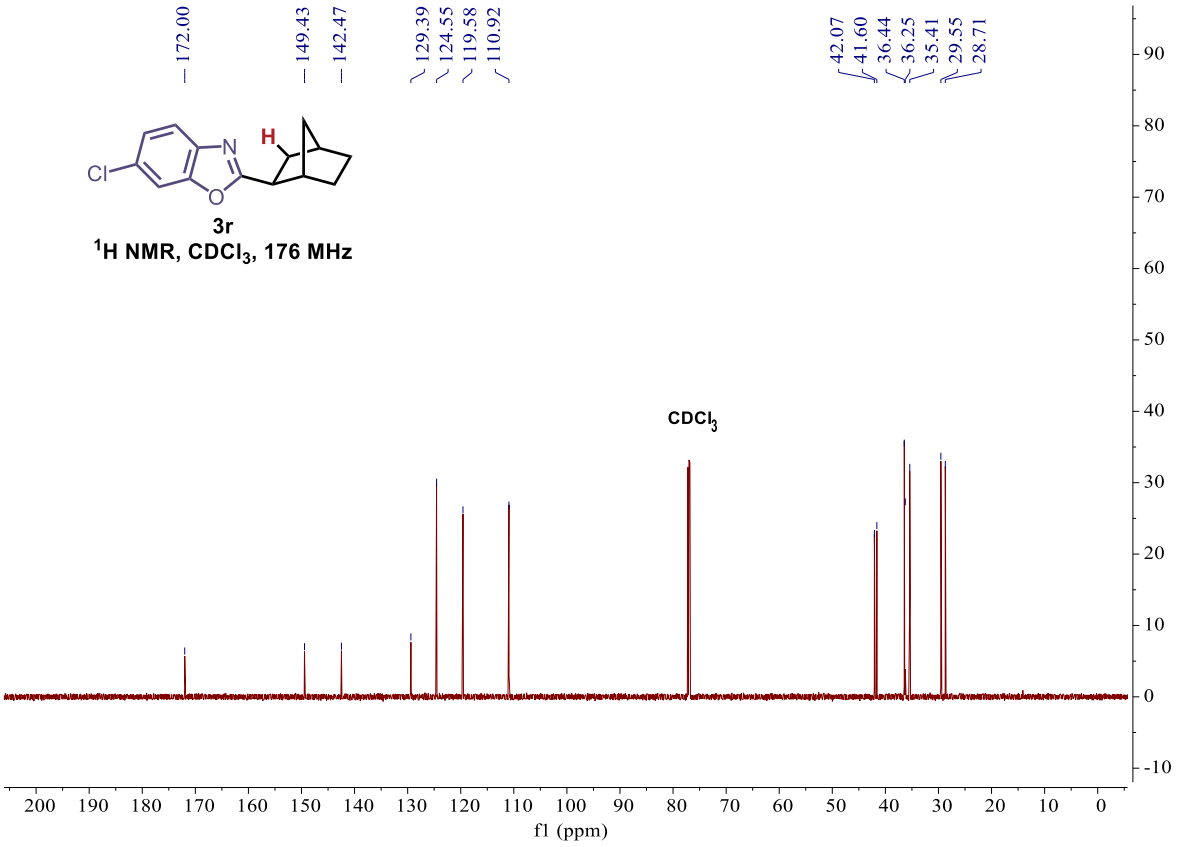
3r
^{1}H NMR, CDCl$_3$, 176 MHz
CDCl$_3$
f1 (ppm)

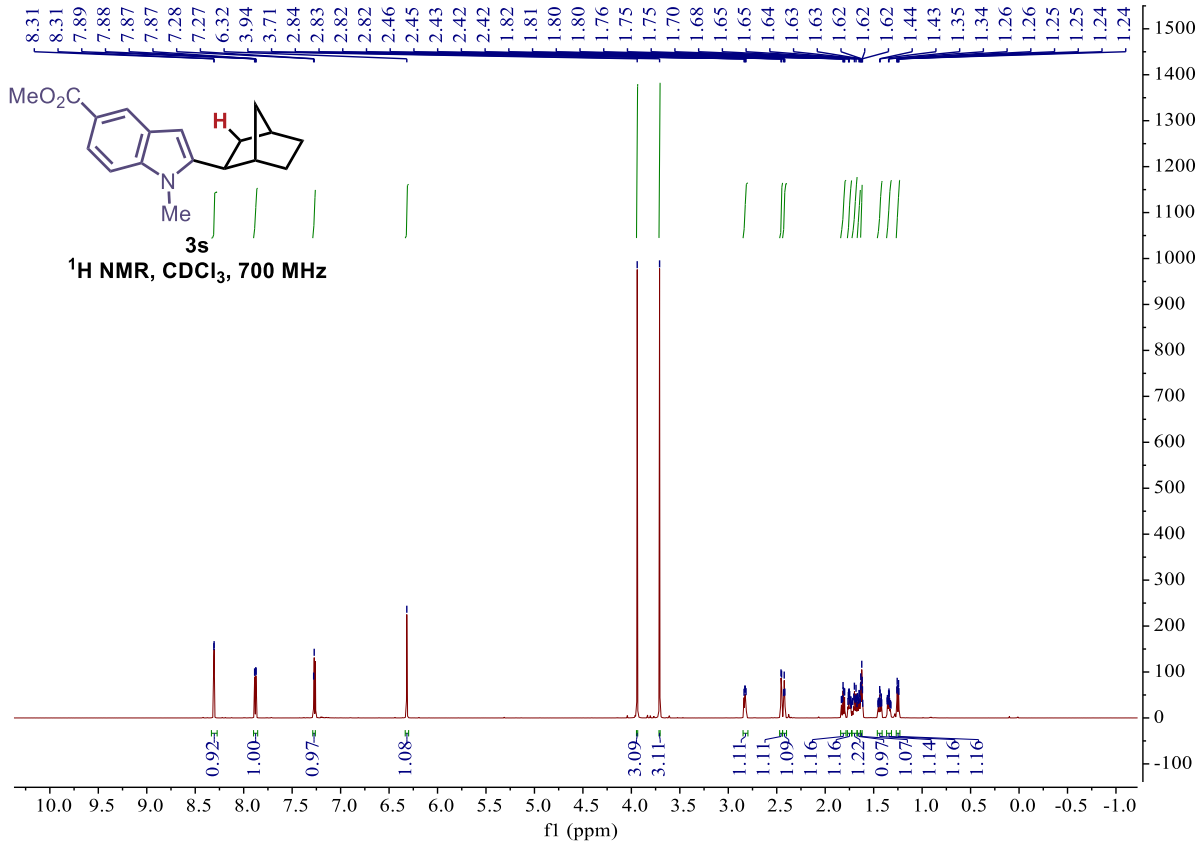

3s

^{1}H NMR, $CDCl_3$, 700 MHz

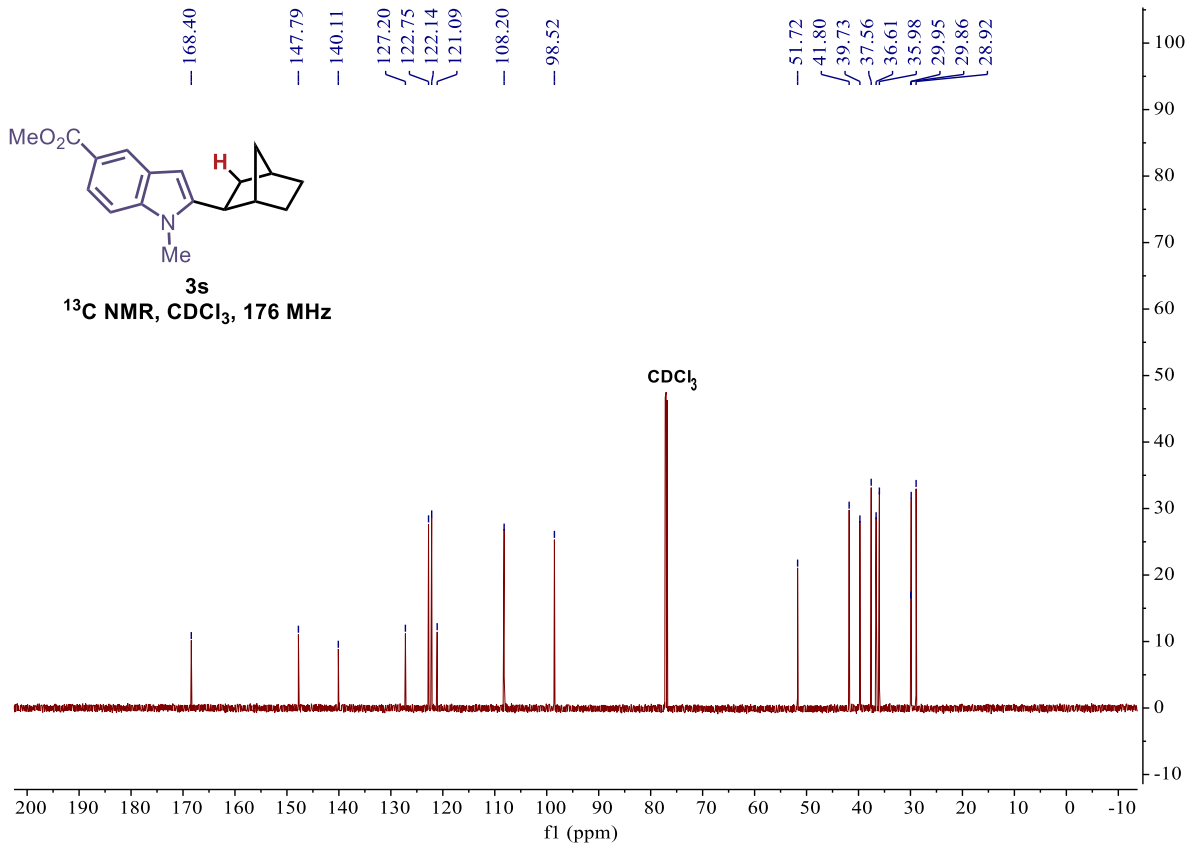

3s

^{13}C NMR, $CDCl_3$, 176 MHz

$CDCl_3$

f1 (ppm)

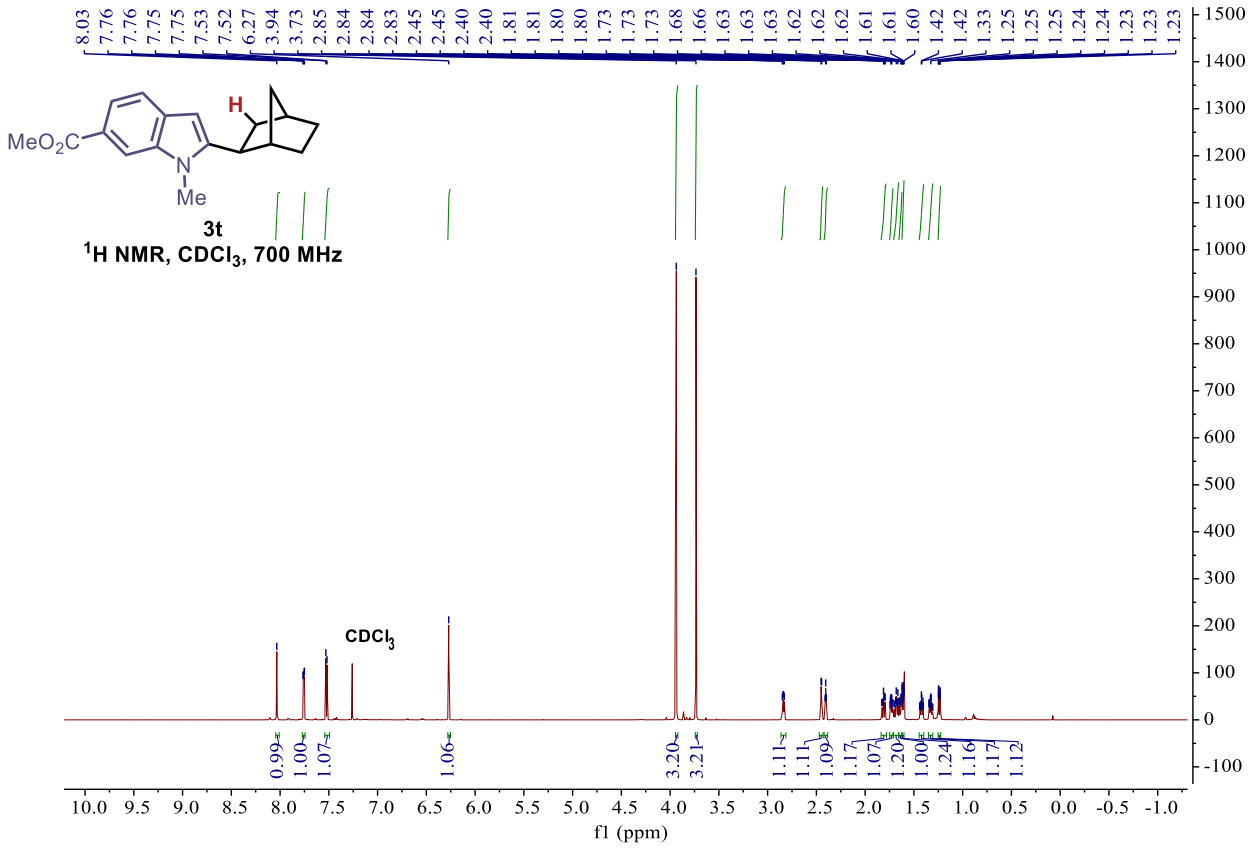
MeO2C
H
N
Me
3t
1H NMR, CDCl3, 700 MHz
CDCl3
f1 (ppm)

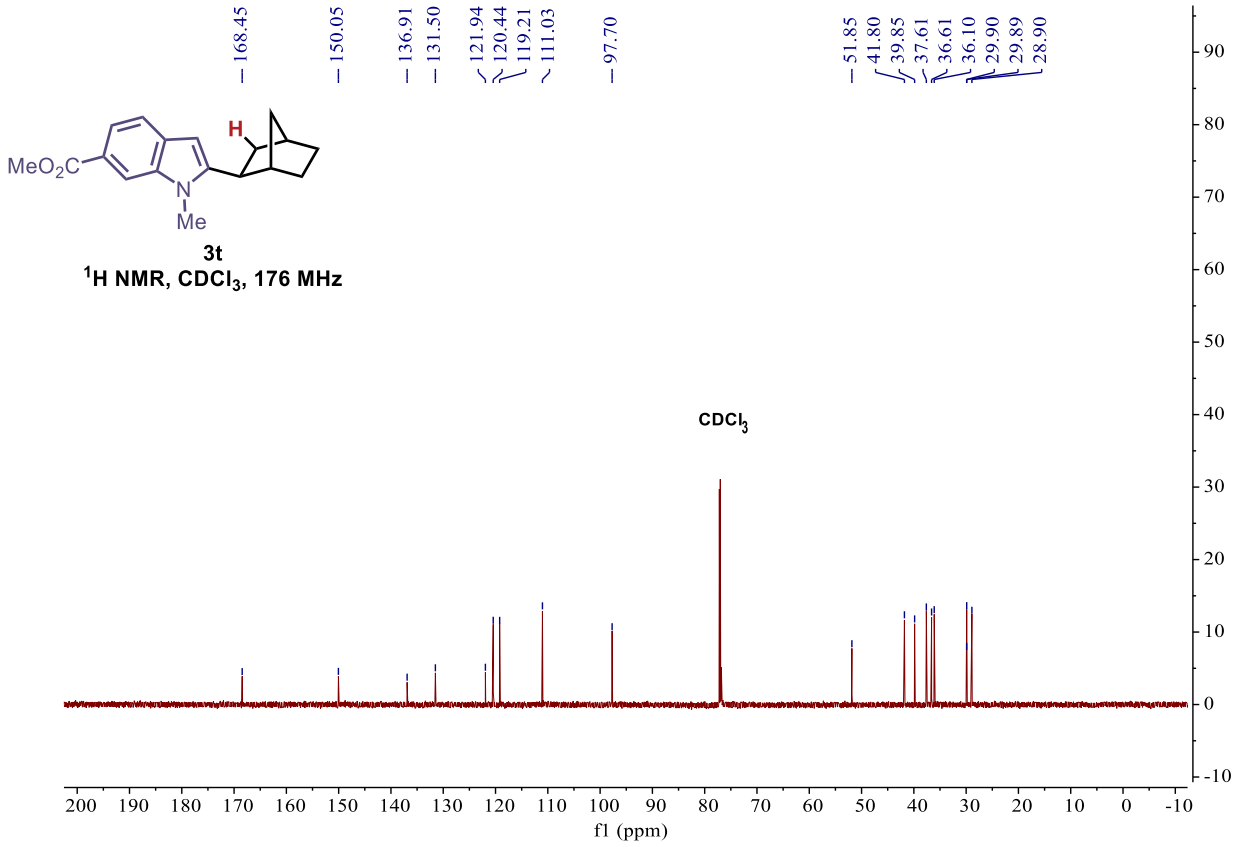
MeO2C
H
N
Me
3t
1H NMR, CDCl3, 176 MHz
CDCl3
f1 (ppm)

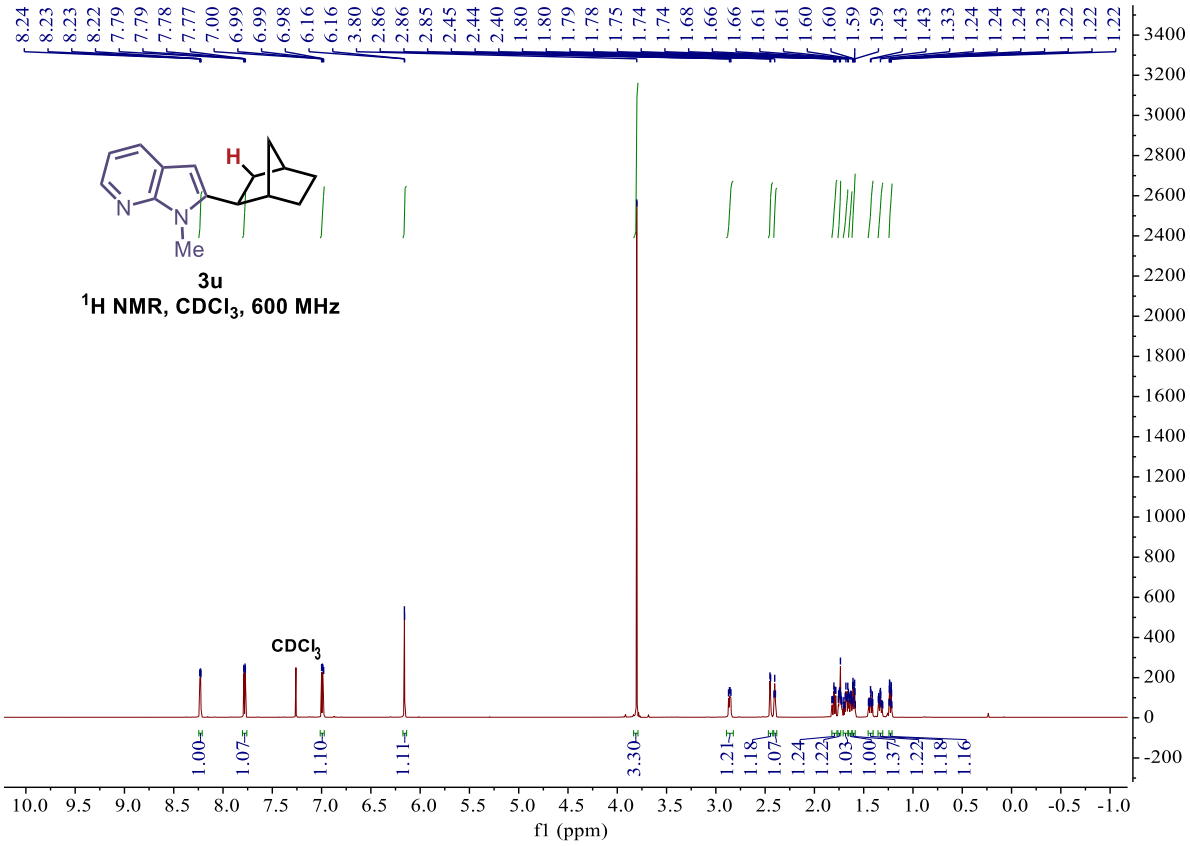

3u

^{1}H NMR, $CDCl_3$, 600 MHz

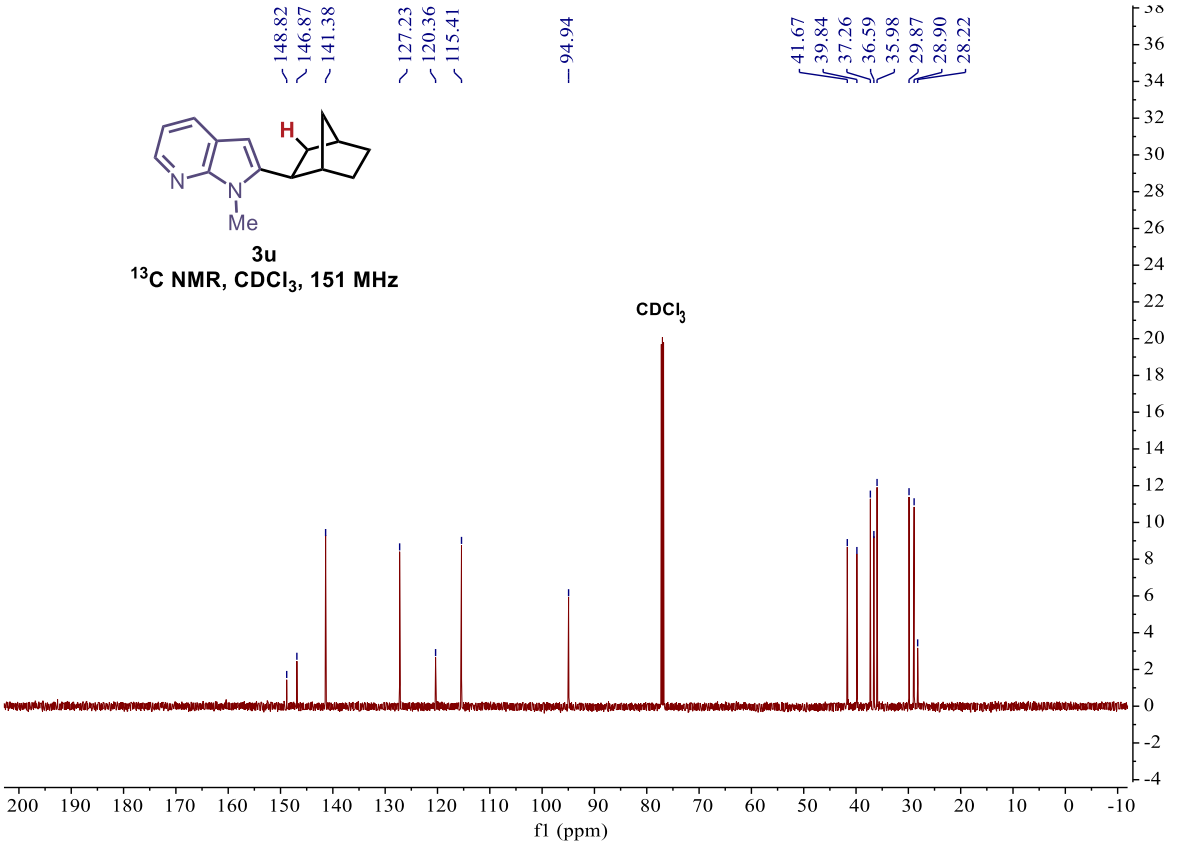

3u

^{13}C NMR, $CDCl_3$, 151 MHz

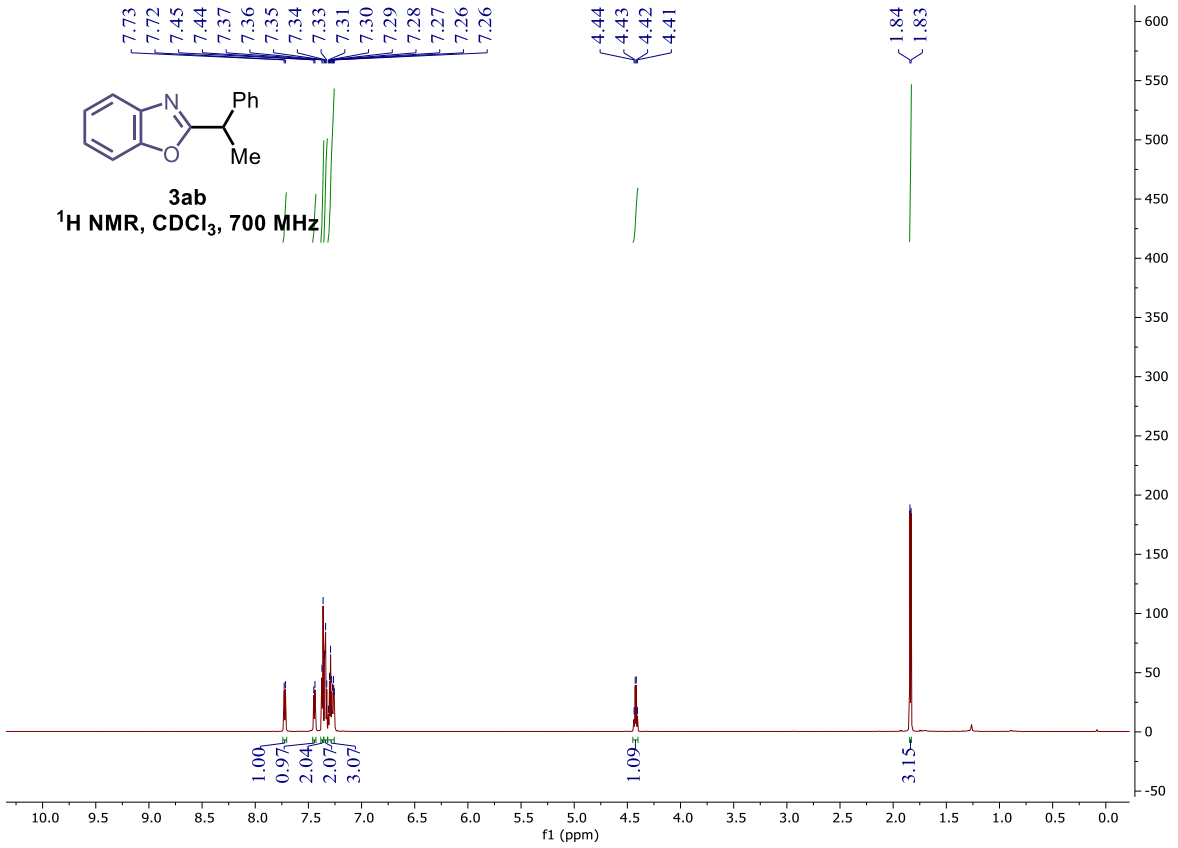

3ab
^{1}H NMR, $CDCl_3$, 700 MHz

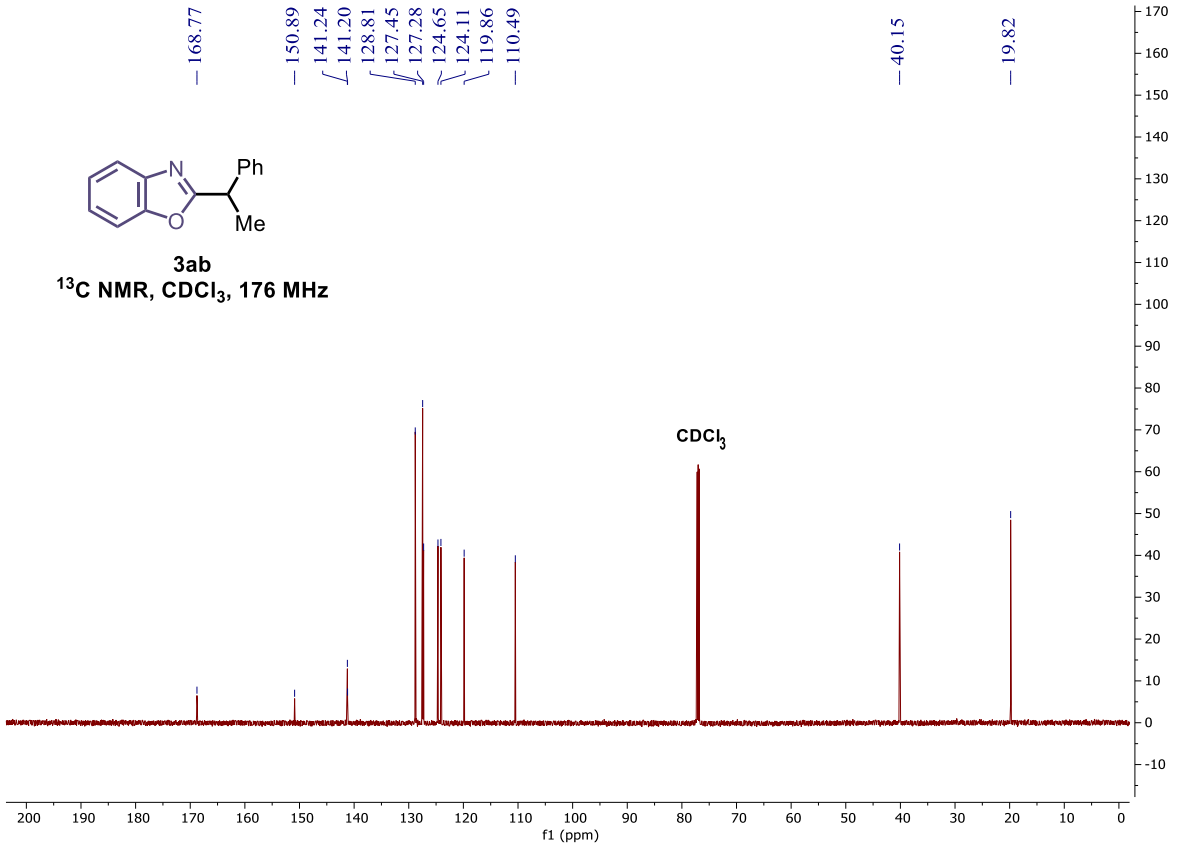

3ab
^{13}C NMR, $CDCl_3$, 176 MHz

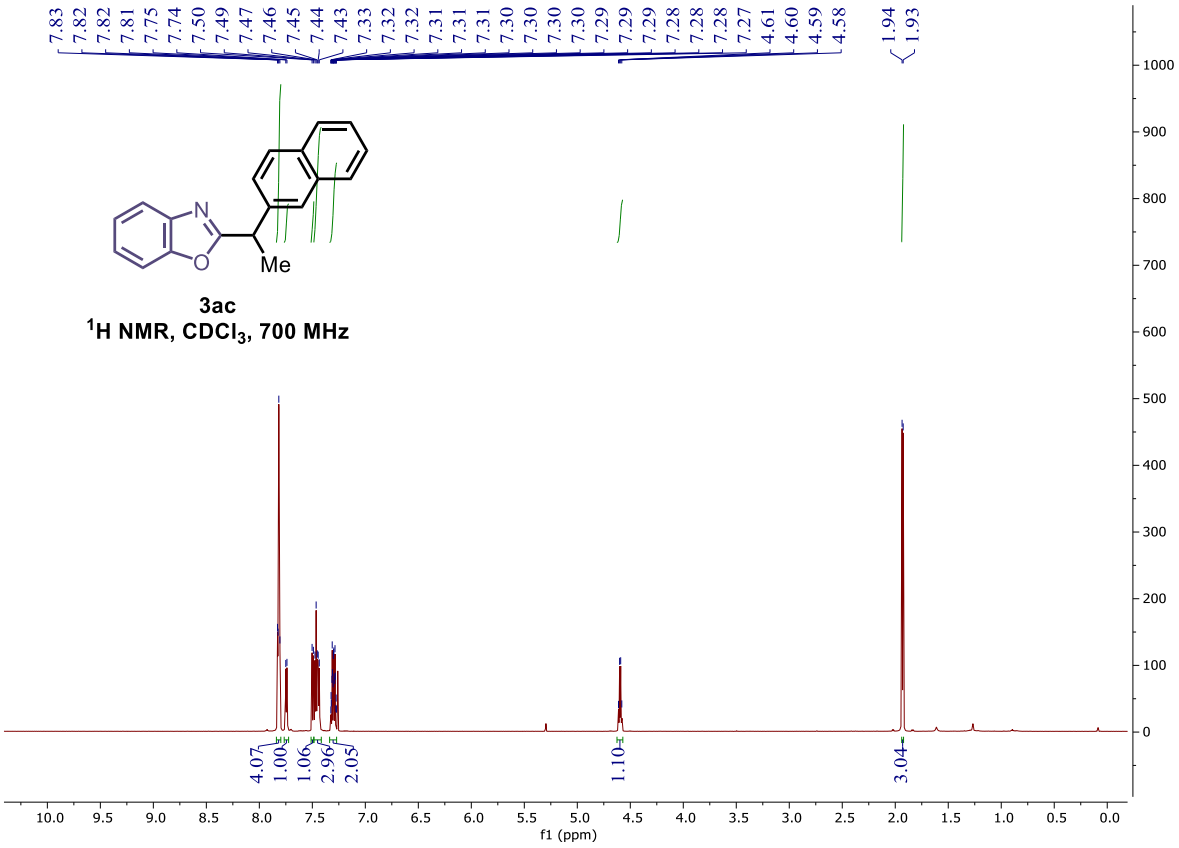

3ac
^{1}H NMR, $CDCl_3$, 700 MHz

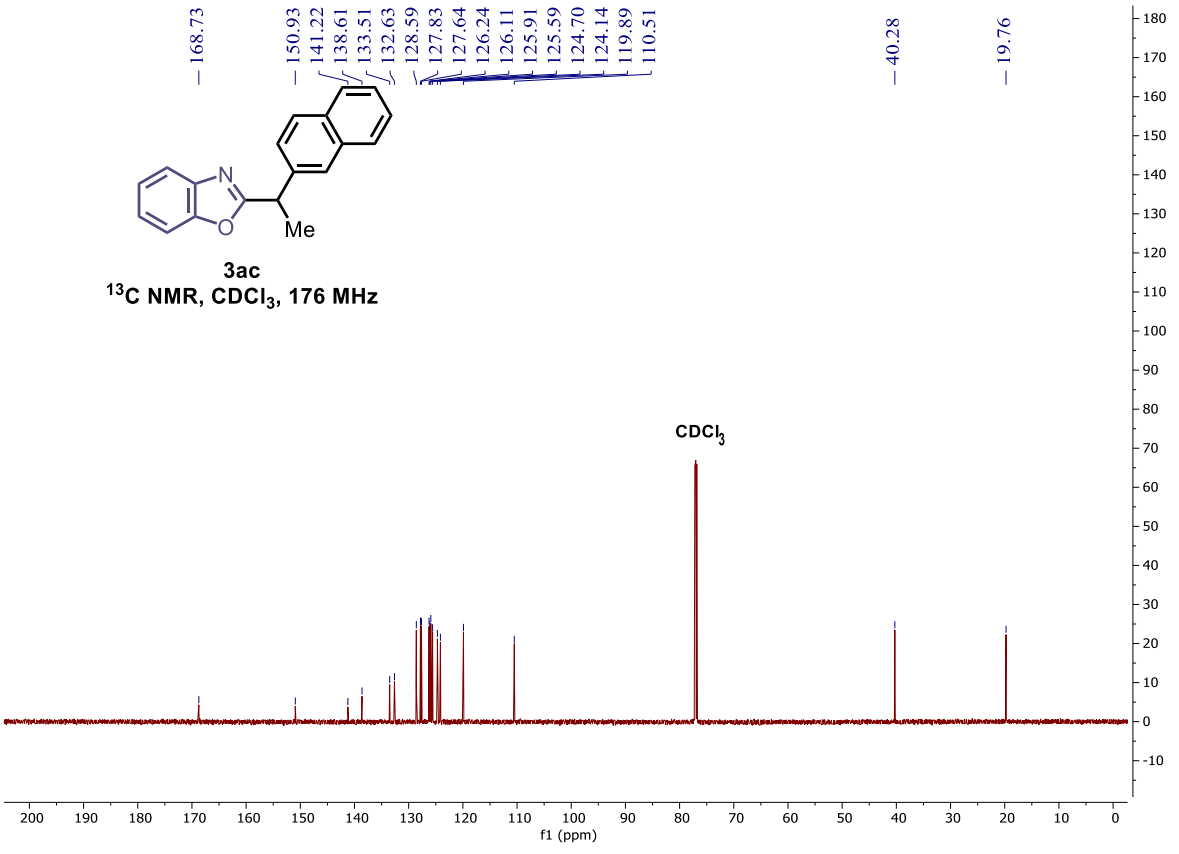

3ac
^{13}C NMR, $CDCl_3$, 176 MHz

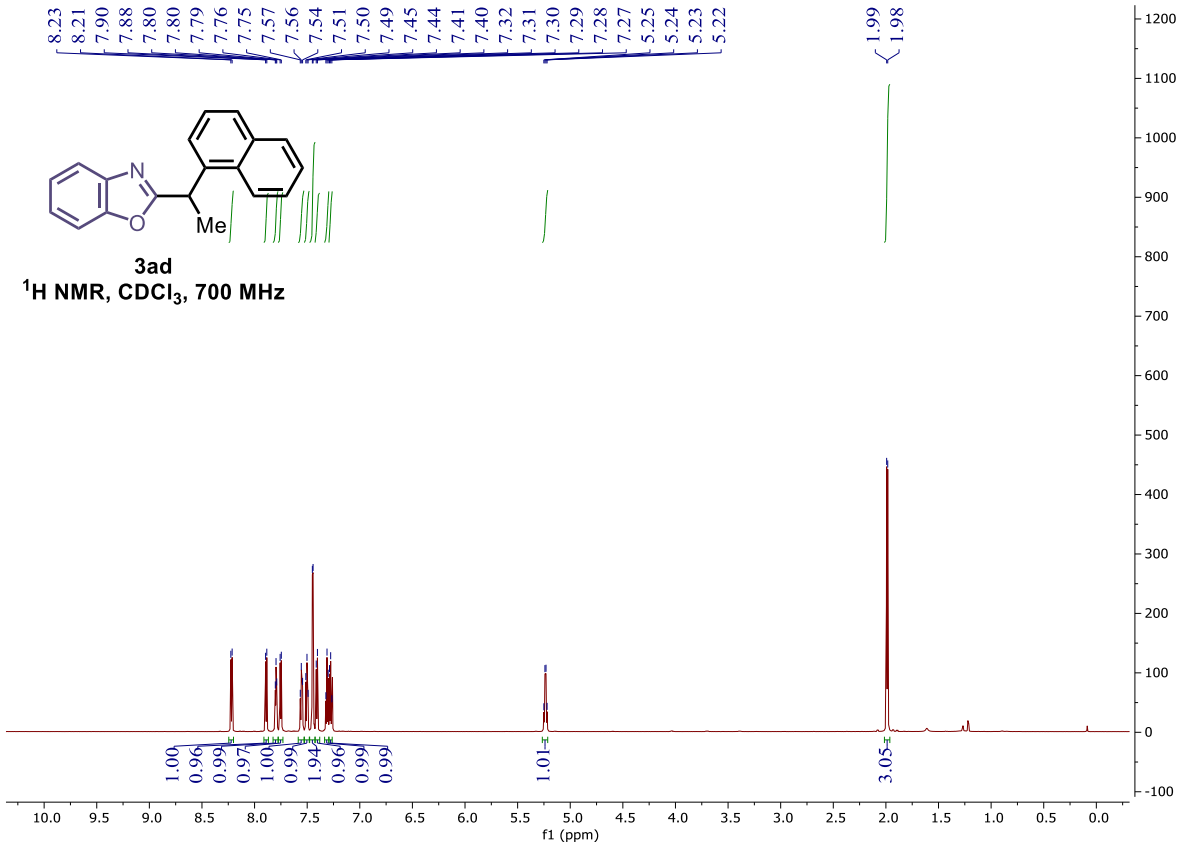

3ad

^{1}H NMR, $CDCl_3$, 700 MHz

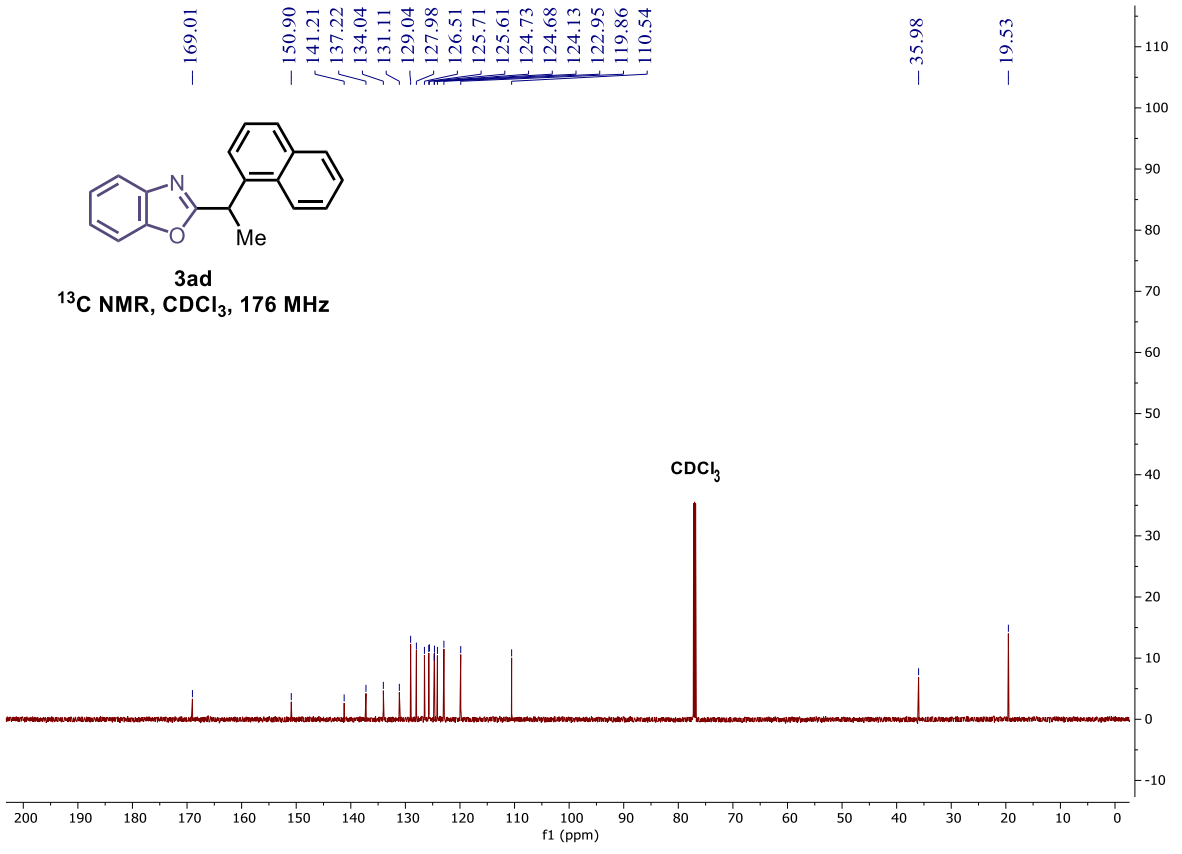

3ad

^{13}C NMR, $CDCl_3$, 176 MHz

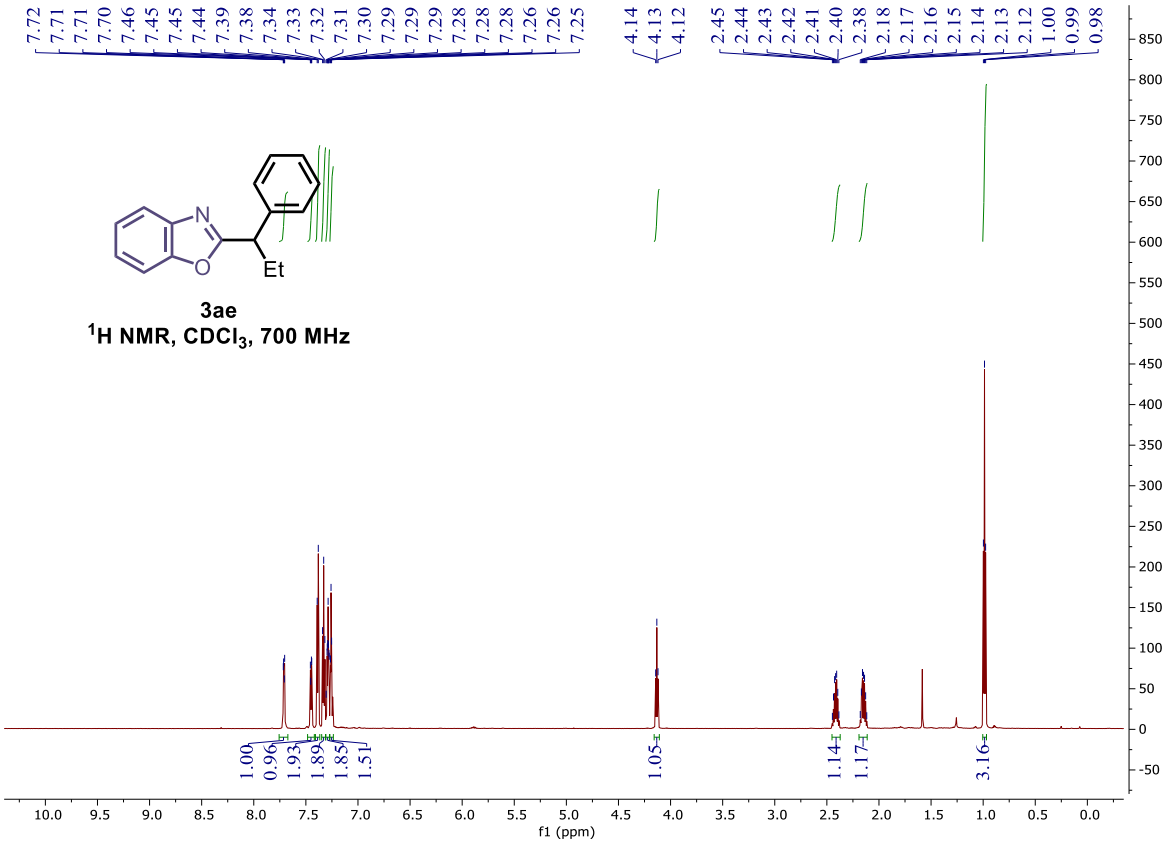

3ae
^{1}H NMR, $CDCl_3$, 700 MHz

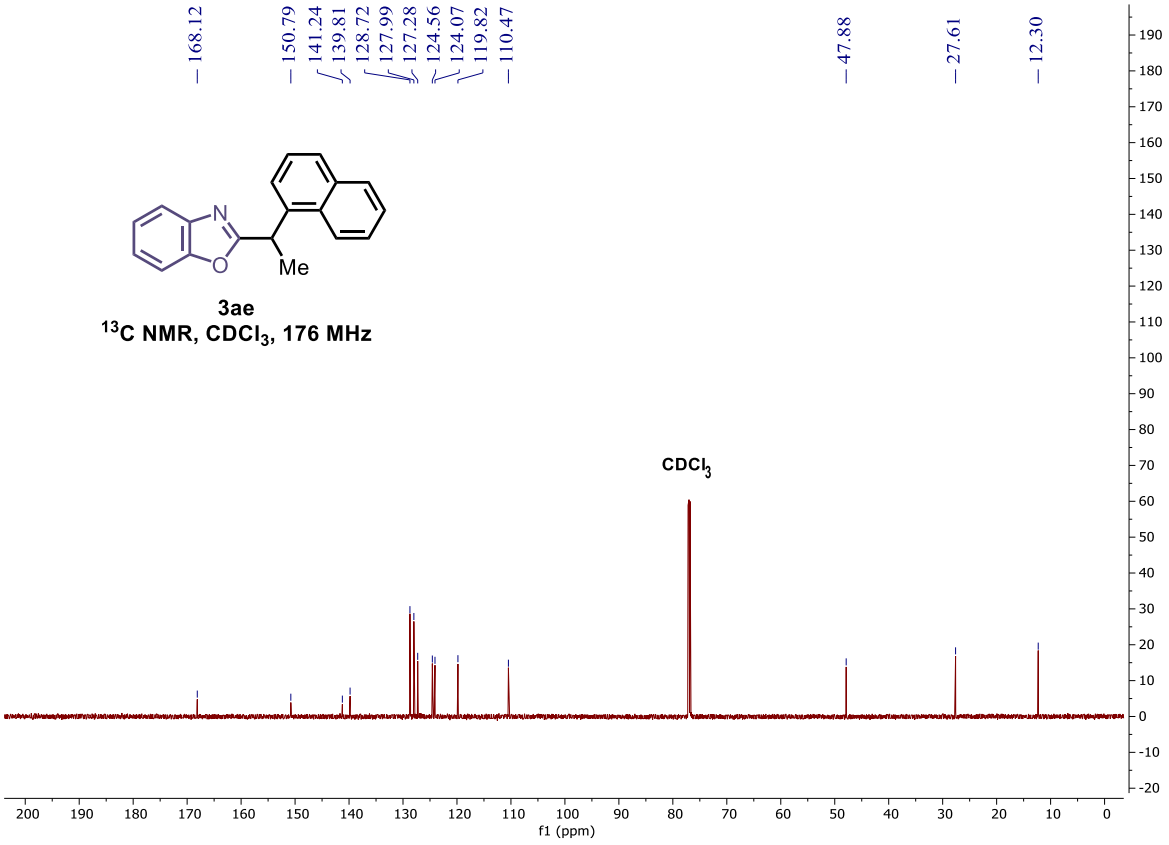

3ae
^{13}C NMR, $CDCl_3$, 176 MHz

8.6.2 Chapter 3

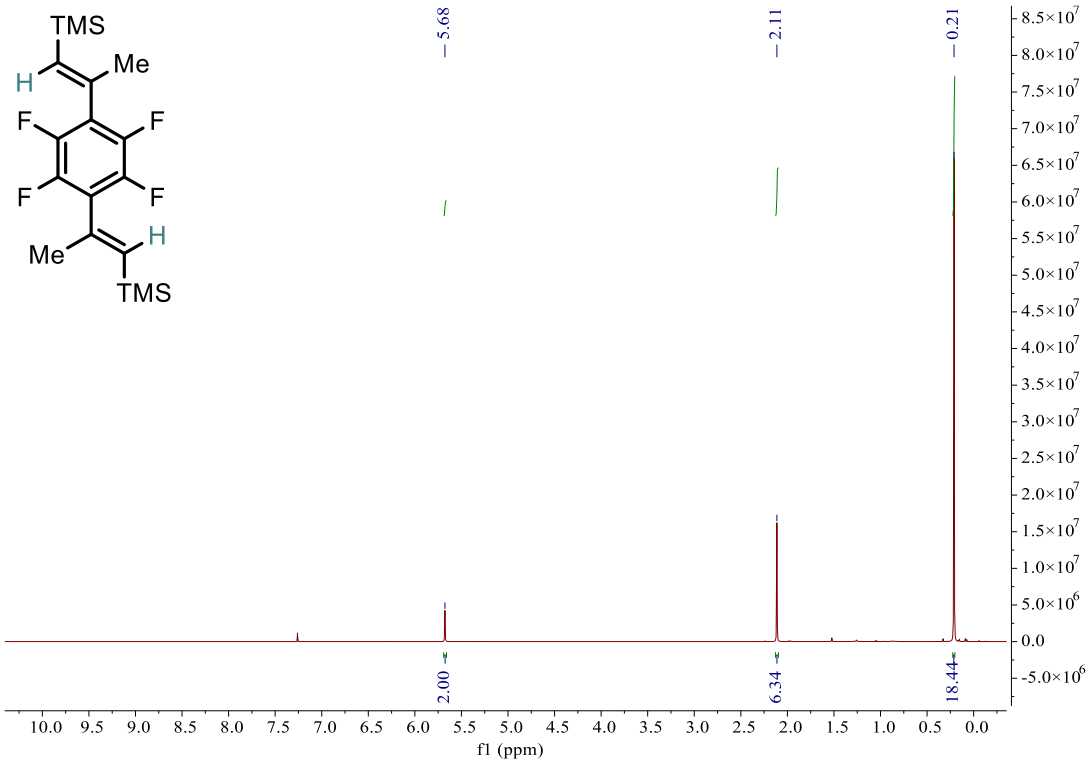

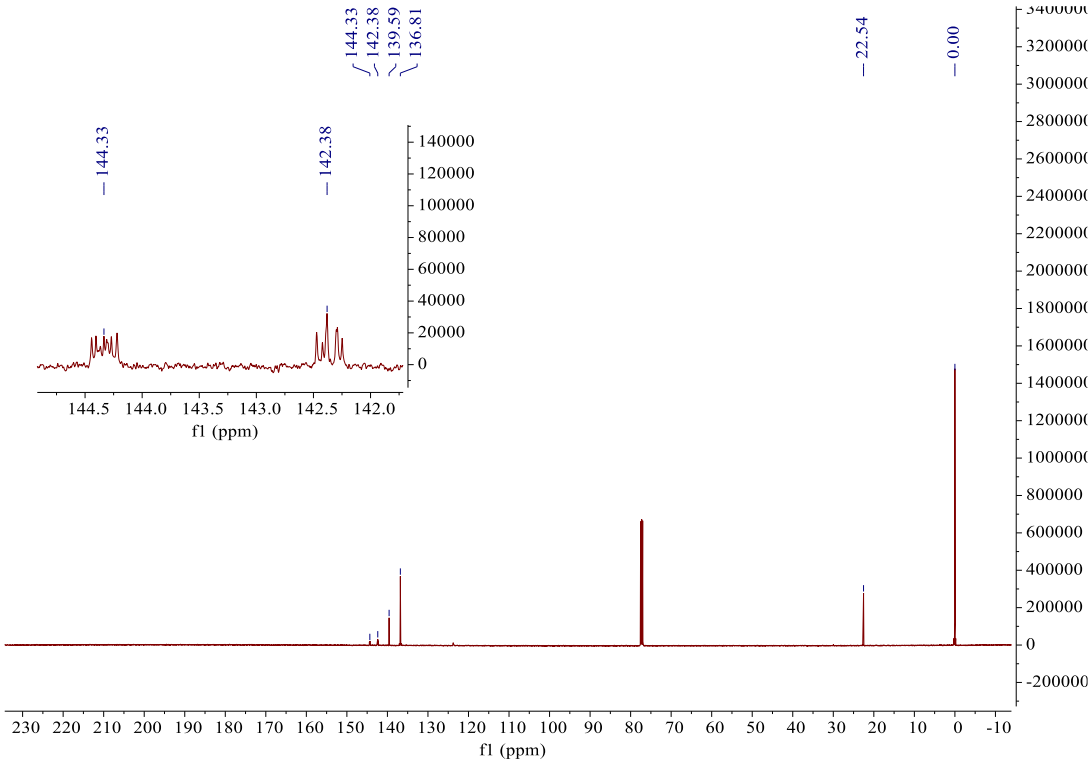

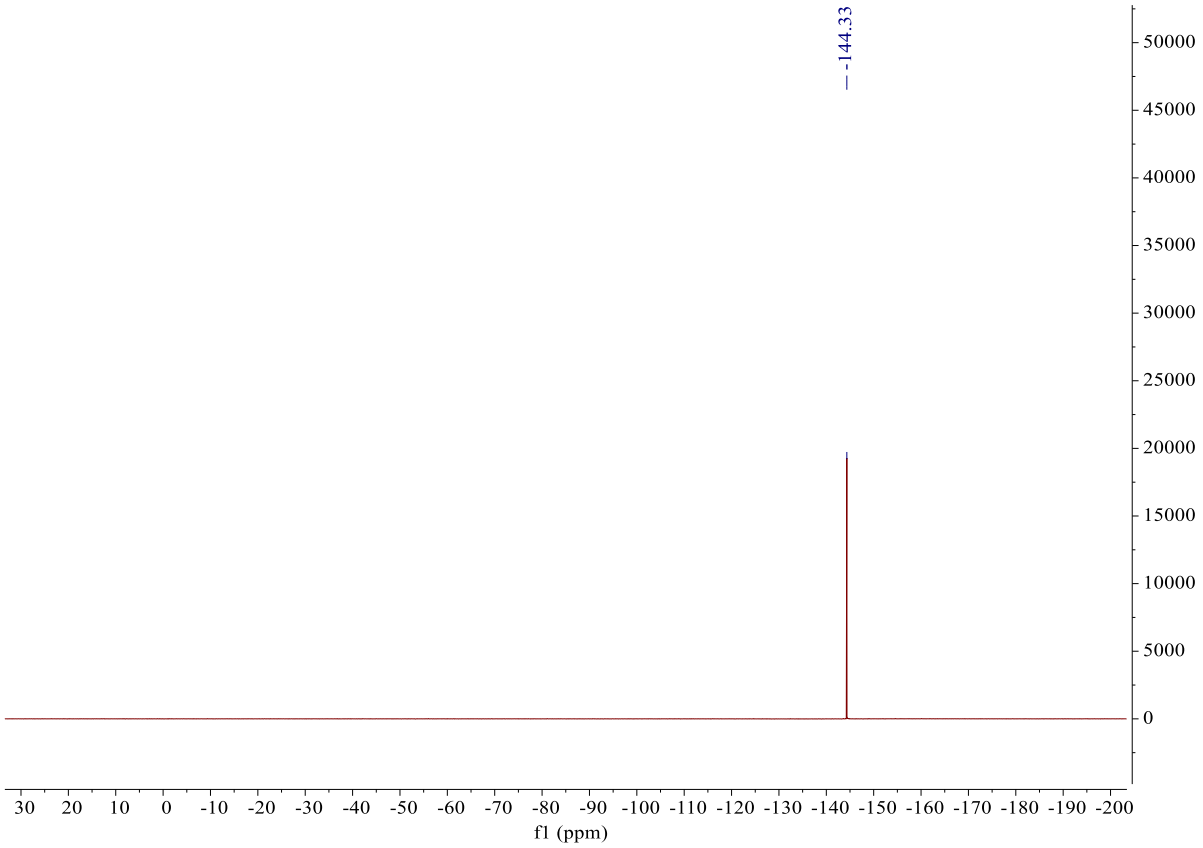
-144.33
50000
45000
40000
35000
30000
25000
20000
15000
10000
5000
0
30 20 10 0 -10 -20 -30 -40 -50 -60 -70 -80 -90 -100 -110 -120 -130 -140 -150 -160 -170 -180 -190 -200
f1 (ppm)

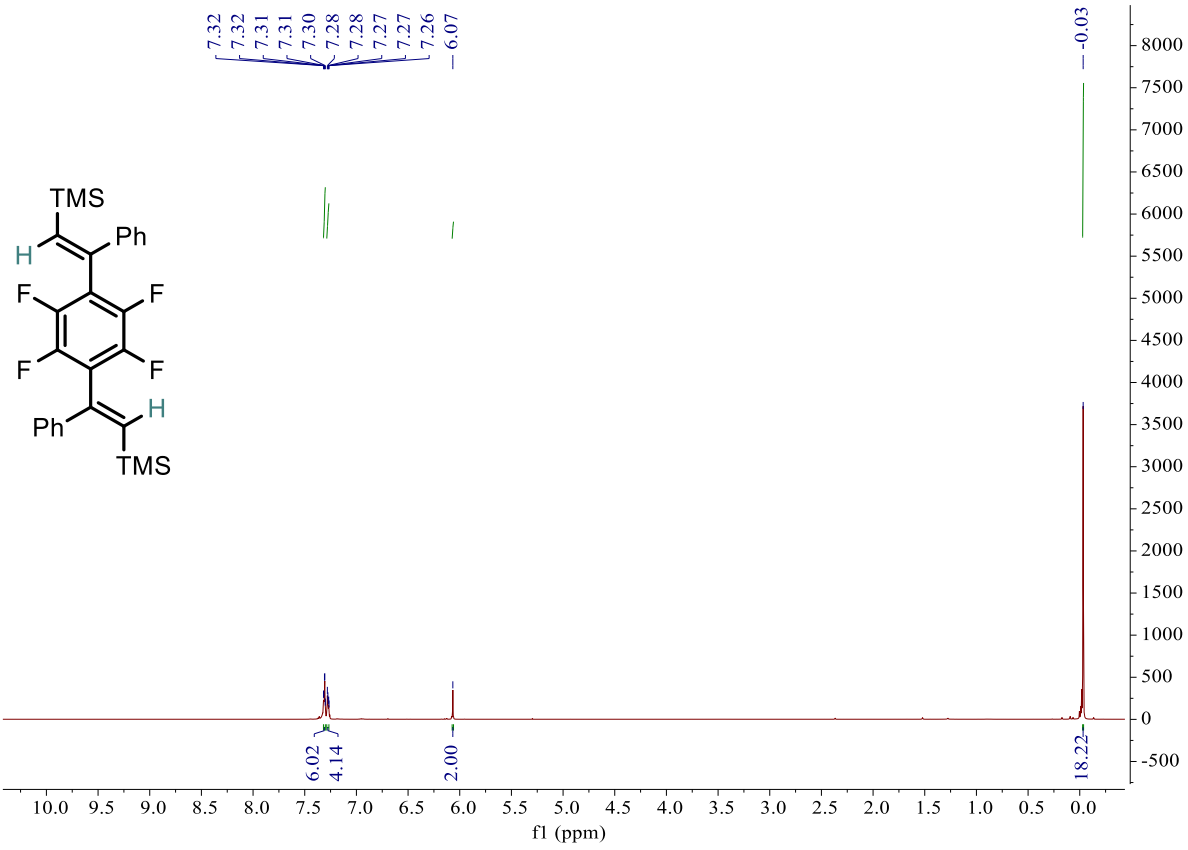
7.32
7.32
7.31
7.31
7.30
7.28
7.28
7.27
7.27
7.26
6.07
-0.03
TMS
Ph
H
F
F
F
F
Ph
H
TMS
6.02
4.14
2.00
18.22
fl (ppm)

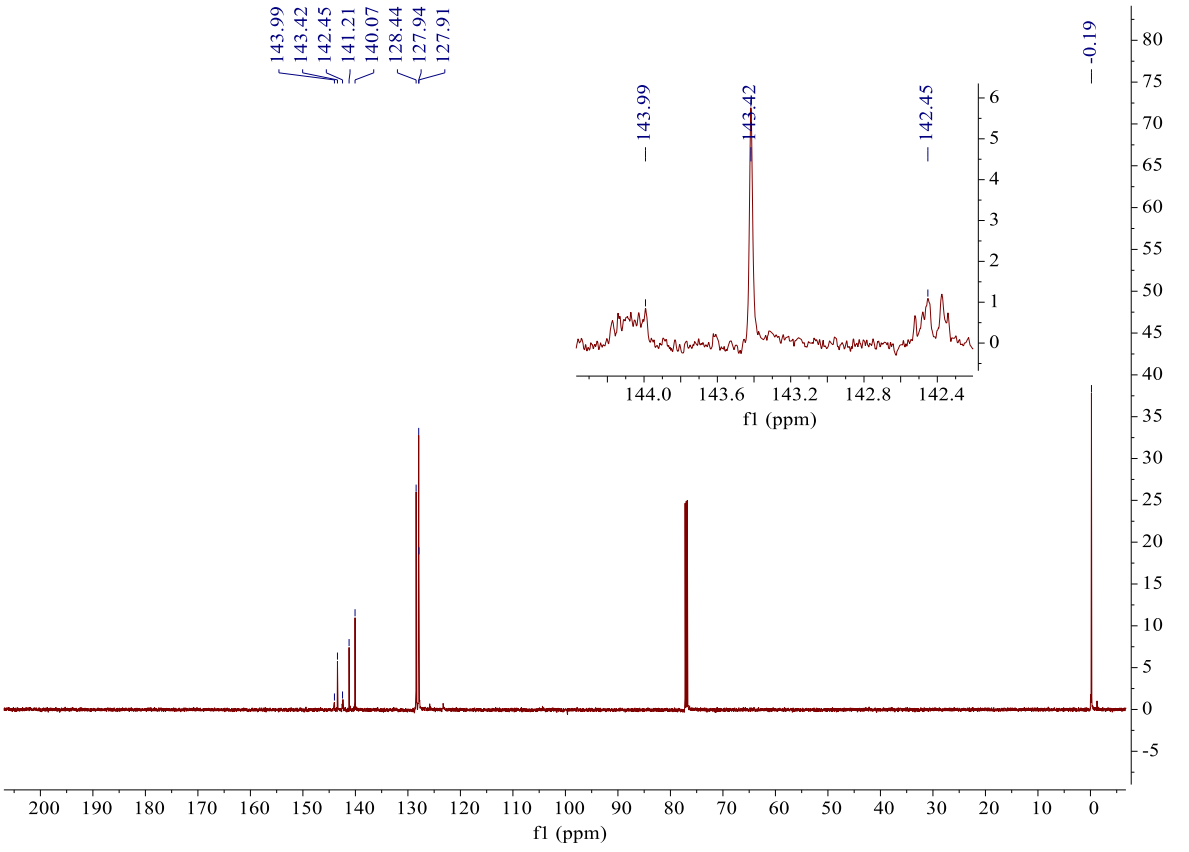
143.99
143.42
142.45
141.21
140.07
128.44
127.94
127.91
-0.19
143.99
143.42
142.45
fl (ppm)

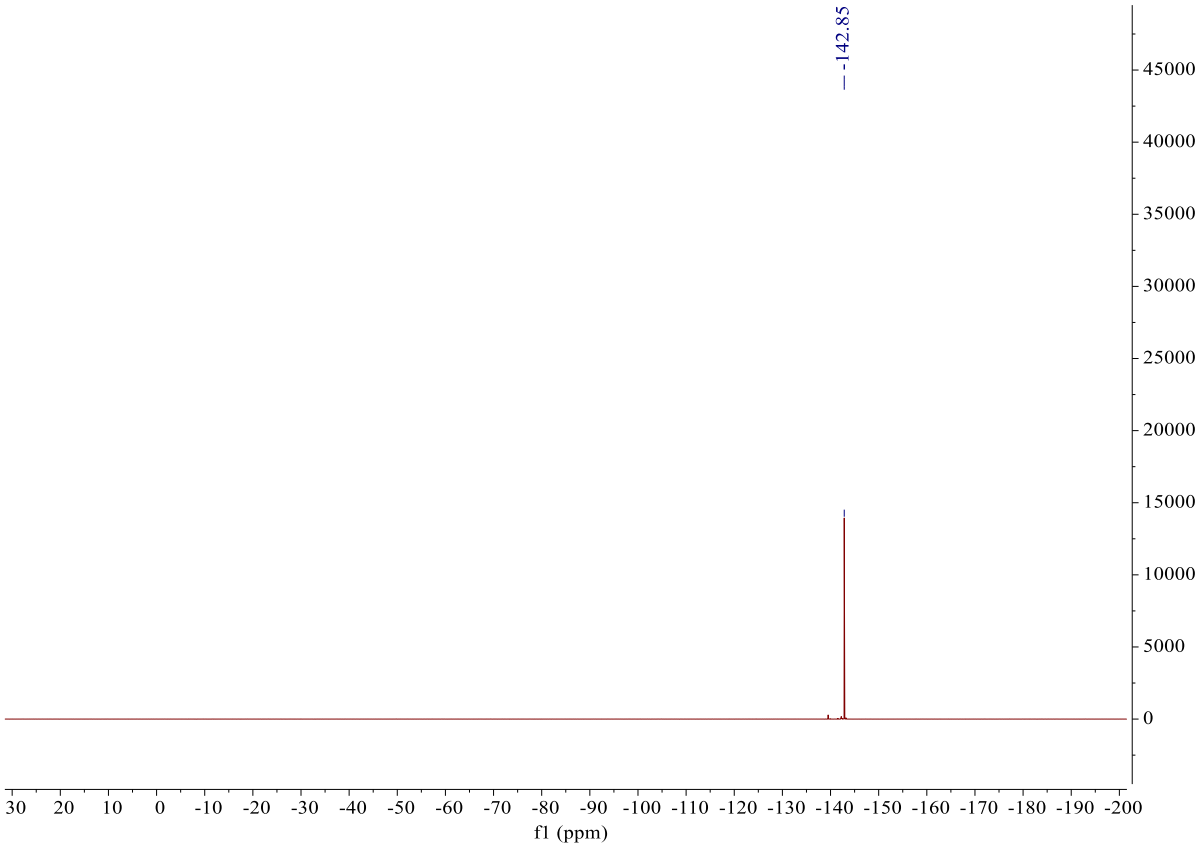
-142.85
45000
40000
35000
30000
25000
20000
15000
10000
5000
0
30 20 10 0 -10 -20 -30 -40 -50 -60 -70 -80 -90 -100 -110 -120 -130 -140 -150 -160 -170 -180 -190 -200
f1 (ppm)

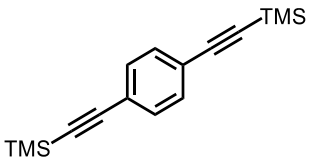
TMS
TMS

BB1

7.37
0.23
4.00
18.20
f1 (ppm)

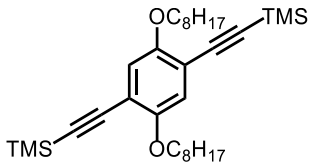
OC8H17
TMS
TMS
OC8H17

BB2

7.06
3.94
3.92
3.91
1.82
1.80
1.78
1.76
1.75
1.50
1.48
1.46
1.44
1.42
1.32
1.31
1.30
1.30
1.29
1.28
1.27
1.26
0.89
0.87
0.86
2.01
4.00
4.03
4.03
15.92
5.87
f1 (ppm)

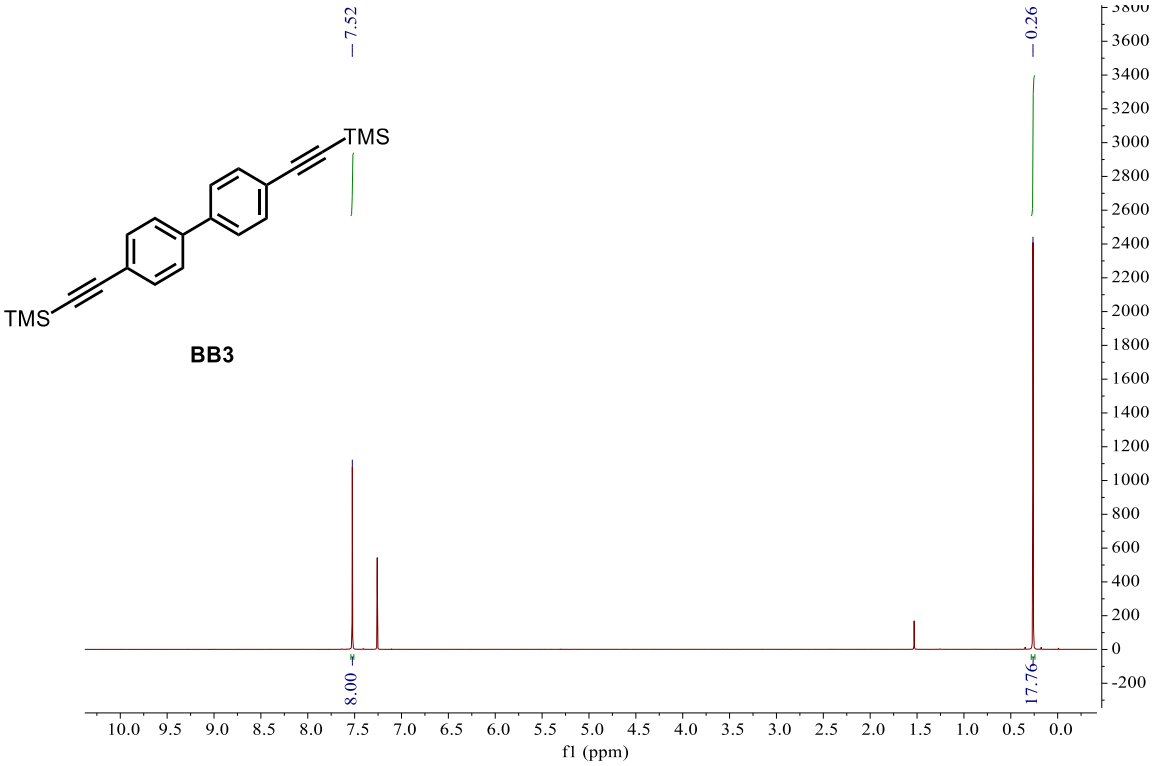

BB3

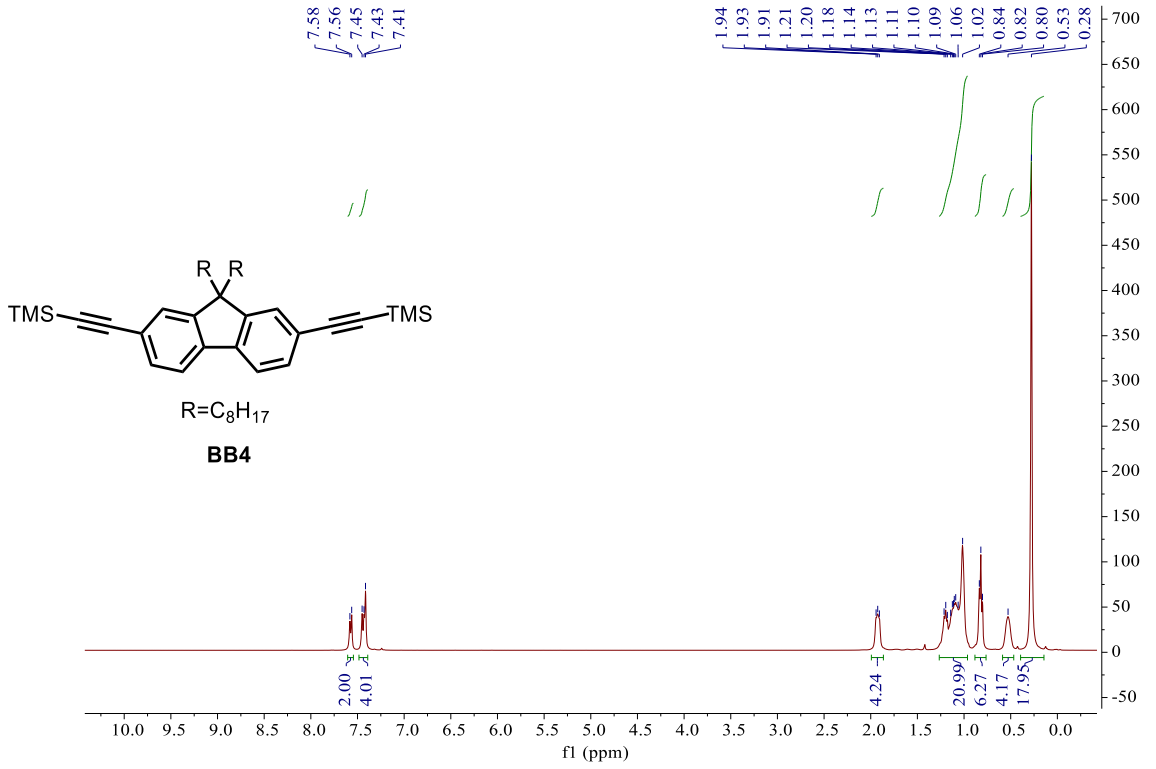

$R=C_8H_{17}$

BB4

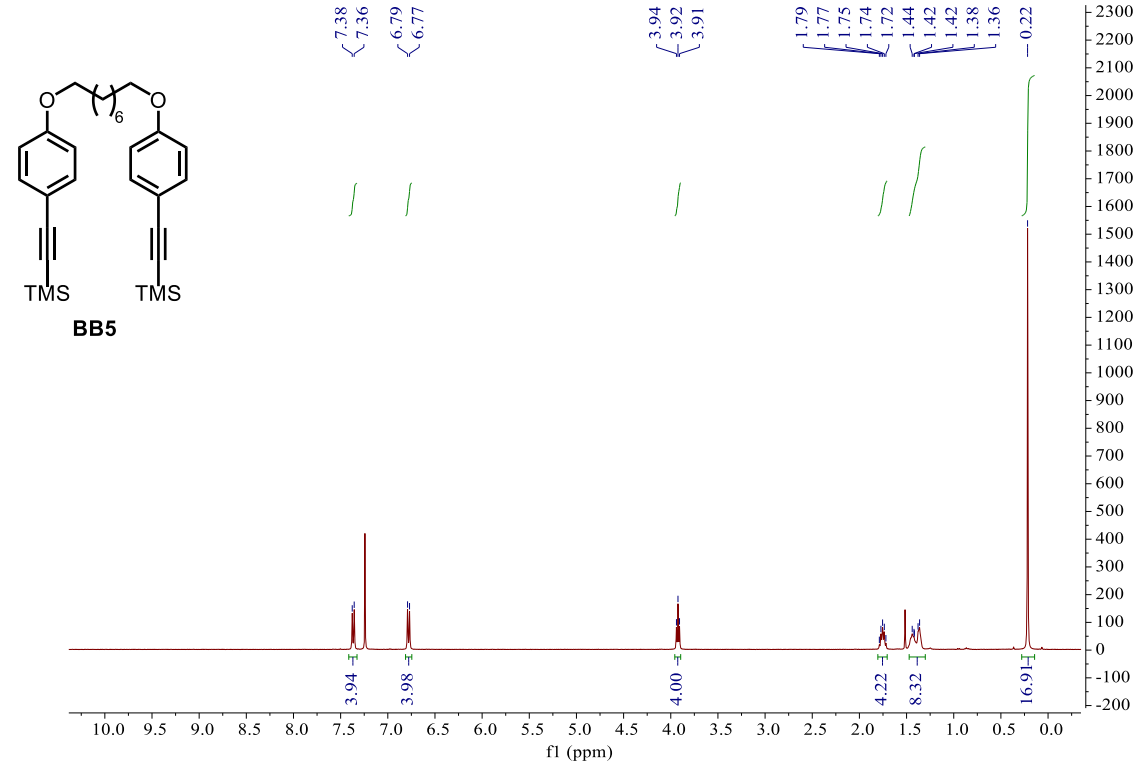
TMS
TMS
BB5
7.38
7.36
6.79
6.77
3.94
3.92
3.91
1.79
1.77
1.75
1.74
1.72
1.44
1.42
1.42
1.38
1.36
0.22
3.94
3.98
4.00
4.22
8.32
16.91
f1 (ppm)

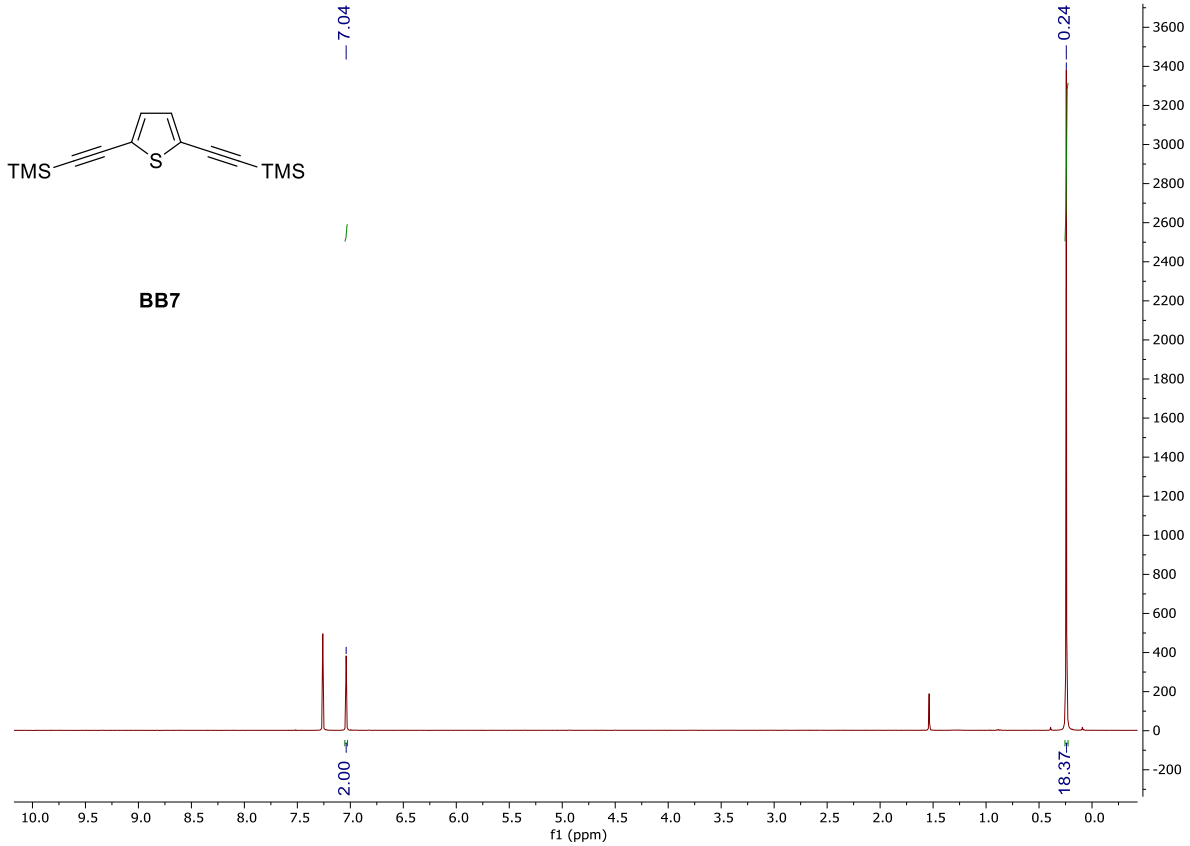
TMS
TMS
S
BB7
7.04
0.24
2.00
18.37
f1 (ppm)

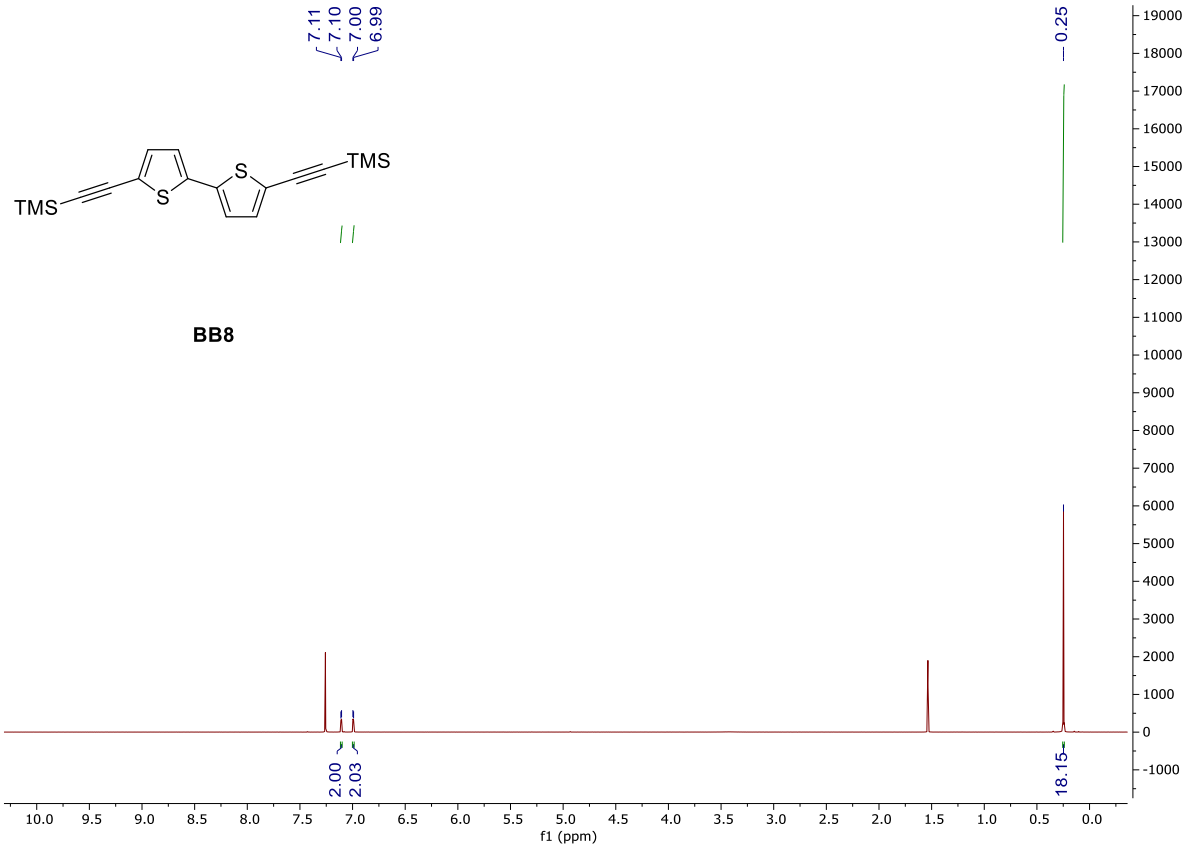
7.11
7.10
7.00
6.99
0.25
TMS
TMS
S
S
2.00
2.03
18.15
f1 (ppm)

BB8

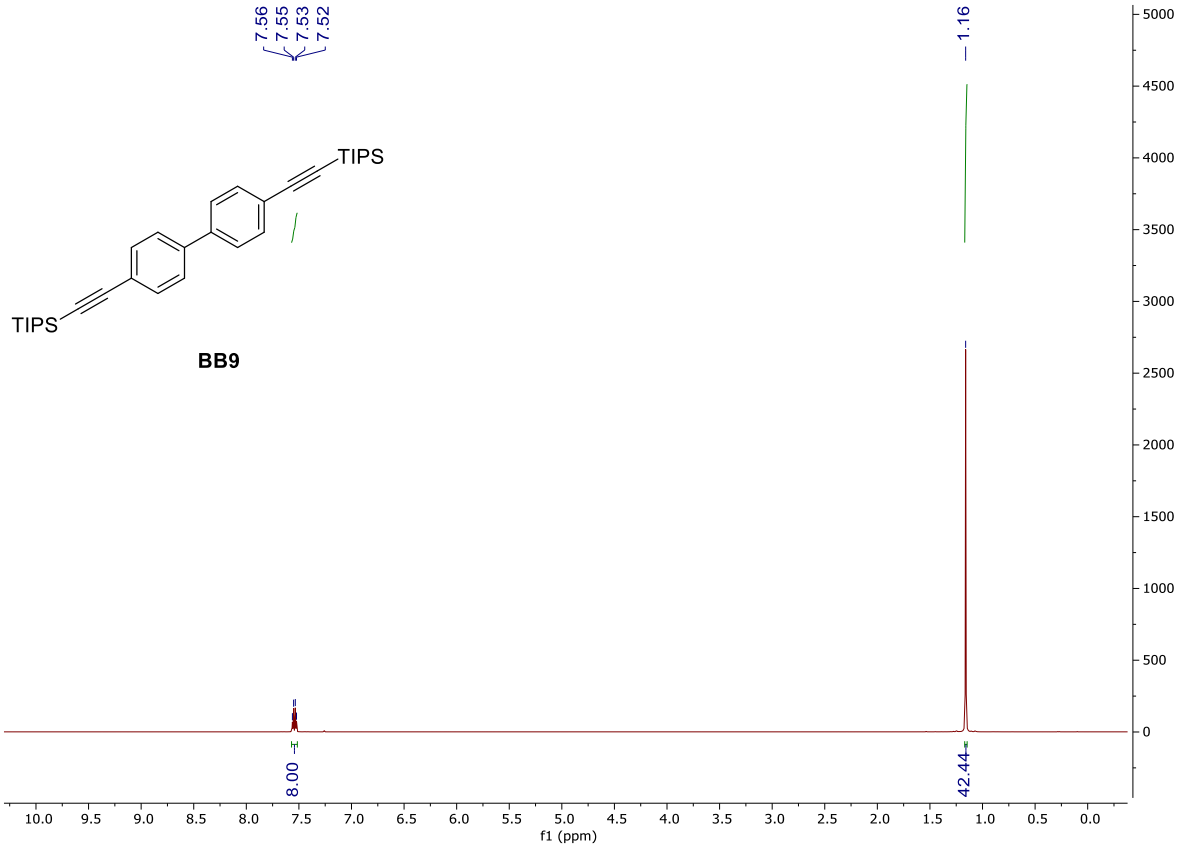
7.56
7.55
7.53
7.52
1.16
TIPS
TIPS
8.00
42.44
f1 (ppm)

BB9

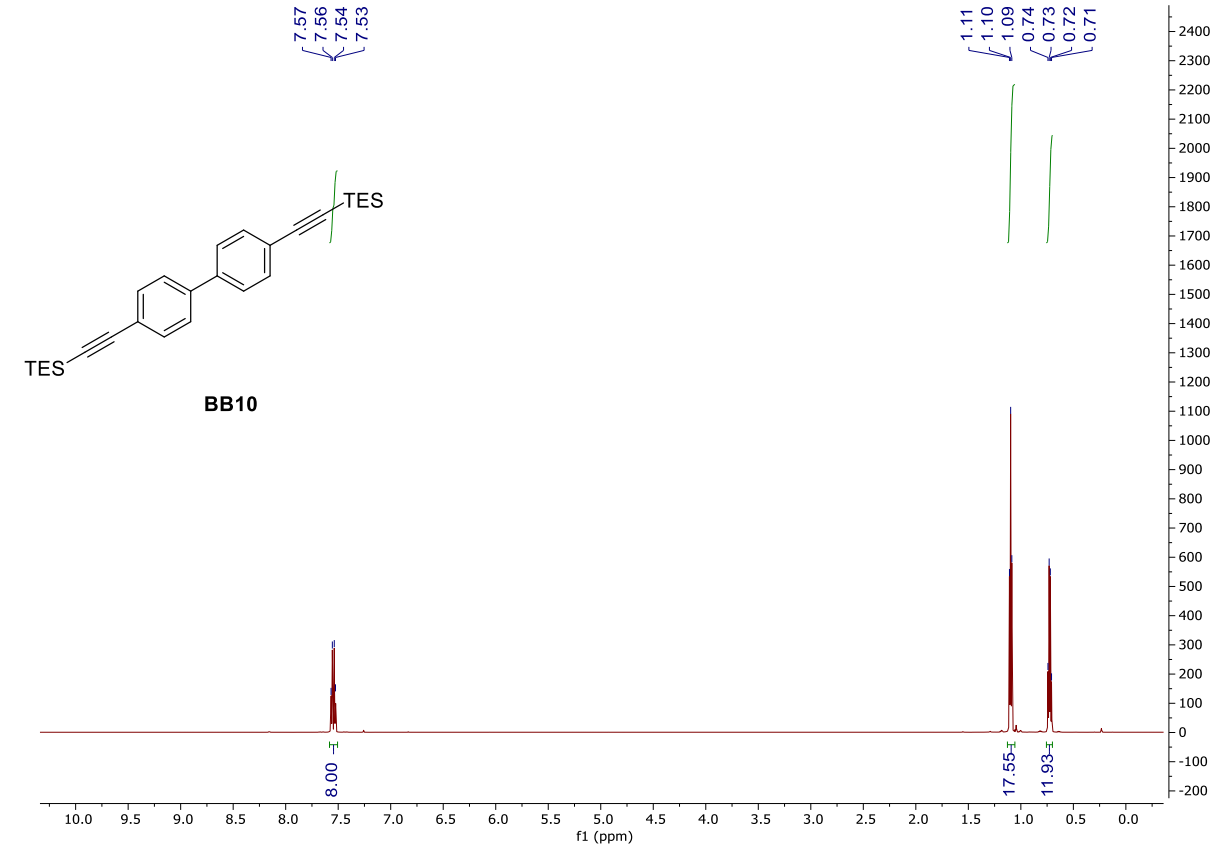
7.57
7.56
7.54
7.53
1.11
1.10
1.09
0.74
0.73
0.72
0.71
TES
TES
8.00
17.55
11.93
f1 (ppm)

BB10

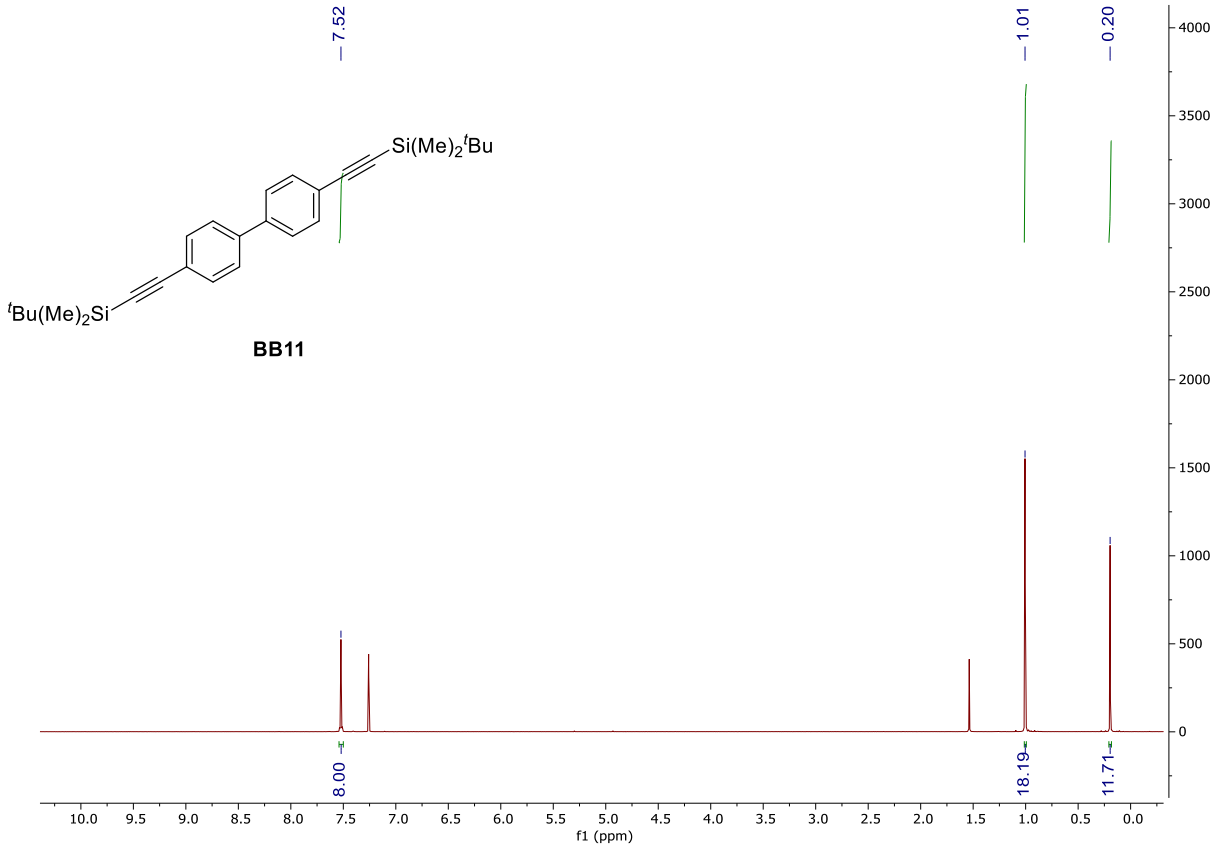
7.52
1.01
0.20
Si(Me)2tBu
tBu(Me)2Si
8.00
18.19
11.71
f1 (ppm)

BB11

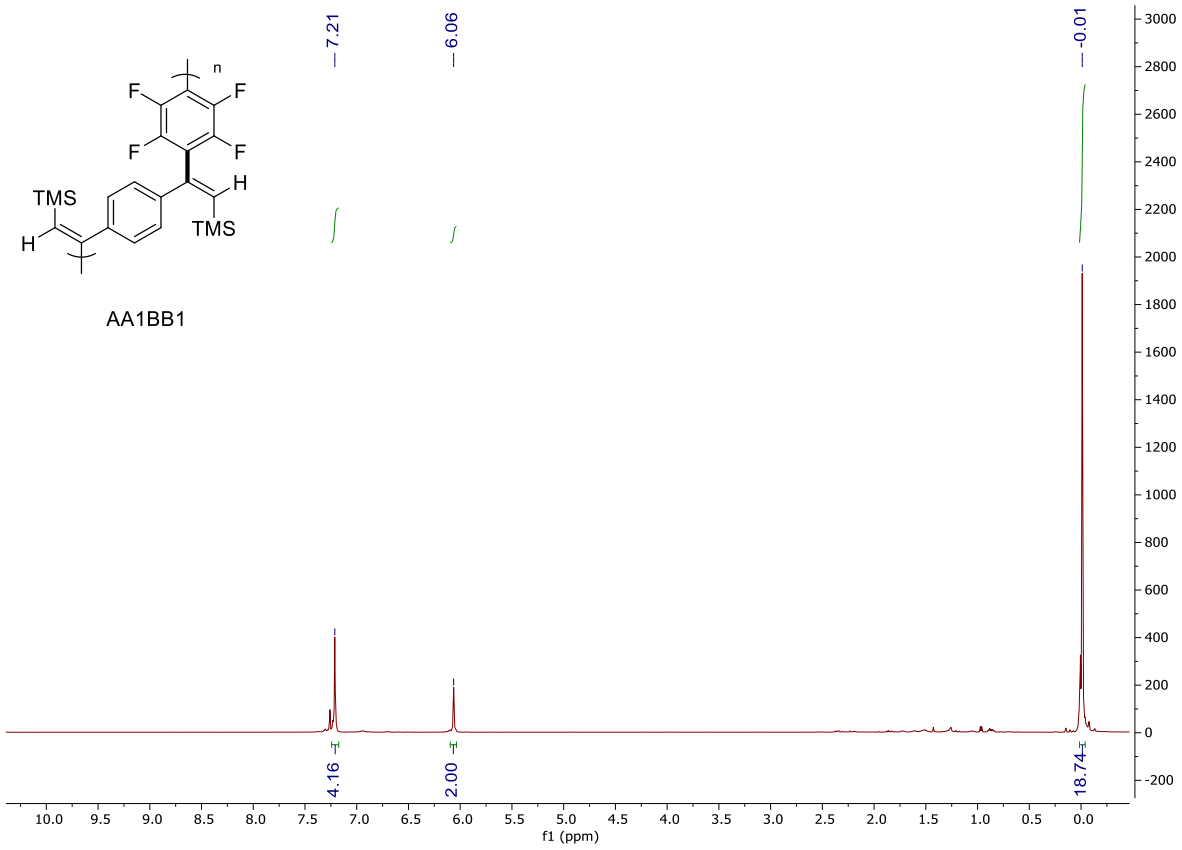

AA1BB1

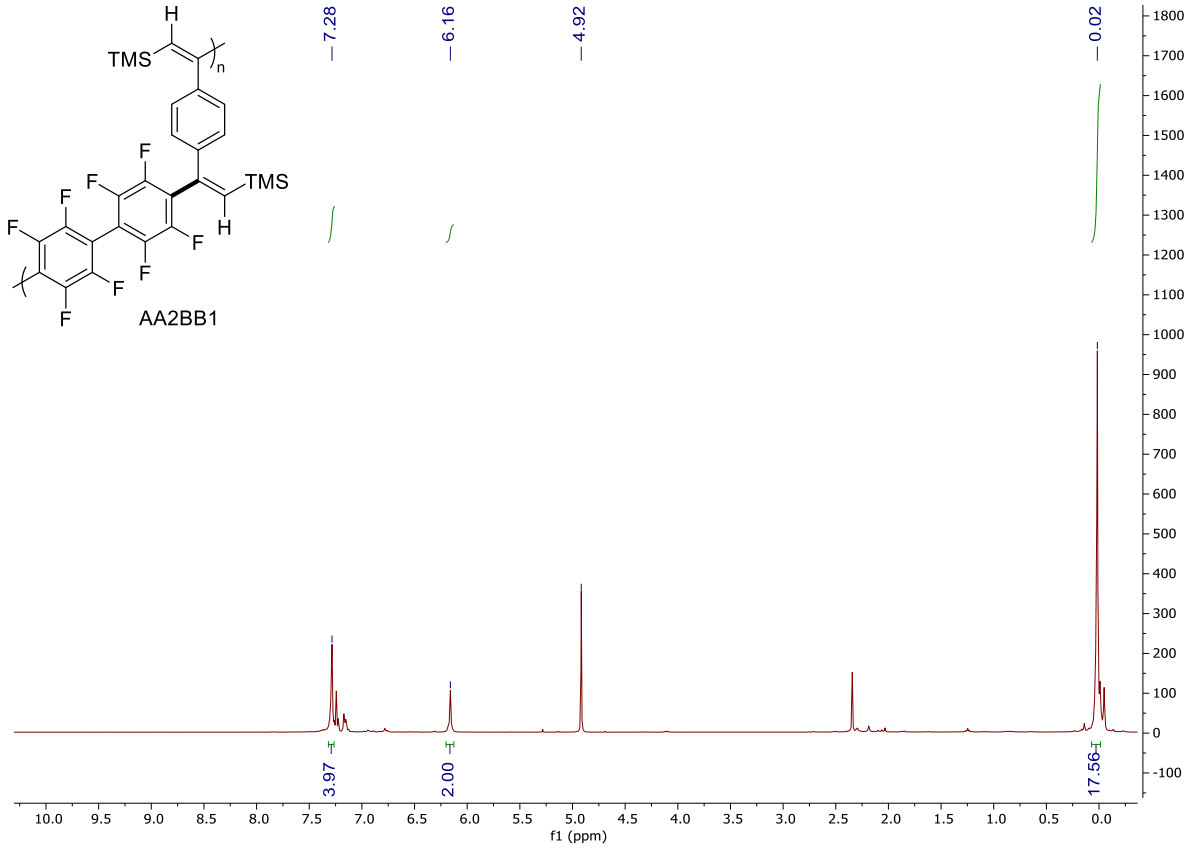

AA2BB1

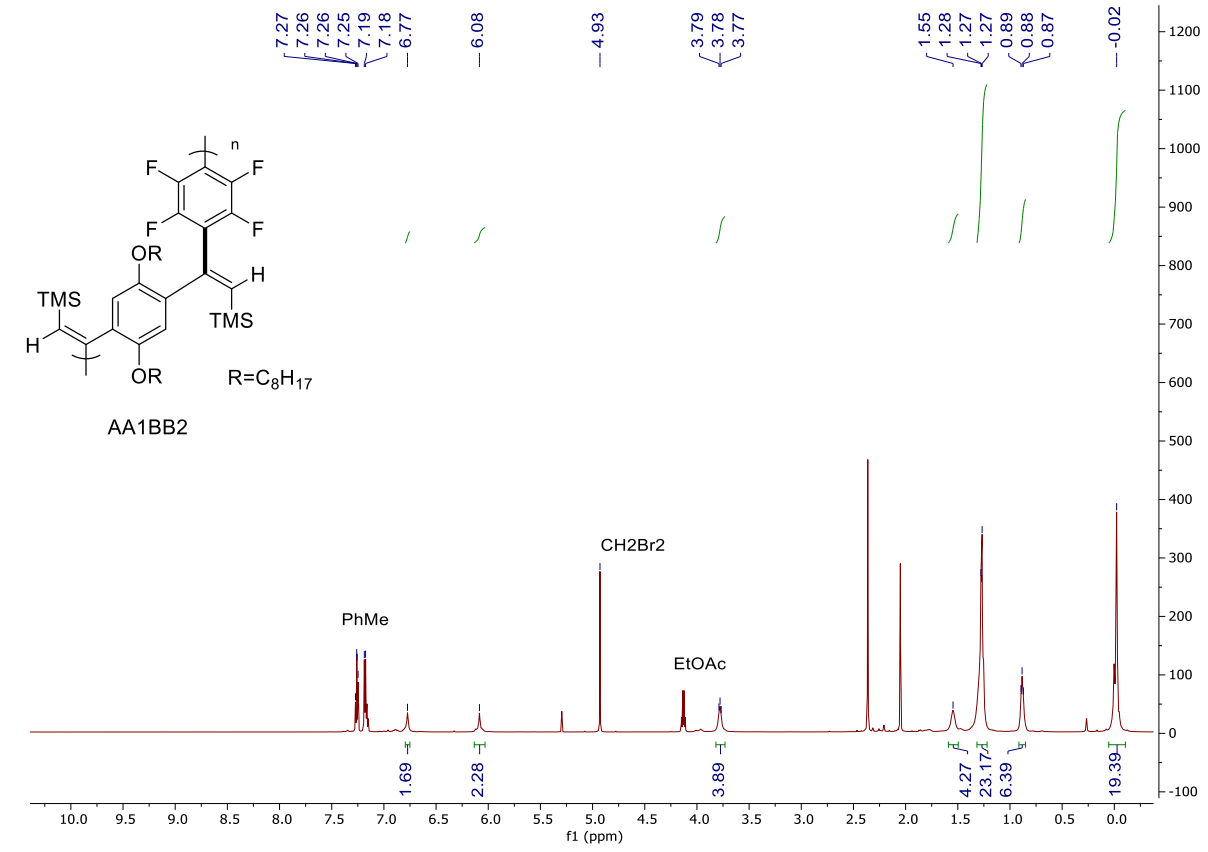
7.27
7.26
7.26
7.25
7.19
7.18
6.77
6.08
4.93
3.79
3.78
3.77
1.55
1.28
1.27
1.27
0.89
0.88
0.87
-0.02
n
F
F
F
F
OR
H
TMS
TMS
H
OR
R=C8H17
AA1BB2
CH2Br2
PhMe
EtOAc
1.69
2.28
3.89
4.27
23.17
6.39
19.39
f1 (ppm)

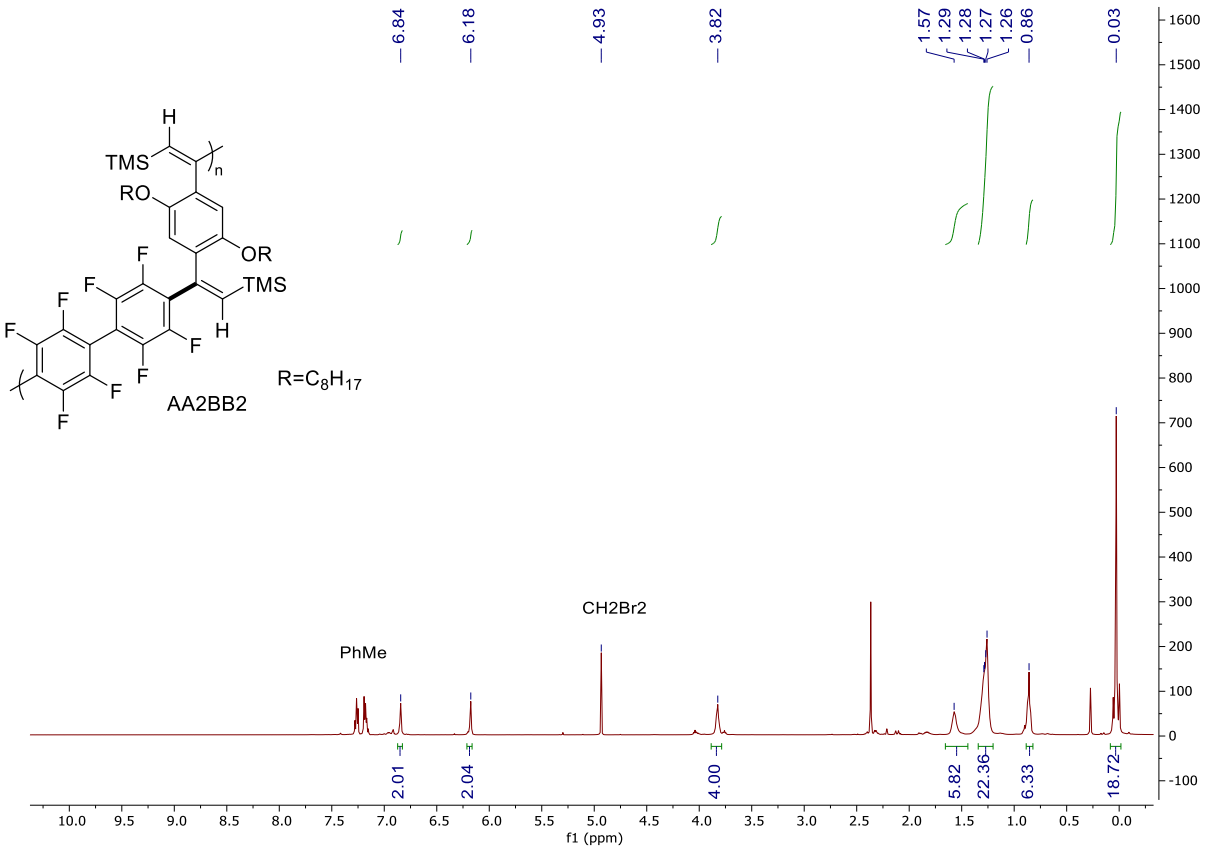
6.84
6.18
4.93
3.82
1.57
1.29
1.28
1.27
1.26
0.86
0.03
H
TMS
n
RO
OR
F
F
TMS
F
H
F
F
F
F
F
R=C8H17
AA2BB2
CH2Br2
PhMe
2.01
2.04
4.00
5.82
22.36
6.33
18.72
f1 (ppm)

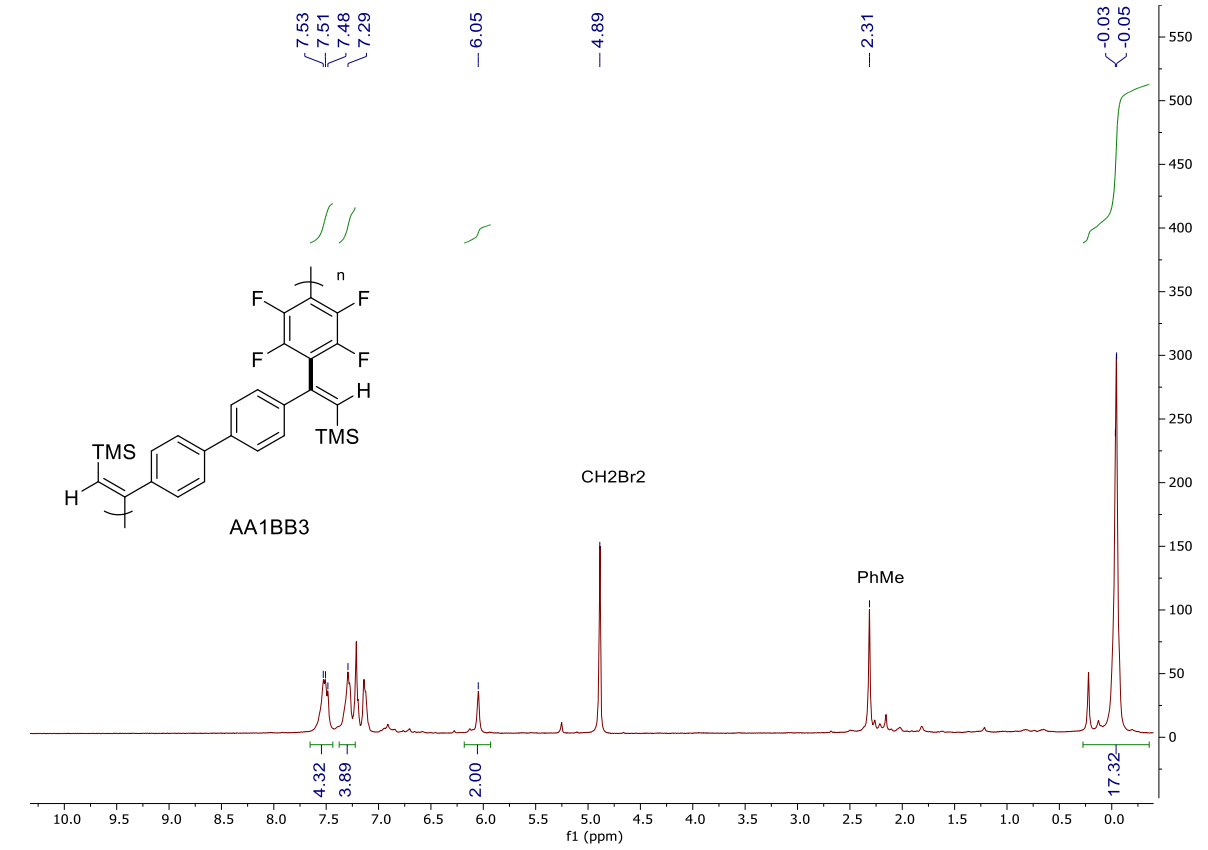
7.53
7.51
7.48
7.29
6.05
4.89
2.31
-0.03
-0.05
n
F
F
F
F
H
TMS
TMS
H
AA1BB3
CH2Br2
PhMe
4.32
3.89
2.00
17.32
f1 (ppm)

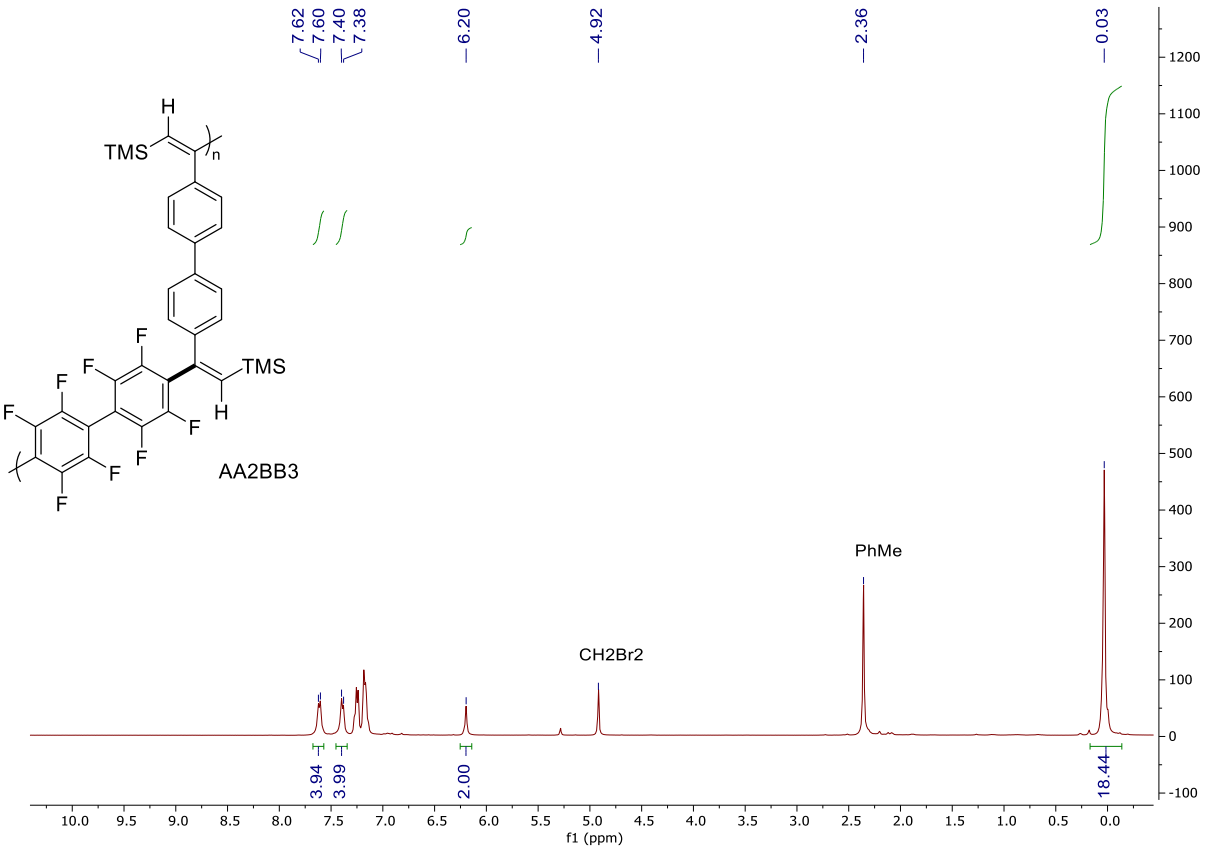
7.62
7.60
7.40
7.38
6.20
4.92
2.36
0.03
H
TMS
n
F
F
F
F
F
F
F
TMS
H
AA2BB3
PhMe
CH2Br2
3.94
3.99
2.00
18.44
f1 (ppm)

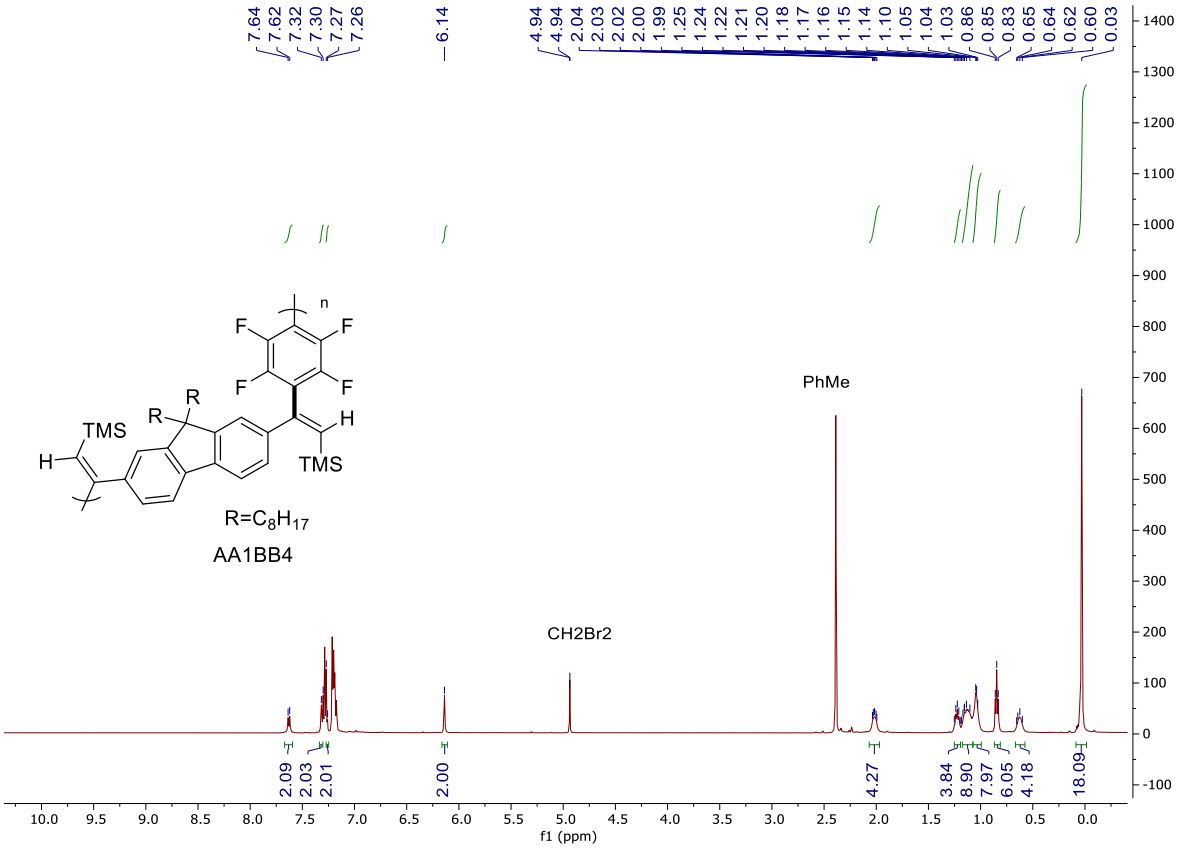
7.64
7.62
7.32
7.30
7.27
7.26
6.14
4.94
4.94
2.04
2.03
2.02
2.00
1.99
1.25
1.24
1.22
1.21
1.20
1.18
1.17
1.16
1.15
1.14
1.10
1.05
1.04
1.03
0.86
0.85
0.83
0.65
0.64
0.62
0.60
0.03
n
F
F
F
F
R
R
TMS
H
H
TMS
R=C8H17
AA1BB4
PhMe
CH2Br2
2.09
2.03
2.01
2.00
4.27
3.84
8.90
7.97
6.05
4.18
18.09
f1 (ppm)

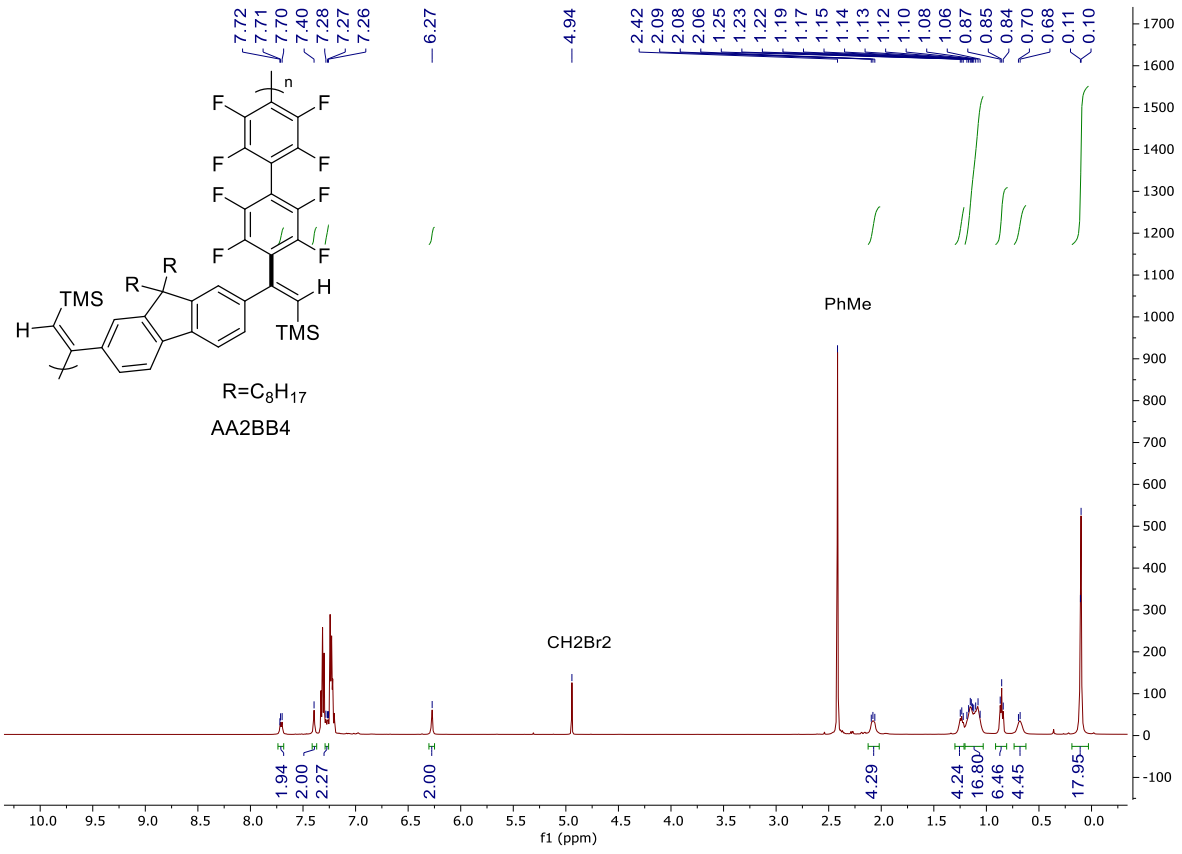
7.72
7.71
7.70
7.40
7.28
7.27
7.26
6.27
4.94
2.42
2.09
2.08
2.06
1.25
1.23
1.22
1.19
1.17
1.15
1.14
1.13
1.12
1.10
1.08
1.06
0.87
0.85
0.84
0.70
0.68
0.11
0.10
n
F
F
F
F
F
F
F
F
R
R
TMS
H
H
TMS
R=C8H17
AA2BB4
PhMe
CH2Br2
1.94
2.00
2.27
2.00
4.29
4.24
16.80
6.46
4.45
17.95
f1 (ppm)

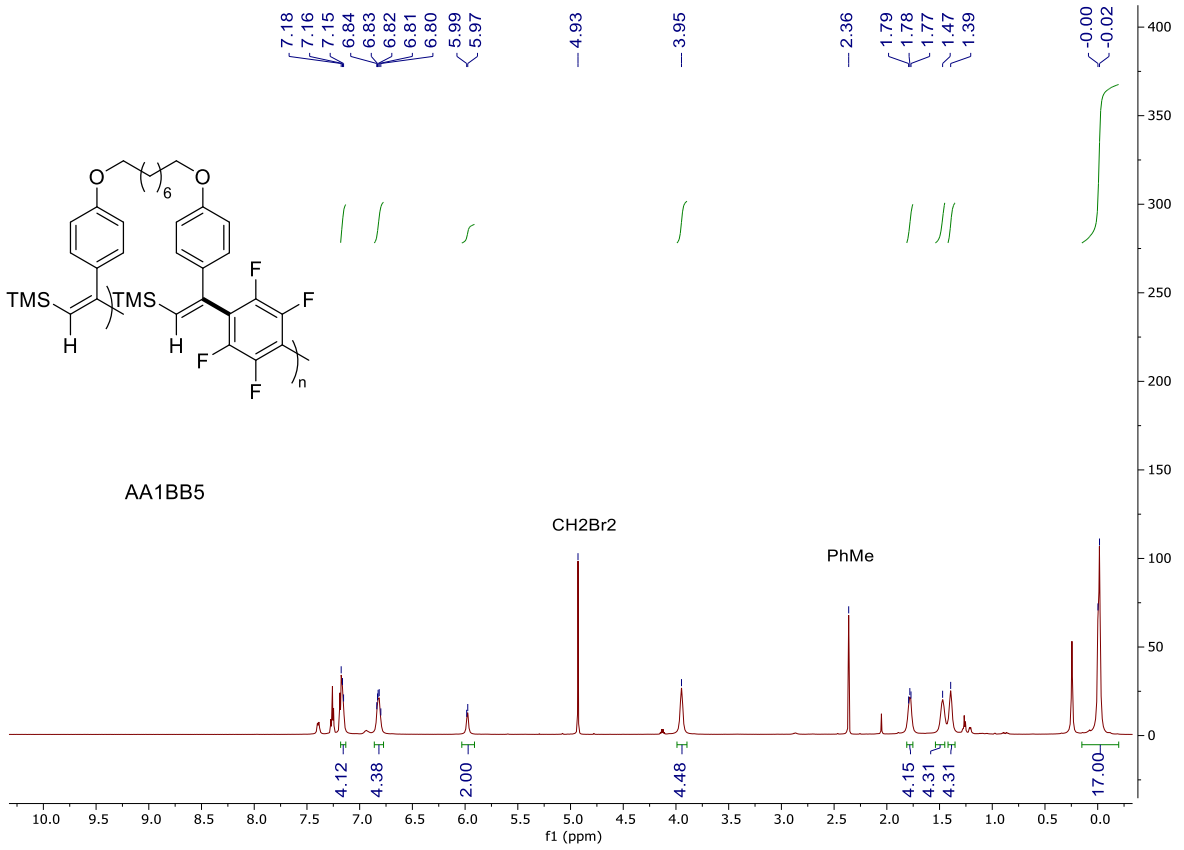
7.18
7.16
7.15
6.84
6.83
6.82
6.81
6.80
5.99
5.97
4.93
3.95
2.36
1.79
1.78
1.77
1.47
1.39
-0.00
-0.02
TMS
TMS
H
H
F
F
F
F
F
n
O
O
6
AA1BB5
CH2Br2
PhMe
4.12
4.38
2.00
4.48
4.15
4.31
4.31
17.00
f1 (ppm)

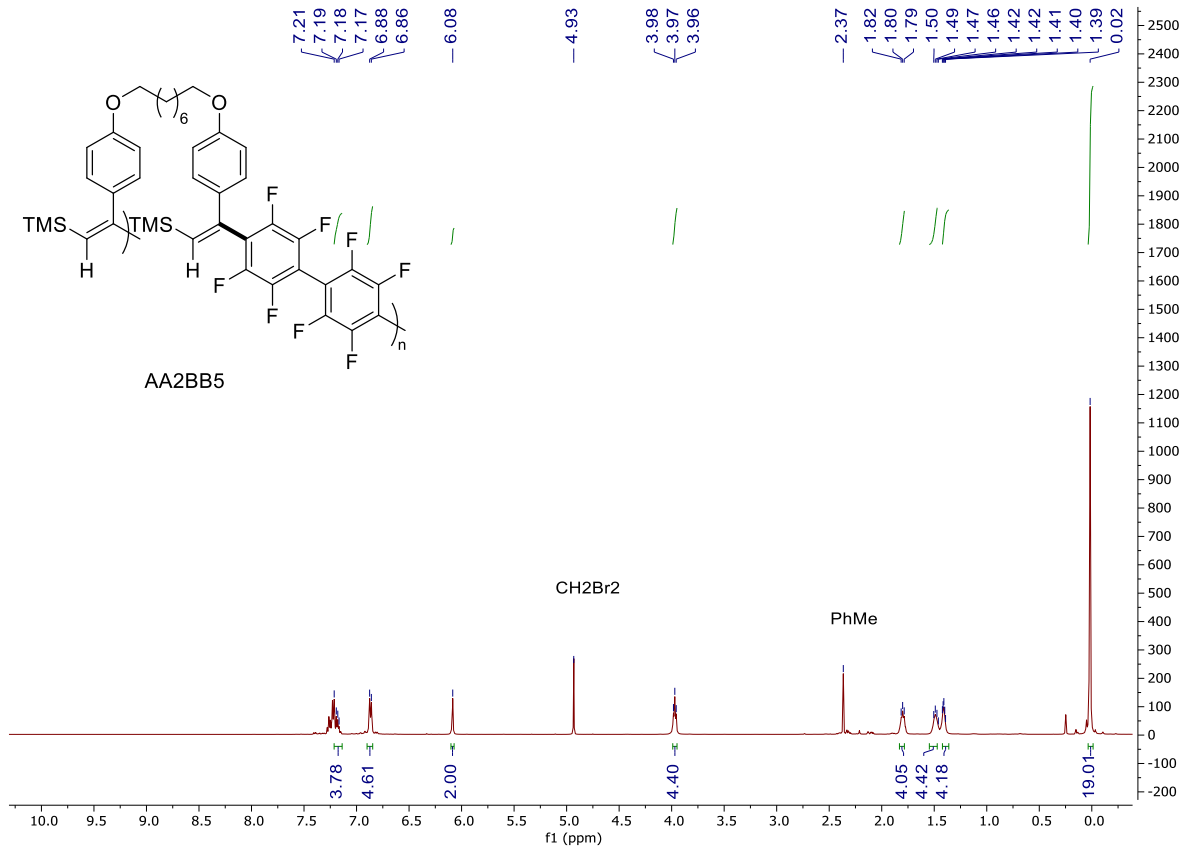
7.21
7.19
7.18
7.17
6.88
6.86
6.08
4.93
3.98
3.97
3.96
2.37
1.82
1.80
1.79
1.50
1.49
1.47
1.46
1.42
1.42
1.41
1.40
1.39
0.02
TMS
TMS
H
H
F
F
F
F
F
F
F
F
n
O
O
6
AA2BB5
CH2Br2
PhMe
3.78
4.61
2.00
4.40
4.05
4.42
4.18
19.01
f1 (ppm)

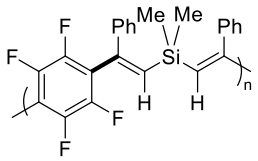

AA1BB6
not observed

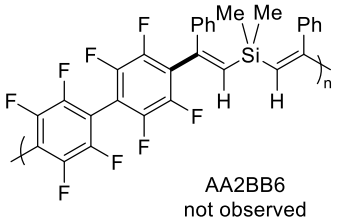

AA2BB6
not observed

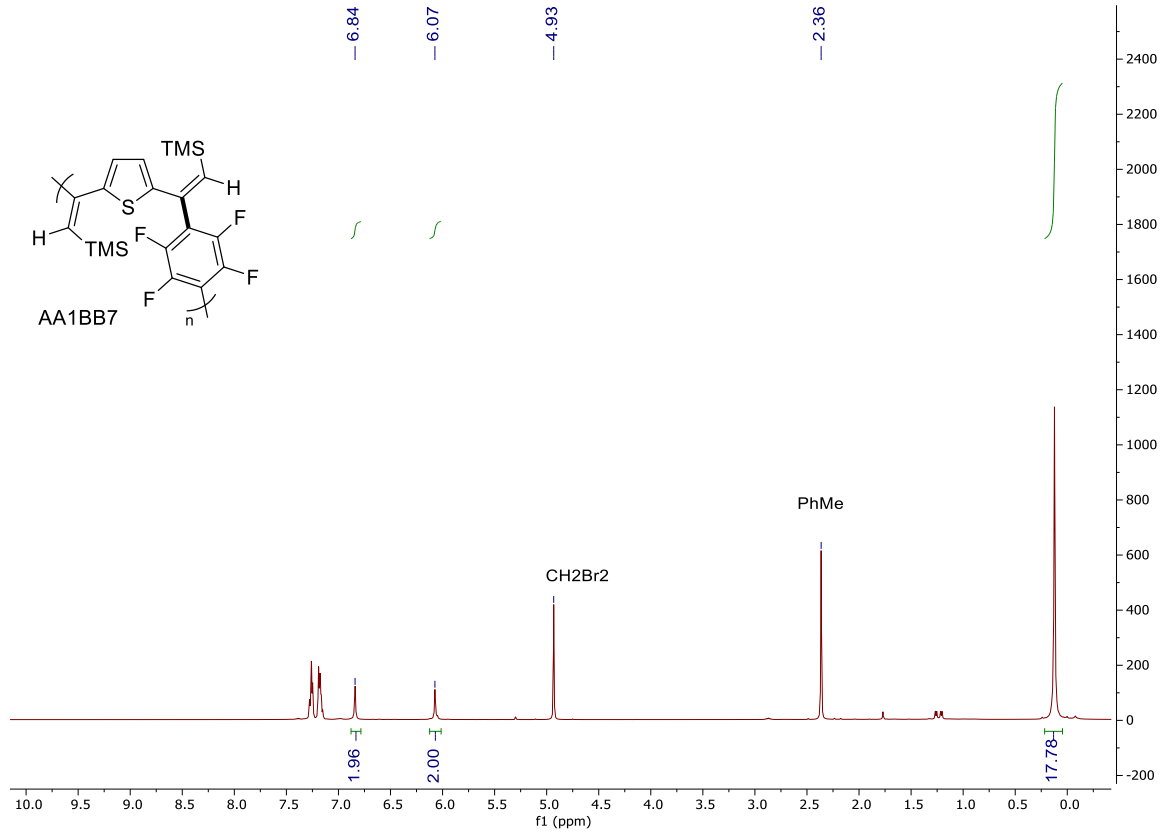
6.84
6.07
4.93
2.36
TMS
H
S
F
H
TMS
F
F
F
n
AA1BB7
PhMe
CH2Br2
1.96
2.00
17.78
f1 (ppm)

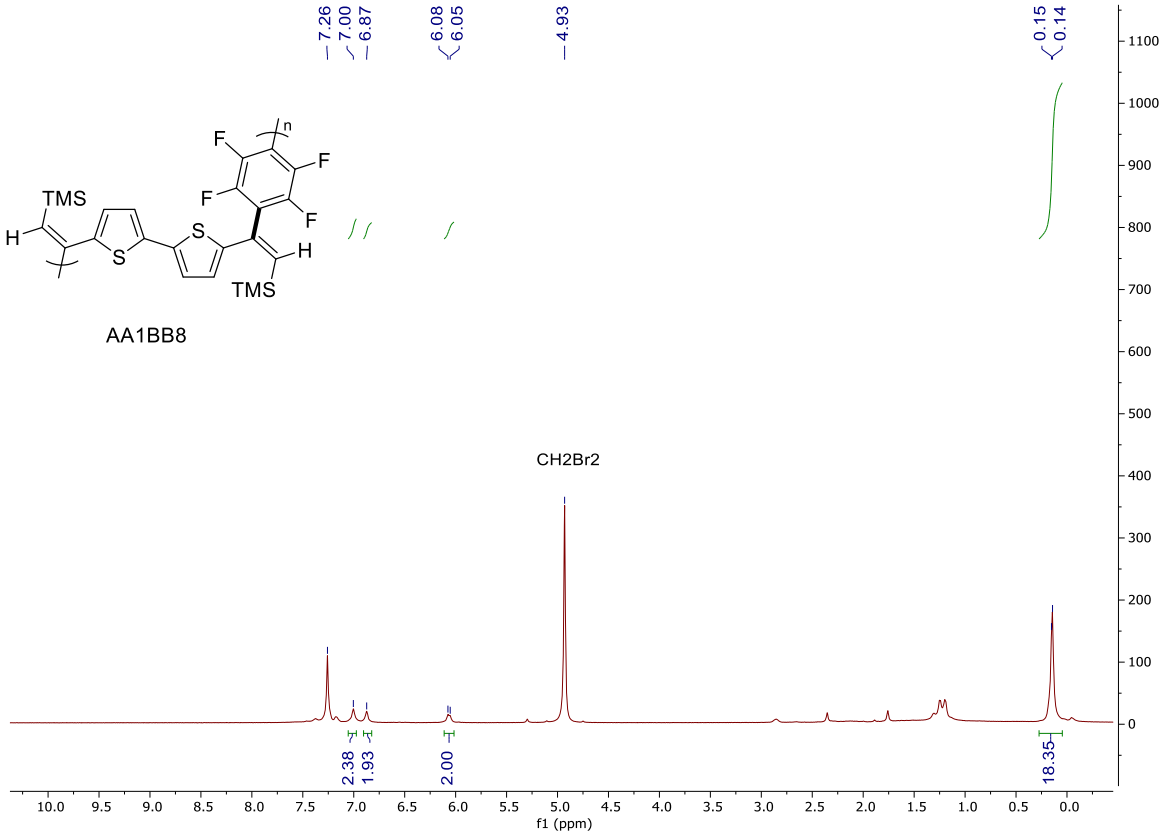
7.26
7.00
6.87
6.08
6.05
4.93
0.15
0.14
F
n
F
F
F
TMS
H
S
S
H
TMS
AA1BB8
CH2Br2
2.38
1.93
2.00
18.35
f1 (ppm)

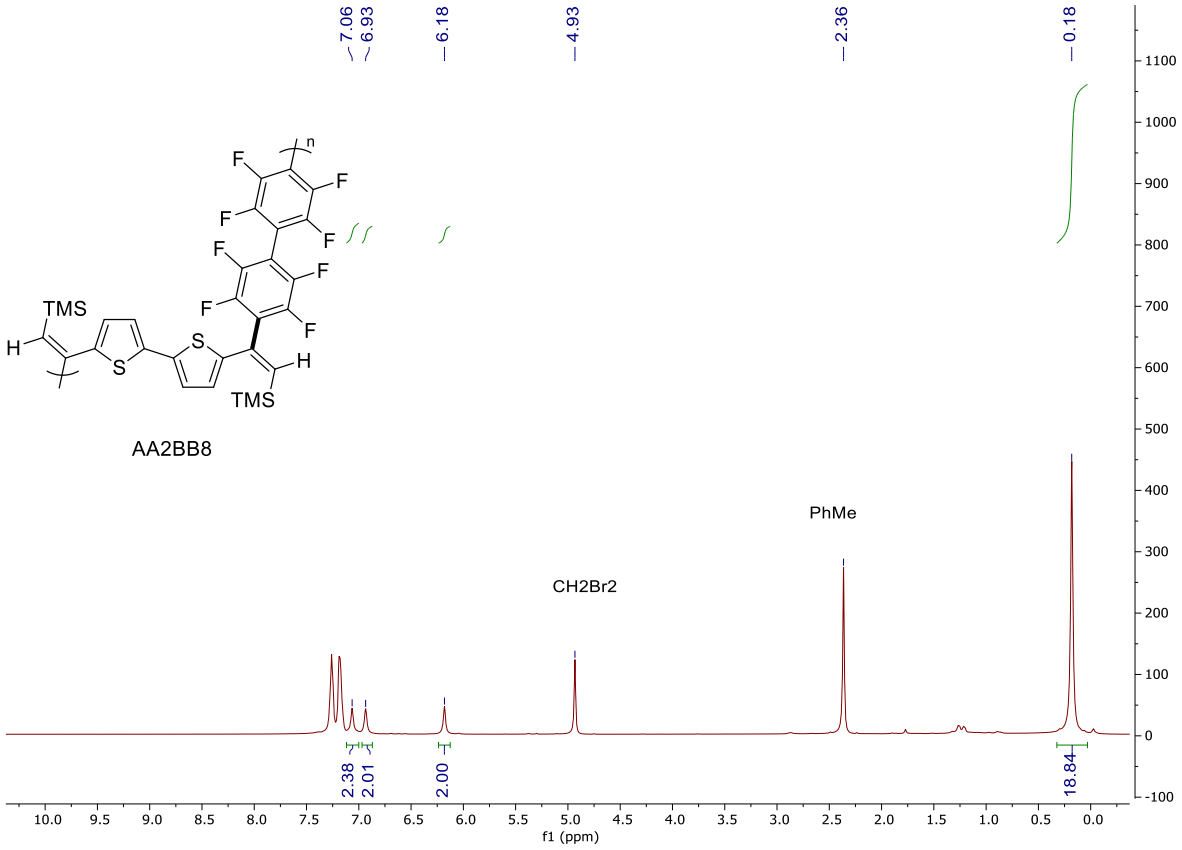
7.06
6.93
6.18
4.93
2.36
0.18
TMS
H
S
S
H
TMS
F
F
F
F
F
F
F
F
n
AA2BB8
PhMe
CH2Br2
2.38
2.01
2.00
18.84
f1 (ppm)

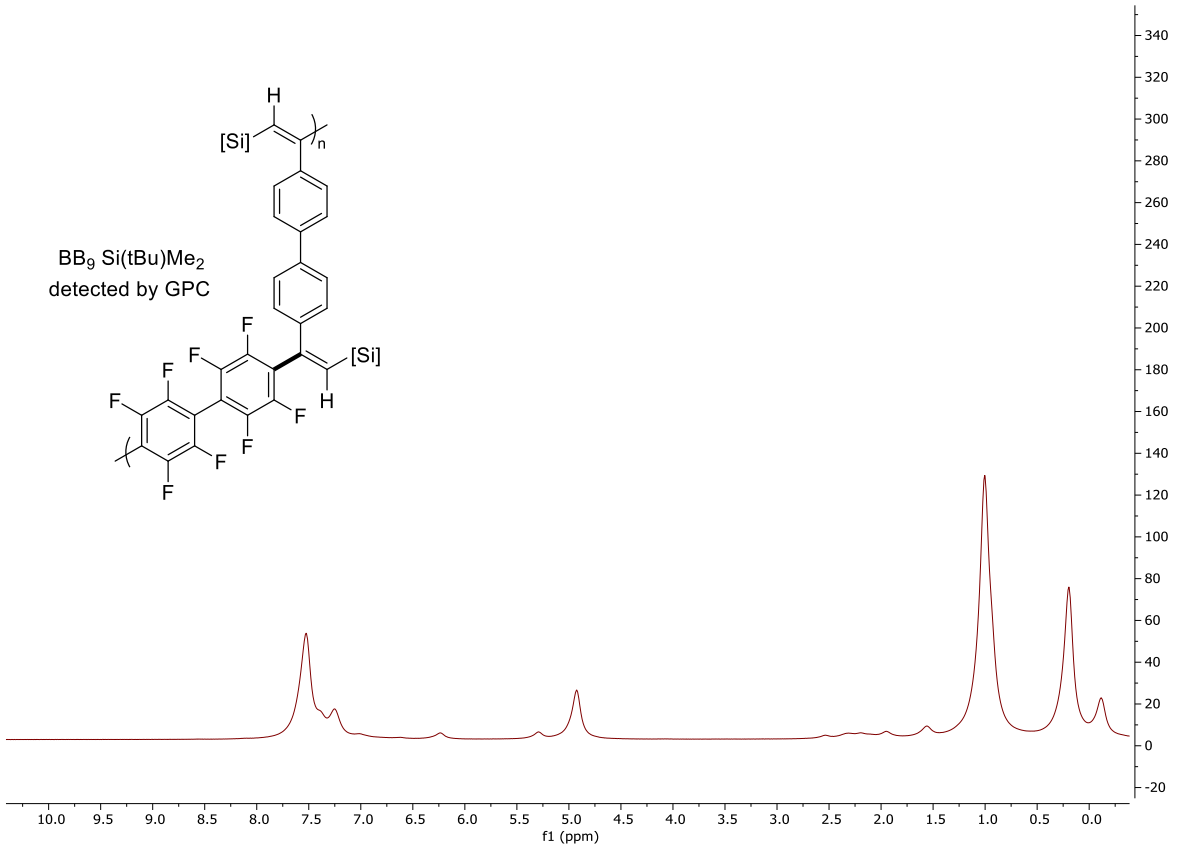
H
[Si]
n
BB9 Si(tBu)Me2
detected by GPC
[Si]
H
F
F
F
F
F
F
F
F
F
f1 (ppm)

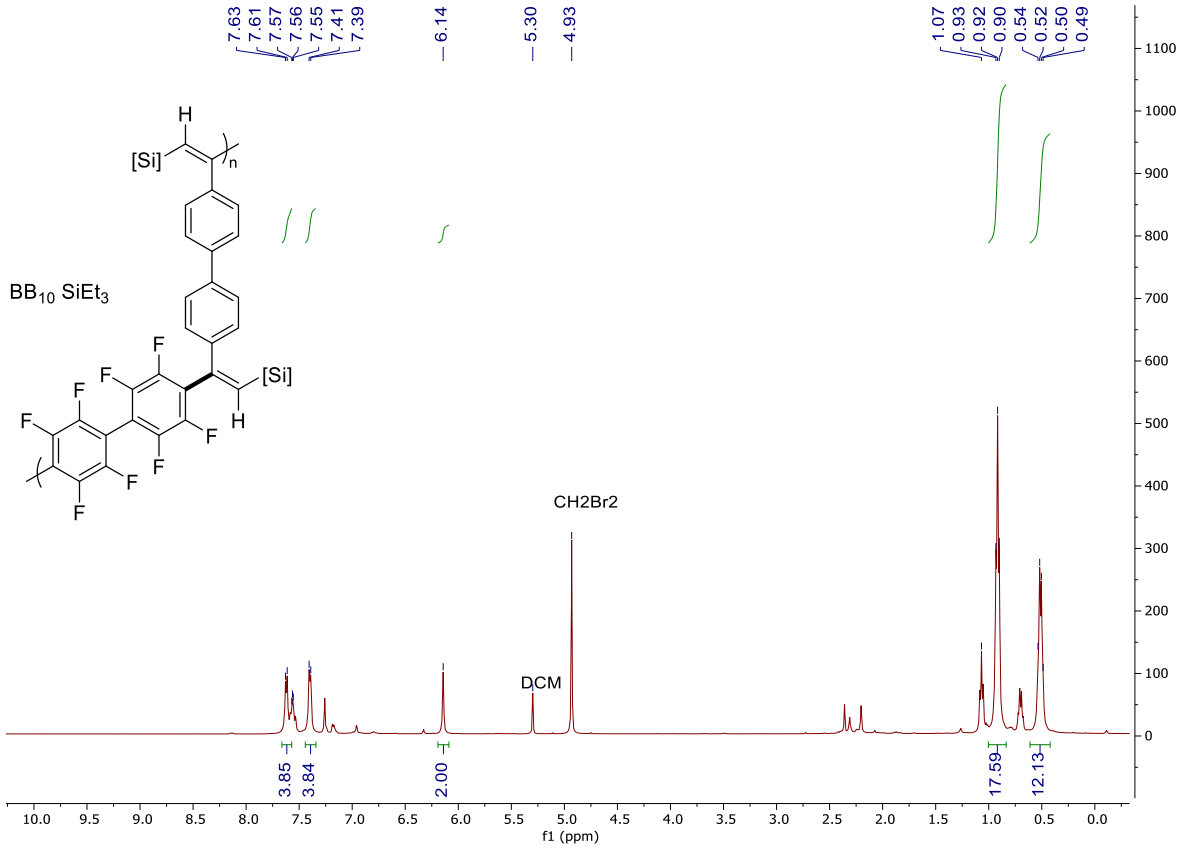
7.63
7.61
7.57
7.56
7.55
7.41
7.39
6.14
5.30
4.93
1.07
0.93
0.92
0.90
0.54
0.52
0.50
0.49
BB10 SiEt3
[Si]
n
H
F
[Si]
H
CH2Br2
DCM
3.85
3.84
2.00
17.59
12.13
f1 (ppm)

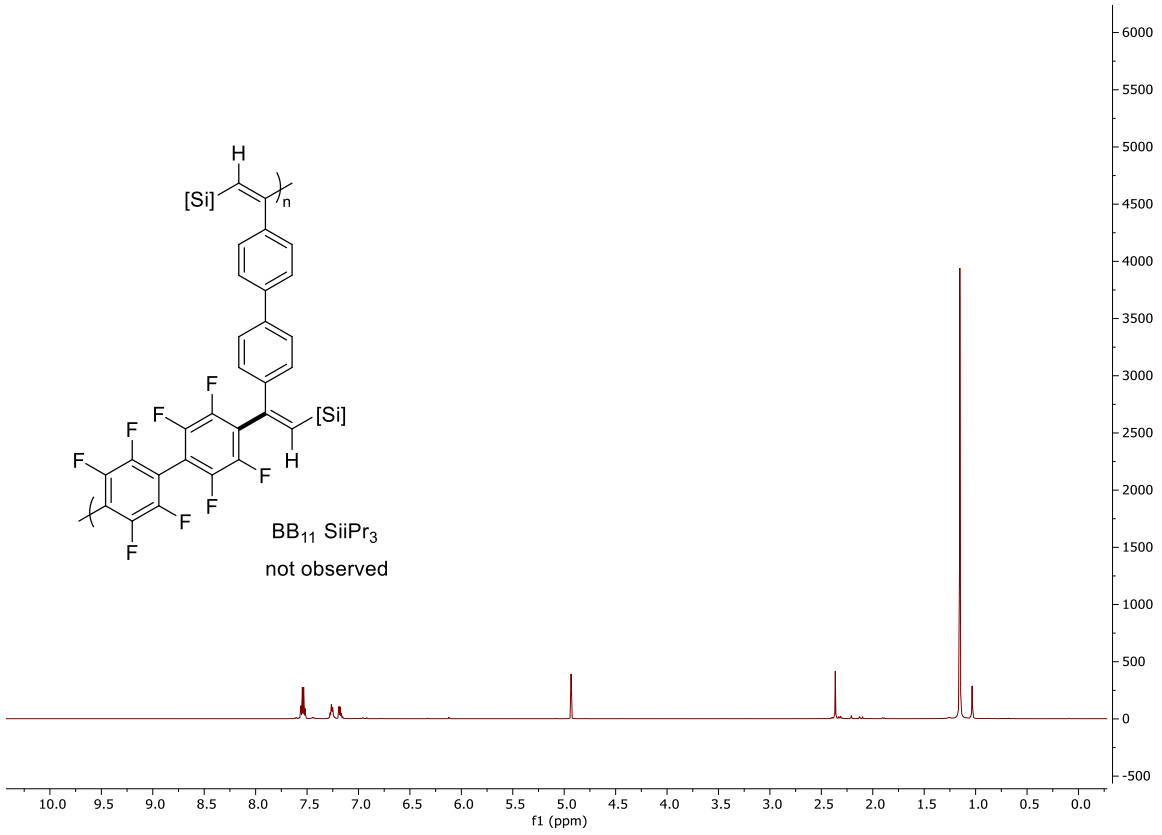
[Si]
n
H
F
[Si]
H
BB11 SiiPr3
not observed
f1 (ppm)

8.6.3 Chapter 5

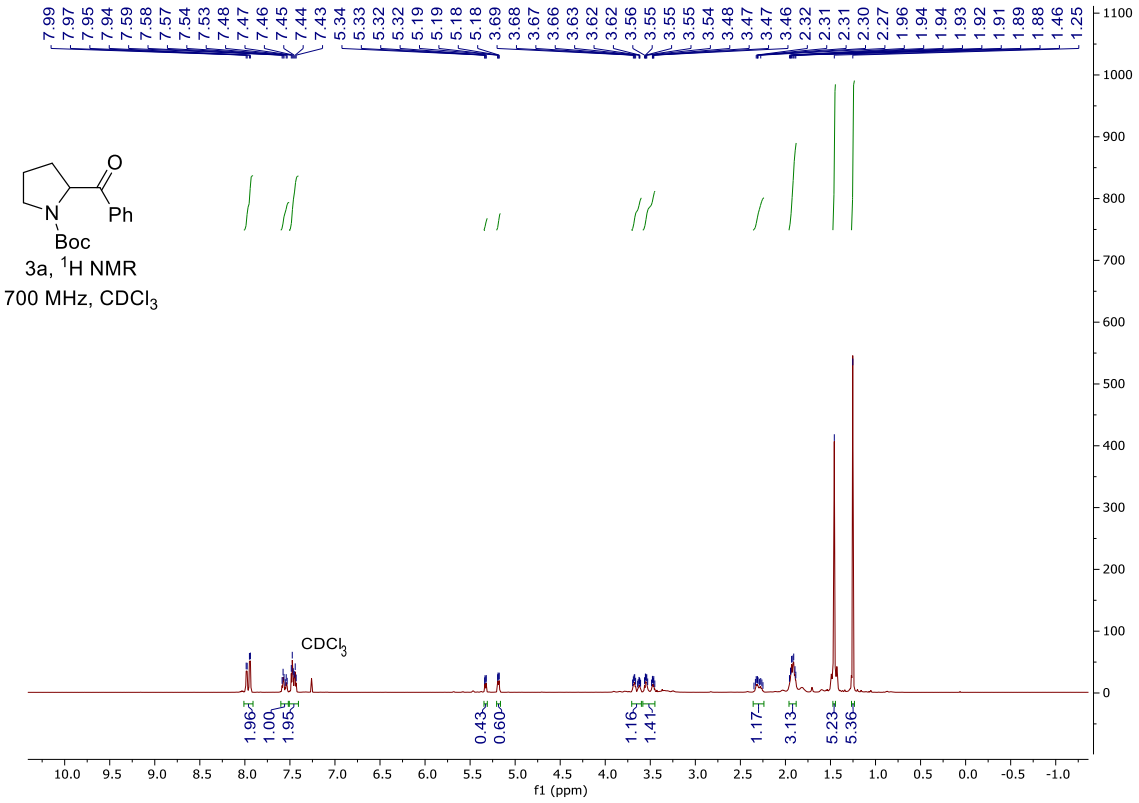

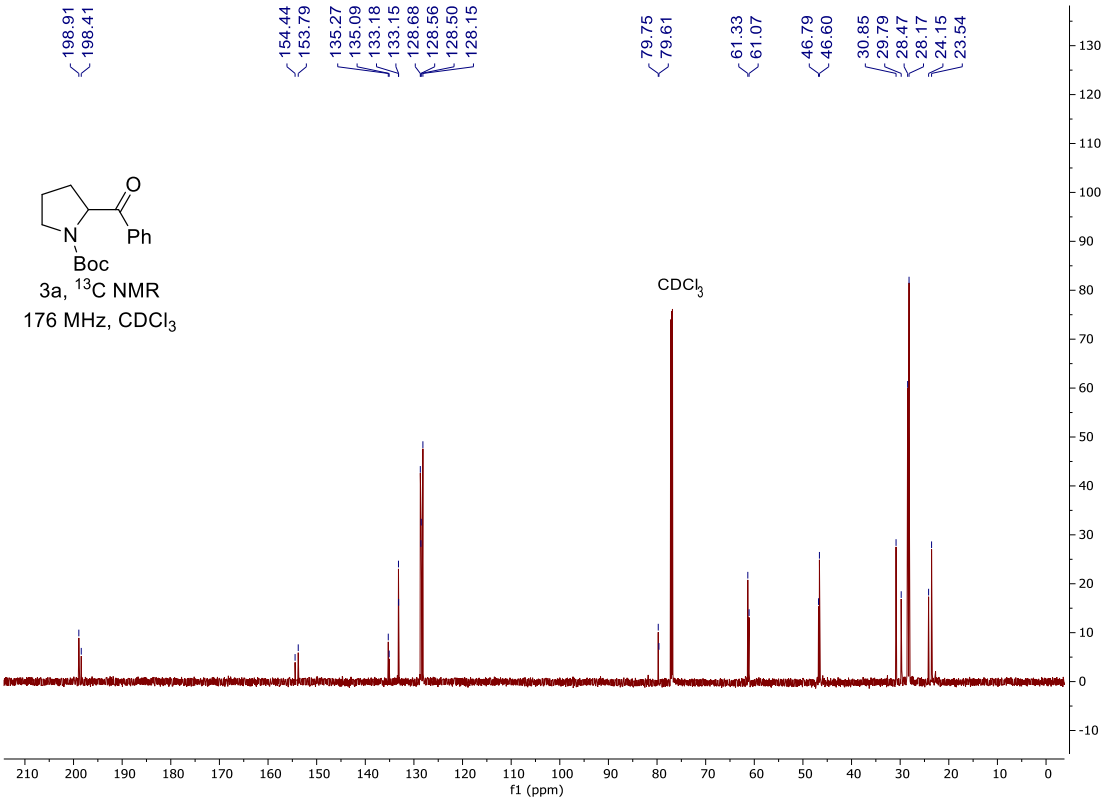

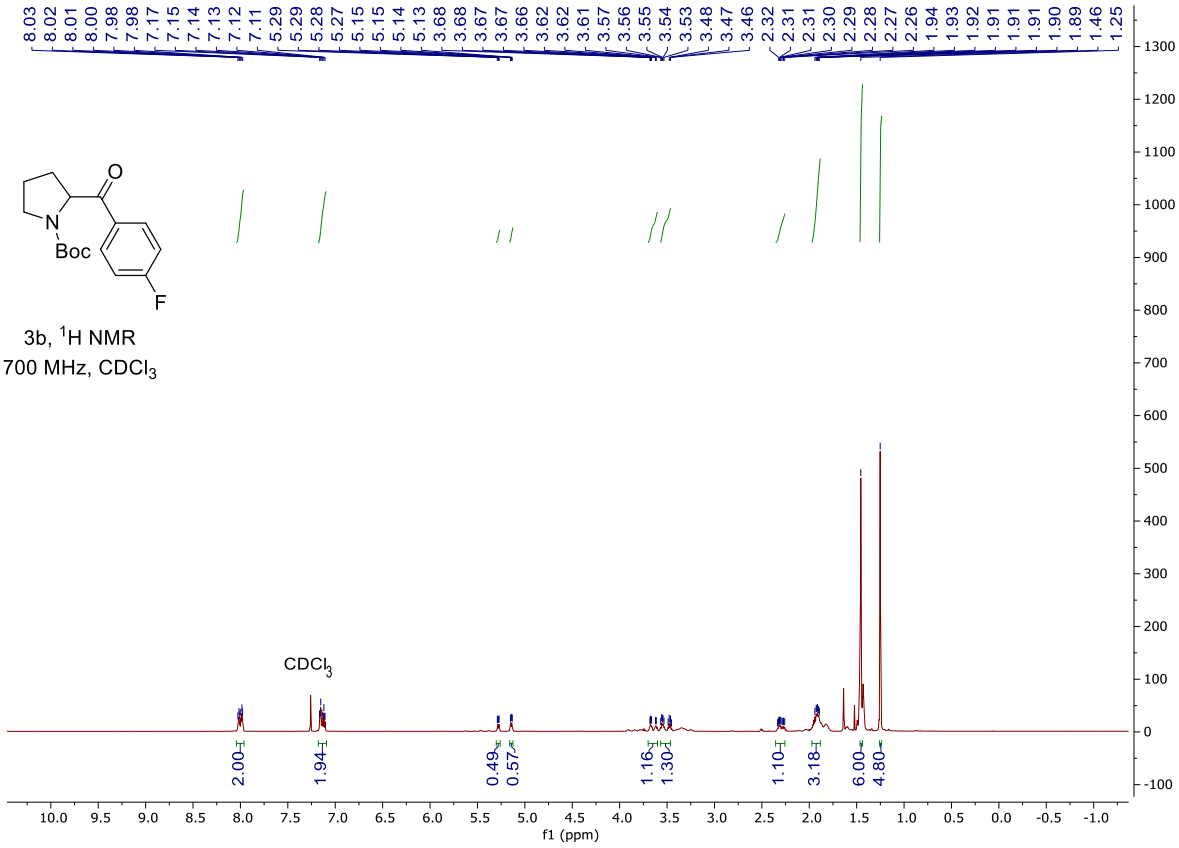
8.03 8.02 8.01 8.00 7.98 7.98 7.17 7.15 7.14 7.13 7.12 7.11 5.29 5.29 5.28 5.27 5.15 5.15 5.14 5.13 3.68 3.68 3.67 3.67 3.66 3.62 3.62 3.61 3.57 3.56 3.55 3.54 3.53 3.48 3.47 3.46 2.32 2.31 2.31 2.30 2.29 2.28 2.27 2.26 1.94 1.93 1.92 1.91 1.91 1.91 1.90 1.89 1.46 1.25
O
N
Boc
F
3b, 1H NMR
700 MHz, CDCl3
CDCl3
2.00 1.94 0.49 0.57 1.16 1.30 1.10 3.18 6.00 4.80
f1 (ppm)

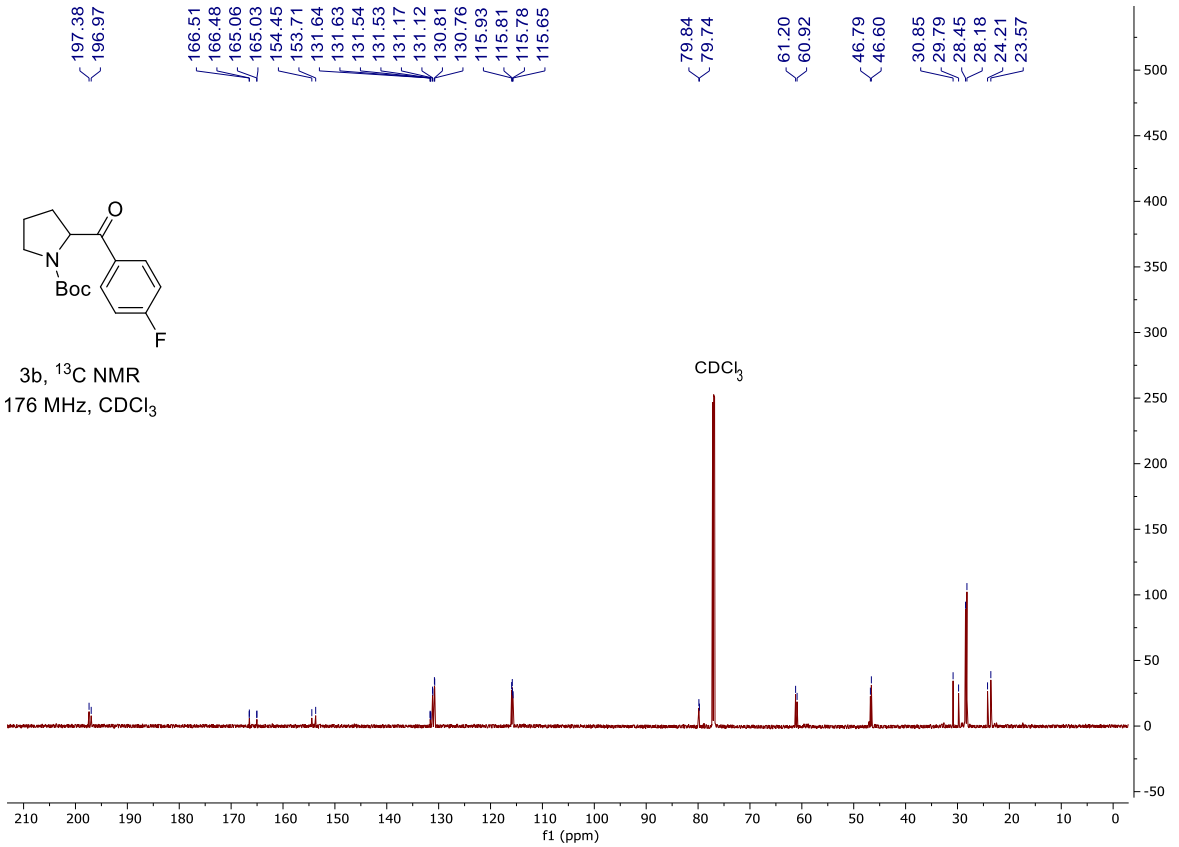
197.38 196.97 166.51 166.48 165.06 165.03 154.45 153.71 131.64 131.63 131.54 131.53 131.17 131.12 130.81 130.76 115.93 115.81 115.78 115.65 79.84 79.74 61.20 60.92 46.79 46.60 30.85 29.79 28.45 28.18 24.21 23.57
O
N
Boc
F
3b, 13C NMR
176 MHz, CDCl3
CDCl3
f1 (ppm)

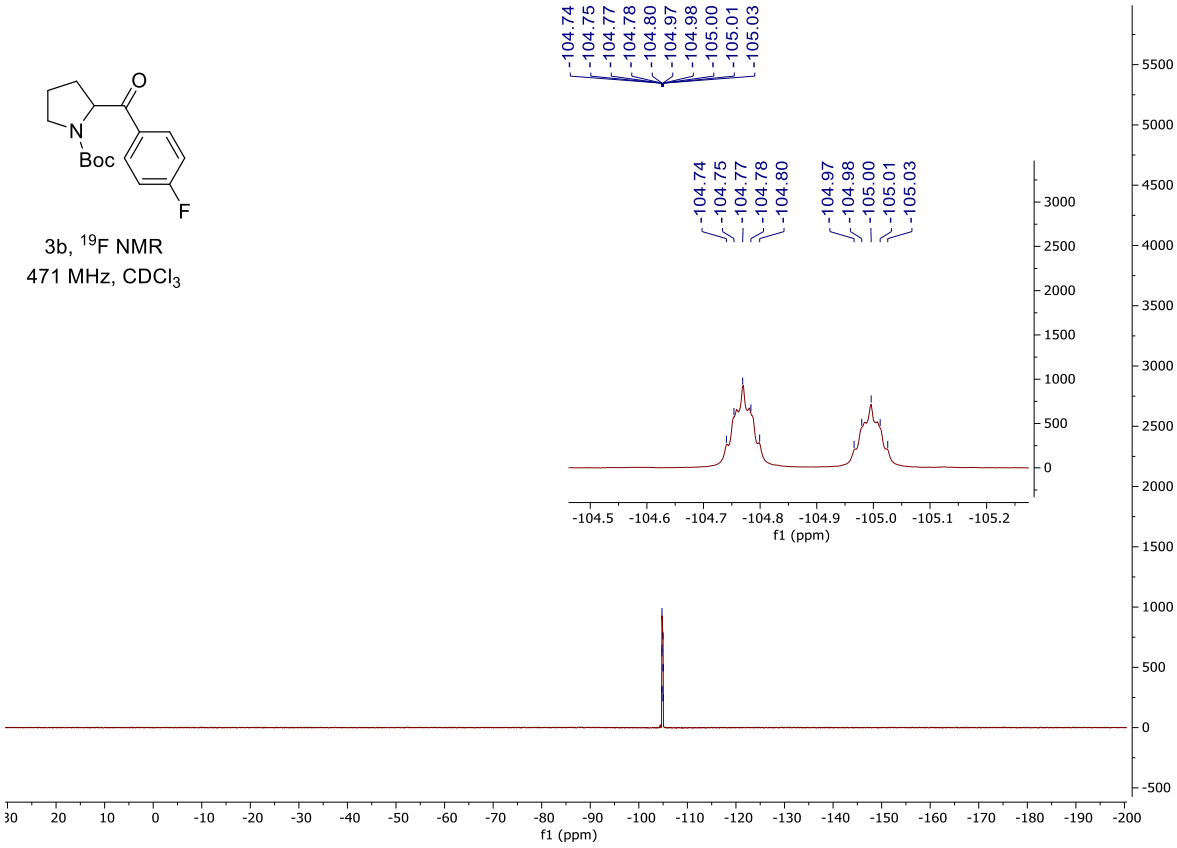
O
N
Boc
F
3b, 19F NMR
471 MHz, CDCl3
-104.74
-104.75
-104.77
-104.78
-104.80
-104.97
-104.98
-105.00
-105.01
-105.03
f1 (ppm)
f1 (ppm)

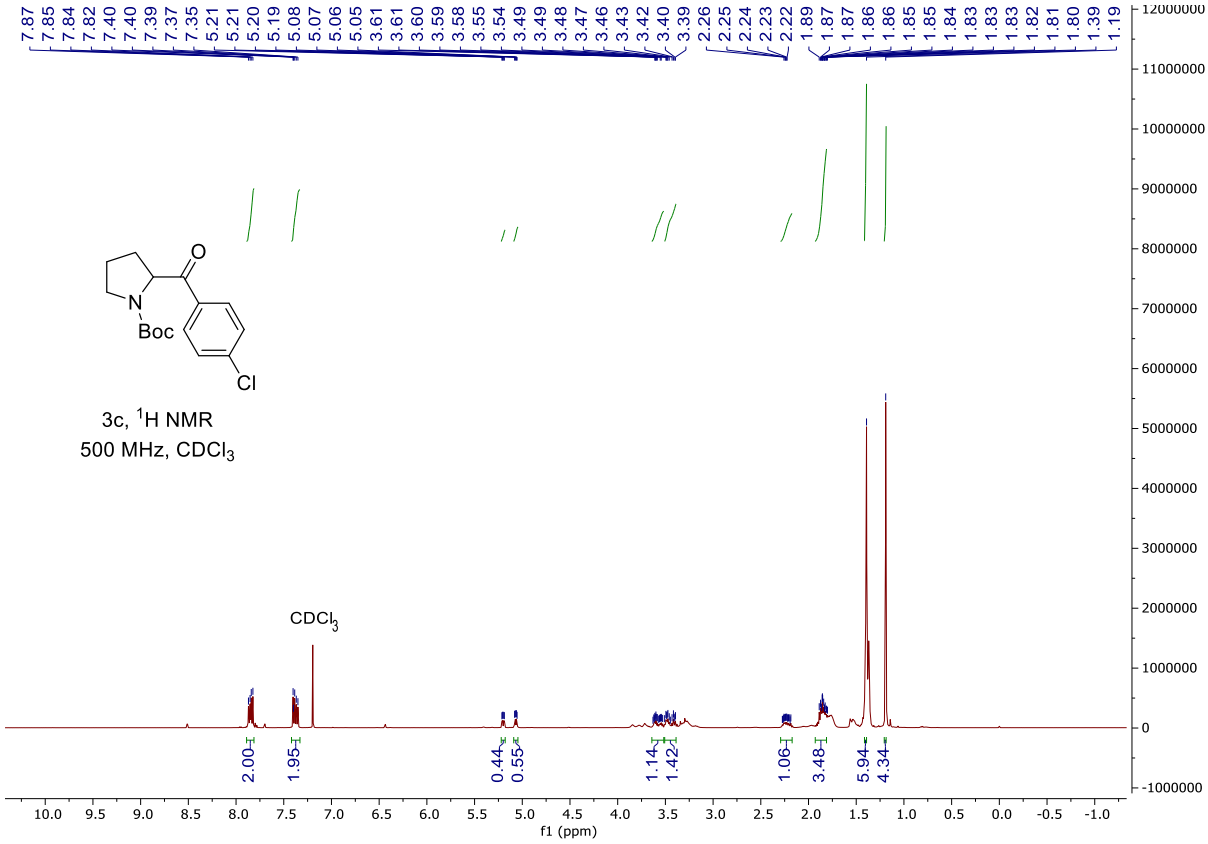
7.87 7.85 7.84 7.82 7.40 7.40 7.39 7.37 7.35 5.21 5.21 5.20 5.19 5.08 5.07 5.06 5.05 3.61 3.61 3.60 3.59 3.58 3.55 3.54 3.49 3.49 3.48 3.47 3.46 3.43 3.42 3.40 3.39 2.26 2.25 2.24 2.23 2.22 1.89 1.87 1.87 1.86 1.86 1.85 1.85 1.84 1.83 1.83 1.82 1.81 1.80 1.39 1.19
O
N
Boc
Cl
3c, 1H NMR
500 MHz, CDCl3
CDCl3
2.00 1.95 0.44 0.55 1.14 1.42 1.06 3.48 5.94 4.34
f1 (ppm)

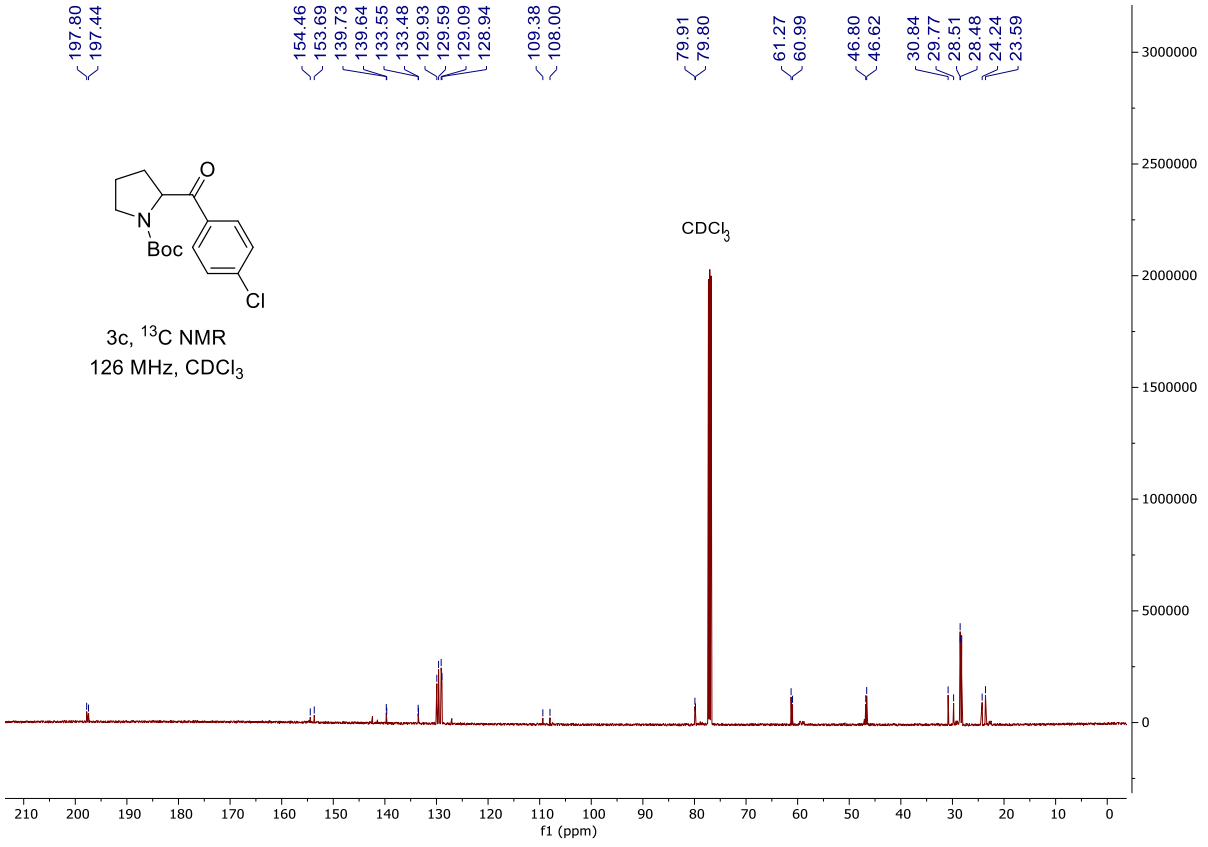
197.80 197.44 154.46 153.69 139.73 139.64 133.55 133.48 129.93 129.59 129.09 128.94 109.38 108.00 79.91 79.80 61.27 60.99 46.80 46.62 30.84 29.77 28.51 28.48 24.24 23.59
O
N
Boc
Cl
3c, 13C NMR
126 MHz, CDCl3
CDCl3
f1 (ppm)

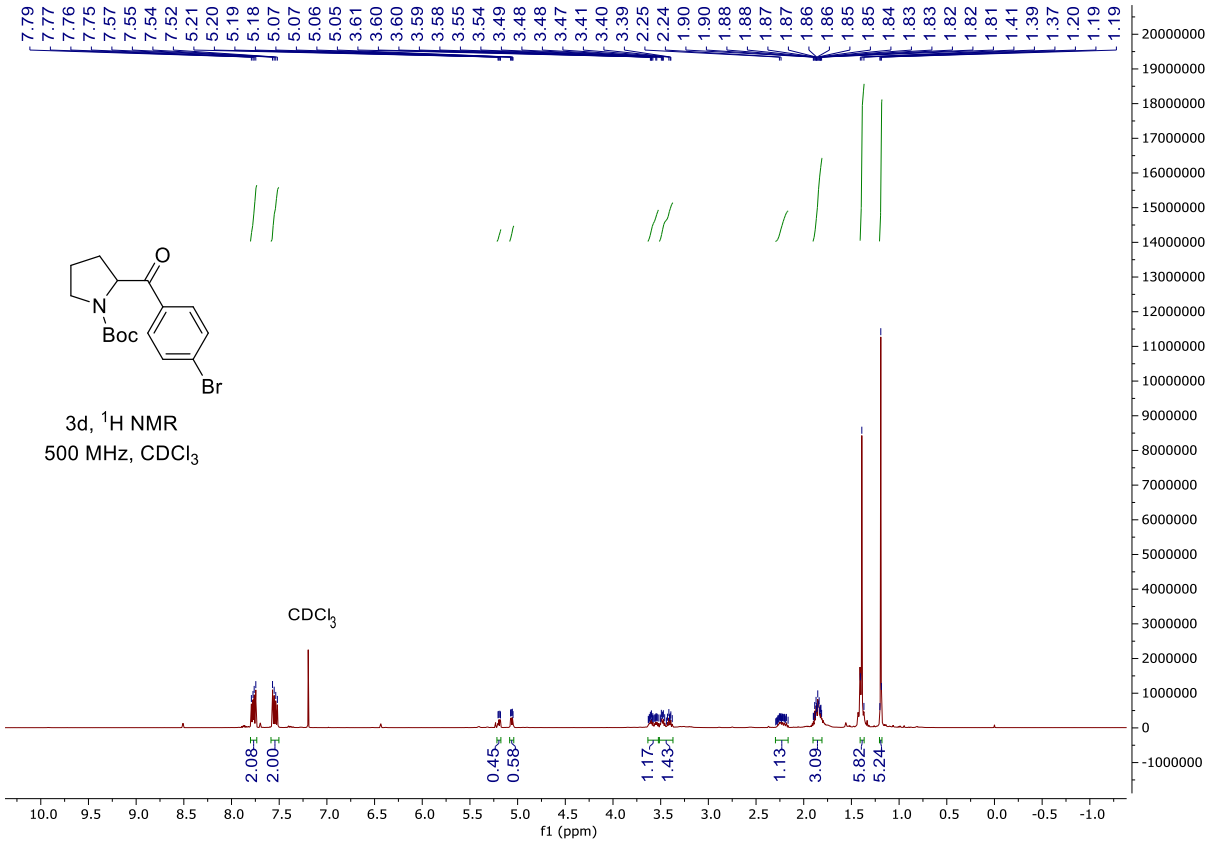
7.79 7.77 7.76 7.75 7.57 7.55 7.54 7.52 5.21 5.20 5.19 5.18 5.07 5.06 5.05 3.61 3.60 3.60 3.59 3.58 3.55 3.54 3.49 3.48 3.48 3.47 3.41 3.40 3.39 2.25 2.24 1.90 1.90 1.88 1.88 1.87 1.87 1.86 1.86 1.85 1.85 1.84 1.83 1.83 1.82 1.82 1.81 1.41 1.39 1.37 1.20 1.19 1.19
O
N
Boc
Br
3d, ^{1}H NMR
500 MHz, $CDCl_3$
$CDCl_3$
2.08 2.00 0.45 0.58 1.17 1.43 1.13 3.09 5.82 5.24
f1 (ppm)

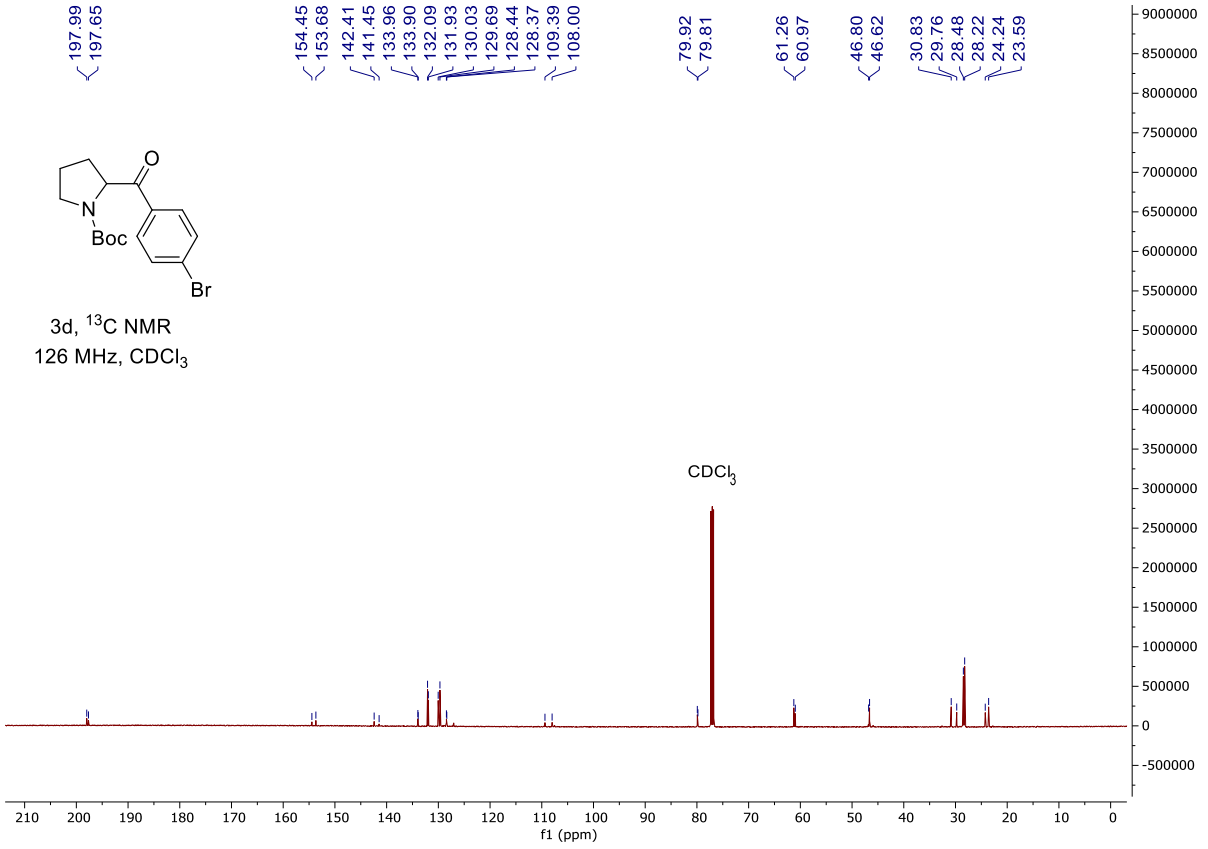
197.99 197.65 154.45 153.68 142.41 141.45 133.96 133.90 132.09 131.93 130.03 129.69 128.44 128.37 109.39 108.00 79.92 79.81 61.26 60.97 46.80 46.62 30.83 29.76 28.48 28.22 24.24 23.59
O
N
Boc
Br
3d, ^{13}C NMR
126 MHz, $CDCl_3$
$CDCl_3$
f1 (ppm)

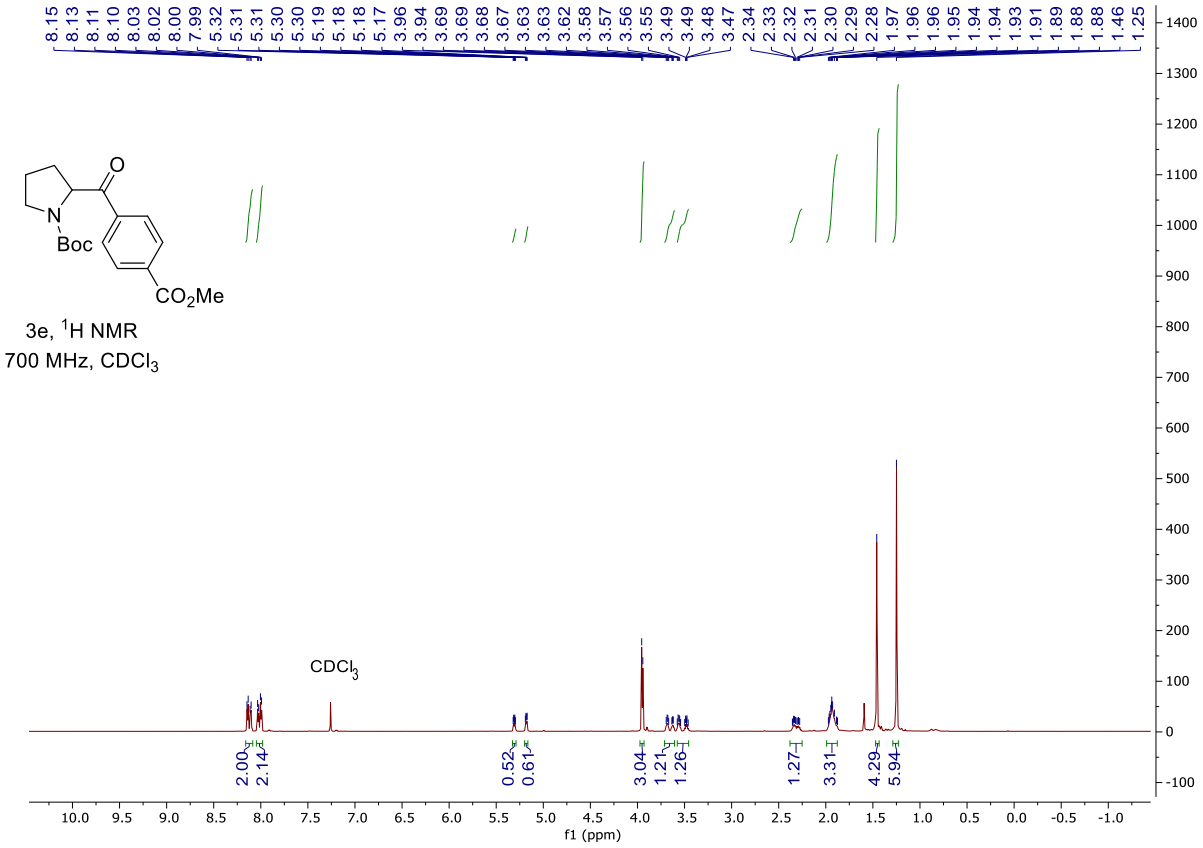

3e, ^{1}H NMR
700 MHz, $CDCl_3$

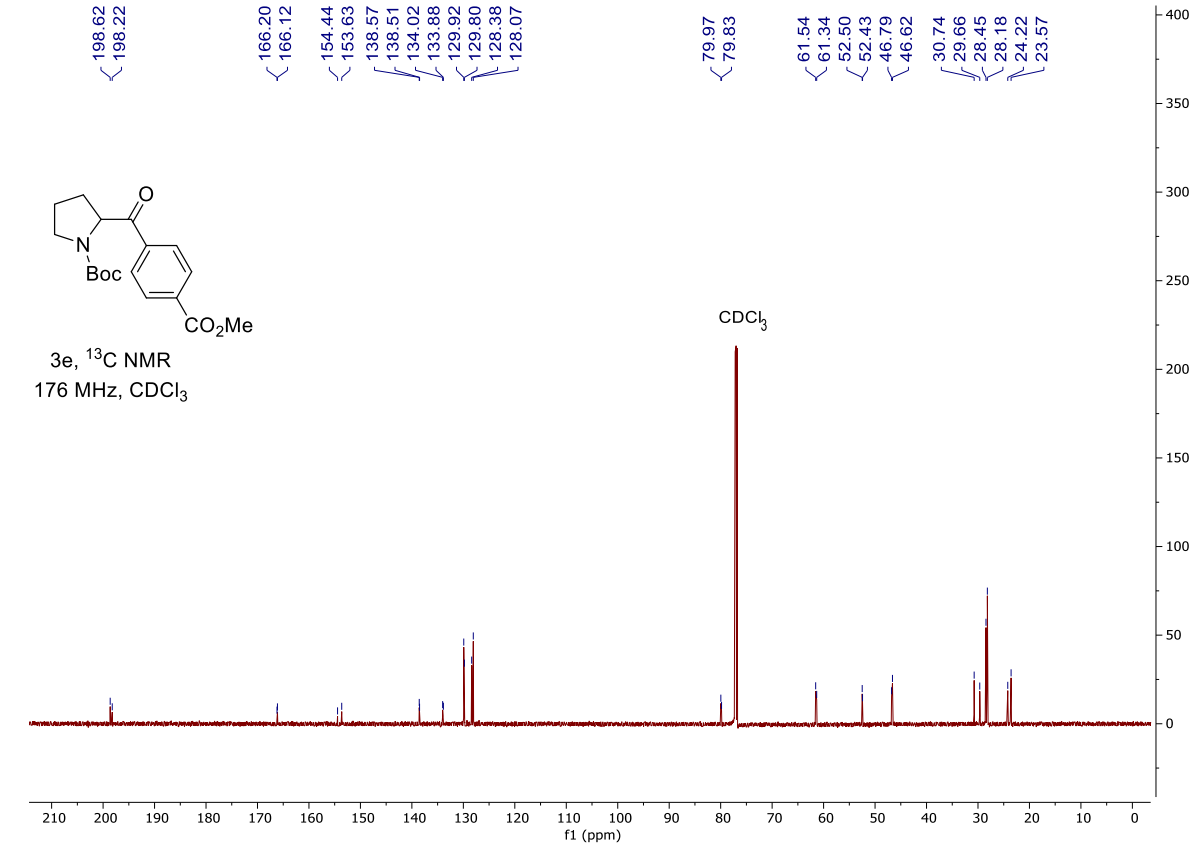

3e, ^{13}C NMR
176 MHz, $CDCl_3$

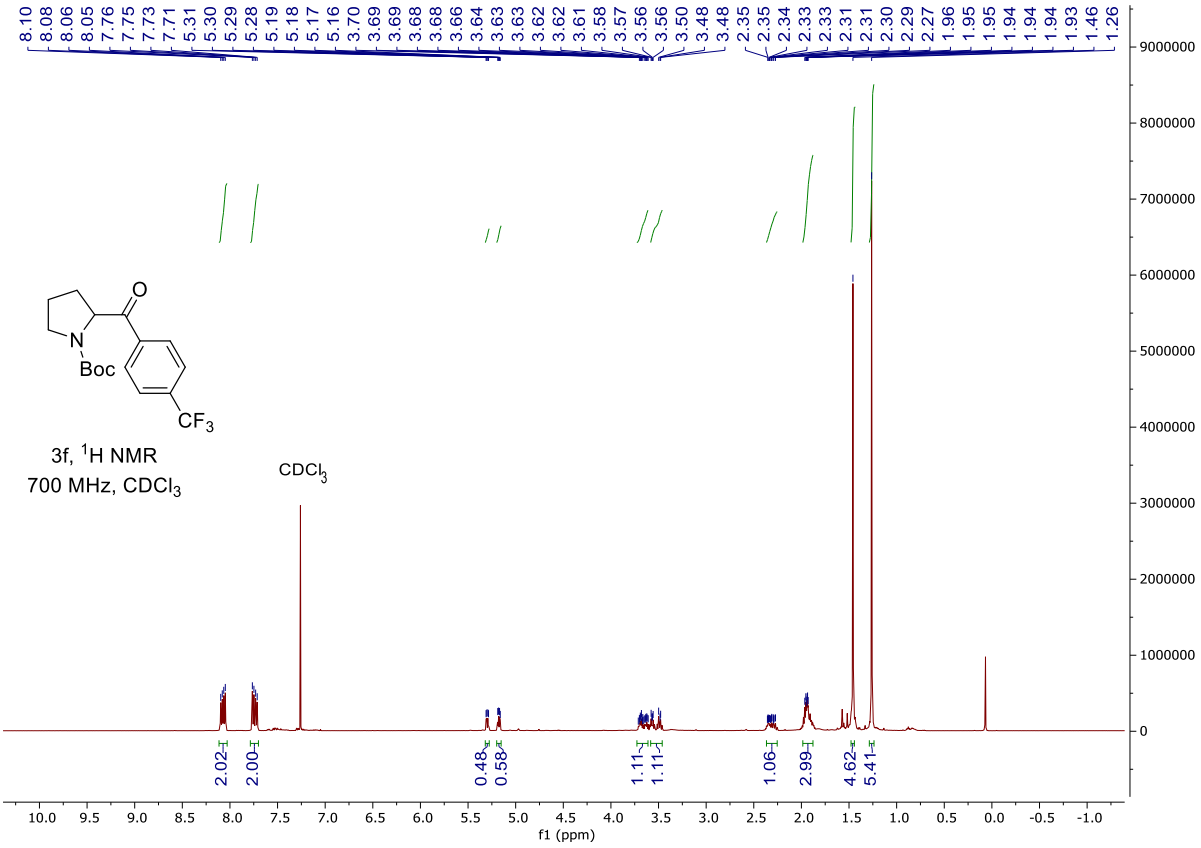
8.10 8.08 8.06 8.05 7.76 7.75 7.73 7.71 5.31 5.30 5.29 5.28 5.19 5.18 5.17 5.16 3.70 3.69 3.69 3.68 3.68 3.66 3.64 3.63 3.63 3.62 3.62 3.61 3.58 3.57 3.56 3.56 3.50 3.48 3.48 2.35 2.35 2.34 2.33 2.31 2.31 2.30 2.29 2.27 1.96 1.95 1.95 1.94 1.94 1.94 1.93 1.46 1.26
O
N
Boc
CF3
3f, 1H NMR
700 MHz, CDCl3
CDCl3
2.02 2.00 0.48 0.58 1.11 1.11 1.06 2.99 4.62 5.41
f1 (ppm)

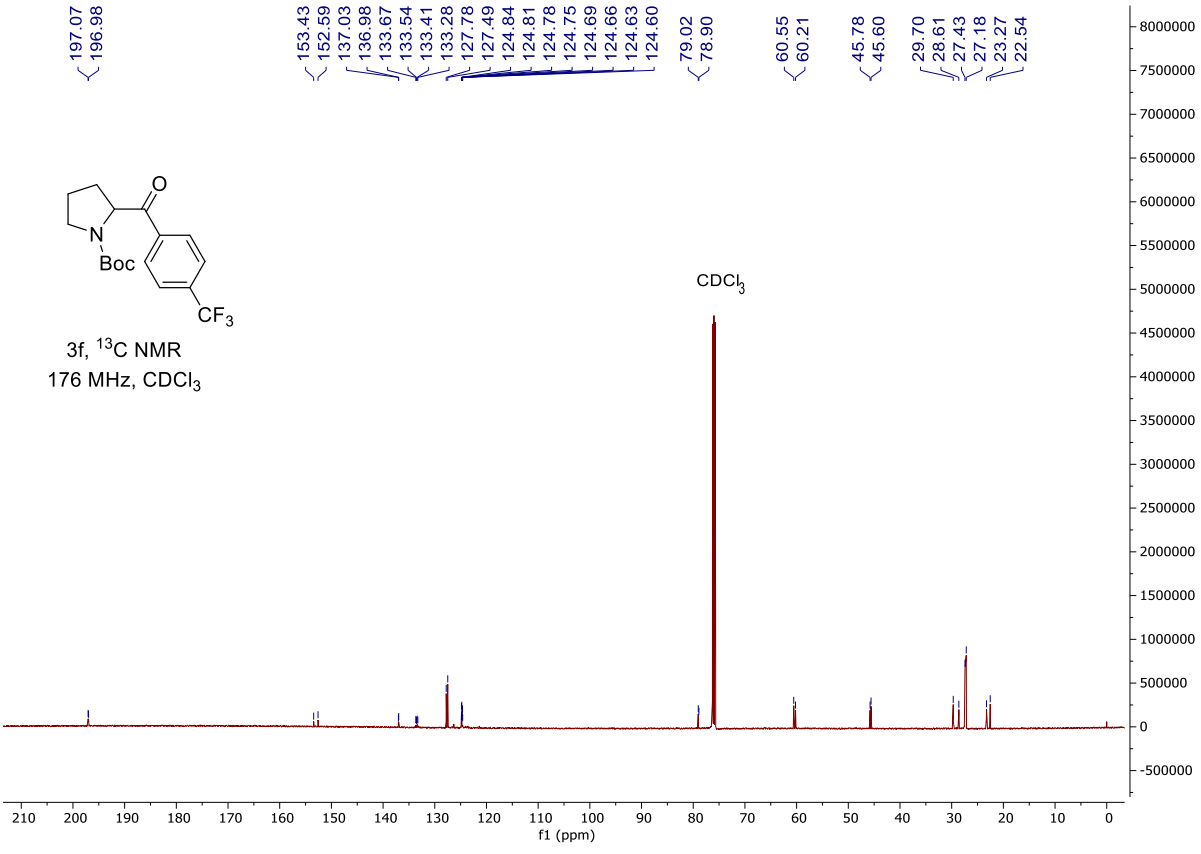
197.07 196.98 153.43 152.59 137.03 136.98 133.67 133.54 133.41 133.28 127.78 127.49 124.84 124.81 124.78 124.75 124.69 124.66 124.63 124.60 79.02 78.90 60.55 60.21 45.78 45.60 29.70 28.61 27.43 27.18 23.27 22.54
O
N
Boc
CF3
3f, 13C NMR
176 MHz, CDCl3
CDCl3
f1 (ppm)

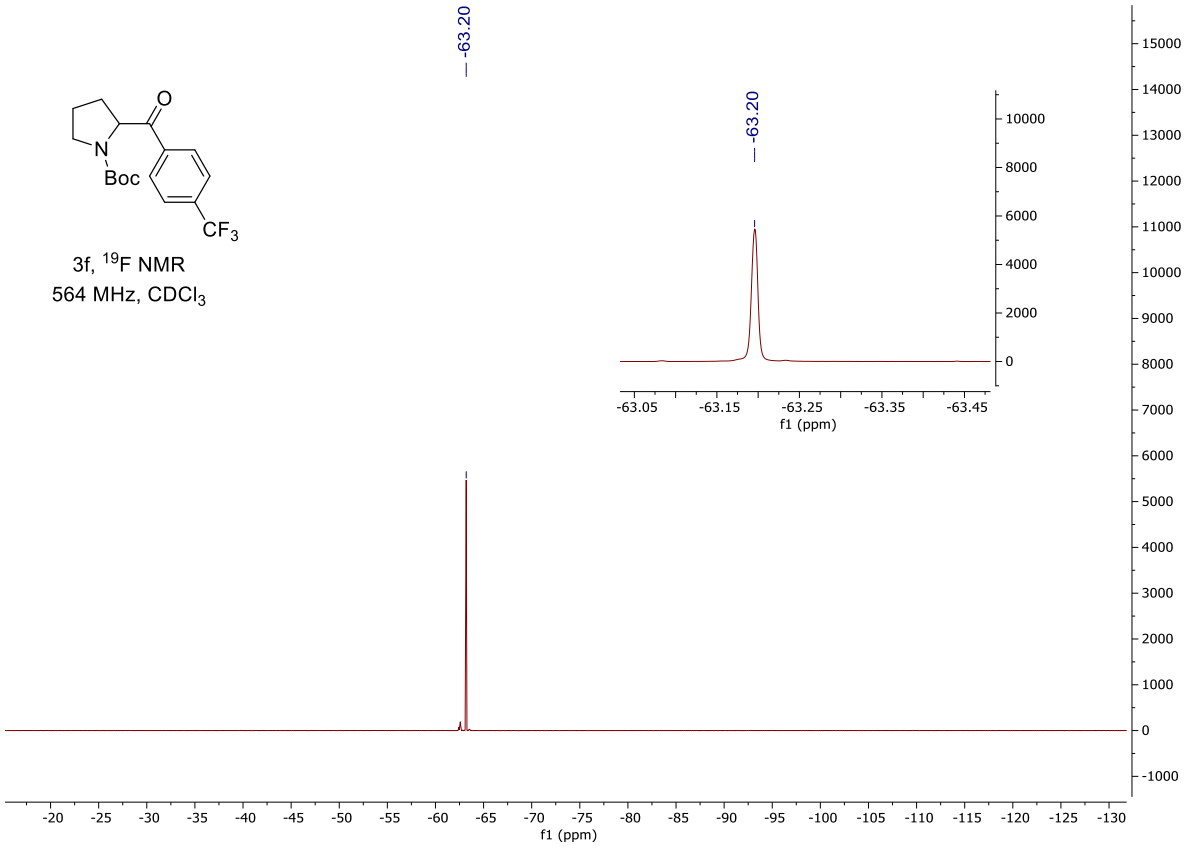
-63.20
O
N
Boc
CF3
3f, 19F NMR
564 MHz, CDCl3
-63.20
f1 (ppm)
f1 (ppm)

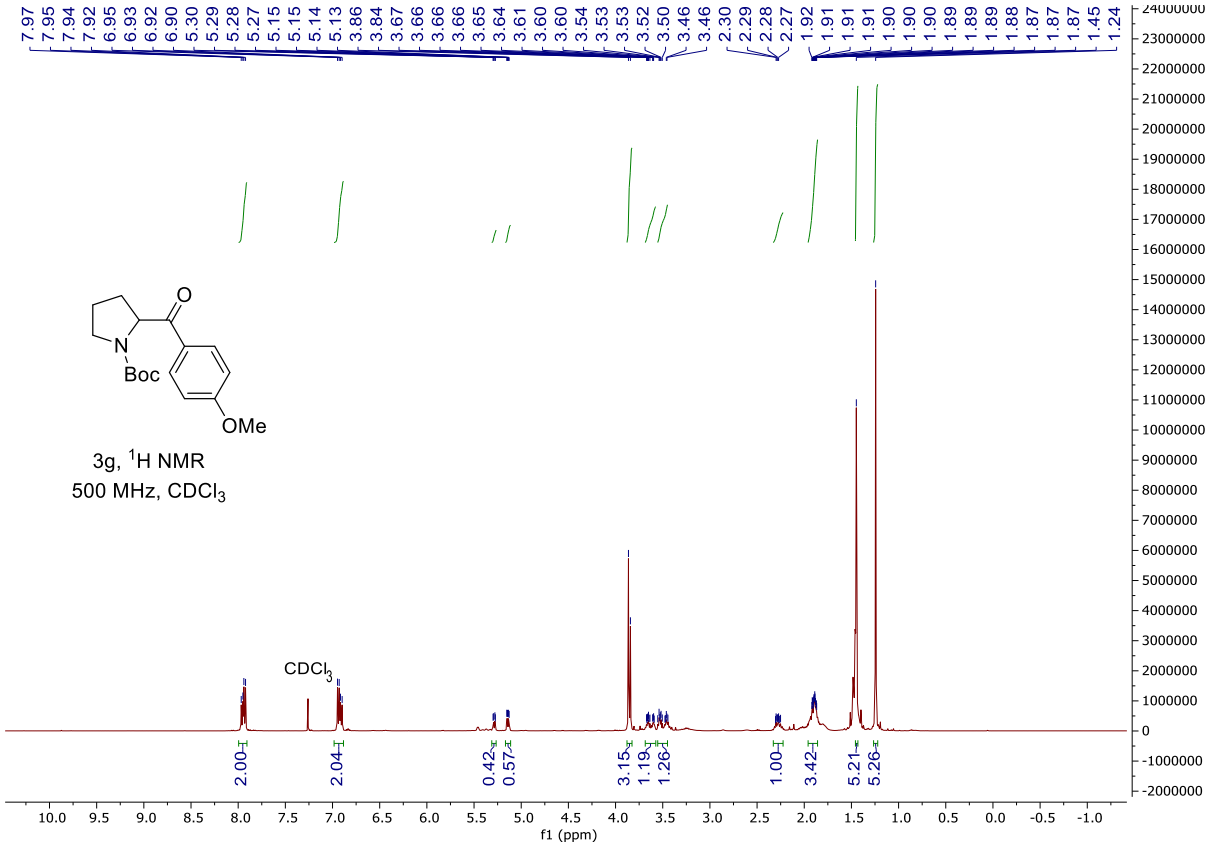
7.97 7.95 7.94 7.92 6.95 6.93 6.92 6.90 5.30 5.29 5.28 5.27 5.15 5.15 5.14 5.13 3.86 3.84 3.67 3.66 3.66 3.66 3.65 3.64 3.61 3.60 3.60 3.54 3.53 3.53 3.52 3.50 3.46 3.46 2.30 2.29 2.28 2.27 1.92 1.91 1.91 1.91 1.90 1.90 1.90 1.89 1.89 1.89 1.88 1.87 1.87 1.87 1.45 1.24
O
N
Boc
OMe
3g, ^{1}H NMR
500 MHz, $CDCl_3$
$CDCl_3$
2.00 2.04 0.42 0.57 3.15 1.19 1.26 1.00 3.42 5.21 5.26
f1 (ppm)

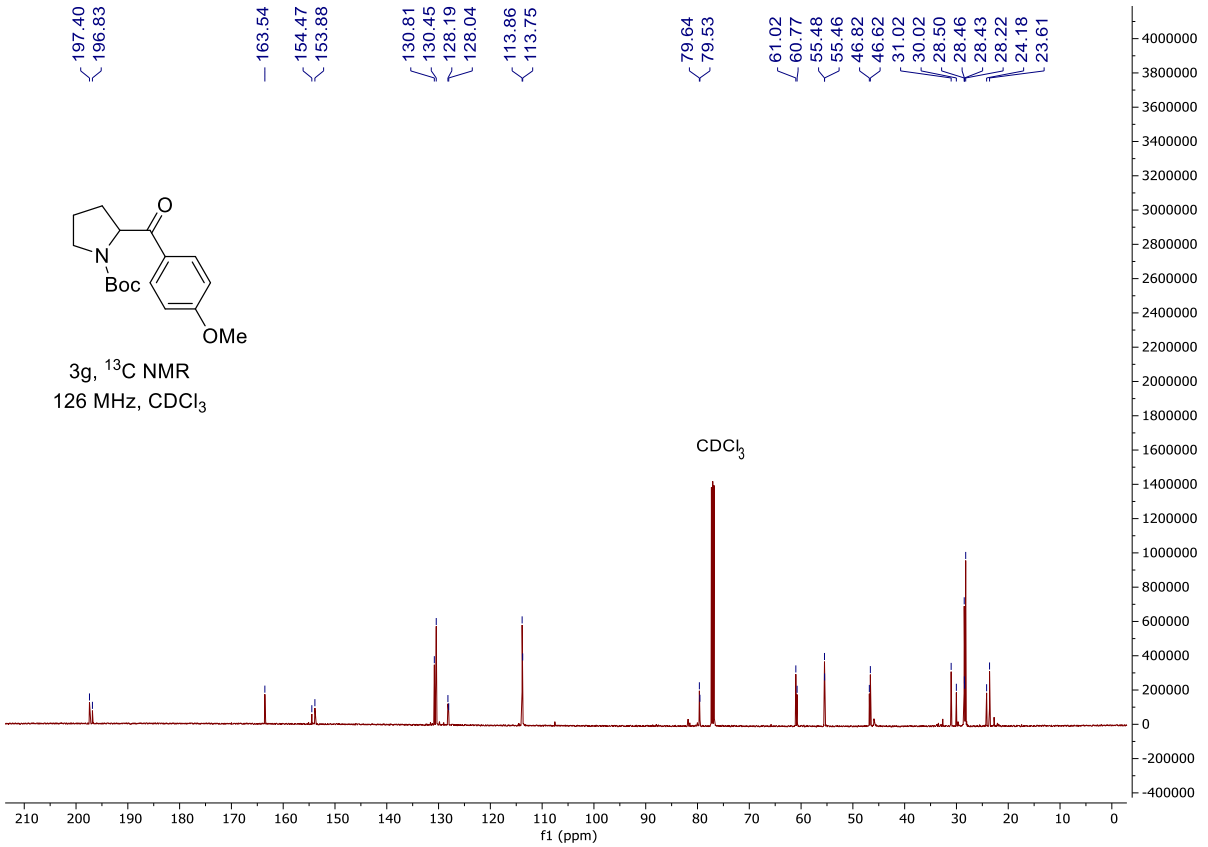
197.40 196.83 163.54 154.47 153.88 130.81 130.45 128.19 128.04 113.86 113.75 79.64 79.53 61.02 60.77 55.48 55.46 46.82 46.62 31.02 30.02 28.50 28.46 28.43 28.22 24.18 23.61
O
N
Boc
OMe
3g, ^{13}C NMR
126 MHz, $CDCl_3$
$CDCl_3$
f1 (ppm)

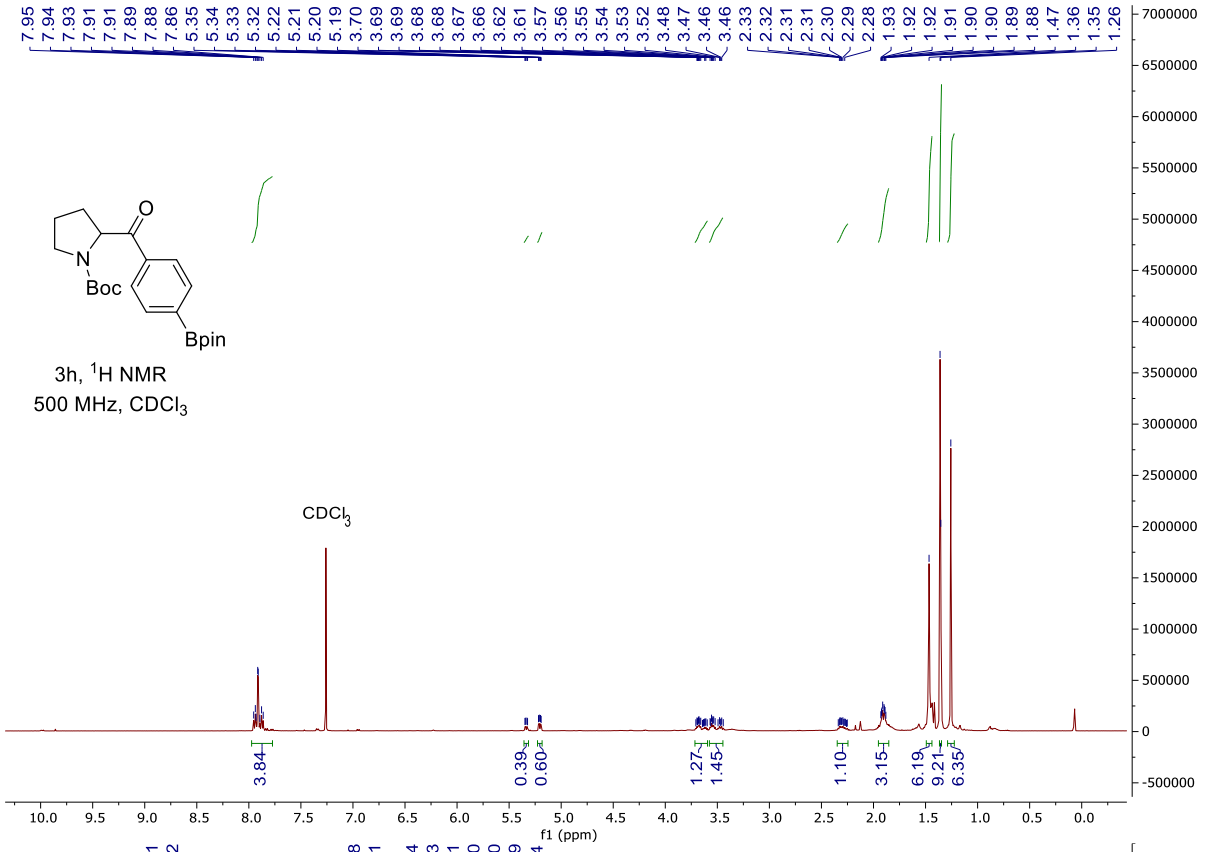
7.95 7.94 7.93 7.91 7.91 7.89 7.88 7.86 5.35 5.34 5.33 5.32 5.22 5.21 5.20 5.19 3.70 3.69 3.69 3.68 3.68 3.67 3.66 3.62 3.61 3.57 3.56 3.55 3.54 3.53 3.52 3.48 3.47 3.46 3.46 2.33 2.32 2.31 2.31 2.30 2.29 2.28 1.93 1.92 1.92 1.91 1.90 1.89 1.88 1.47 1.36 1.35 1.26
O
N
Boc
Bpin
3h, 1H NMR
500 MHz, CDCl3
CDCl3
3.84 0.39 0.60 1.27 1.45 1.10 3.15 6.19 9.21 6.35
f1 (ppm)

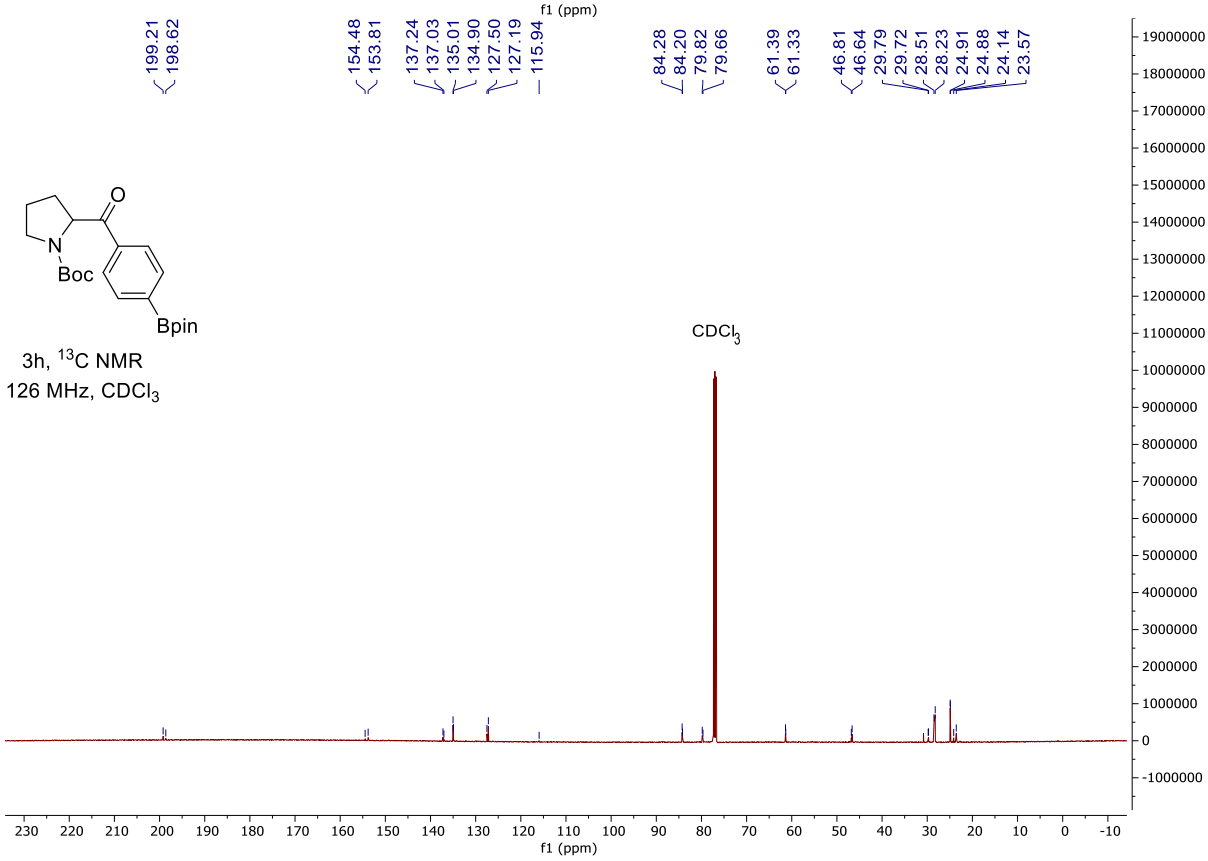
199.21 198.62 154.48 153.81 137.24 137.03 135.01 134.90 127.50 127.19 115.94 84.28 84.20 79.82 79.66 61.39 61.33 46.81 46.64 29.79 29.72 28.51 28.23 24.91 24.88 24.14 23.57
O
N
Boc
Bpin
3h, 13C NMR
126 MHz, CDCl3
CDCl3
f1 (ppm)

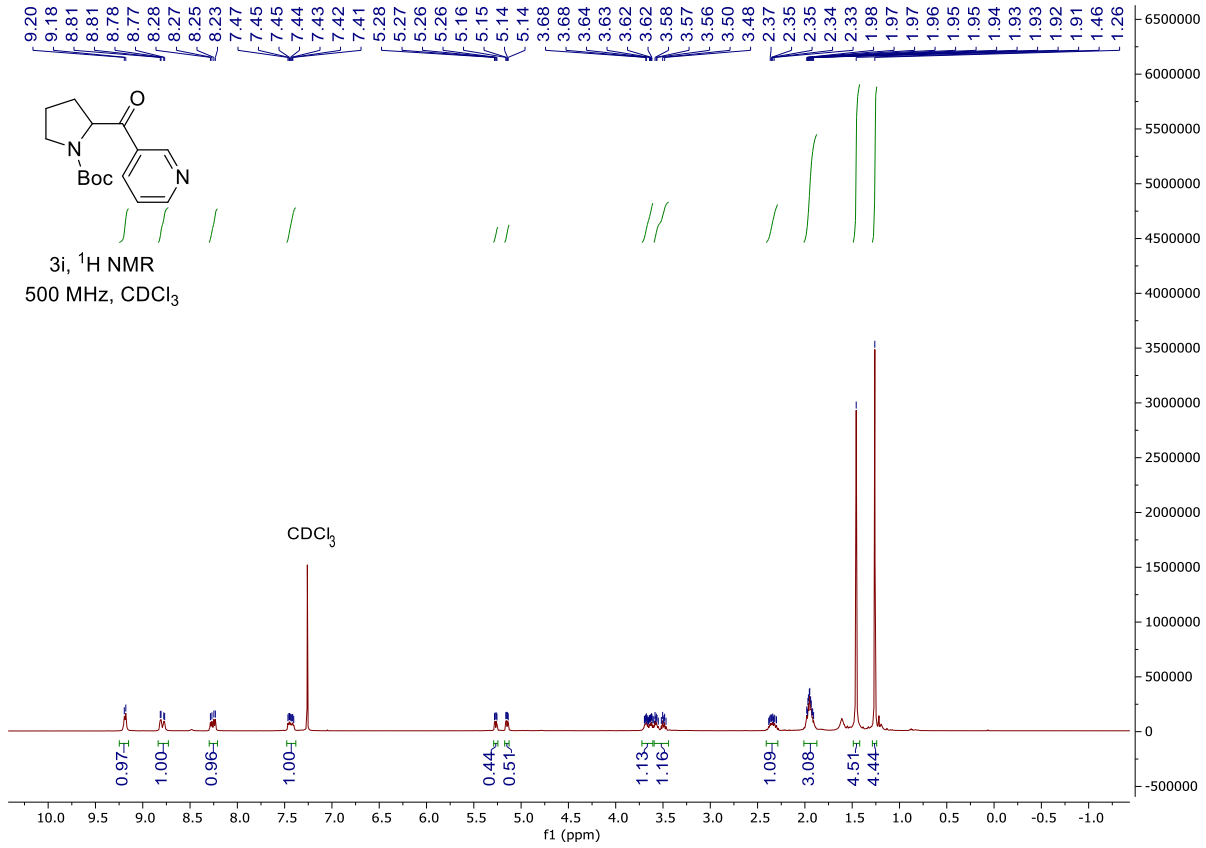
9.20 9.18 8.81 8.81 8.78 8.77 8.28 8.27 8.25 8.23 7.47 7.45 7.45 7.44 7.43 7.42 7.41 5.28 5.27 5.26 5.26 5.16 5.15 5.14 5.14 3.68 3.68 3.64 3.63 3.62 3.62 3.58 3.57 3.56 3.50 3.48 2.37 2.35 2.35 2.34 2.33 1.98 1.97 1.97 1.96 1.95 1.95 1.94 1.93 1.93 1.92 1.91 1.46 1.26
O
N
Boc
N
3i, ^{1}H NMR
500 MHz, $CDCl_3$
$CDCl_3$
0.97 1.00 0.96 1.00 0.44 0.51 1.13 1.16 1.09 3.08 4.51 4.44
f1 (ppm)

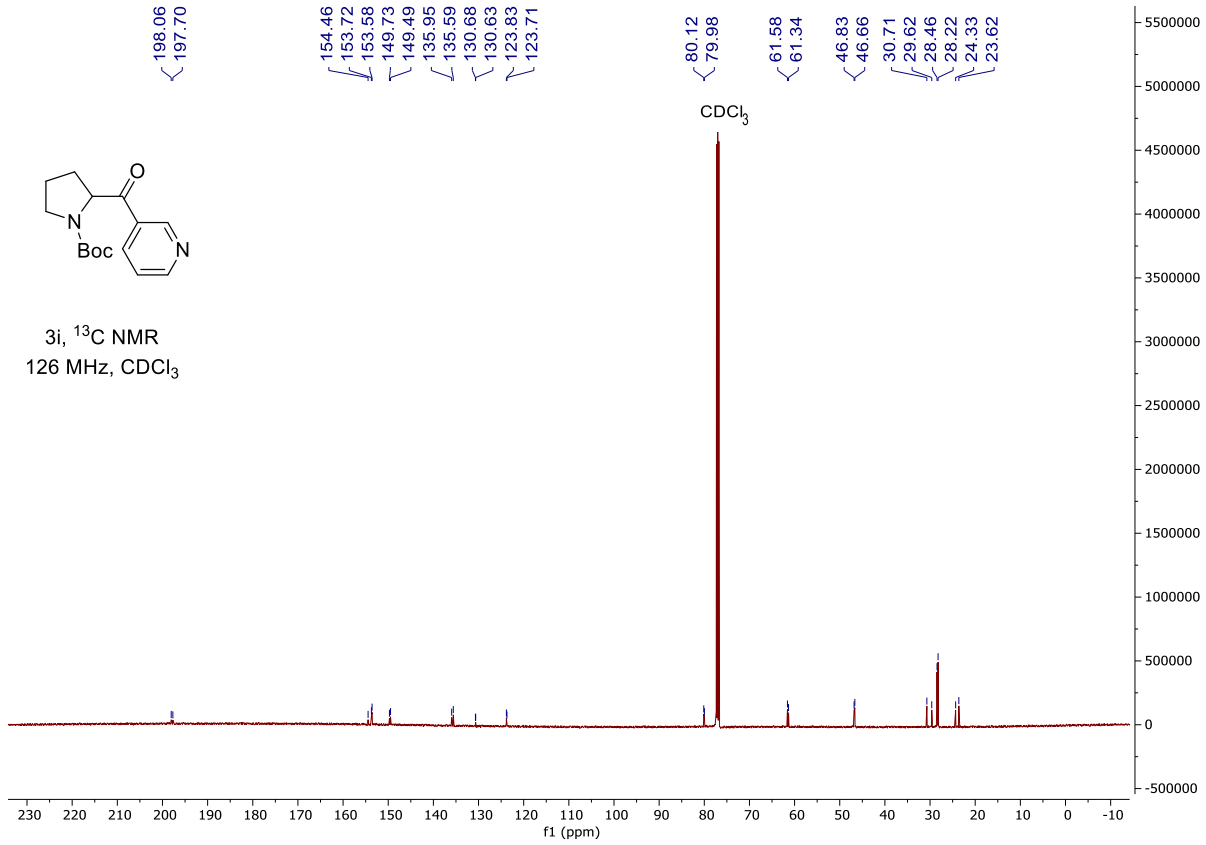
198.06 197.70 154.46 153.72 153.58 149.73 149.49 135.95 135.59 130.68 130.63 123.83 123.71 80.12 79.98 61.58 61.34 46.83 46.66 30.71 29.62 28.46 28.22 24.33 23.62
$CDCl_3$
O
N
Boc
N
3i, ^{13}C NMR
126 MHz, $CDCl_3$
f1 (ppm)

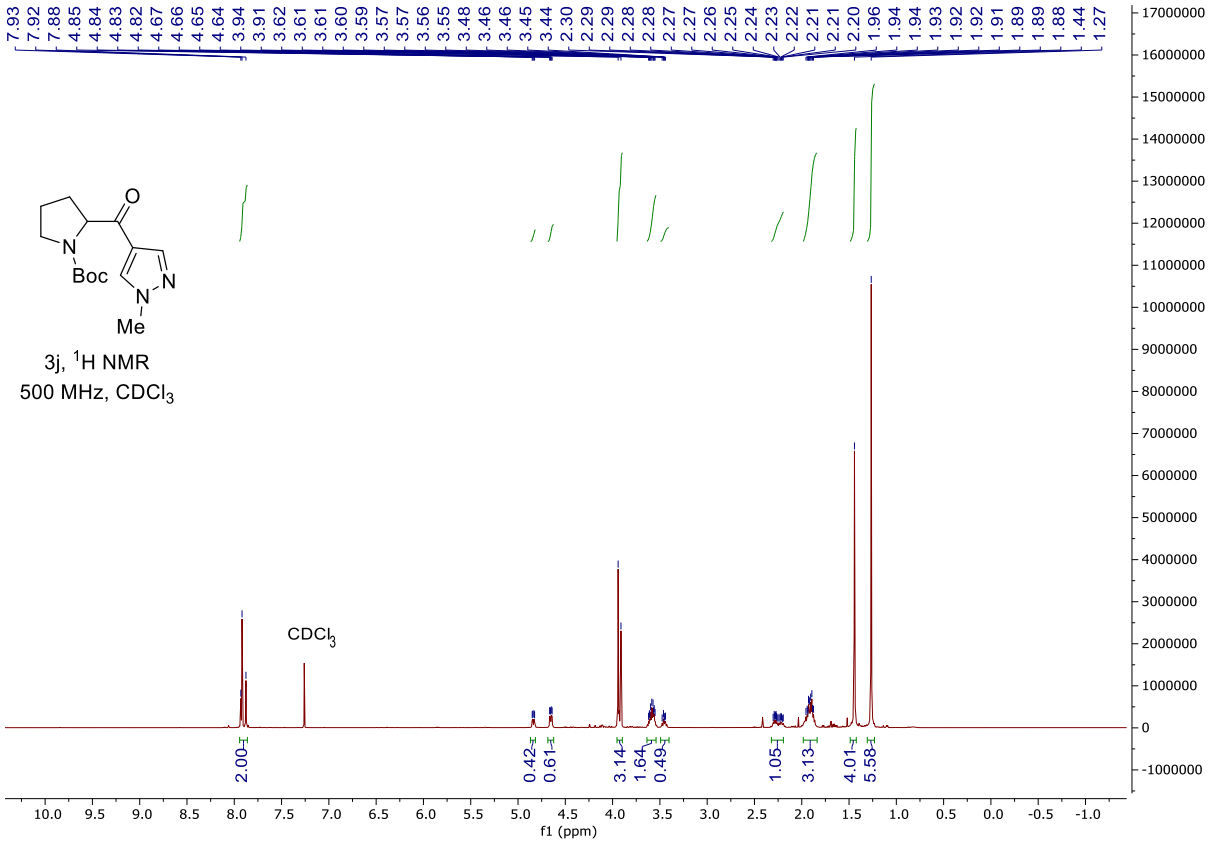

3j, ^{1}H NMR
500 MHz, $CDCl_3$

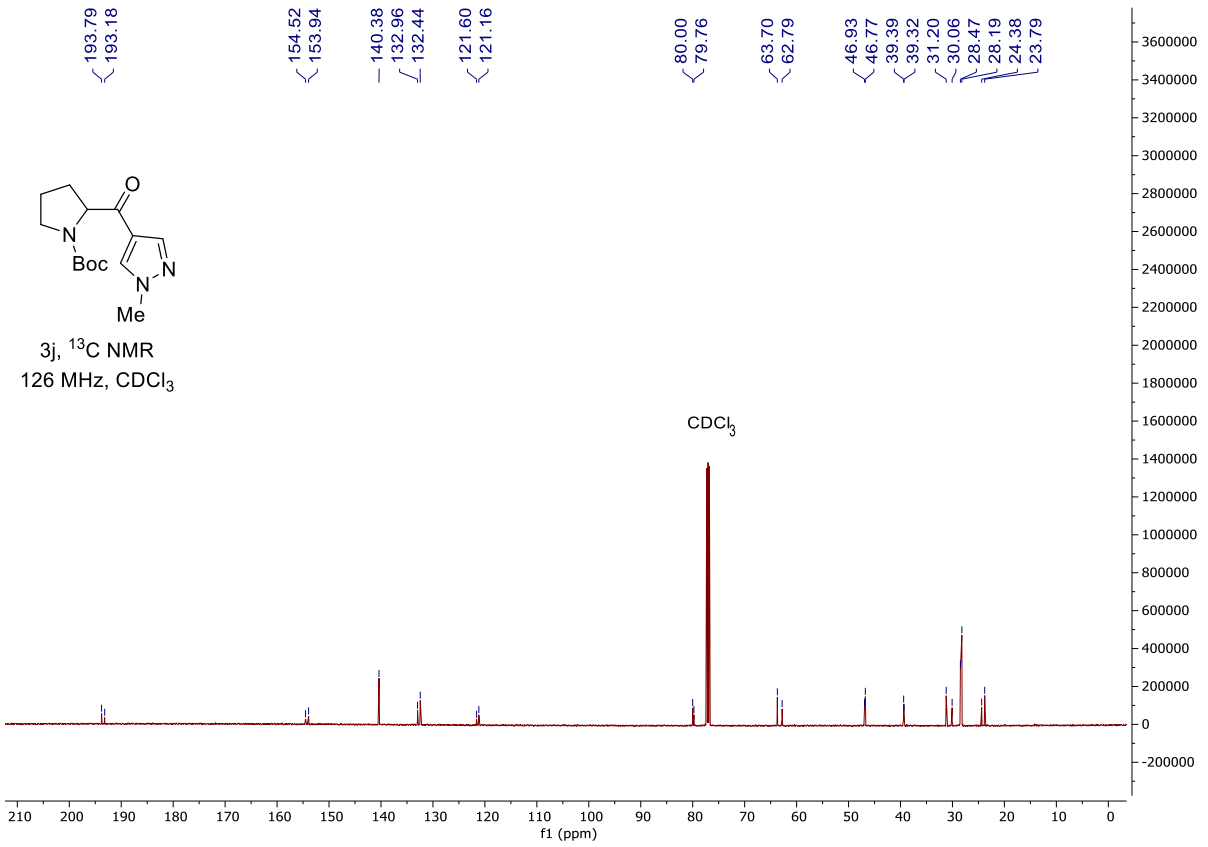

3j, ^{13}C NMR
126 MHz, $CDCl_3$

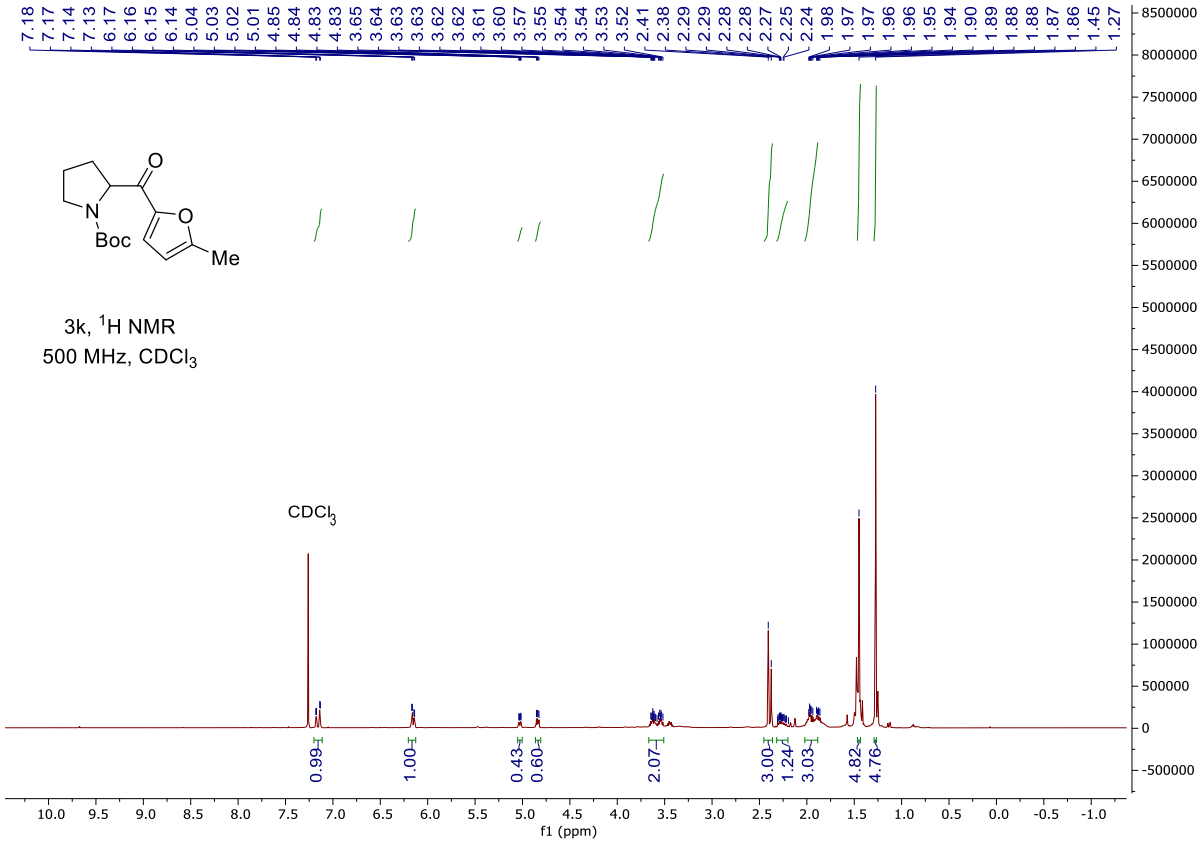
7.18 7.17 7.14 7.13 6.17 6.16 6.15 6.14 5.04 5.03 5.02 5.01 4.85 4.84 4.83 4.83 3.65 3.64 3.63 3.63 3.62 3.62 3.61 3.60 3.57 3.55 3.54 3.54 3.53 3.52 2.41 2.38 2.29 2.29 2.28 2.28 2.27 2.25 2.24 1.98 1.97 1.97 1.96 1.96 1.95 1.94 1.90 1.89 1.88 1.88 1.87 1.86 1.45 1.27
O
N
Boc
O
Me
3k, ^{1}H NMR
500 MHz, $CDCl_3$
$CDCl_3$
0.99 1.00 0.43 0.60 2.07 3.00 1.24 3.03 4.82 4.76
f1 (ppm)

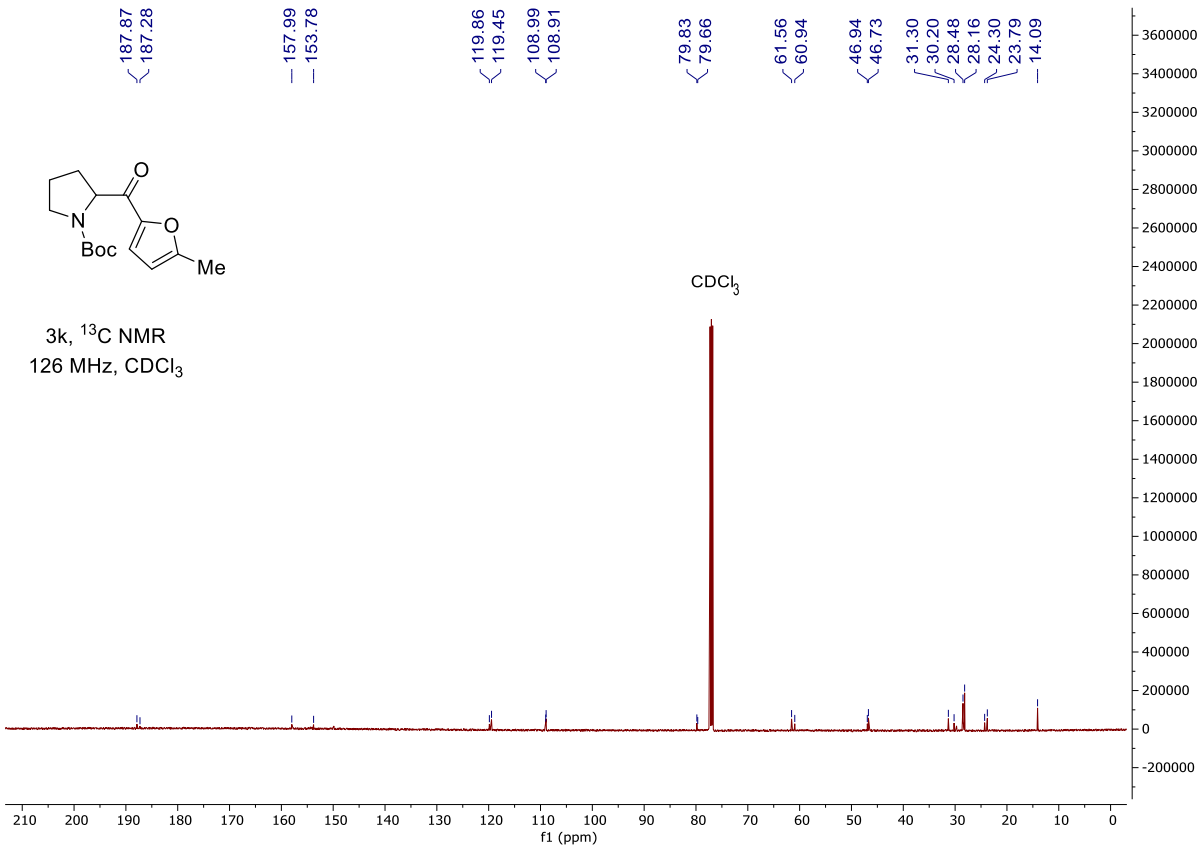
187.87 187.28 157.99 153.78 119.86 119.45 108.99 108.91 79.83 79.66 61.56 60.94 46.94 46.73 31.30 30.20 28.48 28.16 24.30 23.79 14.09
O
N
Boc
O
Me
3k, ^{13}C NMR
126 MHz, $CDCl_3$
$CDCl_3$
f1 (ppm)

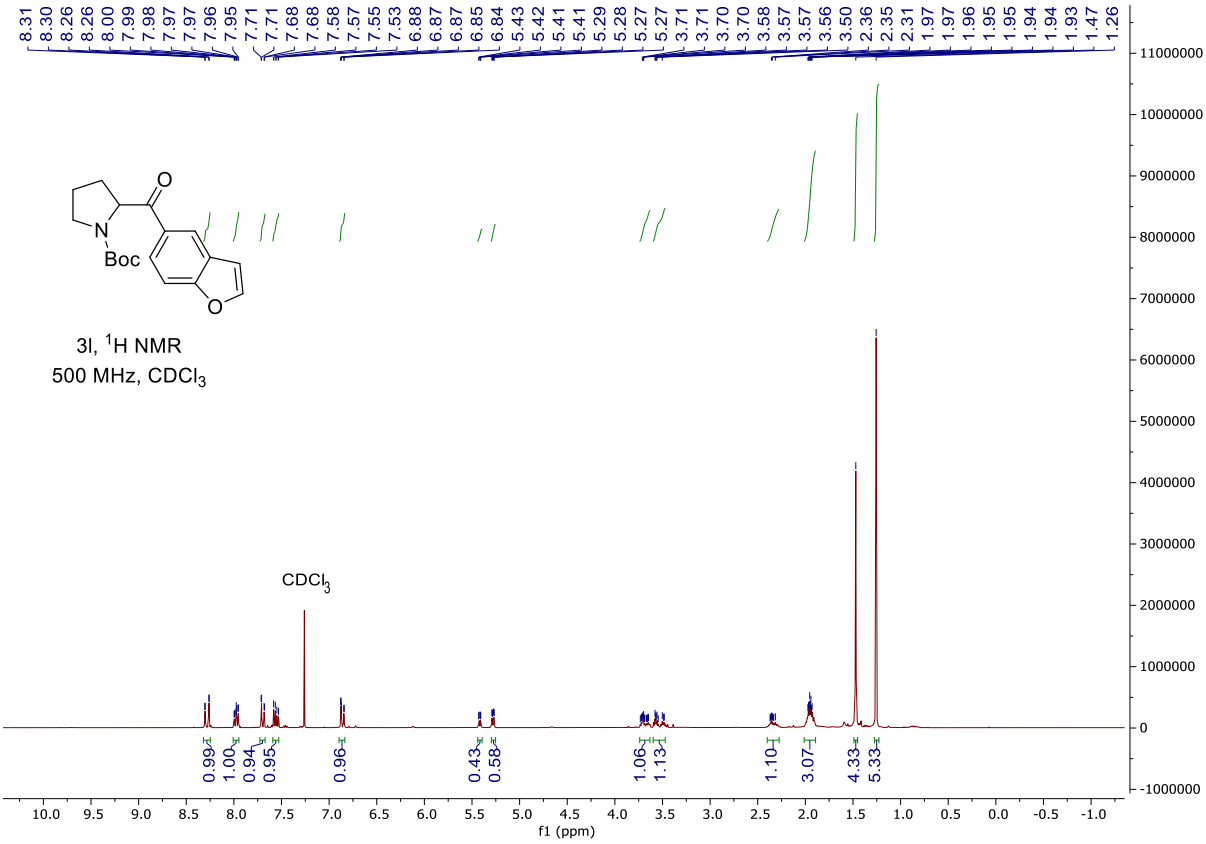
8.31 8.30 8.26 8.26 8.00 7.99 7.98 7.97 7.97 7.96 7.95 7.71 7.71 7.68 7.68 7.58 7.57 7.55 7.53 6.88 6.87 6.87 6.85 6.84 5.43 5.42 5.41 5.41 5.29 5.28 5.27 5.27 3.71 3.71 3.70 3.70 3.58 3.57 3.57 3.56 3.50 2.36 2.35 2.31 1.97 1.97 1.96 1.95 1.95 1.94 1.94 1.93 1.47 1.26
O
N
Boc
O
3l, ^{1}H NMR
500 MHz, $CDCl_3$
$CDCl_3$
0.99 1.00 0.94 0.95 0.96 0.43 0.58 1.06 1.13 1.10 3.07 4.33 5.33
f1 (ppm)

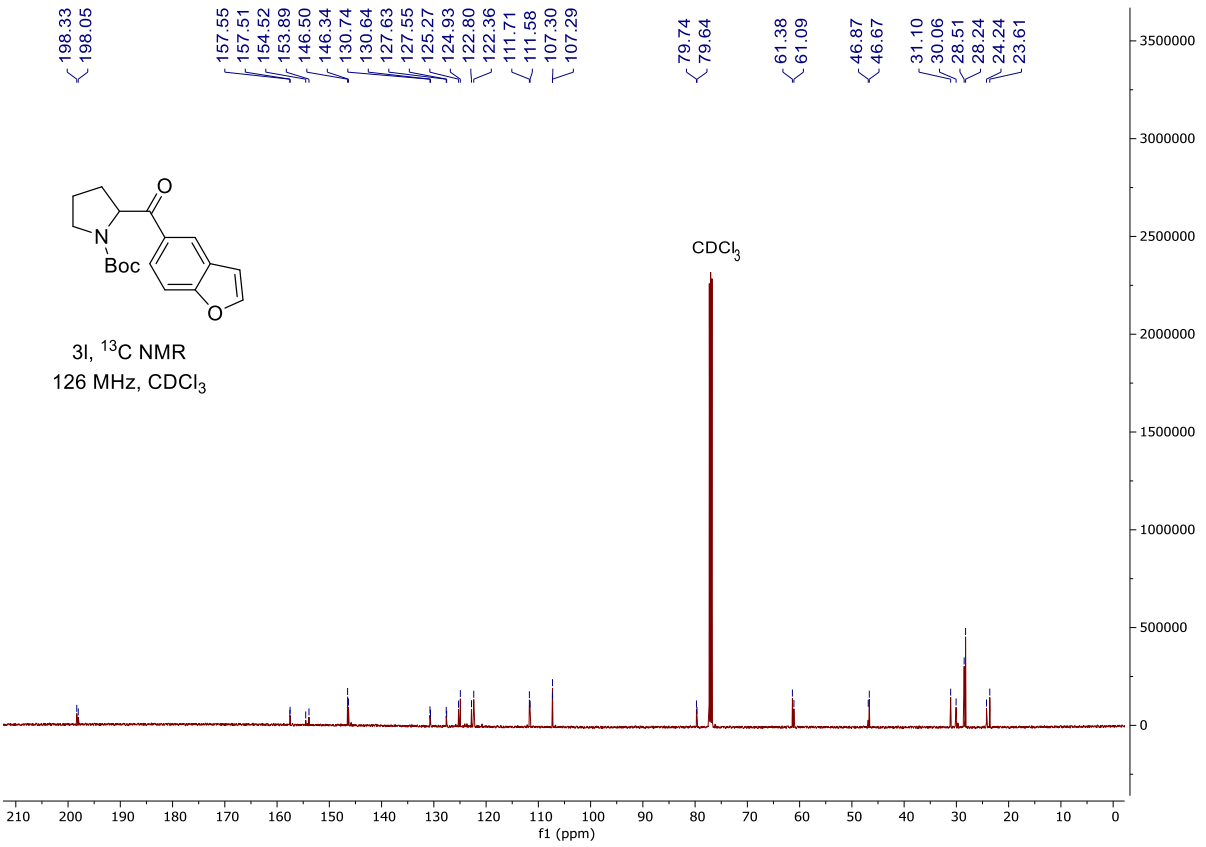
198.33 198.05 157.55 157.51 154.52 153.89 146.50 146.34 130.74 130.64 127.63 127.55 125.27 124.93 122.80 122.36 111.71 111.58 107.30 107.29 79.74 79.64 61.38 61.09 46.87 46.67 31.10 30.06 28.51 28.24 24.24 23.61
O
N
Boc
O
3l, ^{13}C NMR
126 MHz, $CDCl_3$
$CDCl_3$
f1 (ppm)

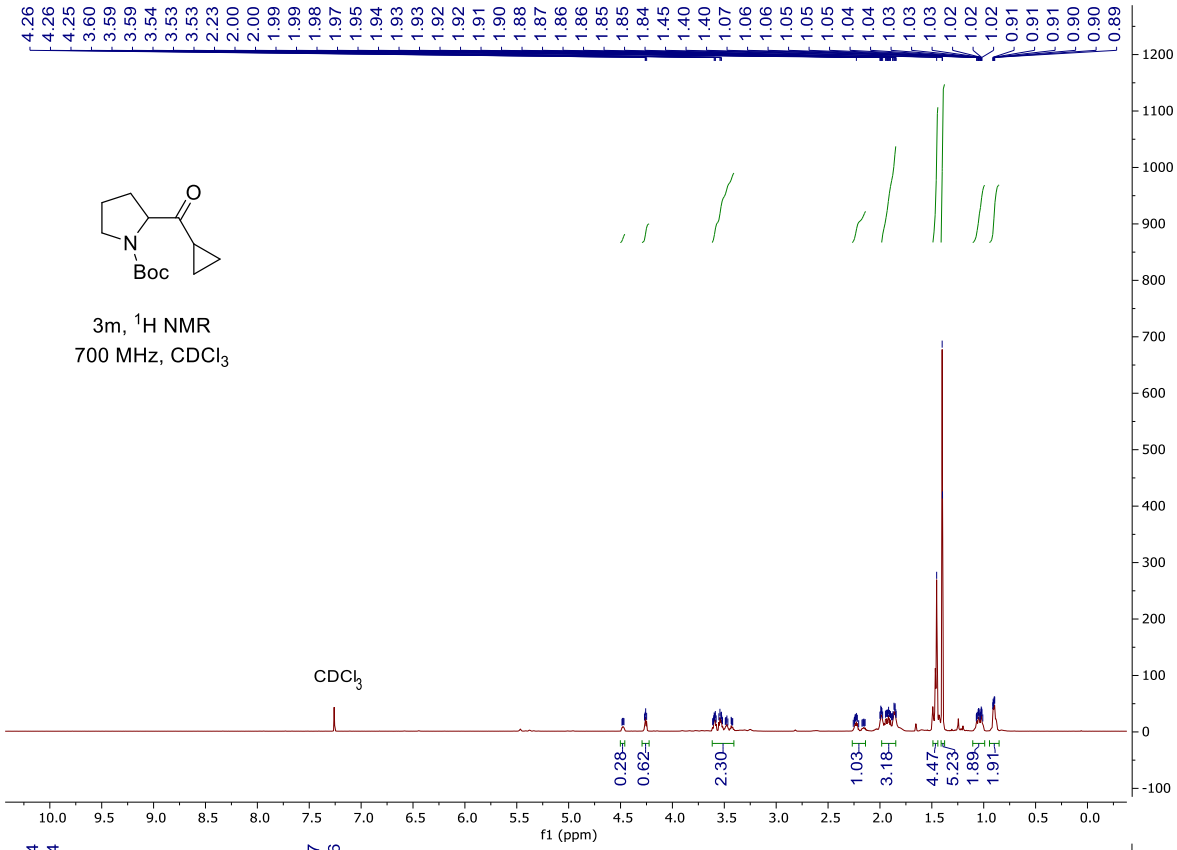
4.26 4.26 4.25 3.60 3.59 3.59 3.54 3.53 3.53 2.23 2.00 2.00 1.99 1.99 1.98 1.97 1.95 1.94 1.93 1.93 1.92 1.92 1.91 1.90 1.88 1.87 1.86 1.86 1.85 1.85 1.84 1.45 1.40 1.40 1.07 1.06 1.06 1.05 1.05 1.05 1.04 1.04 1.03 1.03 1.03 1.02 1.02 1.02 0.91 0.91 0.91 0.90 0.90 0.89
O
N
Boc
3m, 1H NMR
700 MHz, CDCl3
CDCl3
0.28 0.62 2.30 1.03 3.18 4.47 5.23 1.89 1.91
f1 (ppm)

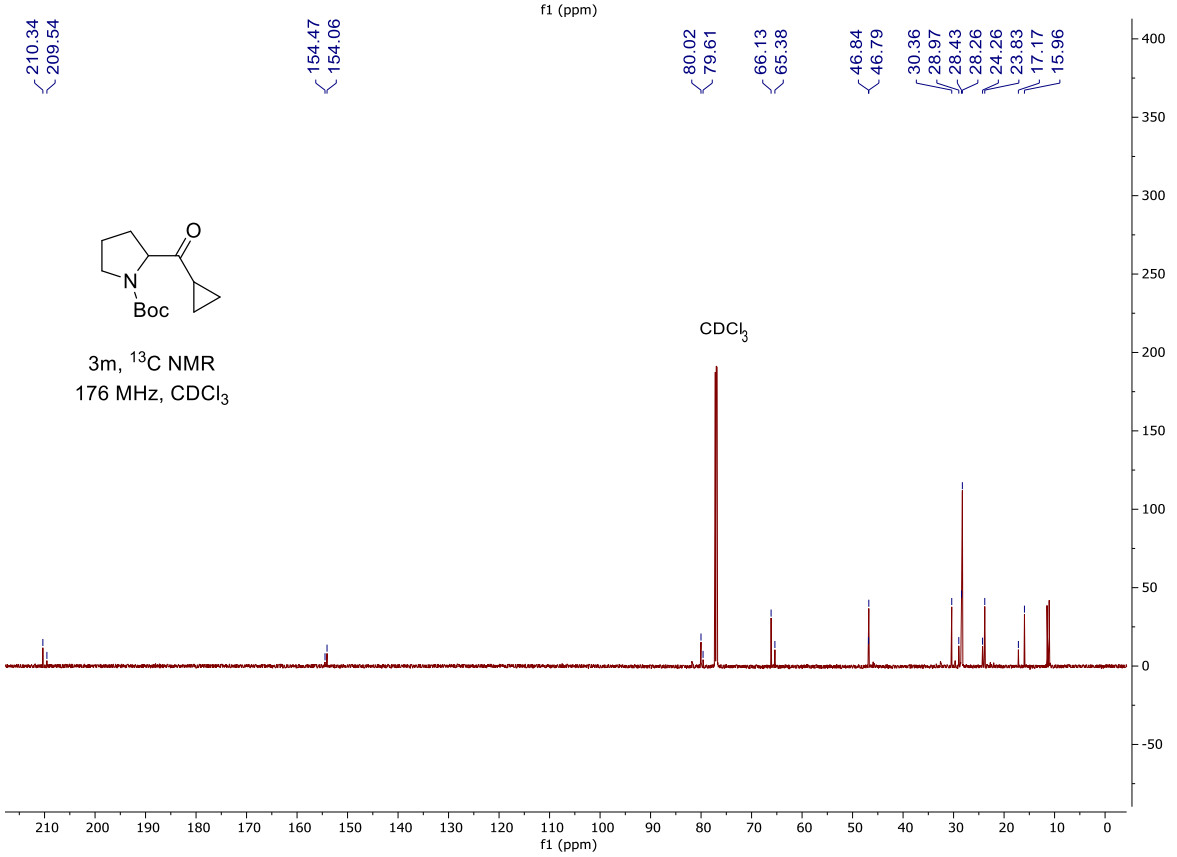
210.34 209.54 154.47 154.06 80.02 79.61 66.13 65.38 46.84 46.79 30.36 28.97 28.43 28.26 24.26 23.83 17.17 15.96
O
N
Boc
3m, 13C NMR
176 MHz, CDCl3
CDCl3
f1 (ppm)

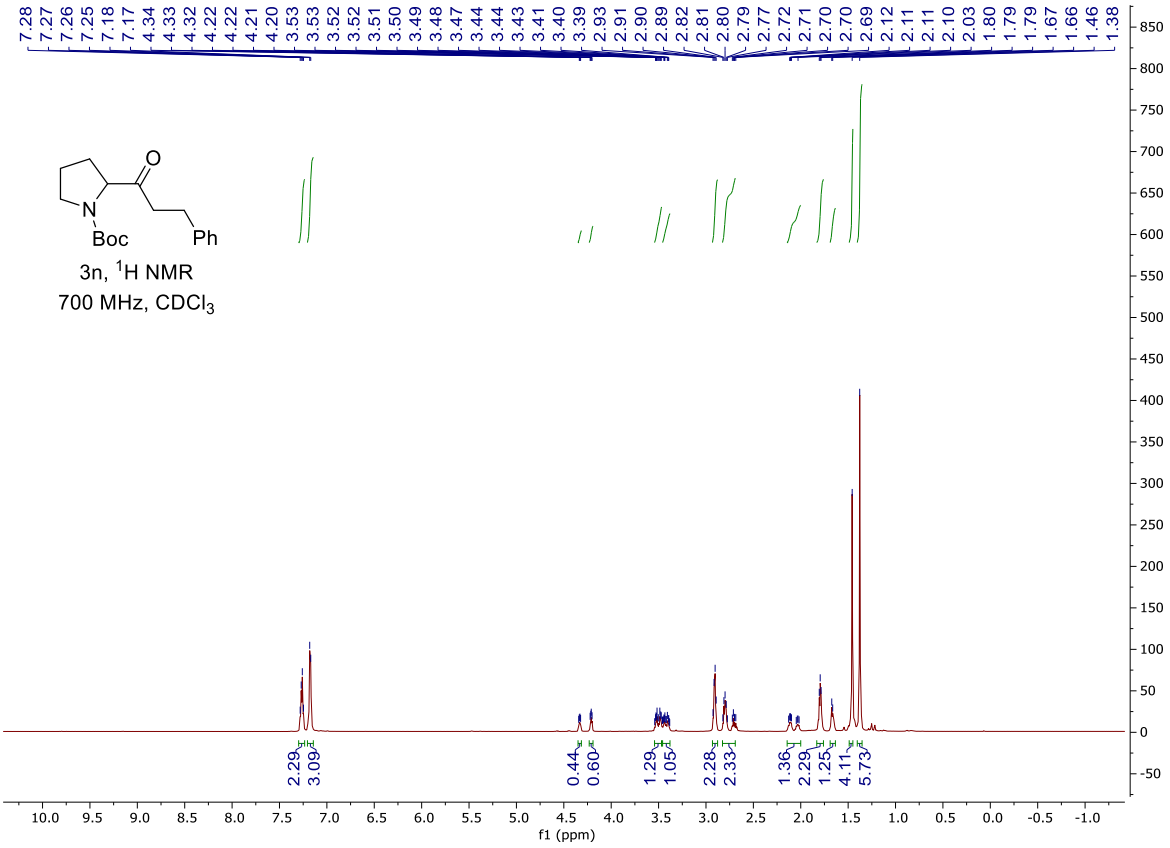
7.28 7.27 7.26 7.25 7.18 7.17 4.34 4.33 4.32 4.22 4.22 4.21 4.20 3.53 3.53 3.52 3.52 3.51 3.50 3.49 3.48 3.47 3.44 3.44 3.43 3.41 3.40 3.39 2.93 2.91 2.90 2.89 2.82 2.81 2.80 2.79 2.77 2.72 2.71 2.70 2.70 2.69 2.12 2.11 2.11 2.10 2.03 1.80 1.79 1.79 1.67 1.66 1.46 1.38
O
N
Boc
Ph
3n, ^{1}H NMR
700 MHz, $CDCl_3$
2.29 3.09 0.44 0.60 1.29 1.05 2.28 2.33 1.36 2.29 1.25 4.11 5.73
f1 (ppm)

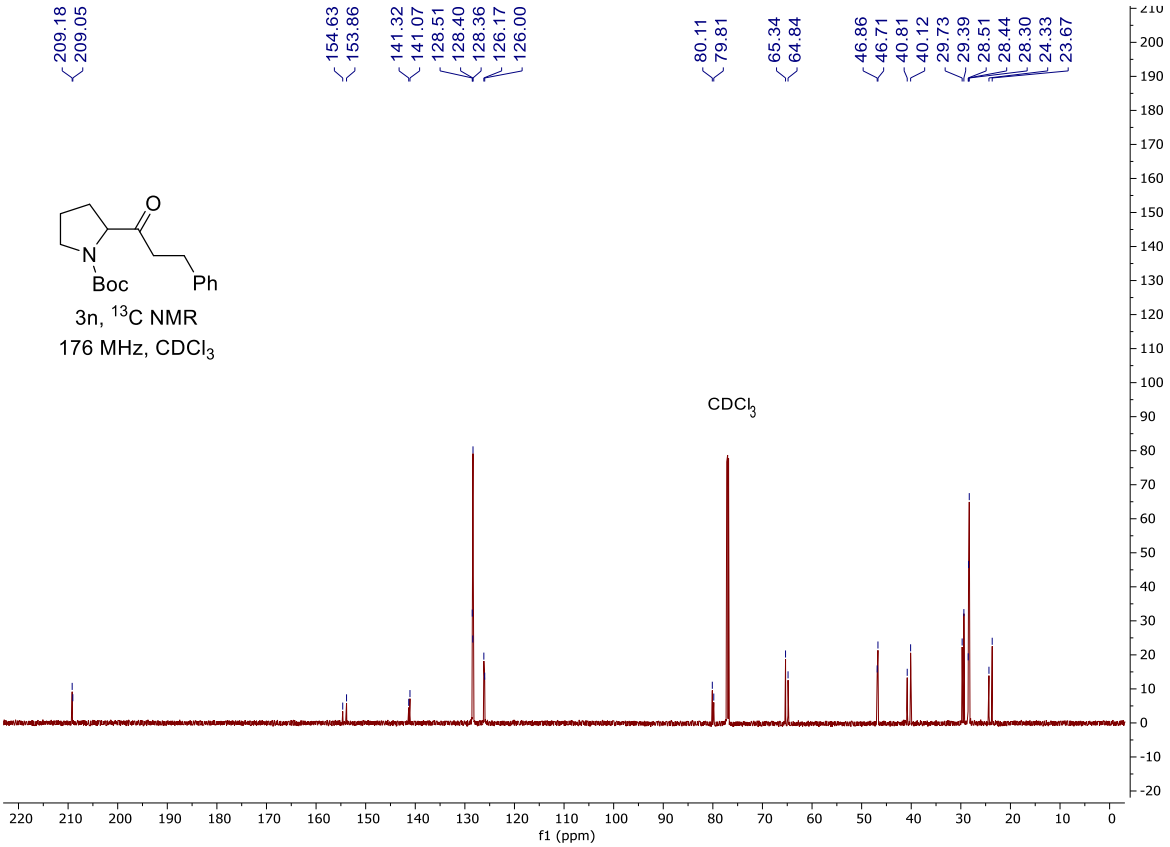
209.18 209.05 154.63 153.86 141.32 141.07 128.51 128.40 128.36 126.17 126.00 80.11 79.81 65.34 64.84 46.86 46.71 40.81 40.12 29.73 29.39 28.51 28.44 28.30 24.33 23.67
O
N
Boc
Ph
3n, ^{13}C NMR
176 MHz, $CDCl_3$
$CDCl_3$
f1 (ppm)

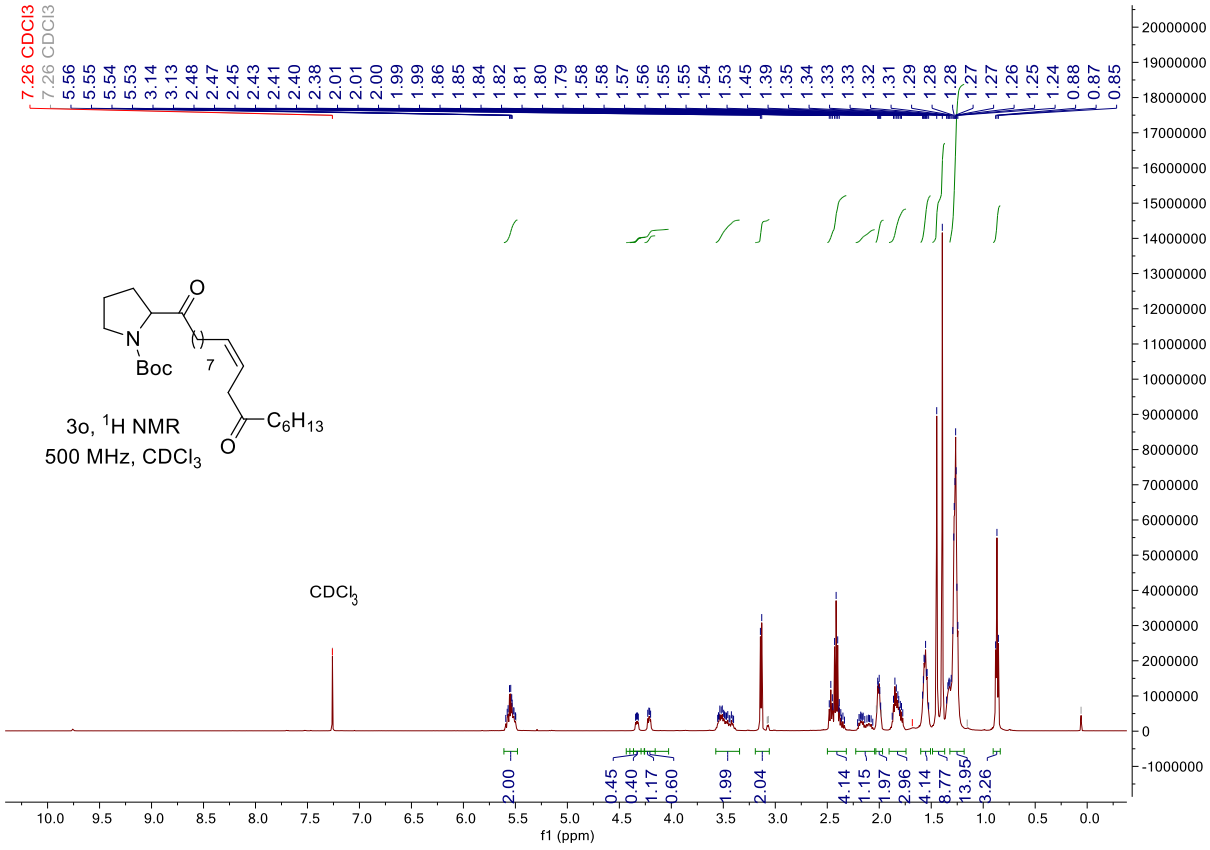
7.26 CDCl3
7.26 CDCl3
5.56 5.55 5.54 5.53 3.14 3.13 2.48 2.47 2.45 2.43 2.41 2.40 2.38 2.01 2.01 2.00 1.99 1.99 1.86 1.85 1.84 1.82 1.81 1.80 1.79 1.58 1.58 1.57 1.56 1.55 1.55 1.54 1.53 1.45 1.39 1.35 1.34 1.33 1.33 1.32 1.31 1.29 1.28 1.28 1.27 1.27 1.26 1.25 1.24 0.88 0.87 0.85
O
N
Boc
7
C6H13
O
3o, 1H NMR
500 MHz, CDCl3
CDCl3
2.00 0.45 0.40 1.17 0.60 1.99 2.04 4.14 1.15 1.97 2.96 4.14 8.77 13.95 3.26
f1 (ppm)

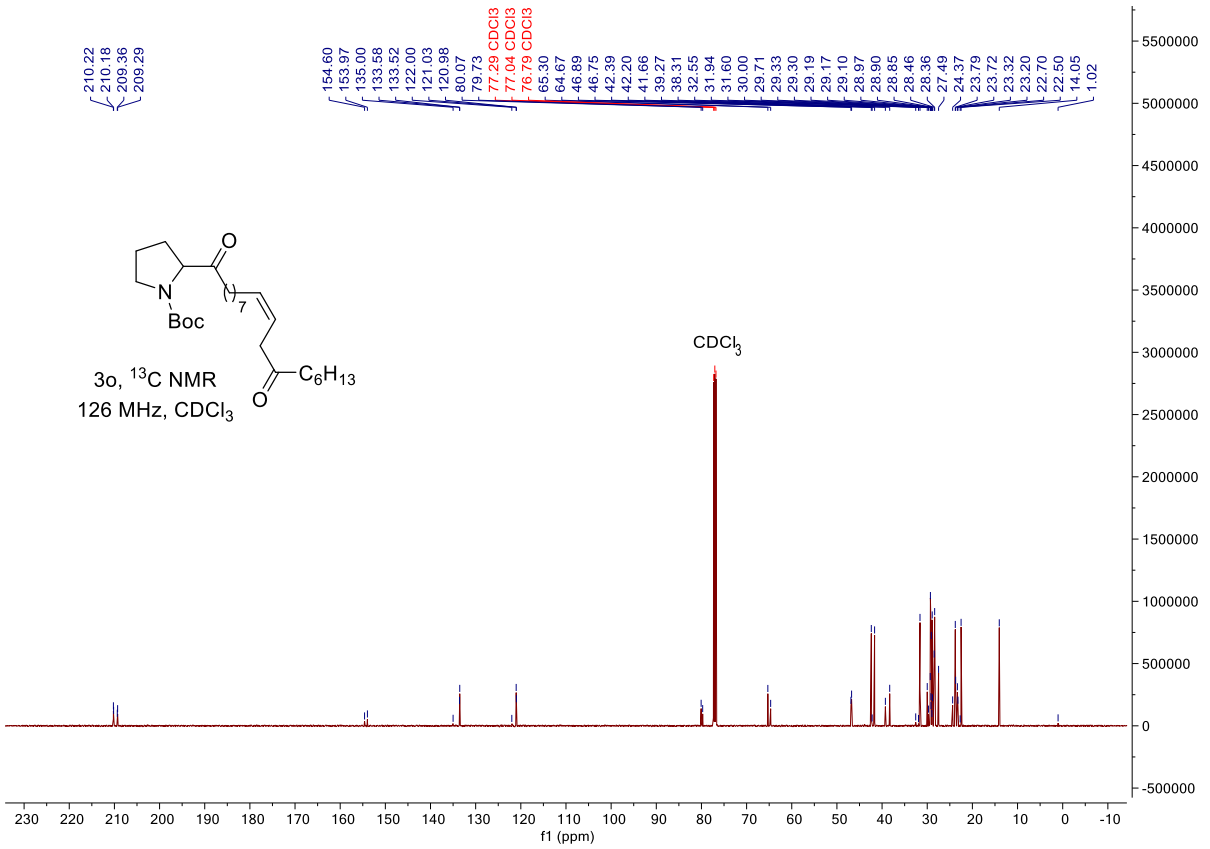
210.22 210.18 209.36 209.29
154.60 153.97 135.00 133.58 133.52 122.00 121.03 120.98 80.07 79.73 77.29 CDCl3 77.04 CDCl3 76.79 CDCl3 65.30 64.67 46.89 46.75 42.39 42.20 41.66 39.27 38.31 32.55 31.94 31.60 30.00 29.71 29.33 29.30 29.19 29.17 29.10 28.97 28.90 28.85 28.46 28.36 27.49 24.37 23.79 23.72 23.32 23.20 22.70 22.50 14.05 1.02
O
N
Boc
7
C6H13
O
3o, 13C NMR
126 MHz, CDCl3
CDCl3
f1 (ppm)

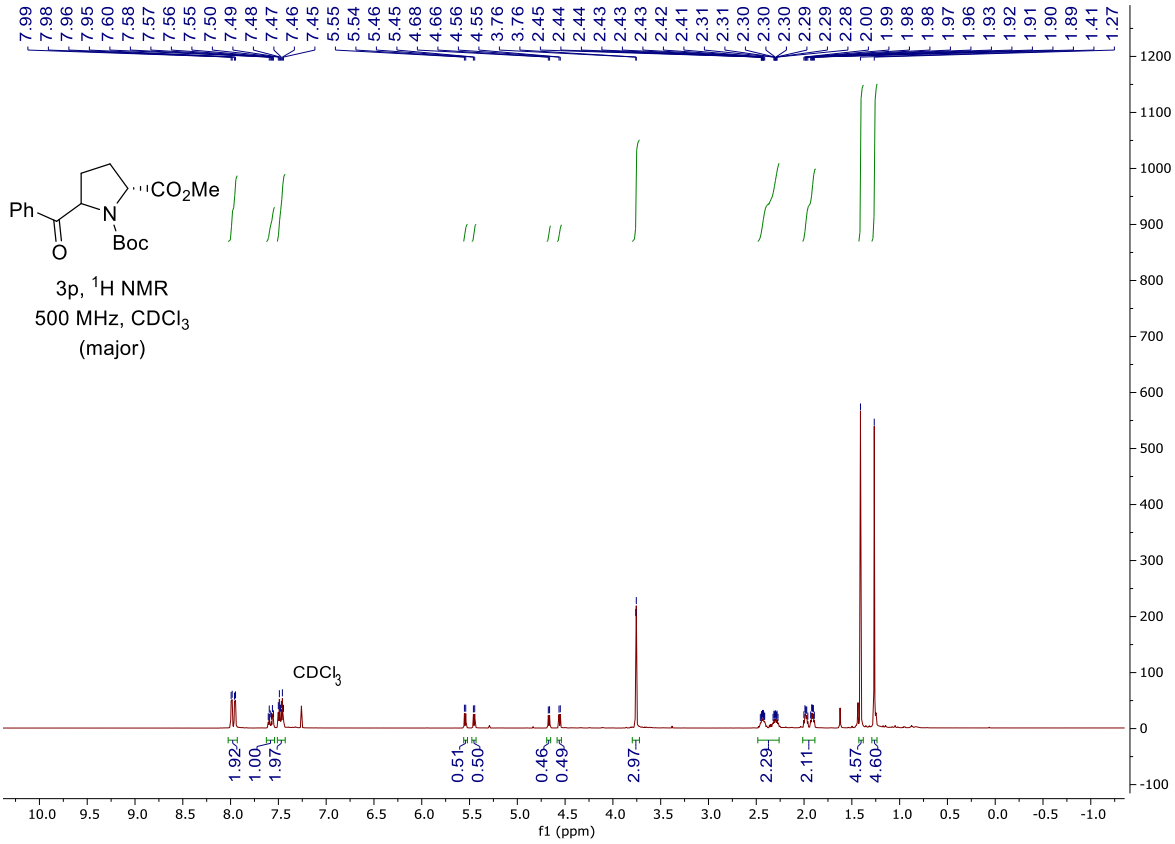
7.99 7.98 7.96 7.95 7.60 7.58 7.57 7.56 7.55 7.50 7.49 7.48 7.47 7.46 7.45 5.55 5.54 5.46 5.45 4.68 4.66 4.56 4.55 3.76 3.76 2.45 2.44 2.44 2.43 2.43 2.43 2.42 2.41 2.31 2.31 2.30 2.30 2.30 2.29 2.29 2.28 2.00 1.99 1.98 1.98 1.97 1.96 1.93 1.92 1.91 1.90 1.89 1.41 1.27
CO2Me
Ph
N
Boc
O
3p, 1H NMR
500 MHz, CDCl3
(major)
CDCl3
1.92 1.00 1.97 0.51 0.50 0.46 0.49 2.97 2.29 2.11 4.57 4.60
f1 (ppm)

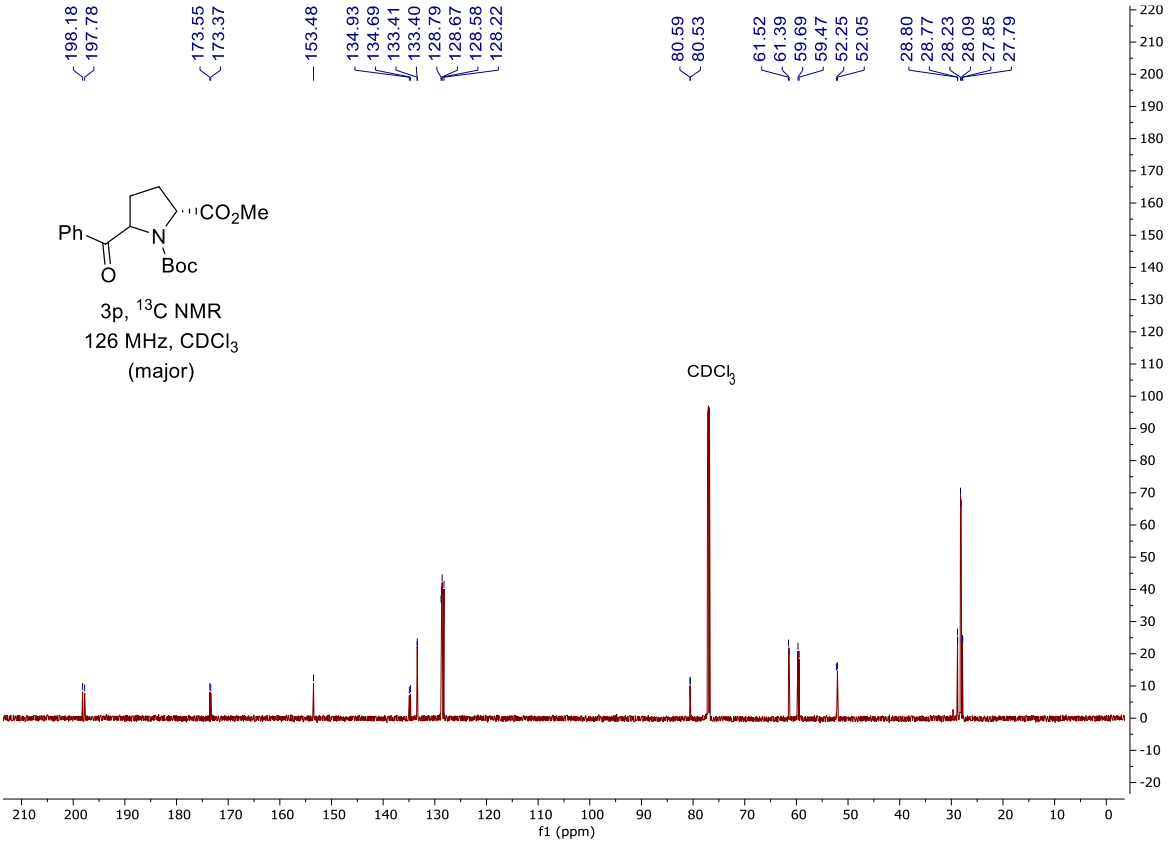
198.18 197.78 173.55 173.37 153.48 134.93 134.69 133.41 133.40 128.79 128.67 128.58 128.22 80.59 80.53 61.52 61.39 59.69 59.47 52.25 52.05 28.80 28.77 28.23 28.09 27.85 27.79
CO2Me
Ph
N
Boc
O
3p, 13C NMR
126 MHz, CDCl3
(major)
CDCl3
f1 (ppm)

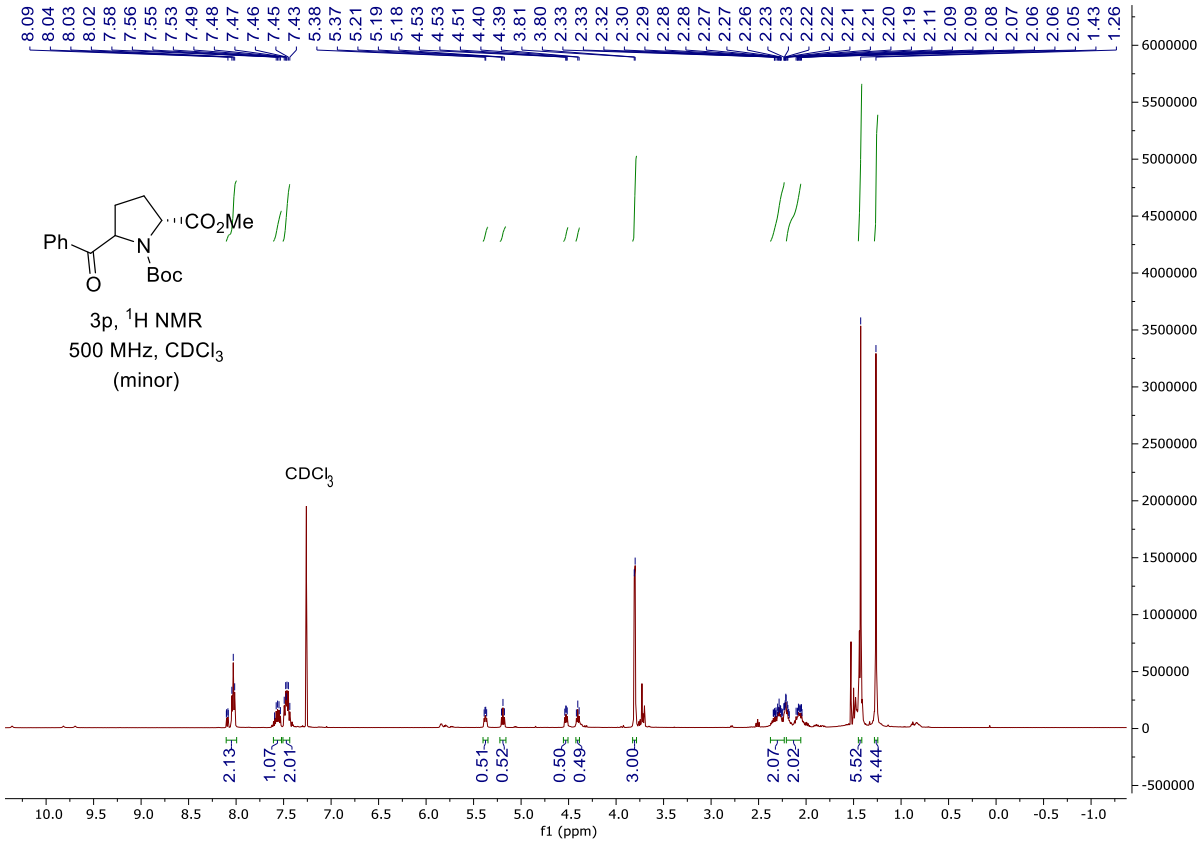
8.09 8.04 8.03 8.02 7.58 7.56 7.55 7.53 7.49 7.48 7.47 7.46 7.45 7.43 5.38 5.37 5.21 5.19 5.18 4.53 4.51 4.40 4.39 3.81 3.80 2.33 2.33 2.32 2.30 2.29 2.28 2.28 2.27 2.27 2.26 2.23 2.23 2.22 2.22 2.21 2.21 2.20 2.19 2.11 2.09 2.09 2.08 2.07 2.06 2.06 2.05 1.43 1.26
CO2Me
Ph
N
Boc
O
3p, 1H NMR
500 MHz, CDCl3
(minor)
CDCl3
2.13 1.07 2.01 0.51 0.52 0.50 0.49 3.00 2.07 2.02 5.52 4.44
f1 (ppm)

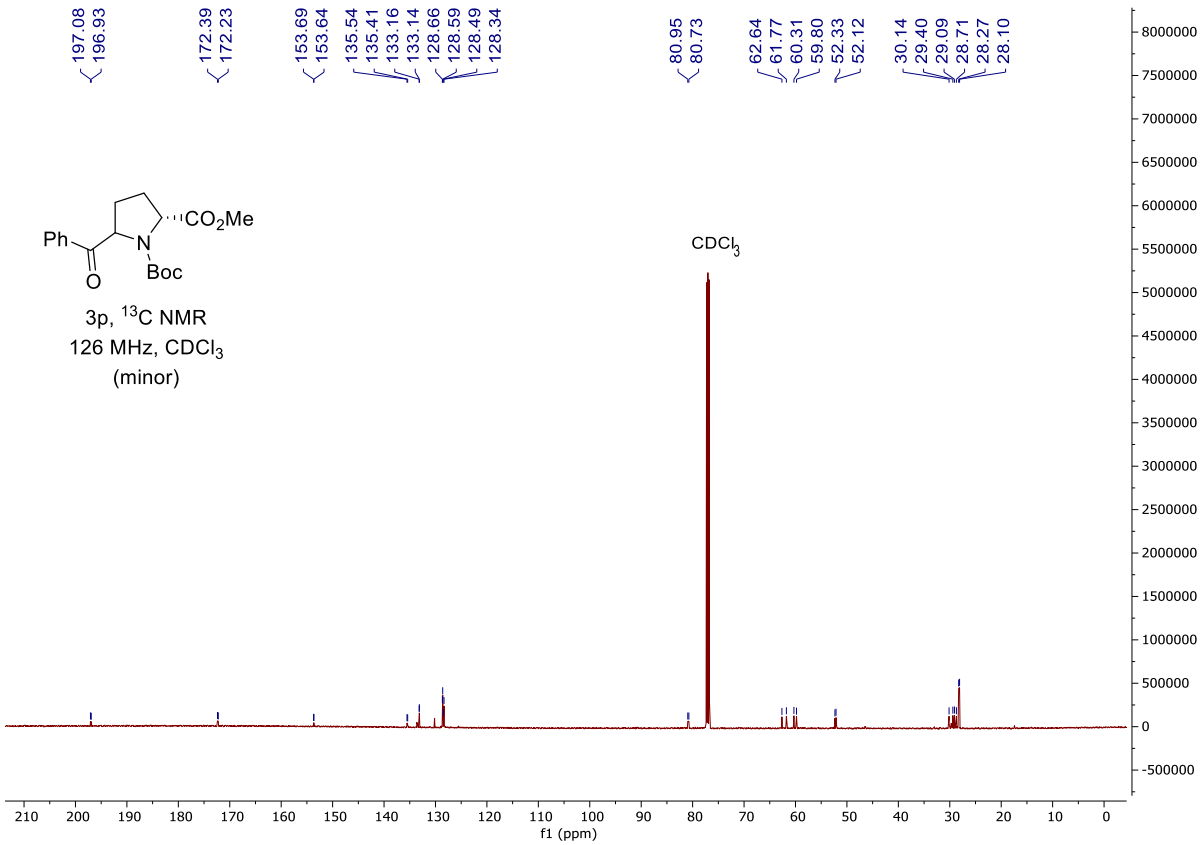
197.08 196.93 172.39 172.23 153.69 153.64 135.54 135.41 133.16 133.14 128.66 128.59 128.49 128.34 80.95 80.73 62.64 61.77 60.31 59.80 52.33 52.12 30.14 29.40 29.09 28.71 28.27 28.10
CO2Me
Ph
N
Boc
O
3p, 13C NMR
126 MHz, CDCl3
(minor)
CDCl3
f1 (ppm)

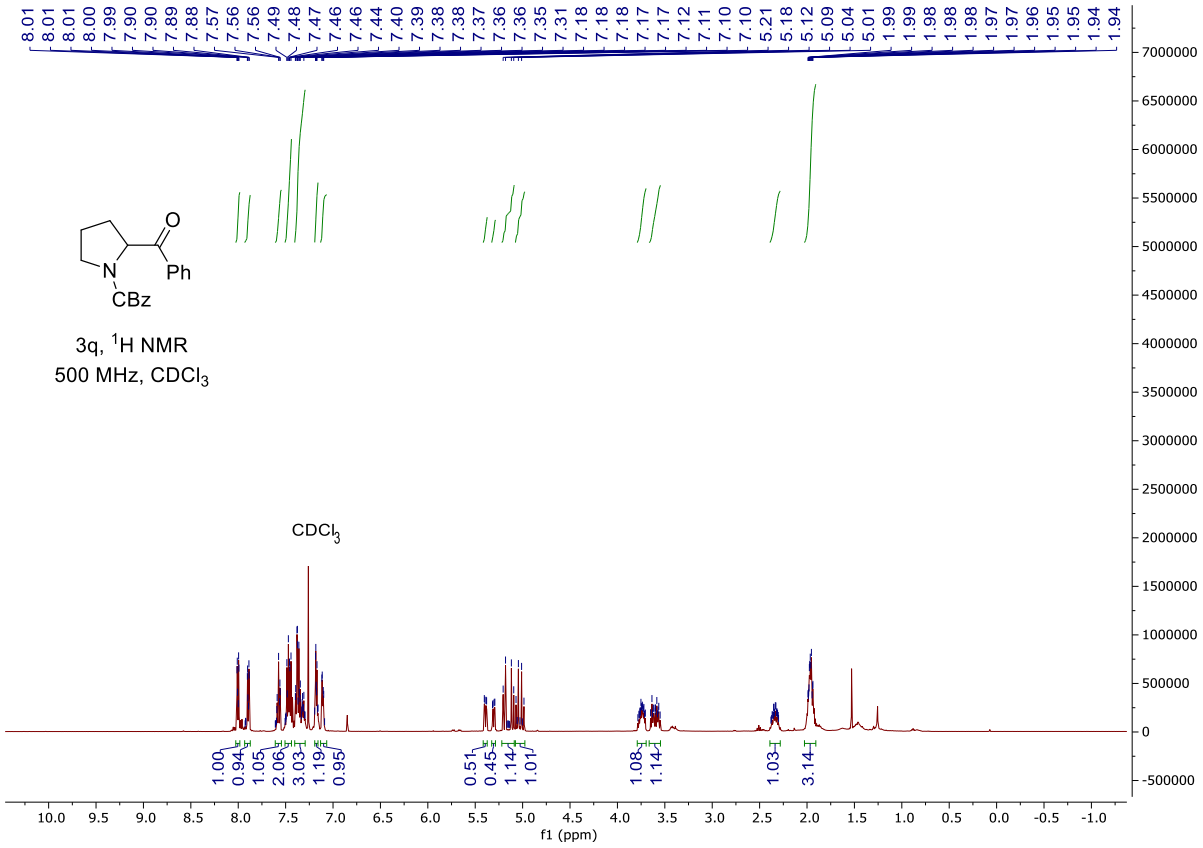
8.01 8.01 8.01 8.00 7.99 7.90 7.90 7.89 7.88 7.57 7.56 7.56 7.49 7.48 7.47 7.46 7.46 7.44 7.40 7.39 7.38 7.38 7.37 7.36 7.36 7.35 7.31 7.18 7.18 7.18 7.17 7.17 7.12 7.11 7.10 7.10 5.21 5.18 5.12 5.09 5.04 5.01 1.99 1.99 1.98 1.98 1.98 1.97 1.97 1.96 1.95 1.95 1.94 1.94
O
N
Ph
CBz
3q, 1H NMR
500 MHz, CDCl3
CDCl3
1.00 0.94 1.05 2.06 3.03 1.19 0.95 0.51 0.45 1.14 1.01 1.08 1.14 1.03 3.14
f1 (ppm)

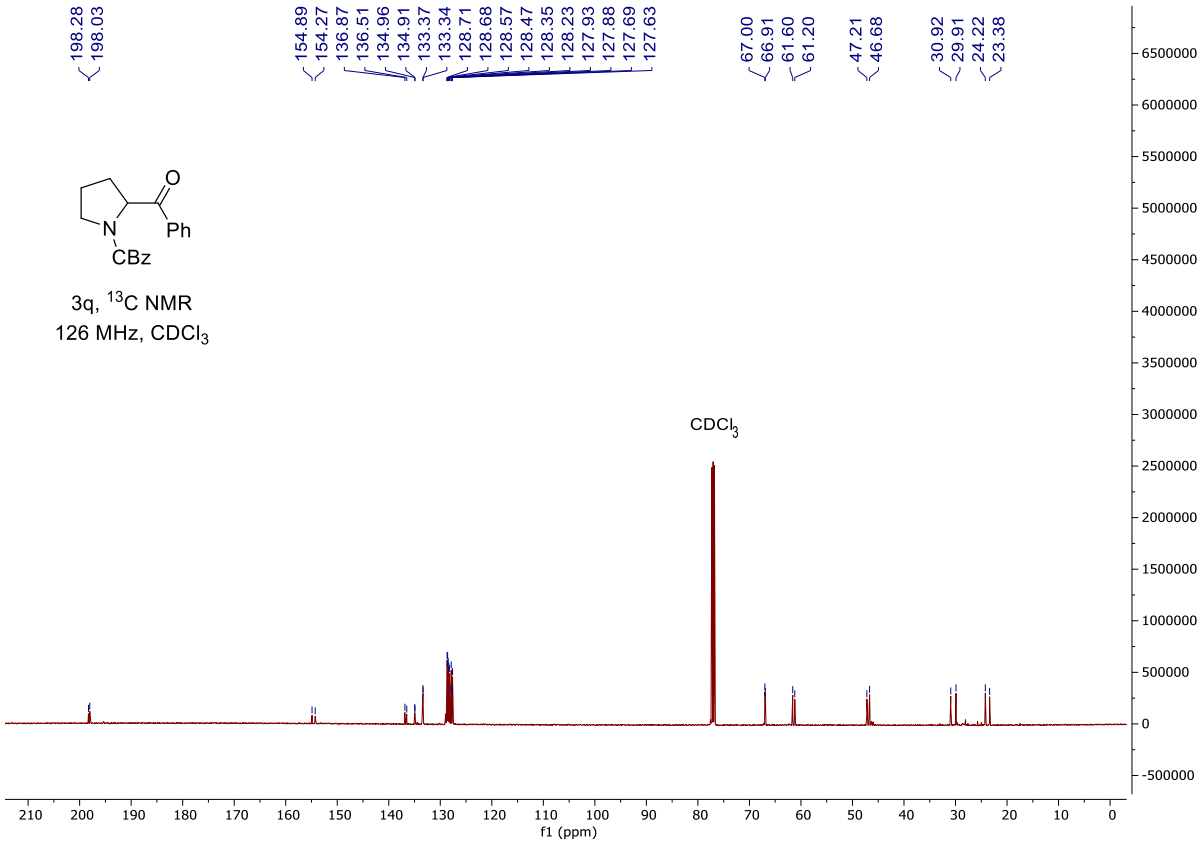
198.28 198.03 154.89 154.27 136.87 136.51 134.96 134.91 133.37 133.34 128.71 128.68 128.57 128.47 128.35 128.23 127.93 127.88 127.69 127.63 67.00 66.91 61.60 61.20 47.21 46.68 30.92 29.91 24.22 23.38
O
N
Ph
CBz
3q, 13C NMR
126 MHz, CDCl3
CDCl3
f1 (ppm)

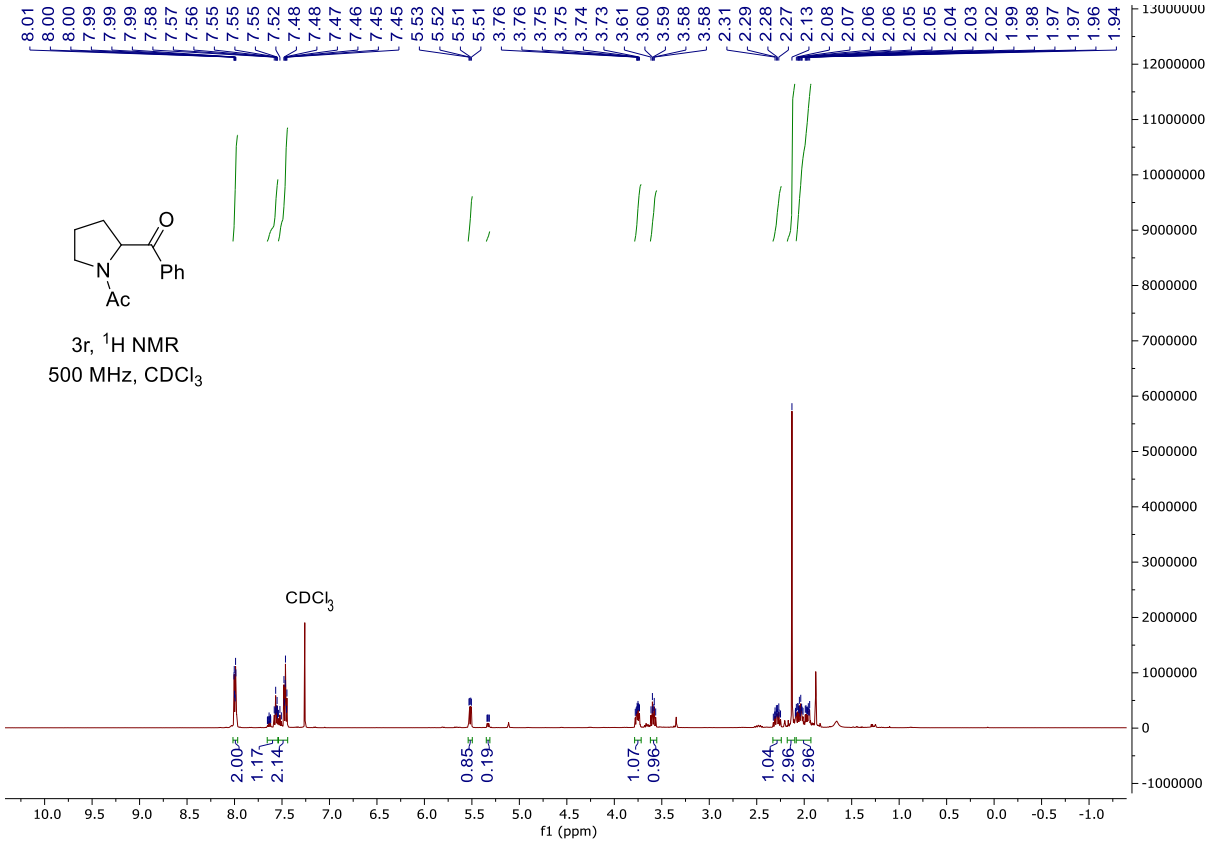
8.01 8.00 8.00 7.99 7.99 7.99 7.58 7.57 7.56 7.55 7.55 7.55 7.52 7.48 7.48 7.47 7.46 7.45 7.45
5.53 5.52 5.51 5.51
3.76 3.76 3.75 3.75 3.74 3.73 3.61 3.60 3.59 3.58 3.58
2.31 2.29 2.28 2.27 2.13 2.08 2.07 2.06 2.06 2.05 2.05 2.04 2.03 2.02 1.99 1.98 1.97 1.97 1.96 1.94
O
N
Ac
Ph
3r, 1H NMR
500 MHz, CDCl3
CDCl3
2.00 1.17 2.14 0.85 0.19 1.07 0.96 1.04 2.96 2.96
f1 (ppm)

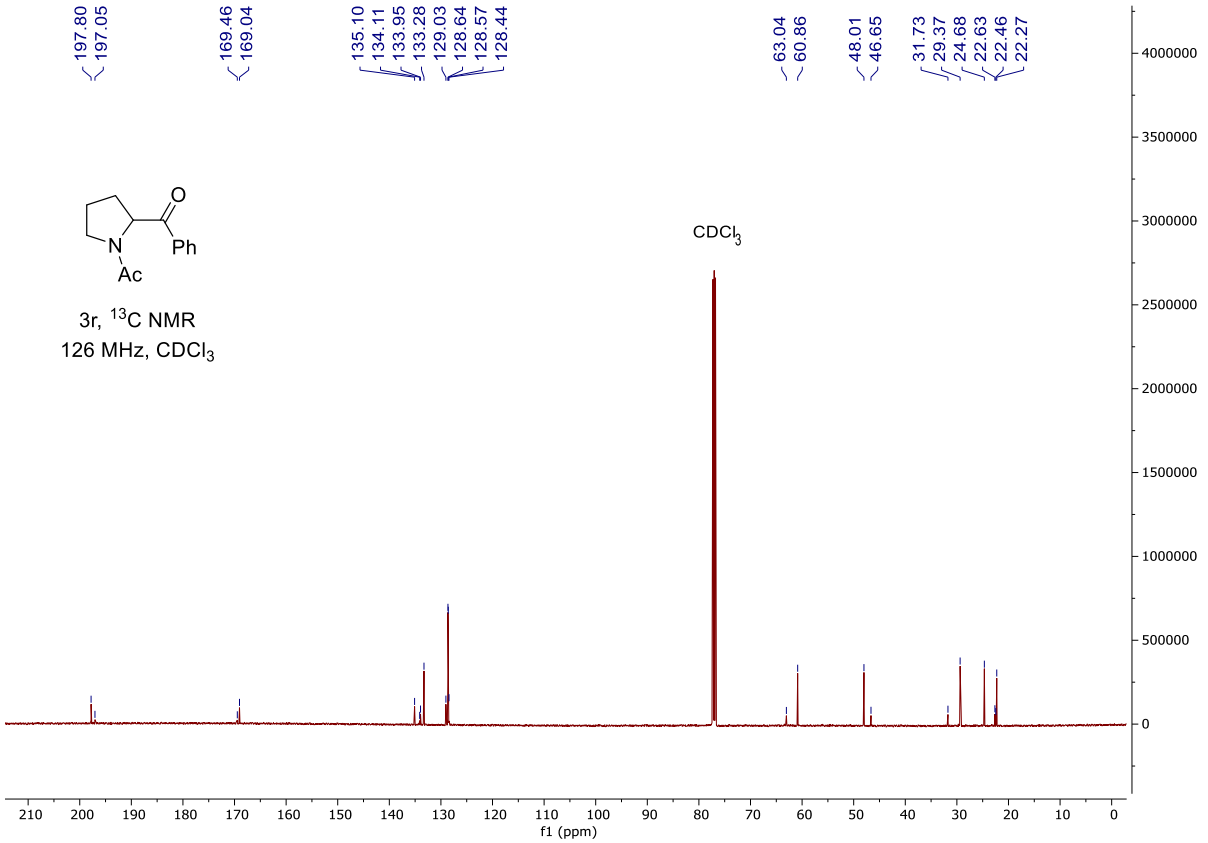
197.80 197.05
169.46 169.04
135.10 134.11 133.95 133.28 129.03 128.64 128.57 128.44
63.04 60.86
48.01 46.65
31.73 29.37 24.68 22.63 22.46 22.27
O
N
Ac
Ph
3r, 13C NMR
126 MHz, CDCl3
CDCl3
f1 (ppm)

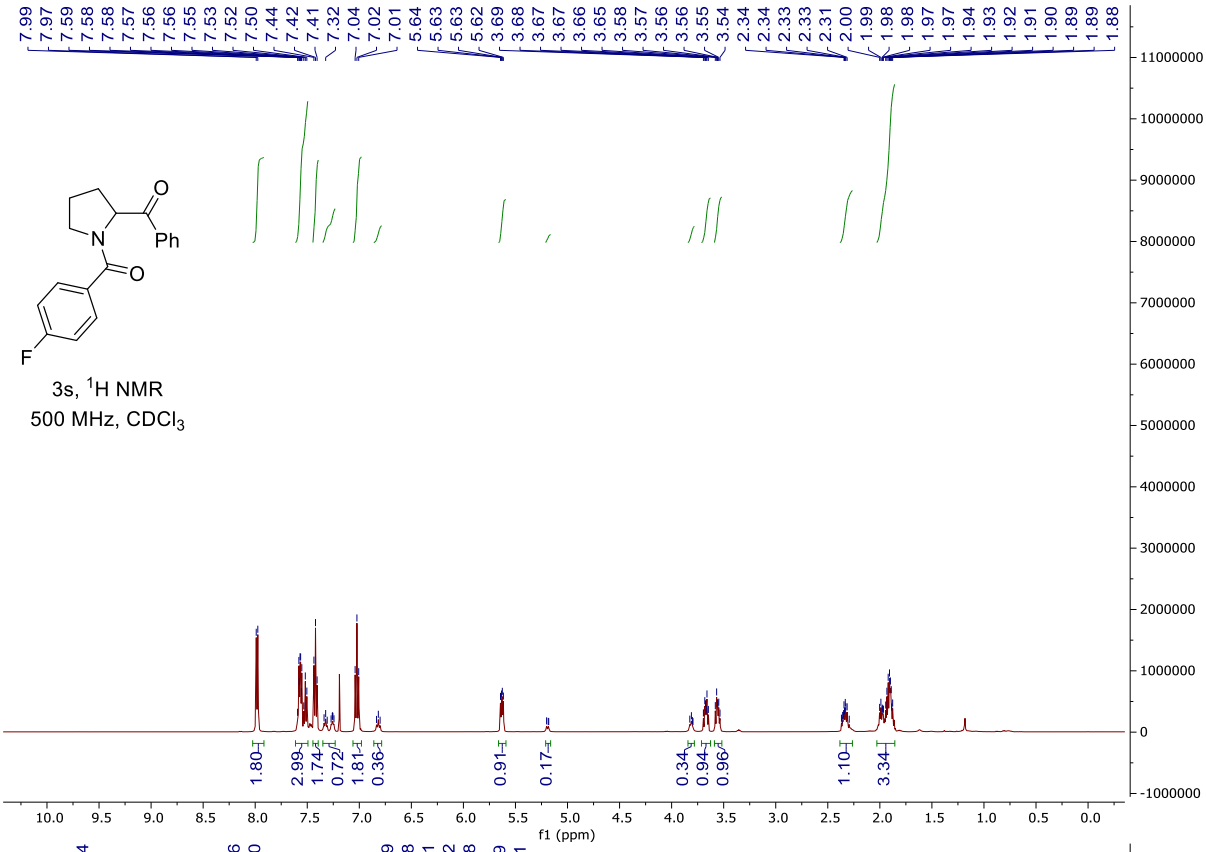
7.99 7.97 7.59 7.58 7.58 7.57 7.56 7.56 7.55 7.53 7.52 7.50 7.44 7.42 7.41 7.32 7.04 7.02 7.01 5.64 5.63 5.63 5.62 3.69 3.68 3.67 3.67 3.66 3.65 3.58 3.57 3.56 3.56 3.55 3.54 2.34 2.34 2.33 2.33 2.31 2.00 1.99 1.98 1.98 1.97 1.97 1.94 1.93 1.92 1.91 1.90 1.89 1.89 1.88
O
Ph
N
O
F
3s, ^{1}H NMR
500 MHz, $CDCl_3$
1.80 2.99 1.74 0.72 1.81 0.36 0.91 0.17 0.34 0.94 0.96 1.10 3.34
f1 (ppm)

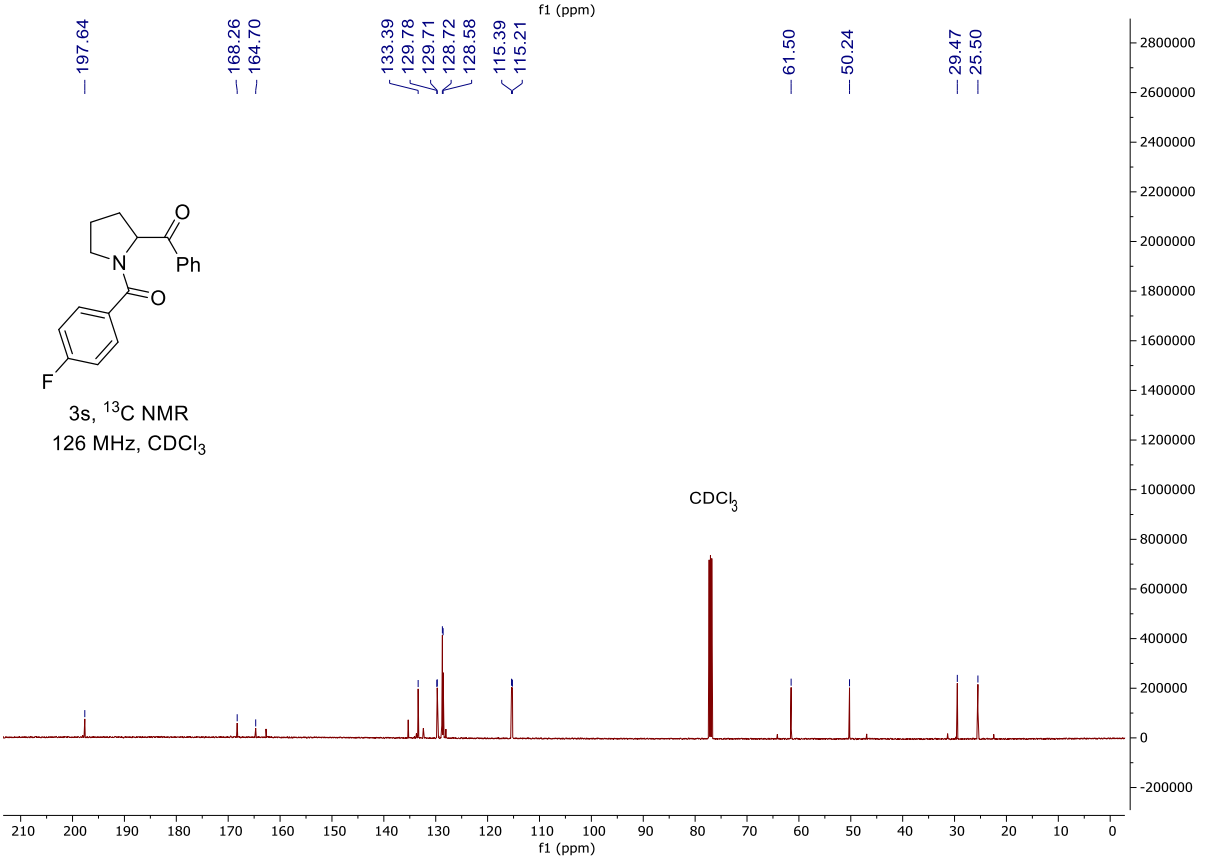
197.64
168.26
164.70
133.39
129.78
129.71
128.72
128.58
115.39
115.21
61.50
50.24
29.47
25.50
O
Ph
N
O
F
3s, ^{13}C NMR
126 MHz, $CDCl_3$
$CDCl_3$
f1 (ppm)

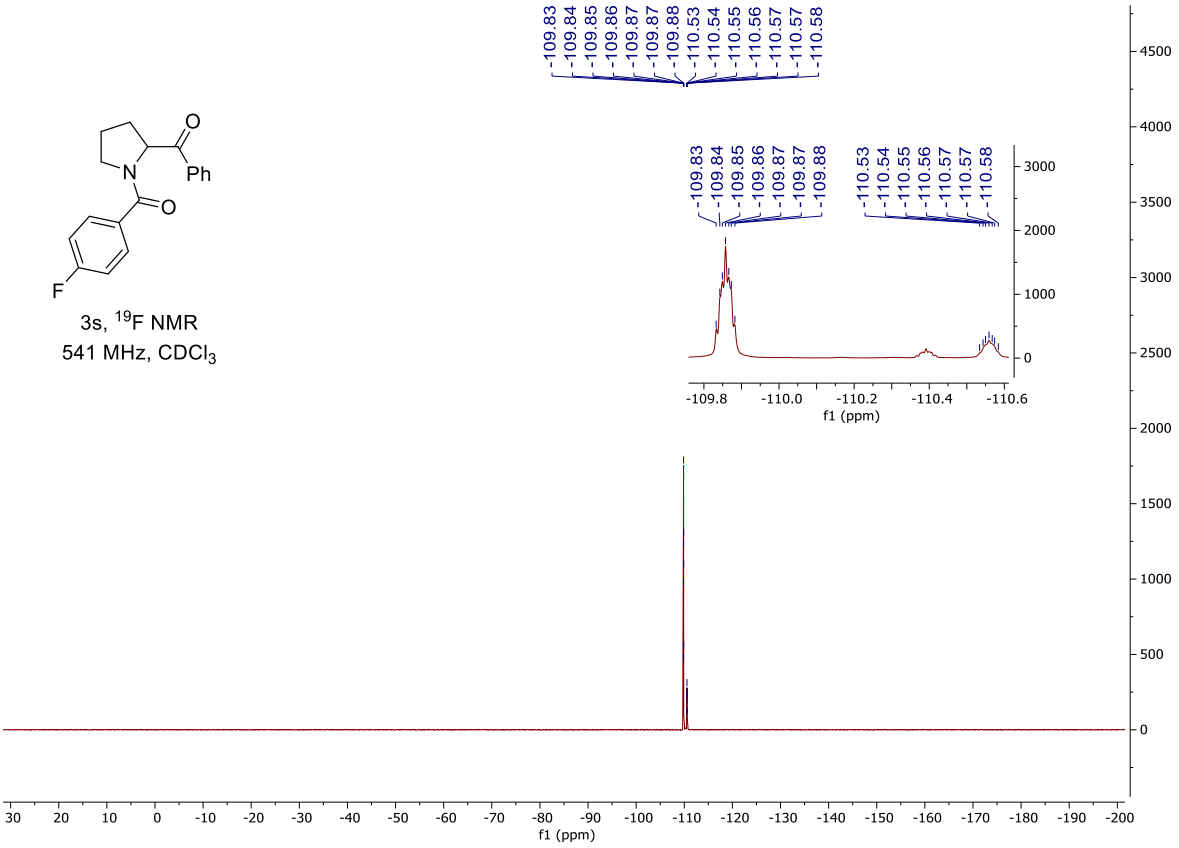
-109.83
-109.84
-109.85
-109.86
-109.87
-109.87
-109.88
-110.53
-110.54
-110.55
-110.56
-110.57
-110.57
-110.58
O
N
Ph
O
F
3s, 19F NMR
541 MHz, CDCl3
f1 (ppm)
f1 (ppm)

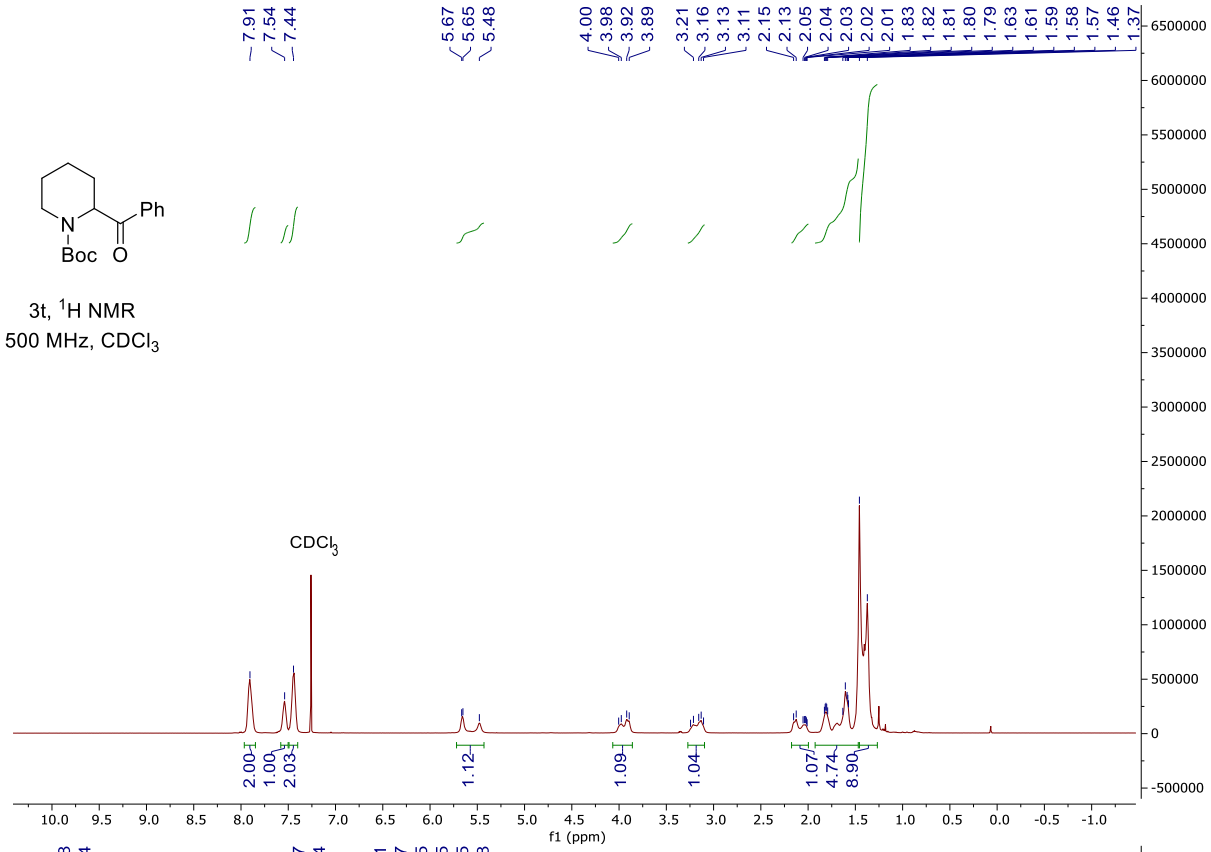

3t, ^{1}H NMR
500 MHz, $CDCl_3$

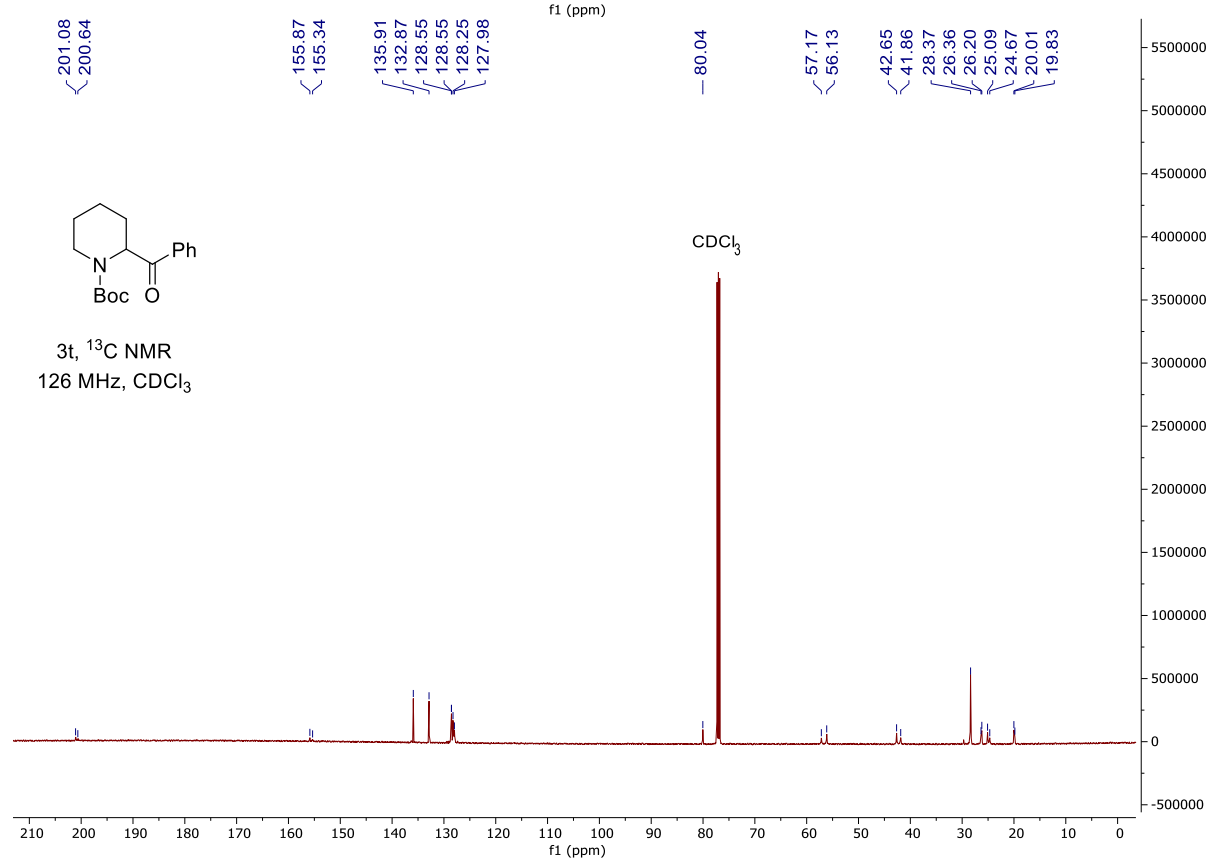

3t, ^{13}C NMR
126 MHz, $CDCl_3$

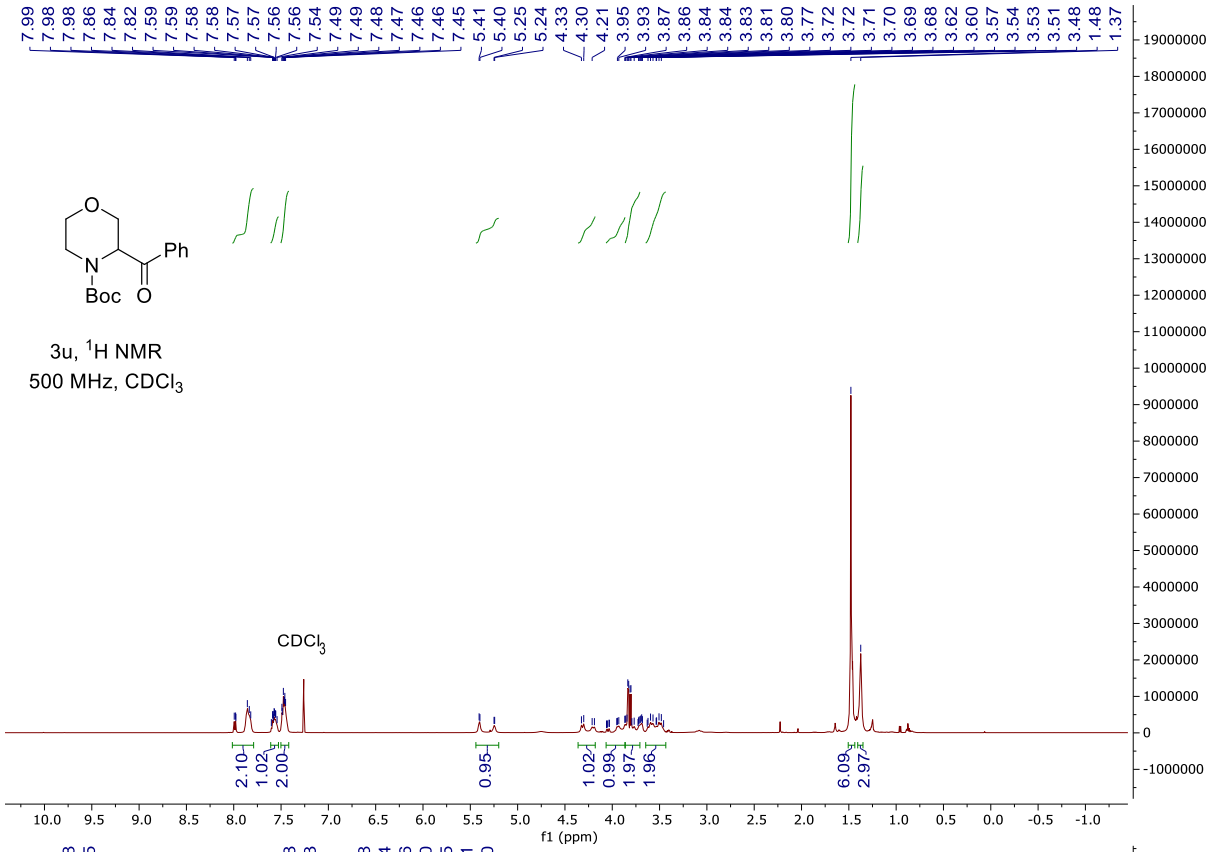
7.99 7.98 7.98 7.86 7.84 7.82 7.59 7.59 7.58 7.58 7.57 7.57 7.56 7.56 7.54 7.49 7.49 7.48 7.47 7.46 7.46 7.45 5.41 5.40 5.25 5.24 4.33 4.30 4.21 3.95 3.93 3.87 3.86 3.84 3.84 3.83 3.81 3.80 3.77 3.72 3.72 3.71 3.70 3.69 3.68 3.62 3.60 3.57 3.54 3.53 3.51 3.48 1.48 1.37
Ph
Boc O
3u, 1H NMR
500 MHz, CDCl3
CDCl3
2.10 1.02 2.00 0.95 1.02 0.99 1.97 1.96 6.09 2.97
f1 (ppm)

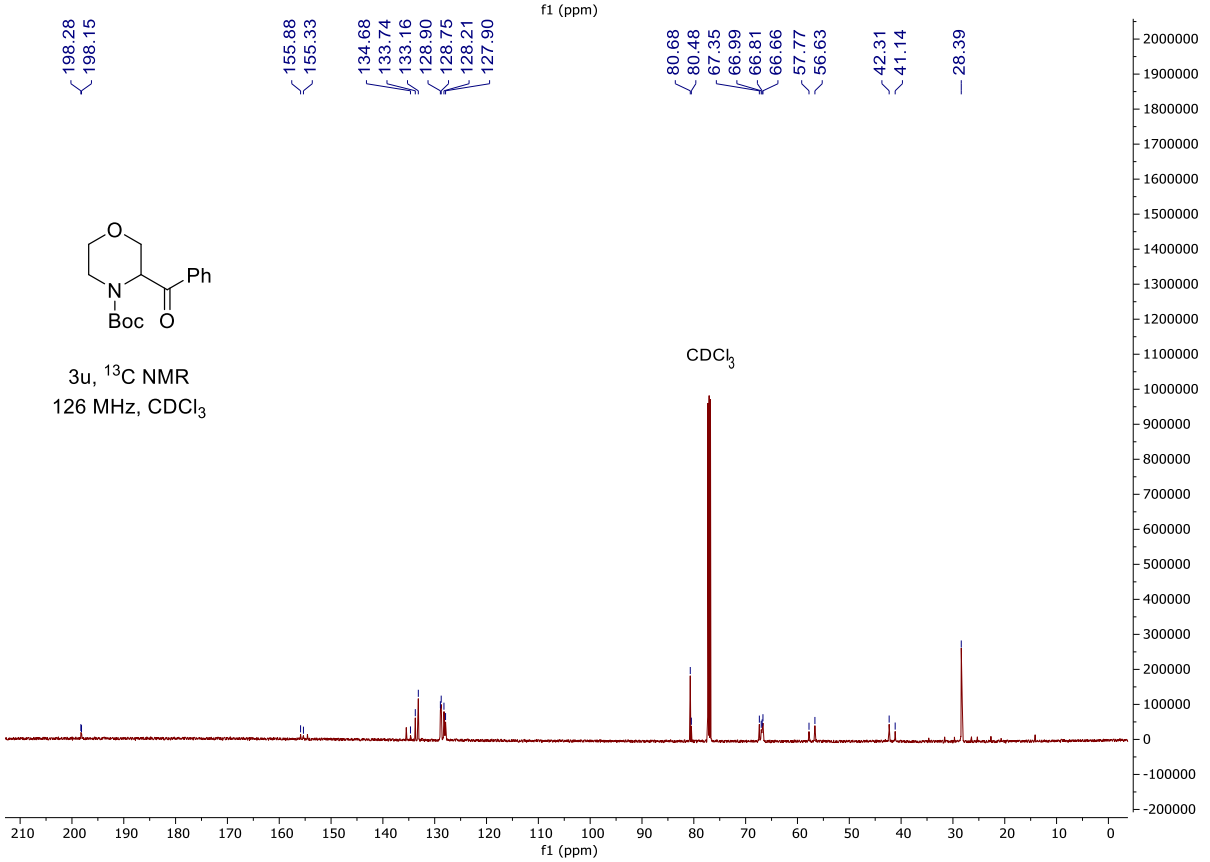
198.28 198.15 155.88 155.33 134.68 133.74 133.16 128.90 128.75 128.21 127.90 80.68 80.48 67.35 66.99 66.81 66.66 57.77 56.63 42.31 41.14 28.39
Ph
Boc O
3u, 13C NMR
126 MHz, CDCl3
CDCl3
f1 (ppm)

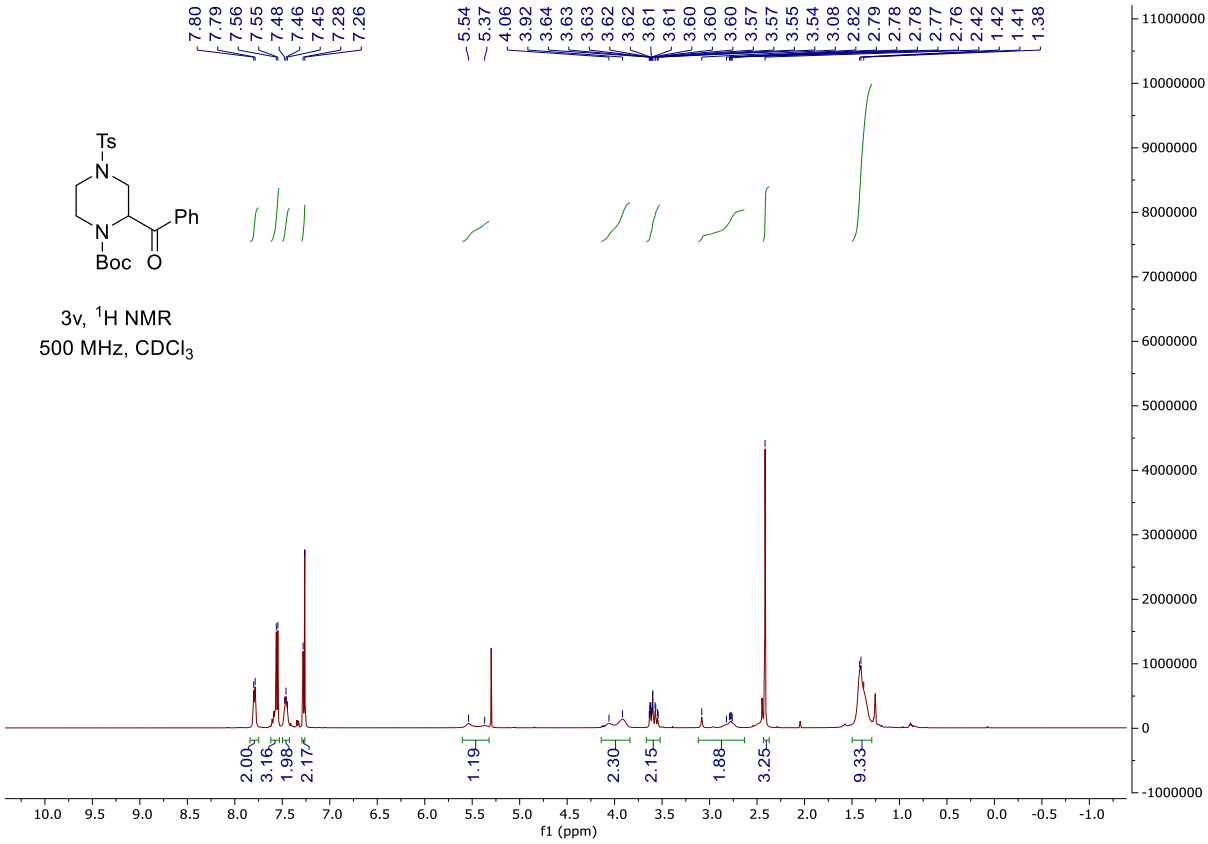

3v, ^{1}H NMR
500 MHz, $CDCl_3$

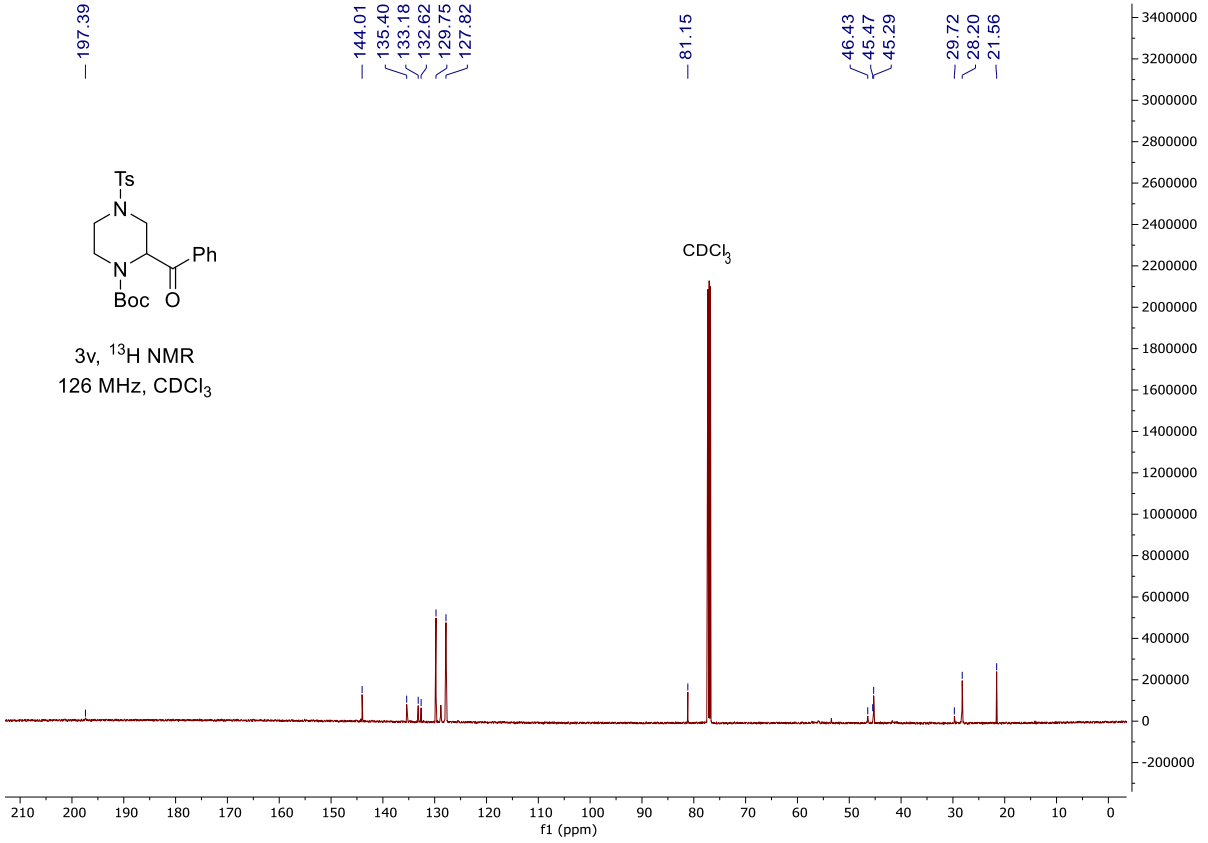

3v, ^{13}H NMR
126 MHz, $CDCl_3$

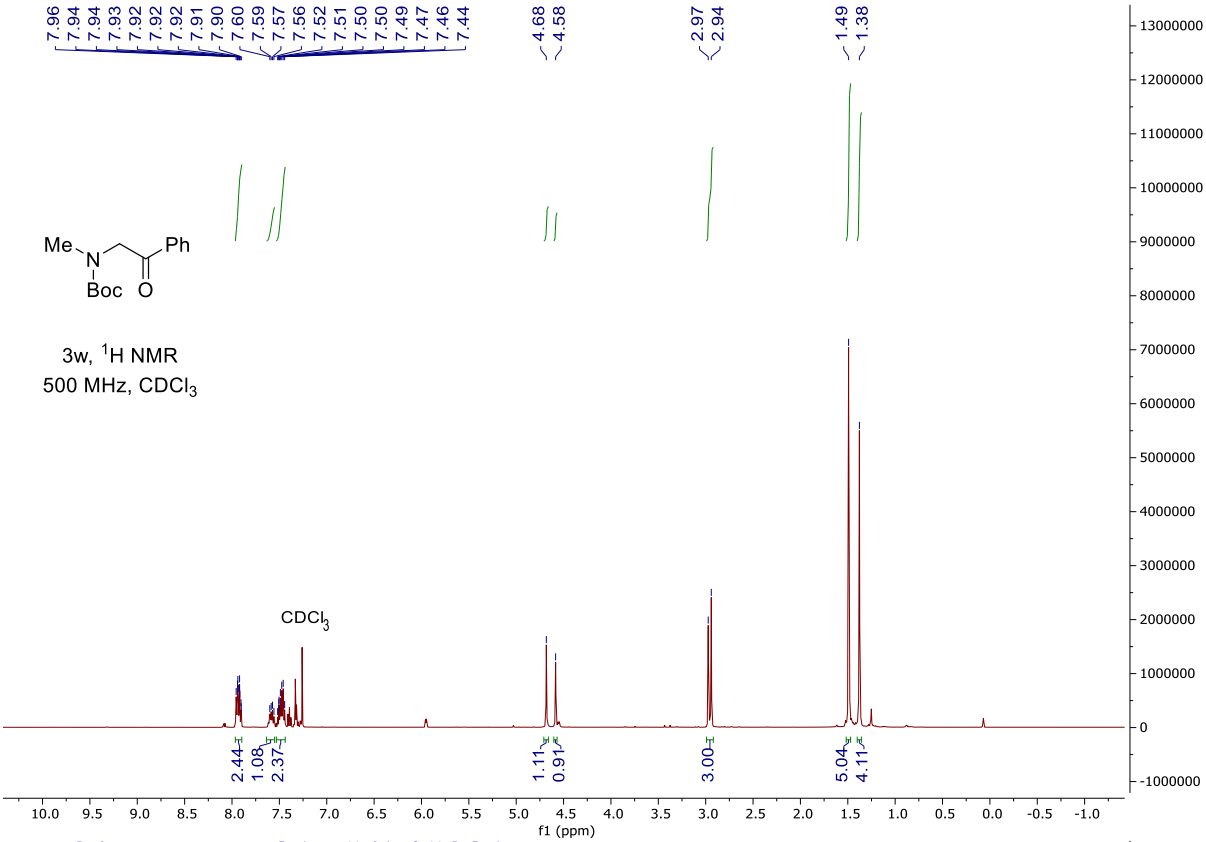
7.96
7.94
7.94
7.93
7.92
7.92
7.92
7.91
7.90
7.60
7.59
7.57
7.56
7.52
7.51
7.50
7.50
7.49
7.47
7.46
7.44
4.68
4.58
2.97
2.94
1.49
1.38
Me
N
Ph
Boc
O
3w, 1H NMR
500 MHz, CDCl3
CDCl3
2.44
1.08
2.37
1.11
0.91
3.00
5.04
4.11
f1 (ppm)

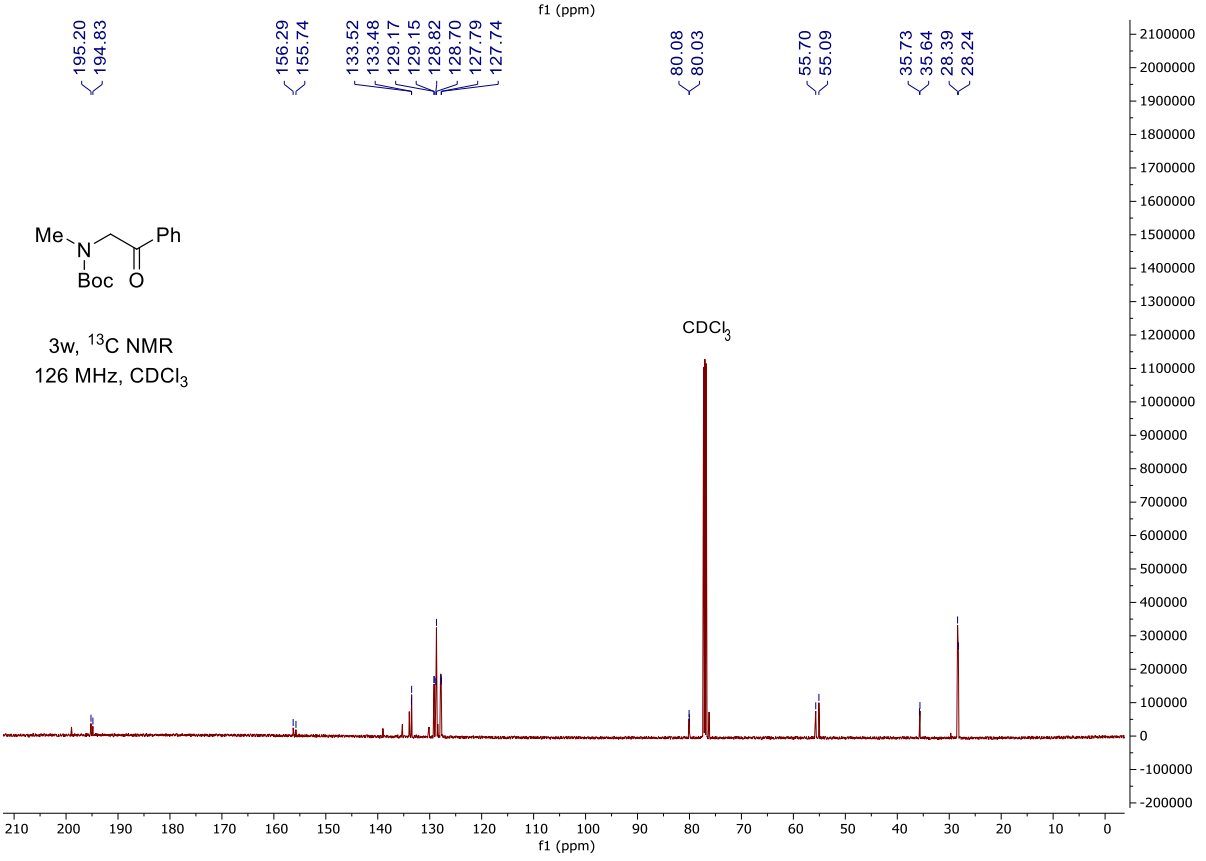
195.20
194.83
156.29
155.74
133.52
133.48
129.17
129.15
128.82
128.70
127.79
127.74
80.08
80.03
55.70
55.09
35.73
35.64
28.39
28.24
Me
N
Ph
Boc
O
3w, 13C NMR
126 MHz, CDCl3
CDCl3
f1 (ppm)

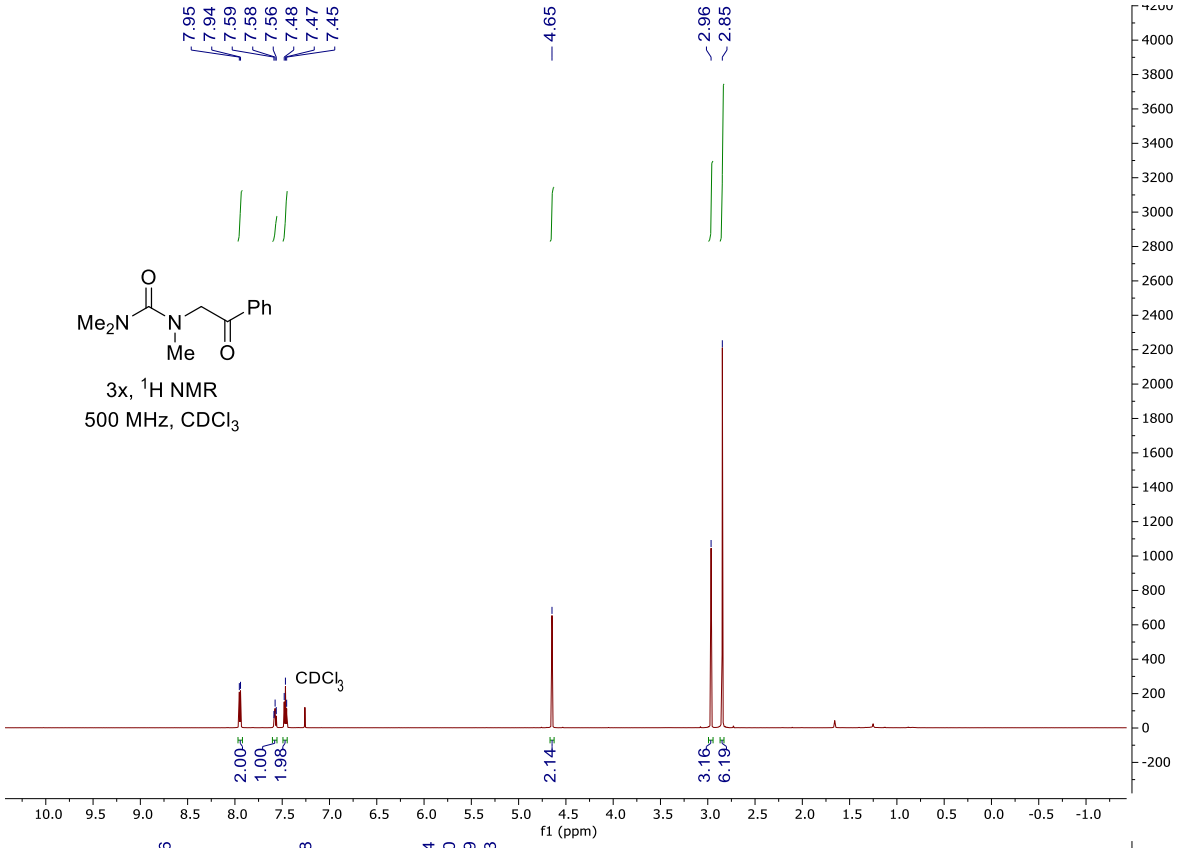
7.95
7.94
7.59
7.58
7.56
7.48
7.47
7.45
4.65
2.96
2.85
Me2N
O
N
Me
O
Ph
3x, 1H NMR
500 MHz, CDCl3
CDCl3
2.00
1.00
1.98
2.14
3.16
6.19
f1 (ppm)

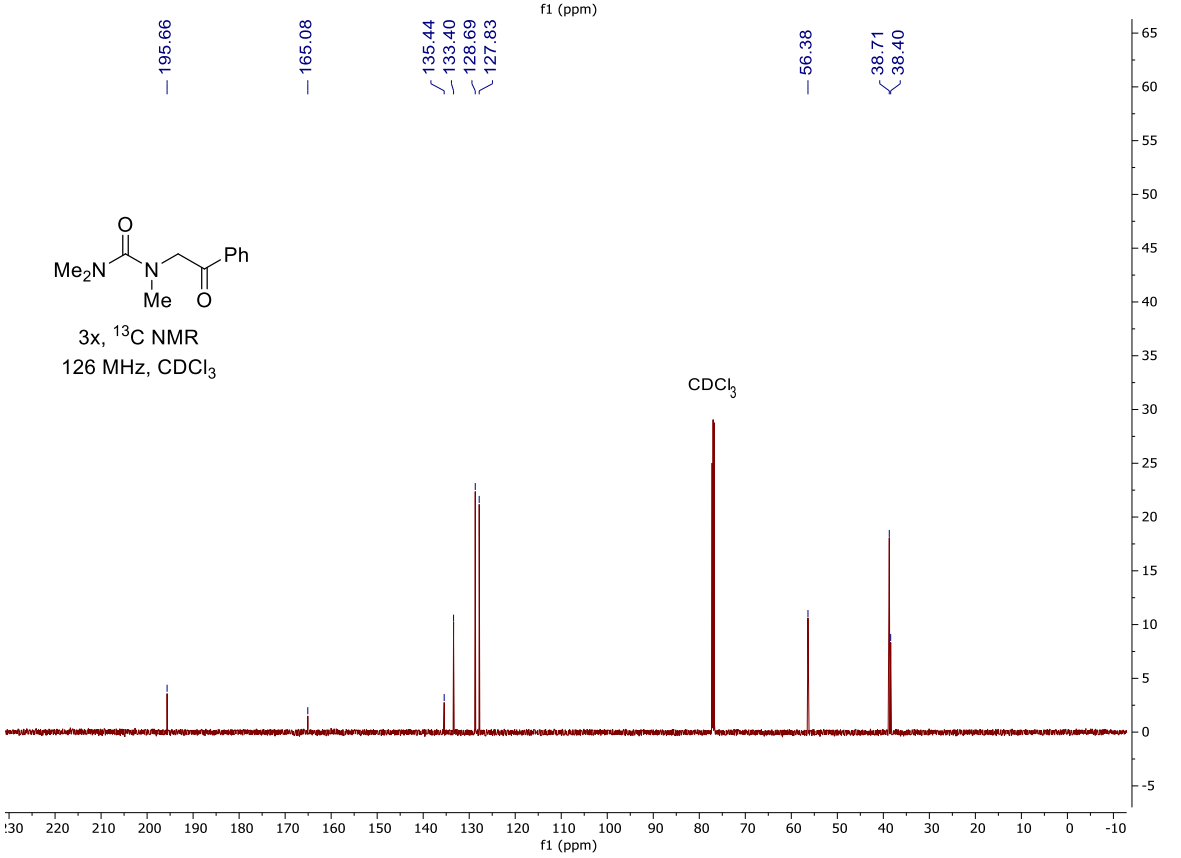
195.66
165.08
135.44
133.40
128.69
127.83
56.38
38.71
38.40
Me2N
O
N
Me
O
Ph
3x, 13C NMR
126 MHz, CDCl3
CDCl3
f1 (ppm)

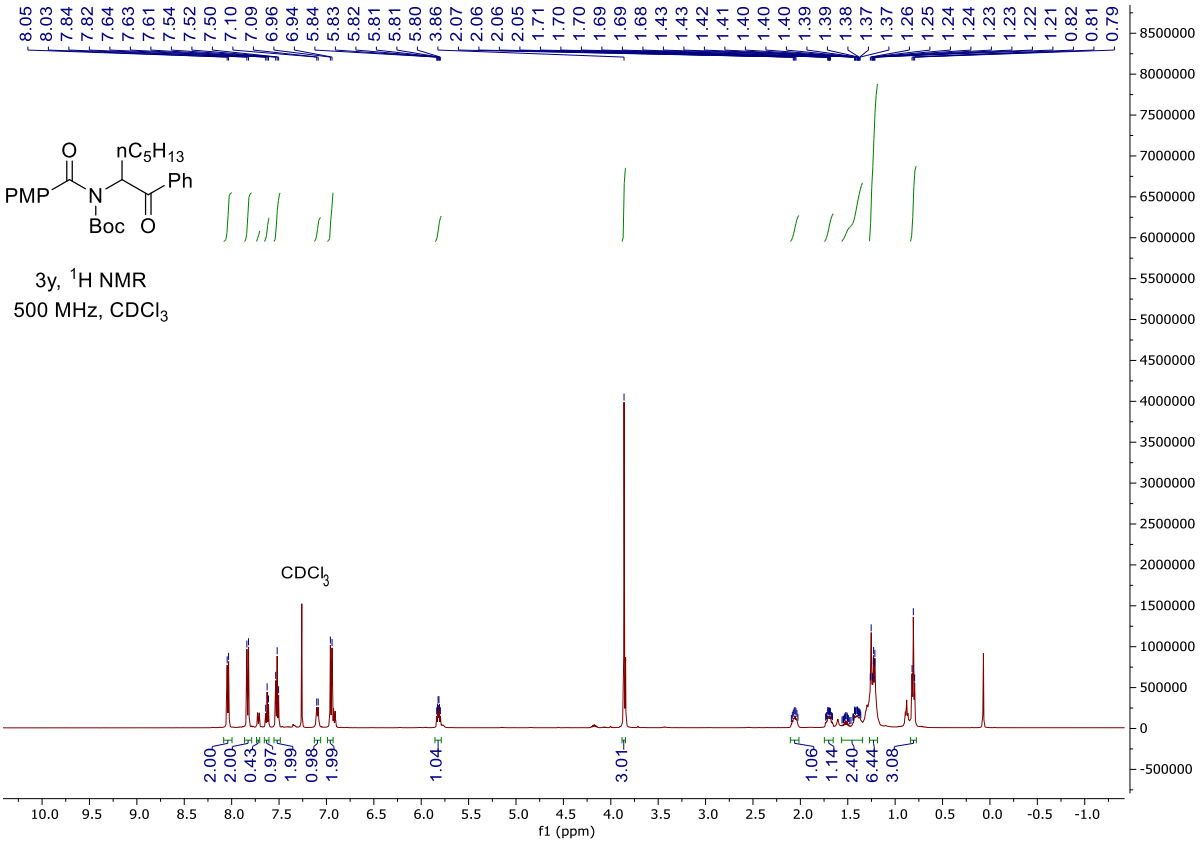

3y, ^{1}H NMR
500 MHz, $CDCl_3$

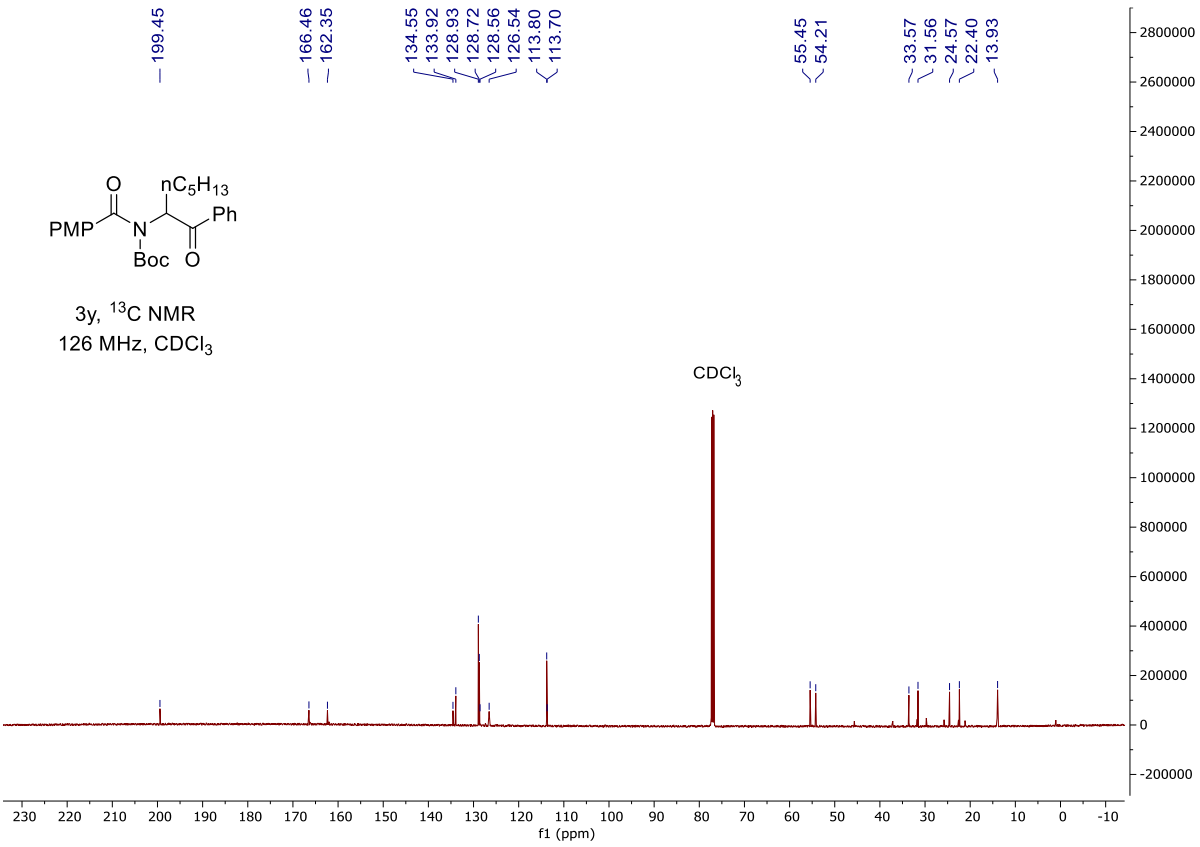

3y, ^{13}C NMR
126 MHz, $CDCl_3$

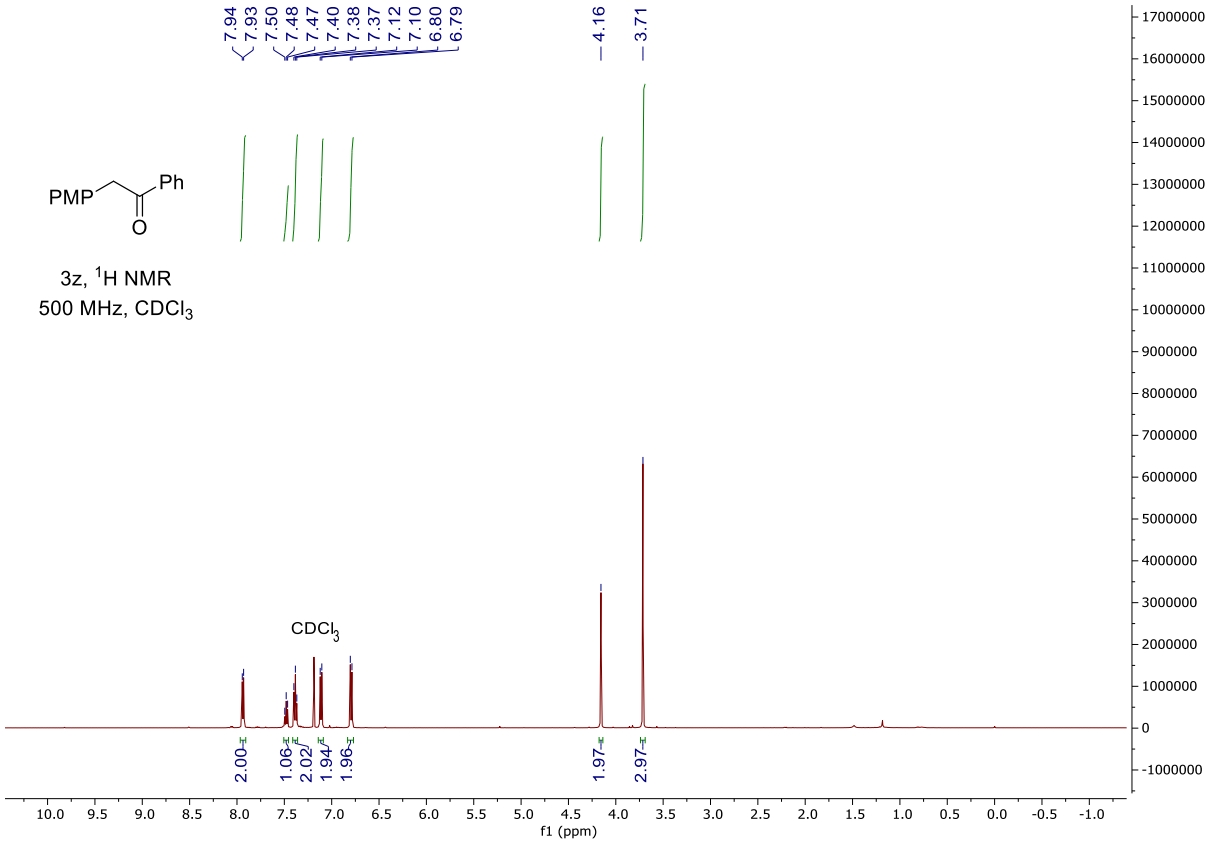
7.94
7.93
7.50
7.48
7.47
7.40
7.38
7.37
7.12
7.10
6.80
6.79
4.16
3.71
PMP
Ph
O
3z, 1H NMR
500 MHz, CDCl3
CDCl3
2.00
1.06
2.02
1.94
1.96
1.97
2.97
f1 (ppm)

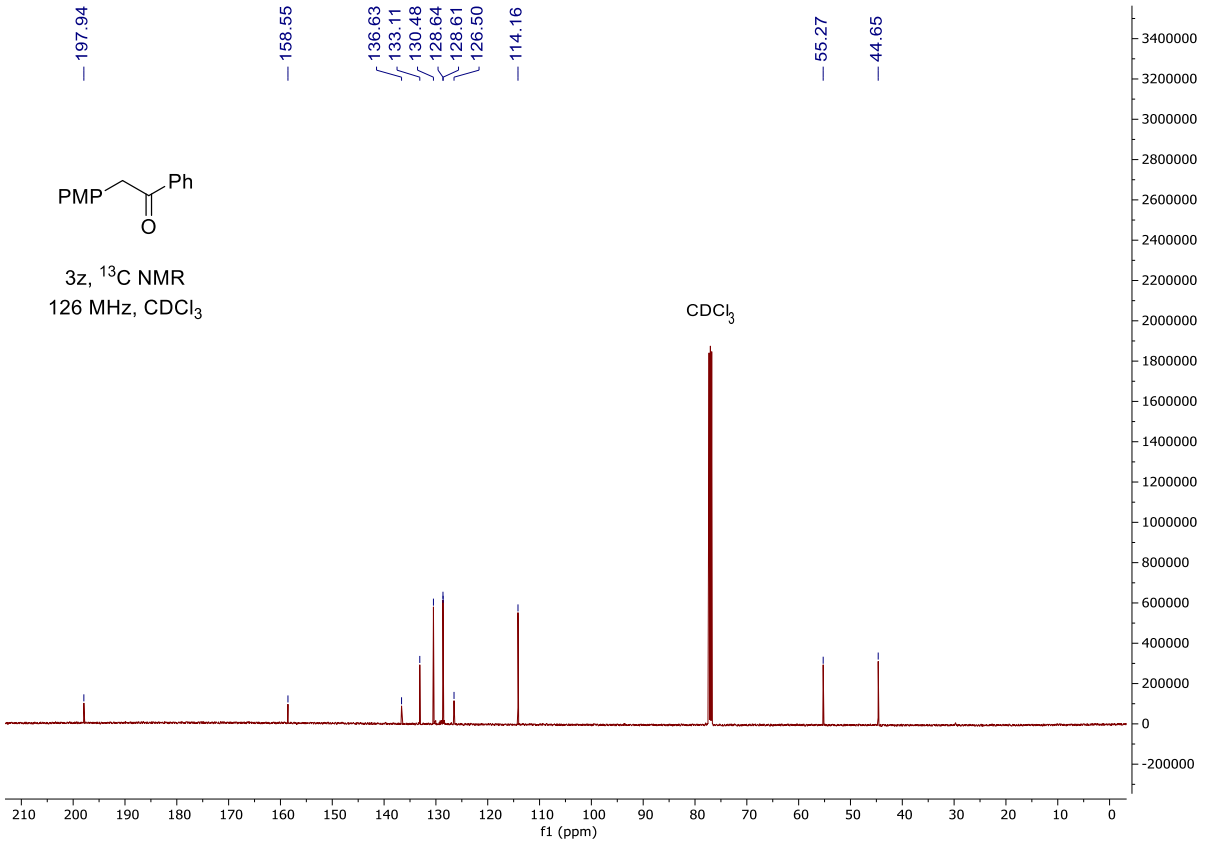
197.94
158.55
136.63
133.11
130.48
128.64
128.61
126.50
114.16
55.27
44.65
PMP
Ph
O
3z, 13C NMR
126 MHz, CDCl3
CDCl3
f1 (ppm)

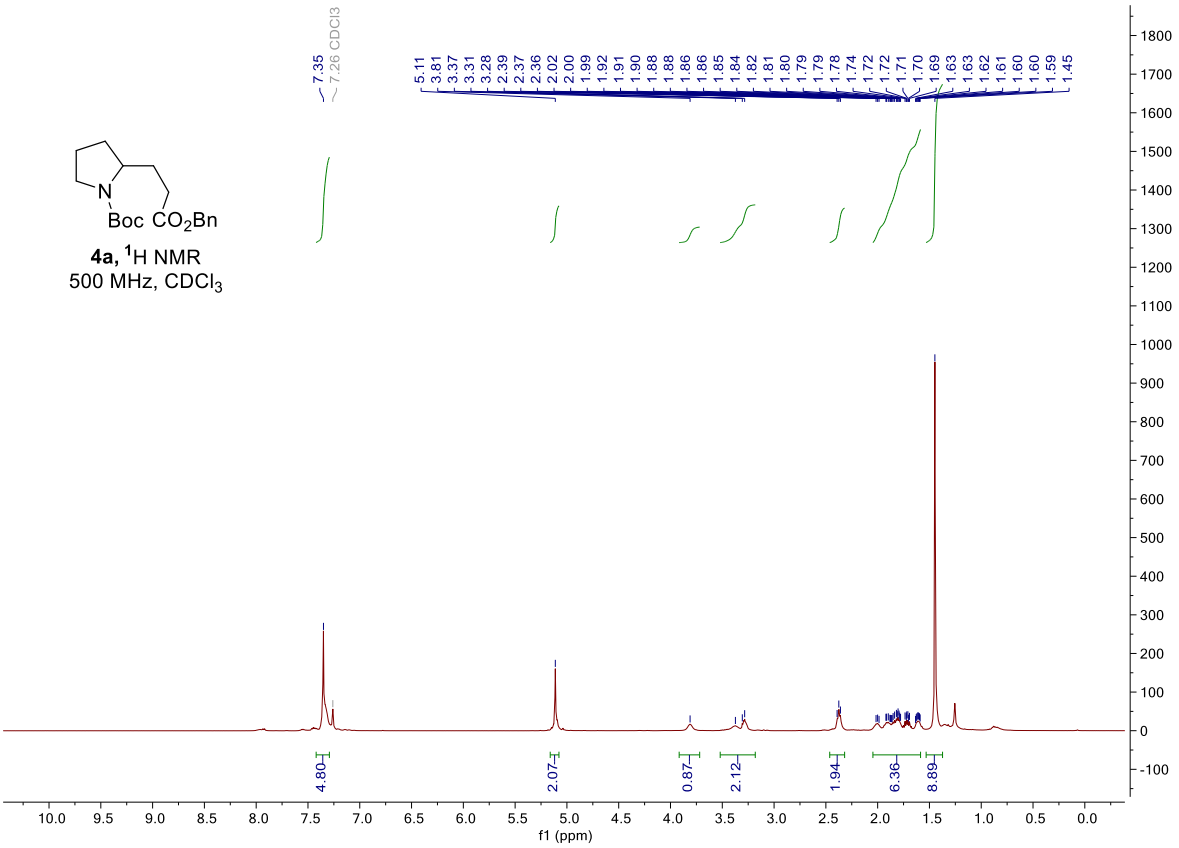
Boc CO2Bn
4a, 1H NMR
500 MHz, CDCl3
7.35
7.26 CDCl3
5.11
3.81
3.37
3.31
3.28
2.39
2.37
2.36
2.02
2.00
1.99
1.92
1.91
1.90
1.88
1.88
1.86
1.86
1.85
1.84
1.82
1.81
1.80
1.79
1.79
1.78
1.74
1.72
1.72
1.71
1.70
1.69
1.63
1.63
1.62
1.61
1.60
1.60
1.59
1.45
4.80
2.07
0.87
2.12
1.94
6.36
8.89
f1 (ppm)

Bibliography

1. Recent Advances in C–H Functionalization. *J. Org. Chem.* **2016,** *81* (2), 343-350.

2. Altus, K. M.; Love, J. A., The continuum of carbon–hydrogen (C–H) activation mechanisms and terminology. *Communications Chemistry* **2021,** *4* (1), 173.

3. Tasker, S. Z.; Standley, E. A.; Jamison, T. F., Recent advances in homogeneous nickel catalysis. *Nature* **2014,** *509* (7500), 299-309.

4. Johnson, S. A., Nickel complexes for catalytic C–H bond functionalization. *Dalton Trans.* **2015,** *44* (24), 10905-10913.

5. Jonas, K.; Wilke, G., Hydrido and Alkyl(aryl)hydrido Complexes of Nickel. *Angew. Chem. Int. Ed.* **1969,** *8* (7), 519-520.

6. (a) Keen, A. L.; Doster, M.; Johnson, S. A., 1,4-Shifts in a Dinuclear Ni(I) Biarylyl Complex: A Mechanistic Study of C−H Bond Activation by Monovalent Nickel. *J. Am. Chem. Soc.* **2007,** *129* (4), 810-819; (b) Khake, S. M.; Chatani, N., Nickel-Catalyzed C−H Functionalization Using A Non-directed Strategy. *Chem* **2020,** *6* (5), 1056-1081; (c) Keen, A. L.; Johnson, S. A., Nickel(0)-Catalyzed Isomerization of an Aryne Complex: Formation of a Dinuclear Ni(I) Complex via C−H Rather than C−F Bond Activation. *J. Am. Chem. Soc.* **2006,** *128* (6), 1806-1807.

7. Kanyiva, K. S.; Kashihara, N.; Nakao, Y.; Hiyama, T.; Ohashi, M.; Ogoshi, S., Hydrofluoroarylation of alkynes with fluoroarenes. *Dalton Trans.* **2010,** *39* (43), 10483-10494.

8. (a) Zhang, Z.; Bera, S.; Fan, C.; Hu, X., Streamlined Alkylation via Nickel-Hydride-Catalyzed Hydrocarbonation of Alkenes. *J. Am. Chem. Soc.* **2022,** *144* (16), 7015-7029; (b) Huang, Q.; Chen, Y.; Zhou, X.; Dai, L.; Lu, Y., Nickel-Hydride-Catalyzed Diastereo- and Enantioselective Hydroalkylation of Cyclopropenes. *Angew. Chem. Int. Ed.* **2022,** *61* (46), e202210560.

9. Doster, M. E.; Hatnean, J. A.; Jeftic, T.; Modi, S.; Johnson, S. A., Catalytic C−H Bond Stannylation: A New Regioselective Pathway to C−Sn Bonds via C−H Bond Functionalization. *J. Am. Chem. Soc.* **2010,** *132* (34), 11923-11925.

10. (a) Johnson, S. A.; Doster, M. E.; Matthews, J.; Shoshani, M.; Thibodeau, M.; Labadie, A.; Hatnean, J. A., A mechanistic investigation of carbon–hydrogen bond stannylation: synthesis and

characterization of nickel catalysts. *Dalton Trans.* **2012,** *41* (26), 8135-8143; (b) Doster, M. E.; Johnson, S. A., Carbon–Hydrogen Bond Stannylation and Alkylation Catalyzed by Nitrogen-Donor-Supported Nickel Complexes: Intermediates with Ni–Sn Bonds and Catalytic Carbostannylation of Ethylene with Organostannanes. *Organometallics* **2013,** *32* (15), 4174-4184.

11. Guihaumé, J.; Halbert, S.; Eisenstein, O.; Perutz, R. N., Hydrofluoroarylation of Alkynes with Ni Catalysts. C–H Activation via Ligand-to-Ligand Hydrogen Transfer, an Alternative to Oxidative Addition. *Organometallics* **2012,** *31* (4), 1300-1314.

12. Winstein, S.; Traylor, T. G., Mechanisms of Reaction of Organomercurials. II. Electrophilic Substitution on Saturated Carbon. Acetolysis of Dialkylmercury Compounds. *J. Am. Chem. Soc.* **1955,** *77* (14), 3747-3752.

13. (a) Gorelsky, S. I.; Lapointe, D.; Fagnou, K., Analysis of the Concerted Metalation-Deprotonation Mechanism in Palladium-Catalyzed Direct Arylation Across a Broad Range of Aromatic Substrates. *J. Am. Chem. Soc.* **2008,** *130* (33), 10848-10849; (b) Zaitsev, V. G.; Shabashov, D.; Daugulis, O., Highly Regioselective Arylation of sp3 C−H Bonds Catalyzed by Palladium Acetate. *J. Am. Chem. Soc.* **2005,** *127* (38), 13154-13155.

14. Gensch, T.; Hopkinson, M. N.; Glorius, F.; Wencel-Delord, J., Mild metal-catalyzed C–H activation: examples and concepts. *Chem. Soc. Rev.* **2016,** *45* (10), 2900-2936.

15. Aihara, Y.; Chatani, N., Nickel-Catalyzed Reaction of C–H Bonds in Amides with I2: ortho-Iodination via the Cleavage of C(sp2)–H Bonds and Oxidative Cyclization to β-Lactams via the Cleavage of C(sp3)–H Bonds. *ACS Catal.* **2016,** *6* (7), 4323-4329.

16. Theoretical Study of Ni-Catalysis. In *Computational Methods in Organometallic Catalysis*, 2021; pp 125-179.

17. Haines, B. E.; Yu, J.-Q.; Musaev, D. G., The mechanism of directed Ni(ii)-catalyzed C–H iodination with molecular iodine. *Chem. Sci.* **2018,** *9* (5), 1144-1154.

18. (a) Muto, K.; Yamaguchi, J.; Itami, K., Nickel-Catalyzed C–H/C–O Coupling of Azoles with Phenol Derivatives. *J. Am. Chem. Soc.* **2012,** *134* (1), 169-172; (b) Amaike, K.; Muto, K.; Yamaguchi, J.; Itami, K., Decarbonylative C–H Coupling of Azoles and Aryl Esters: Unprecedented Nickel Catalysis and Application to the Synthesis of Muscoride A. *J. Am. Chem. Soc.* **2012,** *134* (33), 13573-13576.

19. Lu, Q.; Yu, H.; Fu, Y., Mechanistic Study of Chemoselectivity in Ni-Catalyzed Coupling Reactions between Azoles and Aryl Carboxylates. *J. Am. Chem. Soc.* **2014,** *136* (23), 8252-8260.

20. Xu, H.; Muto, K.; Yamaguchi, J.; Zhao, C.; Itami, K.; Musaev, D. G., Key Mechanistic Features of Ni-Catalyzed C–H/C–O Biaryl Coupling of Azoles and Naphthalen-2-yl Pivalates. *J. Am. Chem. Soc.* **2014,** *136* (42), 14834-14844.

21. Kleiman, J. P.; Dubeck, M., The Preparation of Cyclopentadienyl [o-(Phenylazo)Phenyl]Nickel. *J. Am. Chem. Soc.* **1963,** *85* (10), 1544-1545.

22. Mader, E. A.; Davidson, E. R.; Mayer, J. M., Large Ground-State Entropy Changes for Hydrogen Atom Transfer Reactions of Iron Complexes. *J. Am. Chem. Soc.* **2007,** *129* (16), 5153-5166.

23. Hofmann, A. W., Zur Kenntniss des Piperidins und Pyridins. *Berichte der deutschen chemischen Gesellschaft* **1879,** *12* (1), 984-990.

24. Barton, D. H. R.; Beaton, J. M.; Geller, L. E.; Pechet, M. M., A NEW PHOTOCHEMICAL REACTION. *J. Am. Chem. Soc.* **1960,** *82* (10), 2640-2641.

25. Curran, D. P.; Chen, M.-H., Radical-initiated polyolefinic cyclizations in condensed cyclopentanoid synthesis. Total synthesis of (±)-Δ9(12)-capnellene. *Tetrahedron Lett.* **1985,** *26* (41), 4991-4994.

26. Stateman, L. M.; Nakafuku, K. M.; Nagib, D. A., Remote C–H Functionalization via Selective Hydrogen Atom Transfer. *Synthesis* **2018,** *50* (08), 1569-1586.

27. Sarkar, S.; Cheung, K. P. S.; Gevorgyan, V., C-H functionalization reactions enabled by hydrogen atom transfer to carbon-centered radicals. *Chem. Sci.* **2020,** *11* (48), 12974-12993.

28. Chan, A. Y.; Perry, I. B.; Bissonnette, N. B.; Buksh, B. F.; Edwards, G. A.; Frye, L. I.; Garry, O. L.; Lavagnino, M. N.; Li, B. X.; Liang, Y.; Mao, E.; Millet, A.; Oakley, J. V.; Reed, N. L.; Sakai, H. A.; Seath, C. P.; MacMillan, D. W. C., Metallaphotoredox: The Merger of Photoredox and Transition Metal Catalysis. *Chem. Rev.* **2022,** *122* (2), 1485-1542.

29. Cao, H.; Tang, X.; Tang, H.; Yuan, Y.; Wu, J., Photoinduced intermolecular hydrogen atom transfer reactions in organic synthesis. *Chem Catalysis* **2021,** *1* (3), 523-598.

30. Zuo, Z.; Ahneman, D. T.; Chu, L.; Terrett, J. A.; Doyle, A. G.; MacMillan, D. W. C., Merging photoredox with nickel catalysis: Coupling of α-carboxyl sp³-carbons with aryl halides. *Science* **2014,** *345* (6195), 437-440.

31. Shaw, M. H.; Shurtleff, V. W.; Terrett, J. A.; Cuthbertson, J. D.; MacMillan, D. W. C., Native functionality in triple catalytic cross-coupling: sp3 C–H bonds as latent nucleophiles. *Science* **2016,** *352* (6291), 1304-1308.

32. Perry, I. B.; Brewer, T. F.; Sarver, P. J.; Schultz, D. M.; DiRocco, D. A.; MacMillan, D. W. C., Direct arylation of strong aliphatic C–H bonds. *Nature* **2018,** *560* (7716), 70-75.

33. Capaldo, L.; Ravelli, D., Hydrogen Atom Transfer (HAT): A Versatile Strategy for Substrate Activation in Photocatalyzed Organic Synthesis. *European Journal of Organic Chemistry* **2017,** *2017* (15), 2056-2071.

34. Tang, S.; Wang, P.; Li, H.; Lei, A., Multimetallic catalysed radical oxidative C(sp3)–H/C(sp)–H cross-coupling between unactivated alkanes and terminal alkynes. *Nat. Commun.* **2016,** *7* (1), 11676.

35. Gong, Y.; Su, L.; Zhu, Z.; Ye, Y.; Gong, H., Nickel-Catalyzed Thermal Redox Functionalization of C(sp3)−H Bonds with Carbon Electrophiles**. *Angew. Chem. Int. Ed.* **2022,** *61* (22), e202201662.

36. Hu, H.; Chen, S.-J.; Mandal, M.; Pratik, S. M.; Buss, J. A.; Krska, S. W.; Cramer, C. J.; Stahl, S. S., Copper-catalysed benzylic C–H coupling with alcohols via radical relay enabled by redox buffering. *Nature Catalysis* **2020,** *3* (4), 358-367.

37. Vasilopoulos, A.; Krska, S. W.; Stahl, S. S., C(sp3)–H methylation enabled by peroxide photosensitization and Ni-mediated radical coupling. *Science* **2021,** *372* (6540), 398-403.

38. Nett, A. J.; Montgomery, J.; Zimmerman, P. M., Entrances, Traps, and Rate-Controlling Factors for Nickel-Catalyzed C–H Functionalization. *ACS Catal.* **2017,** *7* (10), 7352-7362.

39. (a) Pitt, W. R.; Parry, D. M.; Perry, B. G.; Groom, C. R., Heteroaromatic Rings of the Future. *J. Med. Chem.* **2009,** *52* (9), 2952-2963; (b) Taylor, A. P.; Robinson, R. P.; Fobian, Y. M.; Blakemore, D. C.; Jones, L. H.; Fadeyi, O., Modern advances in heterocyclic chemistry in drug discovery. *Org. Biomol. Chem.* **2016,** *14* (28), 6611-6637; (c) Jampilek, J., Heterocycles in Medicinal Chemistry. *Molecules* **2019,** *24* (21), 3839.

40. (a) Mei, T. S.; Kou, L.; Ma, S.; Engle, K. M.; Yu, J. Q., Heterocycle Formation via Palladium-Catalyzed C-H Functionalization. *Synthesis* **2012,** *44* (12), 1778-1791; (b) Yang, Y.; Nishiura, M.; Wang, H.; Hou, Z., Metal-catalyzed CH activation for polymer synthesis and functionalization. *Coordination Chemistry Reviews* **2018,** *376*, 506-532.

41. (a) Shilov, A. E.; Shul'pin, G. B., Activation of C−H Bonds by Metal Complexes. *Chem. Rev.* **1997,** *97* (8), 2879-2932; (b) Kakiuchi, F.; Murai, S., Catalytic C−H/Olefin Coupling. *Acc. Chem. Res.* **2002,** *35* (10), 826-834; (c) Labinger, J. A.; Bercaw, J. E., Understanding and exploiting C-H bond activation. *Nature* **2002,** *417* (6888), 507-514; (d) Davies, H. M. L.;

Beckwith, R. E. J., Catalytic enantioselective C-H activation by means of metal-carbenoid-induced C-H insertion. *Chem. Rev.* **2003,** *103* (8), 2861-2903; (e) Zheng, C.; You, S. L., Recent development of direct asymmetric functionalization of inert C-H bonds. *Rsc Adv.* **2014,** *4* (12), 6173-6214; (f) Yang, L.; Huang, H., Transition-Metal-Catalyzed Direct Addition of Unactivated C–H Bonds to Polar Unsaturated Bonds. *Chem. Rev.* **2015,** *115* (9), 3468-3517; (g) Gensch, T.; Hopkinson, M. N.; Glorius, F.; Wencel-Delord, J., Mild metal-catalyzed C-H activation: examples and concepts. *Chem. Soc. Rev.* **2016,** *45* (10), 2900-36; (h) Ping, L.; Chung, D. S.; Bouffard, J.; Lee, S. G., Transition metal-catalyzed site- and regio-divergent C-H bond functionalization. *Chem. Soc. Rev.* **2017,** *46* (14), 4299-4328; (i) Newton, C. G.; Wang, S.-G.; Oliveira, C. C.; Cramer, N., Catalytic Enantioselective Transformations Involving C–H Bond Cleavage by Transition-Metal Complexes. *Chem. Rev.* **2017,** *117* (13), 8908-8976; (j) He, J.; Wasa, M.; Chan, K. S. L.; Shao, Q.; Yu, J.-Q., Palladium-Catalyzed Transformations of Alkyl C–H Bonds. *Chem. Rev.* **2017,** *117* (13), 8754-8786; (k) Park, Y.; Kim, Y.; Chang, S., Transition Metal-Catalyzed C–H Amination: Scope, Mechanism, and Applications. *Chem. Rev.* **2017,** *117* (13), 9247-9301; (l) Dong, Z.; Ren, Z.; Thompson, S. J.; Xu, Y.; Dong, G., Transition-Metal-Catalyzed C–H Alkylation Using Alkenes. *Chem. Rev.* **2017,** *117* (13), 9333-9403.

42. (a) Davies, H. M. L.; Morton, D., Collective Approach to Advancing C–H Functionalization. *ACS Cent. Sci.* **2017,** *3* (9), 936-943; (b) Newhouse, T.; Baran, P. S.; Hoffmann, R. W., The economies of synthesis. *Chem. Soc. Rev.* **2009,** *38* (11), 3010-3021; (c) Pouliot, J. R.; Grenier, F.; Blaskovits, J. T.; Beaupre, S.; Leclerc, M., Direct (Hetero)arylation Polymerization: Simplicity for Conjugated Polymer Synthesis. *Chem Rev* **2016,** *116* (22), 14225-14274; (d) Zhang, J.; Kang, L. J.; Parker, T. C.; Blakey, S. B.; Luscombe, C. K.; Marder, S. R., Recent Developments in C–H Activation for Materials Science in the Center for Selective C–H Activation. *Molecules* **2018,** *23* (4), 922; (e) Cernak, T.; Dykstra, K. D.; Tyagarajan, S.; Vachal, P.; Krska, S. W., The medicinal chemist's toolbox for late stage functionalization of drug-like molecules. *Chem. Soc. Rev.* **2016,** *45* (3), 546-76.

43. (a) Villuendas, P.; Ruiz, S.; Urriolabeitia, E. P., Functionalization of Heteroaromatic Substrates using Groups 9 and 10 Catalysts. *Catalytic Hydroarylation of Carbon-Carbon Multiple Bonds* **2018**, 5-47; (b) Hirano, K.; Miura, M., C□H Activation of Heteroaromatics. In *Sustainable Catalysis*, 2013; pp 233-267.

44. (a) Danopoulos, A. A.; Simler, T.; Braunstein, P., N-Heterocyclic Carbene Complexes of Copper, Nickel, and Cobalt. *Chem. Rev.* **2019,** *119* (6), 3730-3961; (b) Loup, J.; Dhawa, U.; Pesciaioli, F.; Wencel-Delord, J.; Ackermann, L., Enantioselective C−H Activation with Earth-Abundant 3d Transition Metals. *Angew. Chem. Int. Ed.* **2019,** *58* (37), 12803-12818; (c) Gandeepan, P.; Muller, T.; Zell, D.; Cera, G.; Warratz, S.; Ackermann, L., 3d Transition Metals for C-H Activation. *Chem. Rev.* **2019,** *119* (4), 2192-2452; (d) Song, G.; O, W. W. N.; Hou, Z., Enantioselective C–H Bond Addition of Pyridines to Alkenes Catalyzed by Chiral Half-Sandwich Rare-Earth Complexes. *J. Am. Chem. Soc.* **2014,** *136* (35), 12209-12212; (e) Lou, S.-J.; Mo, Z.; Nishiura, M.; Hou, Z., Construction of All-Carbon Quaternary Stereocenters by Scandium-Catalyzed Intramolecular C–H Alkylation of Imidazoles with 1,1-Disubstituted Alkenes. *J. Am. Chem. Soc.* **2020,** *142* (3), 1200-1205.

45. Nakao, Y.; Kashihara, N.; Kanyiva, K. S.; Hiyama, T., Nickel-Catalyzed Alkenylation and Alkylation of Fluoroarenes via Activation of C−H Bond over C−F Bond. *J. Am. Chem. Soc.* **2008,** *130* (48), 16170-16171.

46. (a) Wang, Y.-X.; Qi, S.-L.; Luan, Y.-X.; Han, X.-W.; Wang, S.; Chen, H.; Ye, M., Enantioselective Ni–Al Bimetallic Catalyzed exo-Selective C–H Cyclization of Imidazoles with Alkenes. *J. Am. Chem. Soc.* **2018,** *140* (16), 5360-5364; (b) Chen, H.; Wang, Y.-X.; Luan, Y.-X.; Ye, M., Enantioselective Twofold C−H Annulation of Formamides and Alkynes without Built-in Chelating Groups. *Angew. Chem. Int. Ed.* **2020,** *59* (24), 9428-9432; (c) Yin, G.; Li, Y.; Wang, R.-H.; Li, J.-F.; Xu, X.-T.; Luan, Y.-X.; Ye, M., Ligand-Controlled Ni(0)–Al(III) Bimetal-Catalyzed C3–H Alkenylation of 2-Pyridones by Reversing Conventional Selectivity. *ACS Catal.* **2021,** *11* (8), 4606-4612.

47. (a) Donets, P. A.; Cramer, N., Ligand-Controlled Regiodivergent Nickel-Catalyzed Annulation of Pyridones. *Angew. Chem. Int. Ed.* **2015,** *54* (2), 633-637; (b) Ahlin, J. S. E.; Cramer, N., Chiral N-Heterocyclic Carbene Ligand Enabled Nickel(0)-Catalyzed Enantioselective Three-Component Couplings as Direct Access to Silylated Indanols. *Org. Lett.* **2016,** *18* (13), 3242-3245; (c) Diesel, J.; Finogenova, A. M.; Cramer, N., Nickel-Catalyzed Enantioselective Pyridone C–H Functionalizations Enabled by a Bulky N-Heterocyclic Carbene Ligand. *J. Am. Chem. Soc.* **2018,** *140* (13), 4489-4493; (d) Diesel, J.; Grosheva, D.; Kodama, S.; Cramer, N., A Bulky Chiral N-Heterocyclic Carbene Nickel Catalyst Enables Enantioselective C−H Functionalizations of Indoles and Pyrroles. *Angew. Chem. Int. Ed.* **2019,** *58* (32), 11044-11048.

48. (a) Loup, J.; Müller, V.; Ghorai, D.; Ackermann, L., Enantioselective Aluminum-Free Alkene Hydroarylations through C−H Activation by a Chiral Nickel/JoSPOphos Manifold. *Angew. Chem. Int. Ed.* **2019,** *58* (6), 1749-1753; (b) Liu, J. B.; Wang, X.; Messinis, A. M.; Liu, X. J.; Kuniyil, R.; Chen, D. Z.; Ackermann, L., Understanding the unique reactivity patterns of nickel/JoSPOphos manifold in the nickel-catalyzed enantioselective C-H cyclization of imidazoles. *Chem. Sci.* **2021,** *12* (2), 718-729.

49. (a) Cai, Y.; Ye, X.; Liu, S.; Shi, S.-L., Nickel/NHC-Catalyzed Asymmetric C−H Alkylation of Fluoroarenes with Alkenes: Synthesis of Enantioenriched Fluorotetralins. *Angew. Chem. Int. Ed.* **2019,** *58* (38), 13433-13437; (b) Shen, D.; Zhang, W.-B.; Li, Z.; Shi, S.-L.; Xu, Y., Nickel/NHC-Catalyzed Enantioselective Cyclization of Pyridones and Pyrimidones with Tethered Alkenes. *Adv. Synth. Catal.* **2020,** *362* (5), 1125-1130; (c) Ma, J.-B.; Zhao, X.; Zhang, D.; Shi, S.-L., Enantio- and Regioselective Ni-Catalyzed para-C–H Alkylation of Pyridines with Styrenes via Intermolecular Hydroarylation. *J. Am. Chem. Soc.* **2022**.

50. (a) Albright, A.; Eddings, D.; Black, R.; Welch, C. J.; Gerasimchuk, N. N.; Gawley, R. E., Design and Synthesis of C2-Symmetric N-Heterocyclic Carbene Precursors and Metal Carbenoids. *J. Org. Chem.* **2011,** *76* (18), 7341-7351; (b) Albright, A.; Gawley, R. E., Application of a C2-Symmetric Copper Carbenoid in the Enantioselective Hydrosilylation of Dialkyl and Aryl–Alkyl Ketones. *J. Am. Chem. Soc.* **2011,** *133* (49), 19680-19683.

51. (a) Cai, Y.; Yang, X.-T.; Zhang, S.-Q.; Li, F.; Li, Y.-Q.; Ruan, L.-X.; Hong, X.; Shi, S.-L., Copper-Catalyzed Enantioselective Markovnikov Protoboration of α-Olefins Enabled by a Buttressed N-Heterocyclic Carbene Ligand. *Angew. Chem. Int. Ed.* **2018,** *57* (5), 1376-1380; (b) Cai, Y.; Zhang, J.-W.; Li, F.; Liu, J.-M.; Shi, S.-L., Nickel/N-Heterocyclic Carbene Complex-Catalyzed Enantioselective Redox-Neutral Coupling of Benzyl Alcohols and Alkynes to Allylic Alcohols. *ACS Catal.* **2019,** *9* (1), 1-6; (c) Zhang, W.-B.; Yang, X.-T.; Ma, J.-B.; Su, Z.-M.; Shi, S.-L., Regio- and Enantioselective C–H Cyclization of Pyridines with Alkenes Enabled by a Nickel/N-Heterocyclic Carbene Catalysis. *J. Am. Chem. Soc.* **2019,** *141* (14), 5628-5634.

52. Li, J.-F.; Pan, D.; Wang, H.-R.; Zhang, T.; Li, Y.; Huang, G.; Ye, M., Enantioselective C2–H Alkylation of Pyridines with 1,3-Dienes via Ni–Al Bimetallic Catalysis. *J. Am. Chem. Soc.* **2022,** *144* (41), 18810-18816.

53. (a) Kakkar, S.; Tahlan, S.; Lim, S. M.; Ramasamy, K.; Mani, V.; Shah, S. A. A.; Narasimhan, B., Benzoxazole derivatives: design, synthesis and biological evaluation. *Chemistry*

Central Journal **2018,** *12* (1), 92; (b) Reddy, G. M.; Kumari, A. K.; Reddy, V. H.; Garcia, J. R., Novel pyranopyrazole derivatives comprising a benzoxazole core as antimicrobial inhibitors: Design, synthesis, microbial resistance and machine aided results. *Bioorganic Chemistry* **2020,** *100*, 103908; (c) Wong, X. K.; Yeong, K. Y., A Patent Review on the Current Developments of Benzoxazoles in Drug Discovery. *ChemMedChem* **2021,** *16* (21), 3237-3262.

54. Wang, H.; Lu, G.; Sormunen, G. J.; Malik, H. A.; Liu, P.; Montgomery, J., NHC Ligands Tailored for Simultaneous Regio- and Enantiocontrol in Nickel-Catalyzed Reductive Couplings. *J. Am. Chem. Soc.* **2017,** *139* (27), 9317-9324.

55. Wu, J.; Faller, J. W.; Hazari, N.; Schmeier, T. J., Stoichiometric and Catalytic Reactions of Thermally Stable Nickel(0) NHC Complexes. *Organometallics* **2012,** *31* (3), 806-809.

56. Saper, N. I.; Ohgi, A.; Small, D. W.; Semba, K.; Nakao, Y.; Hartwig, J. F., Nickel-catalysed anti-Markovnikov hydroarylation of unactivated alkenes with unactivated arenes facilitated by non-covalent interactions. *Nat. Chem.* **2020,** *12* (3), 276-283.

57. Benn, R.; Bussemeier, B.; Holle, S.; Jolly, P. W.; Mynott, R.; Tkatchenko, I.; Wilke, G., Transition-Metal Allyls .6. The Stoichiometric Reaction of 1,3-Dienes with Ligand Modified Zerovalent-Nickel Systems. *J. Organomet. Chem.* **1985,** *279* (1-2), 63-86.

58. Iglesias, M. J.; Blandez, J. F.; Fructos, M. R.; Prieto, A.; Álvarez, E.; Belderrain, T. R.; Nicasio, M. C., Synthesis, Structural Characterization, and Catalytic Activity of IPrNi(styrene)2 in the Amination of Aryl Tosylates. *Organometallics* **2012,** *31* (17), 6312-6316.

59. Nickel, T.; Goddard, R.; Krüger, C.; Pörschke, K.-R., Cyclotrimerization of Ethyne on the Complex Fragment [(η1-tBu2PCH2PtBu2)Ni0] with Formation of an η6-Benzene-Nickel(0) Complex. *Angew. Chem. Int. Ed.* **1994,** *33* (8), 879-882.

60. Lee, W.-C.; Shih, W.-C.; Wang, T.-H.; Liu, Y.; Yap, G. P. A.; Ong, T.-G., Nickel promoted switchable hydroheteroarylation of cyclodienes via C–H bond activation of heteroarenes. *Tetrahedron* **2015,** *71* (26), 4460-4464.

61. Nett, A. J.; Zhao, W.; Zimmerman, P. M.; Montgomery, J., Highly Active Nickel Catalysts for C–H Functionalization Identified through Analysis of Off-Cycle Intermediates. *J. Am. Chem. Soc.* **2015,** *137* (24), 7636-7639.

62. (a) Cheltsov, A. V.; Aoyagi, M.; Aleshin, A.; Yu, E. C.-W.; Gilliland, T.; Zhai, D.; Bobkov, A. A.; Reed, J. C.; Liddington, R. C.; Abagyan, R., Vaccinia Virus Virulence Factor N1L is a Novel Promising Target for Antiviral Therapeutic Intervention. *J. Med. Chem.* **2010,** *53* (10),

3899-3906; (b) Ameen, D.; Snape, T. J., Chiral 1,1-diaryl compounds as important pharmacophores. *Med. Chem. Comm.* **2013,** *4* (6), 893-907.

63. Blackmond, D. G., Kinetic Profiling of Catalytic Organic Reactions as a Mechanistic Tool. *J. Am. Chem. Soc.* **2015,** *137* (34), 10852-10866.

64. Bair, J. S.; Schramm, Y.; Sergeev, A. G.; Clot, E.; Eisenstein, O.; Hartwig, J. F., Linear-Selective Hydroarylation of Unactivated Terminal and Internal Olefins with Trifluoromethyl-Substituted Arenes. *J. Am. Chem. Soc.* **2014,** *136* (38), 13098-13101.

65. While C-H oxidative addition cannot be rigorously excluded, an abundance of evidence supports LLHT pathways in reactions of this type (see reference 6e).

66. Zhu, W.; Gunnoe, T. B., Advances in Group 10 Transition-Metal-Catalyzed Arene Alkylation and Alkenylation. *J. Am. Chem. Soc.* **2021,** *143* (18), 6746-6766.

67. (a) Guo, H.; Weber, W. P., Ruthenium catalyzed regioselective copolymerization of acetophenone and α,ω-dienes. *Polymer Bulletin* **1994,** *32* (5), 525-528; (b) Se´vignon, M.; Papillon, J.; Schulz, E.; Lemaire, M., New synthetic method for the polymerization of alkylthiophenes. *Tetrahedron Lett.* **1999,** *40* (32), 5873-5876; (c) Jo, T. S.; Kim, S. H.; Shin, J.; Bae, C., Highly Efficient Incorporation of Functional Groups into Aromatic Main-Chain Polymer Using Iridium-Catalyzed C−H Activation and Suzuki−Miyaura Reaction. *J. Am. Chem. Soc.* **2009,** *131* (5), 1656-1657; (d) Yoon, K.-Y.; Dong, G., Modular In Situ Functionalization Strategy: Multicomponent Polymerization by Palladium/Norbornene Cooperative Catalysis. *Angew. Chem. Int. Ed.* **2018,** *57* (28), 8592-8596; (e) Chen, L.; Malollari, K. G.; Uliana, A.; Sanchez, D.; Messersmith, P. B.; Hartwig, J. F., Selective, Catalytic Oxidations of C–H Bonds in Polyethylenes Produce Functional Materials with Enhanced Adhesion. *Chem* **2021,** *7* (1), 137-145; (f) Menendez Rodriguez, G.; Díaz-Requejo, M. M.; Pérez, P. J., Metal-Catalyzed Postpolymerization Strategies for Polar Group Incorporation into Polyolefins Containing C ‑ C, C═C, and Aromatic Rings. *Macromolecules* **2021,** *54* (11), 4971-4985; (g) Mayhugh, A. L.; Yadav, P.; Luscombe, C. K., Circular Discovery in Small Molecule and Conjugated Polymer Synthetic Methodology. *J. Am. Chem. Soc.* **2022,** *144* (14), 6123-6135; (h) Xing, L.; Liu, J.-R.; Hong, X.; Houk, K. N.; Luscombe, C. K., An Exception to the Carothers Equation Caused by the Accelerated Chain Extension in a Pd/Ag Cocatalyzed Cross Dehydrogenative Coupling Polymerization. *J. Am. Chem. Soc.* **2022,** *144* (5), 2311-2322.

68. (a) Yamamoto, A.; Nishiura, M.; Oyamada, J.; Koshino, H.; Hou, Z., Scandium-Catalyzed Syndiospecific Chain-Transfer Polymerization of Styrene Using Anisoles as a Chain Transfer Agent. *Macromolecules* **2016,** *49* (7), 2458-2466; (b) Shi, X.; Nishiura, M.; Hou, Z., C–H Polyaddition of Dimethoxyarenes to Unconjugated Dienes by Rare Earth Catalysts. *J. Am. Chem. Soc.* **2016,** *138* (19), 6147-6150; (c) Liang, T.; Goudari, S. B.; Chen, C., A simple and versatile nickel platform for the generation of branched high molecular weight polyolefins. *Nat. Commun.* **2020,** *11* (1), 372; (d) Doba, T.; Ilies, L.; Sato, W.; Shang, R.; Nakamura, E., Iron-catalysed regioselective thienyl C–H/C–H coupling. *Nature Catalysis* **2021,** *4* (7), 631-638; (e) Zhou, L.; Xu, L.; Song, X.; Kang, S.-M.; Liu, N.; Wu, Z.-Q., Nickel(II)-catalyzed living polymerization of diazoacetates toward polycarbene homopolymer and polythiophene-block-polycarbene copolymers. *Nat. Commun.* **2022,** *13* (1), 811.

69. (a) Johnson, L. K.; Killian, C. M.; Brookhart, M., New Pd(II)- and Ni(II)-Based Catalysts for Polymerization of Ethylene and .alpha.-Olefins. *J. Am. Chem. Soc.* **1995,** *117* (23), 6414-6415; (b) Younkin, T. R.; Connor, E. F.; Henderson, J. I.; Friedrich, S. K.; Grubbs, R. H.; Bansleben, D. A., Neutral, Single-Component Nickel (II) Polyolefin Catalysts That Tolerate Heteroatoms. *Science* **2000,** *287* (5452), 460-462; (c) Keim, W., Oligomerization of Ethylene to α-Olefins: Discovery and Development of the Shell Higher Olefin Process (SHOP). *Angew. Chem. Int. Ed.* **2013,** *52* (48), 12492-12496; (d) Kaiser, J. M.; Long, B. K., Recent developments in redox-active olefin polymerization catalysts. *Coordination Chemistry Reviews* **2018,** *372*, 141-152; (e) Lutz, J. P.; Hannigan, M. D.; McNeil, A. J., Polymers synthesized via catalyst-transfer polymerization and their applications. *Coordination Chemistry Reviews* **2018,** *376*, 225-247; (f) Wang, F.; Chen, C., A continuing legend: the Brookhart-type α-diimine nickel and palladium catalysts. *Polymer Chemistry* **2019,** *10* (19), 2354-2369.

70. Ziegler, K., A Forty Years' Stroll through the Realms of Organometallic Chemistry. In *Advances in Organometallic Chemistry*, Stone, F. G. A.; West, R., Eds. Academic Press: 1968; Vol. 6, pp 1-17.

71. Wilke, G., Fifty Years of Ziegler Catalysts: Consequences and Development of an Invention. *Angew. Chem. Int. Ed.* **2003,** *42* (41), 5000-5008.

72. Yamamoto, T.; Sanechika, K.; Yamamoto, A., Preparation of thermostable and electric-conducting poly(2,5-thienylene). *Journal of Polymer Science: Polymer Letters Edition* **1980,** *18* (1), 9-12.

73. Lin, J. W. P.; Dudek, L. P., Synthesis and properties of poly(2,5-thienylene). *Journal of Polymer Science: Polymer Chemistry Edition* **1980,** *18* (9), 2869-2873.

74. (a) McCullough, R. D.; Lowe, R. D., Enhanced electrical conductivity in regioselectively synthesized poly(3-alkylthiophenes). *Journal of the Chemical Society, Chemical Communications* **1992,** (1), 70-72; (b) Sheina, E. E.; Liu, J.; Iovu, M. C.; Laird, D. W.; McCullough, R. D., Chain Growth Mechanism for Regioregular Nickel-Initiated Cross-Coupling Polymerizations. *Macromolecules* **2004,** *37* (10), 3526-3528.

75. (a) Leone, A. K.; Goldberg, P. K.; McNeil, A. J., Ring-Walking in Catalyst-Transfer Polymerization. *J. Am. Chem. Soc.* **2018,** *140* (25), 7846-7850; (b) Lee, J.; Kim, H.; Park, H.; Kim, T.; Hwang, S.-H.; Seo, D.; Chung, T. D.; Choi, T.-L., Universal Suzuki–Miyaura Catalyst-Transfer Polymerization for Precision Synthesis of Strong Donor/Acceptor-Based Conjugated Polymers and Their Sequence Engineering. *J. Am. Chem. Soc.* **2021,** *143* (29), 11180-11190; (c) Kobayashi, S.; Ashiya, M.; Yamamoto, T.; Tajima, K.; Yamamoto, Y.; Isono, T.; Satoh, T. Suzuki–Miyaura Catalyst-Transfer Polycondensation of Triolborate-Type Carbazole Monomers *Polymers* [Online], 2021.

76. (a) Obata, A.; Ano, Y.; Chatani, N., Nickel-catalyzed C–H/N–H annulation of aromatic amides with alkynes in the absence of a specific chelation system. *Chem. Sci.* **2017,** *8* (9), 6650-6655; (b) Obata, A.; Sasagawa, A.; Yamazaki, K.; Ano, Y.; Chatani, N., Nickel-catalyzed oxidative C–H/N–H annulation of N-heteroaromatic compounds with alkynes. *Chem. Sci.* **2019,** *10* (11), 3242-3248.

77. Wang, X.-C.; Li, B.; Ju, C.-W.; Zhao, D., Nickel(0)-catalyzed divergent reactions of silacyclobutanes with internal alkynes. *Nat. Commun.* **2022,** *13* (1), 3392.

78. (a) Cheng, L.; Li, M.-M.; Xiao, L.-J.; Xie, J.-H.; Zhou, Q.-L., Nickel(0)-Catalyzed Hydroalkylation of 1,3-Dienes with Simple Ketones. *J. Am. Chem. Soc.* **2018,** *140* (37), 11627-11630; (b) Chen, M.; Montgomery, J., Nickel-Catalyzed Intermolecular Enantioselective Heteroaromatic C–H Alkylation. *ACS Catal.* **2022,** *12* (18), 11015-11023.

79. (a) Flory, P. J.; Leutner, F. S., Occurrence of head-to-head arrangements of structural units in polyvinyl alcohol. *J. Poly. Sci.* **1948,** *3* (6), 880-890; (b) Starnes Jr, W. H., Structural defects in poly(vinyl chloride). *Journal of Polymer Science Part A: Polymer Chemistry* **2005,** *43* (12), 2451-2467; (c) Heintges, G. H. L.; Janssen, R. A. J., On the homocoupling of trialkylstannyl monomers

in the synthesis of diketopyrrolopyrrole polymers and its effect on the performance of polymer-fullerene photovoltaic cells. *Rsc Adv.* **2019,** *9* (28), 15703-15714.

80. Nakao, Y.; Kashihara, N.; Kanyiva, K. S.; Hiyama, T., Nickel-Catalyzed Hydroheteroarylation of Vinylarenes. *Angew. Chem. Int. Ed.* **2010,** *49* (26), 4451-4454.

81. (a) Garlets, Z. J.; Davies, H. M. L., Harnessing the β-Silicon Effect for Regioselective and Stereoselective Rhodium(II)-Catalyzed C–H Functionalization by Donor/Acceptor Carbenes Derived from 1-Sulfonyl-1,2,3-triazoles. *Org. Lett.* **2018,** *20* (8), 2168-2171; (b) Roberts, D. D.; McLaughlin, M. G., Strategic Applications of the β-Silicon Effect. *Adv. Synth. Catal.* **2022,** *364* (14), 2307-2332.

82. Mooney, M.; Wang, Y.; Nyayachavadi, A.; Zhang, S.; Gu, X.; Rondeau-Gagné, S., Enhancing the Solubility of Semiconducting Polymers in Eco-Friendly Solvents with Carbohydrate-Containing Side Chains. *ACS Applied Materials & Interfaces* **2021,** *13* (21), 25175-25185.

83. Kaloni, T. P.; Giesbrecht, P. K.; Schreckenbach, G.; Freund, M. S., Polythiophene: From Fundamental Perspectives to Applications. *Chemistry of Materials* **2017,** *29* (24), 10248-10283.

84. (a) Fujiwara, Y.; Dixon, J. A.; O'Hara, F.; Funder, E. D.; Dixon, D. D.; Rodriguez, R. A.; Baxter, R. D.; Herlé, B.; Sach, N.; Collins, M. R.; Ishihara, Y.; Baran, P. S., Practical and innate carbon–hydrogen functionalization of heterocycles. *Nature* **2012,** *492* (7427), 95-99; (b) Mayol-Llinàs, J.; Nelson, A.; Farnaby, W.; Ayscough, A., Assessing molecular scaffolds for CNS drug discovery. *Drug Discovery Today* **2017,** *22* (7), 965-969.

85. (a) He, J.; Hamann, L. G.; Davies, H. M. L.; Beckwith, R. E. J., Late-stage C–H functionalization of complex alkaloids and drug molecules via intermolecular rhodium-carbenoid insertion. *Nat. Commun.* **2015,** *6* (1), 5943; (b) Seidel, D., The Azomethine Ylide Route to Amine C–H Functionalization: Redox-Versions of Classic Reactions and a Pathway to New Transformations. *Acc. Chem. Res.* **2015,** *48* (2), 317-328.

86. (a) McGrath, N. A.; Brichacek, M.; Njardarson, J. T., A Graphical Journey of Innovative Organic Architectures That Have Improved Our Lives. *J. Chem. Edu.* **2010,** *87* (12), 1348-1349; (b) Kerru, N.; Gummidi, L.; Maddila, S.; Gangu, K. K.; Jonnalagadda, S. B. A Review on Recent Advances in Nitrogen-Containing Molecules and Their Biological Applications *Molecules* [Online], 2020.

87. (a) Phillips, M. W. A., Agrochemical industry development, trends in R&D and the impact of regulation. *Pest Management Science* **2020,** *76* (10), 3348-3356; (b) Balba, H., Review of strobilurin fungicide chemicals. *Journal of Environmental Science and Health, Part B* **2007,** *42* (4), 441-451.

88. (a) Winnacker, M.; Rieger, B., Poly(ester amide)s: recent insights into synthesis, stability and biomedical applications. *Polymer Chemistry* **2016,** *7* (46), 7039-7046; (b) Froidevaux, V.; Negrell, C.; Caillol, S.; Pascault, J.-P.; Boutevin, B., Biobased Amines: From Synthesis to Polymers; Present and Future. *Chem. Rev.* **2016,** *116* (22), 14181-14224.

89. Boström, J.; Brown, D. G.; Young, R. J.; Keserü, G. M., Expanding the medicinal chemistry synthetic toolbox. *Nature Reviews Drug Discovery* **2018,** *17* (10), 709-727.

90. Vitaku, E.; Smith, D. T.; Njardarson, J. T., Analysis of the Structural Diversity, Substitution Patterns, and Frequency of Nitrogen Heterocycles among U.S. FDA Approved Pharmaceuticals. *J. Med. Chem.* **2014,** *57* (24), 10257-10274.

91. Campos, K. R., Direct sp3 C–H bond activation adjacent to nitrogen in heterocycles. *Chem. Soc. Rev.* **2007,** *36* (7), 1069-1084.

92. (a) Holmberg-Douglas, N.; Nicewicz, D. A., Photoredox-Catalyzed C–H Functionalization Reactions. *Chem. Rev.* **2022,** *122* (2), 1925-2016; (b) Qin, Q.; Jiang, H.; Hu, Z.; Ren, D.; Yu, S., Functionalization of C-H Bonds by Photoredox Catalysis. *The Chemical Record* **2017,** *17* (8), 754-774.

93. Schmidt, V. A.; Quinn, R. K.; Brusoe, A. T.; Alexanian, E. J., Site-Selective Aliphatic C–H Bromination Using N-Bromoamides and Visible Light. *J. Am. Chem. Soc.* **2014,** *136* (41), 14389-14392.

94. Wolff, M. E., Cyclization of N-Halogenated Amines (The Hofmann-Löffler Reaction). *Chem. Rev.* **1963,** *63* (1), 55-64.

95. (a) Chen, K.; Richter, J. M.; Baran, P. S., 1,3-Diol Synthesis via Controlled, Radical-Mediated C−H Functionalization. *J. Am. Chem. Soc.* **2008,** *130* (23), 7247-7249; (b) Liu, T.; Mei, T.-S.; Yu, J.-Q., γ,δ,ε-C(sp3)–H Functionalization through Directed Radical H-Abstraction. *J. Am. Chem. Soc.* **2015,** *137* (18), 5871-5874.

96. Bonardi, A.-H.; Dumur, F.; Noirbent, G.; Lalevée, J.; Gigmes, D., Organometallic vs organic photoredox catalysts for photocuring reactions in the visible region. *Beilstein J. Org. Chem.* **2018,** *14*, 3025-3046.

97. Choi, G. J.; Zhu, Q.; Miller, D. C.; Gu, C. J.; Knowles, R. R., Catalytic alkylation of remote C–H bonds enabled by proton-coupled electron transfer. *Nature* **2016,** *539* (7628), 268-271.

98. Bordwell, F. G.; Zhang, S.; Zhang, X.-M.; Liu, W.-Z., Homolytic Bond Dissociation Enthalpies of the Acidic H-A Bonds Caused by Proximate Substituents in Sets of Methyl Ketones, Carboxylic Esters, and Carboxamides Related to Changes in Ground State Energies. *J. Am. Chem. Soc.* **1995,** *117* (27), 7092-7096.

99. Zard, S. Z., Recent progress in the generation and use of nitrogen-centred radicals. *Chem. Soc. Rev.* **2008,** *37* (8), 1603-1618.

100. Pattabiraman, V. R.; Bode, J. W., Rethinking amide bond synthesis. *Nature* **2011,** *480* (7378), 471-479.

101. Kerru, N.; Gummidi, L.; Maddila, S.; Gangu, K. K.; Jonnalagadda, S. B., A Review on Recent Advances in Nitrogen-Containing Molecules and Their Biological Applications. *Molecules* **2020,** *25* (8).

102. Thullen, S. M.; Treacy, S. M.; Rovis, T., Regioselective Alkylative Cross-Coupling of Remote Unactivated C(sp3)–H Bonds. *J. Am. Chem. Soc.* **2019,** *141* (36), 14062-14067.

103. Xu, B.; Tambar, U. K., Remote Allylation of Unactivated C(sp3)–H Bonds Triggered by Photogenerated Amidyl Radicals. *ACS Catal.* **2019,** *9* (5), 4627-4631.

104. (a) Twilton, J.; Le, C.; Zhang, P.; Shaw, M. H.; Evans, R. W.; MacMillan, D. W. C., The merger of transition metal and photocatalysis. *Nature Reviews Chemistry* **2017,** *1* (7), 0052; (b) Skubi, K. L.; Blum, T. R.; Yoon, T. P., Dual Catalysis Strategies in Photochemical Synthesis. *Chem. Rev.* **2016,** *116* (17), 10035-10074; (c) Prier, C. K.; Rankic, D. A.; MacMillan, D. W. C., Visible Light Photoredox Catalysis with Transition Metal Complexes: Applications in Organic Synthesis. *Chem. Rev.* **2013,** *113* (7), 5322-5363.

105. Rand, A. W.; Yin, H.; Xu, L.; Giacoboni, J.; Martin-Montero, R.; Romano, C.; Montgomery, J.; Martin, R., Dual Catalytic Platform for Enabling sp3 α C–H Arylation and Alkylation of Benzamides. *ACS Catal.* **2020,** *10* (8), 4671-4676.

106. (a) Heitz, D. R.; Tellis, J. C.; Molander, G. A., Photochemical Nickel-Catalyzed C–H Arylation: Synthetic Scope and Mechanistic Investigations. *J. Am. Chem. Soc.* **2016,** *138* (39), 12715-12718; (b) Shields, B. J.; Doyle, A. G., Direct C(sp3)–H Cross Coupling Enabled by Catalytic Generation of Chlorine Radicals. *J. Am. Chem. Soc.* **2016,** *138* (39), 12719-12722; (c) Shu, X.; Zhong, D.; Huang, Q.; Huan, L.; Huo, H., Site- and enantioselective cross-coupling of

saturated N-heterocycles with carboxylic acids by cooperative Ni/photoredox catalysis. *Nat. Commun.* **2023,** *14* (1), 125.

107. Godula, K.; Sames, D., C-H Bond Functionalization in Complex Organic Synthesis. *Science* **2006,** *312* (5770), 67-72.

108. (a) Lam, N. Y. S.; Wu, K.; Yu, J.-Q., Advancing the Logic of Chemical Synthesis: C−H Activation as Strategic and Tactical Disconnections for C−C Bond Construction. *Angew. Chem. Int. Ed.* **2021,** *60* (29), 15767-15790; (b) Blakemore, D. C.; Castro, L.; Churcher, I.; Rees, D. C.; Thomas, A. W.; Wilson, D. M.; Wood, A., Organic synthesis provides opportunities to transform drug discovery. *Nat. Chem.* **2018,** *10* (4), 383-394; (c) Cernak, T.; Dykstra, K. D.; Tyagarajan, S.; Vachal, P.; Krska, S. W., The medicinal chemist's toolbox for late stage functionalization of drug-like molecules. *Chem. Soc. Rev.* **2016,** *45* (3), 546-576.

109. (a) Mahatthananchai, J.; Dumas, A. M.; Bode, J. W., Catalytic Selective Synthesis. *Angew. Chem. Int. Ed.* **2012,** *51* (44), 10954-10990; (b) Afagh, N. A.; Yudin, A. K., Chemoselectivity and the Curious Reactivity Preferences of Functional Groups. *Angew. Chem. Int. Ed.* **2010,** *49* (2), 262-310; (c) Trost, B. M., Selectivity: A Key to Synthetic Efficiency. *Science* **1983,** *219* (4582), 245-250.

110. (a) Malik, H. A.; Baxter, R. D.; Montgomery, J., Nickel-Catalyzed Reductive Couplings and Cyclizations. In *Catalysis without Precious Metals*, 2010; pp 181-212; (b) Montgomery, J., Nickel-Catalyzed Reductive Cyclizations and Couplings. *Angew. Chem. Int. Ed.* **2004,** *43* (30), 3890-3908.

111. Bakhoda, A. G.; Wiese, S.; Greene, C.; Figula, B. C.; Bertke, J. A.; Warren, T. H., Radical Capture at Nickel(II) Complexes: C–C, C–N, and C–O Bond Formation. *Organometallics* **2020,** *39* (10), 1710-1718.

112. Joe, C. L.; Doyle, A. G., Direct Acylation of C(sp3)−H Bonds Enabled by Nickel and Photoredox Catalysis. *Angew. Chem. Int. Ed.* **2016,** *55* (12), 4040-4043.

113. Wotal, A. C.; Weix, D. J., Synthesis of Functionalized Dialkyl Ketones from Carboxylic Acid Derivatives and Alkyl Halides. *Org. Lett.* **2012,** *14* (6), 1476-1479.

114. Cuthbertson, J. D.; MacMillan, D. W. C., The direct arylation of allylic sp3 C–H bonds via organic and photoredox catalysis. *Nature* **2015,** *519* (7541), 74-77.

115. Mao, E.; MacMillan, D. W. C., Late-Stage C(sp3)–H Methylation of Drug Molecules. *J. Am. Chem. Soc.* **2023**.

116. McManus, J. B.; Onuska, N. P. R.; Jeffreys, M. S.; Goodwin, N. C.; Nicewicz, D. A., Site-Selective C–H Alkylation of Piperazine Substrates via Organic Photoredox Catalysis. *Org. Lett.* **2020,** *22* (2), 679-683.

117. Zhu, J. L.; Schull, C. R.; Tam, A. T.; Rentería-Gómez, Á.; Gogoi, A. R.; Gutierrez, O.; Scheidt, K. A., Photoinduced Acylations Via Azolium-Promoted Intermolecular Hydrogen Atom Transfer. *J. Am. Chem. Soc.* **2023,** *145* (3), 1535-1541.

118. (a) Xie, J.; Xu, P.; Zhu, Y.; Wang, J.; Lee, W.-C. C.; Zhang, X. P., New Catalytic Radical Process Involving 1,4-Hydrogen Atom Abstraction: Asymmetric Construction of Cyclobutanones. *J. Am. Chem. Soc.* **2021,** *143* (30), 11670-11678; (b) Wang, X.; Ke, J.; Zhu, Y.; Deb, A.; Xu, Y.; Zhang, X. P., Asymmetric Radical Process for General Synthesis of Chiral Heteroaryl Cyclopropanes. *J. Am. Chem. Soc.* **2021,** *143* (29), 11121-11129; (c) Liu, W.; Lavagnino, M. N.; Gould, C. A.; Alcázar, J.; MacMillan, D. W. C., A biomimetic SH2 cross-coupling mechanism for quaternary sp3-carbon formation. *Science* **2021,** *374* (6572), 1258-1263; (d) Bour, J. R.; Ferguson, D. M.; McClain, E. J.; Kampf, J. W.; Sanford, M. S., Connecting Organometallic Ni(III) and Ni(IV): Reactions of Carbon-Centered Radicals with High-Valent Organonickel Complexes. *J. Am. Chem. Soc.* **2019,** *141* (22), 8914-8920; (e) Tsymbal, A. V.; Bizzini, L. D.; MacMillan, D. W. C., Nickel Catalysis via SH2 Homolytic Substitution: The Double Decarboxylative Cross-Coupling of Aliphatic Acids. *J. Am. Chem. Soc.* **2022,** *144* (46), 21278-21286.

119. (a) Leifert, D.; Studer, A., The Persistent Radical Effect in Organic Synthesis. *Angew. Chem. Int. Ed.* **2020,** *59* (1), 74-108; (b) Fischer, H., The Persistent Radical Effect: A Principle for Selective Radical Reactions and Living Radical Polymerizations. *Chem. Rev.* **2001,** *101* (12), 3581-3610; (c) Ke, J.; Tang, Y.; Yi, H.; Li, Y.; Cheng, Y.; Liu, C.; Lei, A., Copper-Catalyzed Radical/Radical C□H/P□H Cross-Coupling: α-Phosphorylation of Aryl Ketone O-Acetyloximes. *Angew. Chem. Int. Ed.* **2015,** *54* (22), 6604-6607.

120. (a) Fu, Y.; Chen, H.; Fu, W.; Garcia-Borràs, M.; Yang, Y.; Liu, P., Engineered P450 Atom-Transfer Radical Cyclases are Bifunctional Biocatalysts: Reaction Mechanism and Origin of Enantioselectivity. *J. Am. Chem. Soc.* **2022,** *144* (29), 13344-13355; (b) Zhou, Q.; Chin, M.; Fu, Y.; Liu, P.; Yang, Y., Stereodivergent atom-transfer radical cyclization by engineered cytochromes P450. *Science* **2021,** *374* (6575), 1612-1616; (c) Coelho, P. S.; Brustad, E. M.; Kannan, A.; Arnold, F. H., Olefin Cyclopropanation via Carbene Transfer Catalyzed by Engineered Cytochrome P450 Enzymes. *Science* **2013,** *339* (6117), 307-310; (d) Farwell, C. C.; McIntosh, J. A.; Hyster, T. K.;

Wang, Z. J.; Arnold, F. H., Enantioselective Imidation of Sulfides via Enzyme-Catalyzed Intermolecular Nitrogen-Atom Transfer. *J. Am. Chem. Soc.* **2014,** *136* (24), 8766-8771; (e) Hyster, T. K.; Farwell, C. C.; Buller, A. R.; McIntosh, J. A.; Arnold, F. H., Enzyme-Controlled Nitrogen-Atom Transfer Enables Regiodivergent C–H Amination. *J. Am. Chem. Soc.* **2014,** *136* (44), 15505-15508.

121. (a) Li, Z.-L.; Sun, K.-K.; Cai, C., Nickel-Catalyzed Cross-Dehydrogenative Coupling of α-C(sp3)–H Bonds in N-Methylamides with C(sp3)–H Bonds in Cyclic Alkanes. *Org. Lett.* **2018,** *20* (20), 6420-6424; (b) Liu, D.; Liu, C.; Li, H.; Lei, A., Direct Functionalization of Tetrahydrofuran and 1,4-Dioxane: Nickel-Catalyzed Oxidative C(sp3)□H Arylation. *Angew. Chem. Int. Ed.* **2013,** *52* (16), 4453-4456.

122. Li, K.; Wu, Q.; Lan, J.; You, J., Coordinating activation strategy for C(sp3)–H/C(sp3)–H cross-coupling to access β-aromatic α-amino acids. *Nat. Commun.* **2015,** *6* (1), 8404.

123. Yi, H.; Zhang, G.; Wang, H.; Huang, Z.; Wang, J.; Singh, A. K.; Lei, A., Recent Advances in Radical C–H Activation/Radical Cross-Coupling. *Chem. Rev.* **2017,** *117* (13), 9016-9085.

124. (a) Li, Z.; Li, C.-J., CuBr-Catalyzed Direct Indolation of Tetrahydroisoquinolines via Cross-Dehydrogenative Coupling between sp3 C−H and sp2 C−H Bonds. *J. Am. Chem. Soc.* **2005,** *127* (19), 6968-6969; (b) Li, Z.; Bohle, D. S.; Li, C.-J., Cu-catalyzed cross-dehydrogenative coupling: A versatile strategy for C–C bond formations via the oxidative activation of sp3 C–H bonds. *Proceedings of the National Academy of Sciences* **2006,** *103* (24), 8928-8933.

125. (a) Ren, X.; Couture, B. M.; Liu, N.; Lall, M. S.; Kohrt, J. T.; Fasan, R., Enantioselective Single and Dual α-C–H Bond Functionalization of Cyclic Amines via Enzymatic Carbene Transfer. *J. Am. Chem. Soc.* **2023,** *145* (1), 537-550; (b) Paul, A.; Seidel, D., α-Functionalization of Cyclic Secondary Amines: Lewis Acid Promoted Addition of Organometallics to Transient Imines. *J. Am. Chem. Soc.* **2019,** *141* (22), 8778-8782; (c) Walker, M. M.; Koronkiewicz, B.; Chen, S.; Houk, K. N.; Mayer, J. M.; Ellman, J. A., Highly Diastereoselective Functionalization of Piperidines by Photoredox-Catalyzed α-Amino C–H Arylation and Epimerization. *J. Am. Chem. Soc.* **2020,** *142* (18), 8194-8202.

126. (a) Xiao, J.; Li, Z.; Montgomery, J., Nickel-Catalyzed Decarboxylative Coupling of Redox-Active Esters with Aliphatic Aldehydes. *J. Am. Chem. Soc.* **2021,** *143* (50), 21234-21240; (b) Cruz, C. L.; Montgomery, J., Nickel-catalyzed reductive coupling of unactivated alkyl bromides and aliphatic aldehydes. *Chem. Sci.* **2021,** *12* (36), 11995-12000; (c) Shimkin, K. W.;

Montgomery, J., Synthesis of Tetrasubstituted Alkenes by Tandem Metallacycle Formation/Cross-Electrophile Coupling. *J. Am. Chem. Soc.* **2018,** *140* (23), 7074-7078.

127. (a) Liu, Z.; Kole, G. K.; Budiman, Y. P.; Tian, Y.-M.; Friedrich, A.; Luo, X.; Westcott, S. A.; Radius, U.; Marder, T. B., Transition Metal Catalyst-Free, Base-Promoted 1,2-Additions of Polyfluorophenylboronates to Aldehydes and Ketones. *Angew. Chem. Int. Ed.* **2021,** *60* (30), 16529-16538; (b) Zheng, Y.-L.; Newman, S. G., Cross-coupling reactions with esters, aldehydes, and alcohols. *Chem Commun* **2021,** *57* (21), 2591-2604.

128. Kawasaki, T.; Ishida, N.; Murakami, M., Dehydrogenative Coupling of Benzylic and Aldehydic C–H Bonds. *J. Am. Chem. Soc.* **2020,** *142* (7), 3366-3370.

129. Taylor, R. D.; MacCoss, M.; Lawson, A. D. G., Rings in Drugs. *J. Med. Chem.* **2014,** *57* (14), 5845-5859.

130. (a) Lahdenperä, A. S. K.; Bacoş, P. D.; Phipps, R. J., Enantioselective Giese Additions of Prochiral α-Amino Radicals. *J. Am. Chem. Soc.* **2022,** *144* (49), 22451-22457; (b) Gant Kanegusuku, A. L.; Roizen, J. L., Recent Advances in Photoredox-Mediated Radical Conjugate Addition Reactions: An Expanding Toolkit for the Giese Reaction. *Angew. Chem. Int. Ed.* **2021,** *60* (39), 21116-21149; (c) Millet, A.; Lefebvre, Q.; Rueping, M., Visible-Light Photoredox-Catalyzed Giese Reaction: Decarboxylative Addition of Amino Acid Derived α-Amino Radicals to Electron-Deficient Olefins. *Chem. Eur. J.* **2016,** *22* (38), 13464-13468.

131. (a) Bath, S.; Laso, N. M.; Lopez-Ruiz, H.; Quiclet-Sire, B.; Zard, S. Z., A practical access to acyl radicals from acyl hydrazides. *Chem Commun* **2003,** (2), 204-205; (b) Crich, D.; Chen, C.; Hwang, J.-T.; Yuan, H.; Papadatos, A.; Walter, R. I., Photoinduced Free Radical Chemistry of the Acyl Tellurides: Generation, Inter- and Intramolecular Trapping, and ESR Spectroscopic Identification of Acyl Radicals. *J. Am. Chem. Soc.* **1994,** *116* (20), 8937-8951.

132. (a) Sun, Z. M.; Tang, B. Q.; Liu, K. K. C.; Zhu, H. Y., Direct photochemical cross-coupling between aliphatic acids and BF3K salts. *Chem Commun* **2020,** *56* (8), 1294-1297; (b) Liu, D.; Li, Y.; Qi, X.; Liu, C.; Lan, Y.; Lei, A., Nickel-Catalyzed Selective Oxidative Radical Cross-Coupling: An Effective Strategy for Inert Csp3–H Functionalization. *Org. Lett.* **2015,** *17* (4), 998-1001.

133. Garcia, K. J.; Gilbert, M. M.; Weix, D. J., Nickel-Catalyzed Addition of Aryl Bromides to Aldehydes To Form Hindered Secondary Alcohols. *J. Am. Chem. Soc.* **2019,** *141* (5), 1823-1827.

134. Mahjour, B.; Shen, Y.; Liu, W.; Cernak, T., A map of the amine–carboxylic acid coupling system. *Nature* **2020,** *580* (7801), 71-75.

135. (a) Li, Q. Y.; Gockel, S. N.; Lutovsky, G. A.; DeGlopper, K. S.; Baldwin, N. J.; Bundesmann, M. W.; Tucker, J. W.; Bagley, S. W.; Yoon, T. P., Decarboxylative cross-nucleophile coupling via ligand-to-metal charge transfer photoexcitation of Cu(ii) carboxylates. *Nat. Chem.* **2022,** *14* (1), 94-99; (b) Liu, C.; Zhang, H.; Shi, W.; Lei, A., Bond Formations between Two Nucleophiles: Transition Metal Catalyzed Oxidative Cross-Coupling Reactions. *Chem. Rev.* **2011,** *111* (3), 1780-1824; (c) Rezayee, N. M.; Lamhauge, J. N.; Jørgensen, K. A., Organocatalyzed Cross-Nucleophile Couplings: Umpolung of Catalytic Enamines. *Acc. Chem. Res.* **2022,** *55* (12), 1703-1717.

136. (a) Hoover, J. M.; Stahl, S. S., Highly Practical Copper(I)/TEMPO Catalyst System for Chemoselective Aerobic Oxidation of Primary Alcohols. *J. Am. Chem. Soc.* **2011,** *133* (42), 16901-16910; (b) Hoover, J. M.; Steves, J. E.; Stahl, S. S., Copper(I)/TEMPO-catalyzed aerobic oxidation of primary alcohols to aldehydes with ambient air. *Nat. Protoc.* **2012,** *7* (6), 1161-1166.

137. Verheyen, T.; van Turnhout, L.; Vandavasi, J. K.; Isbrandt, E. S.; De Borggraeve, W. M.; Newman, S. G., Ketone Synthesis by a Nickel-Catalyzed Dehydrogenative Cross-Coupling of Primary Alcohols. *J. Am. Chem. Soc.* **2019,** *141* (17), 6869-6874.

138. Cheng, L.; Liu, J.; Chen, Y.; Gong, H., Nickel-catalysed hydrodimerization of unactivated terminal alkenes. *Nature Synthesis* **2023**.

139. Hoque, M. A.; Twilton, J.; Zhu, J.; Graaf, M. D.; Harper, K. C.; Tuca, E.; DiLabio, G. A.; Stahl, S. S., Electrochemical PINOylation of Methylarenes: Improving the Scope and Utility of Benzylic Oxidation through Mediated Electrolysis. *J. Am. Chem. Soc.* **2022,** *144* (33), 15295-15302.

140. (a) Zhao, G.; Yao, W.; Kevlishvili, I.; Mauro, J. N.; Liu, P.; Ngai, M.-Y., Nickel-Catalyzed Radical Migratory Coupling Enables C-2 Arylation of Carbohydrates. *J. Am. Chem. Soc.* **2021,** *143* (23), 8590-8596; (b) Hu, X., Nickel-catalyzed cross coupling of non-activated alkyl halides: a mechanistic perspective. *Chem. Sci.* **2011,** *2* (10), 1867-1886.

141. Xu, G.-Q.; Xiao, T.-F.; Feng, G.-X.; Liu, C.; Zhang, B.; Xu, P.-F., Metal-Free α-C(sp3)–H Aroylation of Amines via a Photoredox Catalytic Radical–Radical Cross-Coupling Process. *Org. Lett.* **2021,** *23* (8), 2846-2852.

142. (a) Kranthikumar, R., Recent Advances in C(sp3)–C(sp3) Cross-Coupling Chemistry: A Dominant Performance of Nickel Catalysts. *Organometallics* **2022,** *41* (6), 667-679; (b) Bera, S.; Mao, R.; Hu, X., Enantioselective C(sp3)–C(sp3) cross-coupling of non-activated alkyl electrophiles via nickel hydride catalysis. *Nat. Chem.* **2021,** *13* (3), 270-277; (c) Li, Y.; Nie, W.; Chang, Z.; Wang, J.-W.; Lu, X.; Fu, Y., Cobalt-catalysed enantioselective C(sp3)–C(sp3) coupling. *Nature Catalysis* **2021,** *4* (10), 901-911.

143. McManus, J. B.; Onuska, N. P. R.; Nicewicz, D. A., Generation and Alkylation of α-Carbamyl Radicals via Organic Photoredox Catalysis. *J. Am. Chem. Soc.* **2018,** *140* (29), 9056-9060.

144. (a) Drache, M.; Stehle, M.; Mätzig, J.; Brandl, K.; Jungbluth, M.; Namyslo, J. C.; Schmidt, A.; Beuermann, S., Identification of β scission products from free radical polymerizations of butyl acrylate at high temperature. *Polymer Chemistry* **2019,** *10* (15), 1956-1967; (b) Offenbach, J. A.; Tobolsky, A. V., The Initiation of Polymerization by Di-t-butyl Peroxide. *J. Am. Chem. Soc.* **1957,** *79* (2), 278-281.

145. Blackmond, D. G., Reaction Progress Kinetic Analysis: A Powerful Methodology for Mechanistic Studies of Complex Catalytic Reactions. *Angew. Chem. Int. Ed.* **2005,** *44* (28), 4302-4320.

146. Hamby, T. B.; LaLama, M. J.; Sevov, C. S., Controlling Ni redox states by dynamic ligand exchange for electroreductive Csp3–Csp2 coupling. *Science* **2022,** *376* (6591), 410-416.

147. Milbauer, M. W.; Kampf, J. W.; Sanford, M. S., Nickel(IV) Intermediates in Aminoquinoline-Directed C(sp2)–C(sp3) Coupling. *J. Am. Chem. Soc.* **2022,** *144* (46), 21030-21034.

148. (a) Ju, L.; Hu, C. T.; Diao, T., Strategies for Promoting Reductive Elimination of Bi- and Bis-Oxazoline Ligated Organonickel Complexes. *Organometallics* **2022,** *41* (14), 1748-1753; (b) Lin, Q.; Fu, Y.; Liu, P.; Diao, T., Monovalent Nickel-Mediated Radical Formation: A Concerted Halogen-Atom Dissociation Pathway Determined by Electroanalytical Studies. *J. Am. Chem. Soc.* **2021,** *143* (35), 14196-14206; (c) Wagner, C. L.; Herrera, G.; Lin, Q.; Hu, C. T.; Diao, T., Redox Activity of Pyridine-Oxazoline Ligands in the Stabilization of Low-Valent Organonickel Radical Complexes. *J. Am. Chem. Soc.* **2021,** *143* (14), 5295-5300; (d) Diccianni, J. B.; Diao, T., Mechanisms of Nickel-Catalyzed Cross-Coupling Reactions. *Trends in Chemistry* **2019,** *1* (9), 830-844.

149. (a) Weix, D. J., Methods and Mechanisms for Cross-Electrophile Coupling of Csp2 Halides with Alkyl Electrophiles. *Acc. Chem. Res.* **2015,** *48* (6), 1767-1775; (b) Biswas, S.; Weix, D. J., Mechanism and Selectivity in Nickel-Catalyzed Cross-Electrophile Coupling of Aryl Halides with Alkyl Halides. *J. Am. Chem. Soc.* **2013,** *135* (43), 16192-16197.

150. Welin, E. R.; Le, C.; Arias-Rotondo, D. M.; McCusker, J. K.; MacMillan, D. W. C., Photosensitized, energy transfer-mediated organometallic catalysis through electronically excited nickel(II). *Science* **2017,** *355* (6323), 380-385.

151. Bantreil, X.; Nolan, S. P., Synthesis of N-heterocyclic carbene ligands and derived ruthenium olefin metathesis catalysts. *Nat. Protoc.* **2011,** *6* (1), 69-77.

152. Guo, S.; Qian, B.; Xie, Y.; Xia, C.; Huang, H., Copper-Catalyzed Oxidative Amination of Benzoxazoles via C−H and C−N Bond Activation: A New Strategy for Using Tertiary Amines as Nitrogen Group Sources. *Org. Lett.* **2011,** *13* (3), 522-525.

153. Lee, J. J.; Kim, J.; Jun, Y. M.; Lee, B. M.; Kim, B. H., Indium-mediated one-pot synthesis of benzoxazoles or oxazoles from 2-nitrophenols or 1-aryl-2-nitroethanones. *Tetrahedron* **2009,** *65* (43), 8821-8831.

154. Filloux, C. M.; Rovis, T., Rh(I)–Bisphosphine-Catalyzed Asymmetric, Intermolecular Hydroheteroarylation of α-Substituted Acrylate Derivatives. *J. Am. Chem. Soc.* **2015,** *137* (1), 508-517.

155. Kim, T.; Lee, S.-A.; Noh, T.; Choi, P.; Choi, S.-J.; Song, B. G.; Kim, Y.; Park, Y.-T.; Huh, G.; Kim, Y.-J.; Ham, J., Synthesis, Structure Revision, and Cytotoxicity of Nocarbenzoxazole G. *J. Nat. Prod.* **2019,** *82* (5), 1325-1330.

156. Li, Y.; Waser, J., Zinc–gold cooperative catalysis for the direct alkynylation of benzofurans. *Beilstein J. Org. Chem.* **2013,** *9*, 1763-1767.

157. Xu-Xu, Q.-F.; Liu, Q.-Q.; Zhang, X.; You, S.-L., Copper-Catalyzed Ring Opening of Benzofurans and an Enantioselective Hydroamination Cascade. *Angew. Chem. Int. Ed.* **2018,** *57* (46), 15204-15208.

158. Saito, H.; Otsuka, S.; Nogi, K.; Yorimitsu, H., Nickel-Catalyzed Boron Insertion into the C2–O Bond of Benzofurans. *J. Am. Chem. Soc.* **2016,** *138* (47), 15315-15318.

159. Brück, A.; Ruhland, K., Investigation of the Dynamic Solution Behavior of Chloro(diene)rhodium(I) Phosphine Complexes with a Pendant Unsaturated Heterocycle at

Phosphorus (2-pyridyl, 2-imidazyl; diene = COD, NBD). *Organometallics* **2009,** *28* (22), 6383-6401.

160. Serradeil-Albalat, M.; Roussel, C.; Vanthuyne, N.; Vallejos, J.-C.; Wilhelm, D., Synthesis of chiral primary amines: diastereoselective alkylation of N-[(1E)-alkylidene]-3,5-bis[(1S)-1-methoxyethyl]-4H-1,2,4-triazol-4-amines and N4–Nexocyclic bond cleavage in the resulting 1,2,4-triazol-4-alkylamines. *Tetrahedron Asymm.* **2008,** *19* (23), 2682-2692.

161. Nakao, Y.; Idei, H.; Kanyiva, K. S.; Hiyama, T., Direct Alkenylation and Alkylation of Pyridone Derivatives by Ni/AlMe3 Catalysis. *J. Am. Chem. Soc.* **2009,** *131* (44), 15996-15997.

162. Desrosiers, V.; Garcia, C. Z.; Fontaine, F.-G., Boron Recycling in the Metal-Free Transfer C–H Borylation of Terminal Alkynes and Heteroarenes. *ACS Catal.* **2020,** *10* (19), 11046-11056.

163. Lane, B. S.; Brown, M. A.; Sames, D., Direct Palladium-Catalyzed C-2 and C-3 Arylation of Indoles: A Mechanistic Rationale for Regioselectivity. *J. Am. Chem. Soc.* **2005,** *127* (22), 8050-8057.

164. Wu, X.; See, J. W. T.; Xu, K.; Hirao, H.; Roger, J.; Hierso, J.-C.; Zhou, J., A General Palladium-Catalyzed Method for Alkylation of Heteroarenes Using Secondary and Tertiary Alkyl Halides. *Angew. Chem. Int. Ed.* **2014,** *53* (49), 13573-13577.

165. Sevov, C. S.; Hartwig, J. F., Iridium-Catalyzed Intermolecular Asymmetric Hydroheteroarylation of Bicycloalkenes. *J. Am. Chem. Soc.* **2013,** *135* (6), 2116-2119.

166. Qi, S.-L.; Li, Y.; Li, J.-F.; Zhang, T.; Luan, Y.-X.; Ye, M., Ni-Catalyzed Dual C–H Annulation of Benzimidazoles with Alkynes for Synthesis of π-Extended Heteroarenes. *Org. Lett.* **2021,** *23* (10), 4034-4039.

167. Vijaykumar, G.; Jose, A.; Vardhanapu, P. K.; P, S.; Mandal, S. K., Abnormal-NHC-Supported Nickel Catalysts for Hydroheteroarylation of Vinylarenes. *Organometallics* **2017,** *36* (24), 4753-4758.

168. Zhao, X.; Wu, G.; Zhang, Y.; Wang, J., Copper-Catalyzed Direct Benzylation or Allylation of 1,3-Azoles with N-Tosylhydrazones. *J. Am. Chem. Soc.* **2011,** *133* (10), 3296-3299.

169. Lee, W.-C.; Wang, C.-H.; Lin, Y.-H.; Shih, W.-C.; Ong, T.-G., Tandem Isomerization and C–H Activation: Regioselective Hydroheteroarylation of Allylarenes. *Org. Lett.* **2013,** *15* (20), 5358-5361.

170. Nieddu, G.; Giacomelli, G., A microwave assisted synthesis of benzoxazoles from carboxylic acids. *Tetrahedron* **2013,** *69* (2), 791-795.

171. Spieß, P.; Berger, M.; Kaiser, D.; Maulide, N., Direct Synthesis of Enamides via Electrophilic Activation of Amides. *J. Am. Chem. Soc.* **2021,** *143* (28), 10524-10529.

172. Rand, A. W.; Chen, M.; Montgomery, J., Investigations into mechanism and origin of regioselectivity in the metallaphotoredox-catalyzed α-arylation of N-alkylbenzamides. *Chem. Sci.* **2022,** *13* (35), 10566-10573.

173. Souza, L. W.; Squitieri, R. A.; Dimirjian, C. A.; Hodur, B. M.; Nickerson, L. A.; Penrod, C. N.; Cordova, J.; Fettinger, J. C.; Shaw, J. T., Enantioselective Synthesis of Indolines, Benzodihydrothiophenes, and Indanes by C−H Insertion of Donor/Donor Carbenes. *Angew. Chem. Int. Ed.* **2018,** *57* (46), 15213-15216.

174. Ishii, T.; Kakeno, Y.; Nagao, K.; Ohmiya, H., N-Heterocyclic Carbene-Catalyzed Decarboxylative Alkylation of Aldehydes. *J. Am. Chem. Soc.* **2019,** *141* (9), 3854-3858.

175. Ren, S.-C.; Yang, X.; Mondal, B.; Mou, C.; Tian, W.; Jin, Z.; Chi, Y. R., Carbene and photocatalyst-catalyzed decarboxylative radical coupling of carboxylic acids and acyl imidazoles to form ketones. *Nat. Commun.* **2022,** *13* (1), 2846.

176. Le, C. C.; MacMillan, D. W. C., Fragment Couplings via CO2 Extrusion–Recombination: Expansion of a Classic Bond-Forming Strategy via Metallaphotoredox. *J. Am. Chem. Soc.* **2015,** *137* (37), 11938-11941.

177. Du, D.; Zhang, K.; Ma, R.; Chen, L.; Gao, J.; Lu, T.; Shi, Z.; Feng, J., Bio- and Medicinally Compatible α-Amino-Acid Modification via Merging Photoredox and N-Heterocyclic Carbene Catalysis. *Org. Lett.* **2020,** *22* (16), 6370-6375.

178. Goliszewska, K.; Rybicka-Jasińska, K.; Szurmak, J.; Gryko, D., Visible-Light-Mediated Amination of π-Nucleophiles with N-Aminopyridinium Salts. *J. Org. Chem.* **2019,** *84* (24), 15834-15844.

179. Huang, H.; Dai, Q.-S.; Leng, H.-J.; Li, Q.-Z.; Yang, S.-L.; Tao, Y.-M.; Zhang, X.; Qi, T.; Li, J.-L., Suzuki-type cross-coupling of alkyl trifluoroborates with acid fluoride enabled by NHC/photoredox dual catalysis. *Chem. Sci.* **2022,** *13* (9), 2584-2590.